UNIVERSITAT POLITÈCNICA DE VALÈNCIA

PhD Thesis in Biotechnology

Regulation of the nitric oxide synthesis and signaling by post-translational modifications and N-end rule pathway-mediated proteolysis in *Arabidopsis thaliana*

Álvaro Costa Broseta

Director: José León Ramos

Tutor: Lynne Yenush

VALENCIA, OCTOBER 2018

CSIC

Consejo Superior de Investigaciones Científicas

ibmcp

Instituto de Biología Molecular y Celular de Plantas

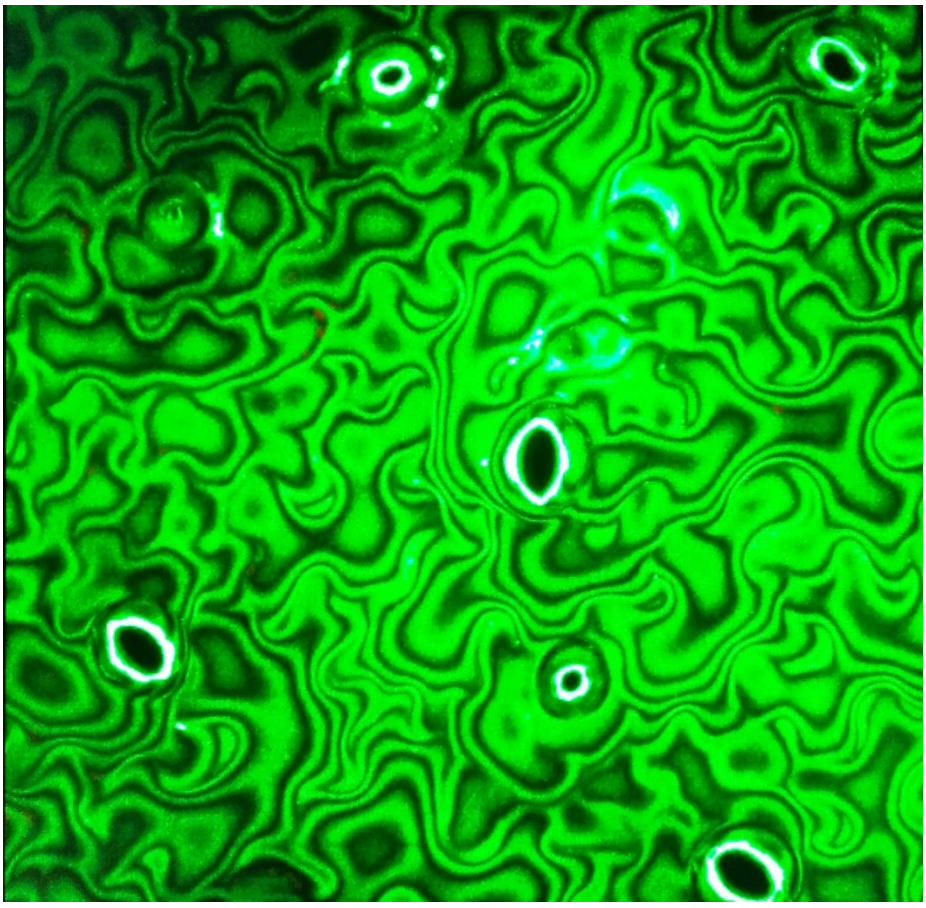

Cover art by Álvaro Costa Broseta. Z stack image of a DAF-FM DA-stained cotyledon obtained by confocal microscopy.

El Dr. José León Ramos, doctor en Ciencias Químicas e Investigador Científico del Consejo Superior de Investigaciones Científicas (CSIC).

CERTIFICA:

Que la presente memoria titulada “Regulation of the nitric oxide synthesis and signaling by post-translational modifications and N-end rule pathway-mediated proteolysis in *Arabidopsis thaliana*”, ha sido realizada por Álvaro Costa Broseta bajo mi dirección y constituye su Memoria de Tesis para optar al grado de Doctor en Biotecnología.

Para que conste a todos los efectos oportunos, firma el presente certificado en Valencia, noviembre del 2018.

Dr. José León Ramos

SUMMARY

Nitric oxide (NO) is a highly reactive gaseous molecule that regulates plant growth and development as well as defense responses. NO is mainly produced from nitrite by nitrate reductases (NRs) in balance with nitrite reductases (NiRs), and is sensed through a mechanism involving the N-end rule pathway-mediated proteolysis of the group VII of ERF transcription factors (ERFVIIs). NO especially exerts its signaling function by triggering post-translational modifications in proteins and altering their function, structure and/or stability. By these means and in collaboration with different phytohormone signaling pathways, NO is capable of regulating a wide array of cell processes in plants, including those related to the acquirement of freezing tolerance.

By using *Arabidopsis thaliana* as model plant, during the development of this work it was found that NO can regulate its own biosynthesis, as NRs and NiR enzymes were regulated by three main factors: nitrate-induced signaling controlled by the function of the NIN-like protein 7 (NLP7) transcription factor, N-end rule proteolytic pathway, and proteasome-mediated degradation, likely triggered by NO-related post-translational modifications. In addition, the ERFVII transcription factor RAP2.3 was found to negatively regulate both the NO biosynthesis and their triggered responses through a rheostat-like mechanism that involves specific NO-related branches of jasmonate and abscisic acid signaling pathways. On the other hand, a combined metabolomic and transcriptomic characterization of NO-deficient *nia1,2noa1-2* mutant plants and NO-fumigated plants allowed to unravel a number of mechanisms that are controlled by NO. First, NO perception in hypocotyls would require various hormones to be fulfilled as it was confirmed by NO-triggered hypocotyl shortening screenings with hormone-related mutants and the TRANSPLANTA collection of transgenic lines conditionally expressing Arabidopsis transcription factors. Second, high NO doses caused a massive but transient reprogramming of primary and secondary metabolism, including alteration of the cellular redox status, alteration of the permeability of lipidic structures or turnover of proteins and nucleic acids. Lastly, NO was found to prevent the development of freezing tolerance under non-stress temperature conditions, while being essential for the low temperature stress-triggered cold acclimation that leads to enhanced freezing tolerance. NO would achieve this fine-tuned modulation of the activation of the cold-related responses by coordinating the accumulation of different metabolites and hormones. Altogether, this work sheds light on the mechanisms by which, by interacting with various signaling and metabolic pathways, NO can regulate several key processes of plant physiology.

RESUMEN

El óxido nítrico (NO) es una molécula gaseosa altamente reactiva que regula el crecimiento y el desarrollo de las plantas así como sus respuestas de defensa. El NO se produce principalmente a partir de nitrito por las nitrato reductasas (NRs) en balance con las nitrito reductasas (NiRs), y es percibido a través de un mecanismo en el que está involucrada la proteólisis dirigida por la secuencia aminoterminal del grupo VII de los factores de transcripción ERF (ERFVIIs). El NO ejerce especialmente su función señalizadora al causar modificaciones postraduccionales en las proteínas y alterar su función, estructura y/o estabilidad. Por estos medios y en colaboración con distintas rutas de señalización fitohormonales, el NO es capaz de regular un amplio abanico de procesos celulares en plantas, incluyendo aquellos relacionados con la adquisición de tolerancia a la congelación.

Utilizando *Arabidopsis thaliana* como planta modelo, en este trabajo se descubrió que el NO puede regular su propia biosíntesis, puesto que las enzimas NRs y NiRs fueron reguladas por tres factores principales: señalización inducida por nitrato y controlada por la función del factor de transcripción NIN-like protein 7 (NLP7), la proteólisis dirigida por la secuencia aminoterminal, y la degradación mediada por el proteasoma, probablemente ocasionada por modificaciones postraduccionales relacionadas con el NO. Adicionalmente, se descubrió que el factor de transcripción ERFVII RAP2.3 regula negativamente tanto la biosíntesis de NO como las respuestas que desencadena a través de un mecanismo similar a un reóstato en el que están involucradas ramas específicas relacionadas con el NO de las rutas de señalización de jasmonato y ácido abscísico. Por otro lado, una caracterización metabolómica y transcriptómica combinada de plantas mutantes *nia1,2noa1-2* deficientes en NO y plantas fumigadas con NO permitió desentrañar una serie de mecanismos que están controlados por NO. En primer lugar, la percepción de NO en los hipocotilos requeriría varias hormonas para ser completada, como fue confirmado por los rastreos de acortamiento de hipocotilo por NO con mutantes relacionados con hormonas y la colección TRANSPLANTA de líneas transgénicas que expresan condicionalmente factores de transcripción de Arabidopsis. En segundo lugar, dosis elevadas de NO causan una reprogramación masiva aunque transitoria de los metabolismos primario y secundario, incluyendo la alteración del estado redox celular, la alteración de la permeabilidad de estructuras lipídicas y el recambio de proteínas y ácidos nucleicos. Por último, se descubrió que el NO previene el desarrollo de la tolerancia a congelación bajo condiciones no estresantes de temperatura, mientras que resulta esencial para la aclimatación a frío desencadenada por bajas temperaturas que conduce a una tolerancia mejorada a congelación. El NO conseguiría esta modulación afinada de la activación de respuestas relacionadas con frío al coordinar la acumulación de diferentes metabolitos y hormonas. En conjunto, este trabajo arroja luz sobre los mecanismos mediante los cuales, al interactuar con varias rutas señalizadoras y metabólicas, el NO puede regular distintos procesos clave de la fisiología vegetal.

RESUM

L'òxid nítric (NO) és una molècula gasosa altament reactiva que regula el creixement i desenvolupament de les plantes així com les seves respostes de defensa. El NO es produeix principalment a partir de nitrit per les nitrat reductases (NRs) en balanç amb les nitrit reductases (NiRs), i és percebut a traves d'un mecanisme que inclou la proteòlisi dirigida per la seqüència aminoterminal del grup VII dels factors de transcripció ERF (ERFVII). El NO exerceix la seva funció senyalitzadora majoritàriament al provocar modificacions postraduccionals en les proteïnes i alterar la seva funció, estructura i/o estabilitat. Mitjançant aquestes modificacions i en col·laboració amb distintes rutes de senyalització fitohormonals, el NO es capaç de regular un ampli espectre de processos cel·lulars en plantes, inclosos aquells relacionats amb l'adquisició de tolerància a la congelació.

Emprant *Arabidopsis thaliana* com a planta model, en aquest treball es va descobrir que el NO regula la seva pròpia biosíntesi, donat que els enzims NRs i NiRs foren regulades per tres factors principals: senyalització induïda per nitrat i controlada per la funció del factor de transcripció NIN-like protein 7 (NLP7), la proteòlisi dirigida per la seqüència aminoterminal, i la degradació mitjançant el proteasoma, probablement a causa de modificacions postraduccionals relacionades amb el NO. A més, es va descobrir que el factor de transcripció ERFVII RAP2.3 regula negativament tant la biosíntesi de NO com les respostes que desencadena aquest a través d'un mecanisme similar a un reòstat en el que estan involucrades branques específiques de les rutes de senyalització de jasmonat i àcid abscísic relacionades amb el NO. Per altre costat, una caracterització metabolòmica i transcriptòmica combinada de plantes mutants *nia1,2noa1-2* deficients en NO i plantes fumigades amb NO va permetre desentranyar una sèrie de mecanismes que estan controlats per NO. En primer lloc, la percepció de NO en els hipocòtils requeriria de varies hormones, com fou confirmat pels rastrejos d'acurtament d'hipocòtil per NO amb mutants relacionats amb hormones i la col·lecció TRANSPLANTA de línies transgèniques d'expressió condicional de factors de transcripció d'Arabidopsis. En segon lloc, dosis elevades de NO causen una reprogramació massiva, encara que transitòria, dels metabolismes primari i secundari, incloent l'alteració de l'estat redox cel·lular, canvis en la permeabilitat de estructures lipídiques i el recanvi de proteïnes i àcids nucleics. Per últim, es va descobrir que el NO prevé el desenvolupament de la tolerància a congelació en condicions no estressants de temperatura, mentre que resulta essencial per a l'aclimatació a fred induïda per baixes temperatures que condueix a una tolerància millorada a congelació. El NO aconseguiria aquesta modulació minuciosa de l'activació de les respostes relacionades amb fred al coordinar l'acumulació de diferents metabòlits i hormones. En conjunt, aquest treball clarifica els mecanismes pels quals el NO pot regular distints processos clau de la fisiologia vegetal al interactuar amb varies rutes senyalitzadores i metabòliques.

Agradecimientos / Acknoledgements

En primerísimo lugar quiero agradecer a Pepe su inestimable labor dirigiendo esta tesis. Tras un TFC, un TFM y esta tesis ya van seis años desde que entré en el labo y Pepe siempre ha sido en la ciencia como un padre para mí. Gracias por haberme soportado todo este tiempo y por haber patrocinado mi doctorado tras mi fracasada búsqueda de financiación. Tu paciencia y tu guía no han caído en saco roto. Gracias también a mi tutora de la UPV, Lynne, por resolverme todas las dudas que me iban surgiendo respecto a los aspectos más burocráticos de la tesis.

Ha sido una tesis cortita (apenas 3 años incluyendo la larga escritura y su correspondiente barba) llena de altibajos y en la que he tenido que despedir varias líneas de investigación que incluían proteínas fantasma, genes inclonables, poblaciones uniforme y eternamente heterocigotas, mutantes imposibles de genotipar y semillas imposibles de resucitar. Lamento la falta de tiempo que me impidió pensar si quiera en la posibilidad de irme de estancia, dar docencia, codirigir el trabajo de algún becario o asistir a un congreso de verdad. Sin embargo creo no equivocarme al decir que ha sido una de las mejores etapas de mi vida. A nivel profesional he tenido más libertad que nunca para diseñar los experimentos e idear la mejor aproximación para cada línea de investigación (aunque rara vez tenía ideas felices). Como recompensa y gracias al duro trabajo de Pepe, hemos publicado tres artículos y hay tres más a la vista. A nivel personal he podido compaginar la tesis con diferentes actividades de ocio que me han llevado a completar varias de mis metas en la vida, incluyendo aprender japonés, ir a Japón, visitar la tumba de Tolkien en Oxford, asistir a un GP de Magic, subir el Veleta en bici, terminar una triatlón (sprint) y terminar una Maratón.

Mi trabajo en el IBMCP no habría sido ni la mitad de llevadero y divertido si no fuera por toda esa gente que ha estado a mi lado. Gracias, Mari, porque llenabas de alegría el laboratorio y tus ausencias eran muy sentidas. No imagino mejor compañera de fatigas. Gracias también a Vicente y Edgar, cuya labor nos allanaba a todos el camino, a pesar de las inevitables y cómicas equivocaciones. A Silvina agradecerle su continuo apoyo durante su breve pero inolvidable estancia en el labo. Gracias a los Rodríguez, especialmente Jorge, Alberto y Marta, por vuestra amistad y por todos los consejos y la ayuda prestada cuando me enfrentaba a nuevos desafíos en la investigación. En especial debo agradecer a Jorge su

asesoramiento en la tinción de DAF y en el uso de la tecnología CRISPR. De la misma forma también agradezco la amistad y los consejos de Leti y las Meloncitas (especialmente Sole, María José y Dorra). Los cafés y las comidas con todos vosotros han sido lo que me ha ayudado a seguir adelante en las malas épocas. A este respecto también valoro mucho las ocasionales reuniones de exleones, donde el intercambio de experiencias con Silbia, Ricardo, Esther o Cristina ha sido de gran provecho. Por otro lado debo agradecer la cálida acogida por parte del laboratorio de Julio Salinas en el CIB. Muchas gracias a Nandy por toda la ayuda que me prestó durante la micro-estancia. También ha sido muy reconfortante y un gran apoyo contar con colegas en mi misma situación como doctorando: agradezco enormemente la comprensión y la empatía de Jorge, Laura, Rosa y Anna. Mención aparte para Laia y mi increíble suerte por conocer a una persona tan valiente y que siempre me ha hecho soñar a lo grande.

Fuera de los ámbitos de la biotecnología, agradezco a mis compañeros del Club Ciclista de Cullera y del curso de Japonés (especialmente Cecilia-san, Mariló-san y Arisa-sensei) por sus ánimos y por ayudarme a desconectar del trabajo. Qué decir del grupo Magic Dance. Alex, Guille, Cat, Diego, Oyan, Tini y Carlitos; alguno de vosotros siempre ha estado ahí dispuesto a ayudarme a relajarme y echarme unas risas con Magic, rol o con cualquier otro juego.

Por último gracias a mi familia, por su apoyo y su afecto impagables. A ellos se lo debo todo.

Table of contents

TABLE OF CONTENTS

FIGURES

TABLES

EQUATIONS

Introduction

1. INTRODUCTION

1.1. *Arabidopsis thaliana* as model organism

The plant *Arabidopsis thaliana* has been used as model organism in the present work. This experimental system has numerous advantages such as: its short life cycle and its manageable size, which allows the analysis of a big number of individuals; its completely sequenced and well annotated genome; the availability of a huge amount of mutants and transgenic lines, organized in stocks of public access, and finally, the availability of a large number of -omic tools. Much of the obtained information in Arabidopsis may be extrapolated to other angiosperms, however those data must be carefully used as a start point for the reconfirmation in other plant species.

1.2. Biosynthesis and metabolism of nitric oxide

Plants are sessile organisms so their development can be compromised by biotic or abiotic stresses coming from an environment they cannot run away from. Plants have acquired plasticity in their development as an adaptation mechanism, therefore the processes related to growth or defense may be enhanced depending on the situation. This distinctive dilemma is controlled on multiple levels through the regulation of transcription, post-transcrition, translation and protein post-translational modifications, in such a way that the development of plants is the outcome of a highly complex network of finely regulated metabolic processes. The control over the metabolism is done via the modulation of the different cell processes in plants, which are determined by the numerous sensed stimuli and signaling pathways. It has been known for a long time that most of these processes are under direct control of regulatory molecules, particularly phytohormones, each of them affecting a wide spectrum of cell events. Nevertheless, even nowadays the details of the mechanisms underlying this complex regulation are not fully understood. Therefore, the characterization of secondary regulators represents the key in deciphering the way the cell machinery is modulated to coordinate plant development and responses to environmental stimuli.

Nitric oxide (NO) is a small gaseous molecule and a free radical that plays numerous key roles in the physiology of living organisms, being particularly important in animal processes like neurotransmission or inflammation response, among others (Schmidt & Walter, 1994). However, it has been in the last twenty years when the function of NO has started to be properly analyzed in plants. Currently, NO is considered a signaling molecule regulating multiple plant physiological processes in collaboration with phytohormones and other growth regulators. However, neither its biosynthesis nor its regulatory involvement in cell processes are fully understood yet (Astier *et al.*, 2017). NO synthesis in plants is enhanced by stress and two main routes have been described for it: one reductive and one oxidative.

The most studied and confirmed biosynthesis pathway of NO in plants is the reduction from nitrite (NO_2^-) (Fig. 1.1). Rarely, this reaction can take place through non-enzymatic means in specific conditions such as low pH or highly reducing environments, or spontaneously in a light-mediated manner (Cooney *et al.*, 1994; Durner *et al.*, 1998; Caro & Puntarulo, 1999; Bethke, 2004). However, various proteins have been described to catalyze this reaction. One of them is the Nitrate Reductase (NR), for which exist two isoforms in *A. thaliana*: NIA1 and NIA2. This protein is a multifunctional cytosolic enzyme that is key for the nitrogen (N) assimilation and metabolism in plants, since it catalyzes the nitrate (NO_3^-) reduction to nitrite by using NADH as an electron donor (Fig. 1.1). In this reaction, the homodimeric complex can only work with molybdopterin, heme and FAD as cofactors (Campbell, 2001). As nitrite is toxic for plants (Wang *et al.*, 2007), usually the next step in the metabolic pathway of nitrogen assimilation is the further reduction of nitrite to ammonium (NH_4^+) by chloroplastic Ferredoxin-Nitrite Reductases (NiR) (Joy & Hageman, 1966; Mikami & Ida, 1984) of which there is only one isoform in *A. thaliana* : NIR1 (Fig. 1.1). Nevertheless, NR has also been described to catalyze the conversion of nitrite to NO (Ni-NR activity) (Fig. 1.1), a marginal reaction that occurs only in specific situations such as high concentration of nitrite and low concentration of nitrate or anoxic or acidic environments (Yamasaki *et al.*, 1999; Yamasaki & Sakihama, 2000; Rockel *et al.*, 2002). Even if NO production by NR is just a secondary role of the enzyme, several pharmacological and genetic approaches have pointed out the importance of this activity for various NO-regulated processes in plant physiology (Astier *et al.*, 2017).

Recently, another NO-producing mechanism has been described. It has been discovered that in the alga *Chlamydomonas reinhardtii*, NO can be produced from nitrite through the interaction of NR with NOFNiR (Nitric Oxide-Forming Nitrite Reductase) (Fig. 1.1). NOFNiR belongs to the Amidoxine Reducing Component (ARC) protein family, whose physiological function is not fully understood yet (Havemeyer *et al.*, 2006). Two genes coding for ARC proteins can be found in the *A. thaliana* genome, but to date the NR:NOFNiR system has not been confirmed in higher plants (Chamizo-Ampudia *et al.*, 2016). Interestingly, it has been described in the same alga that NR can supply electrons from NADPH through its diaphorase/dehydrogenase domain to the Truncated Hemoglobin 1 (THB1), which oxidizes NO to nitrate by its dioxygenase activity in the presence of oxygen (Fig. 1.1) (Sanz-Luque *et al.*, 2015). These two contradictory roles of NR in NO signaling fit the complex modulation of the nitrate cycle of the algae (Calatrava *et al.*, 2017), and highlight also how NR may play a key function in the regulation of the NO homeostasis in plants (Chamizo-Ampudia *et al.*, 2017).

Both NRs and ARCs present a molybdenum cofactor (Moco) in their structure. Other Moco-containing enzymes has been described in plants, such as Xanthine Oxidases (XOs), Aldehyde Oxidases (AOs), and Sulfite Oxidases (SOs), and are suspected to be able to reduce nitrite to NO. XO is a highly conserved enzyme responsible for purine catabolism, and hydroxylating hypoxanthine to xanthine and

xanthine to urea. Two isoforms in plants have been reported to support the reactive oxygen species (ROS) homeostasis during biotic stress (Yesbergenova *et al.*, 2005), but the implication of XOs in NO production is still unclear, with very little evidence (Planchet *et al.*, 2005). AOs are cytoplasmic enzymes with a very similar structure to that of the XOs, which mainly catalyze the oxidation of aldehydes to carboxylates, producing superoxide anions. In plants, AOs play important roles in several defense and development processes, but its implication in the production of NO has not been described yet (Astier *et al.*, 2017). Lastly, SO is a conserved peroxysomal enzyme that catalyzes the oxidation of sulfite to sulfate, but as it occurs with AOs, despite some research with mammalian isoforms, its implication in NO synthesis in plants hasn't been addressed yet (Astier *et al.*, 2017).

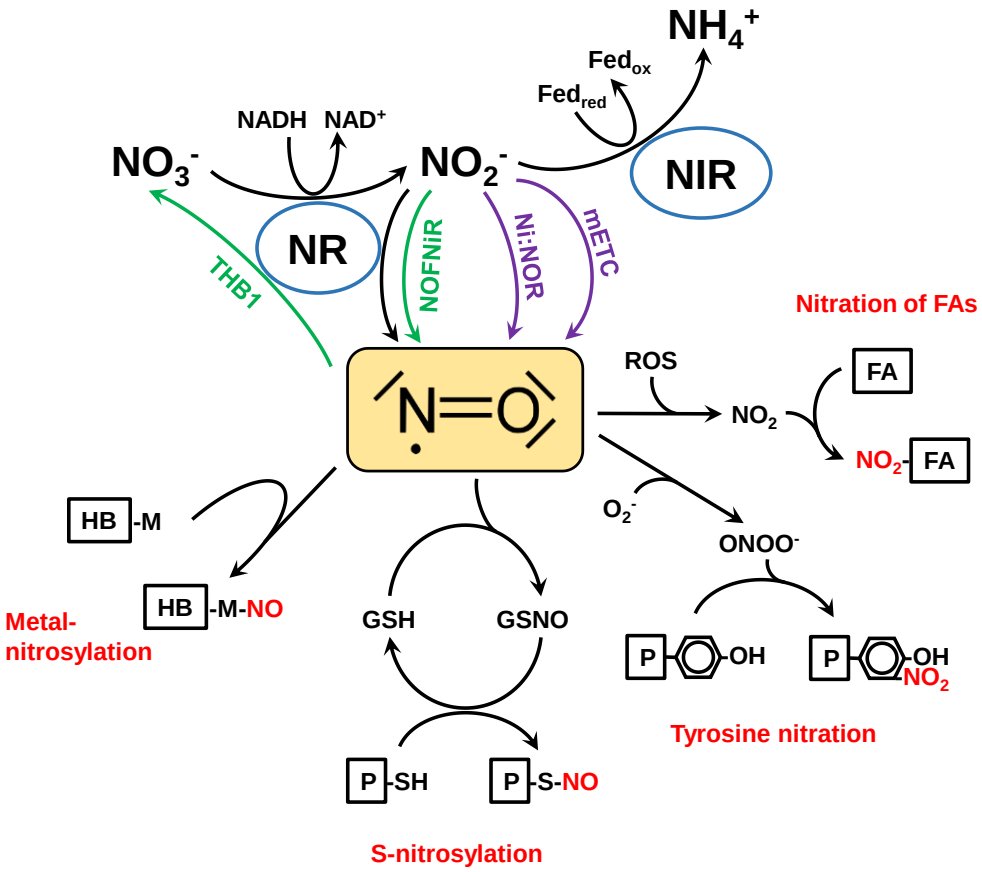

Figure 1.1. Scheme of the main biosynthetic and metabolic pathways of NO. Pathways only confirmed in algae are shown in green; hypoxia-dependent pathways are shown in purple, and post-translational modifications are shown in red. NAD, Nicotinamide adenine dinucleotide; Fed, ferredoxin; NR, Nitrate Reductase; NIR, Nitrite Reductase; THB1, Truncated Hemoglobin 1; NOFNiR, Nitric Oxide-Forming Nitrite Reductase; Ni:NOR, Nitrite-Nitric Oxide Reductase; mETC, mitochondrial Electron Transport Chain; ROS, Reactive Oxygen Species; HB, Hemoglobin; M, transition metal; P, protein; FA, unsaturated fatty acid.

Besides the cytosolic NR, a putative plasma membrane-bound Nitrite-Nitric Oxide Reductase (Ni:NOR) has been described to produce NO in plants. This unidentified protein would produce NO from the nitrite provided by an apoplastic membrane-bound NR, using NADPH as an electron donor, but only in roots and under a very low oxygen pressure (Fig. 1.1) (Stöhr *et al.*, 2001; Stöhr & Ullrich, 2002). In addition, nitrite can be reduced to NO in plants by the mitochondrial electron transport chain (mETC) (Fig. 1.1). This process involves mainly complex III and IV, and is dependent on the concentration of nitrite and oxygen, requiring anaerobic conditions (Gupta *et al.*, 2005). Therefore, it is a process that takes place only in tissues exposed to hypoxia such as roots, and its existence could be a way to preserve respiration when oxygen is scarce, by using nitrite as an electron acceptor (Gupta & Igamberdiev, 2011). Hence, not only the balance between NR and NiR activities but also the levels of available O_2 determine the degree of reduction that nitrate undergoes and the amount of NO synthesized. It has been recently reported that NO production under hypoxia seems to be partially mediated by alternative oxidase (AOX) activity (Vishwakarma *et al.*, 2018).

Similar to the main pathway of NO production in animals via the Nitric Oxide Synthases (NOSs), there is evidence that plants possess an oxidative pathway of NO synthesis in addition to the reductive one. In the search for a NOS homolog in plants, an enzyme was identified in Arabidopsis that seemed to be implicated in NO synthesis (Guo *et al.*, 2003). Initially named AtNOS1, the protein was renamed as Nitric Oxide Associated 1 (AtNOA1) and turned out to be a small GTPase (Moreau *et al.*, 2008). Although the way this protein contributes to the NO production is still unclear, the *noa1* mutant is widely used as a genetic tool due to its low endogenous NO content (Astier *et al.*, 2017). To date, the only NOSs from the plant kingdom that have been described belong to algal species (Foresi *et al.*, 2015; Jeandroz *et al.*, 2016), suggesting that is not likely that canonical NOSs exist in land plants. Because of this, efforts have been lately focused on finding the responsible for the NOS-like activity that for a long time has been described in plants (Astier *et al.*, 2017). Several groups have reported measurements of NOS-like activity strictly dependent on arginine, NADPH and various NOS co-factors in plant tissues, thus supporting the potential existence of a NOS homolog in plants (Durner *et al.*, 1998; Barroso *et al.*, 1999; Corpas & Barroso, 2014). Moreover, the use of NOS inhibitors in pharmacological approaches as well as the heterologous expression of NOS in plants, which have demonstrated that the cofactors and conditions needed for NOS activity indeed occur in plants have been used to support the existence of plant NOS-like enzymes (Frungillo *et al.*, 2014; Astier *et al.*, 2017). Taken together these results, the existence of an oxidative NO synthesis route in higher plants remains controversial.

Currently, the reductive pathway of nitrite to NO by NRs is considered the most relevant route of NO production in higher plants. This pathway is directly integrated in the inorganic nitrogen assimilatory metabolism, as NRs and NiRs compete for the reduction of nitrite, generated upon nitrate reduction (Fig. 1.1). Nitrate and

ammonium are the most available inorganic sources for nitrogen acquisition, without considering atmospheric dinitrogen (N_2) which can only be used by some prokaryotic organisms (Bloom, 2015). However nitrate is both a nutrient and a signal for plants: its signaling is crucial to regulate nitrate assimilation, the expression and activity of assimilatory enzymes and the whole N status of the plant (Armijo & Gutiérrez, 2017; Gent & Forde, 2017; Xuan *et al.*, 2017). The transcription factor NIN-Like Protein7 (NLP7) is the master regulator of nitrate signaling and assimilation (Castaings *et al.*, 2009; Marchive *et al.*, 2013; Yu *et al.*, 2016; Cao *et al.*, 2017; Zhao *et al.*, 2018).

As usual in signaling, the NO pathway in plants is strongly controlled by the action of several specific enzymes. Levels of cytosolic NO are the result of the balance between its synthesis and its turnover. NO can react with glutathione (GSH), thus producing S-nitrosylated glutathione (GSNO), considered a reservoir of NO and a signal for protein nitrosylation (Fig. 1.1). GSNO is metabolized to glutathione disulfide (GSSG) and ammonia (NH_3) by GSNO Reductase (GSNOR) (Wilson *et al.*, 2008). In addition, NO can be scavenged by reacting with ROS. The reaction of NO and superoxide anion (O_2^-) generates peroxynitrite ($ONOO^-$), which is a powerful nitrating agent able to cause tyrosine nitration of some proteins (Fig. 1.1) (Gaupels *et al.*, 2011; Begara-Morales *et al.*, 2014). NO can react chemically with oxygen and generate nitrite and nitrate (Hancock, 2012) and through a mechanism still unknown, can react with ROS and lipid peroxyl radical ($LOO^{\cdot}$) to produce nitro-fatty acids (NO_2-FAs) (Fig. 1.1) (Rubbo, 2013). Finally, the homeostasis of NO can also be regulated through its oxidization to nitrate by non-symbiotic and truncated hemoglobins (HB) (Fig. 1.1). HBs must be reduced to Fe(II)HB to dioxygenate NO (Chamizo-Ampudia *et al.*, 2017). Nitrate has been proposed to regulate coordinately HB expression and NO homeostasis (Trevisan *et al.*, 2011).

1.3. NO as a regulator

Plants may be affected by both exogenous (air and ground) and endogenous (biosynthesized) NO. The major sources of NO in the atmosphere are those derived from industrial activity and car engines (Skalska *et al.*, 2010) as well as the microbial-related release from soils (Pilegaard, 2013). Due to the spontaneous conversion of NO to NO_2 under aerobic conditions, it is frequent to use the term NOx when NO is supplied in an oxygenated environment (Kasten *et al.*, 2017). Levels of NO have been increasing continuously in the Earth atmosphere since industrial revolution started (Jaeglé *et al.*, 2005). Considering this tendency, plants may be exposed in the future to relatively high NO concentrations thus potentially altering their physiology.

NO is a gasotransmitter-diffusible multitasked messenger in a wide range of organisms that belongs to the group of reactive nitrogen species (RNS). Its nature as a free radical is in the basis of its regulatory activity, which is often exerted through interaction with the signaling pathway of most of the phytohormones,

including the five so-called classical plant hormones (gibberellins, auxins, abscisic acid, cytokinins and ethylene) and some of the most recently characterized (brassinosteroids, salicylic acid, jasmonates and strigolactones) (Durbak *et al.*, 2012; Freschi, 2013; Simontacchi *et al.*, 2013). The NO-hormone functional interaction has been reported to regulate numerous physiological processes in plants such as seed dormancy and germination, skotomorphogenic and photomorphogenic vegetative development, root growth, stomatal closure, pollination, flowering, fructification or leaf senescence (Beligni & Lamattina, 2000; He *et al.*, 2004; Bethke *et al.*, 2006; Tsai *et al.*, 2007; Qiao & Fan, 2008; Prado *et al.*, 2008; De Michele *et al.*, 2009; Manjunatha *et al.*, 2010; Lozano-Juste & Leon, 2011; Arc *et al.*, 2013; Liu & Guo, 2013; Du *et al.*, 2014).

NO is able to act as a regulator at two different levels: regulating gene expression and triggering post-translational modifications (PTMs) in proteins. This is because NO is able to react with proteins and alter their activity, subcellular localization, function, structure or stability, and when the affected protein is a transcription factor likely induces transcriptome changes (Bruckdorfer, 2005; Grün *et al.*, 2006; Palmieri *et al.*, 2008). Thus, NO can regulate the expression of numerous genes involved in hormonal signaling, primary metabolism or stress responses (Grün *et al.*, 2006; Besson-Bard *et al.*, 2009) and usually it impacts on the signaling of many phytohormones involved in developmental or defense processes against biotic and abiotic stresses (Freschi, 2013; Fancy *et al.*, 2017). Some examples of transcription factor regulation by NO include the repression of Phytochrome Interacting Factors (PIF) gene family controlling skotomorphogenenic growth (Lozano-Juste & Leon, 2011), the promotion of the TGA1 action in salicylic acid-dependent defense processes (Lindermayr *et al.*, 2010; Gupta, 2011) or the inhibition of AtMYB2 function in ABA signaling pathway (Serpa *et al.*, 2007).

NO can induce PTMs such as the nitrosylation of thiols and amines; the nitration of tyrosine, tryptophan and phenylalanine, the ubiquitylation of lysine, the phosphorylation of serine, threonine and tyrosine or the oxidation of tyrosine and thiols (Gow *et al.*, 2004; Hess & Stamler, 2012). However, due to its potential signaling effect in the plant physiology, the three main specific PTMs caused by NO are the S-nitrosylation of cysteines, the tyrosine nitration and the binding to metallic centers of proteins (Fig. 1.1) (Astier & Lindermayr, 2012). Alternatively, acting as a molecular messenger, NO can also regulate gene expression through the interaction and modulation of secondary messengers of signaling pathways dependent on cGMP, cADP-ribose, Ca_2^+, and notably with reactive oxygen species (ROS) (Durner *et al.*, 1998; Lamotte *et al.*, 2006; Astier *et al.*, 2010; Mur *et al.*, 2013).

S-nitrosylation (or S-nitrosation) is a redox modification consisting in the reversible covalent binding of an NO moiety to the thiol group of a cysteinyl residue (Cys) of a target protein, leading to the formation of an S-nitrosothiol (SNO) (Fig.

1.1) (Astier *et al.*, 2011). This modification is restricted to specific Cys residues and it is completely dependent on the nature of the surrounding amino acids (Seth & Stamler, 2011). GSNO seems to be one of the main donors for the transnitrosylase activity in plants, modulating the total SNO content (Wang *et al.*, 2006; Yu *et al.*, 2012). Tyrosine (Tyr) nitration is the mainly irreversible reaction of a nitrating agent with a tyrosine residue of a protein. It results in the addition of a nitro group (NO_2) in the ortho position of the phenolic hydroxyl group, leading to the formation of 3-nitrotyrosine (3-NY) (Fig. 1.1) (Schopfer *et al.*, 2003). The NO_2 group originates mainly from peroxynitrite ($ONOO^-$). Like in S-nitrosylation, Tyr nitration is also restricted to specific target tyrosine residues (Bayden *et al.*, 2011) and can trigger conformational changes that lead to the activation or the inhibition of the target proteins. These conformational changes seem to promote the polyubiquitylation and subsequent proteasomal degradation of the affected proteins (Castillo *et al.*, 2015). Because of its chemical properties, NO can also interact reversibly with the transition metals (iron, zinc or copper) at the heme center of metalloproteins to form metal-nitrosyl complexes through coordination chemistry (Fig. 1.1) (Ford, 2010; Astier & Lindermayr, 2012). The bound NO group is then susceptible to further nucleophilic or less frequently electrophilic attacks, depending on the protein bounded (Astier & Lindermayr, 2012; Toledo & Augusto, 2012). The formation of the metal-nitrosyl complex can induce conformational changes that compromise the proper functioning of the affected protein (Ford, 2010; Toledo & Augusto, 2012). The best characterized plant proteins undergoing metal nitrosylation are hemoglobins (HB), which are separated in three groups based on their structural properties: class 1, 2 and truncated hemoglobin class 3 (Gupta *et al.*, 2011). The oxidation of HBs by NO produces nitrate, thus scavenging the NO in what is considered a general mechanism modulating NO bioavailability, participating in the regulation and detoxification of NO in plants (Gupta *et al.*, 2011; Igamberdiev *et al.*, 2011). Recently, the nitration of fatty acids by NO has also been demonstrated to be an important part of NO signaling in plants (Mata-Pérez et al., 2017). This reaction would consist in the nitration of unsaturated fatty acids through a redox reaction to form electrophilic nitro-fatty acids (NO_2-FAs) (Fig. 1.1), although the exact molecule responsible for the modification is still unknown (Rubbo, 2013; Mata-Pérez *et al.*, 2017).

In contrast to the increasing knowledge of the effect of NO on protein function, our current knowledge on the NO impact on global metabolome of plants is scarce, being limited to a small number of stress-related processes. Both ROS and NO are produced in stressed plants, where NO seems to be able to alleviate the oxidative status by enhancing the antioxidant capacity and thus contributing to the redox homeostasis (Correa-Aragunde *et al.*, 2015). However, extensive evidence suggest that NO is involved in somehow paradoxical processes exerting sometimes opposing regulatory functions. For instance, NO has been described to enhance or reduce the redox status of the plants depending on either acting in a chronic or acute mode (Groß *et al.*, 2013). This paradox could be due to multiple

factors such as the relative NO cellular concentration, the location where it is produced or the complex interacting microenvironment.

1.4. NO sensing

If the biosynthesis of NO still remains controversial, the way plants sense NO is even less known. NO perception in animals is performed through NO-inducible Guanylate Cyclases (GC) that synthesize the second messenger 3´,5´-cyclic guanosine monophosphate (cGMP) from guanosine triphosphate (GTP) (Friebe & Koesling, 2003; Russwurm & Koesling, 2004). Although a flavin monoxygenase called NO-dependent Guanylate Cyclase 1 (NOGC1), with higher affinity for NO than for molecular oxygen, was identified in Arabidopsis (Mulaudzi *et al.*, 2011), it is not clear yet if this enzyme produces enough cGMP to work as a truly NO receptor (Gross & Durner, 2016). Moreover, it is also still unknown whether enzymes involved in cGMP degradation and downstream signaling, such as phosphodiesterases, are functional in plants (Gross & Durner, 2016), which makes the functionality of a NO-cGMP signaling pathway in plants even more uncertain. In the absence of a GC receptor for NO in plants, plants seem to sense NO mostly through chemical interaction with cofactor metals or with specific amino acid residues of proteins that often undergo NO-triggered post-translational modifications (Astier & Lindermayr, 2012). Nevertheless, alternative NO sensing mechanisms have been searched for and it was recently reported one involving the so called Cys-Arg/N-end rule proteolytic pathway (Gibbs *et al.*, 2014a). It consists in the specific oxidation of the C2 residue of transcription factors of the group VII of Ethylene Response Factors or ERF/AP2 family (ERFVIIs), which is strictly dependent on NO and molecular oxygen, and allows further arginylation, polyubiquitylation and proteasome-mediated degradation of ERFVIIs through the N-end rule proteolytic pathway (Fig. 1.2) (Gibbs *et al.*, 2014a). This pathway acts as a sensor that integrates both NO and O_2 (Gibbs *et al.*, 2014a) and it has been proposed to function as a general sensor of abiotic stress (Vicente *et al.*, 2017) besides being essential for responses to anaerobiosis (Gibbs *et al.*, 2014b; Pucciariello & Perata, 2017). The turnover of regulatory proteins through focused proteolysis by an ATP-dependent proteasome machinery is a conserved mechanism in eukaryotes (Gibbs *et al.*, 2014b).

ERFVIIs can undergo degradation through the cysteine (Cys) subdivision of the Arg/N-end rule pathway (Cys-Arg/N-end rule pathway) (Gibbs *et al.*, 2014a). The beginning of this proteolytic pathway consists in the removal of the methionine by a Methionine Aminopeptidase (MAP), thus exposing the tertiary destabilizing cysteine residue (which constitutes an N-degron) to direct oxidation (Fig. 1.2). The specificity of this reaction depends on the Plant Cysteine Oxidase 1 (PCO1) and PCO2 enzymes, which catalyze the oxidation of the thiol group in the N-terminal Cys of the substrate to sulphinic acid using molecular O_2 and NO as co-substrates (Fig. 1.2) (Gibbs *et al.*, 2014a; Weits *et al.*, 2014). Once it is oxidized, the Cys acts as a secondary destabilizing residue that becomes the substrate for arginylation

by Arg-tRNA Transferase (ATE) ATE1 and ATE2 enzymes (Fig. 1.2). This transfer of an Arg to the N-terminal residue of the target protein constitutes a signal for the N-recognin E3 ubiquitin ligase Proteolysis6 (PRT6) for polyubiquitinylation and further degradation by the proteasome (Fig. 1.2) (Gibbs *et al.*, 2014b). The N-end rule proteolysis of ERFVIIs takes place only under O_2-rich conditions, being deactivated under low O_2 (Pucciariello & Perata, 2017).

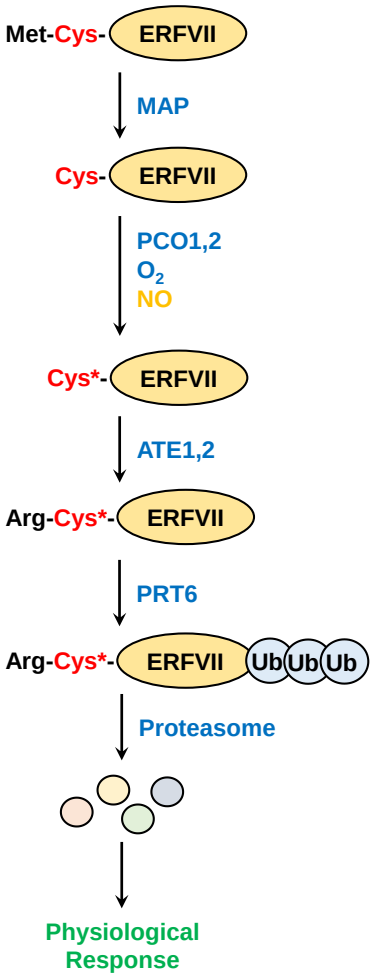

Figure 1.2. Scheme of the Cys-Arg/N-end rule pathway-mediated degradation of ERFVII transcription factors as sensor mechanism of NO in plants. MAP, Methionine Aminopeptidase; PCO1,2, Plant Cysteine Oxidase 1 and 2; ATE1,2, Arginyl tRNA Transferase 1 and 2; PRT6, Proteolysis6 E3 ligase; Cys*, oxidized cysteine.

The ERFVIIs comprise five proteins. Three of them are constitutively expressed transcription factors: Related to AP 2.12 (RAP2.12), RAP2.2 and RAP2.3/EBP. The other two are hypoxia-inducible factors: Hypoxia Responsive ERF 1 (HRE1) and HRE2. All five contain a cysteine residue right after the initial methionine and have been demonstrated to be substrates of the N-end rule pathway (Gibbs *et al.*, 2015). Initially, RAP2.3 was isolated as a suppressor of Bax-induced cell death by functional screening in yeast, and further confirmed its cell death suppressing activity and its capacity to induce resistance to hydrogen peroxide and heat stress

(Ogawa *et al.*, 2005). Moreover, RAP2.3 seems to regulate also defense against pathogens likely through interaction with acyl-CoA binding proteins ACBP2 and 4 (Li *et al.*, 2008), and also with bZIP transcription factors (Buttner & Singh, 1997). Despite their stress-related functions, RAP2.3 has also development-related regulatory functions. It has been identified as a protein interacting with the Gibberellin Insensitive (GAI) DELLA protein in such a way that the interaction impaired the activity of RAP2.3 on target promoters, thus controlling the differential growth during apical hook development (Marín-de la Rosa *et al.*, 2014; Abbas *et al.*, 2015). On the other hand, RAP2.3 together with the other members of ERFVII group have been extensively characterized as key regulators in the expression of hypoxia-responsive anaerobic metabolism-related genes involved in different abiotic stresses (Bui *et al.*, 2015; Gasch *et al.*, 2015; Papdi *et al.*, 2015). However, despite the relevance of ERFVIIs in sensing NO and regulating all this aspects of plant physiology, other still not deciphered components should be likely involved in mediating NO sensitivity and responsiveness.

1.5. NO and stress-triggered responses. The role on plant tolerance to freezing

Plants face two different environmental stresses: those caused by other living organisms or biotic stresses, and those caused by non-living factors or abiotic stresses. Nowadays, abiotic stresses constitute the bigger impact (up to 70%) on crop growth and yield (Mantri *et al.*, 2012) and it is estimated that 90% of cultivable land is exposed to salinity, drought, low or high temperature, heavy metal exposure or high light, among other abiotic stresses (dos Reis *et al.*, 2012). Plants display an array of adaptation responses to ensure their survival against abiotic stress (Nakashima *et al.*, 2009), leading to two possible outcomes: programmed cell death or stress acclimation (Kreps *et al.*, 2002). The stress-triggered production of redox active molecules like ROS or RNS (including NO) is a common trait of plant responses to abiotic stress as a mechanism to ameliorate the resultant oxidative stress (Mittler, 2006). On the other hand, besides its function as regulator of several developmental processes (including seed germination, seed dormancy, and closure of stomata), major phytohormone abscisic acid (ABA) plays an essential role in the plant response against a wide range of biotic and abiotic stresses (Vishwakarma *et al.*, 2017). In several of these processes, NO is a downstream regulator of ABA signaling (Hancock *et al.*, 2011) and an increment of the ABA content correlates with the induction of NO production (Neill *et al.*, 2002; Lozano-Juste & León, 2010). However, NO can also exert a negative effect on ABA signaling by reducing the hormone perception (Castillo *et al.*, 2015), as seen in the NO-deficient *nia1,2noa1-2* triple mutant, which is hypersensitive to ABA (Lozano-Juste & León, 2010). This complex relation between NO and ABA would be another scenario in which NO regulatory effect would depend on factors such as the nature of the process and the site and timing of production of the both regulators (León *et al.*, 2014).

One of the main abiotic stresses whose response is regulated by ABA is cold. This stress factor triggers the accumulation of endogenous ABA in many plants (Mantyla *et al.*, 1995) while exogenous ABA treatment leads to enhanced cold resistance (Kumar *et al.*, 2008; Kim *et al.*, 2016). Among abiotic stresses, stress by low temperatures is one of the most important barriers for productivity in agriculture along with drought, salinity and heat (Calanca, 2017). Unlike the stress caused by cold (5-15 ºC, chilling stress), very few crops can face freezing stress (below 0 º C), which interestingly is a kind of stress more similar to drought stress due to the formation of intracellular ice crystals. When facing these temperatures, plants respond by reprogramming metabolism in order to attenuate the cell damage caused by freezing (Fowler & Thomashow, 2002; Cook *et al.*, 2004; Hannah *et al.*, 2005; Lee *et al.*, 2005; Chinnusamy *et al.*, 2007; Kaplan *et al.*, 2007; Guy *et al.*, 2008). The tolerance to freezing is achieved through endogenous components of the plant and inducible environmental factors. The main endogenous plant components that favor constitutive freezing tolerance seem to be the accumulation of metabolites with osmoprotective activities that limit freeze-induced dehydration and avoid ice nucleation inside the cells (Janská *et al.*, 2010), hormones (Eremina *et al.*, 2016a) and antioxidants (Winkel-Shirley, 2002). Other responses include changes in membrane structure and function, and growth arrest (Renaut *et al.*, 2004; Eremina *et al.*, 2016a). On the other hand, among the environmental factors that enhance freezing tolerance, likely the most efficient is the cold acclimation, consisting in the previous exposure of plants to low non-freezing temperatures (Thomashow, 1999; Knight & Knight, 2012). This is an adaptive process that allows plants to survive the freezing winters. Cold acclimation and freezing tolerance are mainly controlled by changes in genes expression, which, in turn, are regulated at the transcriptional and post-transcriptional levels (Barrero-Gil & Salinas, 2013; Miura & Furumoto, 2013).

Among the cold-induced signaling pathways, the one mediated by the C-repeat/dehydration-responsive element Binding Factors (CBFs/DREB1s) is probably the most important and the best characterized (Gilmour *et al.*, 2004; Medina *et al.*, 2011). This pathway is controlled by Inducer of CBF Expression1 (ICE1), a MYC-type transcriptional activator that enhances freezing tolerance upon binding to the promoters of *CBF* genes (Fig. 1.3) (Chinnusamy *et al.*, 2003). The so-called CBF regulon is not only regulated by the ICE1-CBF pathway but by other transcription factors that are rapidly induced by cold and work as a complex regulatory network only partially dependent on CBFs (Fowler & Thomashow, 2002; Park *et al.*, 2015). Both CBF-dependent and –independent pathways converge into the activation of *Cold-Responsive* (*COR*) genes (Fig. 1.3) (Gilmour *et al.*, 1998), which are key for cold acclimation-induced freezing tolerance. *COR* genes code for dehydrins, heat shock proteins, glucanases and chitinases that are important to prevent membrane alterations, protein aggregation and the formation of inter- and intra-cellular ice crystals (Griffith *et al.*, 2005).

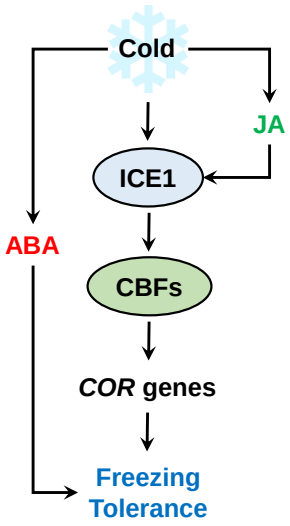

Figure 1.3. Scheme summarizing the CBF-dependent pathway of cold acclimation-induced freezing tolerance. JA, jasmonate; ABA, abscisic acid; ICE1, Inducer of CBF Expression1; CBFs, C-repeat/dehydration-responsive element Binding Factors; *COR*, *Cold-Responsive.*

Cold acclimation is also regulated by plant hormones. Besides ABA, whose quantitative and qualitative contribution is decisive (Nakashima *et al.*, 2014), other phytohormones, including jasmonates, salicylates, auxins, cytokinins, gibberellins, and brassinosteroids, have important functions in cold acclimation (Fig. 1.3) (Jeon *et al.*, 2010; Miura & Ohta, 2010; Rahman, 2013; Richter *et al.*, 2013; Eremina *et al.*, 2016b; Sharma & Laxmi, 2016). Moreover, other non-hormone regulatory molecules such as polyamines, lipids, reactive oxygen species and NO have been described to be involved in freezing tolerance and cold acclimation (Cuevas *et al.*, 2008; Zhao *et al.*, 2009; Puyaubert & Baudouin, 2014; Chen & Thelen, 2016; Takahashi *et al.*, 2016; van Buer *et al.*, 2016).

In the last years, several studies have reported an increased production of NO in cold-stressed plants using many different species and detection methods (Shimoda *et al.*, 2005; Corpas *et al.*, 2008; Zhao *et al.*, 2009; Liu *et al.*, 2010; Cantrel *et al.*, 2011; Bai *et al.*, 2012; Majláth *et al.*, 2012; Xu *et al.*, 2012; Puyaubert & Baudouin, 2014). Therefore, cold-induced NO production appears as a general response taking place in diverse plant species and organs such as leaves, fruits or seeds. However, most of the details behind this process are still unknown and further investigation would now require a more specific analysis of the respective functions of short- and long-term NO signaling during the cold response and acclimation (Puyaubert & Baudouin, 2014). Also, the mechanisms used by NO to control cold acclimation could be part of the discrimination between tolerant and sensitive species to freezing stress (Puyaubert & Baudouin, 2014).

Objectives

2. OBJECTIVES

The present work aims to unravel the mechanisms underlying the regulation of the nitric oxide synthesis as well as its signaling by post-translational modifications and N-end rule pathway-mediated proteolysis in *Arabidopsis thaliana*. Therefore, the following objectives were proposed:

1) Characterization of the effect of NO and post-translational modifications in proteins on the NO homeostasis.
2) Characterization of the genome-wide NO-responsive transcriptome and metabolome.
3) Functional characterization of the N-end rule pathway-mediated control of NO responses by ERFVIIs.
4) Evaluation of the role of NO as a regulator of plant responses to abiotic stress. The case of responses to low temperatures.

Materials and Methods

3. MATERIALS AND METHODS

3.1. Biological material

3.1.1. Plant material

3.1.1.1. Plant species used

Arabidopsis thaliana Columbia-0 (Col-0) ecotype was the wild-type genetic background used in this work. The following knockout mutant lines were obtained from the Nottingham Arabidopsis Stock Centre (NASC) seed bank: *nlp7-1* (SALK_026134C), *prt6-1* (SAIL_1278_H11), *ein2-5* (N16707), *etr1-3* (N3070), *pyl6,7, sid2-1eds5-3nahG, det2-1* (N65989)*, bes1-d* (N65988)*, nia1nia2* (N2356) and *noa1-2* (SAIL_507_E11). Other mutants used include: *jaz10, jaz1,3,5,9,10 or qjaz, myc2, myc2,3,4* (donated by Roberto Solano, CNB, Madrid, Spain)*, hai1,2,3* (donated by Paul E. Verslues, Academia Sinica, Taipei, Taiwan)*, max1, max2, max4* (donated by Javier Agustí, IBMCP, Valencia, Spain), quintuple *erfvii* or *qerfvii* (*rap2.12rap2.2rap2.3hre1hre2*) and *qerfviiprt6-1* (donated by Michael Holdsworth, University of Nottingham, UK). The double *snrk2.3,2.9* mutant was generated by crossing *snrk2.3* and *snrk2.9* (donated by Hiroaki Fujii, Center for Plant Cell Biology, Riverside, USA). The double *nlp7-1prt6-1, 35S::NLP7nlp7-1prt6-1* and *pNLP7::NLP7nlp7-1prt6-1* plants were generated by crossing *nlp7-1, 35S::NLP7nlp7-1* and *pNLP7::NLP7nlp7-1* plants (Marchive *et al.*, 2013) with *prt6-1* plants and screening for homozygous mutations and transgenes in the F3 generation by PCR with specific gene and T-DNA primers (Table A3). The triple *nia1,2noa1-2* mutant seeds were obtained by crossing *nia1nia2* and *noa1-2* as previously reported (Lozano-Juste & León, 2010). Genotyping by PCR and Cleaved Amplified Polymorphic Sequences (CAPS) with specific primers (Table A3) were used to select triple homozygous mutant plants and to ensure that triple homozygous mutant plants were used from every seed stock obtained. A knockout mutant *nir1-1* was obtained by using the CRISPR/Cas9 technology.

Plants over-expressing HA-tagged versions of NR1, NR2 and NiR1 were generated by subcloning the full-length cDNAs in pAlligator 2 vector (Bensmihen *et al.*, 2004) (Fig. A2), and further transformation of *Agrobacterium tumefaciens* with the corresponding constructs. Plants were then genetically transformed by dipping floral organs in a suspension of transformed Agrobacterium (Clough & Bent, 1998) and selected (via a GFP reporter gene expressed in the seed) for homozygotic transgenes (Fig. 4.3). The transgenic plants *35S::MC-RAP2.3-HA* and *35S::MA-RAP2.3-HA* were obtained from Michael J. Holdsworth's lab (University of Nottingham, UK). Around 1000 different transgenic lines from the TRANSPLANTA (TPT) project expressing Arabidopsis transcription factors under the control of a β-estradiol-inducible promoter (Coego *et al.*, 2014) were also used (Supplementary Table S4 in Castillo *et al.*, 2018).

3.1.1.2. Plant growth

3.1.1.2.1. Growing media for plants

For propagation purposes and when indicated, plants were grown in soil mixture (50% blond Kekkilä peat, 25% perlite, 25% vermiculite) irrigated with a nutritive solution (34.95 mg/l gFe, 9.76 mg/l $ZnSO_4 \cdot 7H_2O$, 28.95 mg/l $MnSO_4 \cdot H_2O$, 2.23 mg/l Cu_2SO_4, 32.55 mg/l H_3BO_3, 1.51 mg/l $(NH_4)6Mo_7O_{24}*4H_2O$, 885 mg/l $Ca(NO_3)_2 \cdot 4H_2O$, 381 mg/l KNO_3, 102 mg/l KH_2PO_4, 367.5 mg/l $MgSO_4 \cdot 7H_2O$, pH 6.5, CE 1.6 mS). For the propagation of *nir1-1* plants (unable to grow with nitrate), only vermiculite was used, irrigated with a modified version of the MS (Murashige & Skoog, 1962) medium containing no nitrogen (Bioworld) and supplemented with 0.5% (w/v) sucrose, 10 mM KH_2PO_4/K_2HPO_4 (pH 6.5), 2.5 mM $(NH_4)_2$-succinate and 2.35 mM MES buffer. For most of the experiments, plants were grown in agar-supplemented MS medium (Duchefa) supplemented with 1% (w/v) sucrose, 2.35 mM MES buffer and vitamins, adjusted to a pH 5,7. For the selection of homozygous plants of *nlp7-1prt6-1*, 35S*::NLP7nlp7-1prt6-1* and *pNLP7::NLP7nlp7-1prt6-1* the MS medium was also supplemented with 10 µg/ml glufosinate ammonium (BASTA) and/or 20 µg/ml Hygromycin. The selection of *pU6::gNIR1* (CRISPR-Cas9 transgenic lines for the generation of *nir1* mutants) T1 transformants was carried out in a medium composed by 4.3 g/l of MS medium salts, 8 g/l phytoagar, 25 µg/mL Hygromycin and 100 ug/ml cefotaxime. The induction of the expression of the transcription factors in the TPT lines was performed by supplementing the MS-MES medium with 10 µM β-estradiol. For the experiments with different nitrogen sources, seedlings were grown in MS media depleted of N (-N) (Bioworld), or supplemented with 5 mM KNO_3, 5 mM $NaNO_2$ or 2.5 mM $(NH_4)_2SO_4$ as the only nitrogen source. These media were supplemented also with agar (or none, as indicated in each experiment), 0.5% (w/v) sucrose, 10 mM KH_2PO_4/K_2HPO_4 pH 6.5 (5 mM in nitrate medium) and 2.35 mM MES buffer. Except when indicated, DAF-FM DA staining was performed on seedlings grown in MS-MES medium with or without agar (depending on the experiment) and without sucrose.

3.1.1.2.2. Growing conditions for plants

Seeds were surface sterilized with chlorine gas (4h incubation) and aerated in laminar flow cabinet for 30 min before sowing in MS media plates. Alternatively, seeds were sterilized by incubating with 70% ethanol and 0.1% Triton X-100 for 2 min, 30% bleach solution with 0.02% Tween-20 for 10 min and 5 washes of sterile water, before sowing in liquid media. After sowing, seeds were stratified at 4ºC under darkness for 4 days. Plants were grown under photoperiodic cycles of 16 h day and 8 h night (long days, at 22 ºC and 20 ºC, respectively), under 150 µE m^{-2} s^{-1} cool-white fluorescent lamps and 60% relative humidity.

3.1.2. Microbiological material

3.1.2.1. Bacterial strains used

For cloning purposes, different strains of *Escherichia coli* were used: One Shot TOP10, DH5α, 5α C2987 and DB3.1. Plant transformation was performed using *Agrobacterium tumefaciens* C58pMP90.

3.1.2.2. Bacterial growth

3.1.2.2.1. Growing media for bacteria

All bacteria were grown in LB medium (Bertani, 1951) with or without agar, supplemented with 100 µg/ml spectinomycin, 100 µg/ml kanamycin or 10 µg/ml gentamicin for the selection of transformants depending on the plasmid used. Agrobacterium growth media were always supplemented with 100 µg/ml rifampicin.

3.1.2.2.2. Growing conditions for bacteria

E.coli was grown at 37 ºC while *A. tumefaciens* was grown at 28 ºC, both kept at 200 rpm shaking if grown on liquid medium.

3.2. Manipulation of the biological material

3.2.1. Plant treatments

3.2.1.1. Plant transformation by floral dipping

For the generation of transgenic plants, 1 month soil-grown plants (T0 generation) were transformed by floral dipping (Clough & Bent, 1998). Shoot apexes were cut after bolting and plants were transformed three days after. Two days before the plant transformation, the Agrobacterium transformed with the desired transgene was grown for 24 h at 28 ºC in 10 ml LB medium with the corresponding antibiotics for selection. This culture was used to inoculate 200 ml of medium, which was again incubated for 24 h. Before plant transformation, bacteria were precipitated by centrifuging at 7000 rpm for 10 min and resuspended in 250 ml of transformation solution (5% (w/v) sucrose, 0.02% (v/v) Silwet L-77). Shoot apexes were submerged in this solution for 30-60 s and kept covered with plastic for two days to maintain humidity. After one month, T1 transgenic seeds were harvested.

3.2.1.2. Generation of a *nir1* mutant by CRISPR-Cas9 technology

A 19 bp target sequence (GCCGCTCAGACCACAGCTC) close to the N-terminus of the *NIR1* locus was chosen followed by the PAM sequence NGG. This sequence was used as guide and subcloned into the entry vector pMTN2982 (a

modified pDONR207) (Fig. A3) by Site-directed, Ligase-Independent Mutagenesis (SLIM) (Chiu *et al.*, 2004), which consists of two separate inverse PCR amplifications with tailed primers: (F+R_tailed) and (F_tailed+R) (Table A3, Fig. 3.1A). Both PCRs were performed with Phusion polymerase on an Applied Byosystems 96-well thermocycler, using 10 ng of template (pMTN2982). The program was 3 min at 98 ºC initialization, 35 cycles of denaturation (15 s at 98 ºC), annealing (30 s at 65ºC) and extension (2.5 min at 72 ºC), and 10 min at 72 ºC of final elongation. After verifying the amplification, both PCR products were mixed and digested with *Dpn*I (to remove template) in a mix consisting of 12,5 µl of each PCR product, 3 µl of commercial 10x buffer and 2 µl of *Dpn*I. Restriction mix was incubated at 37 ºC for 12 h and inactivated by incubating at 80º C for 20 min. The hybridization was performed by mixing 30 µl of the digestion and 30 µl of H-buffer (300 mM NaCl, 50 mM Tris-HCl pH 9, 20 mM EDTA) and incubating at 99 ºC for 3 min (melting) and two cycles of annealing of 65 ºC for 5 min and 30 ºC for 15 min. The resultant linear vector was transformed into *E. coli* 5α C2987, in which the 19mer sticky ends were ligated and the vector was circularized. The vector contained the guide (named *gNIR1*), following the structure: pDONR207 flanks; A.t. U6 promoter; *NIR1* target sequence; Guide RNA scaffold; Pol III terminator; pDONR207 flanks (Fig. 3.1A). The guide clone was verified with the primers pDNOR_F and pDONR_R (Table A3).

The pHEE2E-TRI plasmid (Fig. A4) was chosen as destination vector, which carries egg cell-specific promoter-controlled CRISPR/Cas9 technology. Thus, homozygous mutant plants can be obtained in the T1 generation (Wang *et al.*, 2015a). In order to mobilize it, the guide was amplified by PCR using the primers P1b-HindIII and P4b-SpeI (Table A3) and the Phusion polymerase in a 50 µl reaction. The product was checked by agarose electrophoresis and the amplicon was purified from the 500 bp sliced band. The clean amplicon was digested with *Hind*III and *Spe*I for 3 h at 37 ºC and cleaned with a kit. 5 µg of pHEE2E-TRI were digested with *Hind*III and *Spe*I for 3 h at 37 ºC and additional 30 min with alkaline-phosphatase at 37ºC, and cleaned with a PCR Clean-Up Kit. The ligation of 90 ng of digested vector with 9 ng of digested insert was carried out with the T4 DNA ligase (Thermo Scientific), at 16 ºC for 24 h (Fig. 3.1A). A 1:5 dilution of this solution was used to transform *E. coli* 5α C2987 and the sequence was verified with the primers pU6seqF and pU6seqR (Table A3). The *gNIR1*-containing pHEE2E-TRI vector was used for transformation of Agrobacterium cells and further plant transformation.

T1 seeds were sown on Hygromycin selection plates (4.3 g/l of MS medium salts, 8 g/l phytoagar, 25 µg/mL Hygromycin and 100 µg/ml cefotaxime), stratified for 3 days and transferred to dark for additional 3 days after a 6 h white light pulse. When returned to long day conditions, transformants were selected by checking hypocotyl length (hygromycin resistant seedlings display larger hypocotyls) and transferred to soil. Genomic DNA was extracted from samples taken from these

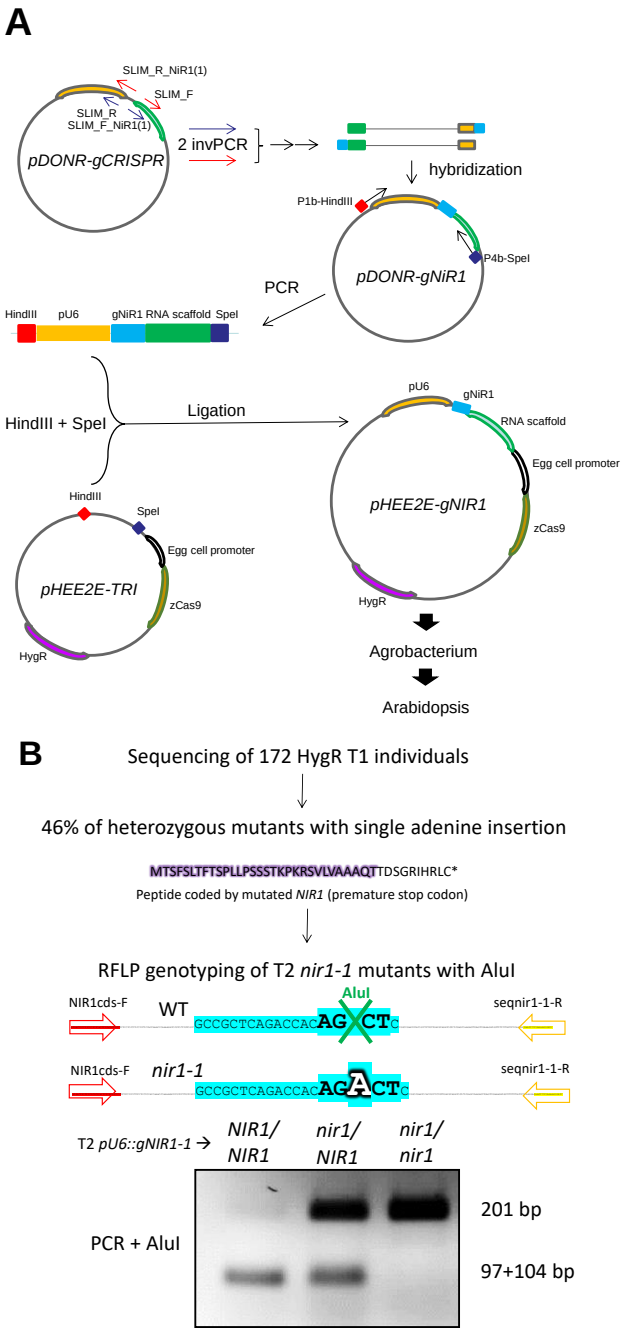

Figure 3.1. Generation of *nir1* mutant plants by CRISPR-Cas9 technology. A, Scheme showing the process for the generation of a transgenic plant expressing both Cas9 and a guide with a scaffold to induce a mutation in the *NIR1* locus. The NiR1 specific guide was subcloned in the pDONR207-Cas9 vector via SLIM (two separate inverse PCRs with tailed primers) and hybridization. The construction was amplified and ligated to pHEE2E-TRI vector that carries with the CRISPR/Cas9 technology components under the control of an egg cell-specific promoter. The names of the primers used for the PCRs are included. B, Scheme showing the process for the generation of a homozygous *nir1* mutant plant. The region of the peptide sequence conserved from the wild type NIR1 protein is highlighted in purple. * represents the stop codon. The region of the *NIR1* gene corresponding to the designed specific NIR1 guide is highlighted in light blue. Bottom panel shows a 2% agarose gel electrophoresis of the RFLP genotyping (amplifying by PCR and cutting with *Alu*I) of a wild type, heterozygous and

homozygous *nir1* plant, all three from a second generation of transgenic *pU6::gNIR1-1* plants. The size of the bands is shown at the right side of panel.

seedlings and used for the amplification of the target sequence of *gNIR1* and its flanking regions with the primers NIR1cdsF and NIR1midR (Table A3) by HF-PCR (to avoid false positive mutations). PCR products were cleaned and checked for mutations by sequencing with the primer seqnir1-1-R (Table A3). The selected *nir1-1* mutation consisted in a single A base insertion in position 98 causing a frame shift leading to a premature stop codon (Fig. 3.1B, Table A5) and a Restriction Fragment Length Polymorphism (RFLP). Genotyping of the RFLP was performed by PCR amplification with primers NIR1cdsF and seqnir1-1-R (Table A3) and subsequent digestion with the restriction enzyme *Alu*I, which cuts the wild type but not the mutant amplicon (Fig. 3.1B).

In order to segregate-out the CRISPR/Cas9 transgene, T2 seeds were sown on Hygromycin inverse selection plates (2.7 g/l of MS medium salts, 8 g/l phytoagar, 20 µg/mL Hygromycin and 0.5% sucrose) and after hypocotyl elongation, Hygromycin sensitive seedlings were selected and transferred to recovery medium plates (2.7 g/l of MS medium salts, 8 g/l phytoagar and 0.5% sucrose). Transgene-free plants were confirmed by PCR with the primers Hyg-F and Hyg-R (Table A3).

3.2.1.3. NO treatments

Pulses of NO were performed by incubating plants for 5 min in a tightly sealed transparent box after injection of 300 ppm of pure NO gas (Linde AG, Germany). For the assays of NO-triggered inhibition of hypocotyl elongation, surface-sterilized seeds were sown in MS-MES media and germination program was activated by exposure to light for 6 h after stratification, and then, incubated in tight-sealed boxes under air supplemented with 300 ppm pure NO gas under darkness for four days. Control seedlings were incubated under the same conditions in air with no supplemented NO. The screenings of TPT transgenic lines (Coego *et al.*, 2014) were performed by using MS-MES media supplemented or not with 10 µM β-estradiol and treated or not with NO. Hypocotyl length was measured for every seedling of genotype and condition tested by using Image J. The experiments were repeated three times with at least 20 individuals per genotype, condition and experiment.

3.2.1.4. Freezing tolerance assays

Seeds from the different genotypes were sown in soil-containing pots and allowed to develop for 7 days. Then, several plants for each pot were removed in order to leave a similar number (25-30) of plants, homogenously distributed in all pots. Before being subjected to freezing temperatures, plants were exposed for 1 h to 4 °C in the freezing chamber. Then, temperature was progressively decreased (−1 °C/30 min) until reaching the indicated freezing temperatures. After exposing

plants to the appropriate freezing temperature for 6 h, temperature was gradually increased to 4 °C (+1 °C/30 min). One hour later, plants were transferred to 20 °C under long-day light regime for recovering and subsequent survival evaluation 7 days later. For cold acclimation assays, the 7 days old plants were acclimated at 4ºC for 7 days prior to the freezing tolerance assay. Control plants were the non-acclimated 14-day old plants grown in standard conditions of temperature.

3.2.1.5. Staining methods

3.2.1.5.1. NO detection by fluorescence and confocal microscopy

The endogenous levels of NO in shoots and roots were determined by staining with 10 µM 4-Amino-5-methylamino-2',7'-difluorofluorescein diacetate (DAF-FM DA) as described (Guo *et al.*, 2003) with some modifications. 4-day old seedlings grown on vertical MS plates (without sucrose) were transferred to the staining buffer (5 mM MES-KOH, pH 5.7; 0.25 mM KCl, 1 mM $CaCl_2$) and incubated on liquid for 24 h at room temperature. For the staining of shoots, DAF-FM DA was added to the buffer used for this 24 h incubation, while for the staining of roots, the dye was added to buffer only during the last hour of incubation. In both cases, plants were kept in dark during the first hour of incubation with the dye and after the 24 h incubation, plants were washed three times for 10 min with staining buffer to remove the excess of DAF. Fluorescence was detected by confocal microscopy with a Zeiss LSM 780 (with excitation at 488 nm and emission at 500-527 nm range) or by fluorescence microscopy with a Leica DM 5000B (with a barrier filter for chlorophyll auto fluorescence), using unchanged parameters for every measurement. The specificity of NO-related fluorescence detection was assessed by a pre-incubation treatment with 0.5 mM of the NO scavenger 2-(4-Carboxyphenyl)-4,4,5,5-tetramethylimidazoline-1-oxyl-3-oxide (cPTIO) (Sigma, USA) and/or with 0.5 mM of the NO inducer salicylic acid (SA). The DAF-FM DA fluorescence intensities were analyzed using Adobe Photoshop by quantifying green pixels in 3 to 6 replicate images of every genotype and condition from three independent experiments.

For the determination of the NO content of cold acclimated plants, seedlings were grown in soil under standard long day photoperiod light conditions and 21ºC for 6 d. Then, plants were either maintained at standard non-acclimated growing conditions or cold acclimated at 4ºC for 7 days. At day 13, plants were sprayed with DAF-FM DA to run-off and kept under darkness for 1 h and later, after extensive washings, transferred to growing conditions at either 4ºC or 21ºC for additional 23 h. Fluorescence was detected by confocal microscopy with a CLSM LEICA TCS SP5.

3.2.1.5.2. Cuticle permeability tests

The toluidine blue test was carried out by placing 10 µl droplets of a 0.025% (w/v) toluidine blue solution in potato dextrose broth (PDB) on the upper side

surface of undetached leaves. After 2 h leaves were washed gently with distilled water to remove excess of the toluidine blue solution, and then leaves were excised and photographed. For Calcofluor white staining, leaves were bleached in absolute ethanol overnight, equilibrated in 0.2 M phosphate buffer (pH 9) for 1 h, and incubated for 1 min in 0.5% (w/v) Calcofluor white in 0.2 M phosphate buffer (pH 9). Leaves were rinsed in phosphate buffer to remove excess of Calcofluor white and viewed under UV light.

3.2.1.5.3. Staining for cell permeability, cell death, superoxide and starch

To assess cell permeability, roots of 10 d-old seedlings were stained with propidium iodide by dipping into a 10 µg/ml solution for 10 min. Stained roots were visualized under confocal microscopy (LSM 780, Zeiss) with excitation at 488 nm and emission at 598-650 nm range. Cell death was assayed by staining seedlings with 2% (w/v) Evans blue solution for 5 min and subsequent extensive washing. Superoxide staining was performed by dipping seedlings in 0.2% (w/v) solution of nitroblue tetrazolium (NBT) in 50 mM sodium phosphate buffer (pH 7.5) overnight at room temperature and protected from light followed by bleaching with hot ethanol. Staining of starch granules was performed by bleaching 7d-old seedlings with 96% ethanol for 5 h and then by incubating bleached seedlings in Lugol´s staining solution (5.7 mM iodine, 43.4 mM KI, 0.2 N HCl) for 30 min and further extensive overnight washing with water.

3.2.1.6. Change of nitrogen source for plant growth

To test the effect of changing the nitrogen source, plants were grown for 11 days in ammonium-supplied MS media without nitrogen and then transferred to media containing either nitrate or ammonium as the only nitrogen source for two additional days.

3.2.1.7. Inhibition of protein synthesis or degradation

To test the effect of proteasome and protein synthesis inhibition, 100 µM MG132 and/or 40 µM cicloheximide (CHX) were added respectively to liquid media, where seedlings were incubated for 16 h.

3.2.2. Bacterial manipulation

3.2.2.1. Genetic transformation by heat shock

Chemically competent *E. coli* cells were transformed by heat shock. For doing so, cells were unfrozen on ice for 15 min, 1-5 µl of variable concentration of the plasmid were added and after another 30 min of incubation on ice, the mixture was kept at 42 ºC for 30 s. After cooling down on ice, 250 µl of LB were added and the mixture was incubated at 37 º C and 200 rpm shaking for 1 h. Transformed bacteria were selected by spreading the mixture on solid LB plates with the corresponding antibiotic and were incubated at 37 ºC for 24 h.

For further plant transformation, chemically competent *A. tumefaciens* cells were transformed by heat shock with the desired plasmid. Cells were unfrozen on ice, 5 µl of variable concentration of the plasmid were added and the mixture was kept at 37 ºC and 200 rpm shaking for 5 min. Then the mixture was frozen on liquid nitrogen and unfrozen on ice. 250 µl of LB were added and the mixture was incubated at 28 º C and 200 rpm shaking for 2-3 h. Transformed Agrobacteria were selected by spreading the mixture on solid LB plates with the corresponding antibiotic and were incubated at 28 ºC for 2-3 days.

3.3. Nucleic acid methods

3.3.1. Extraction and purification of nucleic acids

3.3.1.1. Extraction of genomic DNA from leaves or seedlings

Extraction of genomic DNA from plant material (usually leaves or full seedlings) for genotyping or other purposes was performed as described by Edwards *et al.* (1991) with minor modifications. Liquid nitrogen frozen samples were homogenized in extraction buffer (200 mM Tris-HCl pH 7.5, 250 mM NaCl, 25 mM EDTA, 0.5% SDS) with a polytron. After a 2 min centrifugation at 4 ºC, supernatant was incubated on ice with 1 volume of ice cold isopropanol for 30 min. The mixture was centrifuged for 5 min at room temperature and the dried pellet was resuspended in TE buffer. Alternatively, genomic DNA was isolated with hexadecyltrimethylammonium bromide (CTAB)-containing buffer. DNA samples were stored at -20 ºC.

3.3.1.2. Cleaning of PCR products

Amplified DNA of PCR products was cleaned for further sequencing or manipulation, removing excess primers and unincorporated nucleotides. To achieve this, 5 µl of PCR product was incubated with 1 µl of ExoSAP-IT PCR Product Cleanup Reagent (Affymetrix). The mix was incubated for 15 min at 37 ºC and the reagent was inactivated by incubating for additional 15 min at 80 ºC. Alternatively, PCR products were cleaned with the ChargeSwitch PCR Clean-Up Kit (Invitrogen).

3.3.1.3. Extraction of DNA from agarose gel

DNA fragments separated by size through agarose gel electrophoresis were recovered from gel slices of specific bands by using the PureLink Quick Gel Extraction Kit (Invitrogen).

3.3.1.4. Extraction and isolation of plasmidic DNA from bacteria

For the extraction and purification of plasmids from transformed bacteria, a liquid culture was prepared in 4-8 ml of LB medium from a single colony. Culture was incubated for at least 10 h at 37 ºC and then was centrifuged at 4500 rpm for 10 min. The pellet was used for the extraction by using the PureLink Plasmid

Miniprep Kit of Invitrogen. Plasmids were collected in MilliQ water. Afterwards, plasmid and transgene were checked by sequencing with specific primes (Table A3). Plasmid samples were stored at -20 ºC.

3.3.1.5. Extraction and isolation of total RNA from seedlings

Total RNA from full seedlings was extracted and purified with Nucleospin RNA Plant kit (Macherey-Nagel). RNA was recovered in diethyl pyrocarbonate (DEPC)-treated water and its quality was checked by running a fraction on an agarose gel electrophoresis. Alternatively, for microarray analyses, plants were frozen in liquid nitrogen and the total RNAs were extracted with Trizol and purified with the RNeasy kit (QIAGEN). RNA samples were stored at -80 ºC.

3.3.2. Manipulation of nucleic acids

3.3.2.1. Methods for quantification and concentration

Nucleic acids in extracts were quantified by measuring with an ND1000 spectrophotometer (NanoDrop Technologies), which allows direct measurements using 1 µl of non-diluted samples. Concentration of DNA samples in water was increased by using a centrifugal evaporator SpeedVac Savant at room temperature. Concentration of RNA samples in water was increased by precipitation after adding 0.05 volumes of 1M acetic acid in DEPC-treated water and 0.7 volumes of absolute ethanol. After incubating at -80 ºC for 30 min, samples were centrifuged at maximum speed and 4º C for 10 min and pellets were re-solubilized in DEPC-treated water.

3.3.2.2. Methods for DNA amplification

For genotyping or other purposes, short DNA sequences were amplified by PCR. For each sample, 1 µl of purified DNA was added to a reaction mix composed by 2.5 µl of 10X reaction buffer with $MgCl_2$, 0.75 µl of 10mM dNTP mix, 0.75 µl of 10 µM forward and reverse primers, 0.5 µl of Biotools DNA polymerase (1U/ µl) and MilliQ water to a total volume of 25 µl. Table A3 gathers all oligonucleotides used in this work. Amplification was carried out with an Applied Byosystems 96-well thermocycler. Standard program featured 2 min at 94 ºC initialization, 35 cycles of denaturation (30 s at 94 ºC), annealing (30 s at 54ºC) and extension (2 min at 72 ºC), and 7 min at 72 ºC of final elongation. Number of cycles, annealing temperature and extension time were modified to suit a few cases. Products of PCR were used immediately for electrophoresis or stored at -20 ºC. For cloning purposes, cDNA was used as template for High Fidelity (HF)-PCR, in which polymerase and reaction buffer were substituted by those provided by Fermentas for HF-PCR.

3.3.2.3. Reverse transcription (RT) of mRNA

Reverse transcription of the polyadenylated fraction of RNA was performed to obtain cDNA. For each sample, 1-2 µl of purified RNA were added to 0.5 µg of

oligo(dT)18 in 12.5 µl of DEPC-treated water and incubated at 65 ºC for 5 min. After cooling down on ice, the following was added to the mix: 4 µl of Fermentas 5X reaction buffer, 0.5 µl of RiboLock RNase inhibitor of Thermo Scientific (40 U/µl), 2 µl of 10mM dNTP mix and 1 µl of Fermentas RevertAid H Minus Reverse Transcriptase (200 U/µl). The mix was incubated at 42 ºC for 90 min and the reaction was stopped by incubation for 10 min at 70 ºC. The resulting cDNA was stored at -20 ºC.

3.3.2.4. Quantification of transcripts by quantitative PCR (qPCR)

Real-time or quantitative PCR (qPCR) was used to quantify the expression level of genes. Reaction mix was composed by 10 µl of SYBR Green PCR Master Mix (Applied Biosystems), 7.8 µl of MilliQ water, 0.6 µl of each specific primer (10 µM) (Table A3) and 1 µl of RT product (cDNA) as template. Reactions were performed in MicroAMPTM Optical 96-well reaction plates (Applied Biosystems) in an ABI 7500 Fast Real-Time Thermocycler, following the recommended program (2 min at 50º C, 10 min at 95 ºC and 40 cycles of 15 s at 95 ºC and 1 min at 60 ºC). For each reaction a Ct value and a melting curve were obtained. For each quantification assay, 3 biological replicates were used and each was used for 3 technical replicates. Relative expression of genes respecting control or mock samples was calculated with Applied Biosystems 7500 Software v.2.0.4 as indicated in equation 3.1, using *ACT2/8* as endogenous gene.

Equation 3.1. Normalized relative expression

$$Relative\ expression = 2^{-\Delta\Delta Ct}$$
$$\Delta\Delta Ct = (Ct_{target\ gene} - Ct_{endogenous\ gene}) - (Ct_{calibrator\ gene} - Ct_{endogenous\ gene})$$

3.3.2.5. Transcriptomic analysis by microarrays

Microarrays were used for a genome-wide analysis of gene expression. Prior to the transcriptomic analysis, RNAs were checked for their integrity and purity by nanocapillary electrophoresis in Bioanalyzer Agilent 2100. Then, RNAs were ligated to an RNA oligonucleotide adaptor (Invitrogen) using T4 RNA ligase (Ambion). The RNAs were extracted once with phenol- chloroform and non-ligated adapter was removed by chromatography with MicroSpin S-300 HR columns (GE Healthcare). Purified ligation products were precipitated in ethanol and used as templates for reverse transcription with Superscript III (Invitrogen) for 3 h at 46 °C, using oligonucleotide oligo(dT) as primer. Template RNA was removed by alkaline hydrolysis and first-strand cDNA purified with S.N.A.P. columns (Invitrogen). Second-strand synthesis was performed with Taq DNA polymerase (Roche) for 5 min at 94 °C, 5 min; 58 °C, 1 min; 72 °C, 10 min. A forward oligonucleotide T7-Adap primer, which was complementary to the RNA adapter and contained the sequence of bacteriophage T7 promoter, was used. Double-stranded cDNA was then purified with MinElute columns (Qiagen) and in vitro transcribed with T7 RNA polymerase, using a MessageAmp aRNA kit

(Ambion). Amplified RNA was treated with DNase I (Roche) to remove cDNA templates, purified with an aRNA Purification Module (Ambion) and then used as template for single-stranded cDNA synthesis, according to Affymetrix instructions as follows: aRNA was reverse transcribed with SuperScript II (Invitrogen) for 1 h at 42 °C with oligo(dT) as primer. After alkaline hydrolysis of aRNA and purification (MinElute columns, Qiagen), cDNA was fragmented with 1.5 units of DNase I (GE Healthcare) into fragments in the 50–200 bp range. Finally, 3' ends of fragmented cDNA were biotin- ddUTP labeled with terminal deoxynucleotidyl transferase (Promega) and GeneChip DNA labeling reagent (Affymetrix).

Three biological replicates and their corresponding negative controls were independently hybridized to ATH1 microarrays (Affymetrix), containing 22 500 transcript variants from 24 000 well-characterized Arabidopsis genes. Each sample was added to a hybridization solution containing 100 mM 2-(N-morpholino) ethanesulfonic acid, 1 mM Na^+, and 20 mM of EDTA in the presence of 0.01% Tween-20. Hybridization was performed for 16 h at 45 °C. Each microarray was washed and stained with streptavidin–phycoerythrin in a Fluidics station 450 (Affymetrix) and scanned at 2.5-μm resolution in a GeneChip Scanner 3000 7G system (Affymetrix). Data analyses were performed using genechip operating software (GCOS), to generate the corresponding CEL files.

Alternatively, sample RNA was amplified and labeled with the Agilent Low Input Quick Amp Labeling Kit and an Agilent Spike-In Kit was used to assess the labeling and hybridization efficiencies. Hybridization and slide washing were performed with the Gene Expression Hybridization Kit and Gene Expression Wash Buffers, respectively. Three biological replicates were hybridized to Arabidposis (V4) Gene Expression Microarray 4x44K, which contained 43,803 probes (60-mer oligonucleotides) and was used in a one-color experimental design. After washing and drying, slides were scanned in an Agilent G2565AA microarray scanner, at 5 μm resolution and using the double scanning, as recommended. Image files were analyzed with the Feature Extraction software 9.5.1. Interarray analyses were performed with the GeneSpring 11.5 software.

3.3.2.6. DNA sequencing

Each bacterial purified plasmid (200 ng/μl) was checked by DNA sequencing with an ABi 3130XL (LifeTechnologies) using the cyclic sequencing kit BigDye Terminator v3.1 (LifeTechnologies). One oligonucleotide was used for the sequencing of every 700 bp of DNA. Cleaned PCR products (2.5 ng/μl) were similarly sequenced.

3.3.2.7. Electrophoretic techniques

DNAs were size-separated by agarose gel electrophoresis. Gel was composed by 1-2% (w/v) agarose and 10 mg/ml ethidium bromide in TAE buffer. Electrophoresis was run at 100 V and gel was visualized in UV transilluminator with

digital camera G:BOX (Syngene). Agarose gel electrophoresis was also used for RNA analysis, but it was performed at 40 V.

Genomic DNA isolated from plants was run in duplicate in 2% (w/v) agarose gels and either ethidium bromide-stained (15 µg) or blotted (5 µg) onto positively charged nylon membranes. DNA digested with *Msp*I was digoxigenin (DIG)-labelled and used as probe for Southern blot with anti-DIG antibody coupled to alkaline phosphatase to amplify the signal.

3.3.2.8. Enzymatic digestion of DNA with restriction enzymes

For different purposes, DNA was cut with restriction endonucleases. Reaction mix was composed by the DNA, 2 µl of specific buffer (Thermo Fisher Scientific), 0.5 µl of each restriction enzyme (Thermo Fisher Scientific) and MilliQ water to a volume of 20 µl. The mix was incubated for 1-18 h at the corresponding temperature for the enzyme. The enzyme was deactivated by incubation at 70 ºC for 10 min. Restriction product was analyzed by electrophoresis or stored at -20 ºC.

3.3.2.9. Southern blot

15 µg of CTAB-isolated genomic DNA were separated through 2% (w/v) agarose gel, blotted onto positively charged nylon membranes, and Southern blot performed with a digoxigenin-labelled probe (DIG High Prime DNA Labeling and Detection Starter Kit II from Roche).

3.3.2.10. Cloning techniques in bacteria

For the generation of transgenic plants overexpressing Arabidopsis NRs and NIR1 genes, Invitrogen's pCR8/GW/TOPO (Fig. A1) was used as entry vector while pAlligator2 (Bensmihen *et al.*, 2004) (Fig. A2) was the destination vector. 3' A-overhangs were added to HF-PCR products from amplifying the cDNA corresponding to the transcripts of the target genes by incubating with Taq polymerase for 10 min at 72 ºC. For the cloning reaction of the desired gene into the entry vector, 4.2 µl of HF-PCR product were added to 1 µl of salt solution and 0.8 µl of vector and incubated for 2 h at 23 ºC. This mix was then used for direct bacterial transformation. The gene of interest was cloned to the destination vector by recombination through the Gateway LR reaction. 100-150 ng of purified entry vector, 200 ng of destination vector and 2 µl of Clonase LR II were added to a total volume of 10 µl of TE buffer. The mixture was incubated at 25 ºC for 1-18 h and finished upon addition of 1 µl of Proteinase K and an incubation of 10 min at 37 ºC. This dilution was then used for bacterial transformation.

3.4. Protein methods

3.4.1. Extraction and purification of proteins

3.4.1.1. Extraction of total proteins from plant tissues

Total crude protein extracts were prepared by grinding liquid nitrogen frozen seedlings with a polytron and further extraction in 50 mM Tris-HCl buffer, pH 8.0, containing 150 mM NaCl, 5% (v/v) glycerol, 5 mM EDTA, 0.05% (v/v) Triton X-100, 10 mM dithiothreitol (DTT), 1% (v/v) protease inhibitor cocktail (Sigma) and 1 mM phenylmethylsulfonyl fluoride (PMSF). Alternatively, in order to achieve non-reducing conditions, extractions were performed in the absence of DTT. Clean soluble protein-containing supernatant after 20 min centrifugation at 16000 g and 4 ºC was stored at -80 ºC.

3.4.1.2. Immunopurification of tagged proteins with magnetic beads

HA-tagged proteins overexpressed in transgenic plants were immunopurified with anti-HA-magnetic beads (Miltenyi Biotec, Germany). Purification was performed with the µMAC Epitope Tag Protein Isolation kit (Miltenyi Biotec, Germany). For further proteomic analysis, proteins were eluted under non-denaturing non-reducing conditions by using 0.1 mM triethylamine (pH 11.8) (Sigma), and proteins were collected in 1 M MES buffer (pH 3.0) for neutralization of the eluted immunopurified proteins. Purified proteins were stored at -80 ºC.

3.4.1.3. Precipitation of proteins

In order to change the buffer of protein extracts or to achieve an increase in their concentration, four volumes of cold acetone were added and incubated overnight at -20 ºC. The solution was centrifuged for 10 min at 4 ºC and the dried pellet was resuspended in the desired volume of buffer.

3.4.2. Manipulation of proteins

3.4.2.1. Quantification of total proteins

Total protein content in extracts was measured by adding Bradford reagent as described by Bradford (1976), measuring absorbance at 595 nm with the 96-well Multiskan GO spectrophotometer (Thermo Scientific), and quantifying with a bovine serum albumin (BSA) calibration curve.

3.4.2.2. Protein separation by SDS-PAGE

Proteins in extracts were separated by their molecular weight by sodium dodecyl sulfate polyacrylamide gel electrophoresis (SDS-PAGE). Samples were loaded with Laemmli 6X (without DTT if non-reducing conditions were required) in 10% acrylamide gels, after denatured by 95 ºC incubation for 10 min. Electrophoresis was performed at 100 V with a protein molecular weight ladder.

Gels were either stained for total protein with Imperial reagent (Thermo Scientific) or semi-dry transferred to nitrocellulose membranes.

3.4.2.3. Protein detection by Western blot analyses

Levels of specific endogenous, tagged- or post-translationally-modified proteins were analyzed in total protein extracts by Western blot. Separated proteins in polyacrylamide gels were semi-dry transferred to nitrocellulose membranes with a Semi-Dry Blotter (Thermo Scientific), running at 140 mA for 45 min per gel. After blocking membranes with TTBS buffer supplemented with either 5% (w/v) non-fat dried milk, 3% (w/v) Top-Block (Fluka) or 3% (w/v) BSA, Western blots were performed by incubating membranes overnight at 4ºC in the following primary antibodies at the indicated dilution factor: polyclonal anti-NR (Agrisera, 1:1000), anti-NiR1 (Davenport *et al.*, 2015, 1:1000), monoclonal anti-3nitroY (Cayman Chemicals, 1:1000) or monoclonal anti-TMT (Thermo Scientific, 1:1000). Polyclonal anti DE-ETIOLATED 3 (DET3) (donated by David Alabadí, IBMCP Valencia, Spain, 1:10000) was used as loading control (Duek *et al.*, 2004). Alternatively, loading control was assessed by staining nitrocellulose membranes after blotting with Ponceau S. Secondary anti-rabbit or anti-mouse antibodies coupled to horseradish peroxidase (HRP) (GE, 1:5000) and Supersignal WestPico Chemiluniscence reagents (Thermo Scientific) were used to visualize bands. HA-tagged proteins were directly detected with monoclonal anti-HA-HRP antibody (Thermo Scientific, 1:1000).

3.4.2.4. LC-MS/MS-based proteomic analyses

Protein extracts obtained from plants expressing HA-tagged versions of NRs and NiR1 were used for proteomic analyses for the identification of *in vivo* PTMs. Protein samples immunopurified under non-reducing conditions were precipitated with six volumes of cold acetone and digested overnight, under non-reducing conditions, with trypsin (mass spectrometry grade, Promega Corp.; 1:10 enzyme/substrate ratio) at 37°C in 6 M urea, 200 mM ABC buffer. The resulting peptides, desalted with UltraMicroSpin columns, were fragmented by collision-induced dissociation in a Thermo LTQ Orbitrap Velos Pro mass spectrometer. Fragmented peptides were separated in a packed nanocapillary column (NTCC-360/75-1.9-25L Nikkyo Technos). Raw data were processed and analyzed by using the Mascot Server v2.4 (Matrix Science) database [false discovery rate (FDR) < 5%, A. thaliana UniProt database including 13,140 proteins, with a mass tolerance of 7 ppm for the precursors and 0.5 Dalton for fragments].

3.4.2.5. NR and NIR activity assays

Nitrate reductase activity assays were performed as reported (Park *et al.*, 2011) with slight modifications. Proteins were extracted by homogenizing liquid nitrogen frozen seedlings in a buffer composed by 250 mM Tris–HCl (pH 8.0), 1 mM EDTA, 1 μM Na_2MoO_4, 5 μM flavin adenine dinucleotide (FAD), 3 mM dithiothreitol (DTT), 12 mM β-mercaptoethanol and 250 μM PMSF. The enzymatic

reaction was carried out by incubating 20 µg of protein extract in a final volume of 250 µl of NR activity reaction buffer (40 mM $NaNO_3$, 80 mM K_2HPO_4, 20 mM KH_2PO_4, 0.2 mM NADH, pH 7.5) at 25 ºC for 30 min. Reaction was initiated by the addition of the $NaNO_3$ and was stopped upon addition of 100 µl of sulfanilamide reagent (1% (w/v) sulfanilamide and 2.4 M HCl) and 100 µl of N-(1-napthyl) ethylenediamine hydrochloride (N-NEDA) reagent (0.02% (w/v)) to 100 µl of the reaction solution. Formation of nitrite was determined by measuring at 540 nm the absorbance of the resultant mixture with the 96-well Multiskan GO spectrophotometer (Thermo Scientific). Quantification of nitrite formation was performed by a nitrite calibration curve and the comparison between samples incubated for 30 min and samples in which the reaction was stopped at the beginning by the addition of the sulfanilamide reagent. For each genotype and condition, 3 biological replicates were used and each was used for 3 technical replicates.

Nitrite reductase activity was assayed as previously reported (Takahashi *et al.*, 2001) with slight modifications. Proteins were extracted by homogenizing liquid nitrogen frozen seedlings in 400 µl of a buffer composed by 50 mM potassium phosphate buffer (pH 7.5), 1 mM EDTA, 10 mM β-mercaptoethanol, 100 µM PMSF and 5 mg PVP. The enzymatic reaction was carried out by incubating 50 µg of protein extract in a final volume of 250 µl of NIR activity reaction buffer (33 mM potassium phosphate buffer, pH 7.5, 1 mM $NaNO_2$, 1 mM methyl viologen, 11.11 mM sodium dithionite) at 30 ºC for 10 min. Reaction was initiated upon addition of the sodium dithionite and stopped by oxidizing the samples with a vortex mixer. Nitrite conversion was determined by measuring with the 96-well Multiskan GO spectrophotometer (Thermo Scientific) at 540 nm the absorbance of a mixture composed by 4 µl of the reaction solution, 96 µl water, 100 µl of sulfanilamide reagent and 100 µl of N-NEDA reagent. Quantification of nitrite conversion was performed by a nitrite calibration curve and the comparison between samples incubated for 10 min and samples in which the reaction was stopped at the beginning by vortexing. For each genotype and condition, 3 biological replicates were used and each was used for 3 technical replicates.

3.5. Metabolic methods

3.5.1. LC/MS- and GC/MS-based analyses of the metabolome

The sample preparation process was carried out using the automated MicroLab STAR system from Hamilton Company. Recovery standards were added prior to the first step in the extraction process for quality Control (QC) purposes. Sample preparation was conducted by series of organic and aqueous extractions to remove the protein fraction while allowing maximum recovery of small molecules. The resulting extract was divided into two fractions; one for analysis by Liquid Chromatography (LC) and one for analysis by Gas Chromatography (GC). Samples were placed briefly on a TurboVap

(Zymark) to remove the organic solvent. Each sample was then frozen, dried under vacuum and prepared for either LC/MS or GC/MS.

The LC/MS portion of the platform was based on a Waters ACQUITY UPLC and a Thermo-Finnigan LTQ mass spectrometer, which consisted of an electrospray ionization (ESI) source and linear ion-trap (LIT) mass analyzer. The sample extract was split into two aliquots, dried, then reconstituted in acidic or basic LC-compatible solvents, each of which contained 11 or more injection standards at fixed concentrations. One aliquot was analyzed using acidic positive ion optimized conditions and the other using basic negative ion optimized conditions in two independent injections using separate dedicated columns. Extracts reconstituted in acidic conditions were gradient eluted using water and methanol both containing 0.1% Formic acid, while the basic extracts, which also used water/methanol, contained 6.5 mM ammonium bicarbonate. The MS analysis alternated between MS and data-dependent MS2 scans using dynamic exclusion. The Thermo-Finnigan LTQ-FT mass spectrometer had a linear ion-trap (LIT) front end and a Fourier transform ion cyclotron resonance (FT-ICR) mass spectrometer back end. For ions with counts greater than 2 million, an accurate mass measurement could be performed. Accurate mass measurements could be made on the parent ion as well as fragments. The typical mass error was less than 5 ppm. Ions with less than two million counts require fragmentation spectra (MS/MS) typically generated in data dependent manner or targeted MS/MS in the case of lower level signals.

The samples destined for GC/MS analysis were re-dried under vacuum desiccation for a minimum of 24 hours prior to being derivatized under dried nitrogen using bistrimethyl-silyl-triflouroacetamide (BSTFA). The GC column was 5% phenyl and the temperature ramp is from 40° to 300° C in a 16 minute period. Samples were analyzed on a Thermo-Finnigan Trace DSQ fast-scanning single-quadrupole mass spectrometer using electron impact ionization.

The data extraction of the raw mass spec data files yielded information that was loaded into a relational database and manipulated without resorting to BLOB manipulation. Peaks were identified using peak integration software, and component parts were stored in a separate and specifically designed complex data structure. Compounds were identified by comparison to library entries of more than 1000 commercially available purified standards. The combination of chromatographic properties and mass spectra gave an indication of a match to the specific compound or an isobaric entity. Additional entities could be identified by virtue of their recurrent nature (both chromatographic and mass spectral). A variety of curation procedures were carried out to ensure accurate and consistent identification of true chemical entities, and to remove those representing system artifacts, misassignments, and background noise.

3.5.2. Quantification of anthocyanins

Anthocyanins were spectrophotometrically determined in methanolic extracts by reading their absorbance at 530 nm as described (Solfanelli *et al.*, 2006).

3.5.3. Phytohormone quantification

Four independent biological replicate samples of around 150-200 mg fresh weight of either non-acclimated or cold-acclimated Col-0 and *nia1,2noa1-2* seedlings were suspended in 80% methanol-1% acetic acid containing internal standards and mixed by shaking during one hour at 4ºC. The extract was kept at 20 ºC overnight, centrifuged, the supernatant dried in a vacuum evaporator, and the dry residue was dissolved in 1% acetic acid and passed through an Oasis HLB (reverse phase) column as described in Seo et al. (2011). The dried eluate was dissolved in 5% acetonitrile-1% acetic acid, and the hormones were separated using an autosampler and reverse phase UHPLC chromatography (2.6 µm Accucore RP-MS column, 50 mm length x 2.1 mm i.d., ThermoFisher Scientific) with a 5 to 50% acetonitrile gradient containing 0.05% acetic acid, at 400 µL/min over 14 min. The phytohormones were analyzed with a Q-Exactive mass spectrometer (Orbitrap detector, ThermoFisher Scientific) by targeted Selected Ion Monitoring (SIM). The concentrations of hormones in the extracts were determined using embedded calibration curves and the Xcalibur 2.2 SP1 build 48 and TraceFinder programs. The internal standard for quantification of ABA was the deuterium-labelled hormone. For JA, dihydrojasmonate (dhJA) was used as internal standard.

3.6. *In silico* and statistical methods

3.6.1. *In silico* analyses

DNA and amino acid sequences were analyzed by using the tools available in the Sequence Manipulation Suite (http://www.bioinformatics.org/sms2/) and the alignments were performed with Clustal Omega (https://www.ebi.ac.uk/Tools/msa/clustalo/). Gene Ontology enrichment of functional categories in gene lists was performed by the Gene Ontology Consortium tools (http://www.geneontology.org/). Comparison of transcriptome profiles with publicly available datasets was performed with AtCAST3.1 tool (http://atpbsmd.yokohama-cu.ac.jp/cgi/atcast/search_input.cgi) by selecting data from different ATH1 experiments with P value of Student's t-test < 0.01. Spearman's rank-order correlation coefficients (SCCs) were used to estimate the functional overlapping/co-expression between experiments (Kakei & Shimada, 2015). Search for the RAP2.3 binding motif MGCCGYM in promoter sequences of Arabidopsis genome was performed with Patmatch tool in the TAIR10 Loci Upstream Sequences -- 1000 bp (DNA) database. Multiple protein sequence alignments were performed by using Clustal Omega (https://www.ebi.ac.uk/Tools/msa/clustalo/). Protein Database Bank

(https://www.rcsb.org/) files were processed with Yasara software (www.yasara.org/) for 3D structure modelling.

3.6.2. Prediction of PTMs

S-nitrosylation and nitration sites on potential NO target proteins were predicted by GPS-SNO (Xue *et al.*, 2010; http://sno.biocuckoo.org/) and iSNOPseAAC (Xu *et al.*, 2013; http://app.aporc.org/iSNO-PseAAC/); and GPS-YNO2 (Liu *et al.*, 2011; http://yno2.biocuckoo.org/) and iNi-tro-Tyr (Xu *et al.*, 2014; http://app.aporc.org/iNitro-Tyr/) tools.

3.6.3. Statistical analyses

Differential gene transcript levels or hypocotyl lengths were statistically analyzed by Student´s t-test and considered significant with p-value ≤ 0.05. The Linear Model Methods (LiMMA) were used for determining differentially expressed genes in microarray-based analyses. To control the false-discovery rate, P-values were corrected using the method of Benjamini and Hochberg (1995). Criteria for selection of genes were fold value >1.5 and false-discovery rate ≤ 0.05. Statistical analysis and graphical visualization of data were performed with the interactive tool FIESTA (http://bioinfogp.cnb.csic.es/tools/FIESTA/).

For metabolomic analyses, following log transformation and imputation with minimum observed values for each compound, Welch's two-sample t-test and ANOVA contrast were used to identify biochemicals that differed significantly between experimental groups. A Two-way ANOVA was also used to identify biochemicals exhibiting a significant time and treatment main effect and the interaction effect between these two variables. An estimate of the false discovery rate (q-value) was calculated to take into account the multiple comparisons. Statistical analyses are performed with the program "R" (http://cran.r-project.org/). Statistically significant differences in hormone quantification and transcript analyses were computed based on Student´s t-tests.

Results

4. RESULTS

4.1. Regulation of NR-dependent NO biosynthesis. Post-translational modifications of the biosynthetic enzymes

This section 4.1 is an excerpt from the research article: "Costa-Broseta, Á., Castillo, M. C., & León, J. (2018). Protein Stabilization and Post-translational Modifications Control NO Homeostasis in Arabidopsis". This research article was submitted to Plant Physiology and was under revision when PhD Thesis writing was finished. All the results and figures that appear here are derived from the work of the PhD student in collaboration with the other authors.

4.1.1. Abstract

Nitric oxide (NO) is mainly produced from nitrite in plants through a reductive mechanism involving nitrate reductases (NRs) in balance with nitrite reductases (NiRs). Arabidopsis has two NADH-dependent NRs, NR1/NIA1 and NR2/NIA2, and one Ferredoxin-dependent NiR called NiR1. We found that NRs and NiR1 enzymes were oppositely regulated by two main factors: nitrate-induced signaling controlled by the function of the NIN-like protein 7 (NLP7) transcription factor, and proteasome-mediated degradation. NLP7 positively regulated NRs but negatively regulated NiR1. Moreover, NRs but not NiR1 were controlled by proteasome-mediated degradation. High rates of NO production were sustained under positive regulation of NRs and negative regulation of NiR1 as demonstrated in a *nir1* loss-of-function mutant generated by CRISPR-Cas9. NR stabilization and NO accumulation under treatment with proteasome inhibitors were potentiated in a *prt6-1* mutant background, thus connecting NO production with the Arg/N-end rule proteolytic pathway. Moreover, PRT6 protected NRs from NO-triggered degradation in a putative auto-regulatory loop controlling NO homeostasis. NO-triggered changes in NRs and NiR1 protein and activity were likely exerted by post-translational modifications (PTMs). We identified nitration of tyrosine residues as well as S-nitrosylation of cysteine residues in NRs and NiR1, which may account for inactivation of the enzymes. Moreover, NO-triggered PTMs were accompanied by lysine ubiquitylation that is likely required for further proteasome-mediated degradation of the enzymes.

4.1.2. Nitrate Reductase is Regulated by Proteasome-mediated Degradation and Nitrate Signaling

Nitrate assimilation, involving the nitrate reductase (NR)-catalyzed conversion of nitrate to nitrite and further reduction to ammonium by nitrite reductase (NiR), may be a source of nitric oxide (NO) when the second redox reaction is replaced by a conversion of nitrite to NO catalyzed by NR or other molybdenum-dependent enzymes (Bender & Schwarz, 2018) (Fig. 4.1A). This alternative function for NR

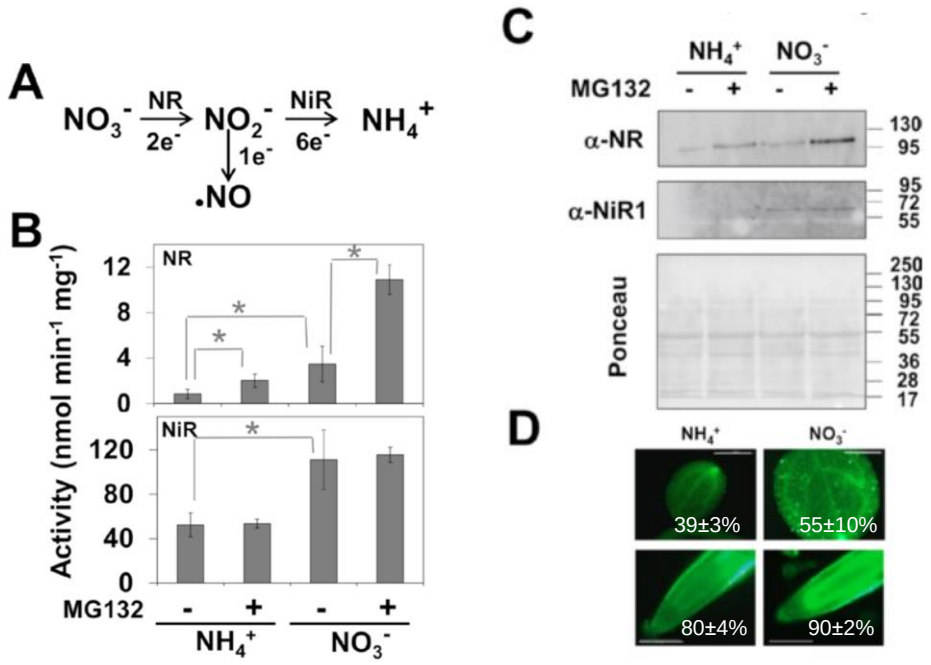

Figure 4.1. Effect of nitrogen source and proteasome-mediated degradation on NR and NiR. A, Scheme of nitrate assimilation and NO production. B, NR and NiR activities; and C, protein levels in plants grown for 11 days in ammonium-supplied media and then transferred to media containing either 5 mM nitrate or 2.5 mM ammonium as indicated for two additional days. By 16 h before collecting samples plants were either untreated (-) or treated with 100 µM MG132 proteasome inhibitor (+). D, NO levels detected in DAF-FM DA stained cotyledons and roots of plants grown with 5 mM nitrate or 2.5 mM ammonium. Quantification of fluorescence is shown as the mean of at least 3 replicate experiments ± standard error. * represents statistically significant with $p<0.05$ in paired Student´s t-test. Size bars represent 100 µm.

place this enzyme as a relevant node in regulating developmental and stress-related responses where NO is involved. However, the conditions favoring this alternative function are not well known. The levels of NR activity and protein are centrally regulated by the availability of nitrate. Nitrate induces gene transcripts, protein synthesis and the activity of nitrate assimilatory enzymes in plants (Aslam & Huffaker, 1989; Cheng *et al.*, 1991). Accordingly, we confirmed that in plants grown in ammonium-supplied media and then transferred to nitrate-supplied media or kept in ammonium as control, the levels of NR and NiR1 proteins and their activities were higher in nitrate-supplied than in ammonium-supplied plants (Fig. 4.1B, C). It is noteworthy mentioning that treatment with the proteasome inhibitor MG132 stabilized NR protein (Fig. 4.1C) and enhanced its activity (Fig. 4.1B), whereas no alterations were detected for NiR1 in the absence or presence of the proteasome inhibitor. The increased NR protein and activity levels correlated well with the increased NO content detected in shoots and roots of nitrate-grown plants when compared to ammonium-grown plants (Fig. 4.1D). All these data together suggest that NR, besides being positively regulated by nitrate, is negatively

regulated by a proteasome-mediated proteolytic process that may be relevant in controlling NO production.

Some previous evidences suggested that the above proposed proteasome-mediated proteolytic process modulating NR function and the subsequent NO production might be related to the N-end rule proteolytic pathway. We previously reported that the degradation of transcription factors of the group VII of Ethylene Responsive Factors (ERFVII) through the arginylation branch of the N-end rule pathway is on the basis of a NO sensor mechanism (Gibbs *et al.*, 2014a). Degradation of ERFVIIs requires their polyubiquitylation by the E3 ubiquitin ligase PRT6 in such a way that *prt6-1* mutant plants were insensitive to NO and, remarkably, contained increased levels of NO in leaf stomata (Gibbs *et al.*, 2014a). On the other hand, it has been reported that the nitrate-triggered induction of genes coding for nitrate assimilation enzymes NR and NiR1 are due to the function of the NLP7 transcription factor that upon nitrate treatment accumulates in the nuclei (Marchive *et al.*, 2013), and binds to specific sites of the promoters of *NR* and *NiR* genes (Guan *et al.*, 2017; Zhao *et al.*, 2018). We have tested whether the levels of NR and NiR1 protein and enzyme activities were altered in the N-end rule pathway *prt6-1* mutant as well as in the nitrate signaling *nlp7-1* mutant plants in nitrate-containing media. Figure 4.2A shows that the levels of NR and NiR1 proteins did not change significantly in *prt6-1* when compared to wild type plants. By contrast, the levels of NR and NiR1 proteins decreased and increased, respectively in *nlp7-1* plants (Fig. 4.2A). These changes in the protein levels matched with decreased and enhanced enzyme NR and NiR activities, respectively (Fig. 4.2B). The effect of *nlp7-1* mutation seems to be epistatic on the *prt6-1* mutation as the double *prt6-1nlp7-1* mutant also showed decreased and increased NR and NiR protein and activities, respectively (Fig. 4.2A, B). Regarding this, *nlp7-1* plants have pale-green normal-size leaves; *prt6-1* plants are smaller with green leaves, and *nlp7-1prt6-1* plants are small pale-green plants combining the parental phenotypes (Fig. 4.3A). Remarkably, the expression of N terminus-tagged NLP7 under the control of the endogenous promoter or the constitutive 35S promoter in the double *nlp7-1prt6-1* background rescued both the small size and the pale green phenotypes (Fig. 4.3A), thus suggesting PRT6 and NLP7 may be somehow functionally linked. It is noteworthy mentioning that expression of *NLP7* in the *nlp7-1* and *nlp7-1prt6-1* mutant backgrounds led to a significant increase in the endogenous NO content even over those detected in *nlp7-1prt6-1* plants (Fig. 4.3B). These data suggest a central role for NLP7 in regulating nitrate assimilation acting oppositely on NRs and NiR1, which might be relevant for the production of NO.

If NLP7 regulates NR positively and NiR negatively it would be expected that the levels of NO decrease in NLP7-defective plants. Figure 4.2C shows that indeed the NO content was slightly lower in *nlp7-1* than in wild type plants. Interestingly, the slightly increased NO levels detected in *prt6-1* plants when compared to wild type plants were substantially larger in *prt6-1nlp7-1* plants (Fig. 4.2C), despite

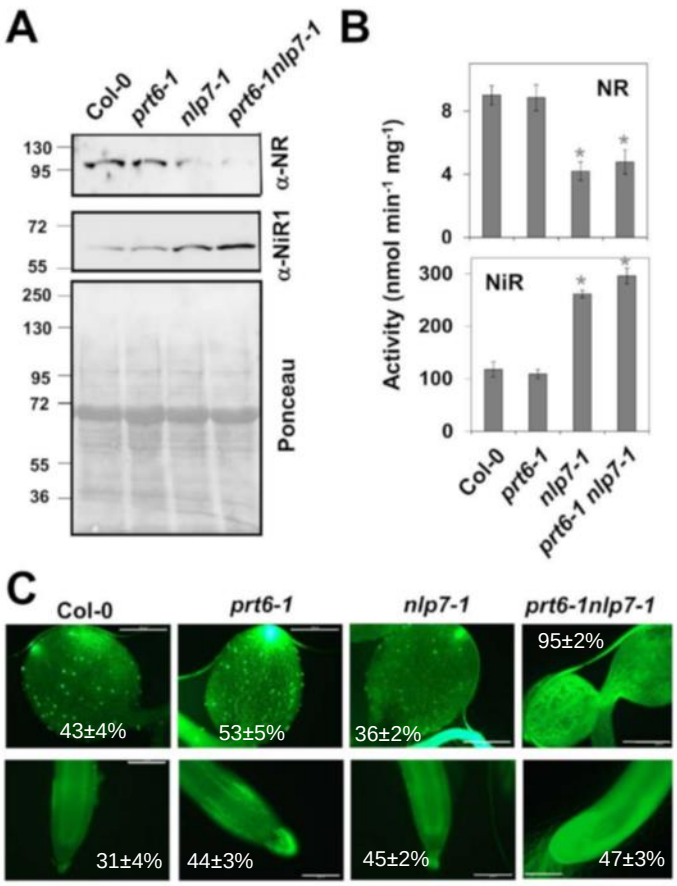

Figure 4.2. Regulation of NR and NiR by NLP7 nitrate signaling factor. A, Protein levels and B, enzyme activities in the indicated mutant plants. Activity values are the mean ± SD of three independent biological replicates and shown Western blots with specific anti-NR and anti-NiR1 proteins are representative. Ponceau S staining was used as loading control and molecular size marker (kDa) locations are shown at the left side of A panels. * Represents statistically significant with $p<0.05$ in paired Student´s t-test comparing to Col-0 levels. C, NO levels detected in DAF-FM DA stained cotyledons and roots of plants of the indicated genotypes. Quantification of fluorescence is shown as the mean of at least 3 replicate experiments ± standard error. Size bars represent 100 µm.

having reduced levels of NR protein and activity (Fig. 4.2A, B). In turn, *prt6-1nlp7-1* plants contained significantly enhanced NiR protein and activity (Fig. 4.2A, B). Therefore, the enhanced NO levels and NiR1 function in *prt6-1nlp7-1* plants could be indicative of NiR1 playing a positive role in NO production. To test this hypothesis, we have generated transgenic 35S:*NiR1* plants (Fig. 4.4) and a *nir1* loss-of-function mutant, by using CRISPR-Cas9 technology (Fig. 3.1). After the analysis of the NO content, we found a large accumulation of NO in *nir1* mutant plants whereas no significant alteration was observed in *35S:NiR1* plants (Fig. 4.5) despite these transgenic plants were in a *prt6-1* background that favors NO production (Fig. 4.2C) (Gibbs *et al.*, 2014a). If the enhanced NO content detected in *prt6-1nlp7-1* plants were not due to increased NiR1 function, it might be alternatively explained by a NLP7-independent PRT6-regulated process. As

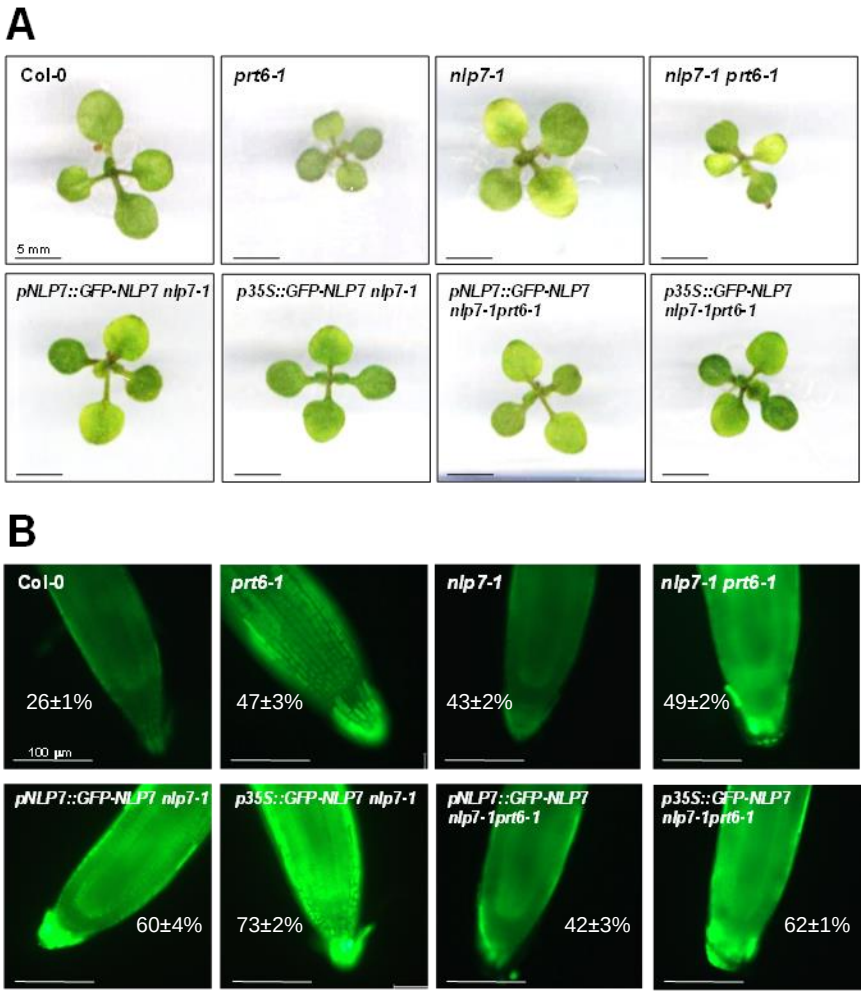

Figure 4.3. Complementation of *nlp7-1* and *prt6-1* related phenotypes and NO production by *NLP7* over-expression. A, Appearance of 11-day old Arabidopsis plants of the indicated genotypes grown under standard conditions. Size bars represent 5 mm. B, NO levels detected by staining with DAF-FM DA in roots of the indicated genotypes. Quantification of fluorescence is shown as the mean of at least 3 replicate experiments ± standard error. Size bars correspond to 100 µm.

shown in Figure 4.6, the levels of NR protein increased upon MG132 treatment and decreased after treatment with the protein synthesis inhibitor cicloheximide (CHX) in wild type plants, thus indicating the levels of NR depend on the *de novo* biosynthesis and further stabilization of the protein. However, the NR levels were lower in *nlp7-1* plants and further decreased upon treatment with MG132 or CHX (Fig. 4.6), thus suggesting the NR stabilization induced by the proteasome inhibitor would require NLP7. Interestingly, the MG132-induced accumulation of NR was strongly potentiated either in *prt6-1* or the quintuple ERFVII (*qerfvii*) mutant plants (Fig. 4.6). These data would be compatible with the accumulation of a potential 26S proteasome substrate, different than ERFVIIs and presumably regulated negatively by them. Upon accumulation, this proteasome substrate would regulate positively NR through NLP7.

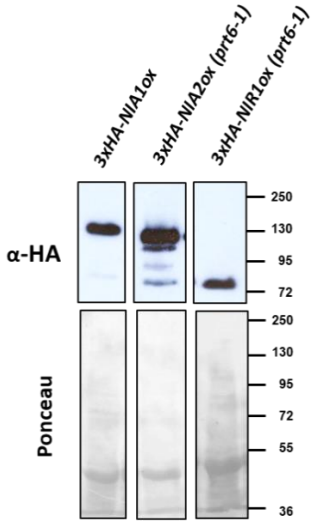

Figure 4.4. Generation of transgenic plants overexpressing HA-tagged versions of NR1, NR2 and NiR1. Representative western blots with specific anti-HA from 27 µg total protein extracted from transgenic lines of Arabidopsis plants overexpressing HA-tagged versions of the NR (NIA1 and NIA2) and NIR1 proteins. Ponceau S staining was used as loading control and molecular size marker (kDa) locations are shown at the right side of panels.

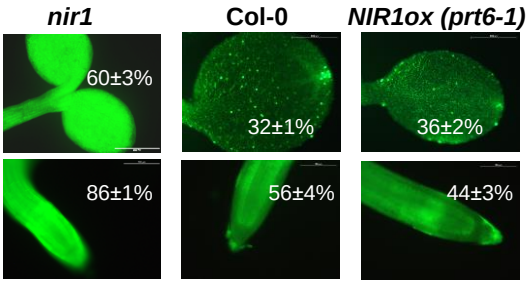

Figure 4.5. NO accumulation in plants altered in nitrite reduction to ammonium. NO levels in CRISPR-Cas9 *nir1* mutant or *NIR1* overexpressing *prt6-1* plants were detected by DAF-FM DA staining of cotyledons and roots. Quantification of fluorescence is shown as the mean of at least 3 replicate experiments ± standard error. Size bars represent 100 µm.

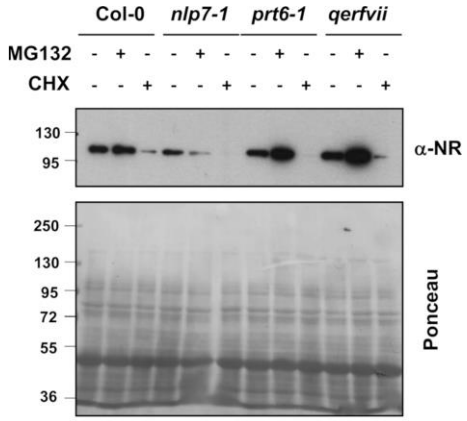

Figure 4.6. NR protein in nitrate signaling and Arg/N-end rule pathway mutants. Effect of proteasome and protein synthesis inhibitors MG132 and cicloheximide (CHX), respectively, on NR protein levels was shown by Western blot using specific anti-NR from 27 µg total protein extracted from plants pretreated with 100 µM MG132 or 40 µM CHX as indicated. Ponceau S staining was used as loading control and molecular size marker (kDa) locations are shown at the left side of panels.

4.1.3. NR and NiR1 proteins are post-translationally regulated by NO

The fact NR function and NO production seems to be tightly controlled by nitrate derived signals points to nitrate signaling as a relevant process in regulating endogenous NO levels. We analyzed the effect of treatment with a pulse of exogenous NO on the levels of NR protein. As shown in Figure 4.7, NR protein accumulated by 1h after exposure of plants to a NO pulse, whereas it was fully degraded in *prt6-1* plants. Because Arabidopsis NR1 and NR2 proteins are not MC-proteins their relationship with PRT6 function must be mediated by an intermediary protein. NR degradation in response to NO exposure occurred also in double *qerviiprt6-1* and *nlp7-1prt6-1* mutant plants (Fig. 4.7), thus suggesting a still unknown negative regulator of NR that is substrate of PRT6 is a target of the negative regulation exerted by NO. All together these data point to the existence of a NO-triggered NR protein stabilization process requiring PRT6 function

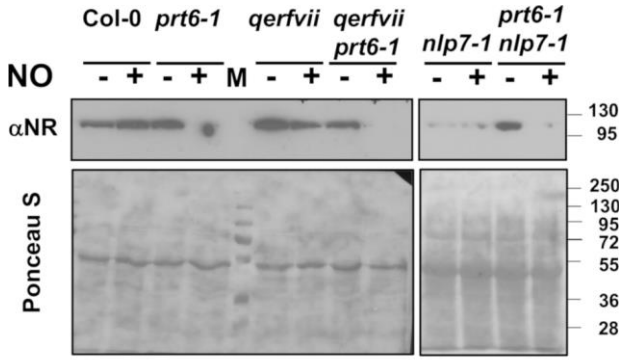

Figure 4.7. Effect of exogenous NO on NR protein stability. Plants of the indicated genotypes were exposed to a 5 min 300 ppm NO pulse (+) or untreated (-) as control and 1 h later samples collected for total protein extraction. Samples of 50 µg protein were loaded per lane and NR levels analyzed by Western blot with anti-NR antibodies. Ponceau S- staining of membranes was performed as loading control. The position of protein size markers (M) in kDa is located at the right side of panels.

independently of ERFVIIs or NLP7. This NO-related protein stabilization processes suggest that NO might act by self-controlling its own biosynthesis by acting on NRs.

Regulation of NR by NO through a PRT6-mediated mechanism, strongly points to post-translational modifications (PTMs) of NR by polyubiquitylation, but also likely by NO-related PTMs. By using proteomic methodologies based on LC-MS/MS techniques on protein extracts from plants expressing HA-tagged protein versions (Fig. 4.4), we have identified that NR1 and NR2 undergo multiple PTMs including ubiquitylation of lysine residues, S-nitrosylation of cysteine residues and nitration or amination of tyrosine residues. As shown in Figure 4.8A, these PTMs were detected in both NR1 and NR2. It is noteworthy mentioning that both proteins were ubiquitylated in lysine residues spanning the whole protein sequences with the only exception of NR2 not being modified in lysine or tyrosine residues inside the cytochrome b5 heme-binding and FAD-binding FR-type domains nor in the lysine residue involved in the sumoylation process of NRs (Fig. 4.9). Moreover,

A

NIA1	NIA2	CONSERVED	Y-NO2	Y-NH2	C-NO	K-GG
	Y24	no	yes	yes		
Y148	Y142	yes	no	yes		
	Y182	no	no	yes		
C197	C191	yes			yes	
K209	K203	no				yes
	K204	no				yes
	K206	no				yes
K272	K269	no				yes
	Y271	no	no	yes		
Y286	Y283	yes	no	yes		
	Y289	no	no	yes		
Y330		yes	no	yes		
Y331	Y328	yes	yes	no		
Y333		yes	no	yes		
K334	K331	yes				yes
Y395	Y392	yes	yes	no		
Y397	Y394	yes	yes	no		
K402	K399	yes				yes
K403	K400	yes				yes
Y431	Y428	yes	yes	no		
K433	K430	yes				yes
K534	K531	no				yes
K546	K543	no				yes
Y548	Y545	no	yes	no		
K555	K552	no				yes
Y571	Y568	yes	no	yes		
C573	C570	yes			yes	
K578		yes				yes
Y614	Y611	yes	yes	no		
K679	K679	no				yes
Y733	Y733	yes	yes	no		
Y771	Y771	yes	no	yes		
K774	K774	no				yes
Y851	Y851	tes	no	yes		

B

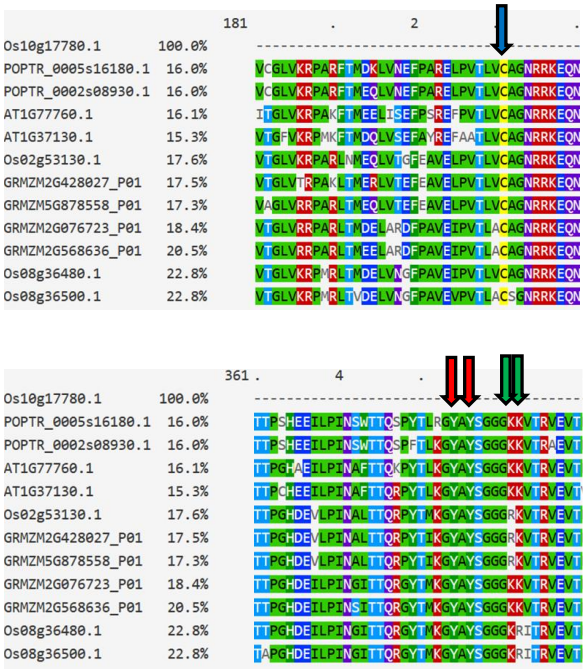

C

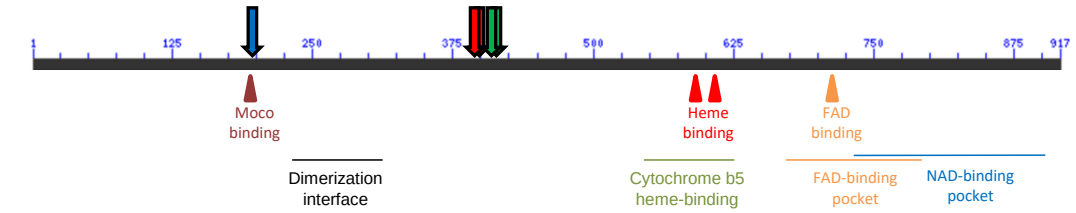

Figure 4.8. Post-translational modifications identified in planta for NR1/NIA1 and NIR2/NIA2. A, Tyrosine (Y), cysteine (C), and lysine (K) residues in red, magenta, violet, blue and green were identified as nitrated, aminated, nitrated and aminated, S-nitrosylated and ubiquitylated, respectively. Homologue residues in gray were not found to be modified. B, Highly conserved cysteine and tyrosine and lysine residues in the motif Y-Y----KK in the N-terminal an central domains of assimilatory NRs, respectively, from rice (Os), Populus (POPTR), Arabidopsis (AT) and maize (GRMZM) plants that were identified as S-nitrosilated (blue vertical arrow), nitrated (red vertical arrow) and ubiquitylated (green vertical arrow) in both NR1 and NR2 proteins. C, Scheme showing the NR protein sequence with the position of the above mentioned conserved residues that were identified as modified and the relative position of Molibdenum Cofactor (MoCO), Heme and Flavin (FAD) binding sites together with the dimerization interface, and cytochrome b5, FAD and NAD binding pockets.

some of the identified PTMs were detected in residues largely conserved not only in Arabidopsis NRs but also in NRs from other plants. Remarkably, we identified S-nitrosylation of the C^{197} and C^{191} from NR1 and NR2, respectively (Fig. 4.8B), which are the amino acids involved in Molybdenum Cofactor (MoCo) binding (Fig. 4.8C). Also nitration and amination of two tyrosine residues in tandem (Y^{395} and Y^{397} from NR1 and Y^{392} and Y^{394} from NR2), and ubiquitylation of two consecutive lysine residues (K^{402} and K^{403} from NR1 and K^{399} and K^{400} from NR2) closed to the tyrosine cluster were identified in NR1 and NR2 (Fig. 4.8A). All these residues were fully conserved in NRs (Fig. 4.8B). This PTM cluster is located in the central part of NR proteins that separate the dimerization domain from the cyt b5-, FAD- and NAD-binding domains in the C-terminal part of the proteins (Fig. 4.8C and 4.9).

As mentioned above, an increased NO production could be the result of enhanced NR function or eventually of reduced NiR1 function (Fig. 4.1 and Fig. 4.5). Therefore, we also checked whether NiR1 may be also target of NO-related PTMs and polyubiquitylation. Similar proteomic analyses than those performed for NRs were also implemented for HA-tagged versions of NiR1. As shown in Figure 4.10, NiR1 was heavily polyubiquitylated in both N- and C-terminal domains in largely conserved lysine residues in nitrite reductases from different plants. NiR1 was also ubiquitylated in non-conserved lysine residues (Fig. 4.10B). Besides, both conserved and non-conserved tyrosine residues were nitrated and/or aminated (Fig. 4.10A, B). Remarkably, conserved C^{464} and C^{470}, involved in binding 4Fe-4S cluster as well as C^{522} involved in siroheme binding were identified as S-nitrosylated (Fig. 4.10B, C). Taking advantage of the homology between the spinach and Arabidopsis NiRs and the reported 3D structure of spinach NiR (Protein Database Code 2akj) we have located the equivalent spinach residues to that identified as modified in Arabidopsis NiR1 (Fig. 4.10). Figure 4.11 shows that whereas nitrated tyrosine residues were located in the uppermost part of the structure relatively far from the 4Fe-4S cluster and siroheme binding pocket, the S-nitrosylation of the two cysteines involved in binding the 4Fe-4S cluster in the catalytic center is very likely to affect the activity of the modified enzyme, presumably by blocking the proper electron transference and thus inhibiting the activity of the enzyme. In comparison, on the other hand, figure 4.12 shows how taking advantage of the availability of the 3D structural model of the corn NR cytochrome FAD- binding domain (PDB code 2cnd) and by amino acid sequence homology with Arabidopsis NRs, we have located a nitrated tyrosine residue in NR1 (Y^{733}) which corresponded to Y^{83} very close to the FAD in the 3D model.

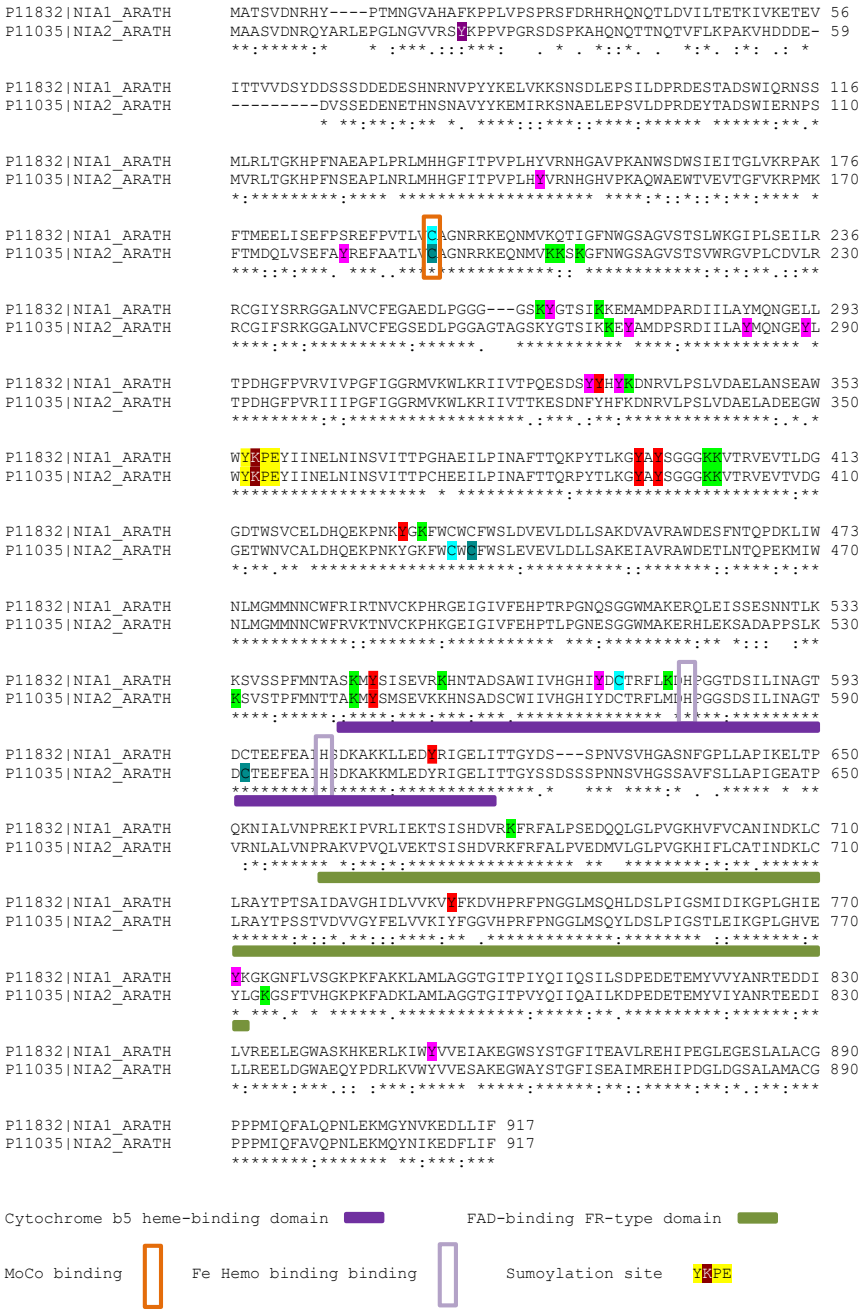

Figure 4.9. Post-translationally modified residues in aligned NR1/NIA1 and NR2/NIA2 proteins. Residues with previously reported regulatory functions and domains with key roles in prosthetic group binding are located as indicated in the sequences. Ubiquitylated lysines, S-nitrosylated cysteines and nitrated or aminated tyrosines are highlighted in green, blue, red and pink, respectively.

A

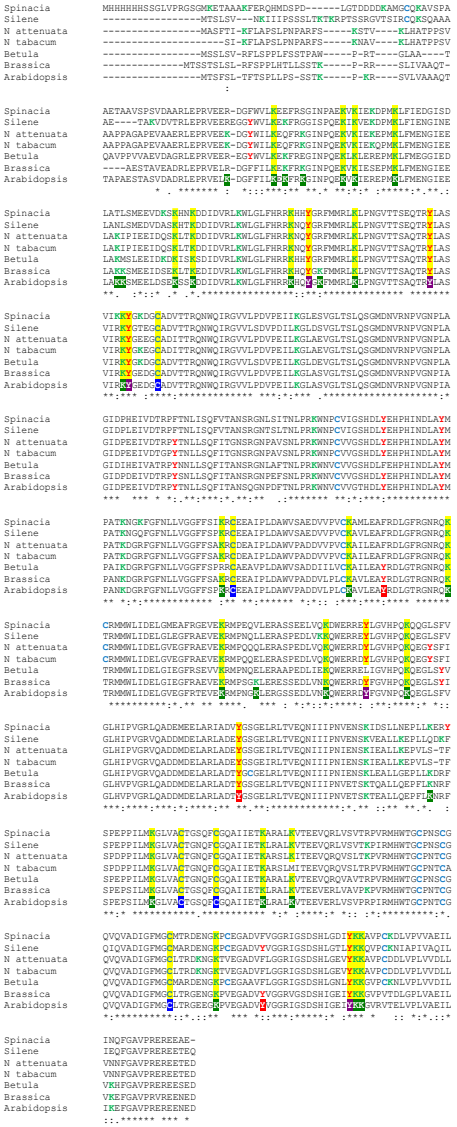

B

NiR1	CONSERVED	Y-NO2	Y-NH2	C-NO	K-GG
K53	no				yes
K60	yes				yes
K62	no				yes
K65	no				yes
K73	yes				yes
K75	yes				yes
K82	yes				yes
K94	no				yes
K95	no				yes
K104	yes				yes
K107	yes				yes
K124	yes				yes
Y127	yes	yes	yes		
K129	no				yes
K135	yes				yes
Y148	yes	yes	yes		
K155	yes				yes
Y156	yes	yes	yes		
C161	yes			yes	
K292	yes				yes
C294	yes			yes	
K314	yes				yes
Y320	no	yes			
K331	yes				yes
K352	yes				yes
K358	no				yes
K370	yes				yes
Y377	yes	yes	yes		
K384	yes				yes
Y414	yes	yes	no		
K447	no				yes
K459	yes				yes
C464	yes			yes	
C470	yes			yes	
K478	yes				yes
K483	yes				yes
C522	yes			yes	
K530	yes				yes
Y538	no	yes	no		
Y553	yes	yes	yes		
K554	yes				yes
K555	yes				yes

C

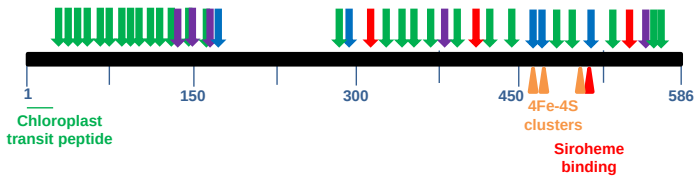

Figure 4.10. Post-translational modifications identified in planta for NiR1. A, Multiple aligned amino acid sequences of different plant NiRs showing conserved residues highlighted in yellow. The Arabidopsis NiR1 tyrosine (Y), cysteine (C), and lysine (K) residues that were identified as nitrated, aminated, nitrated and aminated, S-nitrosylated and ubiquitylated are shown in white characters on red, magenta, violet, blue and green backgrounds, respectively. B, Amino acid residues that were identified as modified (same colour code than in A) in NiR1. Those highly conserved are highlighted in gray background. C, Scheme showing the NiR1 protein sequence with the position (marked with vertical arrows) of the above mentioned conserved residues that were identified as modified, and the relative position of 4Fe-4S cluster and Siroheme binding sites.

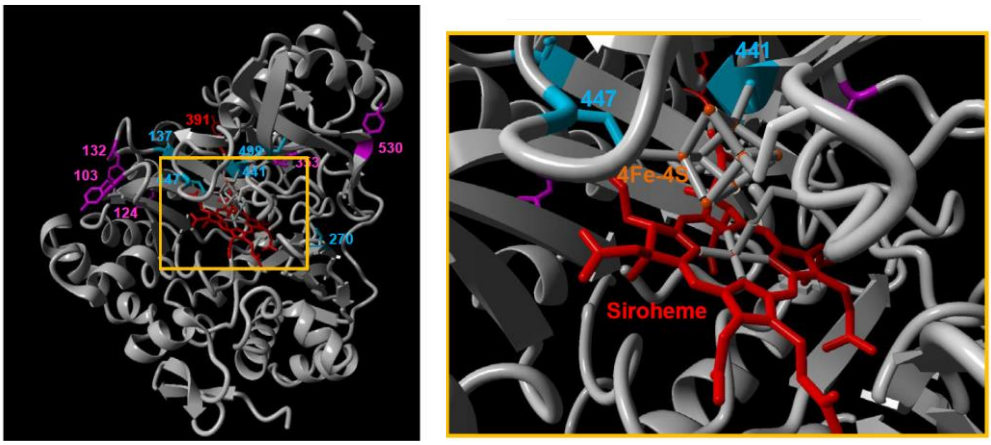

Figure 4.11. Location of S-nitrosylated cysteines and nitrated/aminated tyrosines in the 3D model of NiR1. The NiR1 3D structure was modelled in the basis of the 3D structure obtained from spinach feredoxin-nitrate reductase crystals (PDB code 2akj) using the Yasara application (www.yasara.org). The position of the siroheme (red) and 4Fe-4S cluster (orange) cofactors together with the number residue of each modified amino acid are shown in left panel. Right panel shows a close-up image of the cofactor binding pocket.

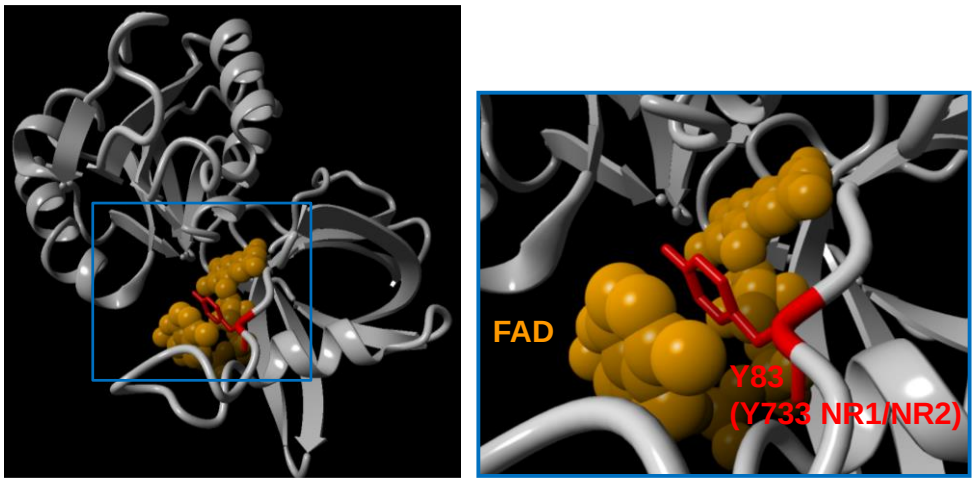

Figure 4.12. 3D modelling of Arabidopsis NRs showing the position of nitrated conserved tyrosine residues close to the FAD binding site. The right panel represents a zoom of the area enclosed by the blue rectangle in the left side image.

4.2. NO-triggered transcriptomic and metabolomic responses. Role of hormones in NO sensing

This section 4.2 is composed by excerpts from the research articles: "Castillo, M. C., Coego, A., Costa-Broseta, Á., & León, J. (2018). Nitric oxide responses in Arabidopsis hypocotyls are mediated by diverse phytohormone pathways. Journal of experimental botany, 69(21), 5265-5278", and "León, J., Costa, Á., & Castillo, M. C. (2016). Nitric oxide triggers a transient metabolic reprogramming in Arabidopsis. Scientific Reports, 6, 37945". All the results and figures that appear here are derived from the work of the PhD student in collaboration with the other authors.

4.2.1. Abstract (1)

Plants are often exposed to high levels of nitric oxide (NO) that affects development and stress-triggered responses. However, the way in which plants sense NO is still largely unknown. Here we combine the analysis of early changes in the transcriptome of plants exposed to a short acute pulse of exogenous NO with the identification of transcription factors (TFs) involved in NO sensing. The NO-responsive transcriptome was enriched in hormone homeostasis- and signaling-related genes. To assess events involved in NO sensing in hypocotyls, we used a functional sensing assay based on the NO-induced inhibition of hypocotyl elongation in etiolated seedlings. Hormone-related mutants and the TRANSPLANTA collection of transgenic lines conditionally expressing Arabidopsis TFs were screened for NO-triggered hypocotyl shortening. These approaches allowed the identification of hormone-related TFs, ethylene perception and signaling, strigolactone biosynthesis and signaling, and salicylate production and accumulation that are essential for or modulate hypocotyl NO sensing. Moreover, NO inhibits hypocotyl elongation through the positive and negative regulation of some abscisic acid (ABA) receptors and transcripts encoding brassinosteroid signaling components thereby also implicating these hormones in NO sensing.

4.2.2. Overrepresentation of hormone- and oxygen-related regulatory components in the early NO-responsive transcriptome

To unravel the sensing mechanism underlying the early plant responses to NO, we have designed an experimental system based on *A. thaliana* seedlings exposed to a short pulse of pure NO gas. We previously reported an increase in NO-related post-translational modification of proteins and an extensive metabolic re-arrangement by 1 h and 6 h after treatment, respectively (León *et al.*, 2016; see next sections 4.2.8-14). These data suggested changes should occur in the time frame between a few minutes and 1 h after NO exposure. Thus, we analyzed

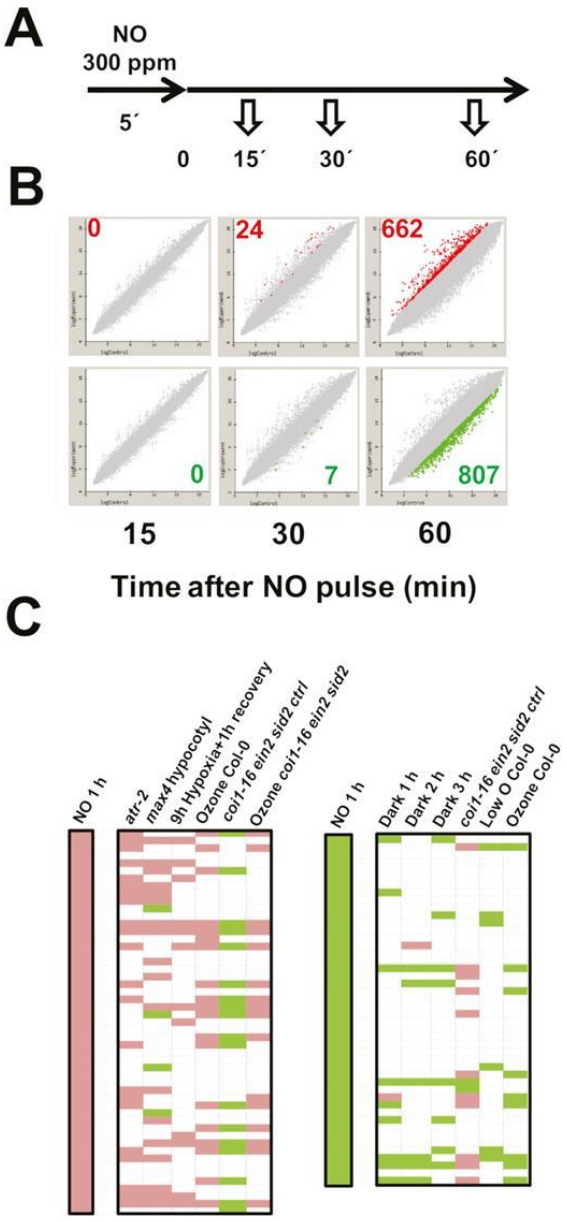

Figure 4.13. Identification and characterization of the NO-responsive transcriptome. A, Experimental scheme of sampling. B, Plots representing the up-regulated (red dots) and down-regulated (green dots) genes at the indicated times after exposure to NO. C, AtCAST3.1-based comparison of the up- and down-regulated transcriptomes at 30 min and 1 h after exposure to NO, respectively, with publicly available hormone- and redox-related transcriptome datasets.

changes in the Arabidopsis transcriptome shortly after exposure to an NO pulse for 5 min. Samples were harvested at 15, 30, and 60 min for subsequent transcriptome analyses (Fig. 4.13A). Overall analyses indicated that by 15 min after exposure to NO, no significant change was observed in any gene transcript when compared to those of untreated seedlings (Fig. 4.13B). By 30 min, 24 and 7 genes were significantly up- or down-regulated, respectively (Fig. 4.13B). After that, more extensive changes in transcript levels were detected by 60 min, with ~1500 genes differentially expressed, representing ~5% of the Arabidopsis genome. A total of

662 and 807 genes were up- and down-regulated, respectively (Fig. 4.13B). The complete list of differentially expressed genes including annotation, fold changes, and P-values corrected for FDRs, as well as a full MIAME-description of the transcriptome analyses is shown in Supplementary Table S2 (in Castillo *et al.*, 2018). A PANTHER over-representation test of Gene Ontology analysis, using the *A. thaliana* database of the Gene Ontology Consortium (http://www.geneontology.org/), with genes differentially expressed by 1 h after NO exposure allowing identification that the response to chitin, the responses to hormones, particularly to ethylene and jasmonates, as well as the responses to hypoxia functional categories were significantly over-represented (Supplementary Table S3 in Castillo *et al.*, 2018). On the other hand, a comparison of the 50 top up-regulated NO-responsive genes identified here at 1 h after NO with publicly available transcriptome data by using AtCAST3.1 (Kakei & Shimada, 2015) (http://atpbsmd.yokohama-cu.ac.jp/cgi/atcast/search_input.cgi) showed significant co-regulation profiles with those also up-regulated in *atr-2* (GEO code GSE63355) and *max4* (GEO code GSE6151) mutants, as well as with the re-oxygenated plants after hypoxia (Branco-Price *et al.*, 2008) (GEO code GSE9719), or the ozone-treated wild-type and *coi1-16ein2sid2ctrl* (GEO code GSE65740) plants (Fig. 4.13 C). Also a significant anti-regulation was observed for the NO-responsive transcriptome at 1 h with the transcriptome of the untreated *coi1-16ein2sid2ctrl* (GEO code GSE65740) mutant (Fig. 4.13C). Genes that were down-regulated by NO showed only a significant co-regulation with the transcriptome of plants under darkness (Fig. 4.13C).

4.2.3. A sensing test based on inhibition of hypocotyl elongation allowed identification of hormone-related transcription factors modulating NO sensitivity

Several of the transcriptomes that display partial overlapping with the transcriptome of NO-exposed plants (Fig. 4.13) corresponded to experiments performed with hypocotyl samples, thus suggesting NO-exerted regulation could be relevant in hypocotyls. Etiolated plants exposed to exogenous NO are characterized by root growth arrest and hypocotyl shortening (Fig. 4.14A). The inhibition of hypocotyl elongation was proportional to NO concentrations, with a 50% inhibition after exposure to 300 ppm NO (Fig. 4.14A). We have used this simple and quantitative NO sensing test to screen 968 Arabidopsis TRANSPLANTA transgenic lines (Supplementary Table S4 in Castillo *et al.*, 2018), conditionally expressing 263 TFs under a β-estradiol-inducible promoter (Coego *et al.*, 2014). Different levels of induced expression ranging from 5- to 250-fold were detected upon β-estradiol treatment of transgenic lines, as shown for a randomly selected group (Fig. 4.15). Several independent transgenic lines for each TF were analyzed for hypocotyl length in etiolated untreated (MS) or β-estradiol-induced (MSE) seedlings, or those conditions plus NO treatment, MS+NO and MSE+NO, respectively. Our screen searched for TFs causing either attenuated inhibition

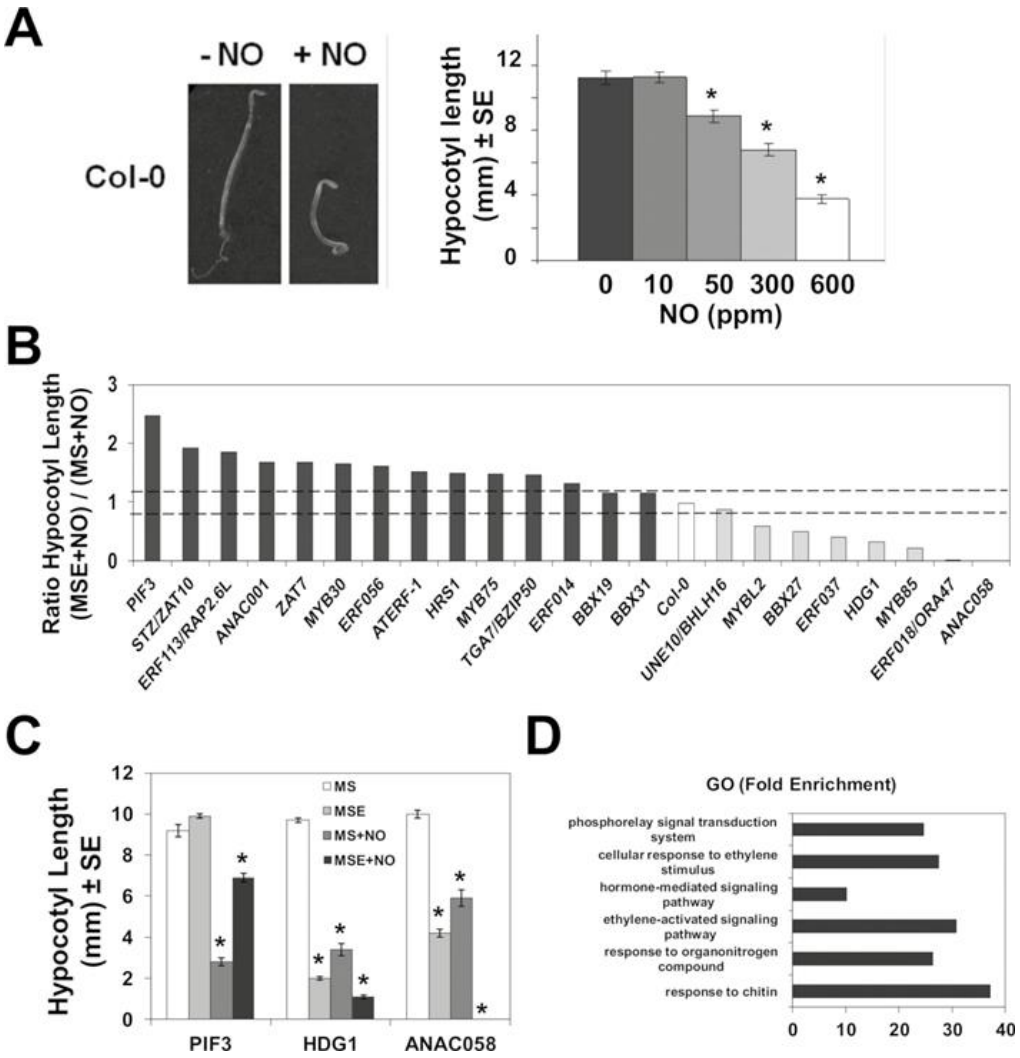

Figure 4.14. Screening of TPT transgenic lines conditionally expressing transcription factor encoding genes through a NO-triggered hypocotyl shortening assay in etiolated seedlings. A, NO triggers a dose-dependent hypocotyl shortening. B, Ratio of the hypocotyl lengths in TPT lines exposed to NO in the absence (MS) or presence of the inducer β-estradiol (MSE). Dashed lines represent the upper and lower variability limits of the ratios of wild type Col-0 hypocotyl lengths. C, Hypocotyl lengths of TPT lines expressing PIF3, HDG1 and ANAC058 transcription factors are altered by β-estradiol treatment even in the absence of NO. D, Gene Ontology (GO) analysis point to a significant enrichment of the hormone and organonitrogen compounds categories among genes triggering significant hypo- or hyper-sensitivity to NO in the screening of TPT lines.

(hyposensitivity) or enhanced inhibition (hypersensitivity) to NO upon conditional β-estradiol-induced expression. The β-estradiol-induced expression of some TFs such as ZAT10 and MYB85 attenuated and potentiated the NO-triggered inhibition of hypocotyl elongation, thus inducing NO hyposensitivity and hypersensitivity, respectively. The ratios between hypocotyl length of β-estradiol-treated and untreated NO-exposed seedlings determined whether the expression of a given TF brings about hyposensitivity or hypersensitivity to NO relative to wild-type Col-0 plants with ratios of ~1 and variability <12% (Fig. 4.14B). Table 4.1 shows the 56

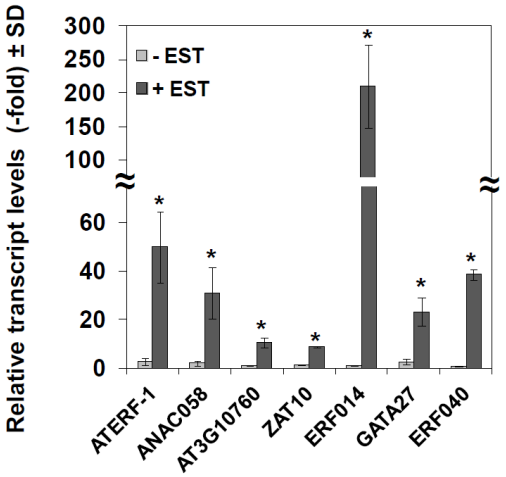

Figure 4.15. β-estradiol induced transcript accumulation in randomly selected TRANSPLANTA transgenic lines. The relative transcript levels were analyzed by RT-qPCR from RNAs obtained from seedlings treated (+EST) or not (-EST) with β-estradiol. Values are normalized to the levels in wild type plant and represent the mean ± SD of three independent replicates. * representing p-values <0.005 in Student´s t-test.

lines corresponding to 22 TFs that showed β-estradiol-dependent hyposensitivity or hypersensitivity to NO. As proofs of concept in our screening, the TF inducing the strongest NO hyposensitivity was PIF3, which has already been reported to promote hypocotyl elongation (Feng *et al.*, 2008). Another TF identified, MYB30, has been reported to be functionally related to NO-triggered responses (Tavares *et al.*, 2014). Moreover, this sort of screening also allows identification of TFs that themselves regulate the elongation of the hypocotyl in the absence of NO treatment, such as HDG1 or ANAC058 that induced shortening, or the above-mentioned PIF3, which promoted elongation (Fig. 4.14C). Paralleling the effects in the absence of NO, those factors also caused hyposensitivity and hypersensitivity to NO, respectively (Fig. 4.14C). Gene Ontology analysis points to a significant over-representation of the functional categories of hormone signaling pathways, particularly ethylene, among the TFs listed in Table 4.1 (Fig. 4.14D). Among the identified TFs, we found the AP2-related and integrase-type ORA47 and RAP2.6L (Krishnaswamy *et al.*, 2011; Chen *et al.*, 2016), as well as four additional integrase-type ERF TFs, ERF014, ERF037, ERF056, and ERF113/RAP2.6L, and the ethylene-responsive element-binding factor 1 (ATERF-1), all of them related to ethylene signaling. Also TFs that are functionally related to ABA homeostasis or signaling such as the MYB-type HRS1 and MYB30 (Wu *et al.*, 2012; Lee & Seo, 2016) and the NAC058 TF (Coego *et al.*, 2014) were identified in the screening. The functional interaction between NO sensitivity and hormone signaling was not restricted to ABA and ethylene. Among TFs identified in the screening, ORA47 and ZAT10 have also been characterized as positive and negative regulators, respectively, of jasmonic acid (JA) signaling (Pauwels *et al.*, 2008), and MYB30 regulates BR signaling (Li *et al.*, 2009). Finally, PAP1/MYB75 and MYBL2 regulate the biosynthesis of anthocyanins and flavonoids, the latter functioning as a node

between JA and gibberellin (GA) signaling (Xie *et al.*, 2016); and MYB75/PAP1 and MYB85 seems to be also involved in the secondary cell wall formation or thickening, and in the lignification of stems (Zhong *et al.*, 2008; Bhargava *et al.*, 2013), a process that tightly controls the growth of hypocotyls and other plant organs (Hamant & Traas, 2010). These data, together with the Gene Ontology analyses (Supplementary Table S3 in Castillo *et al.*, 2018) and the co-regulation of transcriptomes (Fig. 4.13) shown above, strongly suggest a determinant involvement of hormone biosynthesis and signaling in NO sensing.

Table 4.1. TPT lines showing hypo- or hyper-sensitivity to NO on hypocotyl elongation of etiolated seedlings upon conditional expression of TF encoding genes

AGI code	Annotation	TPT lines	NO sensitivity
AT1G09530	PIF3_ phytochrome interacting factor 3	1.09530.1F4	Hyposensitive
AT4G17500	ATERF-1_ ethylene responsive element binding factor 1	4.17500.1B3, E2, I7	Hyposensitive
AT1G01010	ANAC001_ NAC domain containing protein 1	1.01010.1E5, F9, G3	Hyposensitive
AT1G13300	HRS1__myb-like transcription factor family protein	1.13300.1A9, D3, E5	Hyposensitive
AT1G56650	MYB75_ PAP1_ production of anthocyanin pigment 1	1.56650.1C5, H3	Hyposensitive
AT3G28910	MYB30_ myb domain protein 30	3.28910.1C1, E5	Hyposensitive
AT5G13330	Rap2.6L__related to AP2 6l	5.13330.1D9, G9, I4	Hyposensitive
AT2G22200	ERF056_Integrase-type DNA-binding superfamily protein	2.22200.1B1, E7, G8	Hyposensitive
AT1G44830	ERF014_Integrase-type DNA-binding superfamily protein	1.44830.1A99, F99, G99	Hyposensitive
AT3G46090	ZAT7__C2H2 and C2HC zinc fingers superfamily protein	3.46090.1B99,E99,H99,I99	Hyposensitive
AT1G27730	STZ_ZAT10__salt tolerance zinc finger	1.27730.1E5, I1	Hyposensitive
AT3G21890	BBX31_B-box type zinc finger family protein	3.21890.1A8, B5, H8	Hyposensitive
AT4G38960	BBX19_B-box type zinc finger family protein	4.38960.1A3, G3	Hyposensitive
AT1G77920	TGA7_bZIP transcription factor family protein	1.77920.1B3, E1, G3, H2	Hyposensitive
AT3G18400	ANAC058_ NAC domain containing protein 58	3.18400.1D3, G9	Hypersensitive
AT1G71030	MYBL2_ MYB-like 2	1.71030.1C5, H9	Hypersensitive
AT4G22680	MYB85_ myb domain protein 85	4.22680.1F1	Hypersensitive
AT1G77200	ERF037_Integrase-type DNA-binding superfamily protein	1.77200.1C99, H99	Hypersensitive
AT1G74930	ERF018/ORA47__Integrase-type DNA-binding protein	1.74930.1E2, F8, H4	Hypersensitive
AT2G30250	WRKY25_ WRKY DNA-binding protein 25	2.30250.1C5, D2, F2	Hypersensitive
AT1G68190	BBX27_B-box zinc finger family protein	1.68190.1D1	Hypersensitive

4.2.4. Ethylene perception and signaling as well as salicylate and strigolactone biosynthesis are required for NO sensing

The transcriptome analyses of NO-exposed seedlings and the screening of transgenic plants conditionally expressing TFs suggested the involvement of ethylene signaling in NO-triggered responses. To check whether ethylene perception and signaling are involved in sensing NO, we tested the sensitivity to NO in hypocotyl shortening assays with the ethylene-insensitive *etr1-3* and *ein2-5* mutants (Roman *et al.*, 1995). Figure 4.16A shows that *etr1-3* and *ein2-5* seedlings

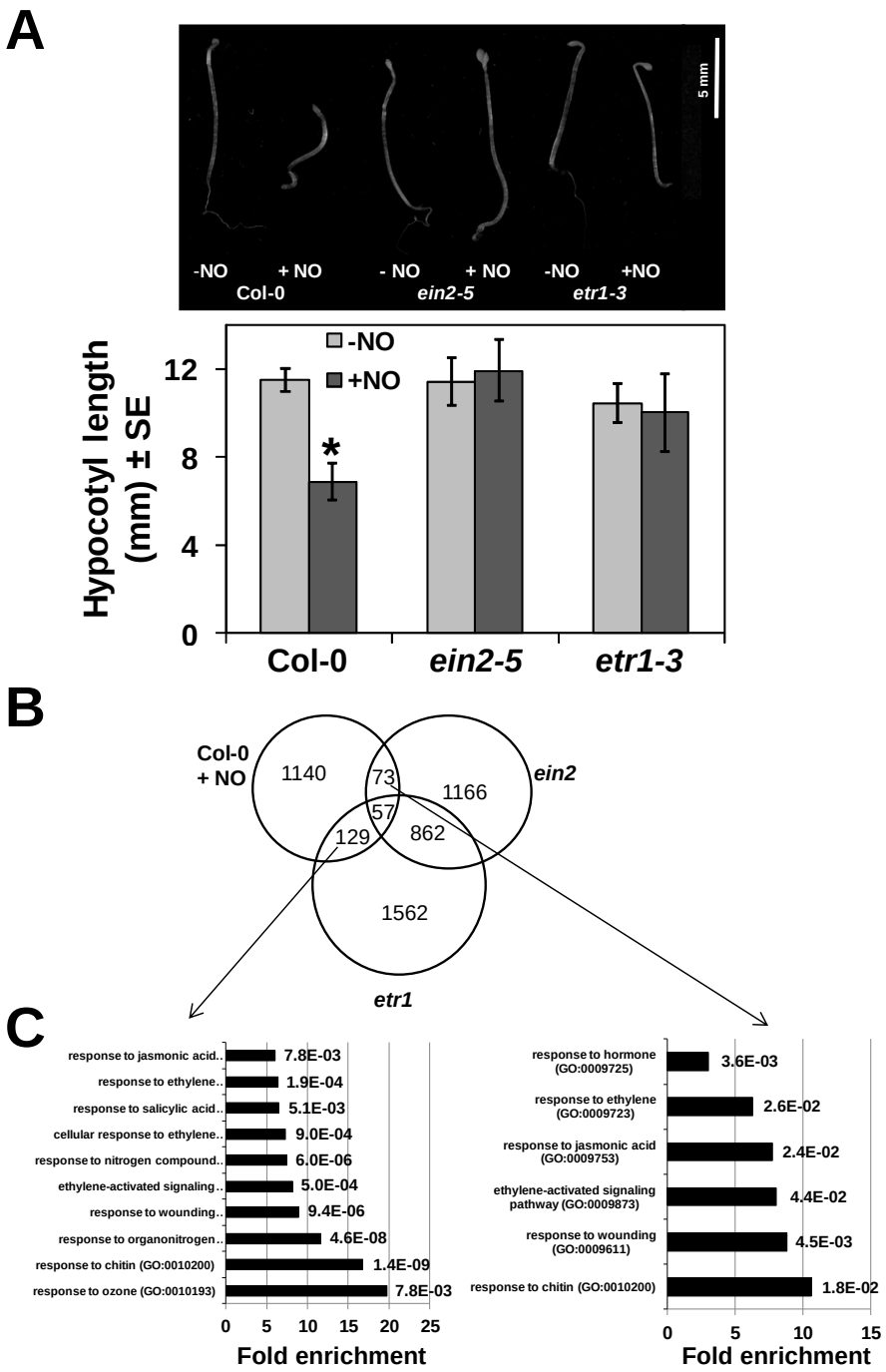

Figure 4.16. Ethylene perception and signaling is required for NO sensing. A, Hypocotyl length of untreated (-NO) and NO-treated (+NO) wild type and ethylene signaling-related mutant seedlings. Values are the mean (n=25) ± standard error with * representing p-values <0.05 in Student´s t-test. B, Venn diagrams representing the intersection between the NO-responsive transcriptome and those differentially regulated in *etr1* and *ein2* mutants. C, Gene Ontology analysis of the genes found in the intersection between the NO-responsive and *etr1*-regulated (left panel) or *ein2*-regulated (right panel) transcriptomes. Fold enrichment (black bars) and the FDR-corrected p-values (at the right side of bars) for the functional categories are shown.

were fully insensitive to NO in inhibiting hypocotyl elongation, thus suggesting that ethylene perception and signaling were essential for NO sensing. The comparison of the NO-responsive transcriptome with the differential transcriptomes previously reported for the *ein2-1* and *etr1-1* mutants (Cheng *et al.*, 2009) (GEO Accession GSE12715) points to a significant overlap (Fig. 4.16B). There were 57 genes that were common for the three transcriptomes and an additional 73 and 129 genes in the intersections of the NO-responsive genes and *ein2-1*, and the NO-responsive genes and *etr1-1*, respectively (Fig. 4.16B), thus supporting a potential relevant involvement of ETR1 and EIN2 in NO sensing. We can rule out that the involvement of ETR1 and EIN2 in NO sensing was due to transcriptional regulation of the corresponding genes by NO, as only slight increases below 1.6-fold in the corresponding transcripts were detected in NO-treated plants (Fig. 4.17). A Gene Ontology analysis with these groups of commonly regulated genes yielded a significant over-representation of the expected functional categories related to ethylene responses but, of note, also of responses to JA- and salicylic acid (SA)-related functional categories (Fig. 4.16C).

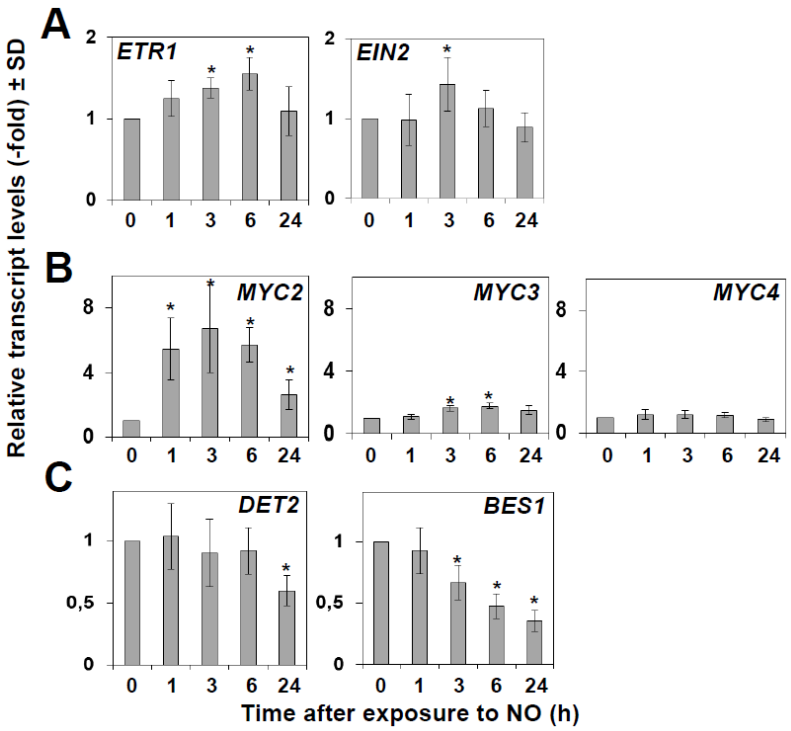

Figure 4.17. Effect of NO treatment on the transcript levels of A, ethylene, B, jasmonate and C, brassinosteroid biosynthetic/or signaling encoding genes. The relative transcript levels were analyzed by RT-qPCR from RNAs obtained at the indicated times after NO exposure of seedlings. Values are the mean ± SD of three independent replicates. * representing p-values <0.05 in Student´s t-test.

Among genes that were similarly regulated by NO treatment in wild-type plants or in untreated ethylene-insensitive mutants (Fig. 4.16B), we found some that participate in SA-triggered responses. SA is synthesized in Arabidopsis mostly

through the isochorismate pathway involving the function of the chloroplast transporter EDS5/SID1 and the isochrorismate synthase 1 (ICS1)/SID2 and ICS2 proteins (Serino *et al.*, 1995; Wildermuth *et al.*, 2001; Garcion *et al.*, 2008). We have tested the sensitivity to NO of SA-deficient *sid2-1eds5-3nahG* plants, which overexpress the *nahG* bacterial gene coding for a SA hydroxylase converting SA to catechol (Gaffney *et al.*, 1993; Delaney *et al.*, 1994) in a genetic background carrying mutations in EDS5/SID1 and ICS1/SID2 genes. Figure 4.18A shows that, in contrast to wild-type plants, the hypocotyls of etiolated *sid2-1eds5-3nahG* plants were not shortened upon exposure to NO, thus suggesting that the biosynthesis and accumulation of SA is essential for NO sensing in hypocotyls.

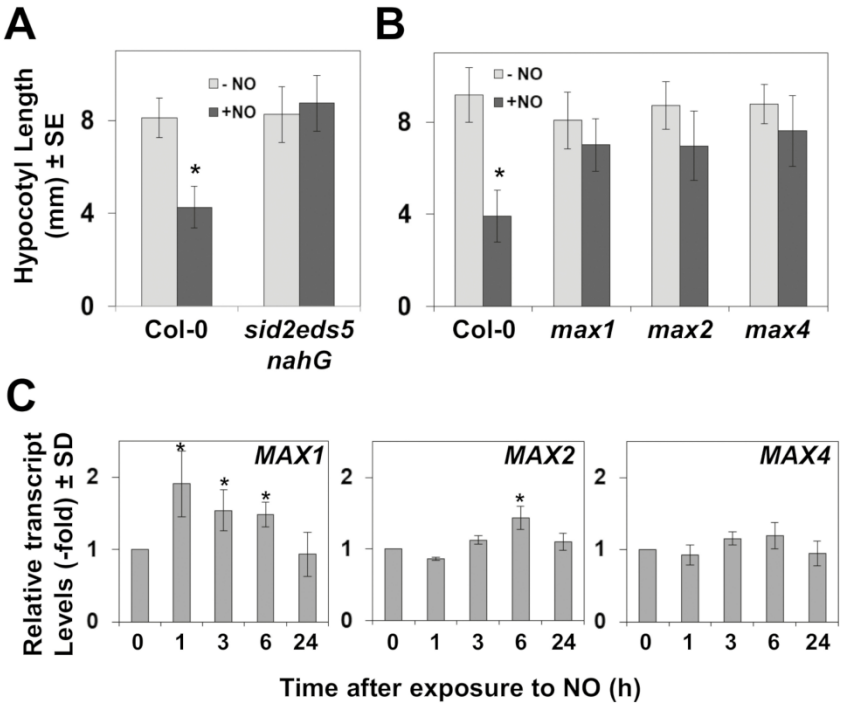

Figure 4.18. Involvement of salicylates and strigolactones in NO sensing. A, Hypocotyl length of untreated (–NO) and NO-treated (+NO) wild-type and salicylate-deficient mutant seedlings; and B, wild-type and strigolactone biosynthesis and signaling mutants. Values are the mean ±SE (*n*=25). C, Effect of NO treatment on the transcript levels of strigolactone biosynthetic/or signaling-encoding genes. The relative transcript levels were analyzed by RT-qPCR from RNAs obtained at the indicated times after NO exposure of seedlings. Values are the mean ±SD of three independent replicates. **P*-values <0.05 in Student's *t*-test.

On the other hand, we found a significant co-regulation between up-regulated genes in NO-treated wild-type plants and in the SL biosynthesis *max4* mutant (Fig. 4.13C). SLs are synthesized from the diterpene all-*trans*-β-carotene by the sequential catalysis of D27, MAX3, MAX4, and MAX1, and then SLs are perceived by the D14 receptor, which interacts with the E3 ubiquitin ligase MAX2 that polyubiquitylates negative regulators of the SMXL family and sends them for proteasome-mediated degradation (Morffy *et al.*, 2016). We have analyzed whether SLs may be relevant for sensing NO by testing NO-triggered hypocotyl

shortening with the biosynthetic and signaling *max1*, *max2*, and *max4* mutants (Sorefan *et al.*, 2003; Booker *et al.*, 2005; Stirnberg *et al.*, 2007). Figure 4.18B shows that all three SL mutants were insensitive to NO, thus indicating that the NO-triggered inhibition of hypocotyl elongation required the biosynthesis and signaling of SLs, and thus the involvement of these hormones in NO sensing. Only the *MAX1* gene was significantly, although moderately, up-regulated upon exposure to NO (Fig. 4.18C), thus suggesting that the transcriptional activation of SL biosynthetic and signaling genes was not the limiting step in the SL-mediated NO response mechanism.

4.2.5. NO sensing and ABA signalling

We have previously reported that NO antagonizes ABA in regulating multiple processes from seed germination and seedling establishment to abiotic stress responses (Lozano-Juste & León, 2010; León *et al.*, 2014). More precisely, the negative effect of NO on ABA perception is mediated, at least in part, by the post-translational Y-nitration and the subsequent inactivation and degradation of PYR/PYL receptors (Castillo *et al.*, 2015). Other positive regulators of the ABA core signaling pathway, such as the kinase OST1/SnRK2.6, were reported to be inactivated through post-translational *S*-nitrosylation of key C residues (Wang *et al.*, 2015b; Wang *et al.*, 2015c). Despite NO exerting regulation on ABA signaling at the post-translational level, our data suggest that NO also regulates ABA signaling at the transcriptional level. The ABA hypersensitivity detected in the NO-deficient *nia1,2noa1-2* mutant plants (Lozano-Juste & León, 2010) correlated well with a significant over-representation of ABA-related genes among up-regulated genes in *nia1,2noa1-2* plants (Gibbs *et al.*, 2014a). Finally, further support for the involvement of ABA signaling in NO-triggered responses comes from the identification of several TFs related to ABA signaling in our screening of NO-triggered shortening of hypocotyls in transgenic conditional overexpressing lines (Fig. 4.14B; Table 4.1). Those include *BBX31*, which is one of the ABA-specific marker genes, as well as the ABA-up-regulated *STZ/ZAT10*, *PIF3*, *ERF056*, and *RAP2.6L* genes and the down-regulated *MYB30* and *HRS1* genes (Nemhauser *et al.*, 2006). Because ABA perception and signaling involve multicomponent families of receptors and regulators, we decided to check first whether a specific NO-regulated ABA signaling pathway might exist in Arabidopsis. To test this hypothesis, the transcript levels of genes coding for core components of the ABA signaling pathway were analyzed by RT-qPCR at different times after exposure to NO. Figure 4.19A shows a transient up-regulation of several ABA receptor-encoding genes by 1–6 h after exposure to NO. PYL3, PYL6, and PYL7 were strongly up-regulated, whereas others, such as PYL4, PYL5, and PYL8, were moderately up-regulated (Fig. 4.19A). Only PYR1 was significantly down-regulated (Fig. 4.19A). In the next step of the signaling pathway, members of the clade A of type 2C phosphatases (PP2Cs) act as negative regulators of ABA signaling. Although most of the genes coding for ABA-related phosphatases, with the

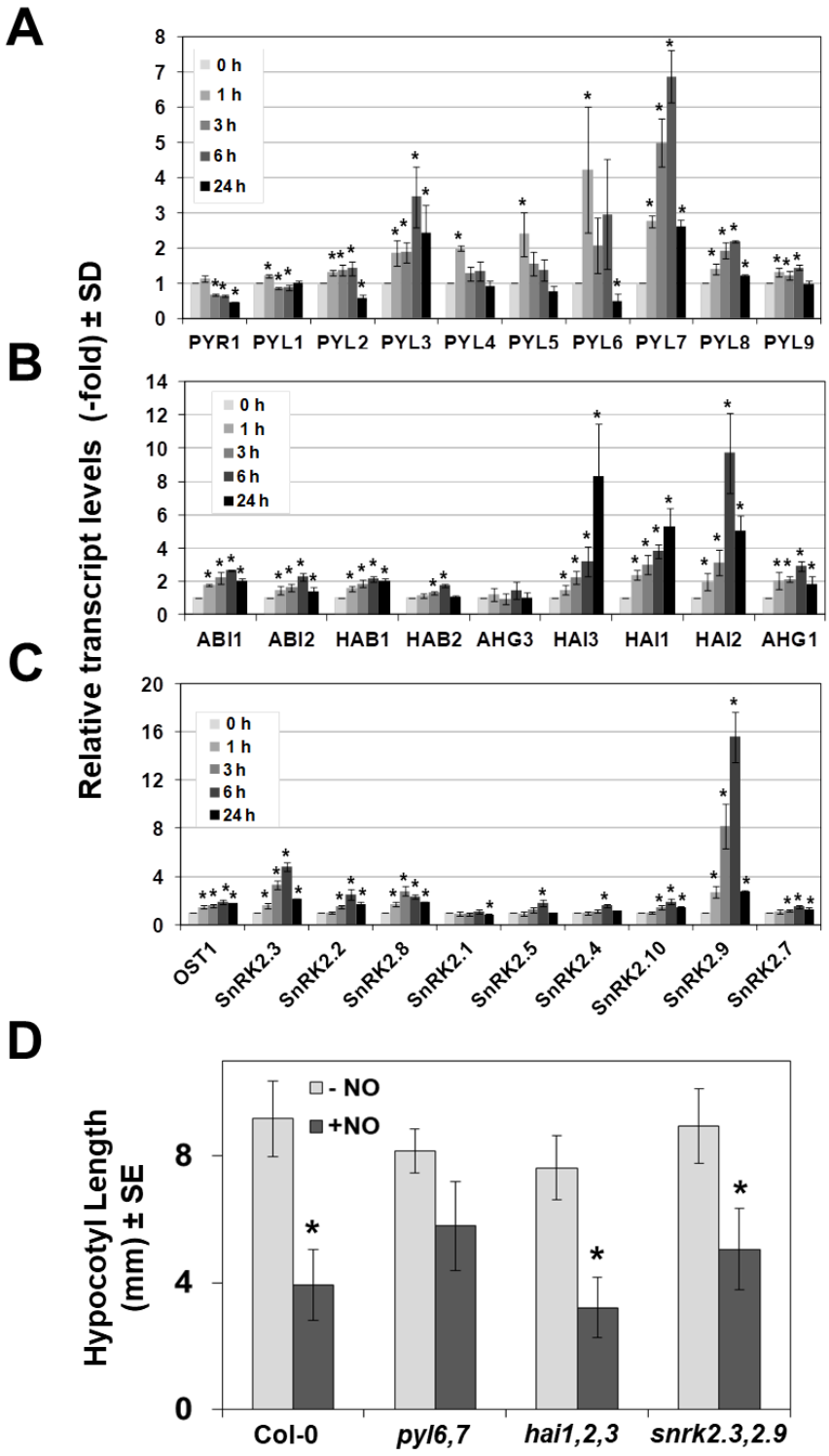

Figure 4.19. Involvement of ABA signaling in NO sensing. The relative transcript levels of A, ABA receptor; B, clade A of protein 2C phosphatase; and C, SnRK2 family of protein kinase encoding genes, were analyzed by RT-qPCR from RNAs obtained at the indicated times (hours) after NO exposure of seedlings. Values are the mean ± SD of three independent replicates. D, Hypocotyl length of untreated control (-NO) and NO-treated (+NO) wild type and ABA signaling mutant seedlings. Values are the mean (n=25) ± standard error with * representing p-values <0.05 in Student´s t-test.

exception of HAB2 and AHG3/PP2CA, were slightly up-regulated in NO-treated plants, only those from the highly ABA-induced subfamily (HAI1, HAI2/AIP1, and HAI3) were strongly up-regulated (>4-fold) by 6–24 h after NO treatment (Fig. 4.19B). Finally, the next step in ABA signaling is carried out by the positive regulation exerted by protein kinases of the Sucrose non-fermenting 1-Related protein Kinase 2 (SnRK2) family. Among SnRK2-encoding genes, only SnRK2.9 and to a lesser extent SnRK2.3 were up-regulated upon NO treatment (Fig. 4.19C). From these data, we identified a subset of NO-responsive ABA signaling components including the receptors PYL6, PYL7, and PYL3, the phosphatases HAI1, HAI2/AIP1, and HAI3, and the SnRK2.9 and SnRK2.3 kinases. To check whether these NO-responsive ABA signaling-encoding genes were involved in regulating the plant sensitivity to NO, we tested the effect of exogenously supplied NO on the elongation of hypocotyls from etiolated seedlings of ABA signaling mutant combinations in the NO-responsive genes identified. We generated double *pyl6,7* and *snrk2.3,2.9* mutants, and, together with the available *hai1,2,3* mutant (Bhaskara *et al.*, 2012), these were analyzed in hypocotyl shortening assays. Figure 4.19D shows that *hai1,2,3* and *snrk2.3,2.9* mutants showed a hypocotyl shortening not significantly different from that detected in wild-type plants, and only the hypocotyls of *pyl6,*7 plants were significantly insensitive to NO.

4.2.6. NO sensing and jasmonate signaling

Three independent transcriptome analysis-based lines of evidence suggest that JA may be important for NO sensing mechanisms. We found a significant over-representation of the JA signaling categories among NO-responsive genes (Supplementary Table S3 in Castillo *et al.*, 2018) but also among the particular set of genes that were also differentially expressed in ethylene signaling-deficient mutants (Fig. 4.16C). Moreover, we found a significant anti-regulation of NO-responsive genes in plants affected in JA perception and signaling (Fig. 4.13C, D). Among NO-responsive genes listed in Supplementary Table S2 (in Castillo *et al.*, 2018), we found that the lipoxygenase-encoding genes *LOX3* and *LOX4*, the 12-oxophytodienoate reductase-encoding gene *OPR1*, and the allene oxide cyclase-encoding gene *AOC3* were all >2-fold up-regulated. Similarly, *JAZ1*, *JAZ5*, *JAZ8*, and *JAZ10* genes coding for different components of the JAZ family of negative regulators of JA signaling were also up-regulated (Supplementary Table S2 in Castillo *et al.*, 2018). Interestingly enough, the gene *JMT* coding for the JA carboxyl methyltransferase, which metabolizes JA to methyl-JA, was strongly down-regulated (Supplementary Table S2 in Castillo *et al.*, 2018). Together, these data suggest the existence of NO-sensitive branches of the JA biosynthetic and signaling pathways. We have confirmed that some JA biosynthetic and signaling genes were up-regulated by NO, thus supporting that the NO-responsive transcriptome identified in the microarray analyses is truly representative. Figure 4.20A shows that *LOX3* and *JAZ10* were strongly up-regulated (>40-fold), whereas *JAZ1* and *JAZ6* were also up-regulated though more slightly (3- to 4-fold) by 1 h

after NO treatment. To explore whether NO-regulated components of the JA signaling pathway modulate NO sensitivity, the response to exogenously supplied NO of JA signaling (*jaz10*, quintuple *jaz1,3,4,9,10*, the single *myc2*, and the triple *myc2,3,4*) mutants was assayed in hypocotyl shortening assays. Figure 4.20B shows that none of them was significantly different in sensitivity to NO-triggered hypocotyl shortening when compared with wild-type plants. We also checked whether the levels of *MYC* transcripts were regulated in NO-treated plants as shown above for some of the *JAZ* genes (Fig. 4.20A). *MYC2* was strongly up-regulated upon exposure to NO, whereas *MYC3* was only slightly up-regulated and *MYC4* was not significantly altered (Fig. 4.17B). These findings together suggest that despite the fact that many of the JA signaling component-encoding genes are regulated by NO, this hormone is not involved in NO sensing.

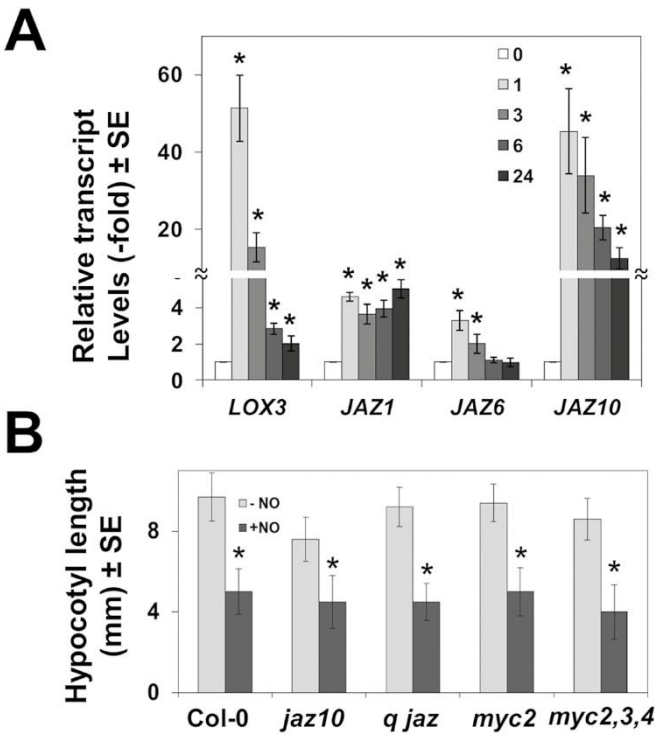

Figure. 4.20. Involvement of jasmonate signaling in NO sensing. A, Relative transcript levels of indicated genes were analyzed by RT-qPCR from RNAs obtained at the indicated times (hours) after NO exposure of seedlings. Values are the mean ± SD of three independent replicates. B, Hypocotyl length of untreated (-NO) and NO-treated (+NO) wild type and jasmonate signaling-related mutant seedlings. *q jaz* stands for the quintuple *jaz1,3,5,9,10* mutant. Values are the mean (n=25) ± standard error with * representing p-values <0.05 in Student´s t-test

4.2.7. Involvement of brassinostereoids in NO sensing

Among genes that were up-regulated by NO at 1 h (Supplementary Table S2 in Castillo *et al.*, 2018), we found a significant overlap (Fig. 4.21) with those that were also up-regulated in responses to BRs (Nemhauser *et al.*, 2006). We also

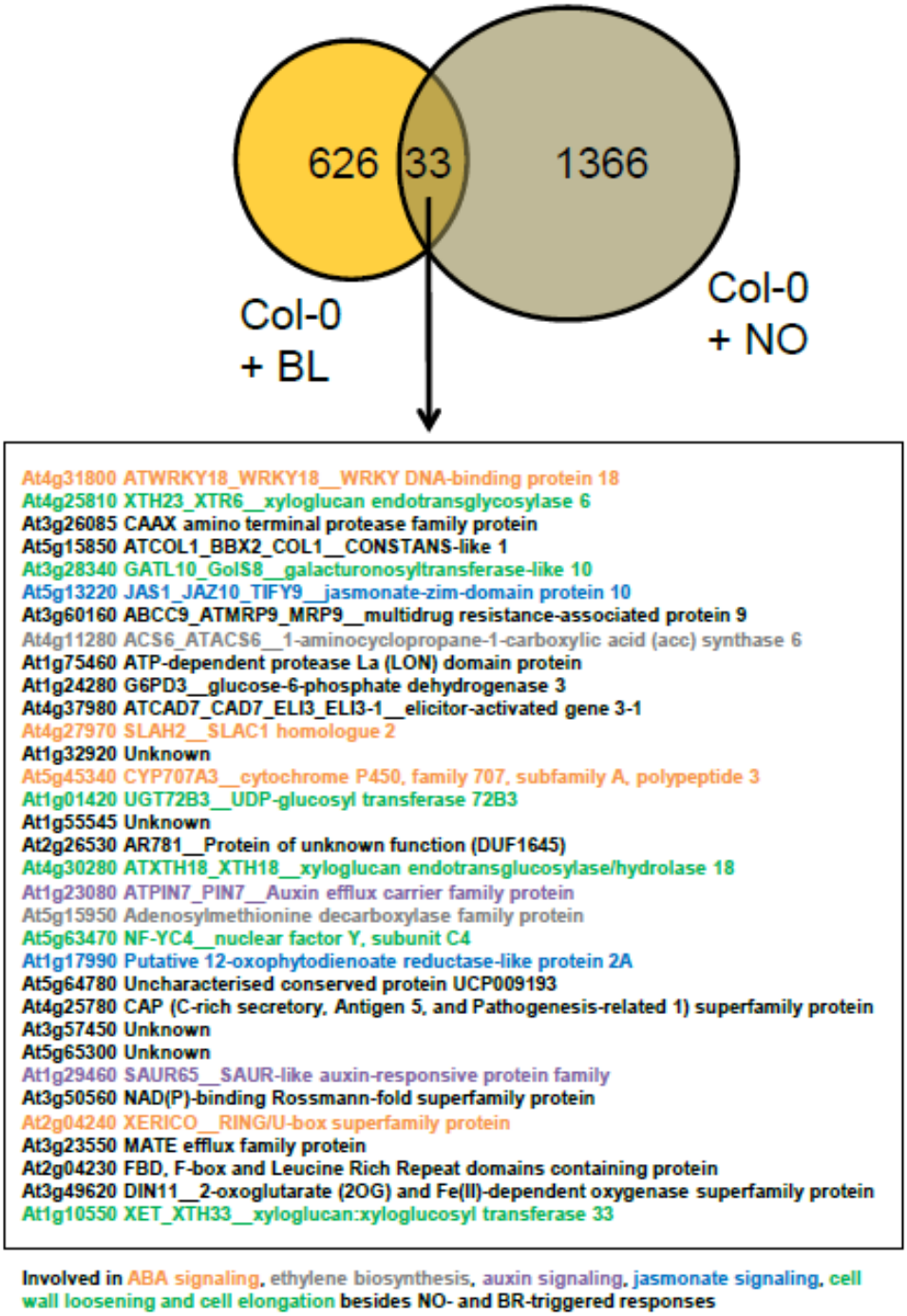

Figure 4.21. Genes up-regulated by either brassinolide (BL) or NO treatments. The color codes corresponded to the functional categories outlined at the end of the table.

found several TF-encoding genes involved in BR-regulated processes. BRs are synthesized from campesterol through a complex pathway involving 11 steps (Fig. 4.22A). The second step catalyzed by DET2 seems to be determinant for BR biosynthesis, in such a way that *det2* mutant plants are severely impaired in BR production (Fujioka *et al.*, 1997; Noguchi *et al.*, 1999). Once the active BR

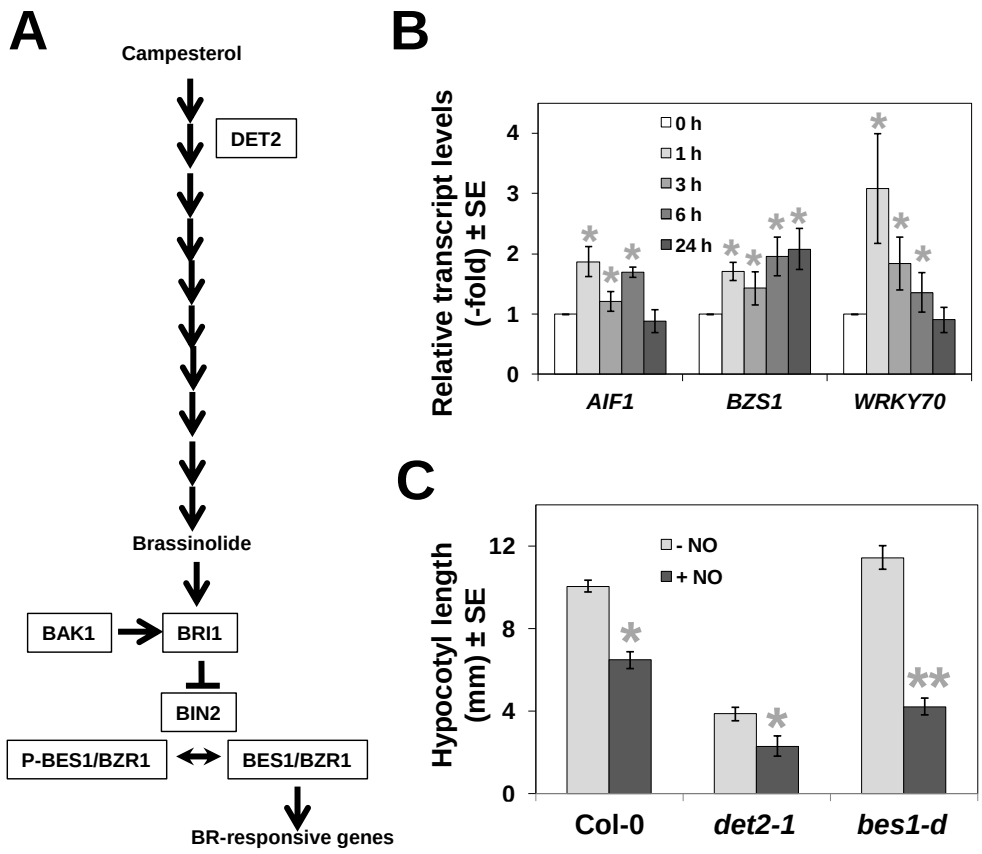

Figure 4.22. Involvement of brassinosteroid signaling in NO sensing. A, Scheme of brassinosteroid biosynthesis and signaling pathways. B, The relative transcript levels of BR-related transcription factor encoding genes were analyzed by RT-qPCR from RNAs obtained at the indicated times (hours) after NO exposure of seedlings. Values are the mean ± SD of three independent replicates. * represents p-values <0.05 in Student´s t-test. C, Hypocotyl length of untreated (-NO) and NO-treated (+NO) wild type and brassinosteroid biosynthesis and signaling mutant seedlings. Values are the mean (n=25) ± standard error. * and ** represent p-values <0.05 and <0,01, respectively, in Student´s t-test.

brassinolide is synthesized, it is further perceived by the BRI1 receptor (Jiang *et al.*, 2013), which is controlled by reversible phosphorylation by BAK1 (He *et al.*, 2013). Then, BRI1 negatively regulates BIN2, which in turn modulates the phosphorylation state of the transcriptional activators BES1 and BZR1 that accumulate in the nucleus (Yin *et al.*, 2002), triggering BR-responsive gene expression (Fig. 4.22A). We have confirmed that *AIF1*, *BZS1* , and *WRKY70*, which are involved in BR-regulated control of plant growth and responses to stress (He *et al.*, 2005; Wang *et al.*, 2009; Chen *et al.*, 2017), were up-regulated by NO to different extents (Fig. 4.22B), thus pointing to BR signaling as a target of NO action. To check whether BR biosynthesis was necessary for NO sensing in hypocotyls, we analyzed the loss-of-function *det2-1* mutant in DE-ETIOLATED2 that is severely BR deficient and dwarf (Chory, 1991). The hypocotyls of etiolated *det2-1* seedlings, despite being short, were still fully sensitive to NO in inhibiting hypocotyl

elongation, thus indicating that biosynthesis of BRs is not required for NO sensing. Moreover, the dominant gain-of-function *bes1-D* mutant in BRI1-EMS-SUPPRESSOR 1 (BES1)/BRASSINAZOLE-RESISTANT 2 (BZR2) (Shin *et al.*, 2016), despite displaying longer hypocotyls in non-treated seedlings, was hypersensitive to NO in shortening their hypocotyls (Fig. 4.22C), thus suggesting that BES1-mediated BR signaling potentiates NO sensing. It is worth mentioning that in accordance with BES1 being an NO target, the *BES1* gene was strongly down-regulated by NO (Fig. 4.17C), thus representing a potential node for self-controlled sensing.

4.2.8. Abstract (2)

Nitric oxide (NO) regulates plant growth and development as well as responses to stress that enhanced its endogenous production. Arabidopsis plants exposed to a pulse of exogenous NO gas were used for untargeted global metabolomic analyses thus allowing the identification of metabolic processes affected by NO. At early time points after treatment, NO scavenged superoxide anion and induced the nitration and the S-nitrosylation of proteins. These events preceded an extensive though transient metabolic reprogramming at 6 h after NO treatment, which included enhanced levels of polyamines, lipid catabolism and accumulation of phospholipids, chlorophyll breakdown, protein and nucleic acid turnover and increased content of sugars. Accordingly, lipid-related structures such as root cell membranes and leaf cuticle altered their permeability upon NO treatment. Besides, NO-treated plants displayed degradation of starch granules, which is consistent with the increased sugar content observed in the metabolomic survey. The metabolic profile was restored to baseline levels at 24h post-treatment, thus pointing up the extraordinary plasticity of plant metabolism in response to nitroxidative stress conditions.

4.2.9. Metabolomic analyses reflect a transient reprogramming response to exogenous NO

Arabidopsis thaliana seedling exposed to a pulse of NO gas were used as model for mimicking an acute exposure of plants to a peak in environmental levels of NO or to intracellular accumulation of large amounts of NO in the production foci in plants under stressful conditions. Seedlings were exposed to a single dose of 300 ppm NO for 5 min and then, samples were harvested for untargeted metabolomic analyses comprising a total of 232 named biochemicals. Similar analyses were also performed in mock treated plants. Samples were collected at the time of the treatment (PRE), and then at 6 h and 24 h after exposure to NO or mock treatment (Fig. 4.23A). Plants exposed to NO underwent a transient though remarkable metabolic alteration by 6 h after treatment. A statistically significant increase in the amount of lipid, carbohydrate, amino acid and nucleotide categories of analyzed metabolites was detected in plants by 6 h after exposure to NO (Fig.

4.23A). By 24 h, the metabolomic status of treated plants was restored to that of untreated plants (Fig. 4.23A). Supplementary Table S1 (can be found in León *et al.*, 2016) includes the complete dataset with pathway heat maps and box and line plots for every analyzed metabolite showing the comparative fold- levels for every metabolite in the different samples as well as the statistical significance for the different comparisons. Only a few metabolites showed a significant difference when PRE and mock 6 h samples were compared, thus indicating only a small proportion of the metabolites analyzed were potentially regulated by circadian-related events in the experiment (Fig. 4.23A and Supplementary Table S1 in León *et al.*, 2016). By contrast, around 70% of the metabolites showed significant alteration in their endogenous levels by 6 h after exposure to NO (Fig. 4.23A and Supplementary Table S1 in León *et al.*, 2016). Significantly lower number of changes were detected in samples collected at 24 h after exposure (Fig. 4.23A and Supplementary Table S1 in León *et al.*, 2016), thus suggesting NO treatment has an extensive though transient metabolic effect on Arabidopsis plants. The Principal Component Analysis (PCA) confirms this general pattern. The PRE and MOCK 6 h or 24 h samples did not separate well, the NOx 24 h samples had only partial separation, and indeed the NOx 6 h samples were all clearly separated from this grouping (Fig. 4.23B). Moreover, to assess the compounds which meet the statistical criteria for significant differentiation between the analyzed samples, we applied two types of tests to compare the five experimental groups. The first approach was to compare each treated or mock-treated group to the PRE samples, using Welch's Two Sample t-Test. This approach yields information on the effect of time parameter on the experiment. A summary of the numbers of biochemicals that achieved statistical significance ($p \leq 0.05$), as well as those approaching significance ($0.05 < p < 0.1$), is shown in Table 4.2. One would expect approximately 10-15 compounds to reach significance by chance alone with 232 compounds tested. In these comparisons the mock samples showed only 12 or 24 compounds

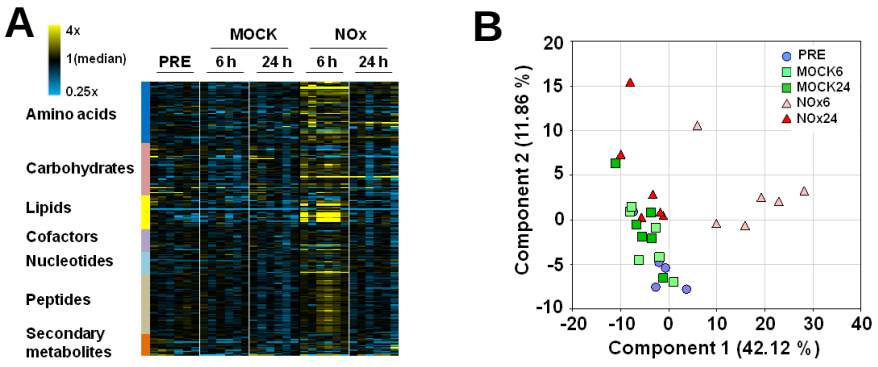

Figure 4.23. **Metabolomic Changes after Applying an NO Pulse to Arabidopsis Plants.** A, Heat map showing the increased (yellow) or decreased (blue) concentration of metabolites at the indicated times after treatment of plants (NOx) or untreated (MOCK) control. B, Principle Component Analysis (PCA) plot. Blue circles represent the samples before treatment, green squares the mock-treated samples and red triangles to NO treated samples at the indicated times after pulse.

at 6 h and 24 h, respectively, which were significant (Table 4.2), thus suggesting the mock treatment had little effect on the metabolome. By contrast, the NOx treatment resulted in 133 compounds being significant at the 6 h time point, and 55 at 24 h (Table 4.2), consistent with a robust experimental effect. To eliminate any diurnal effects in the data, we used an ANOVA Contrast test to compare the NOx to MOCK plants at each time point individually, and to score the time-related differences within each treatment pair. Again, the results were quite consistent with the observations taken from the heat map (Fig. 4.23A), PCA (Fig. 4.23B), and t-test results (Table 4.2). There were 154 compounds meeting the cut-off when comparing NOx 6 h to MOCK 6 h, but only 29 when compared at the 24 h time point (Table 4.2 and Supplementary Table S1 in León *et al.*, 2016), consistent with the idea that plants experienced a transient and acute response to NO exposure, and then, most metabolites returned to baseline levels after 24 h.

Table 4.2. Statistical comparisons in the metabolomic analyses

Welch´s Two Sample t-test	Total number of metabolites p≤0.05	Metabolites up p≤0.05	Metabolites down p≤0.05	Total number of metabolites 0.05<p<0.1	Metabolites up 0.05<p<0.1	Metabolites down 0.05<p<0.1
MOCK 6/PRE	12	1	11	17	1	16
MOCK 24/PRE	24	2	22	22	4	18
NOx6 /PRE	133	114	19	15	10	5
NOx24/PRE	55	17	38	29	7	22
ANOVA contrast						
NOx6/MOCK6	154	138	16	14	9	5
NOx24/MOCK24	29	18	11	17	7	10
MOCK24/MOCK6	27	16	11	17	6	11
NOx24/NOx6	155	12	143	9	2	7

PRE, Pre-treatment; MOCK6, Mock-treated; harvested after 6 h; MOCK24, Mock-treated harvested after 24 h; NOx6, Nitric oxide treatment harvested after 6 h; NOx24, Nitric oxide treatment harvested after 24 h. n=6 biological independent replicates.

4.2.10. Altered levels of amino acids and dipeptides suggests NO treatment increased protein breakdown

The elevated content of proteinogenic amino acids and dipeptides in the NOx 6 h compared to the MOCK 6 h or PRE samples (Supplementary Table S1 in León

et al., 2016) strongly suggest NO is inducing protein degradation. The exceptions to this pattern were amino acids that serve important metabolic functions in addition to protein synthesis. This includes glutamate, glutamine, and arginine, which are involved in nitrogen trafficking and storage, and glycine and serine, which are utilized in the photorespiration reactions, which endogenous content did not change significantly by NO treatment (Supplementary Table S1 in León *et al.*, 2016). The branched chain amino acids, leucine, isoleucine, and valine are typically at relatively low levels in cells, and function almost exclusively in protein synthesis, so an increase in their levels often indicates net protein turnover. These compounds, as well as the aromatic amino acids were more than twice the levels in NOx 6 h samples relative to MOCK 6 h (Supplementary Table S1 in León *et al.*, 2016). The aromatic amino acids are involved in other important pathways, such as the large phenylpropanoid family pathways (phenylalanine), tocopherol production (tyrosine), and hormone and glucosinolate synthesis (tryptophan), which were relatively unchanged or even dropped by NOx treatment (Supplementary Table S1 in León *et al.*, 2016). Moreover, the content of a common precursor of aromatic amino acid biosynthesis such as shikimate was lower in NO-treated relative to mock-treated plants at both 6 and 24 h time points (Supplementary Table S1 in León *et al.*, 2016), thus suggesting either the increased levels of aromatic amino acids caused a feed-back inhibition on the biosynthetic pathway or, alternatively, their increased levels are the result of active protein turnover.

We have observed that by 30 min after exposure to NO the nitroblue tetrazolium staining of superoxide anion in Arabidopsis seedlings was significantly reduced, thus suggesting NO efficiently scavenged superoxide (Fig. 4.24A). Peroxynitrite, a potent nitrating agent, is formed upon superoxide scavenging by NO, thus suggesting nitration of target proteins may occur in plants exposed to NO. We have analyzed the total and NO-related modified protein profile in plants after the NO pulse. No general changes were observed in the total protein pattern detected after monodimensional electrophoresis (Fig. 4.24B). Exogenous NO enables the modification of proteins through S-nitrosylation or nitration of cysteine and tyrosine residues, respectively (Astier & Lindermayr, 2012). We found that many nitrated and S-nitrosylated proteins started to accumulate by 1 h and reached maximum accumulation between 3 and 6 h after exposure of plants to NO (Fig. 4.24B).

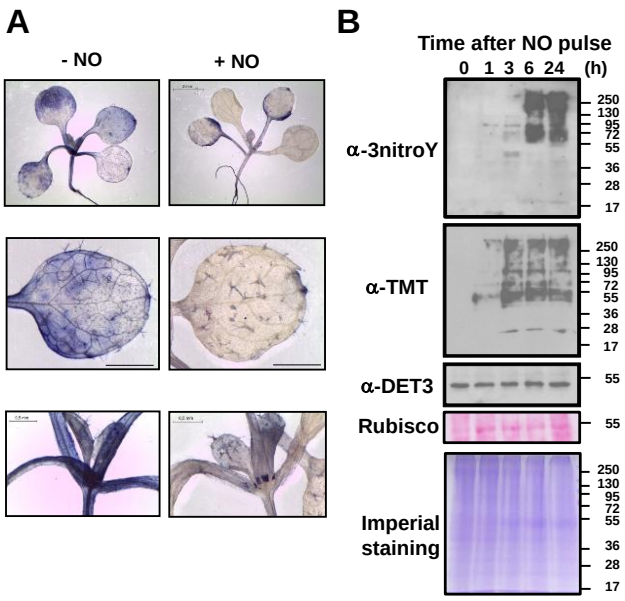

Figure 4.24. Superoxide content reduction and post-translational modifications induced by NO. A, Control untreated seedlings (-NO) and NO-exposed seedlings (+ NO) were stained with Nitroblue tetrazolium from 30 min to 20 h after treatment. B, Nitration and S-nitrosyltion of proteins in NO-treated plants. Each lane was loaded with 10 µg of proteins. The marks and numbers at the right side of panels indicate the position of molecular weight markers in kDa. The general pattern of protein is shown by staining of a replicate gel with Imperial (Thermo Scientific). Blot replicates were probed with the antibodies indicated at the left side of panels. α3-nitroY, anti-3-nitrated-Y; αTMT, anti-Tandem Mass Tagged-S-nitrosylated proteins. Equal loading was checked by Coomassie-stained large subunit of Ribulose-1,5-Bisphosphate Carboxylase / Oxygenase (Rubisco) and by using αDET3, anti-De-Etiolated 3. Data shown are representative of three independent experiments with similar results.

4.2.11. Acute exposure to NO triggers the accumulation of polyamines and responses to oxidative stress

Plants exposed to NO also showed specific effects on α-ketoglutarate-derived amino acids of the glutamate family. The levels of γ-aminobutyrate (GABA) and 2-aminobutyrate were slightly increased, and the increase was higher (4.3-fold) for γ -hydroxybutyrate (GBH) by 6 h after exposure to NO (Supplementary Table S1 in León *et al.*, 2016). It has been reported that the metabolism of GABA leads to accumulation of GBH when plants are exposed to low oxygen or high light conditions, and also that under those stress conditions accumulation of GABA and alanine was also detected (Allan *et al.*, 2008), which is in agreement with our data (Supplementary Table S1 in León *et al.*, 2016). Also in the glutamate family of amino acids, the levels of proline and ornithine were 1.8- and 4-fold increased, respectively, and also their corresponding N-acetyl derivatives were 1,7- and 5.8-fold augmented, respectively (Supplementary Table S1 in León *et al.*, 2016). The increased levels of proline and ornithine were also accompanied by significant increases in the content of polyamines such as putrescine (2.3-fold) and

spermidine (1.4-fold) as well as the precursor agmatine (2.8-fold) in NO-exposed plants after 6 h (Fig. 4.25 and Supplementary Table S1 in León *et al.*, 2016).

Cysteine is an unique example where active synthesis of an amino acid was evident in response to NO treatment. It is formed from serine in two steps, through the O-acetylation of serine by acetyl-CoA to form O-acetylserine, followed by the incorporation of hydrogen sulfide, displacing the acetyl group (Romero *et al.*, 2014). Cysteine synthesis is often the rate limiting step for the formation of glutathione, a critical compound in cellular redox responses (Noctor *et al.*, 2012). We found an increase above 2-fold in all these compounds in NOx 6 h plants. O-

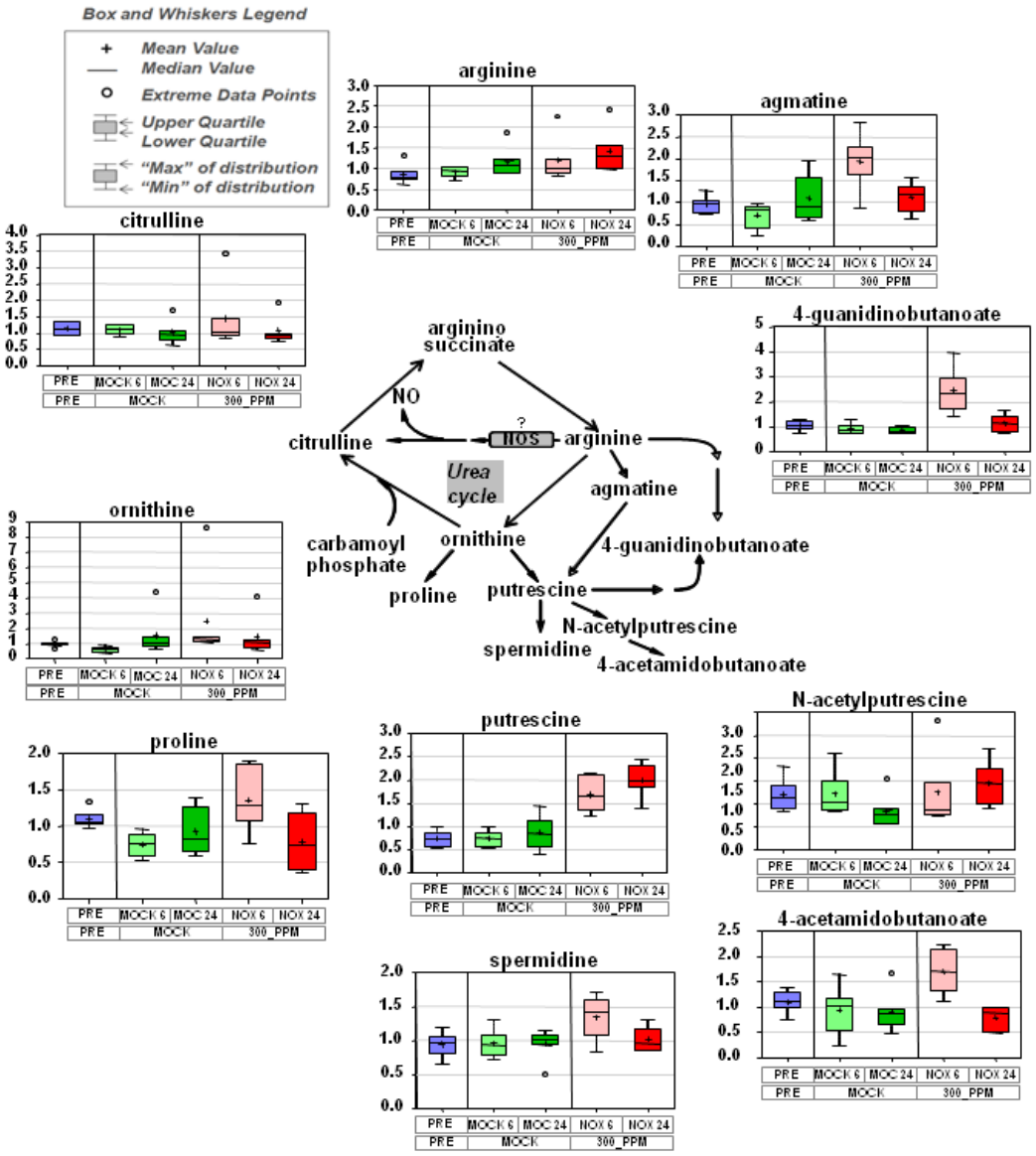

Figure 4.25. Enhanced polyamine content in plants exposed to NO. Scheme showing the biosynthesis of polyamines derived from the urea cycle and the box plots for every metabolite before treatment (blue) and at indicated times after mock- (green) or NO-treatment (red). Light and dark tones correspond to 6 h and 24 h, respectively, after treatment.

acetylserine and the non-enzymatically rearranged N-acetylserine were 17- and 11-fold increased, respectively (Supplementary Table S1 in León *et al.*, 2016), thus suggesting the exposure to NO triggered a strong demand for cysteine production as a mean to remediate oxidative stress. In agreement with that, perturbations of several other oxidative markers, namely increased of oxylipins 13-HODE, 9-HODE and 9,10-hydroxyoctadec-12(Z)-enoic acid produced through the LOX pathway (Feussner & Wasternack, 2001), were detected. Also consistent with NO-treated plants undergoing oxidative stress, the endogenous content of threonate, which is a downstream product of ascorbate metabolism (Green & Fry, 2005), were more than 4-fold higher in NO-treated plants by 6 h, and also a moderate increase in both oxidized and reduced glutathione content was detected (Supplementary Table S1 in León *et al.*, 2016). By contrast, the content of α-tocopherol, which together with glutathione and ascorbate constitute the triad of main antioxidants in plants undergoing oxidative stress (Szarka *et al.*, 2012), were around 50% lower by 6 h after NO treatment (Supplementary Table S1 in León *et al.*, 2016). These data together suggest that NO-exposed plants respond to oxidative stress through a complex process.

4.2.12. Altered lipidome reflects changes in lipidic structures such as membranes and cuticle in NO-exposed plants

The content of compounds belonging to the lipid category underwent large changes in NO-treated plants. Alterations were strictly limited to the six hour time point (Fig. 4.26). A significant increase in the free polyunsaturated fatty acids (PUFAs) content of around 4-fold for linoleate and linolenate, and around 2-fold increase for the C20 PUFAs dihomolinoleate and dihomolinolenate was detected (Supplementary Table S1 in León *et al.*, 2016 and Fig. 4.26). We also found a strong increase in several lyso-lipids such as 1-palmitoyl-GPC (8.9-fold), 1-palmitoyl-GPE (13.2-fold), 1-stearoyl-GPC (5.7-fold), 1-linoleoyl-GPC (10.8-fold), 1-linoleoyl-GPE (8.9-fold), 2-linoleoyl-GPC (4.8-fold) and 2-linoleoyl-GPE (5.4-fold) (Supplementary Table S1 in León *et al.*, 2016 and Fig. 4.26). Altered content of free fatty acids and phospholipids are likely connected to processes of lipid trafficking in either membrane remodeling or alteration of lipidic leaf structures such as cuticles (Hurlock *et al.*, 2014). We tested whether cell membranes or cuticles were altered in Arabidopsis plants upon exposure to NO. Nitrooxidative stress produced by the acute pulse of NO can severely damage membranes by lipid peroxidation (Blokhina *et al.*, 2003), thus altering their permeability. The integrity of membranes was monitored *in vivo* by staining roots with propidium iodide that only stains nuclei if membranes become permeable, but it remains staining membranes and walls if cell membranes are intact. Roots of untreated plants display non altered plasma membranes as demonstrated by propidium iodide decorating the cell membrane with no permeation into the cells (Fig. 4.27A). By contrast, by 30 min after exposure to NO the roots of NO-treated plants displayed numerous cells

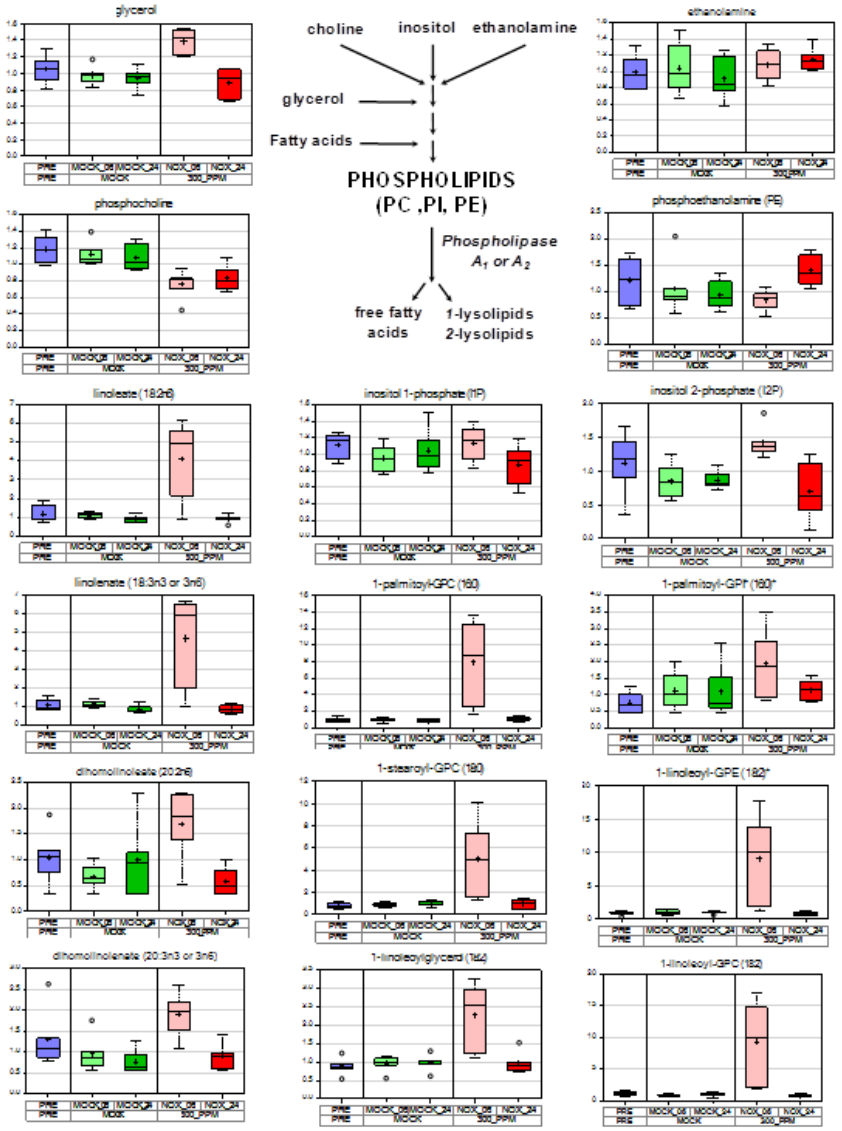

Figure 4.26. Altered phospholipid catabolism in plants after exposure to NO. Scheme showing the metabolism of phospholipids and the box plots for fatty acids and lipids before treatment (blue) and at indicated times after mock- (green) or NO-treatment (red). Light and dark tones correspond to 6 h and 24 h after treatment, respectively.

with propidium iodide-stained nuclei, thus indicating the permeability of their membranes was altered (Fig. 4.27A). Also the formation, integrity and permeability of the leaf cuticle are highly connected to lipid metabolism in Arabidopsis (Yeats & Rose, 2013). We checked whether the permeability of the leaf cuticle was influenced by the exposure to NO. Wild type Arabidopsis plants treated with exogenous NO as well as the Arabidopsis *nia1nia2noa1-2* triple mutant, depleted of endogenous NO (Lozano-Juste & León, 2010), were tested for cuticle permeability. Assays of cuticle permeability after application of toluidine blue or calcofluor white demonstrated an enhanced permeability of the cuticle in NO-deficient leaves that was reversed by treatment with exogenous NO (Fig. 4.27B).

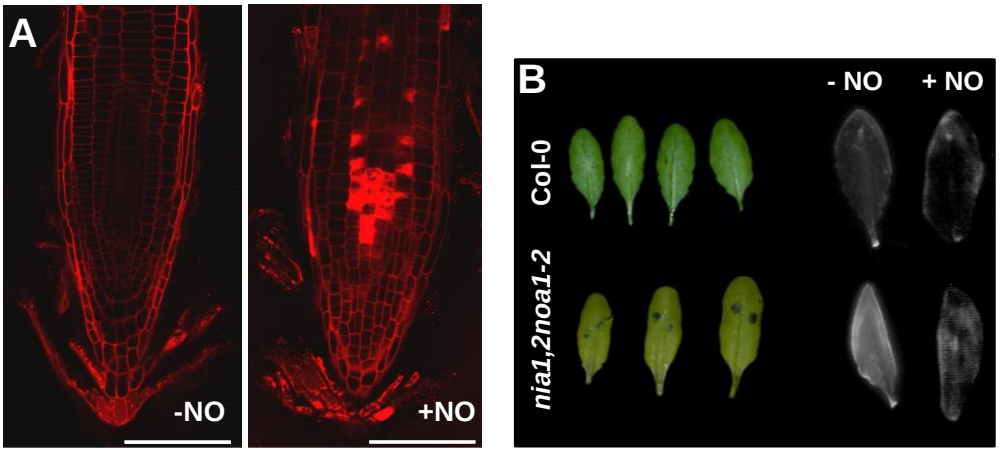

Figure 4.27. Alterations in the permeability of lipidic structures. A, Permeability of plasma membrane in roots of NO-treated plants. Untreated (-NO) or NO-treated (+NO) roots from wild type Col-0 plants were stained with propidium iodide at 30 min after exposure to NO. Images were obtained with a confocal microscope Leica TCS SL with excitation at 488 nm and emission at 598-650 nm range. Scale bars: 50 µm. B, Effect of NO on leaf cuticle permeability. In the left panel, two drops of 10 µl of toluidine blue solution were applied on the upper side of undetached leaves from wild type Col-0 and NO-deficient *nia1,2noa1-2* mutant plants. After 2 h, leaves were extensively washed with water, excised and photographed to show penetration or not of toluidine blue through cuticle. In the right panel, leaves from untreated (-NO) or NO-treated (+NO) plants were detached at 6 h after NO pulse, bleached with ethanol, stained for 1 min with calcolfluor white and extensively rinsed with water before photographed under UV light. Data shown are representative of five and three independent toluidine blue and calcofluor white experiments, respectively, with similar results.

4.2.13. Altered purine, pyrimidine and chlorophyll metabolism suggest NO enhanced nucleic acid turnover, chlorophyll degradation and non-programmed cell death

The metabolomic data also reflected a significant increase in metabolites involved in purine and pyrimidine metabolism. The levels of allantoin, guanine, urate, cytidine, cytosine-2',3'-cyclic monophosphate, pseudouridine, uridine and uracil were all increased (between 1.5- and 7.6-fold) by 6 h after NO treatment (Supplementary Table S1 in León *et al.*, 2016). However, all these metabolites returned to the baseline levels by 24 h, with special emphasis on uracil, which moved from a 7.6-fold increase by 6 h to non-significantly changed levels by 24 h (Supplementary Table S1 in León *et al.*, 2016). It is noteworthy mentioning that, in turn, the levels of nucleosides such as adenosine, adenosine-2´-monophosphate and inosine are between 20 and 45% reduced by 6 h after plants were exposed to NO (Supplementary Table S1 in León *et al.*, 2016). In agreement with the enhanced metabolism of purines and pyrimidines, we found a pattern of progressive genomic DNA degradation upon exposure of plants to the NO pulse (Fig. 4.28A).

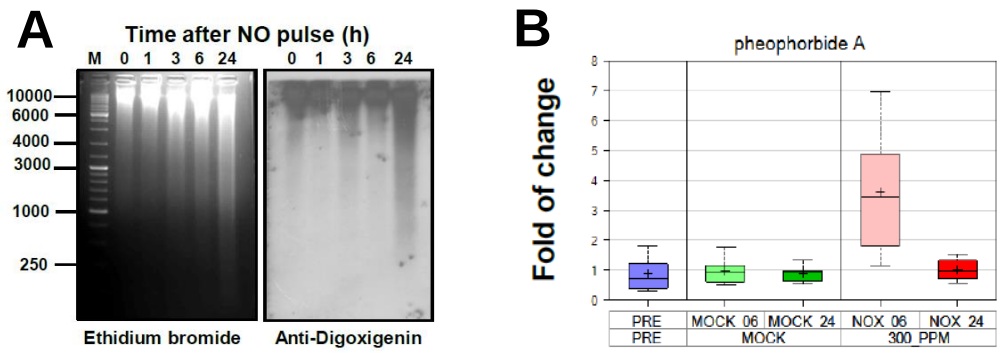

Figure 4.28. NO triggers DNA and chlorophyll degradation. A, Genomic DNA isolated from NO-exposed plants at the indicated times after application of NO pulse. Genomic DNA was run in duplicate in 2% agarose gels and either ethidium bromide-stained (15 µg) or blotted (5 µg) onto positively charged nylon membranes. DNA digested with *Msp*I was digoxigenin (DIG)-labelled and use as probe for Southern blot with anti-DIG antibody coupled to alkaline phosphatase to amplify the signal. DNA ladder marker (M) in base pairs is shown in the left side. B, y-axis shows Fold of Change as Group Means Ratios in Scaled Imputed Data for pheophorbide a. + represents mean value; ___ represents median value; boxes indicate the limits of upper and lower quartile; and error bars represent the maximum and minimum of distribution.

On the other hand, the metabolomic data also suggest NO induces chlorophyll degradation. Pheophorbide a, which has been identified as a genuine intermediate of chlorophyll breakdown (Hörtensteiner, 2013), was 3.7-fold increased by 6 h after NO treatment (Fig. 4.28B), thus suggesting Pheophorbide a oxidase (PAO) activity should be reduced in NO-exposed plants. The absence of PAO activity in different plants has been correlated with increased cell death, and pheophorbide a has been reported to be involved in both light-dependent and light-independent cell death mechanisms (Pruzinská *et al.*, 2005; Hirashima *et al.*, 2009). We checked whether treatment with exogenous NO alters the endogenous levels and leads to cell death in exposed leaves. Figure 4.29A shows the endogenous levels of NO after staining roots with DAF-FM diacetate. The endogenous levels slightly decreased by 2 and 4 h after exposure to exogenous NO and modest increases were observed by 6 and 24 h (Fig. 4.29A) but increases were far below those detected in plants treated with a known inducer of NO such as salicylic acid (Zottini *et al.*, 2007) (Fig. 4.29B). Evans blue staining of plants at different times after NO treatment showed blue stained spots of dead cells at 6 h and 24 h after exposure to NO (Fig. 4.29C) and although seedlings were slightly chlorotic by 24 h plants they were fully viable showing normal growth by seven days after treatment (Fig. 4.29C).

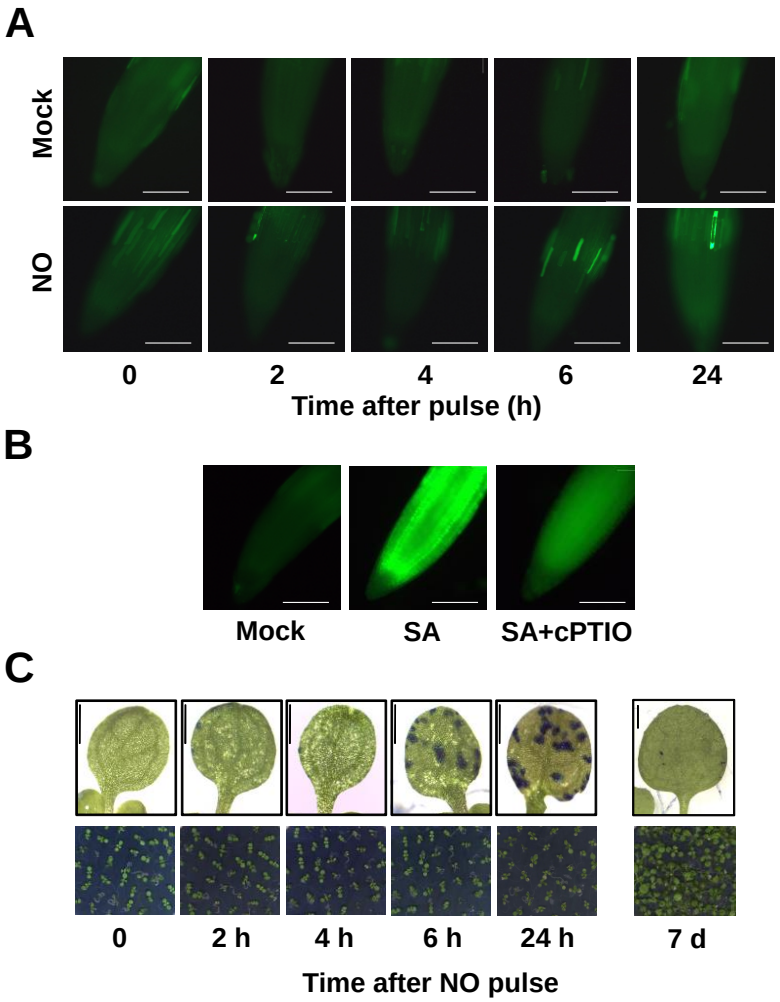

Figure 4.29. Endogenous NO content and cell death upon exposure to exogenous NO. Seedlings (8 day-old) were treated with A, exogenous NO or treated with air as control (Mock) and B, mock treated or treated with 0.5 mM salicylic acid (SA) or with SA plus 0.5 mM 2-(4-Carboxyphenyl)-4,4,5,5-tetramethylimidazoline-1-oxyl-3-oxide (SA+cPTIO) for 1 h, and at the indicated times after exposure, the endogenous NO content was assayed by root staining with DAF-FM DA. Scale bars: 100 µm. C, Cell death was assayed by Evans blue staining of plants at the indicated times after exposure to NO. Scale bars: 1 mm. The appearance of the plants for every time point is shown in the bottom panels. The experiments were repeated three times with similar results and representative images are shown.

4.2.14. Exposure to NO affected photorespiration and central carbon metabolism

By 6 h after exposure to NO, the content of the glycolisis intermediates glucose-6-phosphate, glycerate and pyruvate decreased (0.57-, 0.59- and 0.83-fold, respectively) if compared to mock-treated plants at the same time point (Fig. 4.30A and Supplementary Table S1 in León *et al.*, 2016). It is noteworthy mentioning that glycerate, which is an intermediate in photorespiration, kept levels significantly reduced by 24 h after exposure to NO (Supplementary Table S1 in León *et al.*, 2016). Also the levels of two metabolites of the TCA cycle such as α-

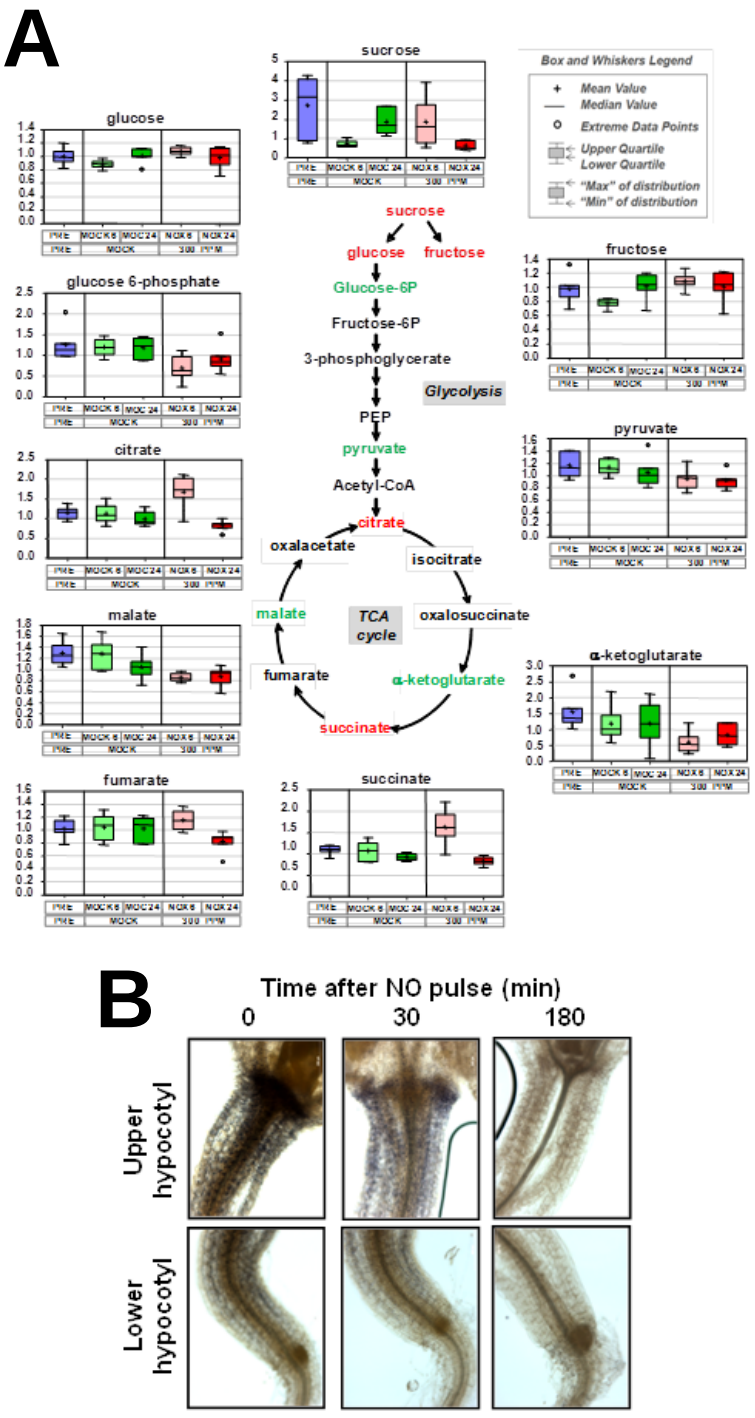

Figure 4.30. Metabolites of glycolysis and TCA cycle in plants exposed to NO. A, Scheme showing the intermediate metabolites (in red increased content; in green reduced content) of the glycolysis and the TCA cycle and the box plots for every metabolite before treatment (blue) and at indicated times after mock- (green) or NO-treatment (red). Light and dark tones correspond to 6 h and 24 h, respectively, after treatment. B, Starch granules were stained with Lugol´s reagent in 7-day old seedlings exposed to a 300 ppm NO pulse for the indicated times. Images for hypocotyls are representative of at least six independent plants per time point.

ketoglutarate and malate were significantly reduced by 6 h in NO-treated plants (Fig. 4.30A and Supplementary Table S1 in León *et al.*, 2016). Finally, sedoheptulose-7-phosphate and ribose-5-phosphate, both intermediates of the Calvin Cycle were not different at the six hour time point, but were significantly lower (0.32-, 0.58-fold, respectively) at 24 hours (Supplementary Table S1 in León *et al.*, 2016). The content of sucrose, the downstream product of photosynthesis, although increased (2.5-fold) by 6 h was significantly reduced (0.33-fold) by 24 h (Fig. 4.30A and Supplementary Table S1). Also different sugars including amino and nucleotide sugars as well as disaccharides were increased (between 1.4- and 3-fold) in the 6 h time point in NO-treated plants (Supplementary Table S1 in León *et al.*, 2016). Remarkably, three of those compounds arabitol, ribulose and ribitol were strongly reduced (0.04-, 0.54- and 0.74-fold, respectively) by 24 h after NO treatment (Supplementary Table S1 in León *et al.*, 2016). In agreement with exogenous NO altering photosynthetic metabolism and triggering differential accumulation of sugars, we have detected a significant reduction in the starch granules in the hypocotyls of NO-treated seedlings by 3 h after exposure to NO (Fig. 4.30B).

4.3. Function of the ERFVII RAP2.3 on the regulation of NO homeostasis and signaling

This section 4.3 is an excerpt from the research article: "León, J., Costa-Broseta, Á., & Castillo, M. C. (2018). RAP2.3 negatively regulates nitric oxide biosynthesis and sensing through a rheostat-like mechanism in Arabidopsis". This research article was submitted to The Plant Journal and was under revision when PhD Thesis writing was finished. All the results and figures that appear here are derived from the work of the PhD student in collaboration with the other authors.

4.3.1. Abstract

Nitric oxide (NO), which regulates development and defense responses in plants, is sensed through a mechanism involving the N-end rule pathway mediated degradation of the group VII of ERF transcription factors (ERFVIIs). A member of the ERFVIIs, RAP2.3, negatively regulates both the NO biosynthesis and their triggered responses. RAP2.3 seems to work as a molecular rheostat maintaining a brake on NO synthesis and responses when accumulated, either by avoiding its degradation or by enhancing its expression. Its degradation would thus release those brakes allowing NO production and the subsequent activated responses. The use of conditionally expressing transgenic lines for *RAP2.3* together with NO treatment and genome-wide transcriptome analyses allowed finding that the enhanced expression of *RAP2.3* largely attenuated the changes in the NO-responsive transcriptome both qualitatively and quantitatively. Transcriptome data uncover the existence of RAP2.3-dependent and –independent NO-responsive branches of jasmonate, and ABA signaling pathways, which seems to be functionally relevant for NO sensing.

4.3.2. A rheostat-like mechanism based on RAP2.3 degradation controls endogenous NO content

RAP2.3 is one of the members of the group VII ERF transcription factors that we previously reported to be involved in NO sensing (Gibbs *et al.,* 2014a). As a substrate of the arginylation branch of the N-end rule pathway of proteolytic degradation (Gibbs *et al.,* 2011; Licausi *et al.,* 2011), the stability of the RAP2.3 protein depends on its N-terminal sequence, in such a way that a wild type version containing the MC- N-terminal motif is degraded upon polyubiquitylation by the proteasome, whereas a mutated MC2A version is resistant to proteasome-mediated degradation. By using plants overexpressing either MC-RAP2.3 or MA-RAP2.3 (Gibbs *et al.,* 2014a), we analyzed the effect of RAP2.3 on the endogenous NO content. After staining with the NO specific fluorophore DAF-FM, plant cotyledons overexpressing the degradable MC-RAP2.3 version contained a 2.3-fold increase in NO-associated fluorescence compared to wild type plants (Fig. 4.31). However, the levels in MC-RAP2.3 overexpressing roots were not

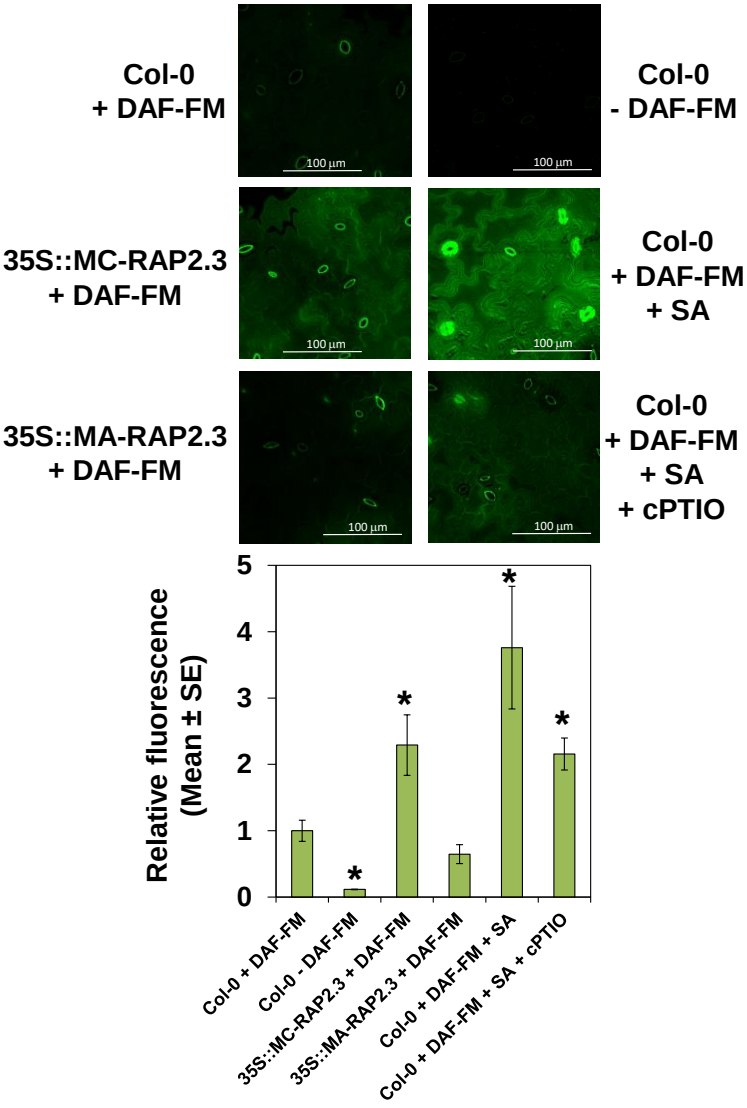

Figure 4.31. NO in cotyledons of plants overexpressing MC- and MA-RAP2.3 versions. Cotyledons from plants of the indicated genotypes were treated (+) or untreated (-) with 10 µM DAF-FM DA, 500 µM of the NO scavenger cPTIO, and 500 µM of the NO inducer salicylic acid (SA) as indicated. Fluorescence was detected by confocal microscopy with Z-stacks equivalents for all the genotypes and conditions tested. Images are representative of 3 to 5 replicate experiments and relative fluorescence is shown as the mean of replicate experiments ± standard error.* means significant with p-value <0.05 in Student´s t-test.

significantly different than those of wild type roots (Fig. 4.33A). The increased fluorescence levels were nevertheless not as high as those detected in plants treated with SA (3.8-fold; Fig. 4.31), which has been reported to be a strong inducer of NO production both in roots and shoots (Zottini *et al.,* 2007). The detected fluorescence was confirmed to be associated to the endogenous content of NO, as samples treated with SA and the NO specific scavenger cPTIO showed lower fluorescence levels than plants treated with SA (Fig. 4.31). Remarkably, the enhanced NO content in *35S::MC-RAP2.3* plants was not directly associated to the protein expression levels, as the over-expression of the non-degradable MA-

RAP2.3 version led to cotyledon fluorescence not significantly different than wild type plants (Fig. 4.31). These data point to a requirement for RAP2.3 degradation to release a brake exerted by RAP2.3 on NO biosynthesis. Since RAP2.3 degradation by the proteasome requires the previous polyubiquitylation mediated by the E3 ubiquitin ligase PRT6, we tested whether NO content in cotyledons was altered in *prt6-1* mutant plants. The overall NO-associated fluorescence in *prt6-1* plants was not significantly different than those from wild type plants either in cotyledons (Fig. 4.32) or in roots (Fig. 4.33B). However, increases in NO levels were detected in the guard cells of stomata (Fig. 4.32), in agreement with previous report (Gibbs *et al*. 2014a). Interestingly, the quintuple mutant with loss of function of all ERFVII transcription factors (*qerfvii*), which contained NO levels similar to wild type plants both in shoots (Fig. 4.32) and roots (Fig. 4.33B), displayed almost no fluorescence in the stomata (Fig. 4.32). A similar pattern of endogenous NO content was also detected in the sextuple *qerfvii prt6-1* mutant (Fig. 4.32 and 4.33B), thus indicating the enhanced NO levels caused by the *prt6* mutation was not dependent on the actual ERFVII levels but on their capacity of being degraded through a PRT6-mediated process. Regarding this, plants expressing a non-

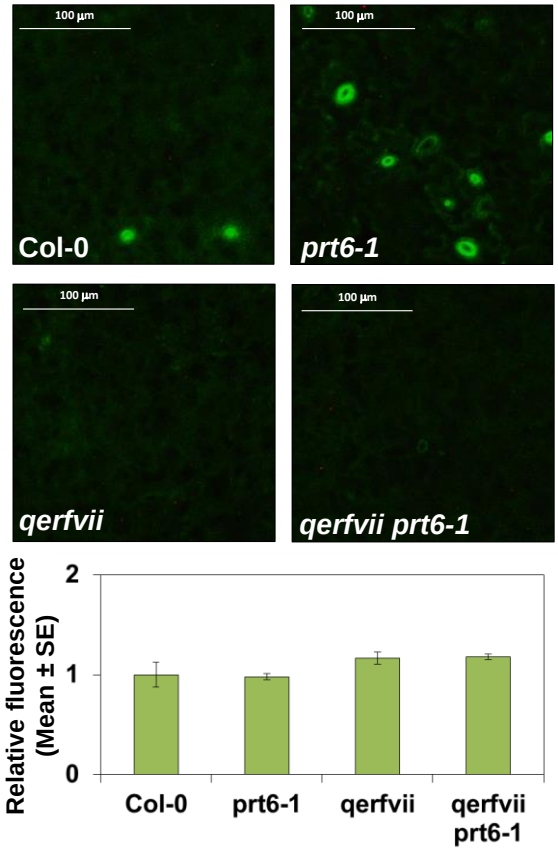

Figure 4.32. NO in cotyledons of N-end rule pathway mutant and wild type plants. Cotyledons from plants of the indicated genotypes were treated with 10 µM DAF-FM DA. Fluorescence was detected by confocal microscopy with Z-stacks equivalents for all the genotypes and conditions tested. Images are representative of 3 to 5 replicate experiments and relative fluorescence is shown as the mean of replicate experiments ± standard error.

degradable version (35S::MA-RAP2.3) of the protein or not expressing the protein at all (*qerfvii* mutant) would behave similarly with low levels of NO. These findings point to a potential role for RAP2.3 working as a molecular rheostat in such a way that the NO synthesis would be limited when RAP2.3 is not degraded but activated upon degradation.

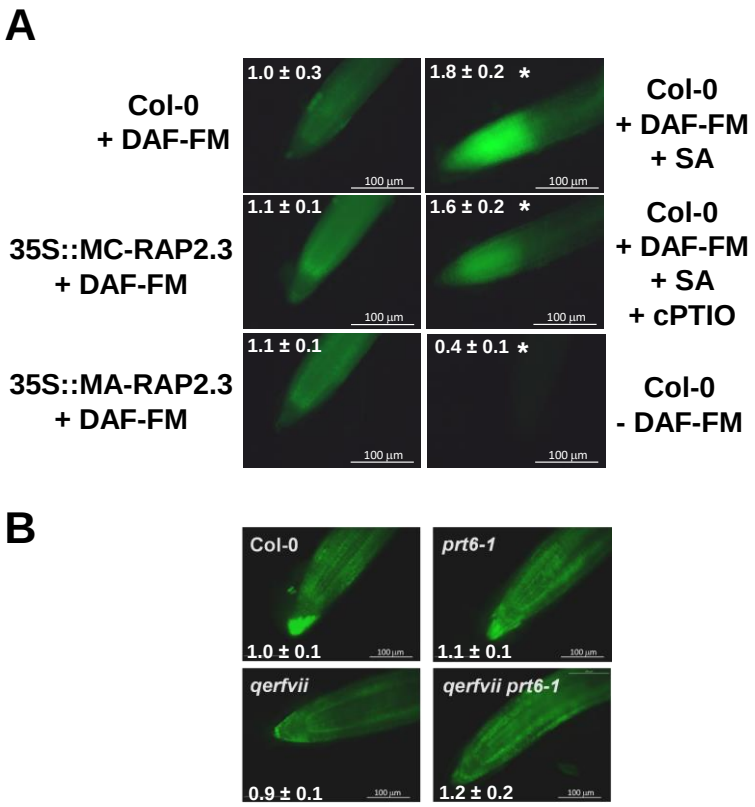

Figure 4.33. NO in roots of mutant and transgenic plants. Roots of the indicated genotypes of A, plants overexpressing MC- and MA-RAP2.3 versions and B, N-end rule pathway mutant plants genotypes were treated (+) or untreated (-) with 10 µM DAF-FM DA, 500 µM of the NO scavenger cPTIO, and 500 µM of the NO inducer salicylic acid (SA) as indicated were treated with 10 µM DAF-FM DA. Plants shown in B were only treated with DAF-FM DA. Fluorescence was detected by fluorescence microscopy. Images are representative of 3 to 5 replicate experiments and quantification of fluorescence is shown as the mean of replicate experiments ± standard error .* means significant with p-value <0.05 in Student´s t-test.

4.3.3. RAP2.3 modulates NO sensing in shoots and roots

Despite the potential role of RAP2.3 in regulating the endogenous NO levels as described above, RAP2.3, together with the rest of ERF VII transcription factors, has been proposed to participate in NO sensing through the arginylation branch of the N-End Rule pathway (Gibbs *et al.*, 2014b; Gibbs *et al.*, 2014a). According to the central role exerted by the E3 ubiquitin ligase PRT6 in that process, we reported that the NO-triggered inhibition of the hypocotyl elongation was impaired in the *prt6*

mutant plants (Gibbs, *et al.*, 2014a). Thus, the stabilization of ERFVIIs seems to be a key factor for the sensitivity of plants to NO. By using plants over-expressing either the wild type MC-version or the mutated MA-version of RAP2.3, we tested whether enhanced levels of RAP2.3 altered the sensitivity to NO in etiolated hypocotyl shortening assays. Figures 4.34A and 4.34B show that plants overexpressing an MC-RAP2.3 version were as sensitive to NO-triggered inhibition of hypocotyl elongation as Col-0 plants. In turn, the over-expression of the non-degradable MA-RAP2.3 version almost fully released the NO-triggered inhibition of hypocotyl elongation. To check whether these differential phenotypes were related to the stability of the RAP2.3 version expressed, we took advantage of the C-terminal HA-tags of both proteins in our constructs. Whereas MC-RAP2.3 was efficiently degraded by NO, the levels of MA-RAP2.3 protein remained high under NO treatment, thus correlating with the NO-sensitive and -resistant phenotypes observed, respectively (Fig. 4.34C). Besides hypocotyl shortening, the response of plants to NO was also characterized by a drastic inhibition of primary root growth in wild type plants (Fig. 4.34A,B). As for hypocotyl shortening, *35S::MC-RAP2.3* plants were also fully inhibited in root growth but, in turn, *35S::MA-RAP2.3* displayed a significant yet defective root growth under the NO treatment applied in this experiment (Fig. 4.34A,B). These data thus suggest the stabilization of RAP2.3 protein made plants less sensitive to NO, so that RAP2.3 likely acts also as a negative regulator of NO sensing and signaling.

4.3.4. Genome-wide transcriptome analyses revealed RAP2.3 as a general negative regulator of NO-triggered responses

Inhibition of root and hypocotyl growth is only part of the NO-triggered responses in plants. We have previously reported that a pulse of NO triggers a transient but extensive metabolic reprogramming that includes enhanced levels of polyamines, lipid catabolism and accumulation of phospholipids, chlorophyll breakdown, protein and nucleic acid turnover and decreased and increased content of starch and sugars, respectively (León *et al.*, 2016). To assess, at the molecular level, how NO triggers multiple responses and what is the regulatory role exerted by RAP2.3, we conducted comparative transcriptome analyses of NO-treated versus untreated plants in TPT (TRANSPLANTA) Arabidopsis transgenic lines (Coego *et al.*, 2014) conditionally expressing *RAP2.3* under a β-estradiol-inducible promoter (Fig. 4.35A). Upon treatment with β-estradiol, those plants specifically expressed *RAP2.3,* as demonstrated by the large accumulation of the *RAP2.3* transcript and the absence of enhanced expression for the highly related *RAP2.12* gene (Fig. 4.35B). Following the experimental scheme shown in Figure 4.35C, β-estradiol treated or control untreated plants were grown for 10 d under standard growing conditions, exposed to a 300 ppm NO pulse for 5 min, and 1 h later samples were collected for RNA isolation and further transcriptome analyses using Arabidopsis whole genome Agilent microarrays. Normalized and filtered data (p-value corrected for FDR < 0.05 and fold change in absolute values > 1.5) from

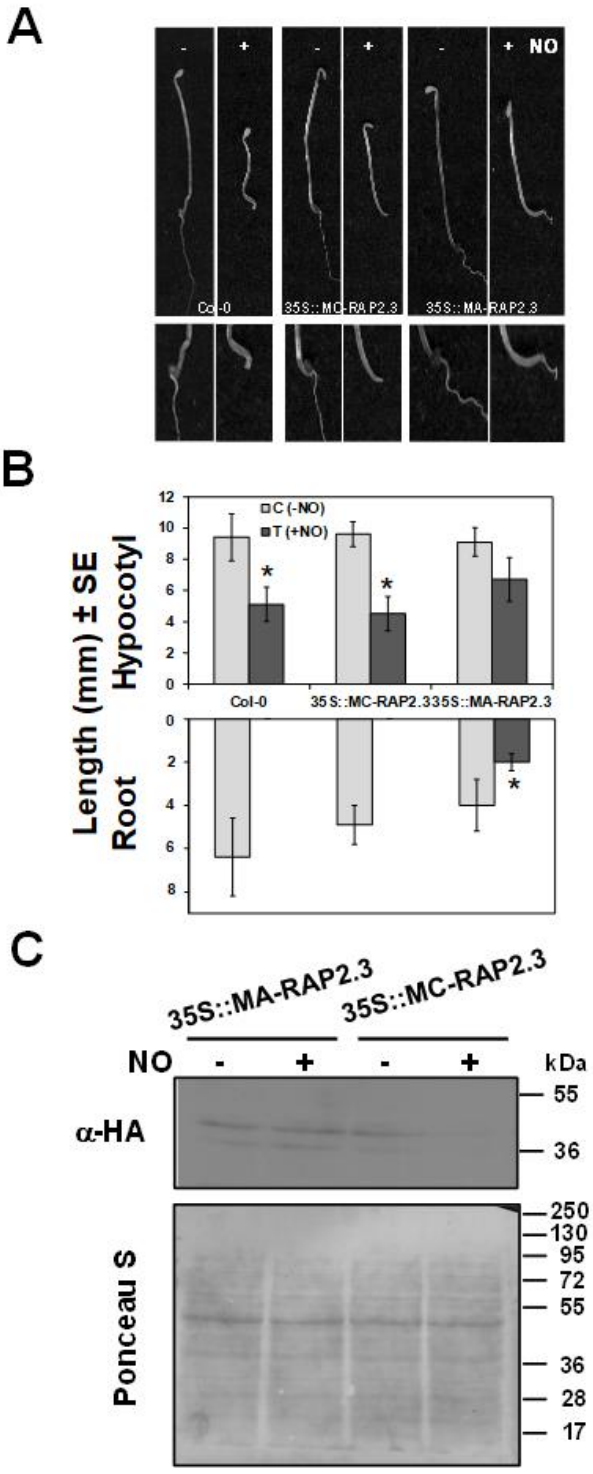

Figure 4.34. Overexpression of non-degradable MA-RAP2.3 confers hyposensitivity to NO. A, Hypocotyls (upper panels) and roots (detail in lower panels) of etiolated seedlings either treated (+) or not (-) with 300 pm NO. B, The length of hypocotyls and primary roots was measured, after scanning at least 20 individuals for every genotype and condition, with Image J. Values are the mean ± SD. * means significant with p-value <0.05 in Student´s t-test. C, The levels of RAP2-3-HA protein were analyzed by Western blot with anti-HA antibodies in protein extracts from NO treated (+) or not (-) etiolated seedlings of the indicated genotypes. Total protein staining with Ponceau S is shown as loading control. The position of molecular weight markers is shown at the right side of panels.

all transcriptome analyses are summarized in Table A9. The NO pulse triggered the rapid and differential regulation of 2097 genes representing roughly 10% of the Arabidopsis genome (Fig. 4.35D), thus pointing to relevant transcriptional regulation of the NO-induced responses. Remarkably, the NO-triggered responses at the transcriptome level were largely attenuated when NO-treated plants over-expressed *RAP2.3* upon activation by β-estradiol treatment (Fig. 4.35D). Around 81% of the up-regulated and 90% of the down-regulated genes by NO in TPT_RAP2.3 plants were differentially expressed only in the absence of β-estradiol treatment (Fig. 4.35D and Table A9). The 1124 and 642 genes that were up- and down-regulated, respectively, by NO in plants not treated with β-estradiol but not in those over-expressing *RAP2.3* represent potential NO targets negatively regulated by RAP2.3. By contrast, only 263 and 68 genes were up- and down-regulated, respectively, by NO regardless of the levels of *RAP2.3* expression (Fig. 4.35D). From those, 56 and 34 genes were up- and down-regulated, respectively, by NO only when *RAP2.3* was over-expressed (Fig. 4.35D), thus suggesting RAP2.3 might act also as a positive regulator of NO-triggered changes in this gene subset. These data support that RAP2.3, in addition to play a role in controlling NO biosynthesis and sensing, exerted an important quantitative and qualitative modulation of the NO-regulated transcriptome. Remarkably, RAP2.3 seems to act mainly as a repressor of NO-responsive genes, although also potential targets of its positive regulation were pinpointed in these analyses. An *in silico* screening of GCC-like boxes, defined previously as putative RAP2.3 binding motifs (Franco-Zorrilla *et al.*, 2014), was performed. Searching the 1000bp promoter sequence upstream of the initiation codon of genes in the whole Arabidopsis genome for the (C/A)GCCG(C/T)(C/A) motif sequence allowed us to find 7994 hits corresponding to 6186 sequences (Fig. 4.35E and Table A7). Among these putative RAP2.3-binding targets, 296 corresponded to genes that were differentially regulated in NO-treated plants of the TPT_RAP2.3 transgenic lines (Fig. 4.35E and Table A7). We found 188 and 97 genes containing the consensus RAP2.3 binding motif that were up- or down-regulated, respectively, by NO only in TPT plants that were not treated with β-estradiol (Fig. 4.35E and Table A7). By contrast, only 7 and 4 genes containing the consensus RAP2.3 binding motif were up- or down-regulated, respectively, by NO only in TPT plants that were treated with β-estradiol (Fig. 4.35E and Table A7), thus suggesting the number of targets negatively regulated by RAP2.3 in NO-triggered responses are by far larger than those positively regulated. We also found a relatively large amount of genes carrying putative RAP2.3-binding motifs, 52 and 7 that were up- or down-regulated by NO in TPT_RAP2.3 plants independently of being treated or not with β-estradiol (Fig. 4.35E and Table A7), thus suggesting they were not truly targets of RAP2.3 regulation.

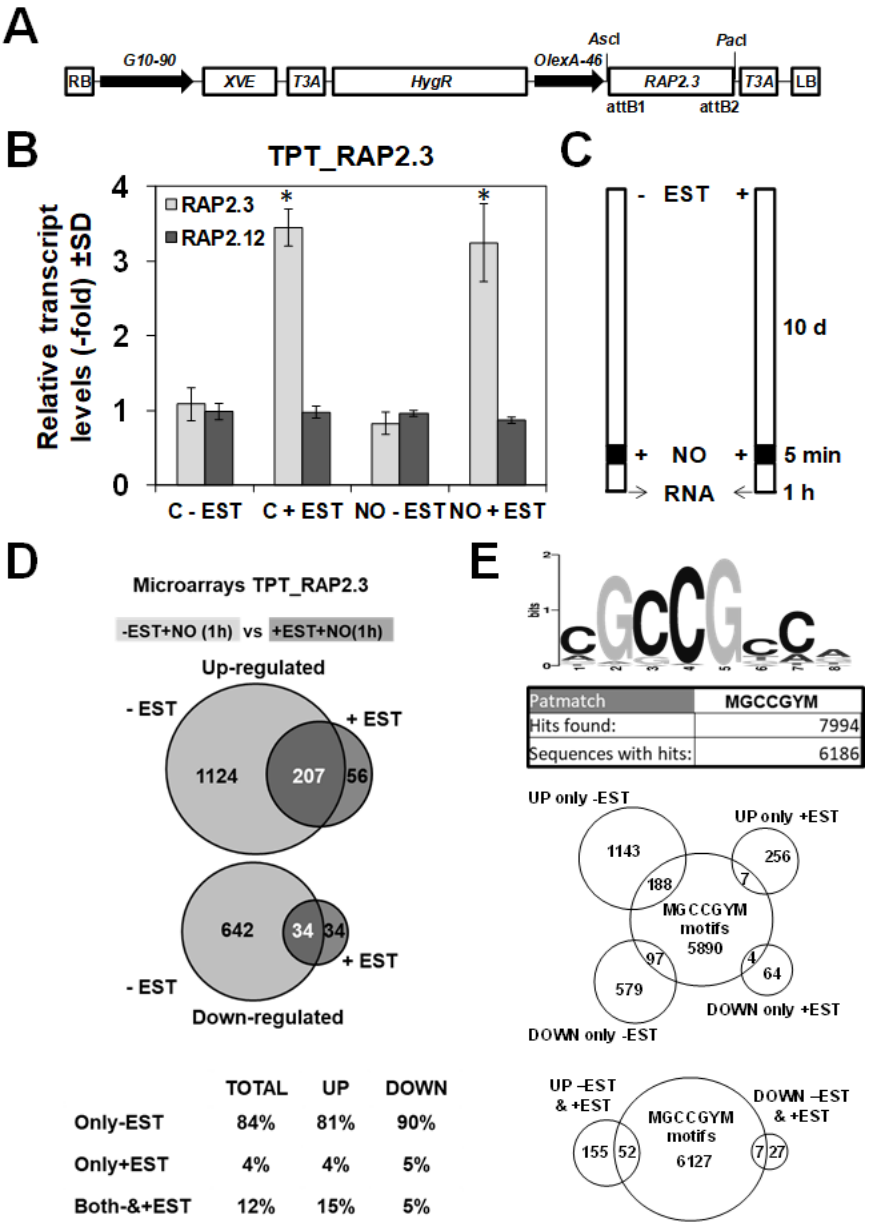

Figure 4.35. Transcriptome analysis of β-estradiol inducible RAP2.3 transgenic lines. A, Construct used to conditionally express *RAP2.3* under the control of a β-estradiol-inducible *XVE* factor that activates the *OlexA-46* promoter. B, *RAP.3* and *RAP2.12* transcript levels were quantified in plants, either not treated (C) or treated (NO) in the presence (+) or absence (-) of β-estradiol (EST), by RT-qPCR with specific primers. Values are the mean ± SD of three independent biological replicates. * mean statistically significant with p-value < 0.05 in Student´s t-test. C, Scheme displaying the times for growing, treatments and sampling designed for the transcriptome analyses. D, Venn diagrams showing differentially up- and down-regulated genes in conditionally expressing TPT-RAP2.3 transgenic lines treated (+) or not (-) with the transgene inducer β-estradiol (EST). E, Putative RAP2.3 binding element and in silico analysis of the presence in promoter genes on the whole Arabidopsis genome. Venn diagrams represent the intersection between genes that were identified as differentially expressed in NO-treated plants and those carrying the binding motif in their promoters.

4.3.5. The NO-responsive RAP2.3-independent transcriptome includes jasmonic acid and ethylene core signaling gene sets

The group of 241 genes that were up- or down-regulated by NO in TPT_RAP2.3 plants independently of being treated or not with β-estradiol (Fig. 4.35D) represents the potential NO-Responsive RAP2.3-independent transcriptome. A Gene Ontology analysis on these genes revealed that the functional categories related to jasmonic acid (JA) biosynthesis, metabolism and signaling as well as the response to ethylene stimulus were the most significantly over-represented. The set of JA-related genes included some coding for biosynthetic enzymes such as LOX3, LOX4, AOC1, AOC3, OPR3 and OPCL1 as well as some coding for different components of JA signaling including the transcription factor MYC2 and the negative regulators JAZ2, 5, 6, 7, 9, 10, CYP94b1 and CYP94c1, which were all strongly up-regulated from 6- to more than 50-fold (Table A9). Similarly, several ethylene response-related genes such as those coding for the ethylene response (ERF) transcription factors RRTF1, ERF13, ERF-2, ERF6, ERF-1, CEJ1/DEAR1 and RAP2.9/DEAR5 were also included in this group of genes. Since these JA- and ethylene-related genes resulted to be up-regulated, it seems that JA and ethylene signaling were both enhanced in response to NO through a process that was not modulated by RAP2.3. Besides JA- and ethylene-regulated processes, also ABA-related processes such as dehydration were also over-represented among up-regulated genes of this group. This subset included genes coding for several dehydrins such as ERD10, ERD12/AOC1, ERD15 or the E3 ubiquitin ligases PUB23 and PUB24, as well as genes coding for water stress-related transcription factors such as MYBR1, MYC2, MBF1C and DREB2b (Table A9). Some of these ABA-responsive genes resulted to be also regulated by other stress-related hormones such as JA or salicylic acid (SA) thus pointing to NO as an enhancer of general RAP2.3-independent stress responses in the plant. Remarkably, some of the above mentioned genes contained (C/A)GCCG(C/T)(C/A) motifs in their promoter sequences (Table A7), thus suggesting not all the *in silico* identified motifs are truly RAP2.3-related and/or that RAP2.3 binding on that motifs are not modifying the regulation exerted by NO on them.

4.3.6. The NO-responsive RAP2.3-dependent transcriptome suggest the existence of NO-sensitive gene-specific hormone signaling pathways

Besides RAP2.3-independent NO-responsive genes, we found two other set of NO-responsive genes showing a RAP2.3-regulated pattern. The smaller set comprised 90 genes that required the over-expression of *RAP2.3* to be up- or down-regulated by NO (Fig. 4.35D). It is noteworthy mentioning that among genes in this set, the cytokinin negative regulator ARR22 encoding gene as well as the auxin responsive proteins SAUR29, 65 and 19, and the auxin metabolic IAA carboxylmethyltransferase 1 (IAMT1) and IAA-amido synthetase GH3.9 encoding genes were strongly down-regulated (Table A9). By contrast, the auxin signaling

enhancer MYB77 transcription factor encoding gene was up-regulated by NO only in *RAP2.3* over-expressing plants (Table A9). All together these data suggest NO may regulate the responses to auxins and cytokinins through RAP2.3-mediated processes. However, only 7 and 4 genes among those up- or down-regulated by NO in β-estradiol treated plants contained the (C/A)GCCG(C/T)(C/A) motif in their promoters, and only SAUR65, from the above mentioned as related to auxin and cytokinin signaling (Table A7). Also remarkably, the phosphate transporters PHT1;4 and PHT2;1 were down-regulated by NO in RAP2.3 over-expressing plants (Table A9). Regarding up-regulated genes in this set, we found that the transcription factors RAV1, BBX20/BZS1 and WRKY28 encoding genes, which are involved in regulating ABA-related stress signaling, brassinosteroid and strigolactone signaling, and SA biosynthesis, respectively (van Verk *et al.*, 2011; Feng *et al.*, 2014; Wei *et al.*, 2016), were only induced by NO in plants that over-express RAP2.3 (Table A9). However, none of them contained RAP2.3-related motifs in their promoters (Table A7), thus suggesting the regulatory effects exerted by RAP2.3 should be not direct on those targets.

The second gene set, by far the greatest group, comprised genes that were up- or down-regulated in NO-treated plants only when *RAP2.3* was not over-expressed, thus suggesting RAP2.3 acted as a negative modulator of the NO-triggered regulation for those genes. Gene Ontology analyses of the genes comprised in this set pointed to the over-representation of the functional categories related to responses to chitin, JA, ABA, temperature, light and SA stimuli. Figure 4.36 shows that JA-related genes coding for biosynthetic and metabolic enzymes (*PLC7, PLDγ1, PLA1/LCAT3, LOX2, AOS/CYP74A, AOC2, OPR1, JAR1, SOT16, CYP94C3, CYP94B1*), for repressors and co-repressors of signaling (*JAZ1, JAZ3, JAZ12* and the NINJA-like AFP2, AFP3, AFP4) and for JA-responsive markers (*VSP1, VSP2, TAT3, JRG21, JR1, CORI3*) were all up-regulated by NO only when *RAP2.3* was not overexpressed, thus suggesting there is a complete JA biosynthesis and signaling pathway induced by NO and repressed by RAP2.3. Remarkably, only the *PLC7*, *LOX4* and *JAR1* jasmonate biosynthetic encoding genes, the latter key for the synthesis of the active form jasmonoyl-isoleucine (Staswick & Tiriyaki, 2004) contained (C/A)GCCG(C/T)(C/A) motifs in their promoters (Table A7). Moreover, as described above there is also a JA pathway, activated by NO independently of RAP2.3, that involve the function of the biosynthetic module comprised by LOX3, AOC1 or AOC3, OPR3, and the signaling module comprising the activator MYC2 and the repressors JAZ5, 6, 7 and 10 (Fig. 4.36 and Table A9). Noteworthy, despite being at principal regulated by NO independently of RAP2.3, the biosynthetic *AOC1* gene and the regulatory *MYC2* and *JAZ6* genes contained (C/A)GCCG(C/T)(C/A) motifs in their promoters (Table A7).

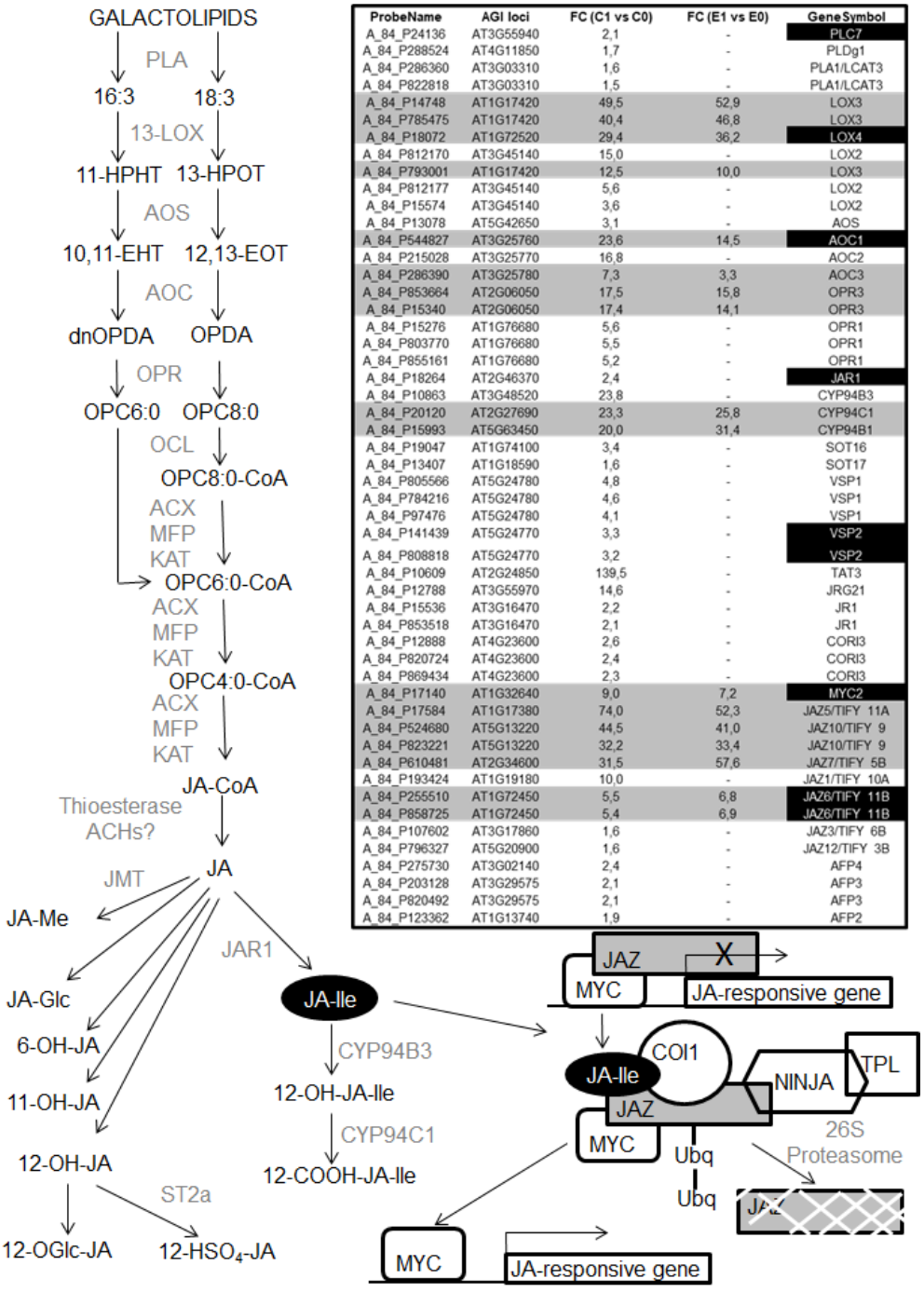

ProbeName	AGI loci	FC (C1 vs C0)	FC (E1 vs E0)	GeneSymbol
A_84_P24136	AT3G55940	2,1	-	PLC7
A_84_P288524	AT4G11850	1,7	-	PLDg1
A_84_P286360	AT3G03310	1,6	-	PLA1/LCAT3
A_84_P822818	AT3G03310	1,5	-	PLA1/LCAT3
A_84_P14748	AT1G17420	49,5	52,9	LOX3
A_84_P785475	AT1G17420	40,4	46,8	LOX3
A_84_P18072	AT1G72520	29,4	36,2	LOX4
A_84_P812170	AT3G45140	15,0	-	LOX2
A_84_P793001	AT1G17420	12,5	10,0	LOX3
A_84_P812177	AT3G45140	5,6	-	LOX2
A_84_P15574	AT3G45140	3,6	-	LOX2
A_84_P13078	AT5G42650	3,1	-	AOS
A_84_P544827	AT3G25760	23,6	14,5	AOC1
A_84_P215028	AT3G25770	16,8	-	AOC2
A_84_P286390	AT3G25780	7,3	3,3	AOC3
A_84_P853664	AT2G06050	17,5	15,8	OPR3
A_84_P15340	AT2G06050	17,4	14,1	OPR3
A_84_P15276	AT1G76680	5,6	-	OPR1
A_84_P803770	AT1G76680	5,5	-	OPR1
A_84_P855161	AT1G76680	5,2	-	OPR1
A_84_P18264	AT2G46370	2,4	-	JAR1
A_84_P10863	AT3G48520	23,8	-	CYP94B3
A_84_P20120	AT2G27690	23,3	25,8	CYP94C1
A_84_P15993	AT5G63450	20,0	31,4	CYP94B1
A_84_P19047	AT1G74100	3,4	-	SOT16
A_84_P13407	AT1G18590	1,6	-	SOT17
A_84_P805566	AT5G24780	4,8	-	VSP1
A_84_P784216	AT5G24780	4,6	-	VSP1
A_84_P97476	AT5G24780	4,1	-	VSP1
A_84_P141439	AT5G24770	3,3	-	VSP2
A_84_P808818	AT5G24770	3,2	-	VSP2
A_84_P10609	AT2G24850	139,5	-	TAT3
A_84_P12788	AT3G55970	14,6	-	JRG21
A_84_P15536	AT3G16470	2,2	-	JR1
A_84_P853518	AT3G16470	2,1	-	JR1
A_84_P12888	AT4G23600	2,6	-	CORI3
A_84_P820724	AT4G23600	2,4	-	CORI3
A_84_P869434	AT4G23600	2,3	-	CORI3
A_84_P17140	AT1G32640	9,0	7,2	MYC2
A_84_P17584	AT1G17380	74,0	52,3	JAZ5/TIFY 11A
A_84_P524680	AT5G13220	44,5	41,0	JAZ10/TIFY 9
A_84_P823221	AT5G13220	32,2	33,4	JAZ10/TIFY 9
A_84_P610481	AT2G34600	31,5	57,6	JAZ7/TIFY 5B
A_84_P193424	AT1G19180	10,0	-	JAZ1/TIFY 10A
A_84_P255510	AT1G72450	5,5	6,8	JAZ6/TIFY 11B
A_84_P858725	AT1G72450	5,4	6,9	JAZ6/TIFY 11B
A_84_P107602	AT3G17860	1,6	-	JAZ3/TIFY 6B
A_84_P796327	AT5G20900	1,6	-	JAZ12/TIFY 3B
A_84_P275730	AT3G02140	2,4	-	AFP4
A_84_P203128	AT3G29575	2,1	-	AFP3
A_84_P820492	AT3G29575	2,1	-	AFP3
A_84_P123362	AT1G13740	1,9	-	AFP2

Figure 4.36. Effect of NO and RAP2.3 on the expression of JA biosynthesis and signaling genes. The scheme shows the biosynthesis and signaling JA pathway and the table the fold change (FC) values for the different transcripts in the comparisons C1 vs C0 of plants not treated with β-estradiol at 1 or 0 h after exposure to NO, and E1 vs E0 for the corresponding β-estradiol-treated plants. Highlighted in grey are NO-regulated genes that were not significantly affected by RAP2.3 overexpression. Those highlighted in black contained putative RAP2.3 binding sites in their promoters.

Similarly, ABA-related biosynthetic and signaling genes were also included in this set. The biosynthetic *BCH1* and *ABA1* genes coding for β-carotene hydroxylase 1 and zeaxanthin epoxidase, respectively, and the metabolic *UGT71B6* gene coding for UDP-glucosyl transferase 71b6 were down- and up-regulated by NO, respectively, only in TPT_RAP2.3 plants that were not treated with β-estradiol (Fig. 4.37). Only the promoter of *UGT71B6* gene contained the (C/A)GCCG(C/T)(C/A) motif (Table A7). We also found that only some genes coding for regulatory components of the core ABA signaling were regulated by NO, and some of them were dependent and other independent of *RAP2.3* expression (Table A9). The ABA receptors PYL7 and PYL4 encoding genes were up-regulated by NO and this induction was repressed by RAP2.3 (Fig. 4.37 and Table A9). In turn, the gene coding for PYL5 receptor was strictly dependent on RAP2.3 over-expression for the NO-induced expression (Fig. 4.37 and Table A9). Finally, the PYL6 encoding gene was up-regulated by NO independently of RAP2.3 (Fig. 4.37 and Table A9). All together these data suggest that NO may control the ABA perception through gene-specific pathways controlled or not by RAP2.3. This sort of gene-specific regulatory effect can be also applied to the positive protein kinase regulators encoded for the *SnRK2* gene family. Only *SnRK2.3* and *SnRK2.9* were up-regulated by NO, being the induced expression of *SnRK2.3* abolished by RAP2.3 over-expression whereas *SnRK2.9* expression was not modulated by RAP2.3 (Fig. 4.37 and Table A9). Only the promoters of genes coding for the positive ABA regulators PYL7, SnRK2.3 and SnRK2.9 contained the (C/A)GCCG(C/T)(C/A) motif (Table A7). However, the existence of gene-specific branch pathways inside the ABA signaling process did not match with the expression pattern of ABA target genes coding for either signaling components or transcription factors, which were mostly up-regulated by NO through a RAP2.3-repressed mechanism (Fig. 4.37). Only the *SLAH2* and *AIB* genes coding for a nitrate-specific anion channel and an ABA-inducible bHLH-type transcription factor, respectively, were up-regulated by NO independently of RAP2.3 (Fig. 4.37 and Table A9). Moreover, we found (C/A)GCCG(C/T)(C/A) motifs in the promoter of genes such as *MYB51* and *LTI30* up-regulated by NO only in the absence of *RAP2.3* over-expression, but also in the *SLAH2* gene, which was up-regulated by NO independently of *RAP2.3* expression levels (Fig. 4.37 and Table A7). Thus our findings suggest that RAP2.3 exerted a very efficient repression of the NO-induced expression of ABA targets genes through either the direct regulation of key targets by binding the promoters containing (C/A)GCCG(C/T)(C/A) motifs or, alternatively, by regulating just some master ABA signaling component, likely coding for a transcription factor.

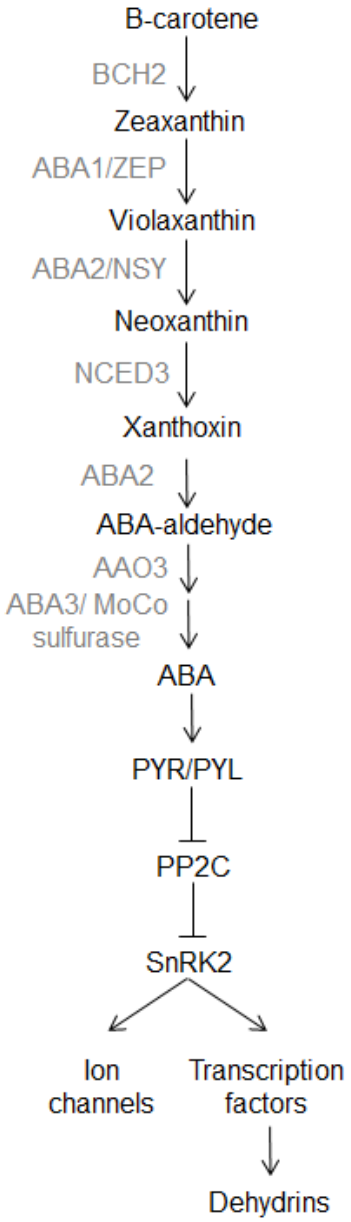

ProbeName	AGI loci	FC ([C1] vs [C0])	FC ([E1] vs [E0])	GeneSymbol
A_84_P763996	AT4G25700	-1,6	-	BCH1
A_84_P832189	AT5G67030	-1,5	-	ABA1
A_84_P20247	AT3G21780	3,0	-	UGT71B6
A_84_P174151	AT2G40330	4,5	5,5	PYL6
A_84_P20389	AT4G01026	2,4	-	PYL7
A_84_P816095	AT4G01026	2,3	-	PYL7
A_84_P197484	AT2G38310	2,2	-	PYL4
A_84_P146199	AT5G05440	-	3,4	PYL5
A_84_P852047	AT5G05440	-	3,3	PYL5
A_84_P817892	AT5G05440	-	3,3	PYL5
A_84_P12575	AT2G23030	3,6	2,7	SnRK2.9
A_84_P16007	AT5G66880	1,6	-	SnRK2.3
A_84_P159915	AT4G27970	5,9	2,4	SLAH2
A_84_P22976	AT2G36270	1,6	-	ABI5
A_84_P164953	AT1G49720	1,9	-	ABF1
A_84_P80879	AT2G46510	3,1	2,7	AIB
A_84_P151138	AT3G63210	-1,7	-	MARD1
A_84_P19130	AT2G46270	1,7	-	GBF3
A_84_P784302	AT1G01720	2,1	-	ATAF1
A_84_P19986	AT1G01720	2,1	-	ATAF1
A_84_P14948	AT5G37260	2,0	-	RVE2
A_84_P18334	AT3G06490	4,9	-	MYB108
A_84_P19074	AT1G18570	3,0	-	MYB51
A_84_P17577	AT1G06180	1,9	-	MYB13
A_84_P14542	AT3G09600	-1,6	-	RVE8
A_84_P860855	AT3G19580	2,4	-	ZF2
A_84_P21219	AT3G19580	2,1	-	ZF2
A_84_P18822	AT5G61420	-2,3	-	MYB28
A_84_P22292	AT4G04020	-2,3	-	FIB
A_84_P79549	AT3G26090	1,6	-	RGS1
A_84_P23251	AT4G09570	1,8	-	CPK4
A_84_P18763	AT5G45820	-1,8	-	CIPK20
A_84_P21126	AT2G32020	3,9	-	GCN5-related
A_84_P853160	AT3G11820	3,0	-	SYP121
A_84_P15485	AT3G11820	2,7	-	SYP121
A_84_P810688	AT5G15960	1,7	-	KIN1
A_84_P258350	AT5G15970	1,9	-	KIN2
A_84_P15372	AT2G38750	1,7	-	ANNAT4
A_84_P10874	AT3G50970	3,5	-	LTI30
A_84_P21026	AT2G33380	1,8	-	RD20
A_84_P22571	AT5G52310	1,8	-	LTI78
A_84_P809384	AT1G76180	1,6	-	ERD4
A_84_P809423	AT1G76180	1,6	-	ERD4
A_84_P12888	AT4G23600	2,6	-	CORI3
A_84_P820724	AT4G23600	2,4	-	CORI3
A_84_P869434	AT4G23600	2,3	-	CORI3

Figure 4.37. Effect of NO and RAP2.3 on the expression of ABA biosynthesis and signaling genes. The scheme shows the biosynthesis and signaling ABA pathway and the table the fold change (FC) values for the different transcripts in the comparisons C1 vs C0 of plants not treated with β-estradiol at 1 or 0 h after exposure to NO, and E1 vs E0 for the corresponding β-estradiol-treated plants. Highlighted in grey are NO-regulated genes that were not significantly affected by RAP2.3 overexpression. Those highlighted in black contained putative RAP2.3 binding sites in their promoters.

4.4. Role of NO in constitutive and cold acclimation induced freezing tolerance

This section 4.4 is composed by excerpts from the research articles: "Costa-Broseta, Á., Perea-Resa, C., Castillo, M. C., Ruíz, M. F., Salinas, J., & León, J. (2018). Nitric Oxide Controls Constitutive Freezing Tolerance in Arabidopsis by Attenuating the Levels of Osmoprotectants, Stress-Related Hormones and Anthocyanins. Scientific Reports, 8(1), 9268" and "Costa-Broseta, Á., Perea-Resa, C., Castillo, M. C., Ruíz, M. F., Salinas, J., & León, J. (2018). Nitric Oxide Deficiency Reduces CBF *Induction, ABA Signaling, Anthocyanin Synthesis and Cold Acclimation in Arabidopsis". The second of these research articles was submitted to Journal of Experimental Botany and was under revision when PhD Thesis writing was finished. All the results and figures that appear here are derived from the work of the PhD student in collaboration with the other authors.*

4.4.1. Abstract (1)

Plant tolerance to freezing temperatures is governed by endogenous constitutive components and environmental inducing factors. Nitric oxide (NO) is one of the endogenous components that participate in freezing tolerance regulation. A combined metabolomic and transcriptomic characterization of NO-deficient *nia1,2noa1-2* mutant plants suggests that NO acts attenuating the production and accumulation of osmoprotective and regulatory metabolites, such as sugars and polyamines, stress-related hormones, such as ABA and jasmonates, and antioxidants, such as anthocyanins and flavonoids. Accordingly, NO-deficient plants are constitutively more freezing tolerant than wild type plants.

4.4.2. The transcriptome of NO-deficient *nia1,2noa1-2* mutant plants is enriched in cold-related transcripts

We previously reported that *nia1,2noa1-2* mutant plants, carrying mutations in both NIA1 and NIA2 nitrate reductases, as well as in the NO-Associated 1 (NOA1) protein, accumulated very low levels of endogenous NO under control and stressed conditions (Lozano-Juste & León, 2010). The strong NO deficiency of the mutant plants correlated with hypersensitivity to ABA in seed germination, stomata closure and tolerance to dehydration (Lozano-Juste & León, 2010). Intriguingly, our transcriptome analysis of *nia1,2noa1-2* mutants grown at 20ºC (GEO identification number GSE41958) (Gibbs *et al.*, 2014a) revealed that around 20% (88/465) of the genes that were up-regulated in the mutant compared to wild-type plants (>2-fold; FDR<0.05) had been related to cold responses (Lee *et al.*, 2005; Kilian *et al.*, 2007). Among those genes (Table A8), some coded for Late Embryogenesis Abundant (LEA) proteins and for transcription factors belonging to the ERF/DREB, Zinc finger and WRKY families. Cold-induced *BCH2* and *NCED3* genes, encoding β-carotene hydroxylase 2 and 9-cis-epoxycarotenoid dioxygenase 3 enzymes involved in ABA biosynthesis, as well as *LOX4* and *OPR1* coding for jasmonate

biosynthesis enzymes were also up-regulated in NO-deficient plants (Table A8). ABA and jasmonates have been reported to positively regulate freezing tolerance in Arabidopsis (Hu *et al.*, 2013; Lee & Seo, 2015). Furthermore, a Gene Ontology analysis performed with the *Arabidopsis thaliana* dataset of the Gene Ontology Consortium (http://www.geneontology.org/) showed that 7 out of 19 and 15 out of 67 genes (20- and 12-fold enrichment with p-values of 2.51E-04 and 1.71E-08) involved in the anthocyanin and flavonoid metabolism functional categories, respectively, were up-regulated in the NO-deficient mutant plants. Accordingly, we found the anthocyanin and flavonoid biosynthesis and metabolism genes *CHS*, *F3´H/TT6*, *DFR/TT3*, *PAP1/MYB75* and *UF3GT* among the cold-induced genes that were up-regulated in *nia1,2noa1-2* plants (Table A8). In addition, genes coding for SUS3, SSP2, and ADC2 enzymes involved in the biosynthesis of sugars and polyamines, respectively, were among the cold-inducible genes up-regulated in NO-deficient plants (Table A8). Sugars and polyamines had been reported to enhance plant-freezing tolerance (Kasukabe *et al.*, 2004; Guy *et al.*, 2008; Korn *et al.*, 2008). To assess the robustness of the over-representation of cold-inducible genes detected in our transcriptomic analysis, the expression levels of 11 cold-induced genes, including *ADH1*, *ZAT10*, *NCED3*, *HAI1*, *SnRK2.9*, *LEA7*, *LEA4-5*, *LTI65*, *PAP1/MYB75* , *DFR* and *CYP707A3*, were determined by RT-qPCR in independent RNA samples from the triple *nia1,2noa1-2* mutant and Col-0 plants grown at 21 ºC. In all cases, the transcript levels were significantly higher in mutant than in wild-type plants (Fig. 4.38), thus validating the microarray data. These observations indicated that, under control conditions, NO functions as a negative regulator of cold-induced gene expression in Arabidopsis.

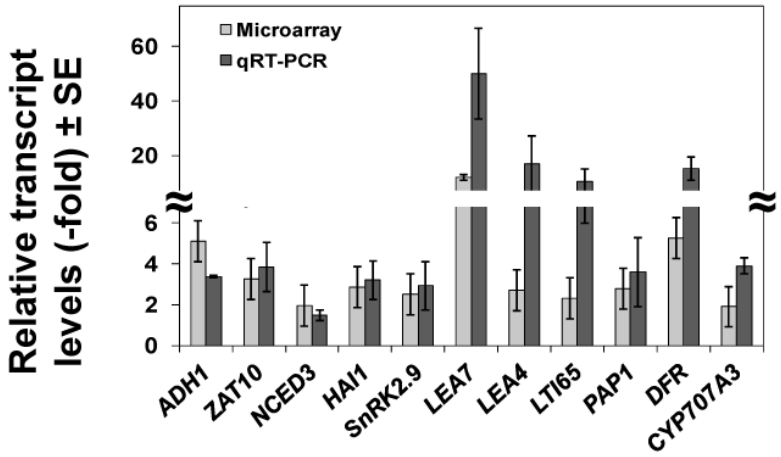

Figure 4.38. Levels of cold-inducible transcripts in Col-0 and *nia1,2noa1-2* plants. Comparative transcript analysis based on microarray data and RT-qPCR of wild-type Col-0 and NO-deficient *nia1,2noa1-2* plants. Ratio (*nia1,2noa1,2*/Col-0) values of RT-qPCR analysis are the mean of three independent biological replicates ± standard deviation.

4.4.3. Enhanced biosynthesis of ABA, JA and osmoprotective metabolites in NO-deficient plants

Data from microarray analyses strongly suggested that NO-deficient mutants should have increased levels of ABA, JA, anthocyanins, flavonoids, sugars and polyamines. Ultra Performance Liquid Chromatography-Mass Spectrometry analysis confirmed that, in fact, the levels of ABA and JA were around 2-fold higher in *nia1,2noa1-2* than in wild-type plants (Fig. 4.39A). On the other hand, a combination of GC-MS and LC-MS techniques allowed quantifying 180 biochemicals including amino acids, carbohydrates, lipids, cofactors and prosthetic groups, nucleotides and secondary metabolites in wild-type and NO-deficient mutant plants (Table S2, which can be found in Costa-Broseta *et al.*, 2018). As expected from the microarray data, the endogenous levels of flavonoids, anthocyanins, polyamines and sugars were significantly higher in mutant than in wild-type plants (Fig. 4.39B-D). The content of the flavonoids/anthocyanins dihydrokaempferol and naringenin in mutant plants were around 6- and 2-fold higher than in wild-type plants, respectively (Fig. 4.39B Table S2 in Costa-Broseta *et al.*, 2018). Similarly, the polyamines agmatine and putrescine were around 30- and 14-fold higher, respectively, in mutant than in wild-type plants (Fig. 4.39C; Table S2 in Costa-Broseta *et al.*, 2018). Finally, the levels of glucose, glucose-1-phosphate, glucose-6-phosphate, sucrose, fructose and maltose were increased from 2- to 18-fold in *nia1,2noa1-2* when compared to wild-type plants (Fig. 4.39D; Table S2 in Costa-Broseta *et al.*, 2018). As shown in Figure 4.40A, the increased levels of polyamines correlated with reduced content of arginine and ornithine and increased levels of citrulline. On the other hand, the increased levels of sugars in *nia1,2noa1-2* plants reflected a general accumulation of glycolisis metabolites and phosphoglycerate-derived amino acids of the serine family (Fig. 4.40B). In turn, metabolites of the tricarboxylic acids (TCA) cycle were significantly less abundant in *nia1,2noa1-2* than in wild-type plants (Fig. 4.40B). Accordingly, the levels of α-ketoglutarate-derived amino acids of the glutaminate synthetase-glutamine oxoglutarate aminotransferase (GS-GOGAT) cycle were also lowered in *nia1,2noa1-2* plants (Fig. 4.40B), likely as a reflection of the impaired nitrate assimilation of the mutant plants. In summary, NO seems to exert a metabolic brake in the production of ABA, JA, anthocyanins, flavonoids, sugars and polyamines under standard conditions.

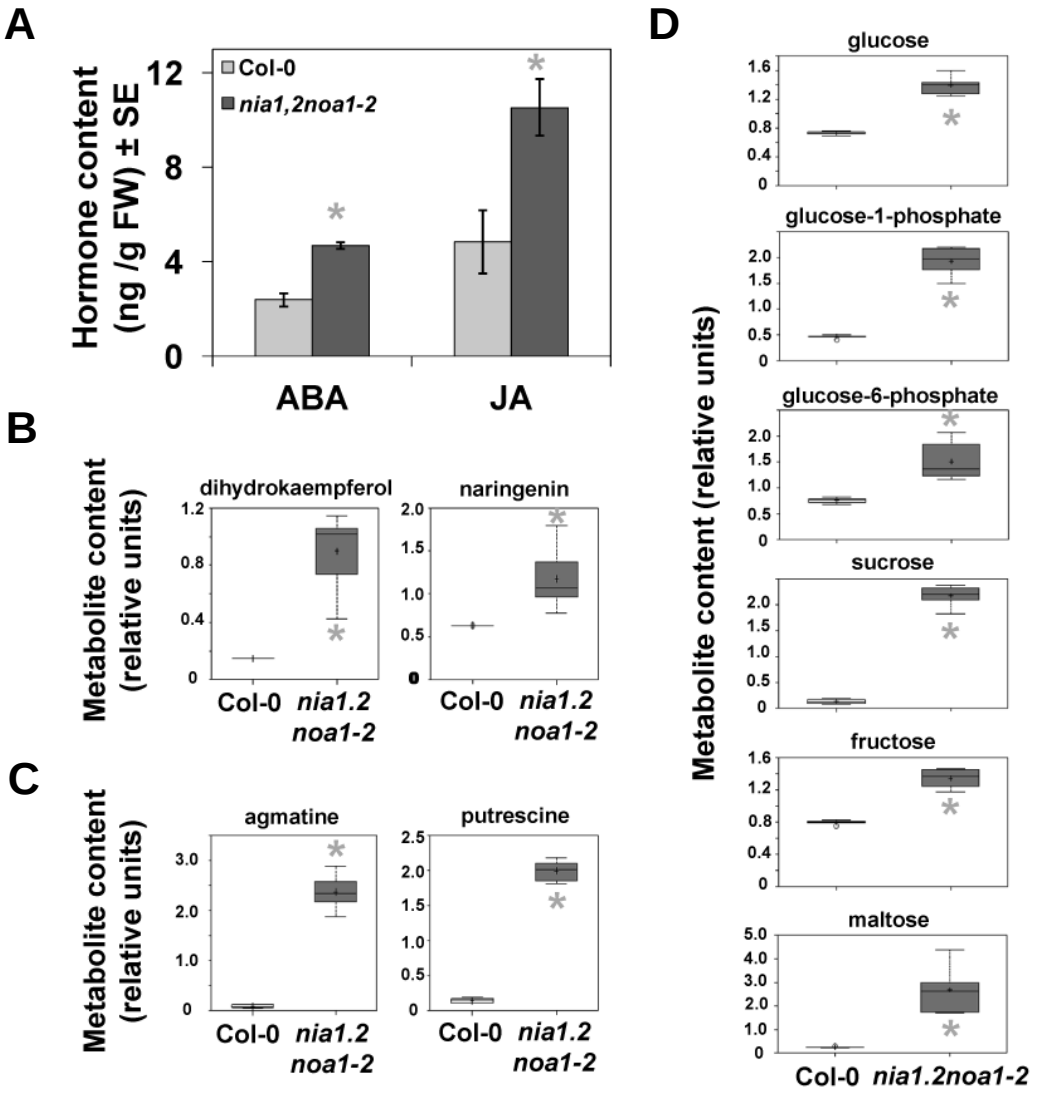

Figure 4.39. Levels of hormones and osmoprotective metabolites in Col-0 and *nia1,2noa1-2* plants. A, Quantification of ABA and JA, B, flavonoids / anthocyanins, C, polyamines, and D, sugars, was performed by GC- and LC-mass spectrometry. Hormone content values represent the mean values of four independent biological replicate samples for each genotype ± standard error. * indicates significantly different with p-value < 0.05 in Student´s t-test. For the metabolomic analyses of the other metabolites, Welch's two-sample t-test was used to identify biochemicals that differed significantly between experimental groups. An estimate of the false discovery rate (q-value) was calculated to take into account the multiple comparisons.

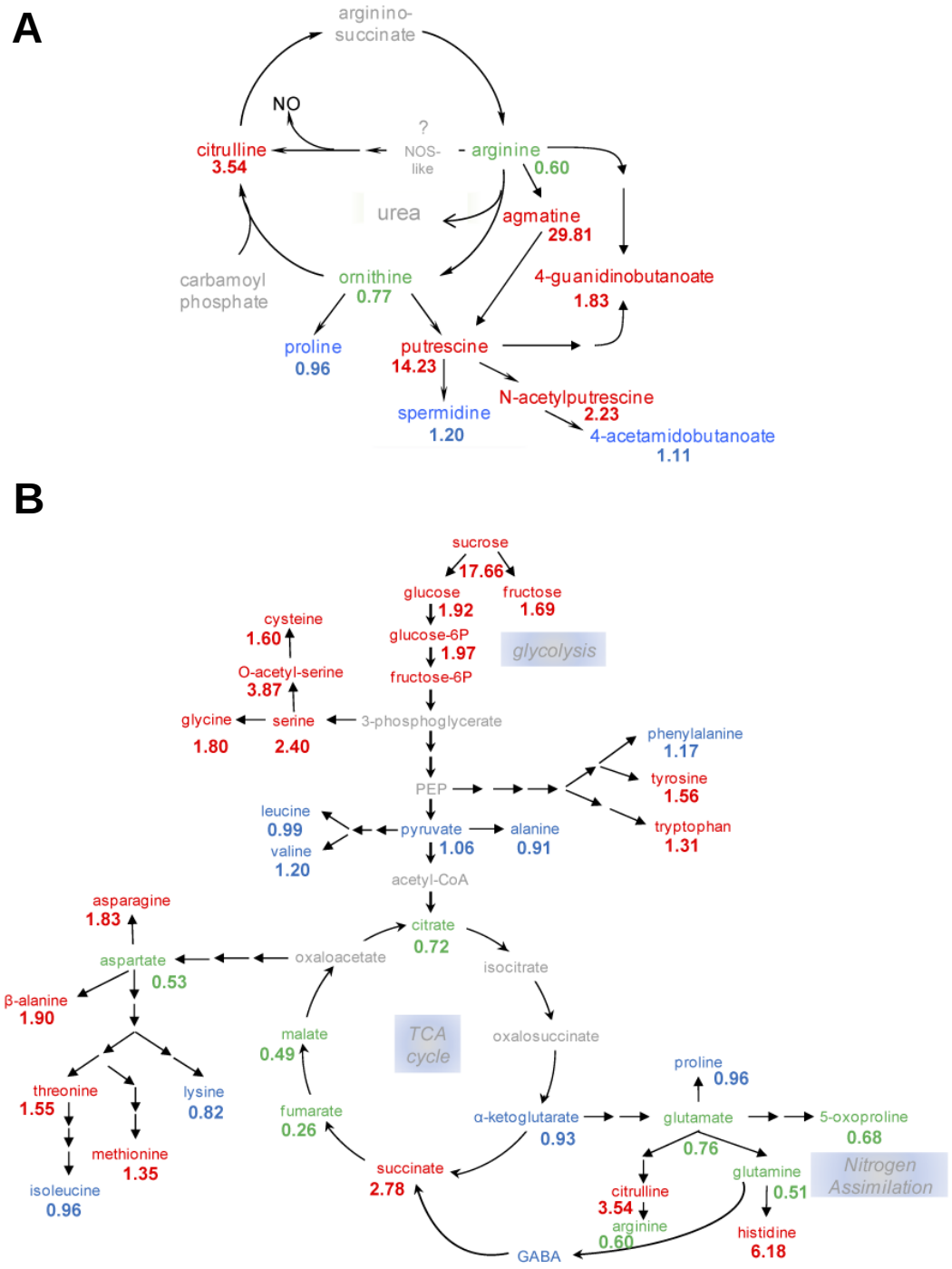

Figure 4.40. Glycolysis and TCA cycle metabolite ratios between *nia1,2noa1-2* and Col-0 plants. Metabolites in red and green were significantly more or less abundant in *nia1,2noa1-2* than in Col-0 plants, respectively. Metabolites in blue were not significantly changed. Values indicated for each metabolite are the mean of six independent replicates performed in the complete metabolomic analyses described in Table S2 in Costa-Broseta *et al.*, 2018.

4.4.4. Increased levels of antioxidant metabolites in *nia1,2noa1-2* plants

As shown in Table S2 (Costa-Broseta *et al.*, 2018), the ascorbate and oxidized glutathione (GSSG) were both elevated in *nia1,2noa1-2* plants. Moreover, other metabolites with antioxidant activity such as the flavonoids dihydrokaempferol and naringenin (Fig. 4.39B) as well as sinapate (Table S2 in Costa-Broseta *et al.*, 2018) accumulated also in NO-deficient plants. We also found around 3-fold accumulation of the oxylipins 9-hydroxyoctadecadienoic acid (9-HODE) and 13-hydroxyoctadecadienoic acid (13-HODE) (Table S2 in Costa-Broseta *et al.*, 2018), which can be synthesized enzymatically by lipoxygenases but also non-enzymatically from ROS (Berger *et al.*, 2001), and are considered good markers of oxidative stress (Yoshida *et al.*, 2013). These data strongly suggested that NO-deficient *nia1,2noa1-2* mutant plants were subjected to constitutive oxidative stress. Under those conditions, the ascorbate-glutathione cycle is in charge of detoxifying reactive oxygen species. As shown in Figure 4.41, the increased levels of ascorbate and oxidized glutathione were accompanied by significant increases of glutathione precursors, such as methionine, S-adenosylhomocysteine, cysteine and glycine, as well as by a reduced content of nitrogen-related amino acids including glutamate, glutamine and aspartate.

4.4.5. NO negatively regulates constitutive freezing tolerance of Arabidopsis

The results described above strongly suggested that NO should have a negative role in the constitutive freezing tolerance of Arabidopsis. To test this possibility, we analyzed the constitutive freezing tolerance of 2-week-old wild-type and *nia1,2noa1-2* plants. Freezing tolerance was determined as the percentage of surviving plants after exposure to different freezing temperatures for 6 h. Figure 4.42A shows that triple *nia1nia2noa1-2* mutant plants displayed significantly greater freezing tolerance than did wild-type plants, the LT_{50} (temperature that causes 50% lethality) value being -5.6ºC and -4.5 ºC, respectively. However, the double *nia1nia2* mutant plants (LT_{50} -4.6 ºC) were not significantly different than wild type plants and the single *noa1-2* mutant plants were slightly more tolerant (LT_{50} -4.8 ºC) than wild type plants. Despite *nia1,2noa1-2* plants being slightly delayed in their development compared to Col-0 plants, the increased freezing tolerance manifested by the mutant with respect to the wild-type plants was very apparent (Fig. 4.42B). The endogenous NO levels of wild type and mutant plants were measured by staining with the NO-specific fluorophore staining DAF-FM DA and we found that, as expected, *nia1,2noa1-2* plants contained significantly less NO than Col-0 plants (Fig. 4.42C). These results demonstrated that NO negatively regulates constitutive freezing tolerance in Arabidopsis, in all likelihood, by controlling the levels of osmoprotectant, hormones and redox metabolites.

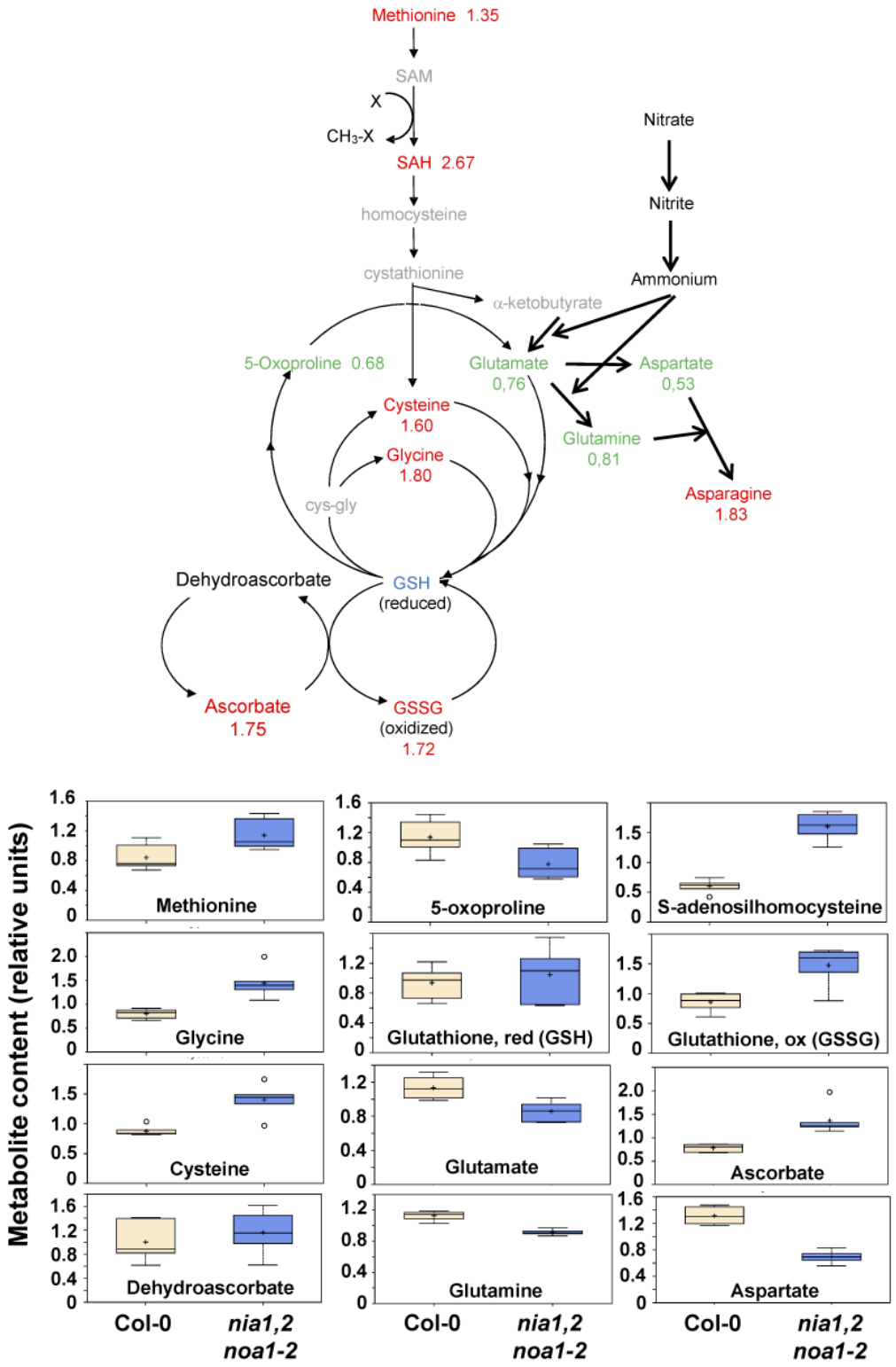

Figure 4.41. Endogenous content of ascorbate-glutathione cycle metabolites in wild type and NO-deficient plants. A diagram of the ascorbate-glutathione cycle is shown at top of the figure. Metabolites in red and green were significantly more or less abundant in *nia1,2noa1-2* than in Col-0 plants, respectively. The box plots corresponding to the metabolites significantly different in both genotypes are shown in the bottom part of the figure. Values indicated for each metabolite are the mean of six independent replicates performed in the complete metabolomic analyses described in Table S2 in Costa-Broseta *et al.*, 2018.

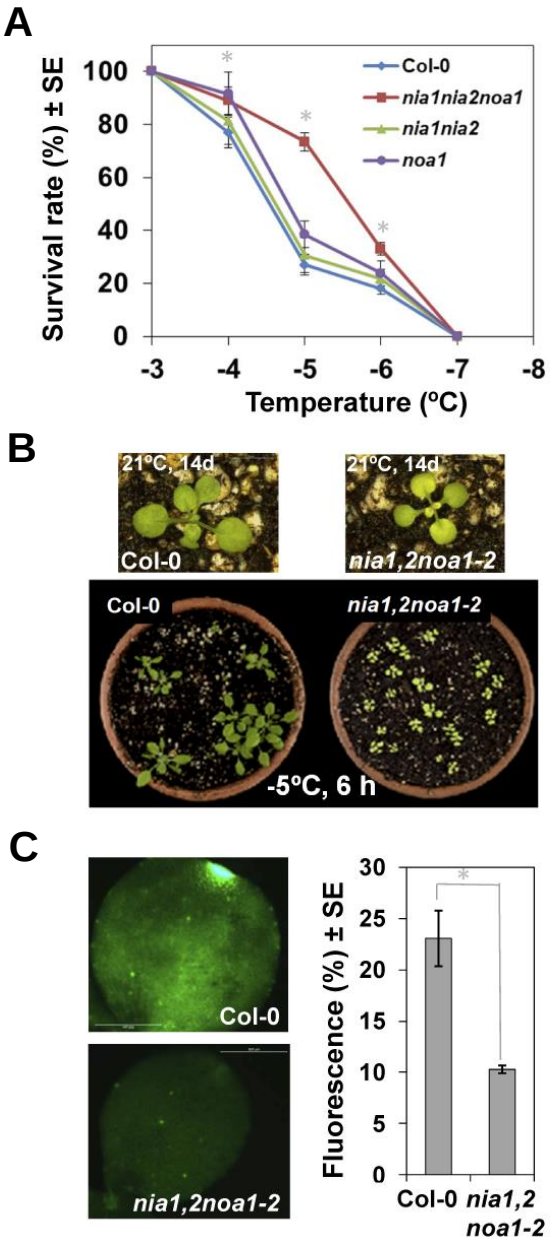

Figure 4.42. Constitutive freezing tolerance of Col-0 and *nia1,2noa1-2* plants. A, Freezing tolerance of 2-week-old plants exposed for 6 h to the indicated freezing temperatures was estimated as the percentage of plants surviving each specific temperature after 7 d of recovery under control conditions at 21ºC. Data are expressed as means of three independent experiments with around 50 plants each indicated genotype ± standard deviation. Asterisks indicate significant differences between *nia1,2noa1-2* and wild-type plants (p-value < 0.05). b, Upper panels show individual plants of wild type and mutant genotypes before freezing to show the difference in size. The bottom panel shows a representative image of plants from both genotypes after freezing at -5ºC and recovery at standard growing temperature for additional 7 days. C, NO levels in Col-0 and *nia1,2noa1-2* plants. Plants were maintained at standard growing conditions for 14 days. The fluorescence of DAF-FM DA-treated plants was detected by confocal microscopy. Shown images are representative of four to six different analyzed plants per genotype and condition, and the quantification values are the mean ± standard error. * indicates significant differences between *nia1,2noa1-2* and wild-type plants (p-value < 0.05).

4.4.6. Abstract (2)

Plant tolerance to freezing temperatures is governed by endogenous components and environmental inducing factors. Exposure to low non-freezing temperatures has been characterized as the main exogenous factor inducing freezing tolerance in a process named cold acclimation. To define the role of nitric oxide (NO) in cold acclimation, we have used triple *nia1,2noa1-2* mutant plants that have impaired not only the nitrate-dependent but also the nitrate-independent NO production, and are thus severe NO-deficient plants. We demonstrate that the cold-induced accumulation of NO is essential to promote full cold acclimation response through the up-regulation of *C-repeat Binding Factor* (*CBF*) gene expression, the perception and signaling of ABA, and the cold-induced production of anthocyanins. Our results reveal ABA perception and signaling as well as anthocyanin production as new relevant factors in the NO-regulated capacity of plants to cold acclimate.

4.4.7. NO functions as a positive regulator of cold acclimation in Arabidopsis

The accumulation of large amounts of NO in Arabidopsis during cold acclimation was previously reported (Zhao *et al.*, 2009; Cantrel *et al.*, 2011). We also found that after cold-acclimation for 7 days at 4ºC, wild-type leaves accumulated 16-fold more NO than non-acclimated leaves (Fig. 4.43). In turn, the levels of NO in triple *nia1,2noa1-2* mutant leaves subjected to the same conditions accumulated only less than 4-fold compared to that in non-acclimated leaves (Fig.

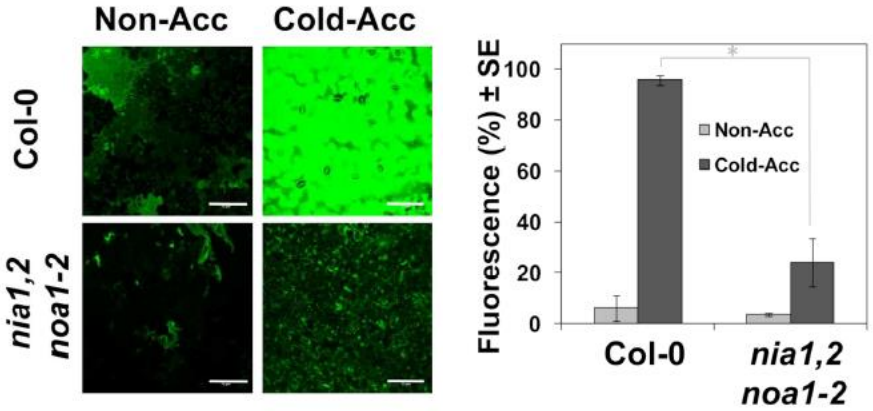

Figure 4.43. NO levels in cotyledons of Col-0 and *nia1,2noa1-2* plants after cold acclimation. Plants were either maintained at standard growing conditions (Non-Acc) or cold acclimated at 4ºC (Cold-Acc) for 7 days. The fluorescence of DAF-FM DA-treated plants was detected by confocal microscopy. Shown images are representative of four to six different analyzed plants per genotype and condition, and the quantification values are the mean ± standard error. * indicates significant differences between *nia1,2noa1-2* and wild-type plants (p-value < 0.05). Scale bars correspond to 25 µm.

4.43). We did not find significant changes in the NO content at shorter times of cold treatment, when full cold acclimation has still not been fully accomplished (Fig. 4.44).

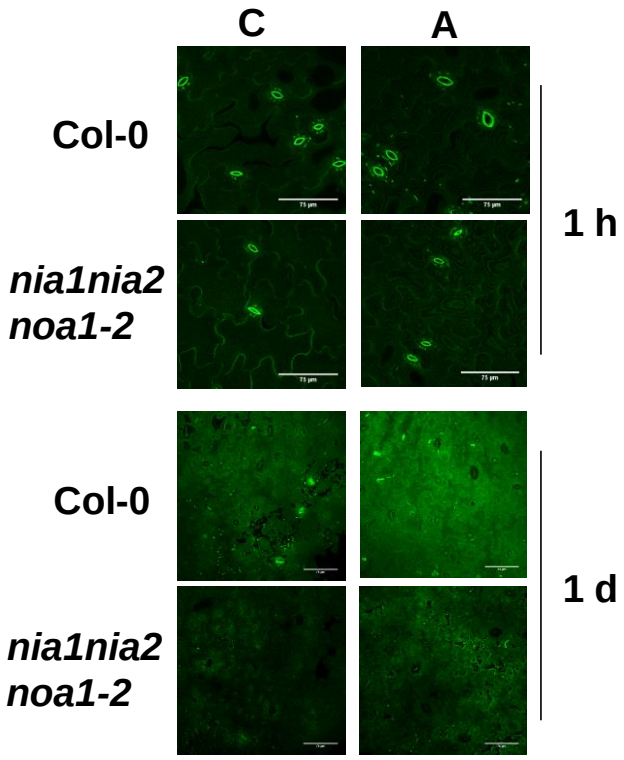

Figure 4.44. NO levels in Col-0 and *nia1,2noa1-2* plants at different times after cold treatment. Plants were grown in soil under standard conditions long day photoperiod light conditions and 21ºC for 14 d, and then, treated with the specific NO stain DAF-FM DA for 1h under darkness. After extensive washings, plants were transferred to 4ºC (A) or kept at 21ºC as control (C) under similar light regime for the indicated times in the right sides of panels. Green fluorescence was visualized with confocal microscopy (40x) of stained cotyledons. Shown images are representative of four to six different analyzed plants per genotype and condition.

Given the remarkable low levels of NO that the triple mutant accumulated in response to 4ºC we decided to determine its capacity to cold acclimate. The analysis of the freezing tolerance of cold acclimated (7d, 4ºC) Col-0 and NO-deficient *nia1,2noa1-2* plants revealed significant differences. As previously reported (Lozano-Juste & León, 2010), *nia1,2noa1-2* plants display smaller size than Col-0 plants when growing under control conditions but both retarded their growth upon exposure at 4ºC (Fig. 4.45A). Freezing tolerance was determined as the percentage of surviving plants after exposure to different freezing temperatures for 6 h. Cold-acclimated mutant plants exhibited significantly lower capacity to tolerate freezing temperatures than cold-acclimated wild-type plants, the LT_{50} being -8.3ºC and -9.8ºC, respectively (Fig. 4.45B). These results indicated that NO plays a positive role in Arabidopsis cold acclimation and also that is required for full development of this adaptive process. However, the defective nitrogen assimilation

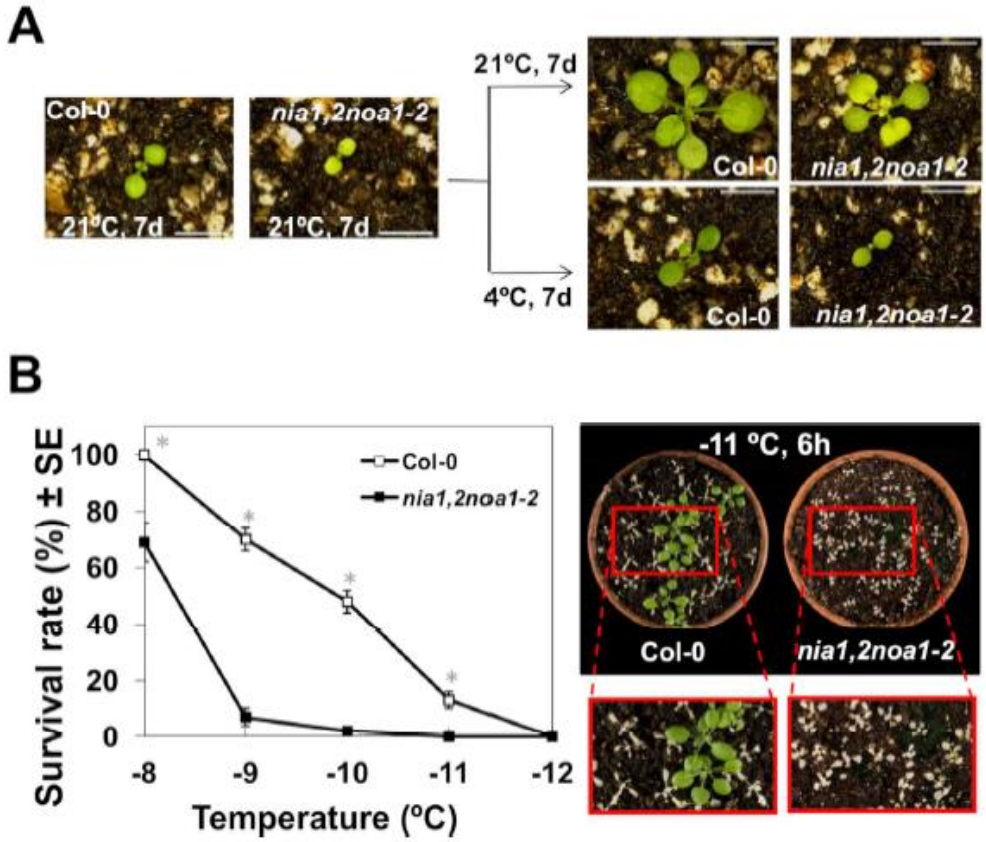

Figure 4.45. Cold acclimation-induced freezing tolerance of Col-0 and *nia1,2noa1-2* plants. A, Panels show representative individual plants of wild type and mutant genotypes grown under standard conditions for 7 d before being shifted to 4ºC for additional 7 d (cold-acclimated) or kept for 7 d more at 21ºC (non-acclimated as control). B, Freezing tolerance of 2-week-old plants exposed for 6 h to the indicated freezing temperatures after being acclimated for 7 d at 4°C. In all cases, freezing tolerance was estimated as the percentage of plants surviving each specific temperature after 7 d of recovery under control conditions at 21ºC. Data are expressed as means of three independent experiments with around 50 plants each ± standard deviation. * indicates significant differences between *nia1,2noa1-2* and wild-type plants (p-value < 0.05). The right panel in B shows a representative image of plants from both genotypes after cold acclimation, freezing and recovery at standard growing temperature for additional 7 days. Close-up images corresponding to the framed areas are included. Scale bars correspond to 5 mm in panel A.

of *nia1,2noa1-2* plants could also be responsible of their reduced cold acclimation-induced freezing tolerance. Regarding this, we have observed that wild type shoots produced more NO when growing in nitrate-containing media than when growing on nitrite or ammonium as unique N sources, or subjected to N starvation (Fig 4.46). This enhanced NO production in nitrate-grown plants was dependent on nitrate reductase activity as it was not detected in *nia1,2* mutant plants (Fig. 4.46).

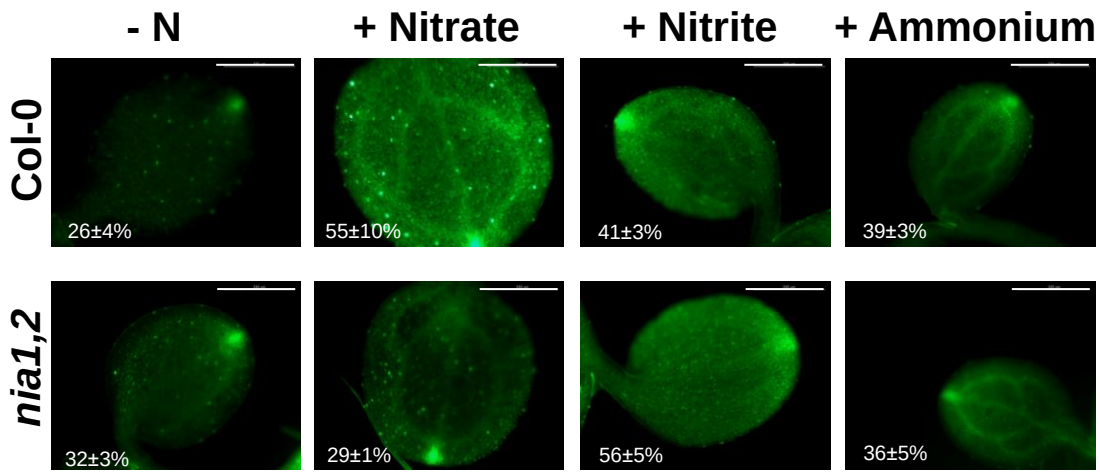

Figure 4.46. Effect of different nitrogen sources on NO production. The NO content was visualized by staining with DAF-FM DA in wild type Col-0 and *nia1,2* seedlings grown in MS media depleted of N (-N), or supplemented with 5 mM of nitrate, 5 mM of nitrite or 2.5 mM of ammonium as indicated as unique nitrogen sources. Quantification of fluorescence is shown as the mean of at least 3 replicate experiments ± standard error. Size bars represent 100 µm.

4.4.8. NO promotes the cold-induced expression of *CBF* genes in Arabidopsis

As already mentioned, the process of cold acclimation involves many physiological and biochemical changes, most of them being controlled by low temperature through changes in gene expression (Knight & Knight, 2012). In Arabidopsis, different signaling pathways have been identified that regulate these changes. The best characterized and, likely, the most relevant is the pathway mediated by the CBFs, a small family of transcription factors (CBF1-3) whose corresponding transcripts accumulate transiently in response to low temperature (Medina *et al.*, 2011; Knight & Knight, 2012). We, therefore, analyzed if the impaired ability to cold acclimate of *nia1,2noa1-2* plants might be due to a reduced cold induction of the *CBF* genes. Figure 4.47A shows that, after 6h of exposure to 4ºC, the induction of *CBF1*, *2* and *3* in *nia1,2noa1-2* was significantly lower than in wild-type plants. This defective induction was specially accentuated in the case of *CBF1* gene. Accordingly, *COR15A, LTI65* and *LTI78* genes, which are well characterized targets of CBFs (Thomashow, 1999), were significantly less induced upon cold treatment in *nia1,2noa1-2* than in Col-0 plants (Fig. 4.47B). NO thus functions as a positive regulator of cold acclimation likely by promoting the cold-induced expression of *CBF* genes and their corresponding gene targets.

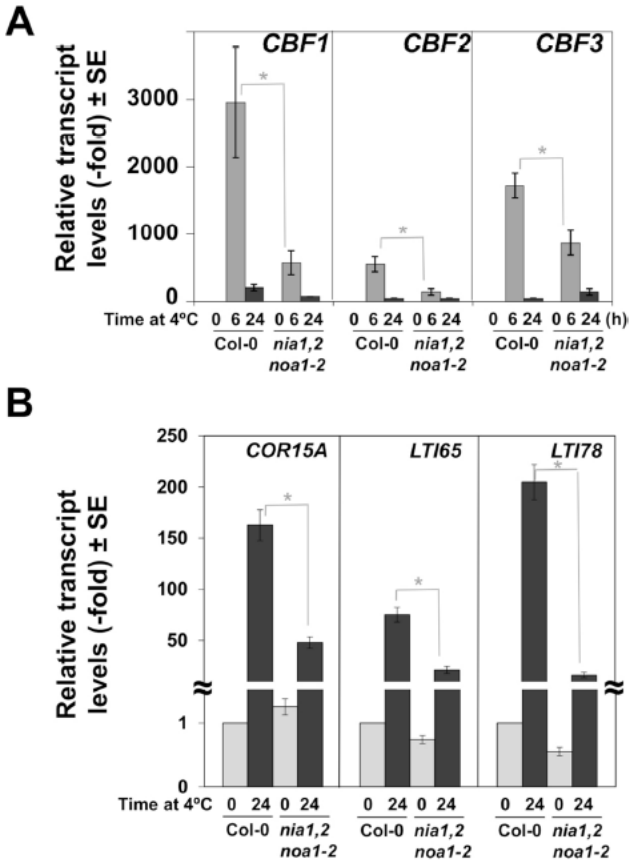

Figure 4.47. Effects of cold acclimation on the *CBFs* and their targets in Col-0 and *nia1,2noa1-2* plants. A, *CBF1*, *CBF2, CBF3* and B, *COR15A, LTI65* and *LTI78* transcript levels were quantified by RT-qPCR from total RNAs isolated from plants of the genotype and time of 4ºC incubation indicated. Values are the mean of three independent biological replicate samples for each genotype and condition ± standard error. * indicates significantly different with p-value ≤ 0.05 in Student´s t-test.

4.4.9. NO regulates the sensitivity of Arabidopsis to ABA in response to low temperature

Phytohormones have also been reported to play important roles in regulating the cold acclimation process in Arabidopsis (Eremina *et al.*, 2016a). In particular, ABA is essential for the adequate development of this adaptive response as evidenced by the fact that low temperature induces increased levels of ABA, and also because ABA-deficient and -insensitive mutants of Arabidopsis are defective in cold acclimation (Nakashima *et al.*, 2014; Ding *et al.*, 2015). To assess whether NO could regulate cold acclimation in Arabidopsis by controlling ABA levels or ABA sensitivity, we first measured the levels of ABA in *nia1,2noa1-2* mutants and wild-type plants after 24 h exposure to 4ºC. Both wild type and NO-deficient plants increased their ABA content and reached values that were not significantly different after exposure to low temperature (Fig. 4.48A), suggesting that ABA homeostasis was not significantly altered in NO-deficient plants during the cold acclimation process. Then, we examined the capacity of *nia1,2noa1-2* mutants to correctly sense and signal ABA by analyzing the levels of different ABA-related signaling

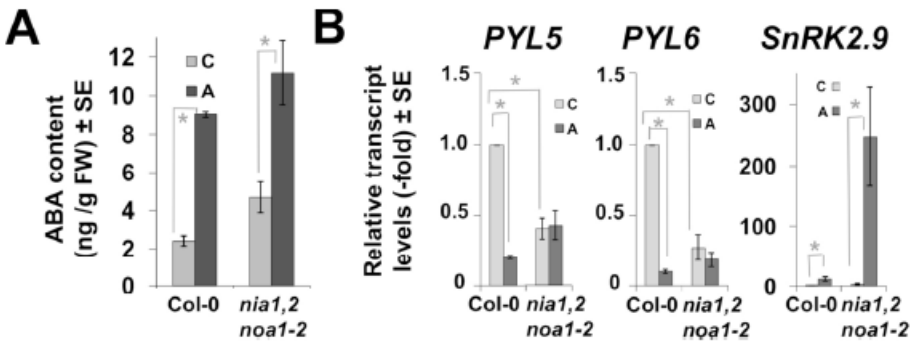

Figure 4.48. ABA homeostasis and signaling in cold acclimated wild-type and NO-deficient plants. A, Quantification of ABA in control non-acclimated C, and cold-acclimated A Col-0 and *nia1,2noa1-2* plants. Values represent the mean values of four independent biological replicate samples for each genotype and condition ± standard error. B, The transcript levels of the ABA signaling genes *PYL5, PYL6* and *SnRK2.9* were quantified by RT-qPCR from three independent total RNAs isolated from plants by 24 h of 4ºC incubation. Values are the mean of three independent biological replicate samples for each genotype and condition ± standard error. * indicates significantly different with p-value ≤ 0.05 in Student´s t-test.

transcripts. As shown in Figure 4.48B, the transcripts of two closely related genes coding for the ABA receptors PYL5 and PYL6 were strongly down-regulated in response to low temperature in wild-type plants. In turn, no such repression was observed in the *nia1,2noa1-2* plants, which indeed showed levels in control plants comparable to those detected under cold conditions in Col-0 plants (Fig. 4.48B). Moreover, the levels of *SnRK2.9* transcripts in *nia1,2noa1-2* plants were more than 20-fold higher than in Col-0 plants after cold treatment (Fig. 4.48B). These findings, together with the ABA hypersensitive phenotype we previously reported for *nia1,2noa1-2* plants (Lozano-Juste & León, 2010), strongly suggested that NO acts on ABA perception and signaling more than in ABA homeostasis to regulate cold acclimation.

4.4.10. NO activates anthocyanin accumulation in Arabidopsis during cold acclimation

It is well documented that, in response to low temperature, anthocyanins accumulate to protect photosystems from photoinhibition, avoiding the concentration of high levels of reactive oxygen species (Krol *et al.*, 1995; Korn *et al.*, 2008; Schulz *et al.*, 2016). Consistent with these results, it has been described that the expression of genes coding for critical enzymes in the anthocyanin and flavonoid biosynthetic pathway were induced by low temperature, and that the accumulation of these pigments was required to ensure full development of cold acclimation in Arabidopsis (Catala *et al.*, 2011; Schulz *et al.*, 2016). Hence, we analyzed the content of anthocyanins in *nia1,2noa1-2* and Col-0 plants after being subjected to 4ºC for 7 days. As shown in Figure 4.49A, wild-type plants increased their anthocyanin content more than 4-fold in response to low temperature. In

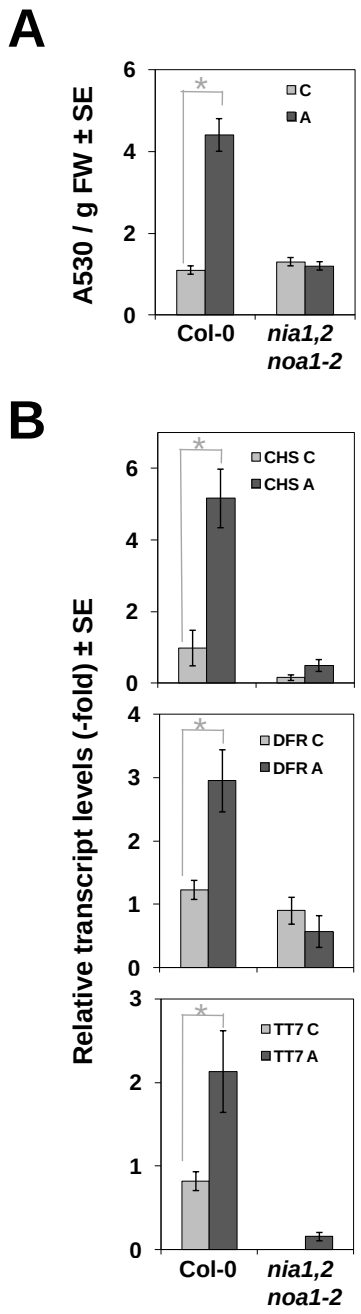

Figure 4.49. Effects of cold acclimation on anthocyanin synthesis in Col-0 and *nia1,2noa1-2* plants. A, Anthocyanin content was spectrophotometrically quantified. Data represent the means of three independent experiments with 25 and 10 plants each. B, Transcript levels of anthocyanin biosynthetic genes chalcone synthase (*CHS*), dihydroflavonol reductase (*DFR*) and flavonol 3-hydroxylase (*TT7/F3H*) genes were quantified by RT-qPCR from total RNAs isolated from plants of the indicated genotype either acclimated A for 24 h at 4ºC or non-acclimated as control C. Values are the mean of three independent biological replicate samples for each genotype and condition ± standard error. * indicates significantly different with p-value ≤ 0.05 in Student´s t-test.

contrast, *nia1,2noa1-2* plants did not accumulate anthocyanins when exposed to cold. As expected from these findings, the cold induction of several genes involved

in anthocyanin biosynthesis, such as *CHS*, *DFR* and *TT7*, was blocked in the NO-deficient plants (Fig. 4.49B). Together, these results indicated that NO positively regulates cold acclimation in Arabidopsis also by activating the cold-induced expression of genes implicated in anthocyanin biosynthesis, hence promoting anthocyanin accumulation.

Discussion

5. DISCUSSION

The figures 5.2, 5.3, 5.5 and 5.6, and part of the information displayed in this section 5 are excerpts of the research articles: "León, J., Costa, Á., & Castillo, M. C. (2016). Nitric oxide triggers a transient metabolic reprogramming in Arabidopsis. Scientific Reports, 6, 37945", "Costa-Broseta, Á., Perea-Resa, C., Castillo, M. C., Ruíz, M. F., Salinas, J., & León, J. (2018). Nitric Oxide Controls Constitutive Freezing Tolerance in Arabidopsis by Attenuating the Levels of Osmoprotectants, Stress-Related Hormones and Anthocyanins. Scientific Reports, 8(1), 9268", "Castillo, M. C., Coego, A., Costa-Broseta, Á., & León, J. (2018). Nitric oxide responses in Arabidopsis hypocotyls are mediated by diverse phytohormone pathways. Journal of experimental botany, 69(21), 5265-5278", "Costa-Broseta, Á., Castillo, M. C., & León, J. (2018). Protein Stabilization and Post-translational Modifications Control NO Homeostasis in Arabidopsis", "León, J., Costa-Broseta, Á., & Castillo, M. C. (2018). RAP2.3 negatively regulates nitric oxide biosynthesis and sensing through a rheostat-like mechanism in Arabidopsis" and "Costa-Broseta, Á., Perea-Resa, C., Castillo, M. C., Ruíz, M. F., Salinas, J., & León, J. (2018). Nitric Oxide Deficiency Reduces CBF *Induction, ABA Signaling, Anthocyanin Synthesis and Cold Acclimation in Arabidopsis". The last three articles were submitted to Plant Physiology, The Plant Journal and Journal of Experimental Botany, respectively and were under revision when PhD Thesis writing was finished. All the results and figures that appear or are discussed here are derived from the work of the PhD student in collaboration with the other authors.*

Plant responses to NO at the molecular level comprise three main different processes: alteration of gene expression, post-translational modification of proteins and metabolism reprogramming. Despite all the efforts to decipher the mechanisms underlying these responses in the last years, NO perception in plants remains mostly unknown. Moreover, researchers have been trying for decades to elucidate the way NO is synthesized and regulated in plants but the picture is still nowadays incomplete. The present work aims to shed light upon NO production and sensing although further research will be required for the full support of the presented hypothesis.

As a free radical gas, NO is very reactive and highly diffusible. This two features make difficult for NO molecules to reach distant locations from the spot they were synthetized in the cell, but, at the same time, very few structures are able to hamper its diffusion. Therefore, NO content inside cells should form sharp concentration gradients, with the highest concentrations around the microenvironment where it is produced. Thus, a short pulse of a high dose of exogenously applied gas represents an attempt to mimic conditions of high local accumulation of NO, similar to those that can occur under stress. On the other hand, the triple *nia1,2noa1-2* mutant plants, which are defective in NO production, represent an invaluable tool

to mimic conditions of NO shortage in plants (Fig. 4.42C). These plants are impaired not only in nitrate reductase-mediated but also in nitrate-independent NOA1-associated production of NO (Lozano-Juste & León, 2010). In this work, NO fumigation and *nia1,2noa1-2* were used as alternative experimental systems to investigate, at genome-wide scale, sensing and signaling associated to NO in plants by conducting two different transcriptomic analyses. First, early plant responses to NO were studied by analyzing changes in the transcriptome shortly after treating plants with a pulse of pure NO gas (Supplementary Tables S2, S3 and S4 in Castillo *et al.*, 2018). Second, the effects of NO endogenous deficit were investigated by comparing the transcriptomes of wild type and *nia1,2noa1-2* plants (GEO code GSE41958).

Endogenous NO has been reported to positively regulate the photomorphogenesis via the control of processes like the hypocotyl elongation (Lozano-Juste & Leon, 2011) and apical hook opening (Abbas *et al.*, 2015) in etiolated seedlings. To identify the regulatory components implicated in NO sensing, the information obtained from the transcriptomic analysis of plants exposed to a NO pulse was combined with a screening of TPT transgenic lines conditionally expressing single TFs (Fig. 4.14, Coego *et al.*, 2014) relying on a NO sensitivity assay that measures the inhibition of hypocotyl elongation after exposure of etiolated seedlings to NO. Despite the high reactivity of NO, most of the changes observed in the transcriptomic data occurred by one hour after the NO pulse (Fig. 4.13B), being consistent with the first significant altered pattern of NO-related post-translational protein modifications, observed also one hour after exposure to NO (Fig. 4.24B), and the later extensive metabolic reprogramming detected six hours after treatment (Fig. 4.23A, B, Supplementary Table S1 in León *et al.*, 2016). Due to the lack of a true NO receptor in plants, the way the plants sense NO would mainly depend on the NO-triggered PTMs in key signaling proteins. Modified proteins would then transmit the signal to other amplifying signaling proteins, thus modulating the transcriptome and eventually the metabolome. A strong evidence suggesting that hormone biosynthesis and signaling pathways are direct targets of NO action came from the characterization of the NO-responsive transcriptome (Supplementary Table S3 in Castillo *et al.*, 2018). Moreover, the genetic approach based on the screening of TPT lines for NO sensitivity allowed confirming the NO-phytohormone connection.

The inability of ethylene-related mutants to properly sense NO (Fig. 4.16A) suggests a key role of ethylene signaling in hypocotyl NO sensing. Both perception and signaling of this hormone would be necessary for NO to trigger inhibition of hypocotyl elongation under darkness. Despite the complex and sometimes controversial interaction between ethylene and NO (Gniazdowska *et al.*, 2007; Montilla-Bascón *et al.*, 2017), it has been recently reported that the NO control on cell cycle progression requires the function of EIN2 in Arabidopsis cell cultures (Novikova *et al.*, 2017), thus suggesting this mechanism could be on the basis of the hypocotyl growth inhibition by NO. Ethylene involvement in NO sensing and

response is further supported by the identification of large number of ethylene-related transcription factors in our screening of TPT lines. Among the identified TFs, the AP2-related and integrase-type ORA47 and RAP2.6L (Krishnaswamy *et al.*, 2011; Chen *et al.*, 2016) were found, as well as four additional integrase-type ERF TFs ERF014, ERF037, ERF056 and ERF113/RAP2.6L and the ethylene responsive element binding factor 1 (ATERF-1), all of them related to ethylene signaling. In addition, the inhibition of hypocotyl elongation by NO requires also the SL biosynthesis and signaling, as SL mutants were insensitive to NO (Fig. 4.18B). These data would be consistent with NO being involved in SL-exerted opposite regulatory effects in root and shoot growth as reported (Jia *et al.*, 2014; Manoli *et al.*, 2016; Sun *et al.*, 2016). Nevertheless, the interaction between NO and SLs seems to be very complex as recently reviewed (Kolbert, 2018). Despite NO lightly induces some of the SL biosynthesis genes (Fig. 4.18C), whether NO can trigger SL production or not will require to measure SL levels in this plants. On the other hand, SA biosynthesis and accumulation seems to be also essential for hypocotyl NO sensing, as a SA-deficient plants were fully insensitive to NO-triggered inhibition of hypocotyl elongation (Fig. 4.18A). The complicated relation reported between the production and signaling of NO, SLs and SA (Tari *et al.*, 2011; Bharti & Bhatla, 2015; Rozpadek *et al.*, 2018) suggests the existence of a self-regulatory hormonal loop involved in ensuring the correct NO sensing under different conditions and/or organ/cellular locations.

A functional interaction between NO and ABA is also depicted by the NO-triggered up-regulation of a subset of ABA signaling genes (Supplementary Table S2 in Castillo *et al.*, 2018, Fig. 4.19A-C). Further support to this interaction comes from the partially insensitive phenotype displayed by the double ABA receptor *pyl6pyl7* mutant plants (Fig. 4.19D). Previously reported data suggest that NO modulates the activity and stability of the ABA receptors through PTMs (Castillo *et al.*, 2015), thus supporting a tight functional link between NO and ABA. Also the ABA involvement in NO sensing was supported by the identification of ABA-related TFs in the screening of TPT lines. Among those TFs, MYB-type HRS1 and MYB30 (Wu *et al.*, 2012; Lee & Seo, 2016) and NAC058 (Coego *et al.*, 2014) are functionally related to ABA homeostasis or signaling.

Lastly, the overlapping found between NO- and BR-responsive transcriptomes (Fig. 4.21) suggested also BRs could be involved in NO sensing. However, a complex connection between NO and BRs in the regulation of the hypocotyl elongation in etiolated seedlings seems to operate. The BR-deficient *det2-1* mutant despite displaying short hypocotyls was fully sensitive to NO (Fig. 4.22C), thus suggesting BR biosynthesis is not required for NO sensing. Besides, the gain-of-function *bes1-D* mutant in BES1/BZR2 BR signaling component was hypersensitive to NO (Fig. 4.22C). Because *BES1/BZR2* gene was found to be downregulated by NO in the transcriptomic analysis (Fig. 4.17C), this TF might represent a potential node for a NO-related regulatory loop.

It is noteworthy mentioning that despite a large amount of jasmonate-related genes were found to be NO-responsive (Supplementary Table S3 in Castillo *et al.*, 2018), none of the mutants in biosynthetic or signaling JA components tested were altered in hypocotyl NO sensing (Fig. 4.20B). These data suggest that JA is likely not implicated in sensing NO in etiolated hypocotyls but do not rule out the potential involvement of JA in NO sensing in other organs/tissues or plants under different conditions.

Potential hormone-related NO targets as described above are likely affected by NO-triggered PTMs. An in silico prediction for these types of post-translational modifications for those potential targets (Table A6) shows that all analyzed proteins may be potentially S-nitrosylated or nitrated. Among them, some residues were predicted to be more likely modified as prediction coincided in two different platforms. This is the case for the S-nitrosylation of C1063 and C1218 of EIN2, and C63 of MAX2, as well as for the nitration of Y783 of EIN2 and Y176 of PYL6 (Table A6). However, these are just predictions and none of these proteins have been identified yet as post-translationally modified. Further proteomic work will clarify whether the NO-related post-translational modifications of these signaling proteins could be important for the NO sensing mechanisms operating in etiolated hypocotyls. Altogether, NO sensing in Arabidopsis hypocotyls needs at least the biosynthesis and/or signaling of ethylene, SLs, SA and ABA, while the negative regulation of BR signaling genes by NO also contributes to the NO-triggered inhibition of hypocotyl elongation (Fig. 5.1). As endogenous levels of NO and hormones may change from one tissue to another, future work will clarify if this model of NO sensing may be extrapolated to other organs.

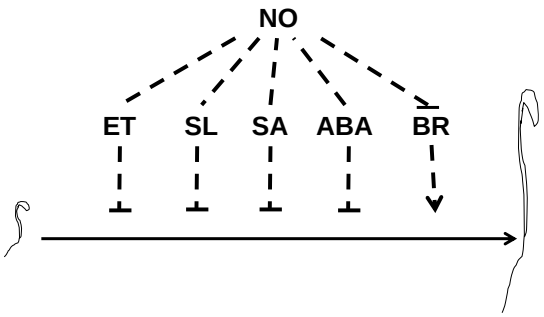

Figure 5.1. Scheme showing the direct involvement of ethylene (ET), strigolactones (SL), salicylates (SA), abscisic acid (ABA) and brassinosteroids (BR) in NO-triggered inhibition of hypocotyl elongation.

As a complementary approach to the analysis of the effects of an acute NO dose, the effects of constitutively low endogenous NO content in *nia1,2noa1-2* plants were also studied in this work. In the analysis of the differential transcriptome of NO-deficient plants (GEO code GSE41958), neither a master regulator of the NO-

triggered responses nor NO-specific gene markers were identified. These data support that regulatory functions of NO are exerted in coordination with other regulators through diverse signaling pathways, as in the above mentioned control over hypocotyl elongation. In agreement with this hypothesis, several genes that were up-regulated in the NO-deficient mutant compared to the wild type, coded for enzymes involved in JA and ABA biosynthesis (Table A8). Supporting these data, *nia1,2noa1-2* plants contain indeed a significantly higher content of ABA and JA than wild-type plants (Fig. 4.39A). Interestingly, an overall analysis of the up-regulated transcriptome in NO-deficient plants showed a significant over representation of genes implicated in cold responses and freezing tolerance (Table A8). ABA and JA have been reported to play a role in plant response to freezing stress (Llorente *et al.*, 2000; Hu *et al.*, 2013), so its higher contents in *nia1,2noa1-2* plants should contribute to their enhanced constitutive freezing tolerance. In addition, a metabolomic analysis of *nia1,2noa1-2* plants compared to Col-0 wild type plants revealed that mutant plants also accumulated high amounts of osmoprotective metabolites such as sugars, polyamines, and antioxidant metabolites, including anthocyanins and other flavonoids (Fig. 4.39B, C, D, Table S2 in Costa-Broseta *et al.*, 2018), which, in all likelihood, limit the impact of the freezing-related damage. Sugars and polyamines have been reported to increase the freezing tolerance (Alet *et al.*, 2011; Nägele *et al.*, 2012) while flavonoids seem to exert a key antioxidant protection against the damage caused by the photoinhibition at low temperatures when the photosynthesis rate decreases (Schulz *et al.*, 2016).

As suggested by the transcriptomic and metabolomic data, the survival assays to freezing conditions showed that indeed NO-deficient mutant plants were constitutively more tolerant to freezing than wild type plants (Fig. 4.42A). However this result comes into conflict with previous works with the double mutant *nia1,2* that describe NO being required for constitutive freezing tolerance (Zhao *et al.*, 2009; Cantrel *et al.*, 2011). This discrepancy could be explained by the differences in the experimental conditions. Freezing assays with the double mutant in previous works were performed in Petri dishes with MS media supplemented with agar and sucrose, whereas in this work the assays were performed using plants grown on soil. These two experimental systems are quite different in terms of humidity and sugar availability, factors that affect freezing tolerance. Another factor that could explain this discrepancy is the difference in NO and proline content between the two mutants used. Due to the additive effect of the mutations, triple mutant has lower endogenous levels of NO than *nia1,2* (Lozano-Juste & León, 2010). The proline content was found to be the same in *nia1,2noa1-2* and wild type plants (Table S2 in Costa-Broseta *et al.*, 2018). It was previously reported an increase in proline in wild type plants exposed to cold but not in *nia1,2* plants (Zhao *et al.*, 2009). However, despite the reported increases in proline content during cold exposure, it has been also proposed that there is no correlation with enhanced freezing tolerance (Zuther *et al.*, 2012).

All these data together suggest that NO would function as a negative regulator of the constitutive freezing tolerance in Arabidopsis by altering hormone homeostasis and by reducing the synthesis of osmoprotective and antioxidant metabolites. Although the mechanisms by which NO exerts this function haven't been properly studied yet, it is very likely that it would regulate these processes by triggering PTMs on proteins with a relevant function in related metabolic routes. Previous work identified several proteins involved in metabolism of C, N and S to be nitrated *in vivo* in a proteomic assay (Lozano-Juste *et al.*, 2011). Besides, it has been reported that several of the enzymes involved in antioxidant systems undergo NO-triggered PTMs (Begara-Morales *et al.*, 2016). Although further investigation will clarify the real relevance of PTMs in the mechanisms underlying the regulation of freezing tolerance, the low levels of NO in the NO-deficient triple mutant should lead to a lower content in nitrated proteins which could explain the great differences between the molecular phenotypes of the wild type and mutant plants (Table S2 in Costa-Broseta *et al.*, 2018). NO would scavenge ROS and suppress the metabolic changes needed for the increase of the content of polyamines, sugars, flavonoids, ABA and JA (Fig. 5.2).

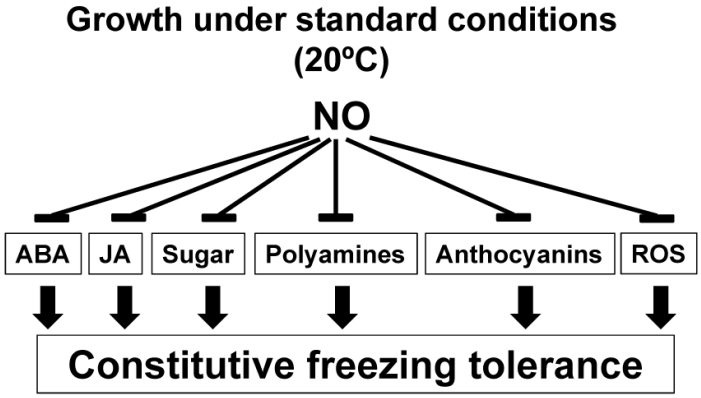

Figure 5.2. Model of NO involvement in the regulation of constitutive freezing tolerance. Blunt ended and black solid arrows represent negative and positive regulation on freezing tolerance, respectively. ABA, JA and ROS mean Abscisic acid, Jasmonates and Reactive Oxygen Species, respectively.

Given the improved constitutive freezing tolerance of *nia1,2noa1-2* plants, their cold acclimated-induced freezing tolerance was also tested and compared to wild type plants. Interestingly, it turned out that the triple mutant was impaired in its ability to cold acclimate (Fig. 4.45B), thus confirming previous research suggesting that NO is required for correct development of cold acclimation (Zhao *et al.*, 2009; Cantrel *et al.*, 2011; Puyaubert & Baudouin, 2014). Supporting this, the cold-induced large increase in the endogenous NO content was observed to be very slight in the NO-deficient mutant (Fig. 4.43) as was previously described for the double mutant *nia1,2* (Zhao *et al.*, 2009). However, it is noteworthy mentioning that

in this work the increase of NO levels during acclimation at 4ºC was not observed after few hours of cold (Fig. 4.44) as previously reported (Zhao *et al.*, 2009; Cantrel *et al.*, 2011), but only after 7 days of cold treatment (Fig. 4.43). These long periods have been reported to be required for full cold-acclimation (Tähtiharjau & Palva, 2001; Kawamura & Uemura, 2003). Differences in humidity conditions between the experimental systems used as well as specific contributions of the *noa1-2* mutation to the cold-acclimation phenotype could be on the basis of the observed changes in the pattern of NO accumulation.

Three main factors have been found to explain the involvement of NO in the regulation of cold acclimation. In first place, as previously described by using the double mutant *nia1,2* (Cantrel *et al.*, 2011), NO would induce the expression of *CBFs* and therefore their gene targets in response to low temperature (Fig. 4.47A,B), but also would control the process of cold acclimation through CBF-independent regulatory pathways. Second, NO was found to promote the induction of genes involved in the biosynthesis of anthocyanin and other flavonoids (Fig. 4.49B). Accordingly, after acclimation anthocyanin levels were strongly increased in wild type but not in *nia1,2noa1-2* plants (Fig. 4.49A). Lastly, a differential expression pattern observed for ABA signaling pathway-related genes under low temperature conditions between the triple mutant and the wild type plants (Fig. 4.48B) suggests that NO controls ABA perception and signaling but not its homeostasis during cold acclimation (Fig. 4.48A). The importance of flavonoids and ABA in cold acclimation and freezing tolerance has been discussed above, but it is important to highlight the role of flavonoids in preventing the accumulation of ROS under cold-induced photoinhibition of photosystems (Havaux & Kloppstech, 2001). Once again, the regulation exerted by NO over cold acclimation is proposed to be performed by triggering PTMs in proteins related to the aforementioned processes. In agreement with this hypothesis, flavonoid-related enzyme quercetin-3-O-methyltransferase 1 was found to be nitrated *in vivo* (Lozano-Juste *et al.*, 2011) while NO has been reported to perform a negative regulation on ABA signaling by causing the nitration and inactivation of its receptors (Castillo *et al.*, 2015).

However, despite all indications suggesting that the lower endogenous NO levels in *nia1,2noa1-2* are the reason for an impaired cold acclimation in this mutant, its defective nitrogen assimilation cannot be ruled out to be behind some of the effects observed. For instance, wild type plants accumulated higher levels of NO when growing in a medium with nitrate as a unique N source than when growing in a medium with nitrite or ammonium or subjected to N starvation, an effect that was not observed in *nia1,2* plants (Fig. 4.46). Therefore this enhanced NO production must be due to the NR activity, as the genes of the two NR enzymes of Arabidopsis are mutated in the triple mutant. Also it has been previously reported that anthocyanins accumulate under deficient nitrogen assimilation (Diaz *et al.*, 2006) but the NO-deficient mutant was unable to induce the anthocyanin biosynthetic genes and produce them during cold acclimation (Fig. 4.49), thus supporting the

hypothesis of NO being essential for the cold-triggered accumulation of anthocyanins and thus for the acclimated-induced freezing tolerance.

All these data suggest that NO would regulate metabolism, hormone signaling and gene expression presumably through PTMs on key regulatory proteins, in such a way that during cold acclimation, NO levels would increase to allow the correct functioning of CBF-dependent and –independent regulatory pathways (Fig. 5.3). Therefore, NO is essential for the full cold-induction of *CBF* genes and flavonoid biosynthesis, as well as for regulating ABA perception and signaling.

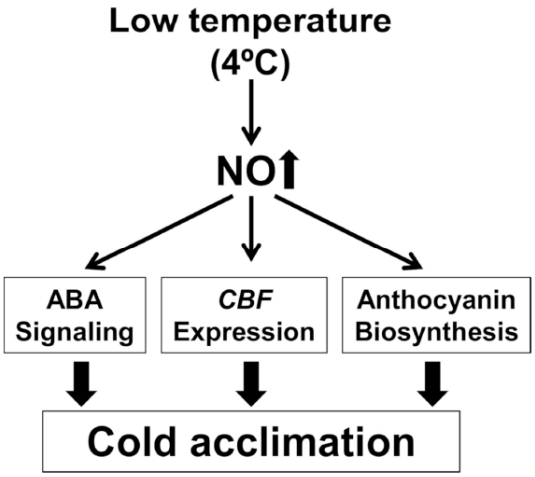

Figure 5.3. Scheme showing the endogenous and environmental factors involved in the positive regulation exerted by NO on cold acclimation-induced freezing tolerance.

A noteworthy issue is the apparently opposite roles of NO in constitutive freezing tolerance and cold acclimation. It is not the first time that a paradoxical function has been attributed to NO, which can exert anti-oxidant or pro-oxidant roles depending on acting in a chronic low or acute doses (Groß *et al.*, 2013). Moreover, the highly reactive nature of NO makes it potentially capable of triggering changes in signaling pathways with different and even opposite regulatory effects. However, the function of NO as a repressor of constitutive freezing tolerance and as an inducer of cold acclimation can be seen as an adaptive mechanism of plants, consisting in a fine tuning of the regulation of the cell processes depending on the concentration of NO in response to the environmental temperature. Since in the absence of stress-related stimuli the allocation of energy and resources to stress responses would entail a waste for the plant, in standard conditions of temperature the equilibrium between development and defense must be unbalanced towards the plant growth. Therefore in this situation NO acts as a brake to those unnecessary mechanisms that are involved in the development of the freezing tolerance. Nevertheless, under cold non-freezing temperatures plants will require the development of cold acclimation, thus anticipating future freezing temperatures. In this process NO is

accumulated and its higher concentrations promote responses that NO would usually be repressing, such as ABA signaling and anthocyanin biosynthesis, leading to a full cold acclimation.

Both aforementioned conducted transcriptomic analyses pointed to NO triggering large metabolic changes that would be responsible for the correct regulation of processes such as hypocotyl elongation, constitutive freezing tolerance and cold acclimation. These suspected metabolic alterations were confirmed in a metabolomic assay that compared the metabolomes of wild type and *nia1,2noa1-2* plants (Table S2 in Costa-Broseta *et al.*, 2018) which helped to figure out the role of NO in repressing freezing tolerance, as mentioned above. This analysis allowed to investigate the effects of a lack of NO in the plant metabolome, but another analysis was pending in order to understand the opposite situation. Therefore, a metabolomic analysis of plants collected at different times after a short pulse of pure NO gas was also performed (Supplementary Table S1 in León *et al.*, 2016). In this analysis a sharp and transient alteration in the metabolome was observed in NO-treated plants by 6 h after treatment, but this response almost disappeared by 24 h after treatment (Fig. 4.23A, B, Supplementary Table S1 in León *et al.*, 2016), showing the extraordinary plasticity of Arabidopsis metabolism.

One of the main NO-triggered effects observed in this analysis was the alleviation of oxidative stress. This response to NO must be understood to be strictly associated to high NO concentrations and would require further investigation to be extrapolated to specific cell events or tissues, as NO has been reported to possess both antioxidant and prooxidants effects (Groß *et al.*, 2013). As observed in the freezing tolerance and cold acclimation, the effect of NO on oxidative stress constitutes another example of the sometimes paradoxical function of NO as a signaling molecule. It could be due to multiple factors including the relative cellular concentration, the location where it is synthetized and the complexity of the interacting microenvironment. When NO palliates oxidative stress, it can be by altering gene expression or by acting as a direct antioxidant. By scavenging ROS such as superoxide anion, NO will be transformed into peroxynitrite, which has been characterized as a potent tyrosine nitration-inducer (Holzmeister *et al.*, 2015). The NO-related activation of processes involved in lowering oxidative stress in NO-treated plants was suggested by a significant increase in the production of polyamines and cysteine (Supplementary Table S1 in León *et al.*, 2016), a reduction of superoxide anions (Fig. 4.24A) and the accumulation of nitrated proteins (Fig. 4.24B). Furthermore, the endogenous content of two important antioxidant molecules such as ascorbate and α-tocopherol (Szarka *et al.*, 2012) were reduced in NO-treated plants (Supplementary Table S1 in León *et al.*, 2016) while the content of threonate increased, suggesting NO would trigger the irreversible catabolism of ascorbate to the non-antioxidant threonate instead of inducing its metabolism through reversible oxidation (Parsons *et al.*, 2011).

Another metabolic disturbance caused by NO was the alteration of central processes of primary metabolism, since several significant changes were observed in the categories of peptides, amino acids, carbohydrates and lipids (Fig. 4.23A). Among these, the changes in the lipidome are of special relevance, as its signaling potential has been reported (Hou *et al.*, 2016). Upon NO treatment, it was observed a significant increase in the content of phospholipids, lyso-lipids, PUFAs and oxylipins (Fig. 4.26 and Supplementary Table S1 in León *et al.*, 2016). The detection of elevated levels of C20 PUFAs could result from the lipase action on trace lipids, or from the enhanced elongase activity (Zhou *et al.*, 2014), while the rise in the oxylipins levels may be indicative of the activation of responses to stress (Pohl & Kock, 2014).

Promotion of cell death was also one of the stress responses that the data from the metabolomic analysis pointed out to be promoted by the NO treatment. The strong increase in pheophorbide a content (Fig. 4.28B) was also accompanied by an alteration in lipidic structures (Fig. 4.27) and metabolic changes associated to massive nucleic acid and protein degradation (Supplementary Table S1 in León *et al.*, 2016), all these processes being usually related to cell death (Hirashima *et al.*, 2009; Araújo *et al.*, 2011; Sakamoto & Takami, 2014). Nevertheless, the absence of DNA ladders in the patterns of DNA degradation in NO-fumigated plants (Fig. 4.28A) suggests that NO would trigger necrotic cell death instead of apoptosis. Confirming all these hints, cell death was detected by Evans blue staining in NO-treated plants (Fig. 4.29C). Besides, other alterations observed in plants upon NO treatment that could be related to NO triggering cell death include an increased nucleic acid metabolism (Supplementary Table S1 in León *et al.*, 2016), the aforementioned increment in the content of polyamines (Fig. 4.25) and a strong accumulation of nitration in tyrosine proteins (Fig. 4.24B). The metabolism of nucleic acids fits the observed DNA degradation (Fig. 4.28A), whereas polyamines have been reported to be able to delay cell death (Del Duca *et al.*, 2014). Regarding protein nitration, as mentioned above, it has been described how this NO-triggered PTM is responsible for the inactivation and further degradation of ABA receptors (Castillo *et al.*, 2015), so, although more work is required to elucidate the connection between NO, protein nitration and protein breakdown, the increase of NO-related PTMs in proteins could be one of the mechanisms leading to the characteristic protein turn-over that is associated with cell death (Araújo *et al.*, 2011). Despite all the observed evidence in this work supporting the role of NO as a cell death inducer, it is noteworthy that the regulation of this process seems to be yet another scenario of paradoxical behavior of this molecule, since NO has been reported to have both promoting and suppressing effects on cell death in plants depending on cell type, redox status and NO concentration (Wang *et al.*, 2010). However, notwithstanding the mentioned multiple metabolic and cellular symptoms of cell death, those were only detected by 6 h after NO treatment, and by 24 h plants recovered its standard metabolic status (Fig 4.23A) and were fully viable, as 7 days after treatment all plants survived and grew normally (Fig. 4.29C).

Therefore, under natural stress conditions, NO would only trigger cell death in a very discrete manner, only in those cell locations where its concentration surpasses a threshold level.

Lastly, a small but statistically significant increase in a wide array of dipeptides was also detected in NO-treated plants (Supplementary Table S1 in León *et al.*, 2016). This accumulation could be due to the N-terminal dipeptide release form target proteins or a plant response to ameliorate the combined effects of NO and O_2 in the cysteine branch of the N-terminal targeted proteolysis of certain protein substrates through the N-end rule pathway. Thus, NO would indirectly promote the accumulation of dipeptides in an attempt by the plant to protect some key proteins from specific N-terminal directed proteolysis, since dipeptides have been described to inhibit the N-end rule pathway proteolysis (Kitamura, 2016).

In brief, data from the metabolomic analysis of NO-treated plants suggest that NO triggers an array of responses to alleviate toxicity and cellular damage that includes massive but transient metabolic reprogramming involving metabolites of both primary and secondary metabolism (Fig. 5.4). As already discussed, this metabolic reprogramming was found to take place by 6 h after an NO pulse, while accordingly effects on the transcriptome and proteome were observed after 1 h (Fig. 4.13B and Fig. 4.24B). This timing would suggest that in order to promote such an extensive metabolic alteration, first NO would have to alter gene expression and cause PTMs in proteins.

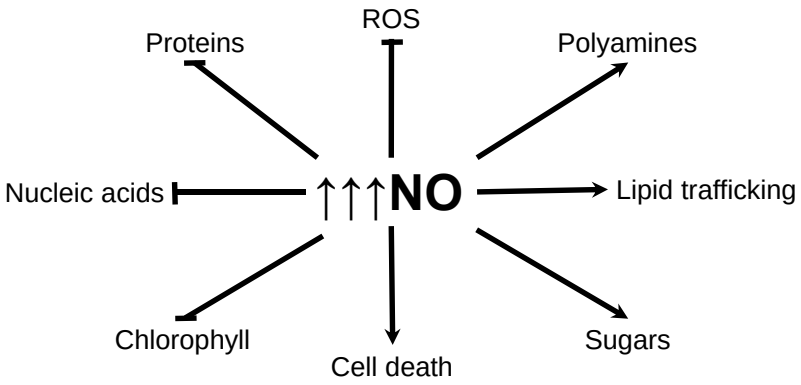

Figure 5.4. Scheme summarizing the regulation that high concentrations of NO exert over different metabolite categories and cell processes.

The results obtained through this metabolomic analysis were not a perfect mirror of those obtained from the metabolomic analysis performed with NO-deficient plants. Since the experimental systems behind these analyses aimed to mimic low and high NO concentration in plants, it could be expected to obtain directly opposing results. Strikingly, that was not the case, as almost the same metabolite categories were altered and in some cases very similar changes were detected in

both analyses. ROS represent one of the few examples of opposing responses. NO-deficient plants displayed the effects of constitutive oxidative stress including the accumulation of ascorbate as a response to ameliorate the redox status, while NO-fumigated plants had its ROS levels decreased and were observed to have a decrease in ascorbate levels and an increase in threonate. By contrast, three metabolite categories that changed in the same direction in NO-treated plants and NO-deficient plants were polyamines, cysteine and cysteine production-related metabolites, and oxylipins, which increased in both cases. It is important to remark that *nia1,2noa1-2* plants have very limited NR activity due to a mutation in the two NR enzymes of Arabidopsis (Wilkinson & Crawford, 1993), so some of the alterations observed may be related to a deficient N assimilation instead of being caused by low endogenous NO levels. Regarding the fumigation with NO, some of the effects observed upon NO treatment could be caused by NO_2 instead, given the rapid NO conversion into NO_2 in the presence of oxygen (Kasten *et al.*, 2017). Also remarkably, the differential transcriptomes of NO-treated plants (Supplementary Tables S2, S3 and S4 in Castillo *et al.*, 2018) and untreated NO-deficient *nia1,2noa1-2* plants (GEO code GSE41958), show a big overlapping, thus suggesting the possibility of NO acting as a repressor of its own biosynthesis when exogenously supplied at high concentrations. Further work will be required to clarify these unexpected results and the true behavior of NO in the regulation of transcriptome and metabolome.

One of the most intriguing metabolic changes observed in NO-fumigated plants was the accumulation of dipeptides. This response has been proposed to be a mechanism to inhibit the N-end rule pathway proteolytic degradation of key proteins in mammals (Baker & Varshavsky, 1991). In plants, the degradation of the ERFVII TFs through this pathway was described to be a mechanism of NO sensing in Arabidopsis (Gibbs *et al.*, 2014a). Given the potential importance of the ERFVIIs in controlling plant responses to NO, an analysis on the modulation of NO homeostasis and signaling by the ERFVII RAP2.3 was performed. The results of the transcriptomic analysis of β-estradiol inducible RAP2.3 TPT transgenic lines (Fig. 4.35C, D) suggest the existence of a regulatory loop involving NO and RAP2.3, with a significant contribution of the transcription factor regulating the plant responses to NO. Specifically, RAP2.3 was found to act mostly as a repressor of NO-triggered responses both at physiological (Fig. 4.31 and 4.34) and molecular (Table A9) levels. RAP2.3 does not contain the Ethylene response factor-associated Amphiphilic Repression (EAR) motif (Ohta *et al.*, 2001), which enable other AP2/ERF transcription factors to act as transcriptional repressors (Tsutsui *et al.*, 2009), so its potential activity as repressor in NO-triggered responses should be due to the RAP2.3-activated expression of a true repressor . However, none of the genes that were up-regulated by NO in TPT-RAP2.3 plants only after β-estradiol treatment and containing the putative RAP2.3 binding motif, codes for an EAR-containing transcription factor (Table A7), so the attenuated NO-triggered response at the transcriptome level could be the result of other non-EAR-containing type of repressor or alternatively of a NO-induced transcriptional activator that is down-regulated upon RAP2.3 overexpression.

Among these candidates, three genes coding for AP2/ERF transcription factors (ERF095/ESE1, RAP2.6 and ERF016) and several genes (*NAC055/NAC3, JAR1* and *MYB113*) containing the putative RAP2.3 binding domain in their promoters were strongly activated by NO only when RAP2.3 was not overexpressed (Table A7 and A10). RAP2.6 has been reported to be activated by NO and be involved in its response in shoot elongation (Imran *et al.*, 2018), while NAC055 has been reported to participate in JA signaling (Bu *et al.*, 2008). Data summarized in Figure 5.5 suggest the existence of RAP2.3-dependent and -independent NO-responsive branch pathways of JA and ABA signaling. Data presented in Figure 4.36 indicate that NO induces the expression of a subset of JA-related genes coding for its biosynthesis and signaling through a process that was repressed by RAP2.3 (Fig. 5.5A). Three different branches of JA signaling can be depicted based on the regulatory role exerted by RAP2.3. A RAP2.3-repressed branch would involve LOX2, AOC2, OPR1 and JAR1, from which only JAR1 would be a direct RAP2.3 target (Fig. 5.5A). JAR1 plays a crucial role in the biosynthesis of the active hormone jasmonoyl-isoleucine (Staswick *et al.*, 2002). A second RAP2.3-activated JA signaling branch would recruit LOX4, AOC1, JAZ1, JAZ6 and MYC2, being LOX4, AOC1 and JAZ6 potential direct targets of RAP2.3 (Fig. 5.5A). Finally, a third RAP2.3-independent branch would involve the participation of LOX3, AOC3, JAZ5, JAZ7 and JAZ10 (Fig. 5.5A). On the other hand, the NO-sensitive ABA signaling pathway could be also split in three branch pathways (Fig. 5.5B). One, repressed by RAP2.3, would involve PYL7 and SnRK2.3, both with potential RAP2.3 binding sites in their promoters (Table A7); the second, involving PYL5 and SnRK2.3 that would require RAP2.3 over-expression for the NO-trigger up-regulation of *PYL5* but RAP2.3 repressing the NO-induced up-regulation of SnRK2.3; and finally, a third branch would comprise the function of the PYL6 receptor and the SnRK2.9 kinase acting through a RAP2.3-independent mechanism. It seems RAP2.3 would control the expression and stability of SnRK2.3 by promoting NO production, since the encoding gene of PP2b11, which modulates ABA signaling by controlling SnRK2.3 degradation (Cheng *et al.*, 2017), was up-regulated by NO only when RAP2.3 is not overexpressed (Table A9). Also it has been reported that the function of SnRK2.3 can be repressed by NO-triggered PTMs (Wang *et al.*, 2015c).

According to all these data, NO would modulate its own biosynthesis and associated responses as well as JA and ABA signaling through RAP2.3-independent and RAP2.3-dependent pathways. In this scenario, RAP2.3 exerts its regulatory effects on plant responses to NO partially through its capacity to be degraded by the N-end rule proteolytic pathway, since the ability of plants to sense NO was reduced when this degradation was blocked, like in a *prt6* mutant or a plant expressing a non-degradable version of the protein (Fig. 4.34). Therefore, NO responses would be modulated by using RAP2.3 as a rheostat, a mechanism already described for other key processes in plants (Baxter-Burrell *et al.*, 2002; Williams *et al.*, 2015; Tischer *et al.*, 2017). Furthermore, RAP2.3 would also

function as a NO- and O_2-modulated rheostat integrating environment-triggered changes in the endogenous levels of NO and oxygen-containing molecules, as well as some hormones such as JA and ABA.

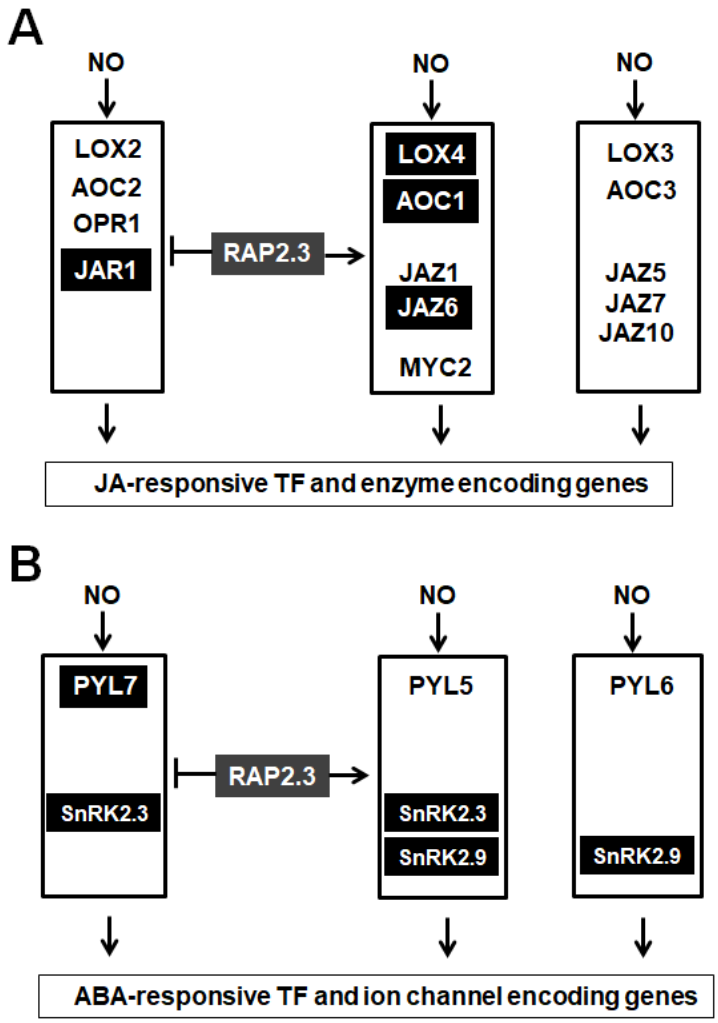

Figure 5.5. RAP2.3-dependent and –independent NO-regulated pathways. A, JA and B, ABA branches of the biosynthesis and signaling pathways and the components involved. Highlighted in black those presumably considered as direct targets of RAP2.3 because contain putative RAP2.3 binding sites in their gene promoters.

The rheostat model for the NO-RAP2.3 regulatory loop constitutes another case of complex regulation exerted by NO. The ability of NO to modulate almost every signaling pathway suggests that the possibility of self-controlled biosynthesis is a highly convenient trait for the plant. In agreement, the similarity of the transcriptomes of NO-treated plants and untreated NO-deficient plants (Supplementary Tables S2, S3 and S4 in Castillo *et al.*, 2018 and GEO code GSE41958), pointed out to the possibility of NO repressing its own production. This

could represent an auto-regulatory mechanism for the plant to keep NO homeostasis under control, which would explain the absence of significant increase in the endogenous NO levels of seedlings treated with exogenous NO (Fig.4.29A).

Since it seems that NO production in plants is largely dependent on the activity of NRs, the balance between NR and NiR activities could be determinant for NO homeostasis, as both kinds of enzymes would compete for nitrite as a substrate for its reduction to NO or ammonium, respectively. Therefore, the accumulation of NO in plants with reduced NiR and enhanced NR activities can be expected, while the opposite situation would result in diminished NO levels. The absence of available T-DNA mutants with a loss-of-function mutation in *NIR1* made necessary the generation of a *nir1-1* full knockout mutant through CRISPR-Cas9 technology. Together with its completely impaired capacity to reduce nitrite to ammonium, this mutant showed a strong increase in NO levels when grown on nitrate-containing media (Fig 4.5). This process is likely the result of the removal of toxic nitrite accumulated after nitrate reduction and incapacity to further reduce nitrite to ammonium. On the other hand, concomitantly, NO production in *nia1,2noa1-2* plants is indeed reduced in both shoot (Fig. 4.42C) and root (Lozano-Juste & León, 2010). This triple mutant has a point mutation that does not truncate the open reading frame of *NIA1* (Lozano-Juste & León, 2010), thus leading to synthesis of NIA1 with null activity.

As nitrate-dependent NO biosynthesis could be considered as a side branch of the nitrate assimilation metabolic pathway, it is expected that nitrate signaling pathway play a major regulatory role on NO production. Some TFs of the NLP family have been reported to act as master regulators in nitrate signaling (Konishi & Yanagisawa, 2013). Among them, NLP7 would regulate mainly NRs and NLP6 would regulate NIR1. NLP7 has been reported as a primary positive regulator of nitrate assimilation that binds to the promoter of *NIA1, NIA2* and *NIR1* to activate their expression (Marchive *et al.*, 2013), but NIR1 protein levels and activity were found to be higher in *nlp7-1* plants (Fig. 4.2A, B). This could be due to a competition between NLP6 (Konishi & Yanagisawa, 2013) and NLP7 that would be unbalanced in the *nlp7-1* mutant. Most likely, NLP7 would be potentially connected to NO homeostasis control, but this relation seems to be quite complex, since *nlp7-1prt6-1* plants, which carry also a mutation in the gene coding for the E3 ubiquitin ligase PRT6 that participates in the Arg/N-end rule pathway, display higher endogenous NO levels than wild type and their parental *nlp7-1* and *prt6-1* plants (Fig 4.2C). These data, together with the enhanced NR protein accumulation and activity observed in proteasome inhibitor-treated plants and the lack of significant effect regarding NIR1 (Fig. 4.1B, C), point to a connection between proteasomal degradation processes modulating NRs activity, the function of PRT6 and the NLP7 regulation of nitrate signaling. The NR protein content was increased in *prt6-1* and *qerfvii* (with mutations in all ERFVII coding genes) plants treated with proteasome inhibitor, whereas NR levels decreased in *nlp7-1* plants (Fig. 4.6). These data suggest that NR stabilization requires NLP7 and the loss of PRT6 function

independently of ERFVIIs. Interestingly, neither NIA1 nor NIA2 can be directly ubiquitylated by PRT6 as they are not MC-proteins. In turn, NLP7 fulfills this requirement and thus could be a potential substrate for the degradation mediated by the Arg/N-end rule pathway. Although this possibility should be further investigated, the functional link between NLP7 and PRT6 was supported by the appearance of plants expressing an N terminus-tagged NLP7 in *nlp7-1prt6-1* background, which rescued the pale green and small size phenotypes that characterize the leaves of *nlp7-1* and *prt6-1*, respectively (Fig. 4.3A). Furthermore, it is noteworthy that the overexpression of NLP7 in *nlp7-1* and *nlp7-1prt6-1* lead to enhanced NO levels (Fig. 4.3B). This functional link between NLP7-1 and PRT6 could be filled by a positive regulator of NLP7 regulated itself by the PRT6-mediated N-end rule pathway. Transcription factors ABR1 and WRKY14 are two candidates, being MC-proteins able to bind the ABRE-like box and the W-boxes present in *NLP7* promoter, respectively (Table A4 and Fig. A5) (Shen & Ho, 1995; Hobo *et al.*, 1999; Maeo *et al.*, 2001).

Besides the regulatory factors related to nitrate signaling and Arg/N-end rule proteolysic pathway, direct NO-related PTM-mediated effect in NR function and the subsequent NO production was suggested by new data. It has been described that phosphorylation and sumoylation can control NR function (Lillo *et al.*, 2004; Park *et al.*, 2011), but an analysis on the effect of NO-triggered PTMs on the NR activity has not been conducted yet. Above has been proposed that NO-triggered PTMs are responsible for the regulation NO exerts over processes such as constitutive freezing tolerance, cold acclimation and hypocotyl elongation, while its implication in ABA sensing has been already confirmed (Castillo *et al.*, 2015). Lysine ubiquitylation, tyrosine nitration and cysteine S-nitrosylation sites were identified *in planta* in NR1, NR2 and NIR1 by using transgenic plants overexpressing HA-tagged versions of these proteins after inmunopurification and LC-MS/MS proteomic analyses (Fig. 4.8, 4.9 and 4.10).

Regarding the NRs, the proteomic analyses showed a differential pattern of PTMs that could account for different regulation for each enzyme, but both were nitrated in two alternate tyrosine residues highly conserved in the central part of NR proteins (Fig. 4.8B) between the sumoylated lysine and the cytochrome b5 heme-binding domain (Fig. 4.9). Interestingly, nitration of those tyrosines was accompanied by ubiquitylation of two close consecutive lysines also highly conserved among plant nitrate reductases (Fig. 4.8B). Whether this cluster of nitration and ubiquitylation of NRs is associated to reduced function or degradation as in the case of ABA receptors (Castillo *et al.*, 2015) would require further work including enzyme assays after *in vitro* nitration of purified recombinant NR1 and NR2 proteins. Taking advantage of the availability of the 3D structural model of the corn NR cytochrome FAD- binding domain (PDB code 2cnd) and by amino acid sequence homology with Arabidopsis NRs, a nitrated tyrosine residue in NR1 (Y^{733}) which corresponded to Y^{83} very close to the FAD in the 3D model was located (Fig. 4.12). The introduction of a nitro group in that residue would largely perturb the

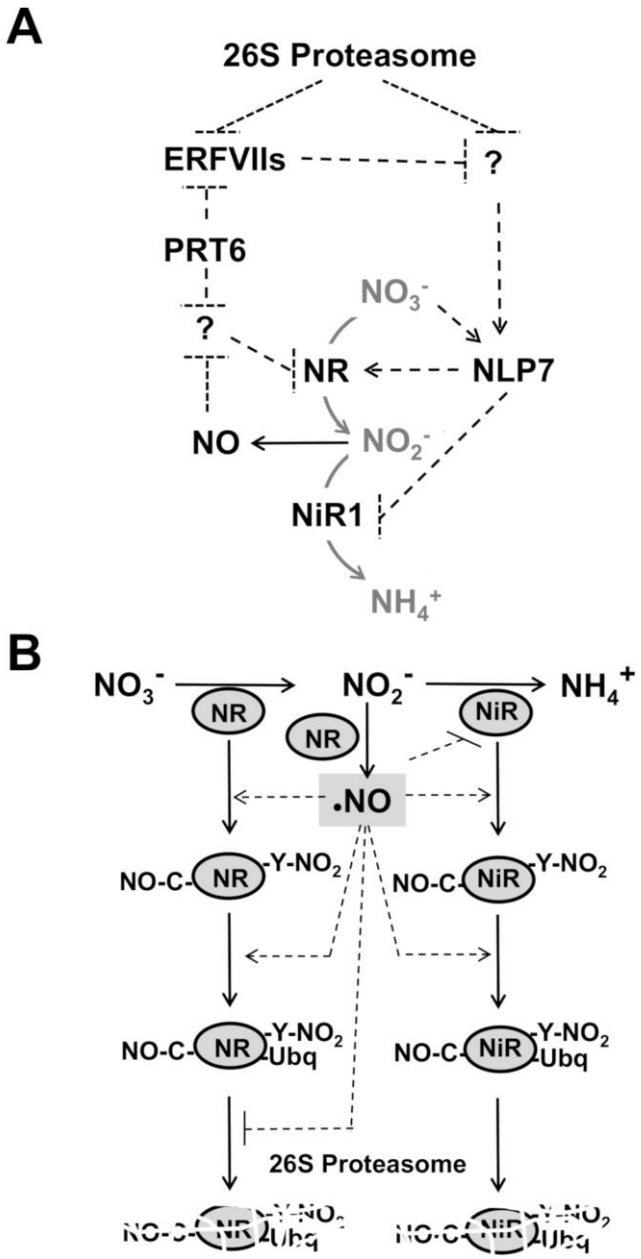

Figure 5.6. Regulation of NRs, NiR1 and NO production. A, The expression of *NRs* and *NiR1* genes and the stability of their corresponding proteins are regulated through NLP7-mediated nitrate signaling and proteasome-mediated degradation. B, NO-triggered post-translational modifications such as tyrosine nitration, cysteine S-nitrosylation, and lysine ubiquitylation control function and stability of NRs and NiR1 involved in NO production.

efficient binding of the flavin, thus likely leading to activity loss. However, we have not found the corresponding tyrosine nitrated in NR2, thus suggesting this could be a differential regulatory mechanism for both NRs. Despite the effect of PTMs in NRs function, the ubiquitylation is likely related to the control of their protein stabilities as treatment with proteasome inhibitor increased NR protein and activity levels, as mentioned above (Fig. 4.1B, C). Altogether, these data suggest that ubiquitylation of NRs is the default condition of NRs when NO-related PTMs affect them, thus triggering the proteolytic action of the proteasome.

In the case of NIR1, among the identified PTMs, a heavy pattern of lysine ubiquitylation was found (Fig. 4.10), however as the inhibition of the proteasome did not affect the activity and stability of NIR1 (Fig. 4.1B, C) it is unlikely that these PTMs represent a relevant factor in controlling its function. On the other hand, the effect of NO-related PTMs on NIR1 activity appears to be decisive, as the cysteines involved in binding the 4Fe-4S cluster and the siroheme group were found to be S-nitrosylated (Fig. 4.10 and 4.11), which would in all likelihood impair the proper functioning of the enzyme. Therefore, NO could induce NIR1 inactivation through S-nitrosylation of these critical cysteine residues. This mechanism would allow NO to enhance its own biosynthesis, by preventing nitrite reduction to ammonium.

Altogether, the aforementioned data suggest that NO can control its own biosynthesis at two complementary levels, through a mechanism that regulates the activity, accumulation and stability of NRs and NiR1. The first level would implicate nitrate signaling and N-terminal guided proteolytic degradation acting on NO-producing enzymes or their upstream regulators (Fig. 5.6A). The other level is the post-translational regulation through nitration of Y residues of NRs and S-nitrosylation of C residues of NiR1 affecting FAD- and siroheme-binding, respectively (Fig. 5.6B). Therefore, NO-triggered control over NRs and NiR1, together with nitrate signaling and proteasomal degradation are thus potentially relevant to control NO production at the transcriptional, translational and post-translational levels.

This ability of the NO to regulate its own biosynthesis would explain the big overlapping of differential transcriptomes of NO-deficient plants and NO-fumigated plants (GEO code GSE41958, Supplementary Tables S2, S3 and S4 in Castillo *et al.*, 2018), likely due to negative effect of NO on its production. As mentioned above, further work will confirm if the positive or negative regulation of NO on its homeostasis is dependent on its concentration (Fig. 5.7). This variable function of the NO resembles that observed for the modulation of cold stress-related plant resources, consisting on a switch from repressor to inducer of freezing tolerance (by enhancing cold acclimation) when cold triggers its accumulation (Fig. 5.7). Such a dramatic alteration in the plant signaling is possible given the capacity of NO to exert massive changes in the plant metabolome when its concentration surpasses a certain threshold (Fig. 5.7). However, it is important to remark that aside from its own concentration, the regulatory effect of NO on cell processes is subjected to multiple factors, including its location and the surrounding molecules. Thus, the highly complex interaction between NO and hormone signaling pathways implies that several hormone-related plant responses are regulated by NO while some NO-triggered responses are regulated by hormones (Fig. 5.7). At the same time, the N-end rule proteolytic pathway is regulated by NO but also is capable to modulate the function and homeostasis of NO (Fig. 5.7). Therefore, it can be concluded that, despite the great capacity of NO to exert extensive and diverse alterations in the plant physiology, unlike other signaling molecules, the regulatory role of NO is highly dependent on its interaction with a wide array of signaling pathways.

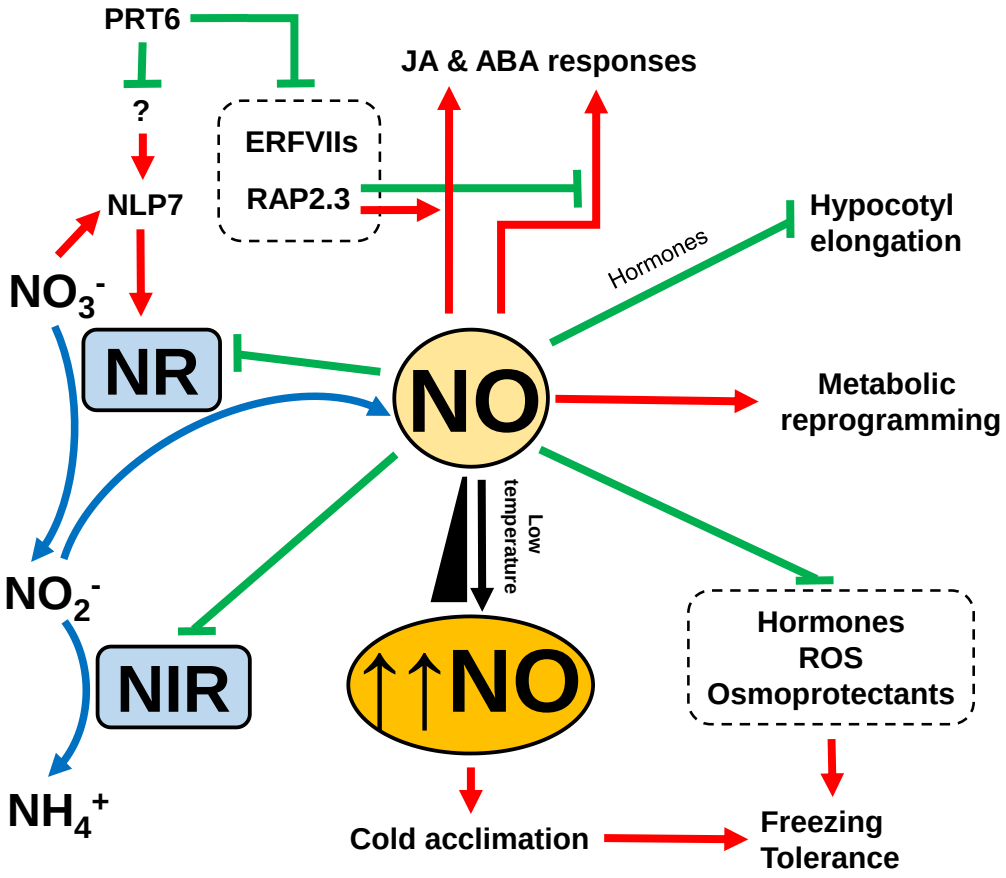

Figure 5.7. Scheme showing processes investigated in this work that regulate NO or are regulated by it. Green and red arrows represent negative and positive regulation, respectively; blue arrows represent catalysis, and the black arrow represents increase in concentration.

Conclusions

6. CONCLUSIONS

1) NO can control its own homeostasis in plants by regulating the function, accumulation and stability of NRs and NIR1 through nitrate signaling, N-end rule proteolytic pathway and post-translational modifications.
2) NO sensing in Arabidopsis hypocotyls requires the biosynthesis and/or signaling of ethylene, strigolactones, salicylates and abscisic acid, and is enhanced by BES1-mediated brassinosteroid signaling.
3) NO triggers an array of responses to alleviate toxicity and cellular damage that includes massive but transient reprogramming of primary and secondary metabolism.
4) RAP2.3 negatively regulates NO biosynthesis and sensing through a NO- and O_2-modulated rheostat-like mechanism in Arabidopsis that involves specific NO-related branches of jasmonate and abscisic acid signaling pathways.
5) NO acts as a sort of endogenous temperature sensor in plants preventing the development of freezing tolerance under non-stress temperature conditions, but triggering cold acclimation-induced freezing tolerance under low temperature stress.

Bibliography

7. BIBLIOGRAPHY

Abbas, M., Berckhan, S., Rooney, D. J., Gibbs, D. J., Conde, J. V., Correia, C. S., ... & Blázquez, M. A. (2015). Oxygen sensing coordinates photomorphogenesis to facilitate seedling survival. Current Biology, 25(11), 1483-1488.

Alet, A. I., Sanchez, D. H., Cuevas, J. C., del Valle, S., Altabella, T., Tiburcio, A. F., ... & Ruiz, O. A. (2011). Putrescine accumulation in Arabidopsis thaliana transgenic lines enhances tolerance to dehydration and freezing stress. Plant Signaling & Behavior, 6(2), 278-286.

Allan, W. L., Simpson, J. P., Clark, S. M., & Shelp, B. J. (2008). γ-Hydroxybutyrate accumulation in Arabidopsis and tobacco plants is a general response to abiotic stress: putative regulation by redox balance and glyoxylate reductase isoforms. Journal of Experimental Botany, 59(9), 2555-2564.

Araújo, W. L., Tohge, T., Ishizaki, K., Leaver, C. J., & Fernie, A. R. (2011). Protein degradation–an alternative respiratory substrate for stressed plants. Trends in Plant Science, 16(9), 489-498.

Arc, E., Sechet, J., Corbineau, F., Rajjou, L., & Marion-Poll, A. (2013). ABA crosstalk with ethylene and nitric oxide in seed dormancy and germination. Frontiers in Plant Science, 4(63), 1-19.

Armijo, G., & Gutiérrez, R. A. (2017). Emerging players in the nitrate signaling pathway. Molecular Plant, 10(8), 1019-1022.

Aslam, M., & Huffaker, R. C. (1989). Role of nitrate and nitrite in the induction of nitrite reductase in leaves of barley seedlings. Plant Physiology, 91(3), 1152-1156.

Astier, J., Besson-Bard, A., Wawer, I., Parent, C., Rasul, S., Jeandroz, S., ... & Wendehenne, D. (2010). Nitric oxide signalling in plants: cross-talk with Ca2+, protein kinases and reactive oxygen species. Annual Plant Reviews Volume 42: Nitrogen Metabolism in Plants in the Post-Genomic Era, Wiley-Blackwell, pp.147-170, 2010.

Astier, J., Gross, I., & Durner, J. (2017). Nitric oxide production in plants: an update. Journal of Experimental Botany, 69(14), 3401-3411.

Astier, J., & Lindermayr, C. (2012). Nitric oxide-dependent posttranslational modification in plants: an update. International Journal of Molecular Sciences, 13(11), 15193-15208.

Astier, J., Rasul, S., Koen, E., Manzoor, H., Besson-Bard, A., Lamotte, O., ... & Wendehenne, D. (2011). S-nitrosylation: an emerging post-translational protein modification in plants. Plant Science, 181(5), 527-533.

Bai, X. G., Chen, J. H., Kong, X. X., Todd, C. D., Yang, Y. P., Hu, X. Y., & Li, D. Z. (2012). Carbon monoxide enhances the chilling tolerance of recalcitrant Baccaurea ramiflora seeds via nitric oxidemediated glutathione homeostasis. Free Radical Biology and Medicine, 53(4), 710-720.

Baker, R. T., & Varshavsky, A. (1991). Inhibition of the N-end rule pathway in living cells. Proceedings of the National Academy of Sciences USA, 88(4), 1090-1094.

Barrero-Gil, J., & Salinas, J. (2013). Post-translational regulation of cold acclimation response. Plant Science, 205, 48-54.

Barroso, J. B., Corpas, F. J., Carreras, A., Sandalio, L. M., Valderrama, R., Palma, J., ... & del Río, L. A. (1999). Localization of nitric-oxide synthase in plant peroxisomes. Journal of Biological Chemistry, 274(51), 36729-36733.

Baxter-Burrell, A., Yang, Z., Springer, P. S., & Bailey-Serres, J. (2002). RopGAP4-dependent Rop GTPase rheostat control of Arabidopsis oxygen deprivation tolerance. Science, 296(5575), 2026-2028.

Bayden, A. S., Yakovlev, V. A., Graves, P. R., Mikkelsen, R. B., & Kellogg, G. E. (2011). Factors influencing protein tyrosine nitration—structure-based predictive models. Free Radical Biology and Medicine, 50(6), 749-762.

Begara-Morales, J. C., Sánchez-Calvo, B., Chaki, M., Valderrama, R., Mata-Pérez, C., López-Jaramillo, J., ... & Barroso, J. B. (2014). Dual regulation of cytosolic ascorbate peroxidase (APX) bytyrosine nitration and S-nitrosylation. Journal of Experimental Botany, 65(2), 527-538.

Begara-Morales, J. C., Sánchez-Calvo, B., Chaki, M., Valderrama, R., Mata-Pérez, C., Padilla, M. N., ... & Barroso, J. B. (2016). Antioxidant systems are regulated by nitric oxide-mediated posttranslational modifications (NO-PTMs). Frontiers in Plant Science, 7, 152.

Beligni, M. V., & Lamattina, L. (2000). Nitric oxide stimulates seed germination and de-etiolation, and inhibits hypocotyl elongation, three light-inducible responses in plants. Planta, 210(2), 215-221.

Bender, D., & Schwarz, G. (2018). Nitrite-dependent nitric oxide synthesis by molybdenum enzymes. FEBS Letters, 592(12), 2126-2139

Benjamini, Y., & Hochberg, Y. (1995). Controlling the false discovery rate: a practical and powerful approach to multiple testing. Journal of the Royal Statistical Society. Series B (Methodological), 289-300.

Bensmihen, S., To, A., Lambert, G., Kroj, T., Giraudat, J., & Parcy, F. (2004). Analysis of an activated ABI5 allele using a new selection method for transgenic Arabidopsis seeds. FEBS Letters, 561(1-3), 127-131.

Berger, S., Weichert, H., Porzel, A., Wasternack, C., Kühn, H., & Feussner, I. (2001). Enzymatic and non-enzymatic lipid peroxidation in leaf development. Biochimica et Biophysica Acta (BBA)-Molecular and Cell Biology of Lipids, 1533(3), 266-276.

Bertani, G. (1951). Studies on lysogenesis i.: The mode of phage liberation by lysogenic Escherichia coli1. Journal of Bacteriology, 62(3), 293.

Besson-Bard, A., Astier, J., Rasul, S., Wawer, I., Dubreuil-Maurizi, C., Jeandroz, S., & Wendehenne, D. (2009). Current view of nitric oxide-responsive genes in plants. Plant Science, 177(4), 302-309.

Bethke, P. C., Badger, M. R., & Jones, R. L. (2004). Apoplastic synthesis of nitric oxide by plant tissues. The Plant Cell, 16(2), 332-341.

Bethke, P. C., Libourel, I. G., & Jones, R. L. (2006). Nitric oxide reduces seed dormancy in Arabidopsis. Journal of Experimental Botany, 57(3), 517-526.

Bhargava, A., Ahad, A., Wang, S., Mansfield, S. D., Haughn, G. W., Douglas, C. J., & Ellis, B. E. (2013). The interacting MYB75 and KNAT7 transcription factors modulate secondary cell wall deposition both in stems and seed coat in Arabidopsis. Planta, 237(5), 1199-1211.

Bharti, N., & Bhatla, S. C. (2015). Nitric oxide mediates strigolactone signaling in auxin and ethylene-sensitive lateral root formation in sunflower seedlings. Plant Signaling & Behavior, 10(8), e1054087.

Bhaskara, G. B., Nguyen, T. T., & Verslues, P. (2012). Unique drought resistance functions of the highly ABA-induced clade A protein phosphatase 2Cs. Plant Physiology, pp-112.

Blokhina, O., Virolainen, E., & Fagerstedt, K. V. (2003). Antioxidants, oxidative damage and oxygen deprivation stress: a review. Annals of Botany, 91(2), 179-194.

Bloom, A. J. (2015). The increasing importance of distinguishing among plant nitrogen sources. Current Opinion in Plant Biology, 25, 10-16.

Booker, J., Sieberer, T., Wright, W., Williamson, L., Willett, B., Stirnberg, P., ... & Leyser, O. (2005). MAX1 encodes a cytochrome P450 family member that acts downstream of MAX3/4 to produce a carotenoid-derived branch-inhibiting hormone. Developmental Cell, 8(3), 443-449.

Bradford, M. M. (1976). A rapid and sensitive method for the quantitation of microgram quantities of protein utilizing the principle of protein-dye binding. Analytical Biochemistry, 72(1-2), 248-254.

Branco-Price, C., Kaiser, K. A., Jang, C. J., Larive, C. K., & Bailey-Serres, J. (2008). Selective mRNA translation coordinates energetic and metabolic adjustments to cellular oxygen deprivation and reoxygenation in Arabidopsis thaliana. The Plant Journal, 56(5), 743-755.

Bruckdorfer, R. (2005). The basics about nitric oxide. Molecular aspects of medicine, 26(1-2), 3-31.

Bu, Q., Jiang, H., Li, C. B., Zhai, Q., Zhang, J., Wu, X., ... & Li, C. (2008). Role of the Arabidopsis thaliana NAC transcription factors ANAC019 and ANAC055 in regulating jasmonic acid-signaled defense responses. Cell Research, 18(7), 756.

van Buer, J., Cvetkovic, J., & Baier, M. (2016). Cold regulation of plastid ascorbate peroxidases serves as a priming hub controlling ROS signaling in Arabidopsis thaliana. BMC Plant Biology, 16(1), 163.

Bui, L. T., Giuntoli, B., Kosmacz, M., Parlanti, S., & Licausi, F. (2015). Constitutively expressed ERF-VII transcription factors redundantly activate the core anaerobic response in Arabidopsis thaliana. Plant Science, 236, 37-43.

Büttner, M., & Singh, K. B. (1997). Arabidopsis thaliana ethylene-responsive element binding protein (AtEBP), an ethylene-inducible, GCC box DNA-binding protein interacts with an ocs element binding protein. Proceedings of the National Academy of Sciences USA, 94(11), 5961-5966.

Calanca, P. P. (2017). Effects of abiotic stress in crop production. In Quantification of Climate Variability, Adaptation and Mitigation for Agricultural Sustainability (pp. 165-180). Springer, Chem.

Calatrava, V., Chamizo-Ampudia, A., Sanz-Luque, E., Ocaña-Calahorro, F., Llamas, A., Fernandez, E., & Galvan, A. (2017). How Chlamydomonas handles nitrate and the nitric oxide cycle. Journal of Experimental Botany, 68(10), 2593-2602.

Campbell, W. H. (2001). Structure and function of eukaryotic NAD (P) H: nitrate reductase. Cellular and Molecular Life Sciences CMLS, 58(2), 194-204.

Cantrel, C., Vazquez, T., Puyaubert, J., Rezé, N., Lesch, M., Kaiser, W. M., ... & Baudouin, E. (2011). Nitric oxide participates in cold-responsive phosphosphingolipid formation and gene expression in Arabidopsis thaliana. New Phytologist, 189(2), 415-427.

Cao, H., Qi, S., Sun, M., Li, Z., Yang, Y., Crawford, N. M., & Wang, Y. (2017). Overexpression of the Maize ZmNLP6 and ZmNLP8 Can Complement the Arabidopsis Nitrate Regulatory Mutant nlp7 by Restoring Nitrate Signaling and Assimilation. Frontiers in Plant Science, 8, 1703.

Caro, A., & Puntarulo, S. (1999). Nitric oxide generation by soybean embryonic axes. Possible effect on mitochondrial function. Free Radical Research, 31(sup1), 205-212.

Castaings, L., Camargo, A., Pocholle, D., Gaudon, V., Texier, Y., Boutet-Mercey, S., ... & Meyer, C. (2009). The nodule inception-like protein 7 modulates nitrate sensing and metabolism in Arabidopsis. The Plant Journal, 57(3), 426-435.

Castillo, M. C., Coego, A., Costa-Broseta, Á., & León, J. (2018). Nitric oxide responses in Arabidopsis hypocotyls are mediated by diverse phytohormone pathways. Journal of Experimental Botany, 69(21), 5265-5278.

Castillo, M. C., Lozano-Juste, J., González-Guzmán, M., Rodriguez, L., Rodriguez, P. L., & León, J. (2015). Inactivation of PYR/PYL/RCAR ABA receptors by tyrosine nitration may enable rapid inhibition of ABA signaling by nitric oxide in plants. Science Signaling, 8(392), ra89-ra89.

Catalá, R., Medina, J., & Salinas, J. (2011). Integration of low temperature and light signaling during cold acclimation response in Arabidopsis. Proceedings of the National Academy of Sciences USA, 108(39), 16475-16480.

Chamizo-Ampudia, A., Sanz-Luque, E., Llamas, A., Galvan, A., & Fernandez, E. (2017). Nitrate reductase regulates plant nitric oxide homeostasis. Trends in Plant Science, 22(2), 163-174.

Chamizo-Ampudia, A., Sanz-Luque, E., Llamas, Á., Ocaña-Calahorro, F., Mariscal, V., Carreras, A., ... & Fernández, E. (2016). A dual system formed by the ARC and NR molybdoenzymes mediates nitrite-dependent NO production in Chlamydomonas. Plant Cell & Environment, 39(10), 2097-2107.

Chen, H. Y., Hsieh, E. J., Cheng, M. C., Chen, C. Y., Hwang, S. Y., & Lin, T. P. (2016). ORA47 (octadecanoid-responsive AP2/ERF-domain transcription factor 47) regulates jasmonic acid

abscisic acid biosynthesis and signaling through binding to a novel cis-element. New Phytologist, 211(2), 599-613.

Chen, J., Nolan, T. M., Ye, H., Zhang, M., Tong, H., Xin, P., ... & Yin, Y. (2017). Arabidopsis WRKY46, WRKY54, and WRKY70 Transcription Factors Are Involved in Brassinosteroid-Regulated Plant Growth and Drought Responses. The Plant Cell, 29(6), 1425-1439.

Chen, M., & Thelen, J. J. (2016). Acyl-lipid desaturase 1 primes cold acclimation response in Arabidopsis. Physiologia Plantarum, 158(1), 11-22.

Cheng, C. L., Acedo, G. N., Dewdney, J., Goodman, H. M., & Conkling, M. A. (1991). Differential expression of the two Arabidopsis nitrate reductase genes. Plant Physiology, 96(1), 275-279.

Cheng, C., Wang, Z., Ren, Z., Zhi, L., Yao, B., Su, C., ... & Li, X. (2017). SCFAtPP2-B11 modulates ABA signaling by facilitating SnRK2. 3 degradation in Arabidopsis thaliana. PLoS Genetics, 13(8), e1006947.

Cheng, W. H., Chiang, M. H., Hwang, S. G., & Lin, P. C. (2009). Antagonism between abscisic acid and ethylene in Arabidopsis acts in parallel with the reciprocal regulation of their metabolism and signaling pathways. Plant Molecular Biology, 71(1-2), 61-80.

Chinnusamy, V., Ohta, M., Kanrar, S., Lee, B. H., Hong, X., Agarwal, M., & Zhu, J. K. (2003). ICE1: a regulator of cold-induced transcriptome and freezing tolerance in Arabidopsis. Genes & Development, 17(8), 1043-1054.

Chinnusamy, V., Zhu, J., & Zhu, J. K. (2007). Cold stress regulation of gene expression in plants. Trends in Plant Science, 12(10), 444-451.

Chiu, J., March, P. E., Lee, R., & Tillett, D. (2004). Site-directed, Ligase-Independent Mutagenesis (SLIM): a single-tube methodology approaching 100% efficiency in 4 h. Nucleic Acids Research, 32(21), e174-e174.

Chory, J., Nagpal, P., & Peto, C. A. (1991). Phenotypic and genetic analysis of det2, a new mutant that affects light-regulated seedling development in Arabidopsis. The Plant Cell, 3(5), 445-459.

Clough, S. J., & Bent, A. F. (1998). Floral dip: a simplified method for Agrobacterium-mediated transformation of Arabidopsis thaliana. The Plant Journal, 16(6), 735-743.

Coego, A., Brizuela, E., Castillejo, P., Ruíz, S., Koncz, C., Del Pozo, J. C., ... & TRANSPLANTA Consortium. (2014). The TRANSPLANTA collection of A rabidopsis lines: a resource for functional analysis of transcription factors based on their conditional overexpression. The Plant Journal, 77(6), 944-953.

Cook, D., Fowler, S., Fiehn, O., & Thomashow, M. F. (2004). A prominent role for the CBF cold response pathway in configuring the low-temperature metabolome of Arabidopsis. Proceedings of the National Academy of Sciences USA, 101(42), 15243-15248.

Cooney, R. V., Harwood, P. J., Custer, L. J., & Franke, A. A. (1994). Light-mediated conversion of nitrogen dioxide to nitric oxide by carotenoids. Environmental Health Perspectives, 102(5), 460.

Corpas, F. J., & Barroso, J. B. (2014). Peroxisomal plant nitric oxide synthase (NOS) protein is imported by peroxisomal targeting signal type 2 (PTS2) in a process that depends on the cytosolic receptor PEX7 and calmodulin. FEBS Letters, 588(12), 2049-2054.

Corpas, F. J., Chaki, M., Fernandez-Ocana, A., Valderrama, R., Palma, J. M., Carreras, A., ... & Barroso, J. B. (2008). Metabolism of reactive nitrogen species in pea plants under abiotic stress conditions. Plant and Cell Physiology, 49(11), 1711-1722.

Correa-Aragunde, N., Foresi, N., & Lamattina, L. (2015). Nitric oxide is a ubiquitous signal for maintaining redox balance in plant cells: regulation of ascorbate peroxidase as a case study. Journal of Experimental Botany, 66(10), 2913-2921.

Costa-Broseta, Á., Perea-Resa, C., Castillo, M. C., Ruíz, M. F., Salinas, J., & León, J. (2018). Nitric Oxide Controls Constitutive Freezing Tolerance in Arabidopsis by Attenuating the Levels of Osmoprotectants, Stress-Related Hormones and Anthocyanins. Scientific Reports, 8(1), 9268.

Cuevas, J. C., López-Cobollo, R., Alcázar, R., Zarza, X., Koncz, C., Altabella, T., ... & Ferrando, A. (2008). Putrescine is involved in Arabidopsis freezing tolerance and cold acclimation by regulating abscisic acid levels in response to low temperature. Plant Physiology, 148(2), 1094-1105.

Davenport, S., Le Lay, P., & Sanchez-Tamburrrino, J. P. (2015). Nitrate metabolism in tobacco leaves overexpressing Arabidopsis nitrite reductase. Plant Physiology and Biochemistry, 97, 96-107.

Delaney, T. P., Uknes, S., Vernooij, B., Friedrich, L., Weymann, K., Negrotto, D., ... & Ryals, J. (1994). A central role of salicylic acid in plant disease resistance. Science, 266(5188), 1247-1250.

Diaz, C., Saliba-Colombani, V., Loudet, O., Belluomo, P., Moreau, L., Daniel-Vedele, F., ... & Masclaux-Daubresse, C. (2006). Leaf yellowing and anthocyanin accumulation are two genetically independent strategies in response to nitrogen limitation in Arabidopsis thaliana. Plant and Cell Physiology, 47(1), 74-83.

Ding, Y., Li, H., Zhang, X., Xie, Q., Gong, Z., & Yang, S. (2015). OST1 kinase modulates freezing tolerance by enhancing ICE1 stability in Arabidopsis. Developmental Cell, 32(3), 278-289.

Du, J., Li, M., Kong, D., Wang, L., Lv, Q., Wang, J., ... & He, Y. (2014). Nitric oxide induces cotyledon senescence involving co-operation of the NES1/MAD1 and EIN2-associated ORE1 signalling pathways in Arabidopsis. Journal of Experimental Botany, 65(14), 4051-4063.

Del Duca, S., Serafini-Fracassini, D., & Cai, G. (2014). Senescence and programmed cell death in plants: polyamine action mediated by transglutaminase. Frontiers in Plant Science, 5, 120.

Duek, P. D., Elmer, M. V., van Oosten, V. R., & Fankhauser, C. (2004). The degradation of HFR1, a putative bHLH class transcription factor involved in light signaling, is regulated by phosphorylation and requires COP1. Current Biology, 14(24), 2296-2301.

Durbak, A., Yao, H., & McSteen, P. (2012). Hormone signaling in plant development. Current Opinion in Plant Biology, 15(1), 92-96.

Durner, J., Wendehenne, D., & Klessig, D. F. (1998). Defense gene induction in tobacco by nitric oxide, cyclic GMP, and cyclic ADP-ribose. Proceedings of the National Academy of Sciences USA, 95(17), 10328-10333.

Edwards, K., Johnstone, C., & Thompson, C. (1991). A simple and rapid method for the preparation of plant genomic DNA for PCR analysis. Nucleic Acids Research, 19(6), 1349.

Eremina, M., Rozhon, W., & Poppenberger, B. (2016a). Hormonal control of cold stress responses in plants. Cellular and Molecular Life Sciences, 73(4), 797-810.

Eremina, M., Unterholzner, S. J., Rathnayake, A. I., Castellanos, M., Khan, M., Kugler, K. G., ... & Poppenberger, B. (2016b). Brassinosteroids participate in the control of basal and acquired freezing tolerance of plants. Proceedings of the National Academy of Sciences USA, 113(40), E5982-E5991.

Fancy, N. N., Bahlmann, A. K., & Loake, G. J. (2017). Nitric oxide function in plant abiotic stress. Plant Cell & Environment, 40(4), 462-472.

Feng, C. Z., Chen, Y., Wang, C., Kong, Y. H., Wu, W. H., & Chen, Y. F. (2014). Arabidopsis RAV 1transcription factor, phosphorylated by S n RK 2 kinases, regulates the expression of ABI 3, ABI 4, and ABI 5 during seed germination and early seedling development. The Plant Journal, 80(4), 654-668.

Feng, S., Martinez, C., Gusmaroli, G., Wang, Y., Zhou, J., Wang, F., ... & Schäfer, E. (2008). Coordinated regulation of Arabidopsis thaliana development by light and gibberellins. Nature, 451(7177), 475.

Feussner, I., & Wasternack, C. (2001). The lipoxygenase pathway. Annual Review of Plant Biology, 53(1), 275-297.

Ford, P. C. (2010). Reactions of NO and nitrite with heme models and proteins. Inorganic Chemistry, 49(14), 6226-6239.

Foresi, N., Mayta, M. L., Lodeyro, A. F., Scuffi, D., Correa-Aragunde, N., García-Mata, C., ... & Lamattina, L. (2015). Expression of the tetrahydrofolate-dependent nitric oxide synthase from the green alga Ostreococcus tauri increases tolerance to abiotic stresses and influences stomatal development in Arabidopsis. The Plant Journal, 82(5), 806-821.

Fowler, S., & Thomashow, M. F. (2002). Arabidopsis transcriptome profiling indicates that multiple regulatory pathways are activated during cold acclimation in addition to the CBF cold response pathway. The Plant Cell, 14(8), 1675-1690.

Franco-Zorrilla, J. M., López-Vidriero, I., Carrasco, J. L., Godoy, M., Vera, P., & Solano, R. (2014). DNA-binding specificities of plant transcription factors and their potential to define target genes. Proceedings of the National Academy of Sciences USA, 111(6), 2367-2372.

Freschi, L. (2013). Nitric oxide and phytohormone interactions: current status and perspectives. Frontiers in Plant Science, 4, 398.

Friebe, A., & Koesling, D. (2003). Regulation of nitric oxide-sensitive guanylyl cyclase. Circulation Research, 93(2), 96-105.

Frungillo, L., Skelly, M. J., Loake, G. J., Spoel, S. H., & Salgado, I. (2014). S-nitrosothiols regulate nitric oxide production and storage in plants through the nitrogen assimilation pathway. Nature Communications, 5, 5401.

Fujioka, S., Li, J., Choi, Y. H., Seto, H., Takatsuto, S., Noguchi, T., ... & Sakurai, A. (1997). The Arabidopsis deetiolated2 mutant is blocked early in brassinosteroid biosynthesis. The Plant Cell, 9(11), 1951-1962.

Gaffney, T., Friedrich, L., Vernooij, B., Negrotto, D., Nye, G., Uknes, S., ... & Ryals, J. (1993). Requirement of salicylic acid for the induction of systemic acquired resistance. Science, 261(5122), 754-756.

Garcion, C., Lohmann, A., Lamodiere, E., Catinot, J., Buchala, A., Doermann, P., & Métraux, J. P. (2008). Characterization and biological function of the ISOCHORISMATE SYNTHASE2 gene of Arabidopsis. Plant Physiology, 147(3), 1279-1287.

Gasch, P., Fundinger, M., Müller, J. T., Lee, T., Bailey-Serres, J., & Mustroph, A. (2015). Redundant ERF-VII transcription factors bind to an evolutionarily conserved cis-motif to regulate hypoxiaresponsive gene expression in Arabidopsis. The Plant Cell, 28(1), 160-180.

Gaupels, F., Spiazzi-Vandelle, E., Yang, D., & Delledonne, M. (2011). Detection of peroxynitrite accumulation in Arabidopsis thaliana during the hypersensitive defense response. Nitric Oxide, 25(2), 222-228.

Gent, L., & Forde, B. G. (2017). How do plants sense their nitrogen status?. Journal of Experimental Botany, 68(10), 2531-2539.

Gibbs, D. J., Bacardit, J., Bachmair, A., & Holdsworth, M. J. (2014b). The eukaryotic N-end rule pathway: conserved mechanisms and diverse functions. Trends in Cell Biology, 24(10), 603-611.

Gibbs, D. J., Conde, J. V., Berckhan, S., Prasad, G., Mendiondo, G. M., & Holdsworth, M. J. (2015). Group VII ethylene response factors coordinate oxygen and nitric oxide signal transduction and stress responses in plants. Plant Physiology, 169(1), 23-31.

Gibbs, D. J., Lee, S. C., Isa, N. M., Gramuglia, S., Fukao, T., Bassel, G. W., ... & Holdsworth, M. J. (2011). Homeostatic response to hypoxia is regulated by the N-end rule pathway in plants. Nature, 479(7373), 415.

Gibbs, D. J., Isa, N. M., Movahedi, M., Lozano-Juste, J., Mendiondo, G. M., Berckhan, S., ... & Bassel, G. W. (2014a). Nitric oxide sensing in plants is mediated by proteolytic control of group VII ERF transcription factors. Molecular Cell, 53(3), 369-379.

Gilmour, S. J., Fowler, S. G., & Thomashow, M. F. (2004). Arabidopsis transcriptional activators CBF1, CBF2, and CBF3 have matching functional activities. Plant Molecular Biology, 54(5), 767-781.

Gilmour, S. J., Zarka, D. G., Stockinger, E. J., Salazar, M. P., Houghton, J. M., & Thomashow, M. F. (1998). Low temperature regulation of the Arabidopsis CBF family of AP2 transcriptional activators as an early step in cold-induced COR gene expression. The Plant Journal, 16(4), 433-442.

Gniazdowska, A., Dobrzyńska, U., Babańczyk, T., & Bogatek, R. (2007). Breaking the apple embryo dormancy by nitric oxide involves the stimulation of ethylene production. Planta, 225(4), 1051-1057.

Gow, A. J., Farkouh, C. R., Munson, D. A., Posencheg, M. A., & Ischiropoulos, H. (2004). Biological significance of nitric oxide-mediated protein modifications. American Journal of Physiology-Lung Cellular and Molecular Physiology, 287(2), L262-L268.

Green, M. A., & Fry, S. C. (2005). Vitamin C degradation in plant cells via enzymatic hydrolysis of 4-O-oxalyl-L-threonate. Nature, 433(7021), 83.

Griffith, M., Lumb, C., Wiseman, S. B., Wisniewski, M., Johnson, R. W., & Marangoni, A. G. (2005). Antifreeze proteins modify the freezing process in planta. Plant Physiology, 138(1), 330-340.

Groß, F., Durner, J., & Gaupels, F. (2013). Nitric oxide, antioxidants and prooxidants in plant defence responses. Frontiers in Plant Science, 4, 419.

Gross, I., & Durner, J. (2016). In search of enzymes with a role in 3′, 5′-cyclic guanosine monophosphate metabolism in plants. Frontiers in Plant Science, 7, 576.

Grün, S., Lindermayr, C., Sell, S., & Durner, J. (2006). Nitric oxide and gene regulation in plants. Journal of Experimental Botany, 57(3), 507-516.

Guan, P., Ripoll, J. J., Wang, R., Vuong, L., Bailey-Steinitz, L. J., Ye, D., & Crawford, N. M. (2017). Interacting TCP and NLP transcription factors control plant responses to nitrate availability. Proceedings of the National Academy of Sciences USA, 114(9), 2419-2424.

Guo, F. Q., Okamoto, M., & Crawford, N. M. (2003). Identification of a plant nitric oxide synthase gene involved in hormonal signaling. Science, 302(5642), 100-103.

Gupta, K. J. (2011). Protein S-nitrosylation in plants: photorespiratory metabolism and NO signaling. Science Signaling, 4(154), jc1.

Gupta, K. J., Hebelstrup, K. H., Mur, L. A., & Igamberdiev, A. U. (2011). Plant hemoglobins: important players at the crossroads between oxygen and nitric oxide. FEBS Letters, 585(24), 3843-3849.

Gupta, K. J., & Igamberdiev, A. U. (2011). The anoxic plant mitochondrion as a nitrite: NO reductase. Mitochondrion, 11(4), 537-543.

Gupta, K. J., Stoimenova, M., & Kaiser, W. M. (2005). In higher plants, only root mitochondria, but not leaf mitochondria reduce nitrite to NO, in vitro and in situ. Journal of Experimental Botany, 56(420), 2601-2609.

Guy, C., Kaplan, F., Kopka, J., Selbig, J., & Hincha, D. K. (2008). Metabolomics of temperature stress. Physiologia Plantarum, 132(2), 220-235.

Hamant, O., & Traas, J. (2010). The mechanics behind plant development. New Phytologist, 185(2), 369-385.

Hancock, J. T. (2012). NO synthase? Generation of nitric oxide in plants. Periodicum Biologorum, 114(1), 19-24.

Hancock, J. T., Neill, S. J., & Wilson, I. D. (2011). Nitric oxide and ABA in the control of plant function. Plant Science, 181(5), 555-559.

Hannah, M. A., Heyer, A. G., & Hincha, D. K. (2005). A global survey of gene regulation during cold acclimation in Arabidopsis thaliana. PLoS Genetics, 1(2), e26.

Havaux, M., & Kloppstech, K. (2001). The protective functions of carotenoid and flavonoid pigments against excess visible radiation at chilling temperature investigated in Arabidopsis npq and tt mutants. Planta, 213(6), 953-966.

Havemeyer, A., Bittner, F., Wollers, S., Mendel, R., Kunze, T., & Clement, B. (2006). Identification of the missing component in the mitochondrial benzamidoxime prodrug-converting system as a novel molybdenum enzyme. Journal of Biological Chemistry, 281(46), 34796-34802.

He, J. X., Gendron, J. M., Sun, Y., Gampala, S. S., Gendron, N., Sun, C. Q., & Wang, Z. Y. (2005). BZR1 is a transcriptional repressor with dual roles in brassinosteroid homeostasis and growth responses. Science, 307(5715), 1634-1638.

He, K., Xu, S., & Li, J. (2013). BAK 1 Directly Regulates Brassinosteroid Perception and BRI 1 Activation. Journal of Integrative Plant Biology, 55(12), 1264-1270.

He, Y., Tang, R. H., Hao, Y., Stevens, R. D., Cook, C. W., Ahn, S. M., ... & Fiorani, F. (2004). Nitric oxide represses the Arabidopsis floral transition. Science, 305(5692), 1968-1971.

Hess, D. T., & Stamler, J. S. (2012). Regulation by S-nitrosylation of protein post-translational modification. Journal of Biological Chemistry, 287(7), 4411-4418.

Hirashima, M., Tanaka, R., & Tanaka, A. (2009). Light-independent cell death induced by accumulation of pheophorbide a in Arabidopsis thaliana. Plant and Cell Physiology, 50(4), 719-729.

Hobo, T., Asada, M., Kowyama, Y., & Hattori, T. (1999). ACGT-containing abscisic acid response element (ABRE) and coupling element 3 (CE3) are functionally equivalent. The Plant Journal, 19(6), 679-689.

Holzmeister, C., Gaupels, F., Geerlof, A., Sarioglu, H., Sattler, M., Durner, J., & Lindermayr, C. (2015). Differential inhibition of Arabidopsis superoxide dismutases by peroxynitrite-mediated tyrosine nitration. Journal of Experimental Botany, 66(3), 989-999.

Hörtensteiner, S. (2013). Update on the biochemistry of chlorophyll breakdown. Plant Molecular Biology, 82(6), 505-517.

Hou, Q., Ufer, G., & Bartels, D. (2016). Lipid signalling in plant responses to abiotic stress. Plant Cell & Environment, 39(5), 1029-1048.

Hu, Y., Jiang, L., Wang, F., & Yu, D. (2013). Jasmonate regulates the inducer of cbf expression-Crepeat binding factor/DRE binding factor1 cascade and freezing tolerance in Arabidopsis. The Plant Cell, 25(8), 2907-2924.

Hurlock, A. K., Roston, R. L., Wang, K., & Benning, C. (2014). Lipid trafficking in plant cells. Traffic, 15(9), 915-932.

Igamberdiev, A. U., Bykova, N. V., & Hill, R. D. (2011). Structural and functional properties of class 1 plant hemoglobins. IUBMB Life, 63(3), 146-152.

Imran, Q. M., Hussain, A., Lee, S. U., Mun, B. G., Falak, N., Loake, G. J., & Yun, B. W. (2018). Transcriptome profile of NO-induced Arabidopsis transcription factor genes suggests their putative regulatory role in multiple biological processes. Scientific Reports, 8(1), 771.

Jaeglé, L., Steinberger, L., Martin, R. V., & Chance, K. (2005). Global partitioning of NO x sources using satellite observations: Relative roles of fossil fuel combustion, biomass burning and soil emissions. Faraday Discussions, 130, 407-423.

Janská, A., Maršík, P., Zelenková, S., & Ovesná, J. (2010). Cold stress and acclimation–what is important for metabolic adjustment?. Plant Biology, 12(3), 395-405.

Jeandroz, S., Wipf, D., Stuehr, D. J., Lamattina, L., Melkonian, M., Tian, Z., ... & Wendehenne, D. (2016). Occurrence, structure, and evolution of nitric oxide synthase–like proteins in the plant kingdom. Science Signaling, 9(417), re2-re2.

Jeon, J., Kim, N. Y., Kim, S., Kang, N. Y., Novák, O., Ku, S. J., ... & Kim, J. (2010). A subset of cytokinin two-component signaling system plays a role in cold temperature stress response in Arabidopsis. The Journal of Biological Chemistry, 285(30), 23371-23386.

Jia, K. P., Luo, Q., He, S. B., Lu, X. D., & Yang, H. Q. (2014). Strigolactone-regulated hypocotyl elongation is dependent on cryptochrome and phytochrome signaling pathways in Arabidopsis. Molecular Plant, 7(3), 528-540.

Jiang, J., Zhang, C., & Wang, X. (2013). Ligand perception, activation, and early signaling of plant steroid receptor brassinosteroid insensitive 1. Journal of Integrative Plant Biology, 55(12), 1198-1211.

Joy, K. W., & Hageman, R. H. (1966). The purification and properties of nitrite reductase from higher plants, and its dependence on ferredoxin. Biochemical Journal, 100(1), 263.

Kakei, Y., & Shimada, Y. (2015). AtCAST3. 0 update: a web-based tool for analysis of transcriptome data by searching similarities in gene expression profiles. Plant and Cell Physiology, 56(1), e7-e7.

Kaplan, F., Kopka, J., Sung, D. Y., Zhao, W., Popp, M., Porat, R., & Guy, C. L. (2007). Transcript and metabolite profiling during cold acclimation of Arabidopsis reveals an intricate relationship of cold-regulated gene expression with modifications in metabolite content. The Plant Journal, 50(6), 967-981.

Kasten, D., Durner, J., & Gaupels, F. (2017). Gas alert: the NO2 pitfall during NO fumigation of plants. Frontiers in Plant Science, 8, 85.

Kasukabe, Y., He, L., Nada, K., Misawa, S., Ihara, I., & Tachibana, S. (2004). Overexpression of spermidine synthase enhances tolerance to multiple environmental stresses and up-regulates the expression of various stress-regulated genes in transgenic Arabidopsis thaliana. Plant and Cell Physiology, 45(6), 712-722.

Kawamura, Y., & Uemura, M. (2003). Mass spectrometric approach for identifying putative plasma membrane proteins of Arabidopsis leaves associated with cold acclimation. The Plant Journal, 36(2), 141-154.

Kilian, J., Whitehead, D., Horak, J., Wanke, D., Weinl, S., Batistic, O., ... & Harter, K. (2007). The AtGenExpress global stress expression data set: protocols, evaluation and model data analysis of UV-B light, drought and cold stress responses. The Plant Journal, 50(2), 347-363.

Kim, Y. H., Choi, K. I., Khan, A. L., Waqas, M., & Lee, I. J. (2016). Exogenous application of abscisic acid regulates endogenous gibberellins homeostasis and enhances resistance of oriental melon (Cucumis melo var. L.) against low temperature. Scientia Horticulturae, 207, 41-47.

Kitamura, K. (2016). Inhibition of the Arg/N-end rule pathway-mediated proteolysis by dipeptidemimetic molecules. Amino Acids, 48(1), 235-243.

Knight, M. R., & Knight, H. (2012). Low-temperature perception leading to gene expression and cold tolerance in higher plants. New Phytologist, 195(4), 737-751.

Kolbert, Z. (2018). Strigolactone-nitric oxide interplay in plants: The story has just begun. Physiologia Plantarum. doi: 10.1111/ppl.12712.

Konishi, M., & Yanagisawa, S. (2013). Arabidopsis NIN-like transcription factors have a central role in nitrate signalling. Nature Communications, 4, 1617.

Korn, M., Peterek, S., MOCK, H. P., Heyer, A. G., & Hincha, D. K. (2008). Heterosis in the freezing tolerance, and sugar and flavonoid contents of crosses between Arabidopsis thaliana accessions of widely varying freezing tolerance. Plant Cell & Environment, 31(6), 813-827.

Kreps, J. A., Wu, Y., Chang, H. S., Zhu, T., Wang, X., & Harper, J. F. (2002). Transcriptome changes for Arabidopsis in response to salt, osmotic, and cold stress. Plant Physiology, 130(4), 2129-2141.

Krishnaswamy, S., Verma, S., Rahman, M. H., & Kav, N. N. (2011). Functional characterization of four APETALA2-family genes (RAP2. 6, RAP2. 6L, DREB19 and DREB26) in Arabidopsis. Plant Molecular Biology, 75(1-2), 107-127.

Krol, M., Gray, G. R., Huner, N. P. A., Hurry, V. M., Öquist, G., & Malek, L. (1995). Low-temperature stress and photoperiod affect an increased tolerance to photoinhibition in Pinus banksiana seedlings. Canadian Journal of Botany, 73(8), 1119-1127.

Kumar, S., Kaur, G., & Nayyar, H. (2008). Exogenous application of abscisic acid improves cold tolerance in chickpea (Cicer arietinum L.). Journal of Agronomy and Crop Science, 194(6), 449-456.

Lamotte, O., Courtois, C., Dobrowolska, G., Besson, A., Pugin, A., & Wendehenne, D. (2006). Mechanisms of nitric-oxide-induced increase of free cytosolic Ca2+ concentration in Nicotiana plumbaginifolia cells. Free Radical Biology and Medicine, 40(8), 1369-1376.

Lee, B. H., Henderson, D. A., & Zhu, J. K. (2005). The Arabidopsis cold-responsive transcriptome and its regulation by ICE1. The Plant Cell, 17(11), 3155-3175.

Lee, H. G., & Seo, P. J. (2015). The MYB 96–HHP module integrates cold and abscisic acid signaling to activate the CBF–COR pathway in Arabidopsis. The Plant Journal, 82(6), 962-977.

Lee, H. G., & Seo, P. J. (2016). The Arabidopsis MIEL1 E3 ligase negatively regulates ABA signalling by promoting protein turnover of MYB96. Nature Communications, 7, 12525.

León, J., Castillo, M. C., Coego, A., Lozano-Juste, J., & Mir, R. (2014). Diverse functional interactions between nitric oxide and abscisic acid in plant development and responses to stress. Journal of Experimental Botany, 65(4), 907-921.

León, J., Costa, Á., & Castillo, M. C. (2016). Nitric oxide triggers a transient metabolic reprogramming in Arabidopsis. Scientific Reports, 6, 37945.

Li, H. Y., Xiao, S., & Chye, M. L. (2008). Ethylene-and pathogen-inducible Arabidopsis acyl-CoAbinding protein 4 interacts with an ethylene-responsive element binding protein. Journal of Experimental Botany, 59(14), 3997-4006.

Li, L., Yu, X., Thompson, A., Guo, M., Yoshida, S., Asami, T., ... & Yin, Y. (2009). Arabidopsis MYB30 is a direct target of BES1 and cooperates with BES1 to regulate brassinosteroid-induced gene expression. The Plant Journal, 58(2), 275-286.

Licausi, F., Kosmacz, M., Weits, D. A., Giuntoli, B., Giorgi, F. M., Voesenek, L. A., ... & van Dongen, J. T. (2011). Oxygen sensing in plants is mediated by an N-end rule pathway for protein destabilization. Nature, 479(7373), 419.

Lillo, C., Meyer, C., Lea, U. S., Provan, F., & Oltedal, S. (2004). Mechanism and importance of posttranslational regulation of nitrate reductase. Journal of Experimental Botany, 55(401), 1275-1282.

Lindermayr, C., Sell, S., Müller, B., Leister, D., & Durner, J. (2010). Redox Regulation of the NPR1-TGA1 System of Arabidopsis thaliana by Nitric Oxide. The Plant Cell, 2894-2907.

Liu, F., & Guo, F. Q. (2013). Nitric oxide deficiency accelerates chlorophyll breakdown and stability loss of thylakoid membranes during dark-induced leaf senescence in Arabidopsis. PLoS One, 8(2), e56345.

Liu, Y., Jiang, H., Zhao, Z., & An, L. (2010). Nitric oxide synthase like activity-dependent nitric oxide production protects against chilling-induced oxidative damage in Chorispora bungeana suspension cultured cells. Plant Physiology and Biochemistry, 48(12), 936-944.

Liu, Z., Cao, J., Ma, Q., Gao, X., Ren, J., & Xue, Y. (2011). GPS-YNO2: computational prediction of tyrosine nitration sites in proteins. Molecular BioSystems, 7(4), 1197-1204.

Llorente, F., Oliveros, J. C., Martínez-Zapater, J. M., & Salinas, J. (2000). A freezing-sensitive mutant of Arabidopsis, frs1, is a new aba3 allele. Planta, 211(5), 648-655.

Lozano-Juste, J., Colom-Moreno, R., & León, J. (2011). In vivo protein tyrosine nitration in Arabidopsis thaliana. Journal of Experimental Botany, 62(10), 3501-3517.

Lozano-Juste, J., & León, J. (2011). Nitric oxide regulates DELLA content and PIF expression to promote photomorphogenesis in Arabidopsis. Plant Physiology, 156(3), 1410-1423.

Lozano-Juste, J., & León, J. (2010). Enhanced abscisic acid-mediated responses in nia1nia2noa1-2 triple mutant impaired in NIA/NR-and AtNOA1-dependent nitric oxide biosynthesis in Arabidopsis. Plant Physiology, 152(2), 891-903.

Maeo, K., Hayashi, S., Kojima-Suzuki, H., Morikami, A., & Nakamura, K. (2001). Role of conserved residues of the WRKY domain in the DNA-binding of tobacco WRKY family proteins. Bioscience, Biotechnology, and Biochemistry, 65(11), 2428-2436.

Majláth, I., Szalai, G., Soós, V., Sebestyén, E., Balázs, E., Vanková, R., ... & Janda, T. (2012). Effect of light on the gene expression and hormonal status of winter and spring wheat plants during cold hardening. Physiologia Plantarum, 145(2), 296-314.

Manjunatha, G., Lokesh, V., & Neelwarne, B. (2010). Nitric oxide in fruit ripening: trends and opportunities. Biotechnology Advances, 28(4), 489-499.

Manoli, A., Trevisan, S., Voigt, B., Yokawa, K., Baluška, F., & Quaggiotti, S. (2016). Nitric oxidemediated maize root apex responses to nitrate are regulated by auxin and strigolactones. Frontiersin Plant Science, 6, 1269.

Mantri, N., Patade, V., Penna, S., Ford, R., & Pang, E. (2012). Abiotic stress responses in plants: present and future. In Abiotic stress responses in plants (pp. 1-19). Springer, New York, NY.

Mantyla, E., Lang, V., & Palva, E. T. (1995). Role of abscisic acid in drought-induced freezing tolerance, cold acclimation, and accumulation of LT178 and RAB18 proteins in Arabidopsis thaliana. Plant Physiology, 107(1), 141-148.

Marchive, C., Roudier, F., Castaings, L., Bréhaut, V., Blondet, E., Colot, V., ... & Krapp, A. (2013). Nuclear retention of the transcription factor NLP7 orchestrates the early response to nitrate in plants. Nature Communications, 4, 1713.

Marín-de la Rosa, N., Sotillo, B., Miskolczi, P., Gibbs, D. J., Vicente, J., Carbonero, P., ... & Blázquez, M. A. (2014). Large-Scale Identification of Gibberellin-Related Transcription Factors Defines Group VII ETHYLENE RESPONSE FACTORS as Functional DELLA Partners. Plant Physiology, 166(2), 1022-1032.

Mata-Perez, C., Sanchez-Calvo, B., Padilla, M. N., Begara-Morales, J. C., Valderrama, R., Corpas, F. J., & Barroso, J. B. (2017). Nitro-fatty acids in plant signaling: new key mediators of nitric oxide metabolism. Redox Biology, 11, 554-561.

Medina, J., Catalá, R., & Salinas, J. (2011). The CBFs: three Arabidopsis transcription factors to cold acclimate. Plant Science, 180(1), 3-11.

De Michele, R., Formentin, E., Todesco, M., Toppo, S., Carimi, F., Zottini, M., ... & Schiavo, F. L. (2009). Transcriptome analysis of Medicago truncatula leaf senescence: similarities and differences in metabolic and transcriptional regulations as compared with Arabidopsis, nodule senescence and nitric oxide signalling. New Phytologist, 181(3), 563-575.

Mikami, B., & Ida, S. (1984). Purification and properties of ferredoxin—nitrate reductase from the cyanobacterium Plectonema boryanum. Biochimica et Biophysica Acta (BBA)-Protein Structure and Molecular Enzymology, 791(3), 294-304.

Mittler, R. (2006). Abiotic stress, the field environment and stress combination. Trends in Plant Science, 11(1), 15-19.

Miura, K., & Furumoto, T. (2013). Cold signaling and cold response in plants. International Journal of Molecular Sciences, 14(3), 5312-5337.

Miura, K., & Ohta, M. (2010). SIZ1, a small ubiquitin-related modifier ligase, controls cold signaling through regulation of salicylic acid accumulation. Journal of Plant Physiology, 167(7), 555-560.

Montilla-Bascón, G., Rubiales, D., Hebelstrup, K. H., Mandon, J., Harren, F. J., Cristescu, S. M., ... & Prats, E. (2017). Reduced nitric oxide levels during drought stress promote drought tolerance in barley and is associated with elevated polyamine biosynthesis. Scientific Reports, 7(1), 13311.

Moreau, M., Lee, G. I., Wang, Y., Crane, B. R., & Klessig, D. F. (2008). AtNOS/AtNOA1 Is a Functional Arabidopsis thaliana cGTPase and Not a Nitric-oxide Synthase. Journal of Biological Chemistry, 283(47), 32957-32967.

Morffy, N., Faure, L., & Nelson, D. C. (2016). Smoke and hormone mirrors: action and evolution of karrikin and strigolactone signaling. Trends in Genetics, 32(3), 176-188.

Mulaudzi, T., Ludidi, N., Ruzvidzo, O., Morse, M., Hendricks, N., Iwuoha, E., & Gehring, C. (2011). Identification of a novel Arabidopsis thaliana nitric oxide-binding molecule with guanylate cyclase activity in vitro. FEBS Letters, 585(17), 2693-2697.

Mur, L. A., Mandon, J., Persijn, S., Cristescu, S. M., Moshkov, I. E., Novikova, G. V., ... & Gupta, K. J. (2013). Nitric oxide in plants: an assessment of the current state of knowledge. AoB PLANTS, 5, pls052.

Murashige, T., & Skoog, F. (1962). A revised medium for rapid growth and bio assays with tobacco tissue cultures. Physiologia Plantarum, 15(3), 473-497.

Nägele, T., Stutz, S., Hörmiller, I. I., & Heyer, A. G. (2012). Identification of a metabolic bottleneck for cold acclimation in Arabidopsis thaliana. The Plant Journal, 72(1), 102-114.

Nakashima, K., Ito, Y., & Yamaguchi-Shinozaki, K. (2009). Transcriptional regulatory networks in response to abiotic stresses in Arabidopsis and grasses. Plant Physiology, 149(1), 88-95.

Nakashima, K., Yamaguchi-Shinozaki, K., & Shinozaki, K. (2014). The transcriptional regulatory network in the drought response and its crosstalk in abiotic stress responses including drought, cold, and heat. Frontiers in Plant Science, 5, 170.

Neill, S. J., Desikan, R., Clarke, A., & Hancock, J. T. (2002). Nitric oxide is a novel component of abscisic acid signaling in stomatal guard cells. Plant Physiology, 128(1), 13-16.

Nemhauser, J. L., Hong, F., & Chory, J. (2006). Different plant hormones regulate similar processes through largely nonoverlapping transcriptional responses. Cell, 126(3), 467-475.

Noctor, G., Mhamdi, A., Chaouch, S., Han, Y., Neukermans, J., Marquez-Garcia, B., ... & Foyer, C. H. (2012). Glutathione in plants: an integrated overview. Plant Cell & Environment, 35(2), 454-484.

Noguchi, T., Fujioka, S., Takatsuto, S., Sakurai, A., Yoshida, S., Li, J., & Chory, J. (1999). Arabidopsis det2 is defective in the conversion of (24R)-24-methylcholest-4-en-3-one to (24R)-24-methyl-5α-cholestan-3-one in brassinosteroid biosynthesis. Plant Physiology, 120(3), 833-840.

Novikova, G. V., Mur, L. A., Nosov, A. V., Fomenkov, A. A., Mironov, K. S., Mamaeva, A. S., ... & Hall, M. A. (2017). Nitric Oxide Has a Concentration-Dependent Effect on the Cell Cycle Acting via EIN2 in Arabidopsis thaliana Cultured Cells. Frontiers in Physiology, 8, 142.

Ogawa, T., Pan, L., Kawai-Yamada, M., Yu, L. H., Yamamura, S., Koyama, T., ... & Uchimiya, H. (2005). Functional analysis of Arabidopsis ethylene-responsive element binding protein conferring resistance to Bax and abiotic stress-induced plant cell death. Plant Physiology, 138(3), 1436-1445.

Ohta, M., Matsui, K., Hiratsu, K., Shinshi, H., & Ohme-Takagi, M. (2001). Repression domains of class II ERF transcriptional repressors share an essential motif for active repression. The Plant Cell, 13(8), 1959-1968.

Palmieri, M. C., Sell, S., Huang, X., Scherf, M., Werner, T., Durner, J., & Lindermayr, C. (2008). Nitric oxide-responsive genes and promoters in Arabidopsis thaliana: a bioinformatics approach. Journal of Experimental Botany, 59(2), 177-186.

Papdi, C., Pérez-Salamó, I., Joseph, M. P., Giuntoli, B., Bögre, L., Koncz, C., & Szabados, L. (2015). The low oxygen, oxidative and osmotic stress responses synergistically act through the ethylene response factor VII genes RAP 2.12, RAP 2.2 and RAP 2.3. The Plant Journal, 82(5), 772-784.

Park, B. S., Song, J. T., & Seo, H. S. (2011). Arabidopsis nitrate reductase activity is stimulated by the E3 SUMO ligase AtSIZ1. Nature Communications, 2, 400.

Park, S., Lee, C. M., Doherty, C. J., Gilmour, S. J., Kim, Y., & Thomashow, M. F. (2015). Regulation of the Arabidopsis CBF regulon by a complex low-temperature regulatory network. The Plant Journal, 82(2), 193-207.

Parsons, H. T., Yasmin, T., & Fry, S. C. (2011). Alternative pathways of dehydroascorbic acid degradation in vitro and in plant cell cultures: novel insights into vitamin C catabolism. Biochemical Journal, 440(3), 375-385.

Pauwels, L., Morreel, K., De Witte, E., Lammertyn, F., Van Montagu, M., Boerjan, W., ... & Goossens, A. (2008). Mapping methyl jasmonate-mediated transcriptional reprogramming of metabolism and cell cycle progression in cultured Arabidopsis cells. Proceedings of the National Academy of Sciences USA, 105(4), 1380-1385.

Pilegaard, K. (2013). Processes regulating nitric oxide emissions from soils. Philosophical Transactions of the Royal Society B: Biological Sciences, 368(1621).

Planchet, E., Jagadis Gupta, K., Sonoda, M., & Kaiser, W. M. (2005). Nitric oxide emission from tobacco leaves and cell suspensions: rate limiting factors and evidence for the involvement of mitochondrial electron transport. The Plant Journal, 41(5), 732-743.

Pohl, C. H., & Kock, J. L. (2014). Oxidized fatty acids as inter-kingdom signaling molecules. Molecules, 19(1), 1273-1285.

Prado, A. M., Colaço, R., Moreno, N., Silva, A. C., & Feijó, J. A. (2008). Targeting of pollen tubes to ovules is dependent on nitric oxide (NO) signaling. Molecular Plant, 1(4), 703-714.

Pružinská, A., Tanner, G., Aubry, S., Anders, I., Moser, S., Müller, T., ... & Hörtensteiner, S. (2005). Chlorophyll breakdown in senescent Arabidopsis leaves. Characterization of chlorophyll catabolites and of chlorophyll catabolic enzymes involved in the degreening reaction. Plant Physiology, 139(1), 52-63.

Pucciariello, C., & Perata, P. (2017). New insights into reactive oxygen species and nitric oxide signalling under low oxygen in plants. Plant Cell & Environment, 40(4), 473-482.

Puyaubert, J., & Baudouin, E. (2014). New clues for a cold case: nitric oxide response to low temperature. Plant Cell & Environment, 37(12), 2623-2630.

Qiao, W., & Fan, L. M. (2008). Nitric oxide signaling in plant responses to abiotic stresses. Journal of Integrative Plant Biology, 50(10), 1238-1246.

Rahman, A. (2013). Auxin: a regulator of cold stress response. Physiologia Plantarum, 147(1), 28-35.

dos Reis, S. P., Lima, A. M., & de Souza, C. R. B. (2012). Recent molecular advances on downstream plant responses to abiotic stress. International Journal of Molecular Sciences, 13(7), 8628-8647.

Renaut, J., Lutts, S., Hoffmann, L., & Hausman, J. F. (2004). Responses of poplar to chilling temperatures: proteomic and physiological aspects. Plant Biology, 6(1), 81-90.

Richter, R., Bastakis, E., & Schwechheimer, C. (2013). Cross-Repressive Interactions between SOC1 and the GATAs GNC and GNL/CGA1 in the Control of Greening, Cold Tolerance, and Flowering Time in Arabidopsis. Plant Physiology, 162(4), 1992-2004.

Rockel, P., Strube, F., Rockel, A., Wildt, J., & Kaiser, W. M. (2002). Regulation of nitric oxide (NO) production by plant nitrate reductase in vivo and in vitro. Journal of Experimental Botany, 53(366), 103-110.

Roman, G., Lubarsky, B., Kieber, J. J., Rothenberg, M., & Ecker, J. R. (1995). Genetic analysis of ethylene signal transduction in Arabidopsis thaliana: five novel mutant loci integrated into a stress response pathway. Genetics, 139(3), 1393-1409.

Romero, L. C., Aroca, M. Á., Laureano-Marín, A. M., Moreno, I., García, I., & Gotor, C. (2014). Cysteine and cysteine-related signaling pathways in Arabidopsis thaliana. Molecular Plant, 7(2), 264-276.

Rozpądek, P., Domka, A. M., Nosek, M., Ważny, R., Jędrzejczyk, R. J., Wiciarz, M., & Turnau, K. (2018). The Role of Strigolactone in the Cross-Talk Between Arabidopsis thaliana and the Endophytic Fungus Mucor sp. Frontiers in Microbiology, 9, 441.

Rubbo, H. (2013). Nitro-fatty acids: novel anti-inflammatory lipid mediators. Brazilian Journal of Medical and Biological Research, 46(9), 728-734.

Russwurm, M., & Koesling, D. (2004). NO activation of guanylyl cyclase. The EMBO Journal, 23(22), 4443-4450.

Sakamoto, W., & Takami, T. (2014). Nucleases in higher plants and their possible involvement in DNA degradation during leaf senescence. Journal of Experimental Botany, 65(14), 3835-3843.

Sanz-Luque, E., Ocaña-Calahorro, F., de Montaigu, A., Chamizo-Ampudia, A., Llamas, Á., Galván, A., & Fernández, E. (2015). THB 1, a truncated hemoglobin, modulates nitric oxide levels and nitrate reductase activity. The Plant Journal, 81(3), 467-479.

Schmidt, H. H., & Walter, U. (1994). NO at work. Cell, 78(6), 919-925.

Schopfer, F. J., Baker, P. R., & Freeman, B. A. (2003). NO-dependent protein nitration: a cell signaling event or an oxidative inflammatory response?. Trends in Biochemical Sciences, 28(12), 646-654.

Schulz, E., Tohge, T., Zuther, E., Fernie, A. R., & Hincha, D. K. (2016). Flavonoids are determinants of freezing tolerance and cold acclimation in Arabidopsis thaliana. Scientific Reports, 6, 34027.

Seo, M., Jikumaru, Y., & Kamiya, Y. (2011). Profiling of hormones and related metabolites in seed dormancy and germination studies. In Seed Dormancy (pp. 99-111). Humana Press.

Serino, L., Reimmann, C., Baur, H., Beyeler, M., Visca, P., & Haas, D. (1995). Structural genes for salicylate biosynthesis from chorismate in Pseudomonas aeruginosa. Molecular and General Genetics, 249(2), 217-228.

Serpa, V., Vernal, J., Lamattina, L., Grotewold, E., Cassia, R., & Terenzi, H. (2007). Inhibition of AtMYB2 DNA-binding by nitric oxide involves cysteine S-nitrosylation. Biochemical and Biophysical Research Communications, 361(4), 1048-1053.

Seth, D., & Stamler, J. S. (2011). The SNO-proteome: causation and classifications. Current Opinion in Chemical Biology, 15(1), 129-136.

Sharma, M., & Laxmi, A. (2016). Jasmonates: emerging players in controlling temperature stress tolerance. Frontiers in Plant Science, 6, 1129.

Shen, Q., & Ho, T. H. (1995). Functional dissection of an abscisic acid (ABA)-inducible gene reveals two independent ABA-responsive complexes each containing a G-box and a novel cis-acting element. The Plant Cell, 7(3), 295-307.

Shimoda, Y., Nagata, M., Suzuki, A., Abe, M., Sato, S., Kato, T., ... & Uchiumi, T. (2005). Symbiotic rhizobium and nitric oxide induce gene expression of non-symbiotic hemoglobin in Lotus japonicus. Plant and Cell Physiology, 46(1), 99-107.

Shin, S. Y., Chung, H., Kim, S. Y., & Nam, K. H. (2016). BRI1-EMS-suppressor 1 gain-of-function mutant shows higher susceptibility to necrotrophic fungal infection. Biochemical and Biophysical Research Communications, 470(4), 864-869.

Simontacchi, M., García-Mata, C., Bartoli, C. G., Santa-María, G. E., & Lamattina, L. (2013). Nitric oxide as a key component in hormone-regulated processes. Plant cell reports, 32(6), 853-866.

Skalska, K., Miller, J. S., & Ledakowicz, S. (2010). Trends in NOx abatement: A review. Science of the Total Environment, 408(19), 3976-3989.

Solfanelli, C., Poggi, A., Loreti, E., Alpi, A., & Perata, P. (2006). Sucrose-specific induction of the anthocyanin biosynthetic pathway in Arabidopsis. Plant Physiology, 140(2), 637-646.

Sorefan, K., Booker, J., Haurogné, K., Goussot, M., Bainbridge, K., Foo, E., ... & Leyser, O. (2003). MAX4 and RMS1 are orthologous dioxygenase-like genes that regulate shoot branching in Arabidopsis and pea. Genes & Development, 17(12), 1469-1474.

Staswick, P. E., Tiryaki, I., & Rowe, M. L. (2002). Jasmonate response locus JAR1 and several related Arabidopsis genes encode enzymes of the firefly luciferase superfamily that show activity on jasmonic, salicylic, and indole-3-acetic acids in an assay for adenylation. The Plant Cell, 14(6), 1405-1415.

Staswick, P. E., & Tiryaki, I. (2004). The oxylipin signal jasmonic acid is activated by an enzyme that conjugates it to isoleucine in Arabidopsis. The Plant Cell, 16(8), 2117-2127.

Stirnberg, P., Furner, I. J., & Ottoline Leyser, H. M. (2007). MAX2 participates in an SCF complex which acts locally at the node to suppress shoot branching. The Plant Journal, 50(1), 80-94.

Stöhr, C., & Ullrich, W. R. (2002). Generation and possible roles of NO in plant roots and their apoplastic space. Journal of Experimental Botany, 53(379), 2293-2303.

Stöhr, C., Strube, F., Marx, G., Ullrich, W. R., & Rockel, P. (2001). A plasma membrane-bound enzyme of tobacco roots catalyses the formation of nitric oxide from nitrite. Planta, 212(5-6), 835-841.

Sun, H., Bi, Y., Tao, J., Huang, S., Hou, M., Xue, R., ... & Shen, Q. (2016). Strigolactones are required for nitric oxide to induce root elongation in response to nitrogen and phosphate deficiencies in rice. Plant Cell & Environment, 39(7), 1473-1484.

Szarka, A., Tomasskovics, B., & Bánhegyi, G. (2012). The ascorbate-glutathione-α-tocopherol triad in abiotic stress response. International Journal of Molecular Sciences, 13(4), 4458-4483.

Tähtiharju, S., & Palva, T. (2001). Antisense inhibition of protein phosphatase 2C accelerates cold acclimation in Arabidopsis thaliana. The Plant Journal, 26(4), 461-470.

Takahashi, D., Kawamura, Y., & Uemura, M. (2016). Cold acclimation is accompanied by complex responses of glycosylphosphatidylinositol (GPI)-anchored proteins in Arabidopsis. Journal of Experimental Botany, 67(17), 5203-5215.

Takahashi, M., Sasaki, Y., Ida, S., & Morikawa, H. (2001). Nitrite reductase gene enrichment improves assimilation of NO2 in Arabidopsis. Plant Physiology, 126(2), 731-741.

Tari, I., Poór, P., & Gémes, K. (2011). Sublethal concentrations of salicylic acid decrease the formation of reactive oxygen species but maintain an increased nitric oxide production in the root apex of the ethylene-insensitive Never ripe tomato mutants. Plant Signaling & Behavior, 6(9), 1263-1266.

Tavares, C. P., Vernal, J., Delena, R. A., Lamattina, L., Cassia, R., & Terenzi, H. (2014). Snitrosylation influences the structure and DNA binding activity of AtMYB30 transcription factor from Arabidopsis thaliana. Biochimica et Biophysica Acta (BBA)-Proteins and Proteomics, 1844(4), 810-817.

Thomashow, M. F. (1999). Plant cold acclimation: freezing tolerance genes and regulatory mechanisms. Annual Review of Plant Biology, 50(1), 571-599.

Tischer, S. V., Wunschel, C., Papacek, M., Kleigrewe, K., Hofmann, T., Christmann, A., & Grill, E. (2017). Combinatorial interaction network of abscisic acid receptors and coreceptors from Arabidopsis thaliana. Proceedings of the National Academy of Sciences USA, 114(38), 10280-10285.

Toledo Jr, J. C., & Augusto, O. (2012). Connecting the chemical and biological properties of nitric oxide. Chemical Research in Toxicology, 25(5), 975-989.

Trevisan, S., Manoli, A., Begheldo, M., Nonis, A., Enna, M., Vaccaro, S., ... & Quaggiotti, S. (2011). Transcriptome analysis reveals coordinated spatiotemporal regulation of hemoglobin and nitrate reductase in response to nitrate in maize roots. New Phytologist, 192(2), 338-352.

Tsai, Y. C., Delk, N. A., Chowdhury, N. I., & Braam, J. (2007). Arabidopsis potential calcium sensors regulate nitric oxide levels and the transition to flowering. Plant Signaling & Behavior, 2(6), 446-454.

Tsutsui, T., Kato, W., Asada, Y., Sako, K., Sato, T., Sonoda, Y., ... & Ichikawa, T. (2009). DEAR1, a transcriptional repressor of DREB protein that mediates plant defense and freezing stress responses in Arabidopsis. Journal of Plant Research, 122(6), 633.

van Verk, M. C., Bol, J. F., & Linthorst, H. J. (2011). WRKY transcription factors involved in activation of SA biosynthesis genes. BMC Plant Biology, 11(1), 89.

Vicente, J., Mendiondo, G. M., Movahedi, M., Peirats-Llobet, M., Juan, Y. T., Shen, Y. Y., ... & Gray, J. E. (2017). The Cys-Arg/N-end rule pathway is a general sensor of abiotic stress in flowering plants. Current Biology, 27(20), 3183-3190.

Vishwakarma, A., Kumari, A., Mur, L. A., & Gupta, K. J. (2018). A discrete role for alternative oxidase under hypoxia to increase nitric oxide and drive energy production. Free Radical Biology and Medicine. 122, 40-51.

Vishwakarma, K., Upadhyay, N., Kumar, N., Yadav, G., Singh, J., Mishra, R. K., ... & Sharma, S. (2017). Abscisic acid signaling and abiotic stress tolerance in plants: a review on current knowledge and future prospects. Frontiers in Plant Science, 8, 161.

Wang, H., Zhu, Y., Fujioka, S., Asami, T., Li, J., & Li, J. (2009). Regulation of Arabidopsis brassinosteroid signaling by atypical basic helix-loop-helix proteins. The Plant Cell, 21(12), 3781-3791.

Wang, P., Du, Y., Hou, Y. J., Zhao, Y., Hsu, C. C., Yuan, F., ... & Zhu, J. K. (2015b). Nitric oxide negatively regulates abscisic acid signaling in guard cells by S-nitrosylation of OST1. Proceedings of the National Academy of Sciences USA, 112(2), 613-618.

Wang, P., Zhu, J. K., & Lang, Z. (2015c). Nitric oxide suppresses the inhibitory effect of abscisic acid on seed germination by S-nitrosylation of SnRK2 proteins. Plant Signaling & Behavior, 10(6), e1031939.

Wang, R., Xing, X., & Crawford, N. (2007). Nitrite acts as a transcriptome signal at micromolar concentrations in Arabidopsis roots. Plant Physiology, 145(4), 1735-1745.

Wang, Y., Chen, C., Loake, G. J., & Chu, C. (2010). Nitric oxide: promoter or suppressor of programmed cell death?. Protein & Cell, 1(2), 133-142.

Wang, Y., Yun, B. W., Kwon, E., Hong, J. K., Yoon, J., & Loake, G. J. (2006). S-nitrosylation: an emerging redox-based post-translational modification in plants. Journal of Experimental Botany, 57(8), 1777-1784.

Wang, Z. P., Xing, H. L., Dong, L., Zhang, H. Y., Han, C. Y., Wang, X. C., & Chen, Q. J. (2015a). Egg cell-specific promoter-controlled CRISPR/Cas9 efficiently generates homozygous mutants for multiple target genes in Arabidopsis in a single generation. Genome Biology, 16(1), 144.

Wei, C. Q., Chien, C. W., Ai, L. F., Zhao, J., Zhang, Z., Li, K. H., ... & Wang, Z. Y. (2016). The Arabidopsis B-box protein BZS1/BBX20 interacts with HY5 and mediates strigolactone regulation of photomorphogenesis. Journal of Genetics and Genomics, 43(9), 555-563.

Weits, D. A., Giuntoli, B., Kosmacz, M., Parlanti, S., Hubberten, H. M., Riegler, H., ... & Licausi, F. (2014). Plant cysteine oxidases control the oxygen-dependent branch of the N-end-rule pathway. Nature Communications, 5, 3425.

Wildermuth, M. C., Dewdney, J., Wu, G., & Ausubel, F. M. (2001). Isochorismate synthase is required to synthesize salicylic acid for plant defence. Nature, 414(6863), 562.

Wilkinson, J. Q., & Crawford, N. M. (1993). Identification and characterization of a chlorate-resistant mutant of Arabidopsis thaliana with mutations in both nitrate reductase structural genes NIA1 and NIA2. Molecular and General Genetics, 239(1-2), 289-297.

Williams, B. P., Pignatta, D., Henikoff, S., & Gehring, M. (2015). Methylation-sensitive expression of a DNA demethylase gene serves as an epigenetic rheostat. PLoS Genetics, 11(3), e1005142.

Wilson, I. D., Neill, S. J., & Hancock, J. T. (2008). Nitric oxide synthesis and signalling in plants. Plant Cell & Environment, 31(5), 622-631.

Winkel-Shirley, B. (2002). Biosynthesis of flavonoids and effects of stress. Current Opinion in Plant Biology, 5(3), 218-223.

Wu, C., Feng, J., Wang, R., Liu, H., Yang, H., Rodriguez, P. L., ... & Wang, D. (2012). HRS1 acts as a negative regulator of abscisic acid signaling to promote timely germination of Arabidopsis seeds. PLoS One, 7(4), e35764.

Xie, Y., Tan, H., Ma, Z., & Huang, J. (2016). DELLA proteins promote anthocyanin biosynthesis via sequestering MYBL2 and JAZ suppressors of the MYB/bHLH/WD40 complex in Arabidopsis thaliana. Molecular Plant, 9(5), 711-721.

Xu, M., Dong, J., Zhang, M., Xu, X., & Sun, L. (2012). Cold-induced endogenous nitric oxide generation plays a role in chilling tolerance of loquat fruit during postharvest storage. Postharvest Biology and Technology, 65, 5-12.

Xu, Y., Ding, J., Wu, L. Y., & Chou, K. C. (2013). iSNO-PseAAC: predict cysteine S-nitrosylation sites in proteins by incorporating position specific amino acid propensity into pseudo amino acid composition. PLoS One, 8(2), e55844.

Xu, Y., Wen, X., Wen, L. S., Wu, L. Y., Deng, N. Y., & Chou, K. C. (2014). iNitro-Tyr: Prediction of nitrotyrosine sites in proteins with general pseudo amino acid composition. PloS One, 9(8), e105018.

Xuan, W., Beeckman, T., & Xu, G. (2017). Plant nitrogen nutrition: sensing and signaling. Current Opinion in Plant Biology, 39, 57-65.

Xue, Y., Liu, Z., Gao, X., Jin, C., Wen, L., Yao, X., & Ren, J. (2010). GPS-SNO: computational prediction of protein S-nitrosylation sites with a modified GPS algorithm. PloS One, 5(6), e11290.

Yamasaki, H., & Sakihama, Y. (2000). Simultaneous production of nitric oxide and peroxynitrite by plant nitrate reductase: in vitro evidence for the NR-dependent formation of active nitrogen species. FEBS Letters, 468(1), 89-92.

Yamasaki, H., Sakihama, Y., & Takahashi, S. (1999). An alternative pathway for nitric oxide production in plants: new features of an old enzyme. Trends in Plant Science, 4(4), 128-129.

Yeats, T. H., & Rose, J. K. (2013). The formation and function of plant cuticles. Plant Physiology, 163(1), 5-20.

Yesbergenova, Z., Yang, G., Oron, E., Soffer, D., Fluhr, R., & Sagi, M. (2005). The plant Mohydroxylases aldehyde oxidase and xanthine dehydrogenase have distinct reactive oxygen species signatures and are induced by drought and abscisic acid. The Plant Journal, 42(6), 862-876.

Yin, Y., Wang, Z. Y., Mora-Garcia, S., Li, J., Yoshida, S., Asami, T., & Chory, J. (2002). BES1 accumulates in the nucleus in response to brassinosteroids to regulate gene expression and promote stem elongation. Cell, 109(2), 181-191.

Yoshida, Y., Umeno, A., & Shichiri, M. (2013). Lipid peroxidation biomarkers for evaluating oxidative stress and assessing antioxidant capacity in vivo. Journal of Clinical Biochemistry and Nutrition, 52(1), 9-16.

Yu, L. H., Wu, J., Tang, H., Yuan, Y., Wang, S. M., Wang, Y. P., ... & Xiang, C. B. (2016). Overexpression of Arabidopsis NLP7 improves plant growth under both nitrogen-limiting and sufficient conditions by enhancing nitrogen and carbon assimilation. Scientific Reports, 6, 27795.

Yu, M., Yun, B. W., Spoel, S. H., & Loake, G. J. (2012). A sleigh ride through the SNO: regulation of plant immune function by protein S-nitrosylation. Current Opinion in Plant Biology, 15(4), 424-430.

Zhao, L., Zhang, W., Yang, Y., Li, Z., Li, N., Qi, S., ... & Wang, Y. (2018). The Arabidopsis NLP7 gene regulates nitrate signaling via NRT1. 1–dependent pathway in the presence of ammonium. Scientific Reports, 8(1), 1487.

Zhao, M. G., Chen, L., Zhang, L. L., & Zhang, W. H. (2009). Nitric reductase-dependent nitric oxide production is involved in cold acclimation and freezing tolerance in Arabidopsis. Plant Physiology, 151(2), 755-767.

Zhong, R., Lee, C., Zhou, J., McCarthy, R. L., & Ye, Z. H. (2008). A battery of transcription factors involved in the regulation of secondary cell wall biosynthesis in Arabidopsis. The Plant Cell, 20(10), 2763-2782.

Zhou, X. R., Callahan, D. L., Shrestha, P., Liu, Q., Petrie, J. R., & Singh, S. P. (2014). Lipidomic analysis of Arabidopsis seed genetically engineered to contain DHA. Frontiers in Plant Science, 5, 419.

Zottini, M., Costa, A., De Michele, R., Ruzzene, M., Carimi, F., & Lo Schiavo, F. (2007). Salicylic acid activates nitric oxide synthesis in Arabidopsis. Journal of Experimental Botany, 58(6), 1397-1405.

Zuther, E., Schulz, E., Childs, L. H., & Hincha, D. K. (2012). Clinal variation in the non-acclimated and cold-acclimated freezing tolerance of Arabidopsis thaliana accessions. Plant, Cell & Environment, 35(10), 1860-1878.

Annexes

A. ANNEXES

Most of the figures and tables displayed in this section A come from the research articles: "León, J., Costa, Á., & Castillo, M. C. (2016). Nitric oxide triggers a transient metabolic reprogramming in Arabidopsis. Scientific Reports, 6, 37945", "Costa-Broseta, Á., Perea-Resa, C., Castillo, M. C., Ruíz, M. F., Salinas, J., & León, J. (2018). Nitric Oxide Controls Constitutive Freezing Tolerance in Arabidopsis by Attenuating the Levels of Osmoprotectants, Stress-Related Hormones and Anthocyanins. Scientific Reports, 8(1), 9268", "Castillo, M. C., Coego, A., Costa-Broseta, Á., & León, J. (2018). Nitric oxide responses in Arabidopsis hypocotyls are mediated by diverse phytohormone pathways. Journal of experimental botany, 69(21), 5265-5278", "Costa-Broseta, Á., Castillo, M. C., & León, J. (2018). Protein Stabilization and Post-translational Modifications Control NO Homeostasis in Arabidopsis", "León, J., Costa-Broseta, Á., & Castillo, M. C. (2018). RAP2.3 negatively regulates nitric oxide biosynthesis and sensing through a rheostat-like mechanism in Arabidopsis" and "Costa-Broseta, Á., Perea-Resa, C., Castillo, M. C., Ruíz, M. F., Salinas, J., & León, J. (2018). Nitric Oxide Deficiency Reduces CBF *Induction, ABA Signaling, Anthocyanin Synthesis and Cold Acclimation in Arabidopsis". The last three articles were submitted to Plant Physiology, The Plant Journal and Journal of Experimental Botany, respectively and were under revision when PhD Thesis writing was finished. All the figures and tables that appear here are derived from the work of the PhD student in collaboration with the other authors.*

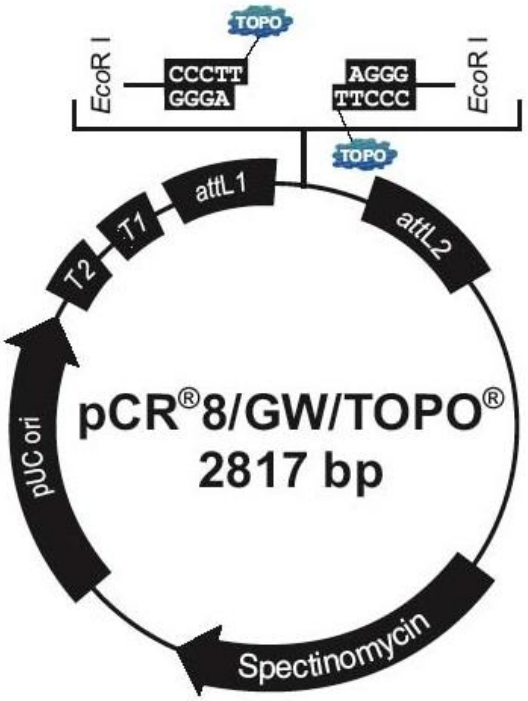

Comments for pCR®8/GW/TOPO®
2817 nucleotides

*rrn*B T2 transcription termination sequence: bases 268-295
*rrn*B T1 transcription termination sequence: bases 427-470
M13 forward (-20) priming site: bases 537-552
*att*L1: bases 569-668
GW1 priming site: bases 607-631
TOPO® recognition site 1: bases 678-682
TOPO® recognition site 2: bases 683-687
*att*L2: bases 696-795
GW2 priming site: bases 733-757
T7 Promoter/priming site: 812-831 (c)
M13 reverse priming site: bases 836-852
Spectinomycin promoter: bases 930-1063
Spectinomycin resistance gene (Spn^R): 1064-2074
pUC origin: bases 2141-2814

Figure A1. Map of pCR8/GW/TOPO vector (Invitrogen).

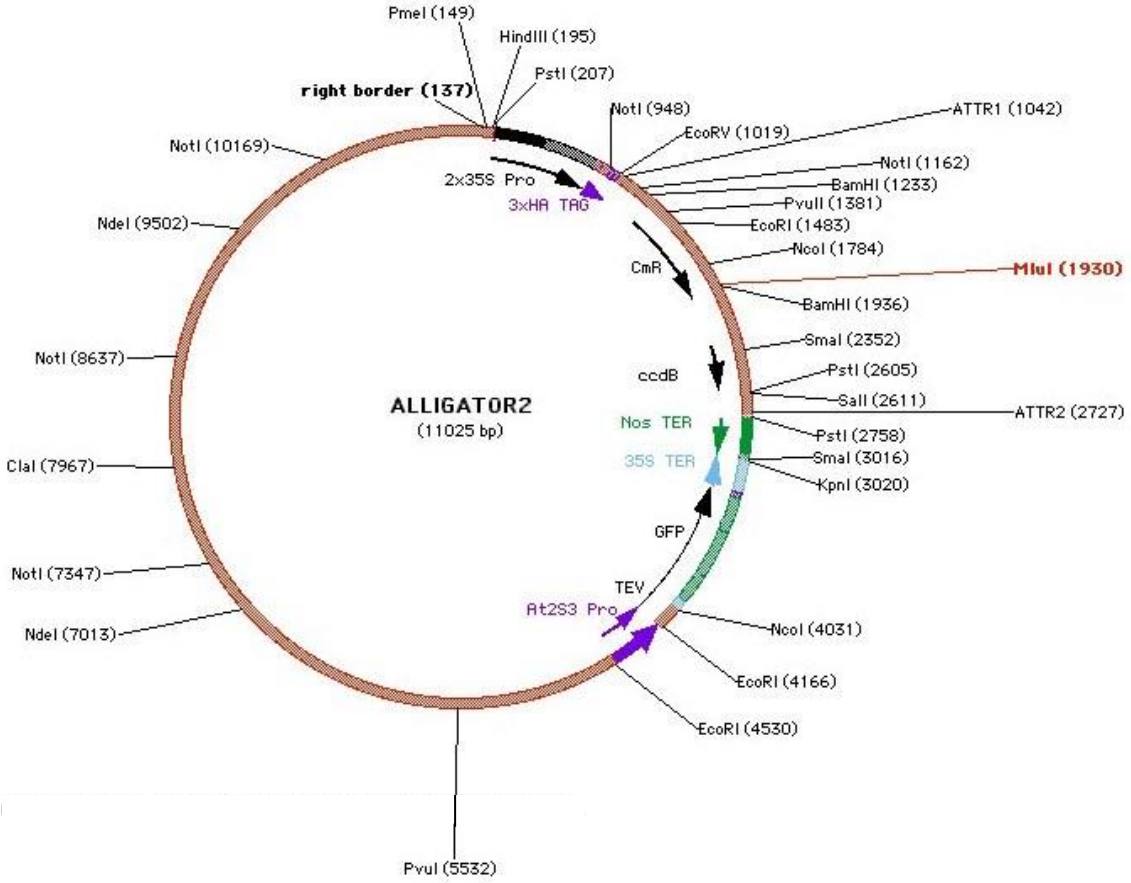

Figure A2. Map of pALLIGATOR2 vector.

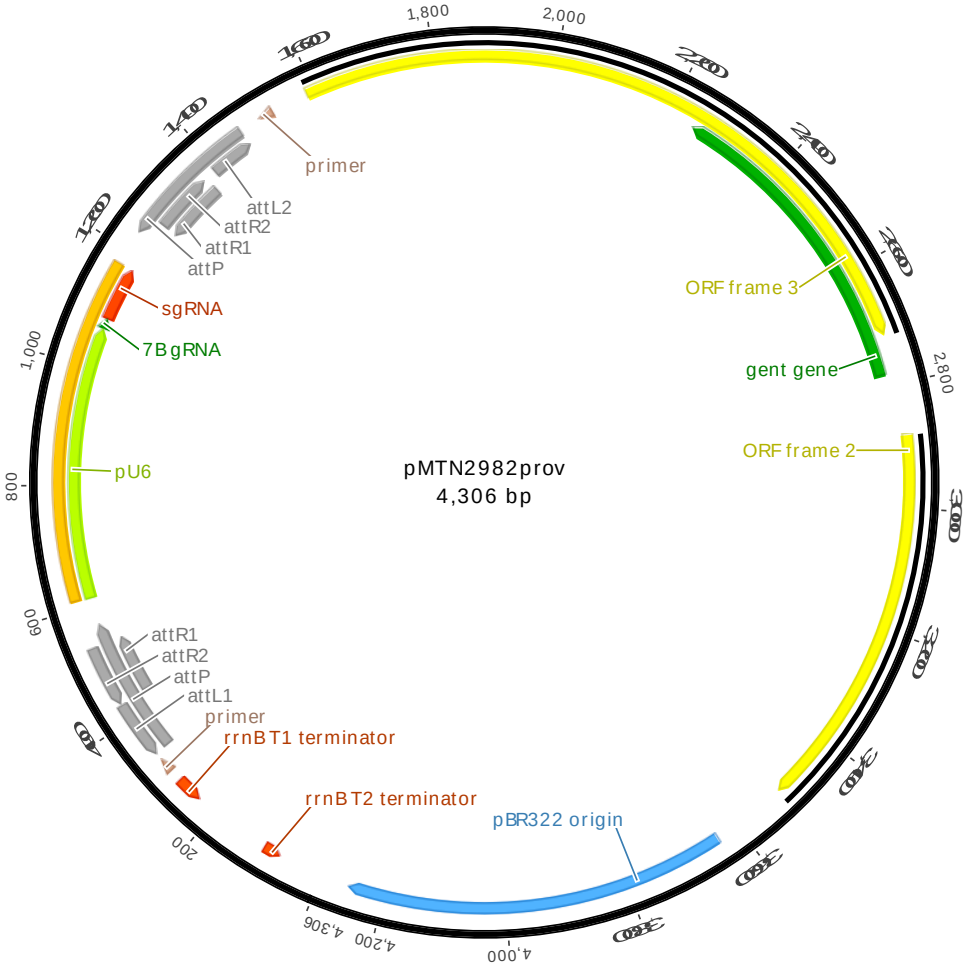

Figure A3. Map of pMTN2982 (pDONR207) vector.

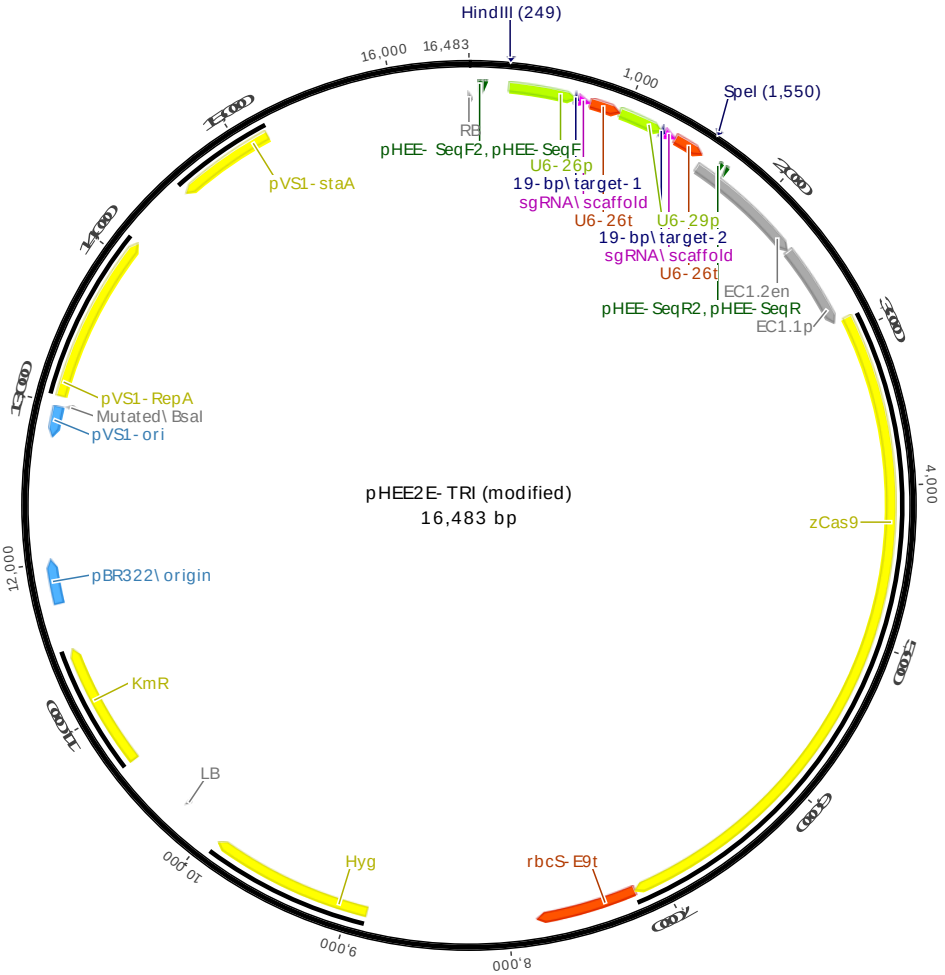

Figure A4. Map of pHEE2E-TRI vector.

gattattttaattctatgttaattccaggcattaaattttaagcgtaatttatagaagaagaaa
aaaaatctagttacattccatctaagataggggtacaaatccatacaagagtctatcttctgta
attcttagcaagttgaacatttcttaatttttatttttatttttattttttggtcaaacgttttctt
taatacaagtggcaaagatattctataacagttataatcatttatagttagggatttttttaatc
attttgtagtatttgtttttctctttttttcctaacaaagtttttggaacttttgatcatctctc
gattgaaagcgaacatataaataatttttactactgcaaatttttaaaaagttaatattcgact
ttataaaagagagatgagagtcaacaaaacaaaaagcaactaatttttggacgtacgaaatgctttg
taaatacattgatatcacttatgtttataatatcactcatcccaagtgttggtcaacatttctt
tgataaaaattaaactattcaatagaacgaaaaccacaaaaaaattataaagaattattgataa
caactcttcatgttaatcttatatatttttttaaaaatatttgtttttaggttttaatacaaac
aacatgattctagtttattaaactaattaacgcaacttgatggattataaaaatatagcttaac
taatccatcaaattaacaagtgaatcgcactataattctaaaagaatcaggtaggtccaggatt
tgtcttttctccacttctcaatttcccattaataatcccgaaaaggcattacgtaataattaat
attttacgctgtagtattattttatgataaacatttccaaattttccaacacttaatcataatt
taaggattaaaggaaatttgattggtgcattccaccacgagtttgcttaacgtgtcgttaaat
gcagccgtcggacttgacaatgcaaaaatgctacataatctaaataattaactctcgcaataag
attcactaataataacatttttaacgacgatatataatttttacaataagaaaaaaaatatgaat
ctaatatttatttaatattaattttactccattatctgaataatctagaatatgtcaaatatcct
tttattattttgtagctgtcgaaactatggtgaataaaatctcgaggaatatattagaaaacaa
aaaagatctagaggaataataatattttaaatatttggggcacagttgtattgtgaagcagaga
atcggttctcaatatattatccgaaaatgtcttaattttaaatttgtttttttgtttgattctg
cgatattggaatcacacactctgccaatttgacctttctctctcgcttctctttctctatccaa
tcggaaagagatcaaccaacgatagaggagaagaagaacttgcatacgcaaaaaaactttcccg
ggaaaattccagaaactgctttggaaaaATG

Site Name	Position	Strand	Matrix score.	sequence	function
ABRE	-1072	-	9	CGTACGTGCA	cis-acting element involved in the abscisic acid responsiveness

Site Name	Position	Strand	Matrix score.	sequence	function
Box-W1	-128	+	6	TTGACC	fungal elicitor responsive element
Box-W1	-1002	-	6	TTGACC	fungal elicitor responsive element

Site Name	Position	Strand	Matrix score.	sequence	function
Box4	-396	+	6	ATTAAT	part of a conserved DNA module involved in light responsiveness
Box4	-674	+	6	ATTAAT	part of a conserved DNA module involved in light responsiveness
Box4	-705	+	6	ATTAAT	part of a conserved DNA module involved in light responsiveness
CATT-motif	-578	+	6	GCATTC	part of a light responsive element
G-Box	-555	-	6	AACGTG	cis-acting regulatory element involved in light responsiveness
GAG-motif	-1109	+	7	AGAGATG	part of a light responsive element
GAG-motif	-1188	-	7	AGAGATG	part of a light responsive element

Figure A5. *In silico* analyses of *NLP7* promoter. Arabidopsis Gene Regulatory Information Server (AGRIS) tools were used to analyze the 1.5 kb *NLP7* promoter sequence upstream of the initiation codon. ABA and light responsiveness cis-acting elements as well as WRKY binding Box W1 consensus sequences are shown.

Table A1. Abbreviations and acronyms.

3-NY	3-nitrotyrosine
A	acclimated
A. thaliana	*Arabidopsis thaliana*
A. tumefaciens	*Agrobacterium tumefaciens*
ABA	abscisic acid
Acc	acclimated
acetyl-CoA	acetyl coenzyme A
ACT	Actin
ANOVA	analysis of variance
AO	Aldehyde Oxidase
AOC	Allene Oxide Cyclase
AOX	Alternative Oxidase
ARC	Amidoxine Reducing Component
Arg	arginine
aRNA	antisense RNA
ATE	Arg-tRNA Transferase
ATP	adenosine triphosphate
BASTA	glufosinate ammonium
BES1	BRI1-EMS-Suppressor 1
bp	base pair, unit of length of double stranded nucleic acids
BR	brassinosteroid
BSA	bovine serum albumin
BSTFA	bistrimethyl-silyl-triflouroacetamide
BZR2	Brassinazole-Resistant 2
C	cysteine
C	control
CAPS	Cleaved Amplified Polymorphic Sequences
Cas9	CRISPR-associated 9
CBF/DREB1	C-repeat/dehydration-responsive element Binding Factor
cDNA	complementary DNA
CDS	coding DNA sequence
cGMP	cyclic guanosine monophosphate
CHS	Chalcone Synthase
CHX	cicloheximide
Col-0	Columbia 0, wild type of *A. thaliana*
COR	Cold-Responsive
cPTIO	2-(4-Carboxyphenyl)-4,4,5,5-tetramethylimidazoline-1-oxyl-3-oxide
CRISPR	Clustered Regularly Interspaced Short Palindromic Repeats
Ct	threshold cycle of qPCR
CTAB	hexadecyltrimethylammonium bromide
Cys	cysteine
cyt	cytochrome
Da	dalton, unified atomic mass unit
DAF-FM DA	4-amino-5-methylamino-2',7'-difluorofluorescein diacetate
ddUTP	dideoxyuridine-5'-triphosphate
DEPC	diethyl pyrocarbonate
DET	De-Etiolated
DFR	Dihydroflavonol Reductase
dhJA	dihydrojasmonate
DIG	digoxigenin
DNA	deoxyribonucleic acid
dNTP	dinucleoside triphosphate
DTT	dithiothreitol
E. coli	*Escherichia coli*
EDTA	ethylenediaminetetraacetic acid
ERF/AP2	Ethylene Response Factors
ERFVIIs	group VII of ERFs
ESI	electrospray ionization
EST	β-estradiol
ET	ethylene
F	forward primer
FA	unsaturated fatty acid
FAD	flavin adenine dinucleotide
FC	fold change
FDR	false discovery rate
fed	ferredoxin
Fig.	Figure
FT	Fourier transform
FW	fresh weight
GA	gibberellin
GABA	γ-aminobutyrate
GAI	Gibberellin Insensitive
GBH	γ -hydroxybutyrate

GC	Guanylate Cyclase
GC	gas chromatograhy
GCOS	genechip operating software
GEO	Gene Expression Omnibus
GFP	Green Fluorescent Protein
GPC	choline glycerophospholipid
GPE	ethanolamine glycerophospholipid
GS-GOGAT	Glutaminate Synthetase-Glutamine Oxoglutarate Aminotransferase
GSH	glutathione
GSNO	S-nitrosylated glutathione
GSNOR	GSNO Reductase
GSSG	glutathione disulfide
GSSG	glutathione disulfide
GTP	guanosine triphosphate
H_2O	water
HA	human influenza Hemagglutinin tag
HAI	Highly ABA-Induced
HB	hemoglobin
HF-PCR	high fidelity PCR
HLB	hydrophilic-lipophilic balance
HODE	hydroxyoctadecadienoic acid
HRE	Hypoxia Responsive ERF
HRP	horseradish peroxidase
Hyg	hygromycin
ICE1	Inducer of CBF Expression1
ICR	ion cyclotron resonance
ICS	Isochrorismate Synthase
JA	jasmonate
K	lysine
LB	lysogeny broth medium for bacteria
LB	left border
LC	liquid chromatography
LiMMA	linear model methods
LIT	linear ion-trap
$LOO^{\cdot}$	lipid peroxyl radical
LT_{50}	temperature that causes 50% lethality
LTQ	Linear Trap Quadrupole
M	DNA ladder marker
MA-	methionine-alanine-
MAP	Methionine Aminopeptidase
MC-	methionine-cysteine-
MES	2-(N-morpholino)ethanesulfonic acid
mETC	mitochondrial electron transport chain
MIAME	minimum information about a microarray experiment
Moco	molybdenum cofactor
mRNA	messenger RNA
MS	Murashige & Skoog medium for plants
MS	mass spectrometer
MSE	β-estradiol-supplemented MS medium
MS-MES	MS medium with MES buffer
NAD	nicotinamide adenine dinucleotide
NBT	nitroblue tetrazolium
NH_3	ammonia
NH_4^+	ammonium
Ni:NOR	Nitrite-Nitric Oxide Reductase
NIA1	Nitrate Reductase 1
NIA2	Nitrate Reductase 2
NiR	nitrite reductase
NIR1	Nitrite Reductase 1
NLP7	NIN-Like Protein 7
N-NEDA	N-(1-napthyl) ethylenediamine hydrochloride
NO	nitric oxide
NO_2^-	nitrite
NO_2-FA	nitro-fatty acid
NO_3^-	nitrate
NOA1	Nitric Oxide Associated 1
NOFNiR	Nitric Oxide-Forming Nitrite Reductase
NOGC1	NO-dependent Guanylate Cyclase 1
NOS	Nitric Oxide Synthase
NOx	Mixture of NO and NO_2
NR	nitrate reductase
O_2	oxygen
O_2^-	superoxide anion
oligo(dT)	short sequence of deoxy-thymidine
$ONOO^-$	peroxynitrite
OPR	Oxophytodienoate Reductase

ORF	open reading frame
ox	overexpressed
p	promoter
PAM	protospacer adjacent motif
PAO	Pheophorbide a Oxidase
PC	phosphatidylcholine
PCA	Principal Component Analysis
PCO	Plant Cysteine Oxidase
PCR	polymerase chain reaction
PDB	potato dextrose broth
PE	phosphatidylethanolamine
PI	phosphatidylinositol
PIF	Phytochrome Interacting Factor
PMSF	phenylmethylsulfonyl fluoride
PRE	before treatment
PRT6	Proteolysis6
PTM	post-translational modification
PUFA	polyunsaturated fatty acid
QC	quality control
qerfvii	*rap2.12rap2.2rap2.3hre1hre2*
qjaz	*jaz10, jaz1,3,5,9,10*
qPCR	quantitative PCR
R	reverse primer
RAP	Related to AP
RB	right border
RFLP	Restriction Fragment Length Polymorphism
RNA	ribonucleic acid
RNS	reactive nitrogen species
ROS	reactive oxygen species
RT	reverse transcription
rubisco	Ribulose-1,5-Bisphosphate Carboxylase / Oxygenase
SA	salicylic acid
SCC	Spearman's rank-order correlation coefficient
SD	standard deviation
SDS	sodium dodecyl sulfate
SDS-PAGE	SDS polyacrylamide gel electrophoresis
SE	standard error
SIM	selected ion monitoring
SL	strigolactone
SLIM	Site-directed, Ligase-Independent Mutagenesis
SNO	S-nitrosothiol
SnRK	Sucrose non-fermenting 1-Related protein Kinase
SO	Sulfite Oxidase
T0	parental generation
T1	first generation
T2	second generation
TAE	Tris, acetic acid and EDTA buffer
TCA	tricarboxcylic acid
T-DNA	transfer DNA, plasmid of Agrobacterium
TE	Tris and EDTA buffer
ter	terminator
TF	transcription factor
THB1	Truncated Hemoglobin 1
TMT	Tandem Mass Tagged-S-nitrosylated protein
TPT	TRANSPLANTA
tRNA	transfer RNA
TT7/F3H	Flavonol 3-Hydroxylase
TTBS	Tris-buffered saline buffer with Tween 20
Tyr	tyrosine
UHPLC	ultra-high-performance liquid chromatography
UPLC	ultra erformance liquid chromatography
UV	ultraviolet light
XO	Xanthine Oxidase
Y	tyrosine
α-	anti-, before the antigen that gives name to an antibody

Table A2. Buffers and solutions used in this work.

Buffer or solution	Composition (in MilliQ water)
Nutritive solution for plants	gFe (34.95 mg/l), $ZnSO_4 \cdot 7H_2O$ (9.76 mg/l), $MnSO_4 \cdot H_2O$ (28.95 mg/l), Cu_2SO_4 (2.23 mg/l), H_3BO_3 (32.55 mg/l), $(NH_4)_6Mo_7O_{24}*4H_2O$ (1.51 mg/l), $Ca(NO_3)_2 \cdot 4H_2O$ (885 mg/l), KNO_3 (381 mg/l), KH_2PO_4 (102 mg/l), $MgSO_4 \cdot 7H_2O$ (367.5 mg/l), pH 6.5, CE 1.6 mS
Floral dipping transformation solution	Sucrose (5%), Silwet L-77 (0.02%)
TTBS	Tris pH 7.4 (10 mM), NaCl (150 µM), Tween 20 (0.1%)
TAE	Tris (40 mM), acetic acid (20 mM), EDTA (1 mM)
TE	Tris pH 8 (0.1 mM), EDTA (2 µM)
SDS-PAGE buffer	Tris (25 mM), Glycine (192 mM), SDS 10% (0,1%)
Semi-dry transference buffer	Tris (25 mM), Glycine (192 mM), methanol (20%)
H-buffer for hybridization	NaCl (300 mM), Tris-HCl pH 9 (50 mM), EDTA (20 mM)
DAF-FM DA staining buffer	MES-KOH pH 5.7 (5 mM), KCl (0.25 mM), $CaCl_2$ (1 mM)
Lugol´s staining solution	Iodine (5.7 mM), KI (43.4 mM), HCl (0.2 N)
DNA extraction buffer	Tris-HCl pH 7.5 (200 mM), NaCl (250 mM), EDTA (25 mM), SDS (0.5%)
Protein extraction buffer	Tris-HCl pH 8.0 (50 mM), NaCl (150 mM), glycerol (5%), EDTA (5 mM), Triton X-100 (0.05%), DTT (10 mM), protease inhibitor cocktail (1%), PMSF (1 mM)
NR activity assay extraction buffer	Tris-HCl pH 8.0 (250 mM), EDTA (1mM), Na_2MoO_4 (1 µM), FAD (5 µM), DTT (3 mM), β-mercaptoethanol (12 mM), PMSF (250 µM)
NR activity reaction buffer	$NaNO_3$ (40 mM), K_2HPO_4 (80 mM), KH_2PO_4 (20 mM), NADH (0.2 mM), pH 7.5
NiR activity assay extraction buffer	Potassium phosphate buffer pH 7.5 (50 mM), EDTA (1 mM), β-mercaptoethanol (10 mM), PMSF (100 µM), PVP (1.25 mg/100 µl)
NiR activity reaction buffer	Potassium phosphate buffer pH 7.5 (33 mM), $NaNO_2$ (1 mM), methyl viologen (1 mM), sodium dithionite (11.11 mM)

Table A3. Oligonucleotides used in this work.

Name	Sequence (5´to 3´)	AGI	Application
M13-F	GTAAAACGACGGCCAG		Cloning pCR8/GW/TOPO
M13-R	CAGGAAACAGCTATGAC		Cloning pCR8/GW/TOPO
35S-seq	CCTTCGCAAGACCCTTCCTCTA		Cloning pAlligator2
NOS-term-rev	GCAAGACCGGCAACAGGATTCAATC		Cloning pAlligator2
NLP7-F	ATGTGCGAGCCCGATGATAATTCCGC	AT4G24020	Cloning *NLP7*
nostop-NLP7-R	CAATTCTCCAGTGCTCTCGCAGG	AT4G24020	Cloning *NLP7*
SeqNLP7_2R	GGTTAGGTGAATTATTGGTG	AT4G24020	Cloning *NLP7*
SeqNLP7_1F	ATAGTGAAAGTGACGTAGAG	AT4G24020	Cloning *NLP7*
SeqNLP7_3R	CGGTTCATCTAATTGGTTAC	AT4G24020	Cloning *NLP7*
NR1cds-F	ATGGCGACCTCCGTCGATAACCGCCATTATCCC	AT1G77760	Cloning *NIA1*
NR1cds-R	GAAGATTAAGAGATCCTCCTTCACGTTGTAACC	AT1G77760	Cloning *NIA1*
seqNR1_F	AGGAGATGGCGATGGATC	AT1G77760	Cloning *NIA1*
SeqNR1_3rev	GATCGAAGTCTTCTCAATG	AT1G77760	Cloning *NIA1*
SeqNR1_2fw	GAGCTAATCTCCGAGTTC	AT1G77760	Cloning *NIA1*
NR2cds-F	ATGGCGGCCTCTGTAGATAATCGCCAATACGCT	AT1G37130	Cloning *NIA2*
NR2cds-R	GAATATCAAGAAATCCTCCTTGATGTTATATTG	AT1G37130	Cloning *NIA2*
seqNR2_F	AGAACATGGTGAAGAAGTC	AT1G37130	Cloning *NIA2*
SeqNR2_2rev	CTAGAACCATATCCTCAAC	AT1G37130	Cloning *NIA2*
NIR1cds-F	ATGACTTCTTTCTCTCTCACTTTCACATCTCC	AT2G15620	Cloning *NIR1*
NIR1cds-R	ATCTTCATTCTCTTCTCTTTCTCTAGGCACAG	AT2G15620	Cloning *NIR1*
seqNIR1_F	GTGGTATGGATAACGTGAG	AT2G15620	Cloning *NIR1*
SLIM_F	gttttagagctagaaatagcaag		Cloning *NIR1guide*
SLIM_R	caatcactacttcgactct		Cloning *NIR1guide*
SLIM_F_NiR1(1)	GCCGCTCAGACCACAGCTCgttttagagctagaaatagcaag	AT2G15620	Cloning *NIR1guide*
SLIM_R_NiR1(1)	GAGCTGTGGTCTGAGCGGCcaatcactacttcgactct	AT2G15620	Cloning *NIR1guide*
pDONR_F	TCGCGTTAACGCTAGCATGGATCTC		Cloning *NIR1guide*
pDONR_R	GTAACATCAGAGATTTTGAGACAC		Cloning *NIR1guide*
P1b-HindIII	TTTTTTAAGCTTGTTTAAACAAGCTTTCGTTGAAC		Cloning *NIR1guide*
P4b-SpeI	TTTTTTACTAGTGGTTTAAACAAAAAAAGCACCG		Cloning *NIR1guide*
pU6seqF	AGGCATCGAACCTTCAAGAATTTG		Cloning *NIR1guide*
pU6seqR	CTTCTCTTCTTTCAGATTCC		Cloning *NIR1guide*
LB3	TAGCATCTGAATTTCATAACCAATCTCGAT		Genotyping SAIL lines
LBb1.3	ATTTTGCCGATTTCGGAAC		Genotyping SALK lines
CAPS_nr1-R	GGCTATAGATCCCGCATCGAC	AT1G77760	Genotyping *nia1*
CAPS_nr1-F	TACGACGACTCCTCAAGCGAC	AT1G77760	Genotyping *nia1*
NR2.1-RP	ACCTTCTTCGTCGGCGAGTTC	AT1G37130	Genotyping *nia2*
NR2.1-LP	ACGGCGTGGTTCGTTCTTACA	AT1G37130	Genotyping *nia2*
AtNOS1.1-RP	GCACCTACACCACAGGCAAGC	AT3G47450	Genotyping *noa1-2*
AtNOS1.1-LP	CCAATTGGCAATGTTGGTCG	AT3G47450	Genotyping *noa1-2*
NIR1cds-F	ATGACTTCTTTCTCTCTCACTTTCACATCTCC	AT2G15620	Genotyping *nir1-1*
seqnir1-1-R	GATCCCTTTTCGAAACTTC	AT2G15620	Genotyping *nir1-1*
SALK_026134C_LP	AAGAATCAACCGAACAACACG	AT4G24020	Genotyping *nlp7-1*
SALK_026134C_RP	CTTCAAAATAGCAGGCCAAATG	AT4G24020	Genotyping *nlp7-1*
SAIL_1278_H11_LP3	AAAATTGATCCTTTCCATGCC	AT5G02310	Genotyping *prt6-1*
SAIL_1278_H11_RP3	CAACATAAGAATCTGCGGGAG	AT5G02310	Genotyping *prt6-1*
Hyg-F	CGGCGAGTACTTCTACACAGC		Genotyping *NIR1* guide
Hyg-R	CTGATCGAAAAGTTCGACAGC		Genotyping *NIR1* guide
qAB1-F	TTCTCCGAAACCCAGATGGA	AT4G26080	qRT-PCR
qABI1-R	CGTTCTCGGAATCTTGATTTGAG	AT4G26080	qRT-PCR
qABI2-F	CTGCAGTCGCTGTTCCATTC	AT5G57050	qRT-PCR
qABI2-R	CACCGTTGCAATAGCCTCTAAGT	AT5G57050	qRT-PCR
qADH1-F	GCACCTGCTGAACATCAAGA	AT1G77120	qRT-PCR
qADH1-R	AGGATGTGGGTGACCTTGTC	AT1G77120	qRT-PCR
qAHG1-F	CGAGGGAGGCTGCGATTT	AT5G51760	qRT-PCR
qAHG1-R	ACAATAATATGATCGTGCGTCAAAA	AT5G51760	qRT-PCR
qAHG3-F	TTGTTGCGGTGTTGTTGGA	AT3G11410	qRT-PCR
qAHG3-R	AGAGAAGCTCGAGAAGTTGAATCA A	AT3G11410	qRT-PCR
qAtNOA-2nd-F	CAATGAAGCAGAGCATGAGATACA	AT3G47450	qRT-PCR
qAtNOA-2nd-R	TGGCAATGTTGGTCGAAGAA	AT3G47450	qRT-PCR
qAXR5-F	TGGATGGCCTCCAGTGAGATCTAACC	AT4G14560	qRT-PCR
qAXR5-R	GGAGCTCCGTCCATACTCACTTTCAC	AT4G14560	qRT-PCR
qCBF1-F	GGAGACAATGTTTGGGATGC	AT4G25490	qRT-PCR
qCBF1-R	TTAGTAACTCCAAAGCGACACG	AT4G25490	qRT-PCR
qCBF2-F	GACGTGTCCTTATGGAGCTATTAAAA	AT4G25470	qRT-PCR
qCBF2-R	TTACCATTTACATTCGTTTCTCACAAC	AT4G25470	qRT-PCR
qCBF3-F	TTCCGTCCGTACAGTGGAAT	AT4G25480	qRT-PCR
qCBF3-R	AACTCCATAACGATACGTCGTC	AT4G25480	qRT-PCR
qCHI-F	ATGTCTTCATCCAACGCCTGCGCC	AT3G55120	qRT-PCR

qCHI-R	GACGGTGAAGATCACGAATTTACC	AT3G55120	qRT-PCR
qCHS-F	AGCTGATGGACCTGCAGGCATCTTGGC	AT5G13930	qRT-PCR
qCHS-R	TGCATGTGACGTTTCCGAATTGTCGAC	AT5G13930	qRT-PCR
qCYP707A3-F	TCTTTTGGGAATGAAGGGTCTG	AT5G45340	qRT-PCR
qCYP707A3-R	TGATGTGCCAAAGGAGGACG	AT5G45340	qRT-PCR
qDFR-F	CGTGCCACCGTTCGAGATCC	AT5G42800	qRT-PCR
qDFR-R	GTGAGTAGCGTCTTGGCGTTTGGC	AT5G42800	qRT-PCR
qF3H/TT7-F	ATGGCTCCAGGAACTTTGACTGAGCTA	AT3G51240	qRT-PCR
qF3H/TT7-R	GATCTGACGGCAGATCTCTCCTCTTTT	AT3G51240	qRT-PCR
qHAB1-F	TCCCGCAGTTGCAATGACT	AT1G72770	qRT-PCR
qHAB1-R	CTGAGTGATCTCGACAGGTGATG	AT1G72770	qRT-PCR
qHAB2-F	CTGTTCAGCGGAGGTACATACTTC	AT1G17550	qRT-PCR
qHAB2-R	CCCACCAGCCGTTTATTCTC	AT1G17550	qRT-PCR
qHAI1-F	ACGCGCATGGACATGGA	AT5G59220	qRT-PCR
qHAI1-R	CTCGCACCGGCATTTTG	AT5G59220	qRT-PCR
qHAI2-F	GCGACGGACGGGCTATG	AT1G07430	qRT-PCR
qHAI2-R	ACACATGCGCACCATCGTA	AT1G07430	qRT-PCR
qHAI3-F	CCGTCGTCGGTTTATGAATCA	AT2G29380	qRT-PCR
qHAI3-R	TGCATCACCGTTTGGAATCTC	AT2G29380	qRT-PCR
qLEA4-5-F	GGAAAAGGCGGAGAAGATGA	AT5G06760	qRT-PCR
qLEA4-5-R	TTGTGCTGACGCGTTTCTCT	AT5G06760	qRT-PCR
qLEA7-F	GTGAGACACAGAGGAAGTGAAGAG	AT1G52690	qRT-PCR
qLEA7-R	CTCACGAACGCAACAAACACTAATC	AT1G52690	qRT-PCR
qLTI65/RD29b-F	CTTGGCACCACCGTTGGGACTA	AT5G52300	qRT-PCR
qLTI65/RD29b-R	TCAGTTCCCAGAATCTTGAACT	AT5G52300	qRT-PCR
q-NCED3-F	CGGTGGTTTACGACAAGAACAA	AT3G14440	qRT-PCR
q-NCED3-R	CAGAAGCAATCTGGAGCATCAA	AT3G14440	qRT-PCR
qNIA1-F	AGGTTTGGAAGGCGAATCG	AT1G77760	qRT-PCR
qNIA1-R	TGGCTGCAACGCAAACTG	AT1G77760	qRT-PCR
qNIA2-F	CCCGTTGCACTACGTTCGTA	AT1G37130	qRT-PCR
qNIA2-R	CGTCCATTCGGCCCATT	AT1G37130	qRT-PCR
qP-ACT2-F	TTGTTCCAGCCCTCGTTTGT	AT3G18780	qRT-PCR
qP-ACT2-R	TGTCTCGTGGATTCCAGCAG	AT3G18780	qRT-PCR
qPAP1-F	GAGGGTTCGTCCAAAGGGCTGCG	AT1G56650	qRT-PCR
qPAP1-R	GCACCGGTTTAGCCCAGCTCTTAC	AT1G56650	qRT-PCR
qPYL1-F	GGCGAATTCAGAGTCCTCCTCC	AT5G46790	qRT-PCR
qPYL1-R	GGGAGAGTTGGGTGAATTCG	AT5G46790	qRT-PCR
qPYL2-F	CAGTACCGAGCGGCTTGAG	AT2G26040	qRT-PCR
qPYL2-R	GCCGACGACCCTGAAGCT	AT2G26040	qRT-PCR
qPYL3-F	CATCACTCATAGCACACCGTGTAG	AT1G73000	qRT-PCR
qPYL3-R	CGAAGTCGCGGACGAATCT	AT1G73000	qRT-PCR
qPYL4-F	GCTTGCCGTTCACCGTCCTTC	AT2G38310	qRT-PCR
qPYL4-R	CGCGATCATCATCGGAATC	AT2G38310	qRT-PCR
qPYL5-F	GGTCACCGGTGCAACTCC	AT5G05440	qRT-PCR
qPYL5-R	CGCGTGGATCATCTGCACC	AT5G05440	qRT-PCR
qPYL6-F	CCAACGTCGATACAGTTTCAG	AT2G40330	qRT-PCR
qPYL6-R	CCTCCACGTCTTGTACCACG	AT2G40330	qRT-PCR
qPYL7-F	GATCGGAGGAGACGATACAGATACA	AT4G01026	qRT-PCR
qPYL7-R	AGTGGTGAAGATGACGCAACCT	AT4G01026	qRT-PCR
qPYL8-F	GGAAGCTAACGGGATTGAG	AT5G53160	qRT-PCR
qPYL8-R	CGGCTTATACTTCTGTGGC	AT5G53160	qRT-PCR
qPYL9-F	GATATGATGGACGGCGTTGAA	AT1G01360	qRT-PCR
qPYL9-R	ATGCGTCCGTACGTATTGCA	AT1G01360	qRT-PCR
qPYR1-F	GCCTTCGGAGTTAACACCAGAAG	AT4G17870	qRT-PCR
qPYR1-R	CGTCGTACGATTGACCAGACGAG	AT4G17870	qRT-PCR
qRAP2.12-F	TGCAGATTTCTCAGCGTCCCCATC	AT1G53910	qRT-PCR
qRAP2.12-R	GCTGCGGAAGGTTCAGTTTTTGGT	AT1G53910	qRT-PCR
qRAP2.3-F	CAAACTCCATCCCACCAACCAAGT	AT3G16770	qRT-PCR
qRAP2.3-R	TCTGTTGCCTGCTCCTTCTTCACT	AT3G16770	qRT-PCR
qSnRK2.10-F	TTCTATCACTTTGTGCCTTTTTTAGC	AT1G60940	qRT-PCR
qSnRK2.10-R	ACTACACAAAGTCACAAACCCAGAAA	AT1G60940	qRT-PCR
qSnRK2.1-F	TGCTCT CTGTTTCTCTTACTTTATTTCTTC	AT5G08590	qRT-PCR
qSnRK2.1-R	TGGCTTTGACAAATGTGTTTTTCT	AT5G08590	qRT-PCR
qSnRK2.2-F	GCAGATAATATCGGAGGCTACGA	AT3G50500	qRT-PCR
qSnRK2.2-R	TCAAGATTATCCGCCATGAAATC	AT3G50500	qRT-PCR
qSnRK2.3-F	TCGAATTTCTCTTTTTGTGATCAGA	AT5G66880	qRT-PCR
qSnRK2.3-R	ACTGTCGTGCATAATCGGCATA	AT5G66880	qRT-PCR
qSnRK2.4-F	CATCGTCATCTCTTTCCCTTT	AT1G10940	qRT-PCR
qSnRK2.4-R	CAAAATCAAGGATGCGATTCC	AT1G10940	qRT-PCR
qSnRK2.5-F	CAACGAGAGATCGTGATCGTACTT	AT5G63650	qRT-PCR
qSnRK2.5-R	CAATACCTTCACAACCTCATACTTGT	AT5G63650	qRT-PCR
qSnRK2.7-F	TTTCCTCCGAGTGCAAGCAT	AT4G40010	qRT-PCR
qSnRK2.7-R	GTGCTTTTCGATTTCCGGTACA	AT4G40010	qRT-PCR
qSnRK2.8-F	GGCAACACATTTGGCGTTAGT	AT1G78290	qRT-PCR
qSnRK2.8-R	CGGCGCTGCAGATTCTTC	AT1G78290	qRT-PCR
qSnRK2.9-F	GGAGAAGTATGAGATGGTGAAGGATT	AT2G23030	qRT-PCR

qSnRK2.9-R	CACAAGCTCGTTTGTTTGCTTATT	AT2G23030	qRT-PCR
qTEM2-F	TGGTCCGAGAGAAAACCCG	AT1G68840	qRT-PCR
qTEM2-R	TCAACTCCGAAAAGCCGAAC	AT1G68840	qRT-PCR
qZF-F	TCATTTCCTCGTAACAATCCTTTATTC	AT4G29190	qRT-PCR
qZF-R	CGGTGTTGTAGGCAGAGACTGA	AT4G29190	qRT-PCR

Table A4. Proteins with the MC- N-terminal amino acid sequence in the Arabidopsis proteome. The Arabidopsis proteome (TAIR 10 protein database) was searched for proteins with MCX sequence starting in position 1 with the PatMatch tool. 247 proteins encoded by 206 genes were identified.

AGI code	Annotation	N-term seq	Transcript
AT1G03106	unknown protein	MCG	AT1G03106.1
AT1G04501	unknown protein	MCI	AT1G04501.1
AT1G05280	Protein of unknown function (DUF604)	MCL	AT1G05280.1
AT1G05550	Protein of unknown function (DUF295)	MCL	AT1G05550.2
AT1G06350	Fatty acid desaturase family protein	MCD	AT1G06350.1
AT1G06360	Fatty acid desaturase family protein	MCD	AT1G06360.1
AT1G06570	HPD_HPPD_PDS1__phytoene desaturation 1	MCL	AT1G06570.1
AT1G06570	HPD_HPPD_PDS1__phytoene desaturation 1	MCL	AT1G06570.2
AT1G09500	NAD(P)-binding Rossmann-fold superfamily protein	MCF	AT1G09500.2
AT1G10657	Plant protein 1589 of unknown function	MCT	AT1G10657.1
AT1G10657	Plant protein 1589 of unknown function	MCT	AT1G10657.2
AT1G10657	Plant protein 1589 of unknown function	MCT	AT1G10657.3
AT1G10657	Plant protein 1589 of unknown function	MCT	AT1G10657.4
AT1G11362	Plant invertase/pectin methylesterase inhibitor superfamily protein	MCL	AT1G11362.1
AT1G11970	Ubiquitin-like superfamily protein	MCH	AT1G11970.1
AT1G14270	CAAX amino terminal protease family protein	MCG	AT1G14270.1
AT1G17235	RTFL11__ROTUNDIFOLIA like 11	MCI	AT1G17235.1
AT1G20240	SWI-SNF-related chromatin binding protein	MCV	AT1G20240.1
AT1G21738	unknown protein	MCV	AT1G21738.1
AT1G22950	2-oxoglutarate (2OG) and Fe(II)-dependent oxygenase superfamily protein	MCN	AT1G22950.1
AT1G24380	unknown protein	MCI	AT1G24380.1
AT1G26770	ATEXP10_expansin A10	MCR	AT1G26770.2
AT1G29010	unknown protein	MCS	AT1G29010.1
AT1G29090	Cysteine proteinases superfamily protein	MCD	AT1G29090.1
AT1G29951	CPuORF35__conserved peptide upstream open reading frame 35	MCI	AT1G29951.1
AT1G30650	**AR411_ATWRKY14_ WRKY DNA-binding protein 14**	**MCS**	**AT1G30650.1**
AT1G44090	ATGA20OX5_GA20OX5__gibberellin 20-oxidase 5	MCI	AT1G44090.1
AT1G49230	RING/U-box superfamily protein	MCT	AT1G49230.1
AT1G52342	unknown protein	MCY	AT1G52342.1
AT1G53625	unknown protein	MCR	AT1G53625.1
AT1G53910	RAP2.12__related to AP2 12	MCG	AT1G53910.1
AT1G53910	RAP2.12__related to AP2 12	MCG	AT1G53910.2
AT1G53910	RAP2.12__related to AP2 12	MCG	AT1G53910.3
AT1G55830	unknown protein	MCC	AT1G55830.1
AT1G58340	BCD1_ZF14_ZRZ__MATE efflux family protein	MCN	AT1G58340.1
AT1G59535	unknown protein	MCS	AT1G59535.1
AT1G62150	Mitochondrial transcription termination factor family protein	MCS	AT1G62150.1
AT1G63200	Cystatin/monellin superfamily protein	MCD	AT1G63200.1
AT1G63535	Defensin-like (DEFL) family protein	MCL	AT1G63535.1
AT1G63610	unknown protein	MCS	AT1G63610.1
AT1G63610	unknown protein	MCS	AT1G63610.2
AT1G65520	ATECI1_ECHIC_ECI1_PEC11__delta(3), delta(2)- enoyl CoA isomerase 1	MCS	AT1G65520.1
AT1G67520	lectin protein kinase family protein	MCS	AT1G67520.1
AT1G68810	basic helix-loop-helix (bHLH) DNA-binding superfamily protein	MCA	AT1G68810.1
AT1G69580	Homeodomain-like superfamily protein	MCL	AT1G69580.1
AT1G69580	Homeodomain-like superfamily protein	MCL	AT1G69580.2
AT1G69710	Regulator of chromosome condensation (RCC1) family with FYVE zinc finger	MCI	AT1G69710.1
AT1G70550	Protein of Unknown Function (DUF239)	MCL	AT1G70550.1
AT1G72360	AtERF73_ERF73_HRE1__Integrase-type DNA-binding superfamily protein	MCG	AT1G72360.2
AT1G72360	AtERF73_ERF73_HRE1__Integrase-type DNA-binding superfamily protein	MCG	AT1G72360.3
AT1G75810	unknown protein	MCL	AT1G75810.1
AT1G75910	EXL4__extracellular lipase 4	MCS	AT1G75910.1
AT1G80220	Protein of unknown function (DUF1644)	MCK	AT1G80220.1
AT1G80640	Protein kinase superfamily protein Protein kinase superfamily protein	MCL	AT1G80640.1
AT1G80640	Protein kinase superfamily protein Protein kinase superfamily protein	MCL	AT1G80640.2
AT2G01170	BAT1__bidirectional amino acid transporter 1	MCV	AT2G01170.2
AT2G02240	MEE66__F-box family protein	MCG	AT2G02240.1
AT2G03667	Asparagine synthase family protein	MCG	AT2G03667.1
AT2G05185	unknown protein	MCK	AT2G05185.1
AT2G05185	unknown protein	MCK	AT2G05185.2
AT2G07362	unknown protein	MCS	AT2G07362.1

AT2G07640	NAD(P)-binding Rossmann-fold superfamily protein	MCH	AT2G07640.1
AT2G10450	14-3-3 family protein	MCC	AT2G10450.1
AT2G10560	unknown protein	MCE	AT2G10560.1
AT2G11405	unknown protein	MCW	AT2G11405.1
AT2G11620	unknown protein	MCN	AT2G11620.1
AT2G14288	unknown protein	MCW	AT2G14288.1
AT2G22802	unknown protein	MCR	AT2G22802.1
AT2G23118	unknown protein	MCL	AT2G23118.1
AT2G26050	Protein of unknown function (DUF1644)	MCE	AT2G26050.1
AT2G26110	Protein of unknown function (DUF761)	MCF	AT2G26110.1
AT2G26470	unknown protein	MCG	AT2G26470.1
AT2G26610	Transducin family protein / WD-40 repeat family protein	MCS	AT2G26610.1
AT2G27110	FRS3__FAR1-related sequence 3	MCW	AT2G27110.3
AT2G29263	unknown protein	MCC	AT2G29263.1
AT2G31090	unknown protein	MCD	AT2G31090.1
AT2G31700	unknown protein	MCQ	AT2G31700.1
AT2G33230	YUC7__YUCCA 7	MCN	AT2G33230.1
AT2G34010	unknown protein	MCS	AT2G34010.1
AT2G34238	unknown protein	MCL	AT2G34238.1
AT2G38570	CONTAINS InterPro DOMAIN/s: PRC-barrel-like	MCN	AT2G38570.1
AT2G39590	Ribosomal protein S8 family protein	MCV	AT2G39590.1
AT2G40140	ATSZF2_CZF1_SZF2_ZFAR1__zinc finger (CCCH-type) family protein	MCG	AT2G40140.1
AT2G40140	ATSZF2_CZF1_SZF2_ZFAR1__zinc finger (CCCH-type) family protein	MCG	AT2G40140.2
AT2G41240	BHLH100__basic helix-loop-helix protein 100	MCA	AT2G41240.1
AT2G41240	BHLH100__basic helix-loop-helix protein 100	MCA	AT2G41240.2
AT2G41470	unknown protein	MCN	AT2G41470.1
AT2G41900	OXS2__CCCH-type zinc finger protein with ARM repeat domain	MCC	AT2G41900.1
AT2G43340	Protein of unknown function (DUF1685)	MCD	AT2G43340.1
AT2G43490	Ypt/Rab-GAP domain of gyp1p superfamily protein	MCS	AT2G43490.1
AT2G43490	Ypt/Rab-GAP domain of gyp1p superfamily protein	MCS	AT2G43490.2
AT2G43490	Ypt/Rab-GAP domain of gyp1p superfamily protein	MCS	AT2G43490.3
AT2G43490	Ypt/Rab-GAP domain of gyp1p superfamily protein	MCS	AT2G43490.4
AT2G43490	Ypt/Rab-GAP domain of gyp1p superfamily protein	MCS	AT2G43490.5
AT2G43490	Ypt/Rab-GAP domain of gyp1p superfamily protein	MCS	AT2G43490.6
AT2G44304	unknown protein	MCE	AT2G44304.1
AT2G45380	unknown protein	MCM	AT2G45380.2
AT2G47520	AtERF71_ERF71_HRE2__Integrase-type DNA-binding superfamily protein	MCG	AT2G47520.1
AT3G01930	Major facilitator superfamily protein	MCI	AT3G01930.1
AT3G02250	O-fucosyltransferase family protein	MCK	AT3G02250.1
AT3G02800	AtPFA-DSP3_PFA-DSP3__Tyrosine phosphatase family protein	MCL	AT3G02800.1
AT3G03720	CAT4__cationic amino acid transporter 4	MCL	AT3G03720.1
AT3G03773	HSP20-like chaperones superfamily protein	MCD	AT3G03773.2
AT3G04732	unknown protein	MCI	AT3G04732.1
AT3G04750	Tetratricopeptide repeat (TPR)-like superfamily protein	MCF	AT3G04750.1
AT3G06019	unknown protein	MCK	AT3G06019.1
AT3G09870	SAUR-like auxin-responsive protein family	MCK	AT3G09870.1
AT3G11000	DCD (Development and Cell Death) domain protein	MCV	AT3G11000.1
AT3G11773	Thioredoxin superfamily protein	MCS	AT3G11773.1
AT3G12600	atnudt16_NUDT16__nudix hydrolase homolog 16	MCD	AT3G12600.1
AT3G13275	unknown protein	MCC	AT3G13275.1
AT3G14230	RAP2.2__related to AP2 2	MCG	AT3G14230.1
AT3G14230	RAP2.2__related to AP2 2	MCG	AT3G14230.2
AT3G14230	RAP2.2__related to AP2 2	MCG	AT3G14230.3
AT3G16770	ATEBP_EBP_ERF72_RAP2.3__ethylene-responsive element binding protein	MCG	AT3G16770.1
AT3G16970	Plant self-incompatibility protein S1 family	MCV	AT3G16970.1
AT3G19560	F-box family protein	MCM	AT3G19560.1
AT3G21890	BBX31, B-box type zinc finger family protein	MCR	AT3G21890.1
AT3G22415	unknown protein	MCM	AT3G22415.1
AT3G23680	F-box associated ubiquitination effector family protein	MCR	AT3G23680.1
AT3G24090	glutamine-fructose-6-phosphate transaminase	MCG	AT3G24090.1
AT3G26100	Regulator of chromosome condensation (RCC1) family protein	MCN	AT3G26100.1
AT3G27130	P-loop containing nucleoside triphosphate hydrolases superfamily protein	MCG	AT3G27130.1
AT3G28193	unknown protein	MCF	AT3G28193.1
AT3G28530	UDP-glucose 4-epimerases	MCR	AT3G28530.1
AT3G42780	unknown protein	MCS	AT3G42780.1
AT3G44713	unknown protein	MCL	AT3G44713.1
AT3G46980	PHT4;3__phosphate transporter 4;3	MCY	AT3G46980.1
AT3G46980	PHT4;3__phosphate transporter 4;3	MCY	AT3G46980.3
AT3G46980	PHT4;3__phosphate transporter 4;3	MCY	AT3G46980.2
AT3G47340	ASN1_AT-ASN1_DIN6__glutamine-dependent asparagine synthase 1	MCG	AT3G47340.1

AT3G47340	ASN1_AT-ASN1_DIN6__glutamine-dependent asparagine synthase 1	MCG	AT3G47340.2
AT3G47340	ASN1_AT-ASN1_DIN6__glutamine-dependent asparagine synthase 1	MCG	AT3G47340.3
AT3G48346	unknown protein	MCA	AT3G48346.1
AT3G49770	unknown protein	MCK	AT3G49770.1
AT3G50440	ATMES10_MES10__methyl esterase 10	MCI	AT3G50440.1
AT3G51640	unknown protein	MCI	AT3G51640.1
AT3G51650	unknown protein	MCI	AT3G51650.1
AT3G53160	UGT73C7__UDP-glucosyl transferase 73C7	MCS	AT3G53160.1
AT3G54510	Early-responsive to dehydration stress protein (ERD4)	MCR	AT3G54510.1
AT3G55980	ATSZF1_SZF1__salt-inducible zinc finger 1	MCS	AT3G55980.1
AT3G56550	Pentatricopeptide repeat (PPR) superfamily protein	MCE	AT3G56550.1
AT3G56970	BHLH038_ORG2__basic helix-loop-helix (bHLH) DNA-binding superfamily protein	MCA	AT3G56970.1
AT3G56980	BHLH039_ORG3__basic helix-loop-helix (bHLH) DNA-binding superfamily protein	MCA	AT3G56980.1
AT3G59680	unknown protein	MCE	AT3G59680.1
AT3G60260	ELMO/CED-12 family protein	MCV	AT3G60260.3
AT3G60890	ZPR2__protein binding ZPR2__protein binding	MCL	AT3G60890.1
AT3G60890	ZPR2__protein binding ZPR2__protein binding	MCL	AT3G60890.2
AT3G61763	unknown protein	MCP	AT3G61763.1
AT3G63220	Galactose oxidase/kelch repeat superfamily protein	MCY	AT3G63220.2
AT4G00180	YAB3__Plant-specific transcription factor YABBY family protein	MCD	AT4G00180.2
AT4G00416	MBD3__methyl-CPG-binding domain 3	MCV	AT4G00416.1
AT4G02860	Phenazine biosynthesis PhzC/PhzF protein	MCD	AT4G02860.1
AT4G04650	RNA-directed DNA polymerase (reverse transcriptase)- related family protein	MCK	AT4G04650.1
AT4G05553	zinc knuckle (CCHC-type) family protein	MCG	AT4G05553.1
AT4G09320	NDPK1__Nucleoside diphosphate kinase family protein	MCG	AT4G09320.1
AT4G11470	CRK31__cysteine-rich RLK (RECEPTOR-like protein kinase) 31	MCL	AT4G11470.1
AT4G11480	CRK32__cysteine-rich RLK (RECEPTOR-like protein kinase) 32	MCL	AT4G11480.1
AT4G11910	unknown protein	MCS	AT4G11910.1
AT4G11911	unknown protein	MCS	AT4G11911.1
AT4G12170	Thioredoxin superfamily protein	MCS	AT4G12170.1
AT4G12382	F-box family protein F-box family protein	MCK	AT4G12382.1
AT4G12382	F-box family protein F-box family protein	MCK	AT4G12382.2
AT4G13395	DVL10_RTFL12__ROTUNDIFOLIA like 12	MCL	AT4G13395.1
AT4G14430	ATECI2_ECHIB_ECI2_IBR10_PEC12__indole-3- butyric acid response 10	MCT	AT4G14430.1
AT4G14440	ATECI3_ECI3_HCD1__3-hydroxyacyl-CoA dehydratase 1	MCT	AT4G14440.1
AT4G15248	BBX30, B-box type zinc finger family protein	MCR	AT4G15248.1
AT4G16845	VRN2__VEFS-Box of polycomb protein	MCR	AT4G16845.1
AT4G20900	MS5_TDM1__Tetratricopeptide repeat (TPR)-like superfamily protein	MCP	AT4G20900.1
AT4G22190	unknown protein	MCY	AT4G22190.1
AT4G22920	ATNYE1_NYE1__non-yellowing 1	MCS	AT4G22920.1
AT4G24020	NLP7__NIN like protein 7	MCE	AT4G24020.1
AT4G24110	unknown protein	MCR	AT4G24110.1
AT4G24973	Plant self-incompatibility protein S1 family	MCP	AT4G24973.1
AT4G28775	unknown protein	MCV	AT4G28775.1
AT4G28820	HIT-type Zinc finger family protein HIT-type Zinc finger family protein	MCP	AT4G28820.1
AT4G28820	HIT-type Zinc finger family protein HIT-type Zinc finger family protein	MCP	AT4G28820.2
AT4G29140	ADS1__MATE efflux family protein	MCN	AT4G29140.1
AT4G29905	unknown protein	MCL	AT4G29905.1
AT4G30760	Putative endonuclease or glycosyl hydrolase	MCA	AT4G30760.1
AT4G30760	Putative endonuclease or glycosyl hydrolase	MCA	AT4G30760.2
AT4G38260	Protein of unknown function (DUF833)	MCI	AT4G38260.1
AT4G38420	sks9__SKU5 similar 9	MCW	AT4G38420.1
AT4G38960	BBX19, B-box type zinc finger family protein	MCN	AT4G38960.2
AT4G39470	Tetratricopeptide repeat (TPR)-like superfamily protein	MCS	AT4G39470.1
AT5G03210	AtDIP2_DIP2__unknown protein	MCF	AT5G03210.1
AT5G07640	RING/U-box superfamily protein	MCV	AT5G07640.1
AT5G10240	ASN3__asparagine synthetase 3	MCG	AT5G10240.1
AT5G10240	ASN3__asparagine synthetase 3	MCG	AT5G10240.2
AT5G10695	unknown protein	MCL	AT5G10695.1
AT5G10695	unknown protein	MCL	AT5G10695.2
AT5G12323	unknown protein	MCE	AT5G12323.1
AT5G12850	CCCH-type zinc finger protein with ARM repeat domain	MCG	AT5G12850.1
AT5G13917	unknown protein	MCS	AT5G13917.1
AT5G14370	CCT motif family protein	MCS	AT5G14370.1
AT5G14602	unknown protein	MCP	AT5G14602.1
AT5G14650	Pectin lyase-like superfamily protein	MCR	AT5G14650.1
AT5G15740	O-fucosyltransferase family protein	MCK	AT5G15740.1

AT5G18150	Methyltransferase-related protein	MCP	AT5G18150.1
AT5G19729	unknown protein	MCV	AT5G19729.1
AT5G20450	unknown protein	MCL	AT5G20450.2
AT5G22545	unknown protein	MCR	AT5G22545.1
AT5G22608	unknown protein	MCK	AT5G22608.1
AT5G22608	unknown protein	MCK	AT5G22608.2
AT5G22608	unknown protein	MCK	AT5G22608.3
AT5G22870	Late embryogenesis abundant (LEA) hydroxyproline-rich glycoprotein family	MCH	AT5G22870.1
AT5G23640	unknown protein	MCV	AT5G23640.1
AT5G24080	Protein kinase superfamily protein	MCL	AT5G24080.1
AT5G26940	DPD1__Polynucleotidyl transferase, ribonuclease H-like superfamily protein	MCI	AT5G26940.1
AT5G26940	DPD1__Polynucleotidyl transferase, ribonuclease H-like superfamily protein	MCI	AT5G26940.2
AT5G26940	DPD1__Polynucleotidyl transferase, ribonuclease H-like superfamily protein	MCI	AT5G26940.3
AT5G26940	DPD1__Polynucleotidyl transferase, ribonuclease H-like superfamily protein	MCI	AT5G26940.4
AT5G29070	unknown protein	MCY	AT5G29070.1
AT5G37478	TPX2 (targeting protein for Xklp2) protein family	MCT	AT5G37478.1
AT5G39720	AIG2L__avirulence induced gene 2 like protein	MCS	AT5G39720.1
AT5G39770	Restriction endonuclease, type II-like superfamily protein	MCP	AT5G39770.1
AT5G42210	Major facilitator superfamily protein	MCI	AT5G42210.1
AT5G44310	Late embryogenesis abundant protein (LEA) family protein	MCE	AT5G44310.1
AT5G44680	DNA glycosylase superfamily protein	MCS	AT5G44680.1
AT5G44830	Pectin lyase-like superfamily protein	MCG	AT5G44830.1
AT5G46270	Disease resistance protein (TIR-NBS-LRR class) family	MCS	AT5G46270.1
AT5G48180	NSP5__nitrile specifier protein 5	MCP	AT5G48180.1
AT5G49480	ATCP1_CP1__Ca2+-binding protein 1	MCP	AT5G49480.1
AT5G50361	unknown protein	MCL	AT5G50361.1
AT5G54830	Dopamine beta-monooxygenase N-terminal domain-containing protein	MCD	AT5G54830.1
AT5G55508	unknown protein	MCN	AT5G55508.1
AT5G55600	agenet domain-containing protein / bromo-adjacent homology (BAH) domain-containing protein	MCE	AT5G55600.1
AT5G55600	agenet domain-containing protein / bromo-adjacent homology (BAH) domain-containing protein	MCE	AT5G55600.2
AT5G55600	agenet domain-containing protein / bromo-adjacent homology (BAH) domain-containing protein	MCE	AT5G55600.3
AT5G56450	PM-ANT__Mitochondrial substrate carrier family protein	MCI	AT5G56450.1
AT5G56720	c-NAD-MDH3__Lactate/malate dehydrogenase family protein	MCN	AT5G56720.1
AT5G57123	unknown protein	MCL	AT5G57123.1
AT5G57340	unknown protein	MCF	AT5G57340.2
AT5G58375	Methyltransferase-related protein	MCP	AT5G58375.1
AT5G59300	ATUBC7_UBC7__ubiquitin carrier protein 7	MCS	AT5G59300.1
AT5G59990	CCT motif family protein CCT motif family protein	MCG	AT5G59990.1
AT5G59990	CCT motif family protein CCT motif family protein	MCG	AT5G59990.2
AT5G60100	APRR3_PRR3__pseudo-response regulator 3	MCF	AT5G60100.1
AT5G60100	APRR3_PRR3__pseudo-response regulator 3	MCF	AT5G60100.2
AT5G60100	APRR3_PRR3__pseudo-response regulator 3	MCF	AT5G60100.3
AT5G64343	CPuORF38__conserved peptide upstream open reading frame 38	MCI	AT5G64343.1
AT5G64750	ABR1__Integrase-type DNA-binding superfamily protein	MCV	AT5G64750.1
AT5G65010	ASN2__asparagine synthetase 2 ASN2__asparagine synthetase 2	MCG	AT5G65010.1
AT5G65010	ASN2__asparagine synthetase 2 ASN2__asparagine synthetase 2	MCG	AT5G65010.2
AT5G65080	AGL68_MAF5__K-box region and MADS-box transcription factor family protein	MCR	AT5G65080.1
AT5G65495	unknown protein	MCY	AT5G65495.1
ATCG00040	MATK__maturase K	MCH	ATCG00040.1

Table A5. Genotyping of T1 generation of *pU6::gNIR1-1.* A total of 172 hygromycin resistant T1 seedlings transformed with *pHEE2E-gNIR1* (carrying both the Cas9 gene under the control of the Egg Cell Promoter and the RNA scaffold with the RNA guide for *NIR1* under the control of the U6 promoter) were genotyped by sequencing the region around the RNA guide target in the *NIR1* locus. The table shows the found mutations.

Genotype	**Number of individuals**	**Percentage**
	172	100%
Wild type	88	51%
Homozygous mutant	0	0%
Heterozygous mutant:	84	49%
• ~10bp deletion	5	3%
• 1bp insertion:	79	46%
– G insertion	1	0.6%
– T insertion	11	6%
– A insertion	67	39%

.

Table A6. Prediction of S-nitrosylation and nitration sites of potential NO targets.

			GPS SNO & YNO2		iNitro -Tyr	iSNO-PseAAC
Protein	**Position**	**Peptide**	**Score**	**Cutoff**	**Δ**	
P49333, ETR1	4	****MEVCNCIEPQW	4.142	1.484		
	65	LVQFGAFIVLCGATHLINLWT				(+)
	99	VLTAVVSCATALMLV	3.549	2.443		
	573	WIESDGLGKGCTAIFDVKLGI				(+)
	634	VTKGLLVHLGCEVTTVSSNEE				(+)
	661	KVVFMDVCMPGVENY	2.832	2.443		
	195	GLELQLSYTLRHQHP			0.556	
	735	LLEPRVLYEGM****	2.766	2.51		
Q9S814, EIN2	344	RILAVAPALYCVWTSGADGIY				(+)
	370	TQVLVAMMLPCSVIPLFRIAS				(+)
	729	SFGKDISSGYCMSPTAKGMDS				(+)
	1063	**LLQSFRHCILKLIKL**	**3.505**	**2.443**		
	1063	**EAKLLQSFRHCILKLIKLEGS**				**(+)**
	1141	ADLIVSFGVWCIHRVLDLSLM				(+)
	1218	**AKPAKGKCTTAVTLL**	**2.897**	**2.443**		
	1218	**PPAAKPAKGKCTTAVTLLDLI**				**(+)**
	32	LLVSVGYIDPGKWV			0.072	
	525	TSVTSSVYDLPENIL	1.116	0.725		
	746	SQMTSSLYDSLKQQR	0.946	0.725		
	783	**RMQMLGAYGNTTNNN**	**1.264**	**0.828**		
	783	**RMQMLGAYGNTTNNN**			**0.548**	
	828	HGYQMKSYVDNLAKE	1.674	1.065		
	859				0.012	
	901	RQSERSYYGVPSSGN	0.757	0.725		
	984	RVGVPSTYDDISQSR	1.114	0.828		
	1099				0.587	
	1161				0.542	
B9DFU2, MAX1	467	FIPFGIGPRACVGQRFALQEI				(+)
	147				0.066	
	316	KNIFTSDYISAVTYE	1.14	1.065		
	341				0.291	
	409	KEVEIGGYLLPKGTW	1.4	1.065		
	504				0.322	
Q9SIM9, MAX2	**63**	**DLSLVPDCFRSISHL**	**2.511**	**2.443**		
	63	**NARDLSLVPDCFRSISHLDLS**				**(+)**
	215	SSEIVSITKSCPNLKTFRVAC				(+)
	317	GVALEALNSKCKKLRVLKLGQ				(+)
	332	VLKLGQFQGVCSATEWRRLDG				(+)
	346	EWRRLDGVALCGGLQSLSIKN				(+)
	372	DMGLVAIGRGCCKLTTFEIQG				(+)
	373	MGLVAIGRGCCKLTTFEIQGC				(+)
	410	KTLTDVRISCCKNLDTAASLK				(+)
	426	AASLKAIEPICDRIKRLHIDC				(+)
	471	DDGYERSQKRCKYSFEEEHCS				(+)
	536	EEIRIKIEGDCRGKRRPAEPE				(+)
	551	RPAEPEFGLSCLALYPKLSKM				(+)
	565	YPKLSKMQLDCGDTIGFALTA				(+)

	111	FVESLNVYTRSPSSL	0.865	0.828		
	169				1.363	
	464	HEEEDDGYERSQKRC	1.189	0.725		
	500				0.415	
Q8VY26, MAX4	-	-	-	-		
	79	EKEKVEGERRCHVAWTSVQQE				(+)
	166	YKAAKKHNRLCYREFSETPKS				(+)
	217	VIKLGDGRVMCLTETQKGSIL				(+)
	395	GKATVIIADCCEHNADTRILD				(+)
	474	LGQKYRYVYACGAQRPCNFPN				(+)
	480	YVYACGAQRPCNFPNALSKVD				(+)
	565	PYGLPYGLHGCWIPKDXXXXX				(+)
	167				0.461	
	313				0.342	
	368				1.265	
	463				1.023	
	566				0.060	
Q8S8E3, PYL6	61	HVVGPSQCFSVVVQD	4.196	2.443		
	96	PQAYKHFVKSCHVVIGDGREV				(+)
	199	TCSFADTIVRCNLQSLAKLAE				(+)
	89				0.187	
	176	**RTRVVESYVVDVPAG**	**1.4**	**1.065**		
	176				**0.739**	
Q1ECF1, PYL7	36	HHCRENQCTSVLVKY	3.549	2.443		
	170	TCYFVESLIKCNLKSLACVSE				(+)
	177	LIKCNLKSLACVSERLAAQDI				(+)
	195	QDITNSIATFCNASNGYREKN				(+)
	14	DDTDTEMYGALVTAQ	1.405	0.725		
	162				0.527	
Q9LN63, BES1/BZR2	62	AQGNYNLPKHCDNNEVLKALC				(+)
	-	-	-	-		
	-	-			-	

Table A7. In silico genome-wide analysis of putative *RAP2.3*-binding motifs and the intersection with NO-regulated genes.

Patmatch	
Hits found:	7994
Sequences with hits:	6186
Sequences searched:	33602
Bytes searched:	33600250
Pattern:	MGCCGYM
Dataset searched:	TAIR10 Loci Upstream Sequences -- 1000 bp (DNA)

188 genes with MGCCGYM motif and UP-regulated by NO only in TPT_RAP2.3 –EST	
At3g09520	ATEXO70H4_EXO70H4__exocyst subunit exo70 family protein H4
At1g03800	ATERF10_ERF10__ERF domain protein 10
At5g06865	other RNA
At1g21120	IGMT2__O-methyltransferase family protein
At1g18570	AtMYB51_BW51A_BW51B_HIG1_MYB51__myb domain protein 51
At3g14590	NTMC2T6.2_NTMC2TYPE6.2__Calcium-dependent lipid-binding (CaLB domain) family protein
At5g58787	RING/U-box superfamily protein
At1g43160	RAP2.6__related to AP2 6
At1g79245	
At5g05140	Transcription elongation factor (TFIIS) family protein
At1g67810	SUFE2__sulfur E2
At1g07500	SMR5__
At4g34135	UGT73B2__UDP-glucosyltransferase 73B2
At4g13110	BSD domain-containing protein
At4g40065	other RNA
At4g21410	CRK29__cysteine-rich RLK (RECEPTOR-like protein kinase) 29
At1g78895	Reticulon family protein
At5g24770	ATVSP2_VSP2__vegetative storage protein 2
At3g55940	PLC7_Phosphoinositide-specific phospholipase C family protein
At2g40095	Alpha/beta hydrolase related protein
At1g73805	SARD1__Calmodulin binding protein-like
At3g50030	ARM-repeat/Tetratricopeptide repeat (TPR)-like protein
At1g27770	ACA1_PEA1__autoinhibited Ca2+-ATPase 1
At5g14700	NAD(P)-binding Rossmann-fold superfamily protein
At3g25790	myb-like transcription factor family protein
At5g27380	AtGSH2_GSH2_GSHB__glutathione synthetase 2
At2g45360	Protein of unknown function (DUF1442)
At4g31980	
At5g63790	ANAC102_NAC102__NAC domain containing protein 102
At1g33560	ADR1__Disease resistance protein (CC-NBS-LRR class) family
At2g31865	PARG2__poly(ADP-ribose) glycohydrolase 2
At1g19770	ATPUP14_PUP14__purine permease 14
At4g05010	AtFBS3_FBS3__F-box family protein
At5g20190	Tetratricopeptide repeat (TPR)-like superfamily protein
At3g21781	other RNA
At3g47960	AtNPF2.10_GTR1_NPF2.10__Major facilitator superfamily protein
At1g56140	Leucine-rich repeat transmembrane protein kinase
At4g39890	AtRABH1c_RABH1c__RAB GTPase homolog H1C
At3g15500	ANAC055_ATNAC3_NAC055_NAC3__NAC domain containing protein 3
At3g25760	AOC1_ERD12__allene oxide cyclase 1
At2g46370	AtGH3.11_FIN219_JAR1__Auxin-responsive GH3 family protein
At3g30405	transposable element gene
At4g27970	SLAH2__SLAC1 homologue 2
At2g21500	RING/U-box superfamily protein
At1g19570	ATDHAR1_DHAR1_DHAR5__dehydroascorbate reductase
At3g21780	UGT71B6__UDP-glucosyl transferase 71B6
At5g61810	APC1__Mitochondrial substrate carrier family protein
At4g03510	ATRMA1_RMA1__RING membrane-anchor 1
At2g24100	ASG1__
At1g27130	ATGSTU13_GST12_GSTU13__glutathione S-transferase tau 13
At1g15430	Protein of unknown function (DUF1644)
At5g35735	Auxin-responsive family protein
At2g05260	alpha/beta-Hydrolases superfamily protein
At1g21000	PLATZ transcription factor family protein
At2g18750	Calmodulin-binding protein
At1g19670	ATCLH1_ATHCOR1_CLH1_CORI1__chlorophyllase 1
At4g18197	ATPUP7_PEX17_PUP7__purine permease 7
At1g53280	AtDJ1B_DJ-1b_DJ1B__Class I glutamine amidotransferase-like superfamily protein
At1g79310	AtMC7_AtMCP2a_MC7_MCP2a__metacaspase 7

At4g01026	PYL7_RCAR2__PYR1-like 7
At3g14660	CYP72A13__cytochrome P450, family 72, subfamily A, polypeptide 13
At1g72850	Disease resistance protein (TIR-NBS class)
At2g17705	
At1g22360	AtUGT85A2_UGT85A2__UDP-glucosyl transferase 85A2
At1g26730	EXS (ERD1/XPR1/SYG1) family protein
At5g27420	ATL31_CNI1__carbon/nitrogen insensitive 1
At5g66880	SNRK2-3_SNRK2.3_SRK2I__sucrose nonfermenting 1(SNF1)-related protein kinase 2.3
At5g49015	Expressed protein
At3g27420	
At4g06529	transposable element gene
At1g50740	Transmembrane proteins 14C
At4g19390	Uncharacterised protein family (UPF0114)
At2g44370	Cysteine/Histidine-rich C1 domain family protein
At1g78410	VQ motif-containing protein
At3g21070	ATNADK-1_NADK1__NAD kinase 1
At3g25070	RIN4__RPM1 interacting protein 4
At4g22690	CYP706A1__cytochrome P450, family 706, subfamily A, polypeptide 1
At2g34930	disease resistance family protein / LRR family protein
At5g20250	DIN10_RS6__Raffinose synthase family protein
At5g18540	
At4g11650	ATOSM34_OSM34__osmotin 34
At1g66370	AtMYB113_MYB113__myb domain protein 113
At1g61370	S-locus lectin protein kinase family protein
At1g01260	JAM2__basic helix-loop-helix (bHLH) DNA-binding superfamily protein
At2g42760	
At3g57760	Protein kinase superfamily protein
At3g57210	Protein of unknown function (DUF626)
At2g43520	ATTI2_TI2__trypsin inhibitor protein 2
At4g36030	ARO3__armadillo repeat only 3
At3g14990	AtDJ1A_DJ-1a_DJ1A__Class I glutamine amidotransferase-like superfamily protein
At4g12005	
At4g39940	AKN2_APK2__APS-kinase 2
At5g10695	
At1g18270	ketose-bisphosphate aldolase class-II family protein
At1g60260	BGLU5__beta glucosidase 5
At5g13550	SULTR4;1__sulfate transporter 4.1
At4g36930	SPT__basic helix-loop-helix (bHLH) DNA-binding superfamily protein
At5g58400	Peroxidase superfamily protein
At2g18200	
At1g78850	D-mannose binding lectin protein with Apple-like carbohydrate-binding domain
At2g27505	FBD-like domain family protein
At5g04020	calmodulin binding
At1g21680	DPP6 N-terminal domain-like protein
At1g13390	
At1g20490	AMP-dependent synthetase and ligase family protein
At1g23850	
At5g07440	GDH2__glutamate dehydrogenase 2
At5g21960	Integrase-type DNA-binding superfamily protein
At3g23220	ESE1__Integrase-type DNA-binding superfamily protein
At5g59730	ATEXO70H7_EXO70H7__exocyst subunit exo70 family protein H7
At5g25210	
At2g44790	UCC2__uclacyanin 2
At1g14860	NUDT18_atnudt18__nudix hydrolase homolog 18
At3g43250	Family of unknown function (DUF572)
At5g56490	AtGulLO4_GulLO4__D-arabinono-1,4-lactone oxidase family protein
At3g47340	ASN1_AT-ASN1_DIN6__glutamine-dependent asparagine synthase 1
At5g10830	S-adenosyl-L-methionine-dependent methyltransferases superfamily protein
At1g77360	APPR6__Tetratricopeptide repeat (TPR)-like superfamily protein
At2g34580	
At4g36140	disease resistance protein (TIR-NBS-LRR class), putative
At4g31875	
At5g14730	
At5g25450	Cytochrome bd ubiquinol oxidase, 14kDa subunit
At3g47210	Plant protein of unknown function (DUF247)
At3g44190	FAD/NAD(P)-binding oxidoreductase family protein
At1g21110	IGMT3__O-methyltransferase family protein
At5g10820	Major facilitator superfamily protein
At2g34355	Major facilitator superfamily protein
At1g69920	ATGSTU12_GSTU12__glutathione S-transferase TAU 12
At1g57990	ATPUP18_PUP18__purine permease 18
At5g01760	ENTH/VHS/GAT family protein
At2g30870	ATGSTF10_ATGSTF4_ERD13_GSTF10__glutathione S-transferase PHI 10
At3g13100	ABCC7_ATMRP7_MRP7__multidrug resistance-associated protein 7
At4g34131	UGT73B3__UDP-glucosyl transferase 73B3
At3g26470	Powdery mildew resistance protein, RPW8 domain

At1g22470	
At5g67410	
At5g66050	Wound-responsive family protein
At2g43550	Scorpion toxin-like knottin superfamily protein
At4g38580	ATFP6_FP6_HIPP26__farnesylated protein 6
At1g66870	Carbohydrate-binding X8 domain superfamily protein
At1g10140	Uncharacterised conserved protein UCP031279
At3g01290	AtHIR2_HIR2__SPFH/Band 7/PHB domain-containing membrane-associated protein family
At1g75000	GNS1/SUR4 membrane protein family
At3g14200	Chaperone DnaJ-domain superfamily protein
At3g56710	SIB1__sigma factor binding protein 1
At4g39675	
At5g63320	NPX1__nuclear protein X1
At1g67365	other RNA
At3g45638	other RNA
At2g44390	Cysteine/Histidine-rich C1 domain family protein
At3g26840	PES2__Esterase/lipase/thioesterase family protein
At5g07890	myosin heavy chain-related
At4g13820	Leucine-rich repeat (LRR) family protein
At5g07460	ATMSRA2_PMSR2__peptidemethionine sulfoxide reductase 2
At5g55460	Bifunctional inhibitor/lipid-transfer protein/seed storage 2S albumin superfamily protein
At4g25030	
At3g50970	LTI30_XERO2__dehydrin family protein
At5g40348	other RNA
At3g25500	AFH1_AHF1_ATFH1_FH1__formin homology 1
At1g28380	NSL1__MAC/Perforin domain-containing protein
At4g14680	APS3__Pseudouridine synthase/archaeosine transglycosylase-like family protein
At5g18470	Curculin-like (mannose-binding) lectin family protein
At1g15125	S-adenosyl-L-methionine-dependent methyltransferases superfamily protein
At1g55850	ATCSLE1_CSLE1__cellulose synthase like E1
At4g13310	CYP71A20__cytochrome P450, family 71, subfamily A, polypeptide 20
At1g73480	alpha/beta-Hydrolases superfamily protein
At4g22710	CYP706A2__cytochrome P450, family 706, subfamily A, polypeptide 2
At1g22890	
At4g28400	Protein phosphatase 2C family protein
At3g60140	BGLU30_DIN2_SRG2__Glycosyl hydrolase superfamily protein
At3g15356	Legume lectin family protein
At1g07890	APX1_ATAPX01_ATAPX1_CS1_MEE6__ascorbate peroxidase 1
At3g14060	
At3g25882	NIMIN-2__NIM1-interacting 2
At5g37250	RING/U-box superfamily protein
At2g45760	BAL_BAP2__BON association protein 2
At1g06000	UDP-Glycosyltransferase superfamily protein
At1g77450	NAC032_anac032__NAC domain containing protein 32
At3g58980	F-box family protein
At4g18510	CLE2__CLAVATA3/ESR-related 2
At1g49650	alpha/beta-Hydrolases superfamily protein
At2g31810	ACT domain-containing small subunit of acetolactate synthase protein
At3g26600	ARO4__armadillo repeat only 4
At2g39420	alpha/beta-Hydrolases superfamily protein
At2g40200	basic helix-loop-helix (bHLH) DNA-binding superfamily protein
At4g38470	STY46__ACT-like protein tyrosine kinase family protein
At1g53440	Leucine-rich repeat transmembrane protein kinase

7 genes with MGCCGYM motif and UP-regulated by NO only in TPT_RAP2.3 plants +EST

At3g53180	NodGS__glutamate-ammonia ligases;catalytics;glutamate-ammonia ligases
At2g41640	Glycosyltransferase family 61 protein
At1g64160	AtDIR5_DIR5__Disease resistance-responsive (dirigent-like protein) family protein
At4g21870	HSP20-like chaperones superfamily protein
At3g19830	NTMC2T5.2_NTMC2TYPE5.2__Calcium-dependent lipid-binding (CaLB domain) family protein
At4g33467	
At1g32460	

52 genes with MGCCGYM motif and UP-regulated by NO in TPT_RAP2.3 plants both -EST & +EST

At1g76600	
At4g18340	Glycosyl hydrolase superfamily protein
At3g03020	
At1g61340	AtFBS1_FBS1__F-box family protein
At3g46640	LUX_PCL1__Homeodomain-like superfamily protein
At4g12720	AtNUDT7_GFG1_NUDT7__MutT/nudix family protein
At1g51780	ILL5__IAA-leucine resistant (ILR)-like gene 5
At2g22880	VQ motif-containing protein
At1g19210	Integrase-type DNA-binding superfamily protein
At5g54940	Translation initiation factor SUI1 family protein
At4g18205	Nucleotide-sugar transporter family protein
At1g28050	BBX13__B-box type zinc finger protein with CCT domain

At1g49520	SWIB complex BAF60b domain-containing protein
At1g59870	ABCG36_ATABCG36_ATPDR8_PDR8_PEN3__ABC-2 and Plant PDR ABC-type transporter family protein
At2g44810	DAD1__alpha/beta-Hydrolases superfamily protein
At4g30350	SMXL2__Double Clp-N motif-containing P-loop nucleoside triphosphate hydrolases superfamily protein
At5g04760	Duplicated homeodomain-like superfamily protein
At5g11650	alpha/beta-Hydrolases superfamily protein
At5g13190	AtGILP_GILP__
At1g30135	JAZ8_TIFY5A__jasmonate-zim-domain protein 8
At3g11020	DREB2_DREB2B__DRE/CRT-binding protein 2B
At3g53600	C2H2-type zinc finger family protein
At1g14480	Ankyrin repeat family protein
At5g25440	Protein kinase superfamily protein
At2g41100	ATCAL4_TCH3__Calcium-binding EF hand family protein
At1g72450	JAZ6_TIFY11B__jasmonate-zim-domain protein 6
At2g23030	SNRK2-9_SNRK2.9__SNF1-related protein kinase 2.9
At4g36150	Disease resistance protein (TIR-NBS-LRR class) family
At5g24590	ANAC091_TIP__TCV-interacting protein
At1g06620	2-oxoglutarate (2OG) and Fe(II)-dependent oxygenase superfamily protein
At1g73500	ATMKK9_MKK9__MAP kinase kinase 9
At3g11840	PUB24__plant U-box 24
At5g52882	P-loop containing nucleoside triphosphate hydrolases superfamily protein
At3g56880	VQ motif-containing protein
At1g72520	ATLOX4_LOX4__PLAT/LH2 domain-containing lipoxygenase family protein
At4g06746	DEAR5_RAP2.9__related to AP2 9
At3g15440	
At1g53430	Leucine-rich repeat transmembrane protein kinase
At3g51450	Calcium-dependent phosphotriesterase superfamily protein
At1g76590	PLATZ transcription factor family protein
At3g29000	Calcium-binding EF-hand family protein
At1g32640	ATMYC2_JAI1_JIN1_MYC2_RD22BP1_ZBF1__Basic helix-loop-helix (bHLH) DNA-binding family protein
At4g11360	RHA1B__RING-H2 finger A1B
At5g16410	HXXXD-type acyl-transferase family protein
At1g74930	ORA47__Integrase-type DNA-binding superfamily protein
At5g05490	AtREC8_DIF1_REC8_SYN1__Rad21/Rec8-like family protein
At4g17500	ATERF-1_ERF-1__ethylene responsive element binding factor 1
At4g35480	RHA3B__RING-H2 finger A3B
At3g24500	ATMBF1C_MBF1C__multiprotein bridging factor 1C
At1g51760	IAR3_JR3__peptidase M20/M25/M40 family protein
At5g67480	ATBT4_BT4__BTB and TAZ domain protein 4
At5g06570	alpha/beta-Hydrolases superfamily protein

97 genes with MGCCGYM motif and DOWN-regulated by NO only in TPT_RAP2.3 plants -EST

At5g47630	mtACP3__mitochondrial acyl carrier protein 3
At5g66460	AtMAN7_MAN7__Glycosyl hydrolase superfamily protein
At1g64370	
At3g20240	Mitochondrial substrate carrier family protein
At1g70120	Protein of unknown function (DUF1163)
At2g37560	ATORC2_ORC2__origin recognition complex second largest subunit 2
At4g22240	Plastid-lipid associated protein PAP / fibrillin family protein
At2g26080	AtGLDP2_GLDP2__glycine decarboxylase P-protein 2
At3g08600	Protein of unknown function (DUF1191)
At4g12320	CYP706A6__cytochrome P450, family 706, subfamily A, polypeptide 6
At1g07490	DVL9_RTFL3__ROTUNDIFOLIA like 3
At3g56870	
At2g36690	2-oxoglutarate (2OG) and Fe(II)-dependent oxygenase superfamily protein
At1g48460	
At1g69160	
At1g71850	Ubiquitin carboxyl-terminal hydrolase family protein
At2g43110	
At2g24820	AtTic55_TIC55-II_Tic55__translocon at the inner envelope membrane of chloroplasts 55-II
At5g16500	LIP1__Protein kinase superfamily protein
At5g43080	CYCA3;1__Cyclin A3;1
At2g32290	BAM6_BMY5__beta-amylase 6
At4g27030	FAD4_FADA__fatty acid desaturase A
At4g09970	
At3g55800	SBPASE__sedoheptulose-bisphosphatase
At3g19270	CYP707A4__cytochrome P450, family 707, subfamily A, polypeptide 4
At5g04950	ATNAS1_NAS1__nicotianamine synthase 1
At3g61550	RING/U-box superfamily protein
At1g17920	HDG12__homeodomain GLABROUS 12
At1g16489	other RNA
At4g26790	GDSL-like Lipase/Acylhydrolase superfamily protein
At1g22850	SNARE associated Golgi protein family
At1g19190	alpha/beta-Hydrolases superfamily protein

At5g18407	Defensin-like (DEFL) family protein
At4g07725	transposable element gene
At5g67200	Leucine-rich repeat protein kinase family protein
At1g10370	ATGSTU17_ERD9_GST30_GST30B_GSTU17__Glutathione S-transferase family protein
At5g51110	Transcriptional coactivator/pterin dehydratase
At3g01060	
At1g79890	RAD3-like DNA-binding helicase protein
At5g23060	CaS__calcium sensing receptor
At3g16870	GATA17__GATA transcription factor 17
At2g31660	EMA1_SAD2_URM9__ARM repeat superfamily protein
At4g31600	UTr7__UDP-N-acetylglucosamine (UAA) transporter family
At3g48160	DEL1_E2FE_E2L3__DP-E2F-like 1
At3g14740	RING/FYVE/PHD zinc finger superfamily protein
At5g61000	ATRPA70D_RPA1D_RPA70D__Replication factor-A protein 1-related
At1g73445	transposable element gene
At5g01410	ATPDX1_ATPDX1.3_PDX1_PDX1.3_RSR4__Aldolase-type TIM barrel family protein
At5g55040	DNA-binding bromodomain-containing protein
At5g65850	F-box and associated interaction domains-containing protein
At4g31330	Protein of unknown function, DUF599
At2g32610	ATCSLB01_ATCSLB1_CSLB01__cellulose synthase-like B1
At4g01037	AtWTF1_WTF1__Ubiquitin carboxyl-terminal hydrolase family protein
At3g18610	ATNUC-L2_NUC-L2_NUC2_PARLL1__nucleolin like 2
At4g14790	ATSUV3_EDA15__ATP-dependent RNA helicase, mitochondrial (SUV3)
At2g28050	Pentatricopeptide repeat (PPR) superfamily protein
At1g69200	FLN2__fructokinase-like 2
At2g32220	Ribosomal L27e protein family
At5g64630	FAS2_MUB3.9_NFB01_NFB1__Transducin/WD40 repeat-like superfamily protein
At1g14430	glyoxal oxidase-related protein
At4g28310	
At1g62250	
At5g43370	APT1_PHT1;2_PHT2__phosphate transporter 2
At5g04230	ATPAL3_PAL3__phenyl alanine ammonia-lyase 3
At5g42445	
At5g22100	RNA cyclase family protein
At1g45201	ATTLL1_TLL1__triacylglycerol lipase-like 1
At5g23300	PYRD__pyrimidine d
At1g78090	ATTPPB_TPPB__trehalose-6-phosphate phosphatase
At1g68570	AtNPF3.1_NPF3.1__Major facilitator superfamily protein
At2g37240	Thioredoxin superfamily protein
At1g08280	GALT29A__Glycosyltransferase family 29 (sialyltransferase) family protein
At5g38100	S-adenosyl-L-methionine-dependent methyltransferases superfamily protein
At2g47490	ATNDT1_NDT1__NAD+ transporter 1
At4g13020	MHK__Protein kinase superfamily protein
At3g14900	EMB3120__
At5g02180	Transmembrane amino acid transporter family protein
At1g56110	NOP56__homolog of nucleolar protein NOP56
At4g29310	Protein of unknown function (DUF1005)
At2g20724	
At4g28630	ABCB23_ATATM1_ATM1__ABC transporter of the mitochondrion 1
At4g15810	P-loop containing nucleoside triphosphate hydrolases superfamily protein
At2g38920	SPX (SYG1/Pho81/XPR1) domain-containing protein / zinc finger (C3HC4-type RING finger) protein-related
At1g27480	alpha/beta-Hydrolases superfamily protein
At1g03020	Thioredoxin superfamily protein
At5g26790	
At2g12462	
At4g33560	Wound-responsive family protein
At1g07010	AtSLP1_SLP1__Calcineurin-like metallo-phosphoesterase superfamily protein
At4g28230	
At3g46870	Pentatricopeptide repeat (PPR) superfamily protein
At4g05410	YAO__Transducin/WD40 repeat-like superfamily protein
At1g16730	UP6__unknown protein 6
At3g56290	
At5g55720	Pectin lyase-like superfamily protein
At1g09890	Rhamnogalacturonate lyase family protein
At1g66250	O-Glycosyl hydrolases family 17 protein

4 genes with MGCCGYM motif and DOWN-regulated by NO only in TPT_RAP2.3 plants +EST

At1g48630	RACK1B_RACK1B_AT__receptor for activated C kinase 1B
At1g29460	SAUR65__SAUR-like auxin-responsive protein family
At3g14570	ATGSL04_GSL04_GSL4_atgsl4__glucan synthase-like 4
At4g04790	Tetratricopeptide repeat (TPR)-like superfamily protein

7 genes with MGCCGYM motif and DOWN-regulated by NO in TPT_RAP2.3 plants both -EST & +EST

At2g27840	HD2D_HDA13_HDT04_HDT4__histone deacetylase-related / HD-related
At4g13710	Pectin lyase-like superfamily protein

At2g46040	ARID/BRIGHT DNA-binding domain;ELM2 domain protein
At3g47430	PEX11B__peroxin 11B
At1g14345	NAD(P)-linked oxidoreductase superfamily protein
At1g14280	PKS2__phytochrome kinase substrate 2
At1g14440	AtHB31_FTM2_HB31_ZHD4__homeobox protein 31

Table A8. Genes that were up-regulated in non-acclimated *nia1,2noa1-2* plants and were reported to be related to cold-triggered responses

Fold Change	FDR (LiMMA)	ProbeID	GI ID Anno	Annotation
11,99	0,00006474	262128_at	At1g52690	LEA7__Late embryogenesis abundant protein (LEA) family protein
10,01	0,00000076	263486_at	At2g22200	AtERF056, DREB subfamily A-6 of ERF/AP2 transcription factor family
9,62	0,00001112	247047_at	At5g66650	Protein of unknown function (DUF607)
8,3	0,00001112	258347_at	At3g17520	Late embryogenesis abundant protein (LEA) family protein
7,72	0,00000449	255479_at	At4g02380	AtLEA5_SAG21__senescence-associated gene 21
7,61	0,00000108	254634_at	At4g18650	Protein DOG1-like 4 transcription factor-related
7,41	0,00002258	258498_at	At3g02480	Late embryogenesis abundant protein (LEA) family protein
6,48	0,00001112	253203_at	At4g34710	ADC2_ATADC2_SPE2__arginine decarboxylase 2
6,16	0,00002258	258349_at	At3g17609	HYH__HY5-homolog
5,1	0,00007264	264953_at	At1g77120	ADH_ADH1_ATADH_ATADH1__alcohol dehydrogenase 1
4,53	0,00596634	252131_at	At3g50930	BCS1__cytochrome BC1 synthesis
4,43	0,0006744	246099_at	At5g20230	ATBCB_BCB_BCB_SAG14__blue-copper-binding protein
4,24	0,00023704	253268_s_at	At4g34131	UGT73B3__UDP-glucosyl transferase 73B3
4,17	0,00010364	247280_at	At5g64260	EXL2__EXORDIUM like 2
4	0,00023961	252367_at	At3g48360	ATBT2_BT2__BTB and TAZ domain protein 2
3,94	0,0013199	262113_at	At1g02820	Late embryogenesis abundant 3 (LEA3) family protein
3,85	0,00007264	256818_at	At3g21420	LBO1__2-oxoglutarate (2OG) and Fe(II)-dependent oxygenase superfamily protein
3,83	0,00004115	260410_at	At1g69870	NRT1.7__nitrate transporter 1.7
3,83	0,00004038	259681_at	At1g77760	GNR1_NIA1_NR1__nitrate reductase 1
3,74	0,00041234	253104_at	At4g36010	Pathogenesis-related thaumatin superfamily protein
3,65	0,00001112	256891_at	At3g19030	unknown protein
3,57	0,00053704	266392_at	At2g41280	ATM10_M10__late embryogenesis abundant protein (M10) / LEA protein M10
3,56	0,00056934	259705_at	At1g77450	anac032_NAC032__NAC domain containing protein 32
3,48	0,00034439	260856_at	At1g21910	DREB26__Integrase-type DNA-binding superfamily protein
3,45	0,00017589	259365_at	At1g13300	HRS1__myb-like transcription factor family protein
3,45	0,00050337	255524_at	At4g02330	AtPME41_ATPMEPCRB_PME41__Plant invertase/pectin methylesterase inhibitor superfamily
3,33	0,00008324	254663_at	At4g18290	KAT2__potassium channel in Arabidopsis thaliana 2
3,3	0,01604548	249527_at	At5g38710	Methylenetetrahydrofolate reductase family protein
3,28	0,00099033	252123_at	At3g51240	F3'H_F3H_TT6__flavanone 3-hydroxylase
3,25	0,01709944	261648_at	At1g27730	STZ_ZAT10__salt tolerance zinc finger
3,08	0,00136951	250207_at	At5g13930	ATCHS_CHS_TT4__Chalcone and stilbene synthase family protein
3,06	0,00045948	263096_at	At2g16060	AHB1_ARATH GLB1_ATGLB1_GLB1_HB1_NSHB1__hemoglobin 1
3,06	0,00004871	262231_at	At1g68740	PHO1;H1__EXS (ERD1/XPR1/SYG1) family protein
3	0,00308858	254707_at	At4g18010	5PTASE2_AT5PTASE2_IP5PII__myo-inositol polyphosphate 5-phosphatase 2
2,99	0,00014127	262644_at	At1g62710	BETA-VPE_BETAVPE__beta vacuolar processing enzyme
2,96	0,00206871	248607_at	At5g49480	ATCP1_CP1__Ca2+-binding protein 1
2,86	0,00057889	247723_at	At5g59220	HAI1_SAG113__highly ABA-induced PP2C gene 1
2,84	0,01284149	266743_at	At2g02990	ATRNS1_RNS1__ribonuclease 1
2,81	0,00003968	255011_at	At4g10040	CYTC-2__cytochrome c-2
2,8	0,00035228	261192_at	At1g32870	ANAC013_ANAC13_NAC13__NAC domain protein 13
2,78	0,00129584	266313_at	At2g26980	CIPK3_SnRK3.17__CBL-interacting protein kinase 3
2,75	0,00450314	245628_at	At1g56650	ATMYB75_MYB75_PAP1_SIAA1__production of anthocyanin pigment 1
2,72	0,00055768	250648_at	At5g06760	AtLEA4-5_LEA4-5__Late Embryogenesis Abundant 4-5
2,72	0,00326299	247925_at	At5g57560	TCH4_XTH22__Xyloglucan endotransglucosylase/hydrolase family protein
2,67	0,01728287	255543_at	At4g01870	tolB protein-related
2,65	0,00054792	246125_at	At5g19875	unknown protein
2,64	0,00751802	252908_at	At4g39670	Glycolipid transfer protein (GLTP) family protein
2,63	0,00024078	266832_at	At2g30040	MAPKKK14__mitogen-activated protein kinase kinase kinase 14
2,6	0,00006604	262262_at	At1g70780	unknown protein
2,6	0,00133771	246310_at	At3g51895	AST12_SULTR3;1__sulfate transporter 3;1
2,56	0,00881697	256576_at	At3g28210	PMZ_SAP12__zinc finger (AN1-like) family protein

2,54	0,00928913	266544_at	At2g35300	AtLEA4-2_LEA18_LEA4-2__Late embryogenesis abundant protein, group 1 protein
2,53	0,00038051	264217_at	At1g60190	AtPUB19_PUB19__ARM repeat superfamily protein
2,51	0,0000475	267254_at	At2g23030	SNRK2-9_SNRK2.9__SNF1-related protein kinase 2.9
2,51	0,0003961	253559_at	At4g31140	O-Glycosyl hydrolases family 17 protein
2,5	0,01480833	264000_at	At2g22500	ATPUMP5_DIC1_UCP5__uncoupling protein 5
2,45	0,00072723	265649_at	At2g27510	ATFD3_FD3__ferredoxin 3
2,45	0,01481085	256442_at	At3g10930	unknown protein
2,44	0,02386155	261892_at	At1g80840	ATWRKY40_WRKY40__WRKY DNA-binding protein 40
2,42	0,00161733	265119_at	At1g62570	FMO GS-OX4__flavin-monooxygenase glucosinolate S-oxygenase 4
2,36	0,00409642	263823_s_at	At2g40340	AtERF48_DREB2C__Integrase-type DNA-binding superfamily protein
2,35	0,00376141	267246_at	At2g30250	ATWRKY25_WRKY25__WRKY DNA-binding protein 25
2,33	0,00002778	260357_at	At1g69260	AFP1__ABI5 binding protein
2,33	0,00009348	263473_at	At2g31750	UGT74D1__UDP-glucosyl transferase 74D1
2,32	0,00227904	251603_at	At3g57760	Protein kinase superfamily protein
2,31	0,00206124	255795_at	At2g33380	AtCLO3_CLO-3_CLO3_RD20__Caleosin-related family protein
2,31	0,00067342	248352_at	At5g52300	LTI65_RD29B__CAP160 protein
2,24	0,00071909	245523_at	At4g15910	ATDI21_DI21__drought-induced 21
2,21	0,00482667	248870_at	At5g46710	PLATZ transcription factor family protein
2,2	0,00663873	256017_at	At1g19180	JAZ1_TIFY10A__jasmonate-zim-domain protein 1
2,2	0,00706728	262050_at	At1g80130	Tetratricopeptide repeat (TPR)-like superfamily protein
2,2	0,00008759	253245_at	At4g34590	ATB2_AtbZIP11_BZIP11_GBF6__G-box binding factor 6
2,2	0,00313122	245711_at	At5g04340	C2H2_CZF2_ZAT6__zinc finger of Arabidopsis thaliana 6
2,2	0,00129607	248381_at	At5g51830	pfkB-like carbohydrate kinase family protein
2,18	0,00102094	265670_s_at	At2g32190	unknown protein
2,17	0,00022176	264436_at	At1g10370	ATGSTU17_ERD9_GST30_GST30B_GSTU17__Glutathione S-transferase family protein
2,17	0,00072928	253097_at	At4g37320	CYP81D5__cytochrome P450, family 81, subfamily D, polypeptide 5
2,12	0,00343103	266545_at	At2g35290	unknown protein
2,1	0,0101275	264758_at	At1g61340	F-box family protein
2,07	0,00372371	256296_at	At1g69480	EXS (ERD1/XPR1/SYG1) family protein
2,07	0,00030772	246495_at	At5g16200	50S ribosomal protein-related
2,05	0,00626975	254432_at	At4g20830	FAD-binding Berberine family protein
2,05	0,00057688	253841_at	At4g27830	BGLU10__beta glucosidase 10
2,04	0,00123699	251827_at	At3g55120	A11_CFI_TT5__Chalcone-flavanone isomerase family protein
2,04	0,00971052	267080_at	At2g41190	Transmembrane amino acid transporter family protein
2,04	0,00575895	258805_at	At3g04010	O-Glycosyl hydrolases family 17 protein
2,04	0,00551881	253485_at	At4g31800	ATWRKY18_WRKY18__WRKY DNA-binding protein 18
2,02	0,00872669	250777_at	At5g05440	PYL5_RCAR8__Polyketide cyclase/dehydrase and lipid transport superfamily protein

(Table A9 is only available in the digital version of the manuscript)

Table A9. Differential transcript levels in TPT-RAP2.3 lines not-treated with β-estradiol. Levels at 1h after treatment with a NO pulse (C1) versus those at 0 time (C0). **Description of microarray experiments according to MIAME**

Investigation Design Format (IDF)	
Investigation title	IBMCP JLeon lab NO-exposed (60 min after pulse of 300 ppm NO during 5 min) TPT-RAP2.3 plants .
Experimental designs	NO-treated (1) vs untreated (0) TPT-RAP2.3 plants in the absence (C) or presence (E) of -estradiol inducer.
Person Last Name	León
Person First Name	José
E-mail	jleon@ibmcp.upv.es
Telephone	(+)3496387782
Affiliation & Address	IBMCP (CSIC-UPV), CPI Edificio 8E, Ingeniero Fausto Elio s/n, 46022 Valencia (Spain)
Person role	Investigator, submitter
Replicate types	3 independent biological replicates per genotype
Experiment description	1. Type of experiment: Compared analysis of the transcriptomes of 10-day old seedlings treated with a NO pulse for 5 min .
	2. Experimental factors: Samples were harvested by 1 h after NO exposure at 6 h after dawn of day 10. Seedlings were grown under long days (16 h light / 8 h darkness) photoperiodic conditions.
	3. Number of hybridizations to Arabidopsis Agilent microarrays): 12 distributed as 3 independent biological replicates of C0, C1, E0 and E1.
	4. Goals of proposed experiments: Identification of the No-regulated transcriptome affected by RAP2.3.

Sample and Data Relationship Format (SDRF)				
1. Hybridization design:				
# Sample	**Label**	**Genotype**	**Growth conditions**	**Tissue**
1	B C0	TPT-RAP2.3 transgenic line B (Coego et al., 2014)	MS media plus 1 % sucrose, 10 days	Seedlings

2	B C1	TPT-RAP2.3 transgenic line B (Coego et al., 2014)	MS media plus 1 % sucrose, 10 days	Seedlings
3	B E0	TPT-RAP2.3 transgenic line B (Coego et al., 2014)	MS media plus 1 % sucrose, 10 days	Seedlings
4	B E1	TPT-RAP2.3 transgenic line B (Coego et al., 2014)	MS media plus 1 % sucrose, 10 days	Seedlings
5	G C0	TPT-RAP2.3 transgenic line G (Coego et al., 2014)	MS media plus 1 % sucrose, 10 days	Seedlings
6	G C1	TPT-RAP2.3 transgenic line G (Coego et al., 2014)	MS media plus 1 % sucrose, 10 days	Seedlings
7	G E0	TPT-RAP2.3 transgenic line G (Coego et al., 2014)	MS media plus 1 % sucrose, 10 days	Seedlings
8	G E1	TPT-RAP2.3 transgenic line G (Coego et al., 2014)	MS media plus 1 % sucrose, 10 days	Seedlings
9	H C0	TPT-RAP2.3 transgenic line H (Coego et al., 2014)	MS media plus 1 % sucrose, 10 days	Seedlings
10	H C1	TPT-RAP2.3 transgenic line H (Coego et al., 2014)	MS media plus 1 % sucrose, 10 days	Seedlings
11	H E0	TPT-RAP2.3 transgenic line H (Coego et al., 2014)	MS media plus 1 % sucrose, 10 days	Seedlings
12	H E1	TPT-RAP2.3 transgenic line H (Coego et al., 2014)	MS media plus 1 % sucrose, 10 days	Seedlings

2. RNA extraction:

Total RNA from wild type and NO-treated plants was isolated and purified by the Micro-to-Midi Total RNA Purification System from Invitrogen (Carlsbad, CA, USA).

3. Quality controls:

RNAs from every genotype were checked by RT-PCR for mRNA levels of the*RAP2.3 and ACT2* genes. Moreover, total RNAs used for further preparation of hybridization probes were analysed to check integrity and purity by nanocapìlar electrophoresis in Bioanalyzer Agilent 2100.

4. Labeling and hybridization protocols:

Sample RNA (0.5 µg) was amplified and labeled with the Agilent Low Input Quick Amp Labeling Kit. An Agilent Spike-In Kit was used to assess the labeling and hybridization efficiencies. Hybridization an slide washing were performed with the Gene Expression Hybridization Kit and Gene Expression Wash Buffers, respectively. Three biological replicates of C0, E0, C1 and E1 were hybridized to Arabidposis (V4) Gene Expression Microarray 4x44K, which contained 43,803 probes (60-mer oligonucleotides) and was used in a one-color experimental design. Chip 1 was hybridized with samples 1,3,2 and 4. Chip 2 was hybridized with samples 8,5,7 and 6. Chipm 3 was hybridixed with samples 10,12,9 and 11. After washing and drying, slides were scanned in an Agilent G2565AA microarray scanner, at 5 µm resolution and using the double scanning, as recommended. Image files were analyzed with the Feature Extraction software 9.5.1. Interarray analyses were performed with the GeneSpring 11.5 software.

5. Sample comparisons:

C1 vs C0 and E1 vs E0 for the three TPT-RAP2.3 incependent transgenic lines.

6. Statistical analysis:

Linear model methods (LiMMA) were used for determining differentially expressed genes. To control the false-discovery rate, P-values were corrected using the method of Benjamini and Hochberg (1995). Criteria for selection of genes were fold value >1.5 and false-discovery rate≤ 0.05. Statistical analysis and graphical visualization of data were performed with the interactive tool fiesta (http://bioinfogp.cnb.csic.es/tools/FIESTA/).

Differential transcript levels in TPT-RAP2.3 lines not-treated with estradiol. Levels at 1h after treatment with a NO pulse (C1) versus those at 0 time (C0).

ProbeName	p (Corr)	p	FC	Log FC	AGI	Symbol	Corrected annotation
A_84_P13535	0,02403887	6,57E-04	447,5877	8,806026	AT2G38240		2-oxoglutarate (2OG) and Fe(II)-dependent oxygenase superfamily protein
A_84_P11046	0,03807803	0,0020636	226,5287	7,82355	AT4G34410	RRTF1	RRTF1__redox responsive transcription factor 1
A_84_P18492	0,00775991	1,58E-05	148,4449	7,213783	AT3G44870		S-adenosyl-L-methionine-dependent methyltransferases superfamily protein
A_84_P10609	0,01106583	6,00E-05	139,5284	7,124415	AT2G24850	TAT, TAT3	TAT_TAT3__tyrosine aminotransferase 3TAT_TAT3__tyrosine aminotransferase 3
A_84_P595141	0,01066107	5,56E-05	130,4175	7,026993	AT1G30135	JAZ8, TIFY5A	JAZ8_TIFY5A__jasmonate-zim-domain protein 8
A_84_P21769	0,00178308	1,41E-07	129,038	7,011652	AT1G61120	GES, TPS04, TPS4	GES_TPS04_TPS4__terpene synthase 04
A_84_P761749	0,00461552	1,91E-06	110,8071	6,791906	AT3G22275		
A_84_P17546	0,00764839	1,21E-05	107,4723	6,74782	AT3G44860	FAMT	FAMT__farnesoic acid carboxyl-O-methyltransferase
A_84_P521598	0,01246891	9,37E-05	97,04614	6,600599	AT2G22760		basic helix-loop-helix (bHLH) DNA-binding superfamily protein
A_84_P544235	0,00387638	8,41E-07	74,76919	6,224372	AT5G28237		Pyridoxal-5'-phosphate-dependent enzyme family protein
A_84_P17584	0,00466105	3,95E-06	73,95527	6,208581	AT1G17380	JAZ5, TIFY11A	JAZ5_TIFY11A__jasmonate-zim-domain protein 5
A_84_P21573	0,00387638	1,08E-06	73,49691	6,199612	AT5G38120	4CL8	4CL8__AMP-dependent synthetase and ligase family protein
A_84_P611898	0,00466105	3,33E-06	72,34635	6,176848	AT5G59580	UGT76E1	UGT76E1__UDP-glucosyl transferase 76E1
A_84_P18113	0,00772467	1,34E-05	58,17991	5,862449	AT1G76640		CML39__Calcium-binding EF-hand family protein
A_84_P91639	0,0352222	0,0017179	54,40184	5,765584	AT2G39030	NATA1	NATA1__Acyl-CoA N-acyltransferases (NAT) superfamily protein
A_84_P832235	0,00574999	5,86E-06	53,84785	5,750817	AT3G44860;	FAMT	
A_84_P762988	0,00894727	3,22E-05	53,5455	5,742693	AT4G36950	MAPKKK21	MAPKKK21__mitogen-activated protein kinase kinase kinase 21
A_84_P14748	0,00477309	4,20E-06	49,46843	5,628436	AT1G17420	ATLOX3, LOX3	ATLOX3_LOX3__lipoxygenase 3
A_84_P18289	0,00772467	1,41E-05	47,09384	5,557467	AT2G44810	DAD1	DAD1__alpha/beta-Hydrolases superfamily protein
A_84_P524680	0,00178308	1,24E-07	44,45429	5,474251	AT5G13220	JAS1, JAZ10, TIFY	JAS1_JAZ10_TIFY9__jasmonate-zim-domain protein 10
A_84_P502791	0,01246891	9,46E-05	42,70589	5,416363	AT1G32910		HXXXD-type acyl-transferase family protein
A_84_P851247	0,00571375	5,55E-06	42,01495	5,392831	AT5G28237		Pyridoxal-5'-phosphate-dependent enzyme family protein
A_84_P785475	0,00571375	5,56E-06	40,4212	5,33704	AT1G17420	ATLOX3, LOX3	ATLOX3_LOX3__lipoxygenase 3
A_84_P19302	0,00935958	4,03E-05	39,88659	5,317832	AT3G23220	ESE1	ESE1__Integrase-type DNA-binding superfamily protein
A_84_P788408	0,00772467	1,49E-05	39,4028	5,300226	AT2G22760		basic helix-loop-helix (bHLH) DNA-binding superfamily protein
A_84_P813757	0,00764839	1,22E-05	36,77208	5,200539	AT3G44860	FAMT	FAMT__farnesoic acid carboxyl-O-methyltransferase
A_84_P17343	0,01766588	2,59E-04	35,66974	5,156629	AT2G44840	ATERF13, EREBP,	ATERF13_EREBP_ERF13__ethylene-responsive element binding factor 13
A_84_P21194	0,01163687	7,28E-05	35,58547	5,153216	AT3G23240	ATERF1, ERF1	ATERF1_ERF1__ethylene response factor 1
A_84_P12324	0,0266426	8,64E-04	33,18674	5,052535	AT1G70130		LecRK-V.2__Concanavalin A-like lectin protein kinase family protein
A_84_P16173	0,00877275	2,26E-05	33,17225	5,051905	AT1G28480	GRX480, roxy19	GRX480_roxy19__Thioredoxin superfamily protein
A_84_P13172	0,02931333	0,0010869	32,58192	5,026	AT5G67080	MAPKKK19	MAPKKK19__mitogen-activated protein kinase kinase kinase 19
A_84_P823221	0,00901326	3,53E-05	32,19144	5,008605	AT5G13220	JAS1, JAZ10, TIFY	JAS1_JAZ10_TIFY9__jasmonate-zim-domain protein 10
A_84_P610481	0,00894727	2,63E-05	31,49779	4,977179	AT2G34600	JAZ7, TIFY5B	JAZ7_TIFY5B__jasmonate-zim-domain protein 7
A_84_P16121	0,00387638	1,24E-06	31,249	4,965738	AT1G43160	RAP2.6	RAP2.6__related to AP2 6
A_84_P18072	0,03349368	0,0015126	29,40931	4,878201	AT1G72520	ATLOX4, LOX4	ATLOX4_LOX4__PLAT/LH2 domain-containing lipoxygenase family protein
A_84_P14331	0,01432252	1,41E-04	28,42864	4,829273	AT1G76650	CML38	CML38__calmodulin-like 38
A_84_P816405	0,02342488	5,82E-04	28,13186	4,814133	AT5G62360		Plant invertase/pectin methylesterase inhibitor superfamily protein
A_84_P20323	0,04056462	0,0024299	27,65687	4,789566	AT3G49620	DIN11	DIN11__2-oxoglutarate (2OG) and Fe(II)-dependent oxygenase superfamily protein
A_84_P23712	0,04917615	0,0038851	26,29377	4,716649	AT1G59860		HSP20-like chaperones superfamily protein
A_84_P16247	0,00952359	4,21E-05	24,47912	4,61348	AT1G12610	DDF1	DDF1__Integrase-type DNA-binding superfamily protein
A_84_P20976	0,00900545	3,45E-05	23,80986	4,573487	AT1G19210		Integrase-type DNA-binding superfamily protein
A_84_P10863	0,00633665	7,48E-06	23,75829	4,570359	AT3G48520	CYP94B3	CYP94B3__cytochrome P450, family 94, subfamily B, polypeptide 3
A_84_P544827	0,01341196	1,14E-04	23,61297	4,561507	AT3G25760	AOC1, ERD12	AOC1_ERD12__allene oxide cyclase 1AOC1_ERD12__allene oxide cyclase 1
A_84_P223429	0,00894727	2,56E-05	23,44203	4,551025	AT5G43650	BHLH92	BHLH92__basic helix-loop-helix (bHLH) DNA-binding superfamily protein
A_84_P20120	0,00124154	2,88E-08	23,30547	4,542597	AT2G27690	CYP94C1	CYP94C1__cytochrome P450, family 94, subfamily C, polypeptide 1
A_84_P768692	0,02248672	5,33E-04	21,88436	4,451829	AT5G40348		other RNA
A_84_P23179	0,00775991	1,58E-05	21,758	4,443474	AT3G53600		C2H2-type zinc finger family protein
A_84_P13031	0,01063389	5,23E-05	21,00736	4,392823	AT5G19110		Eukaryotic aspartyl protease family protein

A_84_P79105	0,0114343	6,36E-05	20,38735	4,349603	AT1G66860		Class I glutamine amidotransferase-like superfamily protein
A_84_P592948	0,00736156	1,04E-05	20,13802	4,33185	AT4G11911		
A_84_P15993	0,01220927	8,85E-05	19,97414	4,320062	AT5G63450	CYP94B1	CYP94B1__cytochrome P450, family 94, subfamily B, polypeptide 1
A_84_P19845	0,01774115	2,74E-04	19,45943	4,282397	AT3G27810	ATMYB21, ATMYB	ATMYB21_ATMYB3_MYB21__myb domain protein 21
A_84_P786477	0,04961063	0,003957	19,42797	4,280063	AT5G05220		
A_84_P786499	0,01163687	7,08E-05	18,72404	4,22682	AT3G25760	AOC1, ERD12	AOC1_ERD12__allene oxide cyclase 1AOC1_ERD12__allene oxide cyclase 1
A_84_P572473	0,03484798	0,0016811	18,15437	4,182245	AT4G21920		
A_84_P815994	0,03807803	0,0020632	17,93385	4,164613	AT1G54020		GDSL-like Lipase/Acylhydrolase superfamily protein
A_84_P232439	0,00772467	1,38E-05	17,75253	4,149953	AT4G31800	ATWRKY18, WRKY	ATWRKY18_WRKY18__WRKY DNA-binding protein 18
A_84_P853664	0,00464882	3,01E-06	17,52594	4,13142	AT2G06050	AtOPR3, DDE1, OP	AtOPR3_DDE1_OPR3__oxophytodienoate-reductase 3
A_84_P15340	0,00412491	1,43E-06	17,36241	4,117895	AT2G06050	AtOPR3, DDE1, OP	AtOPR3_DDE1_OPR3__oxophytodienoate-reductase 3
A_84_P272600	0,01785415	2,84E-04	17,31235	4,11373	AT5G21960	ERF016	Integrase-type DNA-binding superfamily protein
A_84_P15194	0,00894727	3,06E-05	17,05285	4,091941	AT1G54020		GDSL-like Lipase/Acylhydrolase superfamily protein
A_84_P215028	0,02308556	5,66E-04	16,78474	4,069078	AT3G25770	AOC2	AOC2__allene oxide cyclase 2
A_84_P10627	0,02277204	5,49E-04	16,25142	4,022494	AT2G20880	AtERF53, ERF53	AtERF53_ERF53__Integrase-type DNA-binding superfamily protein
A_84_P611334	0,02676006	8,71E-04	16,00674	4,000608	AT2G22880		VQ motif-containing protein
A_84_P604601	0,04572882	0,0032095	15,74719	3,977023	AT4G37140	ATMES20, MEE69,	ATMES20_MEE69_MES20__alpha/beta-Hydrolases superfamily protein
A_84_P537220	0,02728939	9,07E-04	15,22946	3,928793	AT5G57510		
A_84_P862159	0,01539257	1,76E-04	15,10558	3,91701	AT2G24850	TAT, TAT3	TAT_TAT3__tyrosine aminotransferase 3TAT_TAT3__tyrosine aminotransferase 3
A_84_P20248	0,03608721	0,001822	15,09034	3,915553	AT3G23230		AtERF98_AtTDR1_ERF98_TDR1__Integrase-type DNA-binding superfamily protein
A_84_P812170	0,00950448	4,18E-05	15,02068	3,908878	AT3G45140	ATLOX2, LOX2	ATLOX2_LOX2__lipoxygenase 2ATLOX2_LOX2__lipoxygenase 2
A_84_P12788	0,01930832	3,49E-04	14,58847	3,866756	AT3G55970	ATJRG21, JRG21	ATJRG21_JRG21__jasmonate-regulated gene 21
A_84_P14985	0,00894727	2,76E-05	14,52517	3,860483	AT5G47220	ATERF2, ATERF-2	ATERF-2_ATERF2_ERF2__ethylene responsive element binding factor 2
A_84_P23517	0,00894727	2,90E-05	14,32943	3,840909	AT5G52320	CYP96A4	CYP96A4__cytochrome P450, family 96, subfamily A, polypeptide 4
A_84_P786287	0,03636191	0,0018611	14,03171	3,810619	AT5G05410	DREB2, DREB2A	DREB2_DREB2A__DRE-binding protein 2
A_84_P22140	0,01163687	7,10E-05	13,89037	3,796013	AT3G23250	ATMYB15, ATY19,	ATMYB15_ATY19_MYB15__myb domain protein 15
A_84_P847119	0,01564355	1,85E-04	13,77601	3,784086	AT5G62360		Plant invertase/pectin methylesterase inhibitor superfamily protein
A_84_P558681	0,00877048	2,08E-05	13,6393	3,769698	AT1G53885;	0	
A_84_P757973	0,01785415	2,84E-04	13,60557	3,766125	AT2G44578		RING/U-box superfamily protein
A_84_P785932	0,0325659	0,0014245	13,55619	3,76088	AT1G25400		
A_84_P164303	0,02449762	6,96E-04	13,4704	3,751721	AT5G58680		ARM repeat superfamily proteinARM repeat superfamily protein
A_84_P812834	0,02060719	4,29E-04	13,43344	3,747757	AT1G28480	GRX480, roxy19	GRX480_roxy19__Thioredoxin superfamily protein
A_84_P11822	0,00764839	1,21E-05	13,39123	3,743217	AT3G51450		Calcium-dependent phosphotriesterase superfamily protein
A_84_P852628	0,01065349	5,39E-05	13,3837	3,742405	AT5G02600	NAKR1, NPCC6	NAKR1_NPCC6__Heavy metal transport/detoxification superfamily protein
A_84_P870349	0,01163687	6,89E-05	13,26385	3,729427	AT3G23250	ATMYB15, ATY19,	ATMYB15_ATY19_MYB15__myb domain protein 15
A_84_P515468	0,0145606	1,52E-04	13,24495	3,727371	AT2G45940		Protein of unknown function (DUF295)
A_84_P17881	0,01246891	9,62E-05	13,1251	3,714256	AT5G62360		Plant invertase/pectin methylesterase inhibitor superfamily protein
A_84_P13271	0,04963833	0,0039626	13,10179	3,711692	AT1G80840	ATWRKY40, WRKY	ATWRKY40_WRKY40__WRKY DNA-binding protein 40
A_84_P287970	0,00466105	3,46E-06	13,01229	3,701803	AT5G65690	PCK2, PEPCK	PCK2_PEPCK__phosphoenolpyruvate carboxykinase 2
A_84_P172281	0,02271562	5,43E-04	12,98571	3,698853	AT5G48850	ATSDI1	ATSDI1__Tetratricopeptide repeat (TPR)-like superfamily protein
A_84_P67084	0,04636379	0,0033147	12,84307	3,682919	AT1G25400		
A_84_P21501	0,03484798	0,0016798	12,79647	3,677674	AT5G05410	DREB2, DREB2A	DREB2_DREB2A__DRE-binding protein 2
A_84_P832673	0,01375994	1,23E-04	12,505	3,644433	AT3G20340		
A_84_P19584	0,01961223	3,70E-04	12,49937	3,643784	AT4G15975		RING/U-box superfamily protein
A_84_P793001	0,04398336	0,0028868	12,48152	3,641722	AT1G17420	ATLOX3, LOX3	ATLOX3_LOX3__lipoxygenase 3
A_84_P11724	0,01163687	6,92E-05	12,47795	3,641309	AT3G16150	ASPGB1	ASPGB1__N-terminal nucleophile aminohydrolases (Ntn hydrolases) superfamily protein
A_84_P529724	0,01785415	2,85E-04	12,32328	3,623315	AT3G20340		
A_84_P829373	0,04674462	0,0034026	12,30838	3,621569	AT5G67080	MAPKKK19	MAPKKK19__mitogen-activated protein kinase kinase kinase 19
A_84_P242975	0,04741487	0,0034965	12,10399	3,597411	AT1G78410		VQ motif-containing protein
A_84_P704033	0,00764839	1,17E-05	12,06141	3,592327	AT1G11185		other RNA
A_84_P15304	0,00606654	6,89E-06	11,94813	3,578713	AT1G65390	ATPP2-A5, PP2-A5	ATPP2-A5_PP2-A5__phloem protein 2 A5

A_84_P13216	0,00894727	3,19E-05	11,93524	3,577156	AT1G20510	OPCL1	OPCL1__OPC-8:0 CoA ligase1
A_84_P553370	0,04036312	0,0024108	11,85587	3,56753	AT1G56240	AtPP2-B13, PP2-B1	AtPP2-B13_PP2-B13__phloem protein 2-B13
A_84_P11789	0,04372359	0,0028553	11,62336	3,538955	AT3G43250		Family of unknown function (DUF572)
A_84_P16877	0,00877275	2,21E-05	11,49364	3,522764	AT5G47240	atnudt8, NUDT8	NUDT8_atnudt8__nudix hydrolase homolog 8
A_84_P18925	0,01163687	7,07E-05	11,45863	3,518363	AT1G61610		S-locus lectin protein kinase family protein
A_84_P19028	0,01066107	5,66E-05	11,13812	3,477434	AT1G74930	ORA47	ORA47__Integrase-type DNA-binding superfamily protein
A_84_P191974	0,00894727	2,73E-05	10,98623	3,457625	AT5G03210	AtDIP2, DIP2	AtDIP2_DIP2__
A_84_P762569	0,0495561	0,0039515	10,96403	3,454706	AT3G27809		
A_84_P209868	0,01372322	1,20E-04	10,89406	3,44547	AT2G32130		Plant protein of unknown function (DUF641)
A_84_P789698	0,00772467	1,50E-05	10,78722	3,431252	AT1G72416		Chaperone DnaJ-domain superfamily proteinChaperone DnaJ-domain superfamily protein
A_84_P11721	0,03914714	0,0022026	10,63132	3,410249	AT3G15500	ANAC055, ATNAC3	ANAC055_ATNAC3_NAC055_NAC3__NAC domain containing protein 3
A_84_P20831	0,01647879	2,16E-04	10,63009	3,410082	AT1G61340		AtFBS1_FBS1__F-box family protein
A_84_P217688	0,0188704	3,32E-04	10,47759	3,389236	AT1G76600		
A_84_P16963	0,03439173	0,0016258	10,37977	3,375703	AT5G16960		Zinc-binding dehydrogenase family protein
A_84_P216248	0,01163687	7,22E-05	10,01018	3,323397	AT1G69890		Protein of unknown function (DUF569)
A_84_P193424	0,00464882	2,97E-06	9,970627	3,317684	AT1G19180	JAZ1, TIFY10A	AtJAZ1_JAZ1_TIFY10A__jasmonate-zim-domain protein 1
A_84_P785249	0,00682995	8,93E-06	9,916223	3,309791	AT4G31800	ATWRKY18, WRKY	ATWRKY18_WRKY18__WRKY DNA-binding protein 18
A_84_P769350	0,04737008	0,003488	9,885389	3,305298	AT5G54165		
A_84_P196714	0,04641205	0,0033429	9,874924	3,30377	AT5G63250		Carbohydrate-binding X8 domain superfamily protein
A_84_P715317	0,01177365	8,01E-05	9,798193	3,292516	AT1G72416		Chaperone DnaJ-domain superfamily proteinChaperone DnaJ-domain superfamily protein
A_84_P586962	0,01624931	2,07E-04	9,748003	3,285107	AT5G56880		
A_84_P503102	0,03707299	0,0019504	9,668864	3,273346	AT3G15440		
A_84_P22519	0,01393426	1,35E-04	9,607289	3,264129	AT5G38130		HXXXD-type acyl-transferase family protein
A_84_P15826	0,02751414	9,30E-04	9,599502	3,26296	AT5G05600		2-oxoglutarate (2OG) and Fe(II)-dependent oxygenase superfamily protein
A_84_P823879	0,00178308	1,70E-07	9,584101	3,260643	AT5G47240	atnudt8, NUDT8	NUDT8_atnudt8__nudix hydrolase homolog 8NUDT8_atnudt8__nudix hydrolase homolog 8
A_84_P575998	0,02568428	7,98E-04	9,582057	3,260335	AT4G14365	XBAT34	XBAT34__XB3 ortholog 4 in Arabidopsis thaliana
A_84_P549255	0,04647869	0,0033487	9,528822	3,252298	AT3G28600		P-loop containing nucleoside triphosphate hydrolases superfamily protein
A_84_P65264	0,02353903	5,90E-04	9,117328	3,188611	AT3G15356		Legume lectin family protein
A_84_P17140	0,00461552	2,11E-06	9,010446	3,171598	AT1G32640	ATMYC2, JAI1, JIN	ATMYC2_JAI1_JIN1_MYC2_RD22BP1_ZBF1__Basic helix-loop-helix (bHLH) DNA-binding family protein
A_84_P11613	0,04806924	0,0036151	8,917522	3,156643	AT2G34930		disease resistance family protein / LRR family protein
A_84_P820417	0,04572882	0,0032087	8,908025	3,155106	AT4G17490	ATERF6, ERF6, ER	ATERF6_ERF-6-6_ERF6__ethylene responsive element binding factor 6
A_84_P860087	0,01715813	2,39E-04	8,857978	3,146977	AT1G27020		
A_84_P300030	0,00877275	2,31E-05	8,842048	3,144381	AT5G08790	anac081, ATAF2	ATAF2_anac081__NAC (No Apical Meristem) domain transcriptional regulator superfamily protein
A_84_P833808	0,00894727	3,13E-05	8,464248	3,081382	AT1G17420	ATLOX3, LOX3	ATLOX3_LOX3__lipoxygenase 3
A_84_P847302	0,04831925	0,0037243	8,443587	3,077856	AT3G60140	BGLU30, DIN2, SR	BGLU30_DIN2_SRG2__Glycosyl hydrolase superfamily protein
A_84_P22274	0,02921359	0,0010751	8,397223	3,069912	AT3G63350	AT-HSFA7B, HSFA	AT-HSFA7B_HSFA7B__winged-helix DNA-binding transcription factor family protein
A_84_P21275	0,01872867	3,26E-04	8,37904	3,066785	AT3G50930	BCS1	BCS1__cytochrome BC1 synthesis
A_84_P20535	0,01457646	1,52E-04	8,298972	3,052933	AT4G17500	ATERF-1, ERF-1	ATERF-1_ERF-1__ethylene responsive element binding factor 1
A_84_P826417	0,04511397	0,0030989	8,288296	3,051076	AT5G24110	ATWRKY30, WRKY	ATWRKY30_WRKY30__WRKY DNA-binding protein 30
A_84_P283560	0,04851664	0,0037686	8,27021	3,047924	AT2G24600		Ankyrin repeat family protein
A_84_P840621	0,01313344	1,06E-04	8,269592	3,047816	AT1G19530		
A_84_P869292	0,01785633	2,87E-04	8,249113	3,044239	AT4G17500	ATERF-1, ERF-1	ATERF-1_ERF-1__ethylene responsive element binding factor 1
A_84_P594805	0,01375994	1,23E-04	8,234659	3,041709	AT4G36820		Protein of unknown function (DUF607)
A_84_P306860	0,03025034	0,0011889	8,159666	3,02851	AT5G10695		
A_84_P18211	0,01830757	3,07E-04	8,049125	3,008832	AT2G26530	AR781	AR781__Protein of unknown function (DUF1645)AR781__Protein of unknown function (DUF1645)
A_84_P159795	0,00532816	4,94E-06	8,029499	3,00531	AT1G19530		
A_84_P840907	0,016924	2,32E-04	8,029396	3,005292	AT5G56880		
A_84_P786720	0,00894727	2,93E-05	8,004184	3,000754	AT5G08790	anac081, ATAF2	ATAF2_anac081__NAC (No Apical Meristem) domain transcriptional regulator superfamily protein
A_84_P857687	0,01304823	1,03E-04	8,001444	3,00026	AT1G73500	ATMKK9, MKK9	ATMKK9_MKK9__MAP kinase kinase 9
A_84_P813646	0,01618926	2,04E-04	7,927353	2,986839	AT2G26530	AR781	AR781__Protein of unknown function (DUF1645)
A_84_P18100	0,04077161	0,0024607	7,915859	2,984746	AT1G69930	ATGSTU11, GSTU	ATGSTU11_GSTU11__glutathione S-transferase TAU 11

A_84_P21851	0,01331538	1,13E-04	7,896535	2,98122	AT1G66370	AtMYB113, MYB11	AtMYB113_MYB113__myb domain protein 113
A_84_P542646	0,00900545	3,43E-05	7,629397	2,931569	AT1G15040		GAT_GAT1_2.1__Class I glutamine amidotransferase-like superfamily protein
A_84_P23284	0,01769782	2,62E-04	7,628701	2,931438	AT4G21680	NRT1.8	AtNPF7.2_NPF7.2_NRT1.8__NITRATE TRANSPORTER 1.8
A_84_P586644	0,01525796	1,72E-04	7,590999	2,92429	AT3G53232	DVL20, RTFL1	DVL20_RTFL1__ROTUNDIFOLIA like 1
A_84_P573393	0,01830216	3,01E-04	7,587153	2,923559	AT4G27654		
A_84_P106016	0,04822512	0,0036633	7,542984	2,915135	AT1G15125		S-adenosyl-L-methionine-dependent methyltransferases superfamily protein
A_84_P16821	0,00640993	7,84E-06	7,536729	2,913939	AT5G24470	APRR5, PRR5	APRR5_PRR5__pseudo-response regulator 5
A_84_P10039	0,02240153	5,27E-04	7,531903	2,913014	AT1G27020		
A_84_P17934	0,01961223	3,65E-04	7,526135	2,911909	AT5G04340	C2H2, CZF2, ZAT6	C2H2_CZF2_ZAT6__zinc finger of Arabidopsis thaliana 6
A_84_P562774	0,01492891	1,61E-04	7,518686	2,910481	AT5G12340		
A_84_P784449	0,0497107	0,0039859	7,514286	2,909636	AT4G23220	CRK14	CRK14__cysteine-rich RLK (RECEPTOR-like protein kinase) 14
A_84_P802615	0,03187662	0,0013502	7,506802	2,908198	AT5G62360		Plant invertase/pectin methylesterase inhibitor superfamily proteinsuperfamily protein
A_84_P826766	0,02884718	0,0010294	7,487862	2,904554	AT5G58680		ARM repeat superfamily proteinARM repeat superfamily protein
A_84_P10495	0,00461552	2,41E-06	7,478293	2,902709	AT1G65890	AAE12	AAE12__acyl activating enzyme 12
A_84_P282640	0,01066107	5,68E-05	7,461075	2,899384	AT2G23170	GH3.3	GH3.3__Auxin-responsive GH3 family protein
A_84_P15720	0,01961223	3,71E-04	7,409588	2,889393	AT4G22620		SAUR34__SAUR-like auxin-responsive protein family
A_84_P818172	0,0145606	1,48E-04	7,380822	2,883781	AT1G15040		GAT_GAT1_2.1__Class I glutamine amidotransferase-like superfamily protein
A_84_P288904	0,01539895	1,77E-04	7,374735	2,882591	AT3G49570	LSU3	LSU3__response to low sulfur 3
A_84_P511454	0,02850118	9,95E-04	7,361979	2,880094	AT5G43570		Serine protease inhibitor, potato inhibitor I-type family protein
A_84_P245475	0,00668285	8,37E-06	7,354634	2,878654	AT2G25460		
A_84_P259470	0,01375994	1,27E-04	7,336154	2,875024	AT1G61890		MATE efflux family protein
A_84_P19511	0,0282192	9,78E-04	7,325701	2,872967	AT4G24380		
A_84_P20466	0,03367831	0,0015599	7,296392	2,867183	AT4G26260	MIOX4	MIOX4__myo-inositol oxygenase 4
A_84_P286390	0,00877048	2,11E-05	7,261025	2,860173	AT3G25780	AOC3	AOC3__allene oxide cyclase 3
A_84_P870348	0,04465805	0,0030167	7,216152	2,85123	AT2G41100	ATCAL4, TCH3	ATCAL4_TCH3__Calcium-binding EF hand family protein
A_84_P559351	0,01305407	1,04E-04	7,170948	2,842164	AT5G55460		Bifunctional inhibitor/lipid-transfer protein/seed storage 2S albumin superfamily protein
A_84_P759481	0,00772467	1,32E-05	7,119588	2,831794	AT3G12145	FLOR1, FLR1	FLOR1_FLR1_FTM4__Leucine-rich repeat (LRR) family protein
A_84_P85269	0,00877275	2,28E-05	7,004758	2,808335	AT1G24909;	ASB1,TRP4,WEI7	
A_84_P10611	0,00903297	3,59E-05	6,996785	2,806692	AT2G43530		Scorpion toxin-like knottin superfamily protein
A_84_P836406	0,01504028	1,66E-04	6,991565	2,805615	AT1G15125		S-adenosyl-L-methionine-dependent methyltransferases superfamily protein
A_84_P609369	0,01177365	7,92E-05	6,945716	2,796124	AT1G31550		GDSL-like Lipase/Acylhydrolase superfamily protein
A_84_P137619	0,030758	0,0012295	6,944105	2,795789	AT5G54490	PBP1	PBP1__pinoid-binding protein 1
A_84_P10561	0,00464882	2,73E-06	6,928264	2,792494	AT1G51780	ILL5	ILL5__IAA-leucine resistant (ILR)-like gene 5
A_84_P302360	0,04465805	0,0030186	6,918314	2,790421	AT5G37490		ARM repeat superfamily protein
A_84_P14490	0,02312214	5,67E-04	6,915822	2,789901	AT2G34180	ATWL2, CIPK13, S	ATWL2_CIPK13_SnRK3.7_WL2__CBL-interacting protein kinase 13
A_84_P21931	0,01961223	3,77E-04	6,88339	2,783119	AT1G28370	ATERF11, ERF11	ATERF11_ERF11__ERF domain protein 11
A_84_P14882	0,00466105	3,99E-06	6,854181	2,776984	AT1G06620		2-oxoglutarate (2OG) and Fe(II)-dependent oxygenase superfamily protein
A_84_P18032	0,03926466	0,0022285	6,777144	2,760677	AT1G54050		HSP20-like chaperones superfamily protein
A_84_P23070	0,01257935	9,79E-05	6,751513	2,755211	AT3G22740	HMT3	HMT3__homocysteine S-methyltransferase 3
A_84_P811729	0,02663922	8,62E-04	6,750648	2,755026	AT2G33830		AtDRM2_DRM2__Dormancy/auxin associated family protein
A_84_P169283	0,01911949	3,43E-04	6,718439	2,748126	AT5G06570		alpha/beta-Hydrolases superfamily protein
A_84_P101246	0,03864233	0,0021259	6,699562	2,744067	AT5G22530		
A_84_P595805	0,02403887	6,53E-04	6,649183	2,733177	AT5G36925		
A_84_P811808	0,00461552	2,28E-06	6,61285	2,725272	AT3G12145	FLOR1, FLR1	FLOR1_FLR1_FTM4__Leucine-rich repeat (LRR) family protein
A_84_P602187	0,03358237	0,0015229	6,596125	2,721619	AT1G05575		
A_84_P548213	0,0293697	0,0010921	6,595964	2,721583	AT2G31945		
A_84_P13376	0,00772467	1,32E-05	6,538024	2,708855	AT1G74430	ATMYB95, ATMYB	ATMYB95_ATMYBCP66_MYB95__myb domain protein 95
A_84_P230699	0,02150118	4,76E-04	6,491094	2,698462	AT5G05530		RING/U-box superfamily protein
A_84_P504336	0,01017677	4,71E-05	6,487664	2,697699	AT5G37250		RING/U-box superfamily protein
A_84_P13607	0,0121042	8,72E-05	6,451693	2,689678	AT3G06830		Plant invertase/pectin methylesterase inhibitor superfamily
A_84_P22892	0,01163687	7,40E-05	6,437172	2,686427	AT1G73500	ATMKK9, MKK9	ATMKK9_MKK9__MAP kinase kinase 9

A_84_P267120	0,00443168	1,64E-06	6,400991	2,678295	AT1G74950	JAZ2, TIFY10B	JAZ2_TIFY10B__TIFY domain/Divergent CCT motif family protein
A_84_P530732	0,0161733	2,03E-04	6,39089	2,676017	AT4G06746	DEAR5, RAP2.9	DEAR5_RAP2.9__related to AP2 9
A_84_P10171	0,00877048	2,02E-05	6,386692	2,675069	AT5G10300	AtHNL, ATMES5, H	ATMES5_AtHNL_HNL_MES5__methyl esterase 5
A_84_P290124	0,02400674	6,44E-04	6,367141	2,670646	AT2G22860	ATPSK2, PSK2	ATPSK2_PSK2__phytosulfokine 2 precursor
A_84_P97916	0,03700301	0,0019445	6,318588	2,659602	AT4G29780		
A_84_P19191	0,00894727	3,23E-05	6,298683	2,65505	AT1G19670	ATCLH1, ATHCOR	ATCLH1_ATHCOR1_CLH1_CORI1__chlorophyllase 1
A_84_P761897	0,02745852	9,21E-04	6,264201	2,647131	AT3G19615		
A_84_P24073	0,02830536	9,83E-04	6,261674	2,646548	AT3G28740	CYP81D11	CYP81D11__Cytochrome P450 superfamily protein
A_84_P10992	0,01526442	1,74E-04	6,249454	2,64373	AT4G21990	APR3, ATAPR3, PR	APR3_ATAPR3_PRH-26_PRH26__APS reductase 3
A_84_P141619	0,01842527	3,13E-04	6,208693	2,63429	AT1G66870		Carbohydrate-binding X8 domain superfamily protein
A_84_P11272	0,01156977	6,67E-05	6,187967	2,629466	AT1G52390		
A_84_P522895	0,04360947	0,0028168	6,178401	2,627234	AT5G10210		
A_84_P290684	0,03913938	0,0021977	6,153355	2,621373	AT4G17490	ATERF6, ERF6, ER	ATERF6_ERF-6-6_ERF6__ethylene responsive element binding factor 6
A_84_P605140	0,00877048	2,06E-05	6,138272	2,617833	AT2G28920		RING/U-box superfamily protein
A_84_P12419	0,01132469	6,27E-05	6,114624	2,612264	AT1G51760	IAR3, JR3	IAR3_JR3__peptidase M20/M25/M40 family protein
A_84_P516067	0,03206014	0,001375	6,113522	2,612004	AT1G17345		SAUR77__SAUR-like auxin-responsive protein family
A_84_P15269	0,01961223	3,70E-04	6,102159	2,60932	AT1G52890	ANAC019, NAC019	ANAC019_NAC019__NAC domain containing protein 19
A_84_P765109	0,04371872	0,002852	6,090106	2,606467	AT4G36052		other RNA
A_84_P15450	0,02054225	4,25E-04	6,062175	2,599835	AT2G32120	HSP70T-2	HSP70T-2__heat-shock protein 70T-2
A_84_P17787	0,02452861	7,06E-04	6,043014	2,595268	AT5G37670		HSP20-like chaperones superfamily protein
A_84_P101906	0,00894727	3,14E-05	6,038961	2,5943	AT1G70700	JAZ9, TIFY7	JAZ9_TIFY7__TIFY domain/Divergent CCT motif family protein
A_84_P712636	0,02524157	7,71E-04	6,017644	2,589199	AT3G27415		
A_84_P811806	0,01403995	1,37E-04	5,975347	2,579022	AT3G12145	FLOR1, FLR1	FLOR1_FLR1_FTM4__Leucine-rich repeat (LRR) family protein
A_84_P16803	0,00466105	3,98E-06	5,929307	2,567864	AT5G14700		NAD(P)-binding Rossmann-fold superfamily protein
A_84_P10330	0,04812316	0,0036404	5,926709	2,567231	AT5G65600		LecRK-IX.2__Concanavalin A-like lectin protein kinase family protein
A_84_P18976	0,0265841	8,57E-04	5,912258	2,563709	AT1G30730		FAD-binding Berberine family protein
A_84_P22732	0,01526442	1,74E-04	5,904238	2,561751	AT1G08860	BON3	BON3__Calcium-dependent phospholipid-binding Copine family protein
A_84_P159915	0,01507741	1,67E-04	5,892859	2,558968	AT4G27970	SLAH2	SLAH2__SLAC1 homologue 2
A_84_P23204	0,02612251	8,34E-04	5,87842	2,555429	AT3G59480		pfkB-like carbohydrate kinase family protein
A_84_P21864	0,03959642	0,0022907	5,832219	2,544045	AT1G73805	SARD1	SARD1__Calmodulin binding protein-like
A_84_P17644	0,03879603	0,002141	5,831932	2,543974	AT4G29710		Alkaline-phosphatase-like family protein
A_84_P582920	0,04066901	0,0024498	5,820572	2,541161	AT2G45760	BAL, BAP2	BAL_BAP2__BON association protein 2
A_84_P787617	0,0127527	9,98E-05	5,801665	2,536467	AT5G03270	LOG6	LOG6__lysine decarboxylase family protein
A_84_P811724	0,03189056	0,0013546	5,79123	2,53387	AT2G33830		AtDRM2_DRM2__Dormancy/auxin associated family protein
A_84_P756822	0,029931	0,0011627	5,765104	2,527347	AT2G07731;	NAD6	
A_84_P606233	0,00918073	3,86E-05	5,76142	2,526424	AT3G56260		
A_84_P76184	0,02626428	8,42E-04	5,750794	2,523761	AT5G24110	ATWRKY30, WRKY	ATWRKY30_WRKY30__WRKY DNA-binding protein 30
A_84_P11239	0,01368821	1,19E-04	5,742682	2,521725	AT5G56840		myb-like transcription factor family protein
A_84_P789539	0,01730775	2,44E-04	5,681701	2,506323	AT4G06746	DEAR5, RAP2.9	DEAR5_RAP2.9__related to AP2 9DEAR5_RAP2.9__related to AP2 9
A_84_P15276	0,0288939	0,001037	5,606352	2,487063	AT1G76680	ATOPR1, OPR1	ATOPR1_OPR1__12-oxophytodienoate reductase 1
A_84_P812177	0,03225273	0,0013988	5,577023	2,479495	AT3G45140	ATLOX2, LOX2	ATLOX2_LOX2__lipoxygenase 2ATLOX2_LOX2__lipoxygenase 2
A_84_P767439	0,00929625	3,98E-05	5,563991	2,47612	AT5G37230;	0	
A_84_P826608	0,01842527	3,14E-04	5,545459	2,471307	AT5G66650		Protein of unknown function (DUF607)Protein of unknown function (DUF607)
A_84_P803770	0,01874703	3,28E-04	5,529426	2,46713	AT1G76680	ATOPR1, OPR1	ATOPR1_OPR1__12-oxophytodienoate reductase 1
A_84_P19710	0,0278461	9,53E-04	5,459477	2,448763	AT5G46040		Major facilitator superfamily protein
A_84_P236643	0,00603258	6,29E-06	5,45451	2,44745	AT1G44350	ILL6	ILL6__IAA-leucine resistant (ILR)-like gene 6
A_84_P255510	0,01063389	5,22E-05	5,451627	2,446687	AT1G72450	JAZ6, TIFY11B	JAZ6_TIFY11B__jasmonate-zim-domain protein 6
A_84_P858725	0,00995117	4,52E-05	5,421475	2,438685	AT1G72450	JAZ6, TIFY11B	JAZ6_TIFY11B__jasmonate-zim-domain protein 6
A_84_P501308	0,03934355	0,002247	5,347799	2,418945	AT3G14260		Protein of unknown function (DUF567)
A_84_P241449	0,01163687	7,34E-05	5,343442	2,417769	AT1G28190		
A_84_P193944	0,0227833	5,50E-04	5,3431	2,417677	AT5G66650		Protein of unknown function (DUF607)Protein of unknown function (DUF607)

A_84_P14417	0,03359263	0,0015462	5,326117	2,413084	AT2G20560		DNAJ heat shock family proteinDNAJ heat shock family protein
A_84_P23398	0,00894727	3,26E-05	5,318908	2,41113	AT5G06870	ATPGIP2, PGIP2	ATPGIP2_PGIP2__polygalacturonase inhibiting protein 2
A_84_P12686	0,04864829	0,003789	5,30064	2,406167	AT3G25180	CYP82G1	CYP82G1__cytochrome P450, family 82, subfamily G, polypeptide 1
A_84_P16831	0,0390369	0,0021726	5,282131	2,40112	AT5G27420	ATL31, CNI1	ATL31_CNI1__carbon/nitrogen insensitive 1
A_84_P855161	0,00894727	2,86E-05	5,194599	2,377012	AT1G76680	ATOPR1, OPR1	ATOPR1_OPR1__12-oxophytodienoate reductase 1
A_84_P154615	0,01785633	2,86E-04	5,181008	2,373233	AT1G76590		PLATZ transcription factor family protein
A_84_P224809	0,02047567	4,17E-04	5,179902	2,372925	AT2G38790		
A_84_P827393	0,0307965	0,0012415	5,178978	2,372667	AT3G48650		
A_84_P19561	0,01176281	7,82E-05	5,163301	2,368294	AT4G35480	RHA3B	RHA3B__RING-H2 finger A3B
A_84_P829388	0,00877275	2,18E-05	5,150688	2,364765	AT1G07150	MAPKKK13	MAPKKK13__mitogen-activated protein kinase kinase kinase 13
A_84_P12418	0,01742975	2,51E-04	5,134507	2,360226	AT1G49530	GGPS6	GGPS6__geranylgeranyl pyrophosphate synthase 6
A_84_P23308	0,01751097	2,55E-04	5,101237	2,350847	AT4G27140	AT2S1, SESA1	AT2S1_SESA1__seed storage albumin 1
A_84_P18198	0,0378567	0,0020381	5,091441	2,348074	AT2G16660		Major facilitator superfamily protein
A_84_P572494	0,00900545	3,50E-05	5,081011	2,345116	AT4G28703		RmlC-like cupins superfamily proteinRmlC-like cupins superfamily protein
A_84_P579612	0,01166756	7,46E-05	5,044079	2,334591	AT4G27652		
A_84_P289964	0,04324035	0,0027782	5,010316	2,324902	AT1G19020		
A_84_P761787	0,03308225	0,0014794	4,998734	2,321563	AT3G14185		other RNA
A_84_P19375	0,01718834	2,40E-04	4,984381	2,317414	AT3G49110	ATPCA, ATPRX33,	ATPCA_ATPRX33_PRX33_PRXCA__peroxidase CA
A_84_P787406	0,00772467	1,48E-05	4,974677	2,314603	AT4G28703		RmlC-like cupins superfamily proteinRmlC-like cupins superfamily protein
A_84_P13315	0,02300682	5,63E-04	4,970052	2,313261	AT1G16370	OCT6, ATOCT6	ATOCT6_OCT6__organic cation/carnitine transporter 6
A_84_P299810	0,0246688	7,24E-04	4,933648	2,302655	AT1G11925		Stigma-specific Stig1 family protein
A_84_P22991	0,0339728	0,0015838	4,92892	2,301271	AT2G37430		ZAT11__C2H2 and C2HC zinc fingers superfamily protein
A_84_P786490	0,0378567	0,0020384	4,92617	2,300467	AT2G46400	ATWRKY46, WRKY	ATWRKY46_WRKY46__WRKY DNA-binding protein 46
A_84_P18334	0,01066107	5,52E-05	4,920482	2,2988	AT3G06490	AtMYB108, BOS1,	AtMYB108_BOS1_MYB108__myb domain protein 108
A_84_P10711	0,0321314	0,0013819	4,912672	2,296508	AT2G39330	JAL23	JAL23__jacalin-related lectin 23
A_84_P16571	0,03927104	0,0022318	4,89059	2,290009	AT3G56400	ATWRKY70, WRKY	ATWRKY70_WRKY70__WRKY DNA-binding protein 70
A_84_P211588	0,02991109	0,0011472	4,877779	2,286224	AT4G24110		
A_84_P16037	0,00857212	1,85E-05	4,875406	2,285523	AT1G56650	ATMYB75, MYB75,	ATMYB75_MYB75_PAP1_SIAA1__production of anthocyanin pigment 1
A_84_P11191	0,02353903	5,88E-04	4,83706	2,27413	AT5G43620		Pre-mRNA cleavage complex II
A_84_P16645	0,03490096	0,0016857	4,828329	2,271524	AT4G13480	AtMYB79, MYB79	AtMYB79_MYB79__myb domain protein 79
A_84_P21473	0,04680366	0,0034123	4,815778	2,267769	AT4G15210	ATBETA-AMY, AT-	AT-BETA-AMY_ATBETA-AMY_BAM5_BMY1_RAM1__beta-amylase 5
A_84_P805566	0,02951533	0,0011157	4,805011	2,26454	AT5G24780	ATVSP1, VSP1	ATVSP1_VSP1__vegetative storage protein 1
A_84_P12975	0,01455063	1,47E-04	4,789286	2,25981	AT1G19550		Glutathione S-transferase family protein
A_84_P16077	0,03484798	0,0016771	4,784685	2,258424	AT1G05100	MAPKKK18	MAPKKK18__mitogen-activated protein kinase kinase kinase 18
A_84_P862058	0,01188738	8,37E-05	4,774704	2,255411	AT3G12145	FLOR1, FLR1	FLOR1_FLR1_FTM4__Leucine-rich repeat (LRR) family protein
A_84_P115562	0,01572616	1,90E-04	4,772359	2,254703	AT1G73325		Kunitz family trypsin and protease inhibitor protein
A_84_P16802	0,03920303	0,0022235	4,756288	2,249836	AT5G14470		AtGALK2_GALK2__GHMP kinase family protein
A_84_P786837	0,00903297	3,61E-05	4,748268	2,247401	AT5G13080	ATWRKY75, WRKY	ATWRKY75_WRKY75__WRKY DNA-binding protein
A_84_P87559	0,02167651	4,88E-04	4,743054	2,245816	AT1G66500		Pre-mRNA cleavage complex II
A_84_P541993	0,01354508	1,16E-04	4,736571	2,243843	AT2G27310		F-box family protein
A_84_P21703	0,01320943	1,08E-04	4,710181	2,235783	AT5G13080	ATWRKY75, WRKY	ATWRKY75_WRKY75__WRKY DNA-binding protein 75
A_84_P15864	0,01424899	1,40E-04	4,658196	2,219771	AT5G18470		Curculin-like (mannose-binding) lectin family protein
A_84_P787776	0,00178308	2,89E-07	4,650138	2,217274	AT3G56260		
A_84_P11731	0,01222481	8,89E-05	4,62808	2,210414	AT3G24500	ATMBF1C, MBF1C	ATMBF1C_MBF1C__multiprotein bridging factor 1C
A_84_P14710	0,0286969	0,0010111	4,622901	2,208798	AT3G56710	SIB1	SIB1__sigma factor binding protein 1
A_84_P92059	0,02237896	5,24E-04	4,619537	2,207748	AT5G67480	ATBT4, BT4	ATBT4_BT4__BTB and TAZ domain protein 4
A_84_P12086	0,01246891	9,59E-05	4,596134	2,200421	AT5G19100		Eukaryotic aspartyl protease family protein
A_84_P10148	0,01797131	2,91E-04	4,589444	2,198319	AT5G03270	LOG6	LOG6__lysine decarboxylase family proteinLOG6__lysine decarboxylase family protein
A_84_P816079	0,0241966	6,69E-04	4,581136	2,195705	AT4G17230	SCL13	SCL13__SCARECROW-like 13SCL13__SCARECROW-like 13
A_84_P819821	0,03879603	0,0021411	4,579017	2,195038	AT2G20560		DNAJ heat shock family proteinDNAJ heat shock family protein
A_84_P504929	0,0373915	0,0019897	4,57067	2,192406	AT3G29000		Calcium-binding EF-hand family proteinCalcium-binding EF-hand family protein

A_84_P301340	0,00764839	1,14E-05	4,567662	2,191456	AT1G80120		Protein of unknown function (DUF567)
A_84_P784216	0,04759051	0,0035292	4,567451	2,191389	AT5G24780	ATVSP1, VSP1	ATVSP1_VSP1__vegetative storage protein 1
A_84_P18553	0,02376995	6,12E-04	4,53024	2,179587	AT4G21390	B120	B120__S-locus lectin protein kinase family protein
A_84_P15209	0,01720161	2,42E-04	4,528386	2,178997	AT1G15330		Cystathionine beta-synthase (CBS) proteinCystathionine beta-synthase (CBS) protein
A_84_P828124	0,01363577	1,17E-04	4,510864	2,173404	AT1G72360	AtERF73, ERF73, H	AtERF73_ERF73_HRE1__Integrase-type DNA-binding superfamily protein
A_84_P174151	0,03189378	0,0013572	4,466162	2,159036	AT2G40330	PYL6, RCAR9	PYL6_RCAR9__PYR1-like 6
A_84_P24128	0,02236889	5,19E-04	4,462134	2,157734	AT3G54150		S-adenosyl-L-methionine-dependent methyltransferases superfamily protein
A_84_P205068	0,01202061	8,62E-05	4,459051	2,156737	AT1G17744		
A_84_P11850	0,00894727	3,01E-05	4,450363	2,153923	AT3G57760		Protein kinase superfamily protein
A_84_P13499	0,02864917	0,0010029	4,445462	2,152333	AT2G14160		RNA-binding (RRM/RBD/RNP motifs) family protein
A_84_P12726	0,01742975	2,52E-04	4,440763	2,150807	AT3G11020	DREB2, DREB2B	DREB2_DREB2B__DRE/CRT-binding protein 2B
A_84_P784935	0,01756549	2,56E-04	4,433978	2,148602	AT1G15330		Cystathionine beta-synthase (CBS) proteinCystathionine beta-synthase (CBS) protein
A_84_P13568	0,01958881	3,59E-04	4,419572	2,143907	AT2G33830		AtDRM2_DRM2__Dormancy/auxin associated family protein
A_84_P156125	0,03585444	0,0018033	4,408545	2,140303	AT3G61190	BAP1	BAP1__BON association protein 1
A_84_P17388	0,00894727	2,89E-05	4,404374	2,138937	AT3G06500	A/N-InvC	A/N-InvC__Plant neutral invertase family protein
A_84_P135945	0,01320943	1,07E-04	4,404077	2,13884	AT3G11840	PUB24	PUB24__plant U-box 24
A_84_P20736	0,02403887	6,57E-04	4,391066	2,134571	AT5G66700	ATHB53, HB53, HB	ATHB53_HB-8_HB53__homeobox 53
A_84_P145309	0,04139324	0,0025452	4,353202	2,122077	AT4G13820		Leucine-rich repeat (LRR) family protein
A_84_P268810	0,01188738	8,40E-05	4,323877	2,112326	AT4G27560		UDP-Glycosyltransferase superfamily proteinUDP-Glycosyltransferase superfamily protein
A_84_P18030	0,02160571	4,83E-04	4,274418	2,095728	AT1G30720		FAD-binding Berberine family protein
A_84_P567982	0,00640993	7,87E-06	4,252192	2,088207	AT4G15210	ATBETA-AMY, AT-	AT-BETA-AMY_ATBETA-AMY_BAM5_BMY1_RAM1__beta-amylase 5
A_84_P549947	0,01771716	2,71E-04	4,248887	2,087085	AT2G18210		
A_84_P20977	0,02353903	5,90E-04	4,23665	2,082924	AT1G14480		Ankyrin repeat family protein
A_84_P139169	0,02401475	6,48E-04	4,205016	2,072111	AT1G67810	SUFE2	SUFE2__sulfur E2
A_84_P849804	0,01961223	3,68E-04	4,187997	2,06626	AT2G18210		
A_84_P15797	0,0364524	0,0018701	4,187597	2,066123	AT4G15100	scpl30	scpl30__serine carboxypeptidase-like 30
A_84_P827867	0,03518269	0,0017128	4,184982	2,065222	AT1G65880	BZO1	BZO1__benzoyloxyglucosinolate 1
A_84_P12963	0,0116891	7,53E-05	4,182253	2,064281	AT4G15440	CYP74B2, HPL1	CYP74B2_HPL1__hydroperoxide lyase 1
A_84_P870191	0,04017467	0,0023847	4,159566	2,056433	AT1G21320;	0	
A_84_P13173	0,02646521	8,51E-04	4,15641	2,055338	AT5G67300	ATMYB44, ATMYB	ATMYB44_ATMYBR1_MYB44_MYBR1__myb domain protein r1
A_84_P12969	0,01390775	1,34E-04	4,153408	2,054296	AT4G17230	SCL13	SCL13__SCARECROW-like 13SCL13__SCARECROW-like 13
A_84_P97476	0,02951533	0,0011131	4,146306	2,051827	AT5G24780	ATVSP1, VSP1	ATVSP1_VSP1__vegetative storage protein 1
A_84_P767469	0,02100477	4,54E-04	4,129149	2,045845	AT5G37270		RING/U-box superfamily protein
A_84_P269630	0,02684096	8,78E-04	4,098218	2,034997	AT2G27505		FBD-like domain family protein
A_84_P834641	0,04908544	0,0038744	4,091984	2,032801	AT3G29000		Calcium-binding EF-hand family proteinCalcium-binding EF-hand family protein
A_84_P23096	0,01686909	2,30E-04	4,089145	2,031799	AT3G26200	CYP71B22	CYP71B22__cytochrome P450, family 71, subfamily B, polypeptide 22
A_84_P847323	0,01156977	6,58E-05	4,084339	2,030103	AT2G18210		
A_84_P22507	0,00772467	1,43E-05	4,082771	2,029549	AT5G27520	AtPNC2, PNC2	AtPNC2_PNC2__peroxisomal adenine nucleotide carrier 2
A_84_P279280	0,01797131	2,91E-04	4,073453	2,026252	AT5G44590		S-adenosyl-L-methionine-dependent methyltransferases superfamily protein
A_84_P23455	0,02943616	0,0011009	4,058723	2,021026	AT1G68620		alpha/beta-Hydrolases superfamily protein
A_84_P10947	0,00387638	1,26E-06	4,050553	2,018119	AT4G04610	APR, APR1, ATAP	APR_APR1_ATAPR1_PRH19__APS reductase 1
A_84_P14013	0,01693314	2,33E-04	4,042065	2,015092	AT5G40000		P-loop containing nucleoside triphosphate hydrolases superfamily protein
A_84_P755325	0,00904516	3,71E-05	4,030572	2,010985	AT2G06045		transposable element gene
A_84_P856887	0,02532245	7,79E-04	4,024943	2,008968	AT3G10985	ATWI-12, SAG20,	ATWI-12_SAG20_WI12__senescence associated gene 20
A_84_P11345	0,00772467	1,46E-05	4,011036	2,003975	AT1G17750	AtPEPR2, PEPR2	AtPEPR2_PEPR2__PEP1 receptor 2
A_84_P179084	0,01504028	1,65E-04	4,010959	2,003947	AT5G35735		Auxin-responsive family protein
A_84_P22015	0,01246891	9,28E-05	3,99287	1,997426	AT1G30040	ATGA2OX2, GA2O	ATGA2OX2_GA2OX2__gibberellin 2-oxidase
A_84_P20910	0,01305407	1,05E-04	3,986538	1,995136	AT1G72360	AtERF73, ERF73, H	AtERF73_ERF73_HRE1__Integrase-type DNA-binding superfamily protein
A_84_P23353	0,02507846	7,59E-04	3,985152	1,994635	AT4G38390	RHS17	RHS17__root hair specific 17
A_84_P56650	0,01305407	1,03E-04	3,940731	1,978463	AT5G41080	AtGDPD2, GDPD2	AtGDPD2_GDPD2__PLC-like phosphodiesterases superfamily protein
A_84_P20428	0,04788074	0,0035903	3,935472	1,976537	AT4G13310	CYP71A20	CYP71A20__cytochrome P450, family 71, subfamily A, polypeptide 20

A_84_P96076	0,01177365	8,02E-05	3,921685	1,971474	AT3G25790	HHO		myb-like transcription factor family protein
A_84_P564464	0,01020095	4,91E-05	3,915044	1,969029	AT4G27460			CBSX5__Cystathionine beta-synthase (CBS) family protein
A_84_P820222	0,02751414	9,28E-04	3,906483	1,96587	AT1G73480			alpha/beta-Hydrolases superfamily proteinalpha/beta-Hydrolases superfamily protein
A_84_P10871	0,01747336	2,53E-04	3,882391	1,956945	AT3G50280			HXXXD-type acyl-transferase family protein
A_84_P18425	0,00178308	2,51E-07	3,86338	1,949863	AT3G47960			AtNPF2.10_GTR1_NPF2.10__Major facilitator superfamily protein
A_84_P24091	0,02009357	3,97E-04	3,862192	1,94942	AT3G45960	ATEXLA3, ATEXPL		ATEXLA3_ATEXPL3_ATHEXP BETA 2.3_EXLA3_EXPL3__expansin-like A3
A_84_P769675	0,029931	0,0011632	3,862049	1,949367	AT5G66210	CPK28		CPK28__calcium-dependent protein kinase 28
A_84_P811178	0,01909557	3,41E-04	3,861123	1,94902	AT4G16146			cAMP-regulated phosphoprotein 19-related protein
A_84_P17461	0,01185074	8,24E-05	3,860947	1,948955	AT3G43430			RING/U-box superfamily protein
A_84_P14693	0,009203	3,92E-05	3,859746	1,948506	AT3G59750			LecRK-V.8__Concanavalin A-like lectin protein kinase family protein
A_84_P210868	0,0110149	5,93E-05	3,855405	1,946882	AT4G16146			cAMP-regulated phosphoprotein 19-related protein
A_84_P21126	0,01961223	3,65E-04	3,853399	1,946132	AT2G32020			Acyl-CoA N-acyltransferases (NAT) superfamily protein
A_84_P790164	0,00682995	9,49E-06	3,85206	1,94563	AT5G41080	AtGDPD2, GDPD2		AtGDPD2_GDPD2__PLC-like phosphodiesterases superfamily protein
A_84_P818318	0,01246891	9,29E-05	3,85125	1,945327	AT4G27560			UDP-Glycosyltransferase superfamily protein
A_84_P22522	0,01386093	1,29E-04	3,847009	1,943737	AT5G39020			Malectin/receptor-like protein kinase family protein
A_84_P11439	0,03764553	0,0020141	3,840557	1,941316	AT1G52560			HSP20-like chaperones superfamily protein
A_84_P169853	0,02114772	4,60E-04	3,820757	1,933858	AT3G49580	LSU1		LSU1__response to low sulfur 1
A_84_P17380	0,0184221	3,11E-04	3,804794	1,927818	AT3G08720	ATPK19, ATPK2, A		ATPK19_ATPK2_ATS6K2_S6K2__serine/threonine protein kinase 2
A_84_P545008	0,0308525	0,0012449	3,796443	1,924648	AT4G31875			
A_84_P132425	0,01971263	3,82E-04	3,789433	1,921982	AT3G46110			Domain of unknown function (DUF966)Domain of unknown function (DUF966)
A_84_P21203	0,02403887	6,56E-04	3,7818	1,919073	AT1G26730			EXS (ERD1/XPR1/SYG1) family protein
A_84_P794434	0,03518269	0,0017138	3,752533	1,907865	AT4G27460			CBSX5__Cystathionine beta-synthase (CBS) family protein
A_84_P12859	0,01439785	1,44E-04	3,741184	1,903495	AT4G12410			SAUR35__SAUR-like auxin-responsive protein family
A_84_P542288	0,01174265	7,69E-05	3,739886	1,902994	AT4G17470			alpha/beta-Hydrolases superfamily proteinalpha/beta-Hydrolases superfamily protein
A_84_P542377	0,03915126	0,0022042	3,729649	1,89904	AT5G03550			
A_84_P20121	0,04708578	0,0034459	3,728491	1,898592	AT1G07860;		0	
A_84_P15366	0,01363577	1,17E-04	3,725646	1,897491	AT1G11210			Protein of unknown function (DUF761)
A_84_P16742	0,00877275	2,28E-05	3,715552	1,893577	AT4G14680	APS3		APS3__Pseudouridine synthase/archaeosine transglycosylase-like family protein
A_84_P72634	0,02740352	9,17E-04	3,712206	1,892277	AT4G36500			
A_84_P10209	0,02069154	4,38E-04	3,706598	1,890096	AT5G25930			Protein kinase family protein with leucine-rich repeat domain
A_84_P20724	0,01961223	3,68E-04	3,698443	1,886918	AT5G63790	ANAC102, NAC102		ANAC102_NAC102__NAC domain containing protein 102
A_84_P16285	0,03529944	0,0017323	3,697263	1,886457	AT2G29720	CTF2B		CTF2B__FAD/NAD(P)-binding oxidoreductase family protein
A_84_P162443	0,03988752	0,0023223	3,686305	1,882175	AT5G64510	TIN1		TIN1__
A_84_P19959	0,04340026	0,0027966	3,652484	1,868878	AT1G32970			Subtilisin-like serine endopeptidase family protein
A_84_P788885	0,02114772	4,59E-04	3,650146	1,867954	AT1G56300			Chaperone DnaJ-domain superfamily proteinChaperone DnaJ-domain superfamily protein
A_84_P14664	0,00772467	1,45E-05	3,64758	1,86694	AT3G53160	UGT73C7		UGT73C7__UDP-glucosyl transferase 73C7
A_84_P111682	0,03146277	0,0013105	3,611352	1,852539	AT5G43520			Cysteine/Histidine-rich C1 domain family protein
A_84_P23394	0,00764839	1,17E-05	3,607725	1,851089	AT5G05730	AMT1, ASA1, JDL1		AMT1_ASA1_JDL1_TRP5_WEI2__anthranilate synthase alpha subunit 1
A_84_P12575	0,01630908	2,10E-04	3,599378	1,847748	AT2G23030	SNRK2.9, SNRK2-9		SNRK2-9_SNRK2.9__SNF1-related protein kinase 2.9
A_84_P567134	0,04661662	0,0033663	3,596957	1,846777	AT4G27657			
A_84_P847558	0,0266426	8,63E-04	3,586693	1,842654	AT1G55450			S-adenosyl-L-methionine-dependent methyltransferases superfamily protein
A_84_P856597	0,01232764	9,08E-05	3,581019	1,84037	AT5G16190	ATCSLA11, CSLA1		ATCSLA11_CSLA11__cellulose synthase like A11
A_84_P210768	0,01961223	3,79E-04	3,572125	1,836783	AT5G19230			Glycoprotein membrane precursor GPI-anchored
A_84_P18856	0,00894727	3,34E-05	3,559658	1,831739	AT5G17490	AtRGL3, RGL3		AtRGL3_RGL3__RGA-like protein 3
A_84_P16133	0,02454009	7,11E-04	3,556661	1,830524	AT1G79310	AtMC7, AtMCP2a,		AtMC7_AtMCP2a_MC7_MCP2a__metacaspase 7
A_84_P17683	0,01592639	1,97E-04	3,545827	1,826122	AT4G39580			Galactose oxidase/kelch repeat superfamily protein
A_84_P796533	0,0116891	7,52E-05	3,541016	1,824163	AT3G46650			UDP-Glycosyltransferase superfamily protein
A_84_P575245	0,01065349	5,36E-05	3,532726	1,820782	AT5G16190	ATCSLA11, CSLA1		ATCSLA11_CSLA11__cellulose synthase like A11
A_84_P856591	0,01756549	2,56E-04	3,532625	1,820741	AT5G63790	ANAC102, NAC102		ANAC102_NAC102__NAC domain containing protein 102
A_84_P203438	0,02774078	9,46E-04	3,526228	1,818126	AT4G34138	UGT73B1		UGT73B1__UDP-glucosyl transferase 73B1
A_84_P603728	0,03916847	0,0022167	3,519121	1,815215	AT5G02600	NAKR1, NPCC6		NAKR1_NPCC6__Heavy metal transport/detoxification superfamily protein

A_84_P23171	0,02114772	4,61E-04	3,518177	1,814828	AT3G51910	AT-HSFA7A, HSFA	AT-HSFA7A_HSFA7A__heat shock transcription factor A7A
A_84_P831247	0,04115299	0,0025123	3,504628	1,809261	AT5G43520		Cysteine/Histidine-rich C1 domain family proteinCysteine/Histidine-rich C1 domain family protein
A_84_P537274	0,03440424	0,0016283	3,48534	1,8013	AT1G66600	ABO3, ATWRKY63	ABO3_ATWRKY63_WRKY63__ABA overly sensitive mutant 3
A_84_P118712	0,01769782	2,64E-04	3,481653	1,799772	AT1G56300		Chaperone DnaJ-domain superfamily proteinChaperone DnaJ-domain superfamily protein
A_84_P54170	0,00992271	4,48E-05	3,478181	1,798333	AT3G57450		
A_84_P10874	0,02582126	8,07E-04	3,475145	1,797073	AT3G50970	LTI30, XERO2	LTI30_XERO2__dehydrin family protein
A_84_P768949	0,03884352	0,0021488	3,469673	1,7948	AT5G35688		
A_84_P12431	0,01771716	2,70E-04	3,452907	1,787811	AT1G74420	ATFUT3, FUT3	ATFUT3_FUT3__fucosyltransferase 3
A_84_P20043	0,03768138	0,0020188	3,451168	1,787085	AT1G54070		Dormancy/auxin associated family protein
A_84_P23164	0,00682995	9,18E-06	3,450413	1,786769	AT3G50260	ATERF#011, CEJ1,	ATERF#011_CEJ1_DEAR1__cooperatively regulated by ethylene and jasmonate 1
A_84_P18141	0,01961223	3,79E-04	3,432829	1,779398	AT1G55450		S-adenosyl-L-methionine-dependent methyltransferases superfamily protein
A_84_P23287	0,00461552	2,37E-06	3,419379	1,773734	AT4G22530		S-adenosyl-L-methionine-dependent methyltransferases superfamily protein
A_84_P15703	0,02244603	5,29E-04	3,41561	1,772143	AT4G18340		Glycosyl hydrolase superfamily protein
A_84_P16727	0,01365065	1,18E-04	3,412288	1,77074	AT4G37390	AUR3, BRU6, GH3.	AUR3_BRU6_GH3-2_GH3.2_YDK1__Auxin-responsive GH3 family protein
A_84_P800816	0,02040927	4,14E-04	3,407377	1,768662	AT3G10985	ATWI-12, SAG20,	ATWI-12_SAG20_WI12__senescence associated gene 20ATWI-12
A_84_P19047	0,01063874	5,27E-05	3,406807	1,76842	AT1G74100	ATSOT16, ATST5A	ATSOT16_ATST5A_CORI-7_SOT16__sulfotransferase 16
A_84_P205978	0,01742975	2,49E-04	3,402426	1,766564	AT4G31950	CYP82C3	CYP82C3__cytochrome P450, family 82, subfamily C, polypeptide 3
A_84_P23838	0,02009357	3,97E-04	3,401447	1,766149	AT1G73480		alpha/beta-Hydrolases superfamily proteinalpha/beta-Hydrolases superfamily protein
A_84_P855665	0,01246891	9,38E-05	3,394857	1,763351	AT2G18200		
A_84_P562234	0,04669211	0,0033886	3,389558	1,761097	AT1G59640	BPE, BPEp, BPEub	BPE_BPEp_BPEub_ZCW32__BIG PETAL
A_84_P763062	0,0151022	1,68E-04	3,389215	1,760951	AT4G22710	CYP706A2	CYP706A2__cytochrome P450, family 706, subfamily A, polypeptide 2
A_84_P582597	0,0457815	0,0032287	3,385733	1,759468	AT1G09932		Phosphoglycerate mutase family protein
A_84_P22853	0,00904516	3,77E-05	3,38344	1,758491	AT1G75960		AMP-dependent synthetase and ligase family protein
A_84_P22308	0,01163687	7,27E-05	3,378833	1,756525	AT4G10390		Protein kinase superfamily protein
A_84_P10305	0,01246891	9,49E-05	3,373704	1,754334	AT5G59730	ATEXO70H7, EXO	ATEXO70H7_EXO70H7__exocyst subunit exo70 family protein H7
A_84_P118462	0,02449875	7,01E-04	3,368924	1,752288	AT2G28400		Protein of unknown function, DUF584
A_84_P752754	0,01020095	4,92E-05	3,368518	1,752114	AT1G64195		Defensin-like (DEFL) family protein
A_84_P13988	0,03707299	0,0019508	3,366215	1,751127	AT5G25450		Cytochrome bd ubiquinol oxidase, 14kDa subunit
A_84_P169053	0,02894387	0,0010428	3,339133	1,739473	AT3G45730		
A_84_P818968	0,01693864	2,33E-04	3,33096	1,735938	AT3G15630		
A_84_P763641	0,03916847	0,002218	3,328925	1,735056	AT4G06529		transposable element gene
A_84_P843872	0,04254071	0,0026896	3,315494	1,729224	AT1G53430		Leucine-rich repeat transmembrane protein kinaseLeucine-rich repeat transmembrane protein kinase
A_84_P868217	0,01828971	3,00E-04	3,31116	1,727337	AT1G52030	F-ATMBP, MBP1.2,	F-ATMBP_MBP1.2_MBP2__myrosinase-binding protein 2F
A_84_P18550	0,0237198	6,06E-04	3,307844	1,725891	AT4G20780	CML42	CML42__calmodulin like 42
A_84_P23721	0,00606654	6,64E-06	3,299227	1,722128	AT1G14200		RING/U-box superfamily protein
A_84_P560583	0,02054225	4,25E-04	3,288508	1,717433	AT2G18670;	0	
A_84_P183724	0,02494651	7,47E-04	3,287958	1,717192	AT2G35290		SAUR79__
A_84_P19046	0,04465805	0,0030117	3,269159	1,708919	AT1G69920	ATGSTU12, GSTU	ATGSTU12_GSTU12__glutathione S-transferase TAU 12
A_84_P69204	0,0215952	4,82E-04	3,265163	1,707155	AT1G21110	IGMT3	IGMT3__O-methyltransferase family protein
A_84_P807259	0,04812316	0,0036429	3,263752	1,706532	AT5G67300	ATMYB44, ATMYB	ATMYB44_ATMYBR1_MYB44_MYBR1__myb domain protein r1
A_84_P141439	0,01911949	3,42E-04	3,263312	1,706337	AT5G24770	ATVSP2, VSP2	ATVSP2_VSP2__vegetative storage protein 2
A_84_P814936	0,02353903	5,92E-04	3,262307	1,705892	AT4G30210	AR2, ATR2	AR2_ATR2__P450 reductase 2AR2_ATR2__P450 reductase 2
A_84_P172941	0,02400674	6,42E-04	3,2618	1,705668	AT2G18690		
A_84_P13022	0,02114772	4,61E-04	3,254941	1,702632	AT5G15250	ATFTSH6, FTSH6	ATFTSH6_FTSH6__FTSH protease 6
A_84_P11679	0,0234887	5,86E-04	3,252398	1,701504	AT2G23680		Cold acclimation protein WCOR413 family
A_84_P611805	0,00606654	6,74E-06	3,251261	1,700999	AT5G26600		Pyridoxal phosphate (PLP)-dependent transferases superfamily protein
A_84_P11802	0,02454009	7,15E-04	3,25068	1,700742	AT3G46690		UDP-Glycosyltransferase superfamily protein
A_84_P763881	0,02353903	5,90E-04	3,248226	1,699652	AT4G20830		FAD-binding Berberine family proteinFAD-binding Berberine family protein
A_84_P15965	0,00900545	3,50E-05	3,245562	1,698468	AT5G56980		
A_84_P136725	0,01177365	8,06E-05	3,228448	1,690841	AT5G36920		
A_84_P133525	0,03051006	0,0012073	3,219433	1,686807	AT3G49780	ATPSK3 (FORMER	ATPSK3 (FORMER SYMBOL)_ATPSK4_PSK4__phytosulfokine 4 precursor

A_84_P12073	0,04543232	0,0031481	3,210028	1,682586	AT1G18290		
A_84_P10473	0,01742975	2,49E-04	3,184558	1,671093	AT1G59870	ABCG36, ATABCG	ABCG36_ATABCG36_ATPDR8_PEN3__ABC-2 and Plant PDR ABC-type transporter family protein
A_84_P813990	0,01375994	1,24E-04	3,183021	1,670397	AT4G30530	GGP1	GGP1__Class I glutamine amidotransferase-like superfamily protein
A_84_P524641	0,02702	8,91E-04	3,181917	1,669896	AT4G39675		
A_84_P816512	0,02430013	6,79E-04	3,171227	1,665041	AT2G18690		
A_84_P598475	0,01842527	3,13E-04	3,161928	1,660805	AT5G26600		Pyridoxal phosphate (PLP)-dependent transferases superfamily protein
A_84_P16642	0,01375994	1,25E-04	3,159096	1,659512	AT4G12720	AtNUDT7, GFG1, N	AtNUDT7_GFG1_NUDT7__MutT/nudix family protein
A_84_P808818	0,02524157	7,71E-04	3,158492	1,659236	AT5G24770;	ATVSP2,VSP2,ATVSP1,VSP1	
A_84_P813874	0,02269863	5,43E-04	3,155744	1,65798	AT4G12720	AtNUDT7, GFG1, N	AtNUDT7_GFG1_NUDT7__MutT/nudix family protein
A_84_P22296	0,01114487	6,07E-05	3,147514	1,654213	AT4G05010		AtFBS3_FBS3__F-box family protein
A_84_P109302	0,01526442	1,74E-04	3,144848	1,65299	AT1G19570	ATDHAR1, DHAR1	ATDHAR1_DHAR1_DHAR5__dehydroascorbate reductase
A_84_P16192	0,02381684	6,25E-04	3,143213	1,65224	AT1G77450	anac032, NAC032	NAC032_anac032__NAC domain containing protein 32
A_84_P798326	0,01830757	3,06E-04	3,136388	1,649104	AT5G50570;	SPL13,SPL13A,SPL13,SPL13B	
A_84_P21924	0,02237896	5,22E-04	3,132248	1,647199	AT1G78050	PGM	PGM__phosphoglycerate/bisphosphoglycerate mutase
A_84_P80879	0,01560944	1,81E-04	3,131741	1,646965	AT2G46510	AIB, ATAIB	AIB_ATAIB_JAM1__ABA-inducible BHLH-type transcription factor
A_84_P784658	0,01948675	3,55E-04	3,126082	1,644356	AT5G56980		
A_84_P547572	0,01020095	4,94E-05	3,125545	1,644108	AT4G02360		Protein of unknown function, DUF538
A_84_P63594	0,03681569	0,0019242	3,123849	1,643325	AT4G18205		Nucleotide-sugar transporter family protein
A_84_P16568	0,02066042	4,31E-04	3,116968	1,640143	AT3G55840		Hs1pro-1 protein
A_84_P810288	0,03518269	0,0017109	3,116542	1,639946	AT3G56880		VQ motif-containing proteinVQ motif-containing protein
A_84_P60830	0,0390369	0,0021757	3,109611	1,636734	AT4G34135	UGT73B2	UGT73B2__UDP-glucosyltransferase 73B2
A_84_P500185	0,03581283	0,0017993	3,108379	1,636162	AT1G63590		Receptor-like protein kinase-related family protein
A_84_P118232	0,02067851	4,35E-04	3,108127	1,636046	AT5G16360		NC domain-containing protein-related
A_84_P812024	0,01100802	5,89E-05	3,102263	1,633321	AT1G28330	DRM1, DYL1	AtDRM1_DRM1_DYL1__dormancy-associated protein-like 1
A_84_P15515	0,01707055	2,36E-04	3,095456	1,630152	AT3G19390		Granulin repeat cysteine protease family protein
A_84_P23064	0,01592639	1,94E-04	3,091225	1,628179	AT3G06850	BCE2, DIN3, LTA1	BCE2_DIN3_LTA1__2-oxoacid dehydrogenases acyltransferase family protein
A_84_P753508	0,03358237	0,0015265	3,085983	1,62573	AT1G55525		other RNA
A_84_P10080	0,03914714	0,0022025	3,085648	1,625574	AT4G29610		Cytidine/deoxycytidylate deaminase family protein
A_84_P10415	0,01771716	2,67E-04	3,073254	1,619767	AT1G52030	F-ATMBP, MBP1.2,	F-ATMBP_MBP1.2_MBP2__myrosinase-binding protein 2F
A_84_P831354	0,01066107	5,66E-05	3,072931	1,619615	AT4G17470		alpha/beta-Hydrolases superfamily proteinalpha/beta-Hydrolases superfamily protein
A_84_P52340	0,01322879	1,10E-04	3,070525	1,618486	AT3G26840		PES2__Esterase/lipase/thioesterase family protein
A_84_P763462	0,01633501	2,12E-04	3,066847	1,616756	AT4G03510	ATRMA1, RMA1	ATRMA1_RMA1__RING membrane-anchor 1ATRMA1_RMA1__RING membrane-anchor 1
A_84_P13078	0,00894727	3,35E-05	3,065897	1,616309	AT5G42650	AOS, CYP74A, DD	AOS_CYP74A_DDE2__allene oxide synthase
A_84_P532079	0,0151022	1,68E-04	3,063726	1,615287	AT1G47510	5PTASE11, AT5PT	5PTASE11_AT5PTASE11__inositol polyphosphate 5-phosphatase 11
A_84_P10329	0,02452861	7,04E-04	3,063496	1,615179	AT5G65280	GCL1	GCL1__GCR2-like 1
A_84_P19210	0,04639193	0,0033254	3,063278	1,615076	AT2G46400	ATWRKY46, WRKY	ATWRKY46_WRKY46__WRKY DNA-binding protein 46
A_84_P604458	0,03956232	0,0022778	3,059521	1,613306	AT3G57210		Protein of unknown function (DUF626)
A_84_P110112	0,02991192	0,0011579	3,058019	1,612598	AT5G09980	PROPEP4	PROPEP4__elicitor peptide 4 precursor
A_84_P72974	0,02100477	4,54E-04	3,056071	1,611678	AT5G50570;	SPL13,SPL13A,SPL13,SPL13B	
A_84_P787273	0,01961223	3,68E-04	3,0525	1,609991	AT5G24600		Protein of unknown function, DUF599
A_84_P12143	0,02582126	8,07E-04	3,045242	1,606557	AT5G45340	CYP707A3	CYP707A3__cytochrome P450, family 707, subfamily A, polypeptide 3CYP707A3
A_84_P509078	0,03367786	0,0015589	3,044057	1,605995	AT1G69900		Actin cross-linking proteinActin cross-linking protein
A_84_P762419	0,03916847	0,0022178	3,039217	1,6037	AT3G15518		
A_84_P784166	0,0265841	8,58E-04	3,03847	1,603345	AT5G45340	CYP707A3	CYP707A3__cytochrome P450, family 707, subfamily A, polypeptide 3CYP707A3
A_84_P514608	0,00961027	4,30E-05	3,033142	1,600813	AT3G09032		
A_84_P284990	0,03255169	0,0014193	3,023977	1,596447	AT4G15610		Uncharacterised protein family (UPF0497)Uncharacterised protein family (UPF0497)
A_84_P21604	0,03993093	0,0023274	3,021445	1,595239	AT5G46590	anac096, NAC096	NAC096_anac096__NAC domain containing protein 96
A_84_P22149	0,01462891	1,55E-04	3,020397	1,594738	AT3G13310		DJC66__Chaperone DnaJ-domain superfamily protein
A_84_P19958	0,02951533	0,001114	3,019281	1,594205	AT1G05560	UGT1, UGT75B1	UGT1_UGT75B1__UDP-glucosyltransferase 75
A_84_P815262	0,03308225	0,0014838	3,015878	1,592578	AT3G06850	BCE2, DIN3, LTA1	BCE2_DIN3_LTA1__2-oxoacid dehydrogenases acyltransferase family protein
A_84_P10136	0,03518269	0,0017144	3,014202	1,591776	AT4G36670	AtPLT6, AtPMT6, P	AtPLT6_AtPMT6_PLT6_PMT6__Major facilitator superfamily protein

A_84_P20247	0,03051006	0,0012132	3,01163	1,590545	AT3G21780	UGT71B6	UGT71B6__UDP-glucosyl transferase 71B6
A_84_P19074	0,04633552	0,0032945	3,008857	1,589215	AT1G18570	AtMYB51, BW51A,	AtMYB51_BW51A_BW51B_HIG1_MYB51__myb domain protein 51
A_84_P22489	0,0111888	6,12E-05	3,000947	1,585418	AT5G22250	AtCAF1b, CAF1b	AtCAF1b_CAF1b__Polynucleotidyl transferase, ribonuclease H-like superfamily protein
A_84_P12120	0,02400674	6,37E-04	2,999374	1,584662	AT5G39050	PMAT1	PMAT1__HXXXD-type acyl-transferase family protein
A_84_P189894	0,04527197	0,0031214	2,997715	1,583863	AT5G22660		FBD, F-box, Skp2-like and Leucine Rich Repeat domains containing protein
A_84_P21591	0,02924256	0,0010816	2,992981	1,581583	AT5G43170	AZF3, ZF3	AZF3_ZF3__zinc-finger protein 3AZF3_ZF3__zinc-finger protein 3
A_84_P817440	0,02454009	7,18E-04	2,989123	1,579722	AT4G15610		Uncharacterised protein family (UPF0497)Uncharacterised protein family (UPF0497)
A_84_P21537	0,00682995	9,40E-06	2,987816	1,579091	AT5G17850		Sodium/calcium exchanger family protein
A_84_P16943	0,02368718	6,04E-04	2,984989	1,577725	AT1G52410	TSA1	AtTSA1_TSA1__TSK-associating protein 1
A_84_P204138	0,02991192	0,001155	2,983229	1,576875	AT1G66080		
A_84_P828333	0,01627859	2,08E-04	2,981689	1,57613	AT2G29740	UGT71C2	UGT71C2__UDP-glucosyl transferase 71C2
A_84_P594466	0,04114922	0,0025111	2,978932	1,574795	AT2G33130	RALF18, RALFL18	RALF18_RALFL18__ralf-like 18
A_84_P13228	0,01686909	2,29E-04	2,978648	1,574657	AT4G34131	UGT73B3	UGT73B3__UDP-glucosyl transferase 73B3
A_84_P809682	0,03784298	0,0020342	2,974286	1,572543	AT5G54940		Translation initiation factor SUI1 family proteinTranslation initiation factor SUI1 family protein
A_84_P853160	0,02963863	0,0011257	2,974284	1,572542	AT3G11820	ATSYP121, ATSYR	AT-SYR1_ATSYP121_ATSYR1_PEN1_SYP121_SYR1__syntaxin of plants 121
A_84_P19057	0,02060719	4,29E-04	2,971792	1,571333	AT1G67970	AT-HSFA8, HSFA8	AT-HSFA8_HSFA8__heat shock transcription factor A8
A_84_P826434	0,04737008	0,0034909	2,971617	1,571248	AT5G43170	AZF3, ZF3	AZF3_ZF3__zinc-finger protein 3
A_84_P89269	0,04017467	0,002366	2,971615	1,571247	AT1G06225	CLE3	CLE3__CLAVATA3/ESR-RELATED 3
A_84_P14672	0,01948675	3,55E-04	2,97068	1,570793	AT1G23850		
A_84_P23654	0,0143883	1,43E-04	2,966837	1,568926	AT1G52000		Mannose-binding lectin superfamily protein
A_84_P500176	0,00894727	2,84E-05	2,95021	1,560818	AT1G61065		Protein of unknown function (DUF1218)
A_84_P17279	0,02704264	8,93E-04	2,947885	1,55968	AT2G25090	CIPK16, SnRK3.18	AtCIPK16_CIPK16_SnRK3.18__CBL-interacting protein kinase 16
A_84_P550101	0,02084717	4,47E-04	2,941421	1,556513	AT3G14660	CYP72A13	CYP72A13__cytochrome P450, family 72, subfamily A, polypeptide 13
A_84_P13560	0,02820842	9,75E-04	2,941267	1,556438	AT2G32150		Haloacid dehalogenase-like hydrolase (HAD) superfamily protein
A_84_P137739	0,01305407	1,04E-04	2,938295	1,554979	AT3G63060	EDL3	EDL3__EID1-like 3
A_84_P824985	0,04465805	0,0030205	2,93521	1,553464	AT2G18670;		0
A_84_P16120	0,01686909	2,31E-04	2,928472	1,550148	AT1G10140		Uncharacterised conserved protein UCP031279
A_84_P23396	0,03782426	0,0020323	2,918577	1,545265	AT5G06320	NHL3	NHL3__NDR1/HIN1-like 3NHL3__NDR1/HIN1-like 3
A_84_P11606	0,01474425	1,57E-04	2,913899	1,542951	AT2G29480	ATGSTU2, GST20,	ATGSTU2_GST20_GSTU2__glutathione S-transferase tau 2
A_84_P572262	0,0467632	0,0034082	2,912071	1,542046	AT3G10815		RING/U-box superfamily protein
A_84_P829722	0,04856481	0,0037753	2,903335	1,537711	AT4G23190	AT-RLK3, CRK11	AT-RLK3_CRK11__cysteine-rich RLK (RECEPTOR-like protein kinase) 11
A_84_P130216	0,03518269	0,0017123	2,899507	1,535808	AT2G37750		
A_84_P84909	0,03558141	0,0017731	2,899047	1,535579	AT3G17110		
A_84_P764548	0,03220695	0,0013912	2,898405	1,535259	AT4G18197	ATPUP7, PEX17, P	ATPUP7_PEX17_PUP7__purine permease 7
A_84_P182564	0,01382326	1,28E-04	2,895632	1,533878	AT4G21323		Subtilase family protein
A_84_P81409	0,02069154	4,37E-04	2,894878	1,533503	AT3G15630		
A_84_P803216	0,02609744	8,26E-04	2,893577	1,532854	AT5G06320	NHL3	NHL3__NDR1/HIN1-like 3NHL3__NDR1/HIN1-like 3
A_84_P857301	0,03330867	0,0014993	2,88175	1,526945	AT2G40140	ATSZF2, CZF1, SZ	ATSZF2_CZF1_SZF2_ZFAR1__zinc finger (CCCH-type) family protein
A_84_P199584	0,01539895	1,77E-04	2,861063	1,516551	AT3G14200		Chaperone DnaJ-domain superfamily protein
A_84_P14864	0,03782426	0,0020321	2,859129	1,515575	AT4G37260	ATMYB73, MYB73	ATMYB73_MYB73__myb domain protein 73
A_84_P12030	0,04036312	0,0024062	2,858766	1,515392	AT5G01100		FRB1__O-fucosyltransferase family protein
A_84_P772475	0,00574999	5,73E-06	2,853494	1,51273	AT1G66760		MATE efflux family proteinMATE efflux family protein
A_84_P552447	0,02376995	6,12E-04	2,852966	1,512463	AT1G44414		
A_84_P19431	0,0246688	7,27E-04	2,852798	1,512378	AT3G62150	ABCB21, PGP21	ABCB21_PGP21__P-glycoprotein 21
A_84_P18081	0,04809133	0,0036197	2,851654	1,511799	AT1G76410	ATL8	ATL8__RING/U-box superfamily protein
A_84_P21661	0,02023179	4,06E-04	2,85125	1,511595	AT5G61590		Integrase-type DNA-binding superfamily protein
A_84_P185784	0,04759051	0,0035302	2,850656	1,511294	AT2G39920		HAD superfamily, subfamily IIIB acid phosphatase
A_84_P167173	0,04887474	0,0038209	2,85026	1,511094	AT4G25480	ATCBF3, CBF3, DR	ATCBF3_CBF3_DREB1A__dehydration response element B1A
A_84_P559517	0,01163687	6,99E-05	2,846862	1,509373	AT1G28330	DRM1, DYL1	AtDRM1_DRM1_DYL1__dormancy-associated protein-like 1
A_84_P17256	0,0409498	0,0024853	2,8438	1,50782	AT2G40140	ATSZF2, CZF1, SZ	ATSZF2_CZF1_SZF2_ZFAR1__zinc finger (CCCH-type) family protein
A_84_P197444	0,03173508	0,0013273	2,843176	1,507504	AT3G22160		JAV1__VQ motif-containing protein

A_84_P10799	0,04473491	0,0030371	2,841544	1,506675	AT3G29190		Terpenoid cyclases/Protein prenyltransferases superfamily protein
A_84_P116712	0,01830757	3,08E-04	2,840573	1,506182	AT1G29180		Cysteine/Histidine-rich C1 domain family protein
A_84_P245685	0,0293697	0,0010918	2,837193	1,504464	AT3G44300	AtNIT2, NIT2	AtNIT2_NIT2__nitrilase 2
A_84_P16624	0,03032501	0,0011939	2,832481	1,502066	AT4G08250		GRAS family transcription factor
A_84_P545146	0,01255292	9,74E-05	2,825738	1,498628	AT5G40180		
A_84_P55660	0,03220695	0,0013931	2,822829	1,497142	AT3G56880		VQ motif-containing proteinVQ motif-containing protein
A_84_P271340	0,04464122	0,0030034	2,811616	1,4914	AT3G09350	Fes1A	Fes1A__Fes1AFes1A__Fes1A
A_84_P821119	0,04927701	0,0039103	2,809513	1,49032	AT3G09350	Fes1A	Fes1A__Fes1AFes1A__Fes1A
A_84_P819884	0,03864233	0,0021264	2,801693	1,486299	AT4G38550		Arabidopsis phospholipase-like protein (PEARLI 4) family
A_84_P609600	0,0143883	1,43E-04	2,799154	1,484991	AT2G40200		basic helix-loop-helix (bHLH) DNA-binding superfamily protein
A_84_P10284	0,02430013	6,76E-04	2,798562	1,484686	AT5G54170		Polyketide cyclase/dehydrase and lipid transport superfamily protein
A_84_P123322	0,01253431	9,70E-05	2,796931	1,483845	AT1G58200	MSL3	MSL3__MSCS-like 3
A_84_P845967	0,02987884	0,0011431	2,796564	1,483655	AT5G22570	ATWRKY38, WRKY	ATWRKY38_WRKY38__WRKY DNA-binding protein 38
A_84_P71564	0,02894719	0,0010504	2,790486	1,480516	AT2G19800	MIOX2	MIOX2__myo-inositol oxygenase 2
A_84_P15041	0,02248672	5,32E-04	2,787846	1,479151	AT5G61890		Integrase-type DNA-binding superfamily protein
A_84_P16057	0,04195379	0,0026195	2,786024	1,478208	AT1G45145	ATH5, ATTRX5, LIV	ATH5_ATTRX5_LIV1_TRX-h5_TRX5__thioredoxin H-type 5
A_84_P809927	0,0209969	4,51E-04	2,784638	1,47749	AT5G07440	GDH2	GDH2__glutamate dehydrogenase 2
A_84_P21022	0,03202478	0,0013684	2,782358	1,476308	AT2G15480	UGT73B5	UGT73B5__UDP-glucosyl transferase 73B5
A_84_P859107	0,04899432	0,0038609	2,777443	1,473757	AT2G17840	ERD7	ERD7__Senescence/dehydration-associated protein-related
A_84_P785967	0,02130474	4,68E-04	2,777187	1,473624	AT5G54940		Translation initiation factor SUI1 family protein
A_84_P828523	0,00894727	2,60E-05	2,774368	1,472159	AT3G46110		Domain of unknown function (DUF966)
A_84_P23419	0,01156977	6,66E-05	2,767869	1,468776	AT5G13200		GRAM domain family protein
A_84_P17231	0,04661662	0,003371	2,76387	1,46669	AT2G29710		UDP-Glycosyltransferase superfamily protein
A_84_P17042	0,04195379	0,0026186	2,757106	1,463155	AT1G24280	G6PD3	G6PD3__glucose-6-phosphate dehydrogenase 3
A_84_P169313	0,01710836	2,38E-04	2,750229	1,459552	AT2G36590	ATPROT3, ProT3	ATPROT3_ProT3__proline transporter 3
A_84_P12066	0,03211456	0,0013797	2,742419	1,455449	AT5G11410		Protein kinase superfamily protein
A_84_P13072	0,01305407	1,04E-04	2,738441	1,453355	AT5G40850	UPM1	UPM1__urophorphyrin methylase 1
A_84_P17400	0,01451385	1,45E-04	2,734765	1,451417	AT3G14050	ATRSH2, AT-RSH2	AT-RSH2_ATRSH2_RSH2__RELA/SPOT homolog 2
A_84_P17802	0,01375994	1,27E-04	2,729744	1,448766	AT5G41610	ATCHX18, CHX18	ATCHX18_CHX18__cation/H+ exchanger 18
A_84_P818633	0,04733288	0,0034826	2,723729	1,445583	AT1G05560	UGT1, UGT75B1	UGT1_UGT75B1__UDP-glucosyltransferase 75
A_84_P19570	0,03580366	0,0017977	2,722464	1,444913	AT4G38550		Arabidopsis phospholipase-like protein (PEARLI 4) family
A_84_P19170	0,0138317	1,28E-04	2,718617	1,442873	AT2G29420	ATGSTU7, GST25,	ATGSTU7_GST25_GSTU7__glutathione S-transferase tau 7
A_84_P15485	0,02581204	8,05E-04	2,716761	1,441888	AT3G11820	ATSYP121, ATSYR	AT-SYR1_ATSYP121_ATSYR1_PEN1_SYP121_SYR1__syntaxin of plants 121
A_84_P211628	0,04417133	0,0029155	2,716733	1,441873	AT2G40080	ELF4	ELF4__Protein of unknown function (DUF1313)
A_84_P767650	0,01679116	2,23E-04	2,716406	1,441699	AT5G23510		
A_84_P15467	0,03822042	0,0020775	2,715343	1,441135	AT3G01290	AtHIR2, HIR2	AtHIR2_HIR2__SPFH/Band 7/PHB domain-containing membrane-associated protein family
A_84_P233859	0,03437764	0,0016186	2,715088	1,440999	AT2G28570		
A_84_P119812	0,01372322	1,19E-04	2,712464	1,439604	AT1G50740		Transmembrane proteins 14C
A_84_P11193	0,02750804	9,25E-04	2,705641	1,43597	AT5G44210	ATERF9, ATERF-9	ATERF-9_ATERF9_ERF9__erf domain protein 9
A_84_P813469	0,01177365	7,89E-05	2,705083	1,435673	AT2G15890	MEE14	MEE14__maternal effect embryo arrest 14
A_84_P22839	0,03518269	0,0017111	2,694863	1,430212	AT1G73260	ATKTI1, KTI1	ATKTI1_KTI1__kunitz trypsin inhibitor 1
A_84_P14602	0,04572882	0,0032069	2,690116	1,427669	AT1G59590	ZCF37	ZCF37__ZCF37
A_84_P556737	0,00894727	2,83E-05	2,687887	1,426473	AT5G65207		
A_84_P858400	0,02548116	7,89E-04	2,687429	1,426227	AT1G76790	IGMT5	IGMT5__O-methyltransferase family proteinIGMT5__O-methyltransferase family protein
A_84_P758905	0,02894387	0,0010451	2,686678	1,425823	AT3G30415		
A_84_P233559	0,02355661	5,95E-04	2,685708	1,425303	AT1G10340		Ankyrin repeat family protein
A_84_P601310	0,02342488	5,84E-04	2,68549	1,425185	AT1G11070		
A_84_P16332	0,03187662	0,0013499	2,683619	1,42418	AT2G29450	AT103-1A, ATGST	AT103-1A_ATGSTU1_ATGSTU5_GSTU5__glutathione S-transferase tau 5
A_84_P813465	0,01375994	1,26E-04	2,682411	1,423531	AT2G15890	MEE14	MEE14__maternal effect embryo arrest 14
A_84_P786976	0,04030779	0,0023982	2,677043	1,42064	AT2G37750		
A_84_P858464	0,00903297	3,64E-05	2,669566	1,416605	AT3G10020		

A_84_P17963	0,0364153	0,0018656	2,659572	1,411194	AT1G13300	HRS1	HRS1__myb-like transcription factor family protein
A_84_P823802	0,03001025	0,001169	2,659334	1,411065	AT3G09830		Protein kinase superfamily protein
A_84_P19214	0,02484235	7,40E-04	2,656492	1,409522	AT2G32510	MAPKKK17	MAPKKK17__mitogen-activated protein kinase kinase kinase 17
A_84_P19413	0,02020679	4,03E-04	2,650528	1,40628	AT3G57530	ATCPK32, CDPK32	ATCPK32_CDPK32_CPK32__calcium-dependent protein kinase 32
A_84_P21381	0,01592639	1,97E-04	2,647591	1,40468	AT4G18950		Integrin-linked protein kinase familyIntegrin-linked protein kinase family
A_84_P16702	0,01386093	1,31E-04	2,645091	1,403317	AT4G30530	GGP1	GGP1__Class I glutamine amidotransferase-like superfamily protein
A_84_P761881	0,04831925	0,003719	2,640671	1,400905	AT3G04640		glycine-rich protein
A_84_P13338	0,01189048	8,43E-05	2,636332	1,398532	AT1G18710	AtMYB47, MYB47	AtMYB47_MYB47__myb domain protein 47
A_84_P786702	0,01782063	2,80E-04	2,635521	1,398088	AT3G09830		Protein kinase superfamily protein
A_84_P12088	0,01961223	3,75E-04	2,626764	1,393287	AT5G22630	ADT5	ADT5__arogenate dehydratase 5
A_84_P21836	0,02732394	9,11E-04	2,626306	1,393035	AT1G72940		Toll-Interleukin-Resistance (TIR) domain-containing protein
A_84_P12888	0,01375994	1,24E-04	2,626245	1,393002	AT4G23600	CORI3, JR2	CORI3_JR2__Tyrosine transaminase family protein
A_84_P17107	0,01433996	1,42E-04	2,622361	1,390866	AT1G73080	ATPEPR1, PEPR1	ATPEPR1_PEPR1__PEP1 receptor 1
A_84_P816048	0,02364189	6,01E-04	2,618699	1,38885	AT1G79245		
A_84_P598498	0,00894727	3,10E-05	2,617607	1,388248	AT5G41120		Esterase/lipase/thioesterase family protein
A_84_P289354	0,01769782	2,65E-04	2,613421	1,38594	AT2G15890	MEE14	MEE14__maternal effect embryo arrest 14
A_84_P816929	0,03049443	0,0012048	2,611863	1,385079	AT5G54170		Polyketide cyclase/dehydrase and lipid transport superfamily protein
A_84_P15250	0,02449762	6,97E-04	2,611232	1,38473	AT1G66760		MATE efflux family proteinMATE efflux family protein
A_84_P548152	0,04811797	0,0036328	2,607072	1,38243	AT2G05400		Ubiquitin-specific protease family C19-related protein
A_84_P16040	0,01742975	2,49E-04	2,606768	1,382262	AT2G17840	ERD7	ERD7__Senescence/dehydration-associated protein-related
A_84_P12642	0,0254004	7,82E-04	2,604687	1,38111	AT3G10020		
A_84_P840707	0,0398743	0,0023188	2,602607	1,379957	AT1G07500		SMR5__SMR5__
A_84_P11917	0,01961223	3,71E-04	2,599207	1,378072	AT4G13180		NAD(P)-binding Rossmann-fold superfamily protein
A_84_P20050	0,03076559	0,0012329	2,595113	1,375797	AT1G14370	APK2A, Kin1, PBL2	APK2A_Kin1_PBL2__protein kinase 2A
A_84_P764555	0,02765526	9,40E-04	2,594751	1,375596	AT4G18195	ATPUP8, PUP8	ATPUP8_PUP8__purine permease 8
A_84_P20057	0,04437989	0,0029652	2,587407	1,371507	AT1G63580		Receptor-like protein kinase-related family protein
A_84_P20399	0,00894727	2,93E-05	2,586013	1,370729	AT4G03400	DFL2, GH3-10	DFL2_GH3-10__Auxin-responsive GH3 family protein
A_84_P825287	0,01961223	3,74E-04	2,584982	1,370154	AT2G15480;	UGT73B5,UGT73B4	
A_84_P17278	0,04040338	0,002416	2,583501	1,369327	AT2G29440	ATGSTU6, GST24,	ATGSTU6_GST24_GSTU6__glutathione S-transferase tau 6
A_84_P13740	0,04260025	0,0026974	2,581705	1,368324	AT3G57740		Protein kinase superfamily protein
A_84_P509290	0,04768498	0,0035489	2,581378	1,368141	AT3G11385		Cysteine/Histidine-rich C1 domain family protein
A_84_P149248	0,03764553	0,0020135	2,577705	1,366087	AT1G21120	IGMT2	IGMT2__O-methyltransferase family protein
A_84_P22843	0,03916847	0,0022089	2,576723	1,365538	AT1G76790	IGMT5	IGMT5__O-methyltransferase family proteinIGMT5
A_84_P816425	0,02974324	0,0011345	2,576313	1,365308	AT3G30415;	UPM1	
A_84_P790545	0,01375994	1,23E-04	2,576044	1,365157	AT1G49520		SWIB complex BAF60b domain-containing protein
A_84_P293774	0,01020095	4,81E-05	2,571634	1,362685	AT5G55120	VTC5	VTC5__galactose-1-phosphate guanylyltransferase (GDP)s;GDP-D-glucose phosphorylases
A_84_P20176	0,03731508	0,001975	2,570201	1,361881	AT2G44790	UCC2	UCC2__uclacyanin 2
A_84_P12990	0,02312453	5,69E-04	2,569164	1,361299	AT5G05490	ATREC8, DIF1, RE	AtREC8_DIF1_REC8_SYN1__Rad21/Rec8-like family protein
A_84_P11918	0,0147321	1,57E-04	2,567422	1,360321	AT4G13410	ATCSLA15, CSLA1	ATCSLA15_CSLA15__Nucleotide-diphospho-sugar transferases superfamily protein
A_84_P556854	0,01163687	7,19E-05	2,566753	1,359944	AT1G25275		
A_84_P18342	0,02400674	6,42E-04	2,565089	1,359009	AT3G16050	A37, ATPDX1.2, PD	A37_ATPDX1.2_PDX1.2__pyridoxine biosynthesis 1.2
A_84_P11961	0,04624212	0,0032824	2,564002	1,358398	AT4G27410	ANAC072, RD26	ANAC072_RD26__NAC (No Apical Meristem) domain transcriptional regulator superfamily protein
A_84_P759616	0,02009357	3,98E-04	2,562804	1,357723	AT3G30405		transposable element gene
A_84_P715787	0,01890162	3,33E-04	2,56263	1,357625	AT1G32928		
A_84_P61100	0,0161733	2,04E-04	2,558041	1,35504	AT5G12010		
A_84_P206968	0,04066901	0,0024447	2,557007	1,354456	AT1G57990	ATPUP18, PUP18	ATPUP18_PUP18__purine permease 18
A_84_P824268	0,04492367	0,0030827	2,555374	1,353535	AT1G56660		
A_84_P544677	0,02300682	5,62E-04	2,545981	1,348222	AT2G30400	ATOFP2, OFP2	ATOFP2_OFP2__ovate family protein 2
A_84_P803184	0,02018128	4,02E-04	2,54226	1,346111	AT3G10020		
A_84_P770411	0,0286969	0,0010119	2,539844	1,34474	ATMG00020	RRN26	RRN26__
A_84_P819429	0,01163687	7,40E-05	2,539609	1,344606	AT1G59640	BPE, BPEp, BPEub	BPE_BPEp_BPEub_ZCW32__BIG PETAL

A_84_P14539	0,01020095	4,94E-05	2,538698	1,344088	AT1G53440		Leucine-rich repeat transmembrane protein kinase
A_84_P21943	0,04769728	0,0035538	2,53539	1,342208	AT1G32170	XTH30, XTR4	XTH30_XTR4__xyloglucan endotransglucosylase/hydrolase 30
A_84_P85009	0,03380537	0,0015721	2,532451	1,340534	AT3G44190		FAD/NAD(P)-binding oxidoreductase family protein
A_84_P227239	0,03184637	0,0013409	2,531027	1,339723	AT5G13210		Uncharacterised conserved protein UCP015417
A_84_P14776	0,03051006	0,0012091	2,522825	1,33504	AT4G23180	CRK10, RLK4	CRK10_RLK4__cysteine-rich RLK (RECEPTOR-like protein kinase) 10
A_84_P22452	0,00857212	1,81E-05	2,515416	1,330797	AT5G06860	ATPGIP1, PGIP1	ATPGIP1_PGIP1__polygalacturonase inhibiting protein 1
A_84_P528136	0,02353903	5,93E-04	2,509955	1,327661	AT4G23190	AT-RLK3, CRK11	AT-RLK3_CRK11__cysteine-rich RLK (RECEPTOR-like protein kinase) 11
A_84_P790566	0,02524157	7,70E-04	2,507474	1,326235	AT1G69900		Actin cross-linking proteinActin cross-linking protein
A_84_P18180	0,03837948	0,002103	2,505292	1,324979	AT2G31880	EVR, SOBIR1	EVR_SOBIR1__Leucine-rich repeat protein kinase family protein
A_84_P14392	0,02612251	8,31E-04	2,503665	1,324041	AT2G43550		Scorpion toxin-like knottin superfamily protein
A_84_P575955	0,04552429	0,003164	2,501719	1,32292	AT3G62990		
A_84_P12402	0,01719517	2,42E-04	2,501221	1,322633	AT1G69370	CM3, cm-3	CM3_cm-3__chorismate mutase 3
A_84_P197554	0,02732394	9,10E-04	2,494302	1,318636	AT2G28650	ATEXO70H8, EXO	ATEXO70H8_EXO70H8__exocyst subunit exo70 family protein H8
A_84_P513046	0,03454188	0,0016501	2,491851	1,317218	AT4G25110	AtMC2, AtMCP1c,	AtMC2_AtMCP1c_MC2_MCP1c__metacaspase 2
A_84_P10026	0,04830764	0,0036958	2,485292	1,313415	AT4G13110		BSD domain-containing proteinBSD domain-containing protein
A_84_P581339	0,01828971	3,00E-04	2,48407	1,312706	AT4G12005		
A_84_P12218	0,02242965	5,28E-04	2,477961	1,309154	AT5G64870		SPFH/Band 7/PHB domain-containing membrane-associated protein family
A_84_P824914	0,04972693	0,003995	2,477426	1,308842	AT4G18197;	ATPUP7,PEX17,PUP7	
A_84_P532052	0,03238549	0,0014086	2,472546	1,305997	AT1G30757		
A_84_P21550	0,01185074	8,29E-05	2,470846	1,305005	AT5G24270	ATSOS3, CBL4, SO	ATSOS3_CBL4_SOS3__Calcium-binding EF-hand family protein
A_84_P16138	0,029571	0,0011218	2,470398	1,304744	AT1G30700		FAD-binding Berberine family protein
A_84_P141219	0,01774115	2,76E-04	2,469971	1,304494	AT5G35320		
A_84_P579587	0,01375994	1,21E-04	2,468474	1,303619	AT4G20830		FAD-binding Berberine family proteinFAD-binding Berberine family protein
A_84_P10613	0,04831925	0,0037168	2,463903	1,300945	AT2G42530	COR15B	COR15B__cold regulated 15b
A_84_P844671	0,02684096	8,78E-04	2,460304	1,298837	AT4G38470	STY46	STY46__ACT-like protein tyrosine kinase family protein
A_84_P13549	0,00764839	1,12E-05	2,458024	1,297499	AT2G39420		alpha/beta-Hydrolases superfamily protein
A_84_P848384	0,00877275	2,32E-05	2,457736	1,29733	AT5G23510		
A_84_P23347	0,01861906	3,20E-04	2,453821	1,29503	AT4G36010		Pathogenesis-related thaumatin superfamily protein
A_84_P168223	0,02894387	0,001045	2,449246	1,292337	AT1G19770	ATPUP14, PUP14	ATPUP14_PUP14__purine permease 14
A_84_P12053	0,03086358	0,0012502	2,448501	1,291899	AT5G07440	GDH2	GDH2__glutamate dehydrogenase 2
A_84_P548542	0,02400674	6,41E-04	2,447158	1,291107	AT4G30090		
A_84_P19196	0,02924256	0,001077	2,445617	1,290198	AT1G75490		Integrase-type DNA-binding superfamily protein
A_84_P786801	0,03006957	0,0011748	2,444663	1,289636	AT5G13210		Uncharacterised conserved protein UCP015417
A_84_P82539	0,03681569	0,0019186	2,444237	1,289384	AT1G14870	AtPCR2, PCR2	AtPCR2_PCR2__PLANT CADMIUM RESISTANCE 2
A_84_P20574	0,02500151	7,52E-04	2,442544	1,288384	AT5G10830		S-adenosyl-L-methionine-dependent methyltransferases superfamily protein
A_84_P868891	0,03051006	0,0012108	2,442013	1,288071	AT1G52400	ATBG1, BGL1, BGL	ATBG1_BGL1_BGLU18__beta glucosidase 18
A_84_P193364	0,03529676	0,0017265	2,439675	1,286689	AT1G56660		
A_84_P16319	0,02381684	6,25E-04	2,439413	1,286534	AT2G20350		Integrase-type DNA-binding superfamily protein
A_84_P10142	0,03308225	0,001484	2,43681	1,284994	AT5G01760		ENTH/VHS/GAT family protein
A_84_P174131	0,02725007	9,04E-04	2,435835	1,284416	AT5G14730		
A_84_P114372	0,01613558	2,02E-04	2,433768	1,283192	AT5G53050		alpha/beta-Hydrolases superfamily protein
A_84_P13322	0,01564355	1,85E-04	2,4328	1,282618	AT1G21680		DPP6 N-terminal domain-like protein
A_84_P175914	0,04669211	0,0033885	2,423554	1,277124	AT4G01895		systemic acquired resistance (SAR) regulator protein NIMIN-1-related
A_84_P816258	0,03204315	0,0013707	2,414566	1,271764	AT2G36220		
A_84_P820724	0,02045072	4,15E-04	2,414354	1,271637	AT4G23600	CORI3, JR2	CORI3_JR2__Tyrosine transaminase family protein
A_84_P11544	0,01911949	3,44E-04	2,403924	1,265391	AT1G33590		Leucine-rich repeat (LRR) family protein
A_84_P811890	0,04760732	0,0035348	2,402274	1,264401	AT4G08950	EXO	EXO__Phosphate-responsive 1 family protein
A_84_P814710	0,03731508	0,0019756	2,400459	1,26331	AT1G14870	AtPCR2, PCR2	AtPCR2_PCR2__PLANT CADMIUM RESISTANCE 2
A_84_P18264	0,01785415	2,85E-04	2,392477	1,258505	AT2G46370	FIN219, JAR1	AtGH3.11_FIN219_JAR1__Auxin-responsive GH3 family protein
A_84_P20835	0,03450806	0,0016363	2,391751	1,258067	AT1G80820	ATCCR2, CCR2	ATCCR2_CCR2__cinnamoyl coa reductase
A_84_P23343	0,02009357	4,00E-04	2,390708	1,257438	AT4G35110		Arabidopsis phospholipase-like protein (PEARLI 4) family

A_84_P75664	0,04418246	0,0029183	2,389869	1,256931	AT2G36220		
A_84_P16180	0,03206007	0,0013729	2,389379	1,256636	AT1G11050		Protein kinase superfamily protein
A_84_P824135	0,01386738	1,34E-04	2,388701	1,256227	AT1G19770	ATPUP14, PUP14	ATPUP14_PUP14__purine permease 14
A_84_P10306	0,04096361	0,0024884	2,386203	1,254717	AT5G59930		Cysteine/Histidine-rich C1 domain family protein
A_84_P96976	0,00904516	3,75E-05	2,385634	1,254373	AT3G10985	ATWI-12, SAG20,	ATWI-12_SAG20_WI12__senescence associated gene 20
A_84_P805135	0,03530139	0,0017332	2,384953	1,253961	AT3G15450		Aluminium induced protein with YGL and LRDR motifs
A_84_P823929	0,02263641	5,38E-04	2,374197	1,247439	AT1G03850	ATGRXS13, GRXS	ATGRXS13_GRXS13__Glutaredoxin family protein
A_84_P843621	0,04831925	0,0037149	2,373633	1,247097	AT2G31010		Protein kinase superfamily proteinProtein kinase superfamily protein
A_84_P21192	0,02998462	0,0011666	2,370026	1,244903	AT3G19930	ATSTP4, STP4	ATSTP4_STP4__sugar transporter 4
A_84_P19368	0,03452952	0,0016402	2,36957	1,244625	AT3G47340	ASN1, AT-ASN1, D	ASN1_AT-ASN1_DIN6__glutamine-dependent asparagine synthase 1
A_84_P18271	0,03910996	0,0021902	2,367633	1,243445	AT1G07500		SMR5__SMR5__
A_84_P576707	0,03367786	0,0015574	2,366442	1,24272	AT3G09020		alpha 1,4-glycosyltransferase family protein
A_84_P20555	0,01790467	2,89E-04	2,357059	1,236988	AT5G05400		LRR and NB-ARC domains-containing disease resistance protein
A_84_P10893	0,01226299	8,95E-05	2,356899	1,23689	AT3G55130	ABCG19, ATWBC1	ABCG19_ATWBC19_WBC19__white-brown complex homolog 19
A_84_P20389	0,01622046	2,05E-04	2,355444	1,235999	AT4G01026	PYL7, RCAR2	PYL7_RCAR2__PYR1-like 7PYL7_RCAR2__PYR1-like 7
A_84_P23258	0,04137047	0,0025352	2,355279	1,235898	AT4G11370	RHA1A	RHA1A__RING-H2 finger A1A
A_84_P11710	0,04975333	0,0040021	2,353234	1,234645	AT1G53080		Legume lectin family protein
A_84_P786905	0,02948737	0,0011067	2,351595	1,23364	AT5G41120		Esterase/lipase/thioesterase family protein
A_84_P11250	0,02991192	0,0011573	2,349519	1,232366	AT5G59570	BOA	BOA__Homeodomain-like superfamily protein
A_84_P845323	0,01396545	1,36E-04	2,348723	1,231876	AT4G08170		Inositol 1,3,4-trisphosphate 5/6-kinase family protein
A_84_P120892	0,01961223	3,76E-04	2,343634	1,228747	AT4G08170		Inositol 1,3,4-trisphosphate 5/6-kinase family protein
A_84_P20495	0,01771716	2,70E-04	2,340631	1,226897	AT4G32800		Integrase-type DNA-binding superfamily protein
A_84_P19755	0,04989897	0,0040283	2,335947	1,224008	AT5G58750		NAD(P)-binding Rossmann-fold superfamily protein
A_84_P103496	0,02364212	6,02E-04	2,332659	1,221975	AT5G05140		Transcription elongation factor (TFIIS) family protein
A_84_P18946	0,02403887	6,54E-04	2,332654	1,221973	AT1G09970	LRR XI-23, RLK7	LRR XI-23_RLK7__Leucine-rich receptor-like protein kinase family protein
A_84_P545592	0,04555509	0,0031725	2,331709	1,221388	AT2G39650		Protein of unknown function (DUF506)
A_84_P10597	0,01785415	2,82E-04	2,327028	1,218489	AT1G27770	ACA1, PEA1	ACA1_PEA1__autoinhibited Ca2+-ATPase 1ACA1_PEA1__autoinhibited Ca2+-ATPase 1
A_84_P830058	0,04899432	0,0038659	2,323218	1,216125	AT1G63860		Disease resistance protein (TIR-NBS-LRR class) family
A_84_P15109	0,01719517	2,41E-04	2,322675	1,215787	AT1G20450	ERD10, LTI29, LTI4	ERD10_LTI29_LTI45__Dehydrin family protein
A_84_P569157	0,01320943	1,09E-04	2,321776	1,215229	AT5G67410		
A_84_P857480	0,01624931	2,07E-04	2,318691	1,21331	AT1G20450	ERD10, LTI29, LTI4	ERD10_LTI29_LTI45__Dehydrin family protein
A_84_P702605	0,04799153	0,0036067	2,317382	1,212496	AT3G14362	DVL19, RTFL10	DVL19_RTFL10__ROTUNDIFOLIA like 10
A_84_P752539	0,00877048	2,10E-05	2,313822	1,210278	AT1G08920	ESL1	ESL1__ERD (early response to dehydration) six-like 1
A_84_P12321	0,04616675	0,0032749	2,30816	1,206743	AT1G61290	ATSYP124, SYP12	ATSYP124_SYP124__syntaxin of plants 124
A_84_P167943	0,03103756	0,001264	2,306531	1,205725	AT3G15210	ATERF4, ATERF-4	ATERF-4_ATERF4_ERF4_RAP2.5__ethylene responsive element binding factor 4
A_84_P23850	0,04379391	0,0028632	2,305991	1,205387	AT2G43520	ATTI2, TI2	ATTI2_TI2__trypsin inhibitor protein 2
A_84_P820727	0,03305386	0,001469	2,305668	1,205185	AT4G24160		alpha/beta-Hydrolases superfamily protein
A_84_P17618	0,02267799	5,40E-04	2,305359	1,204991	AT4G24160		alpha/beta-Hydrolases superfamily protein
A_84_P750801	0,04465805	0,0030131	2,303411	1,203772	AT1G42490		
A_84_P79769	0,03172537	0,0013245	2,303389	1,203758	AT4G38470	STY46	STY46__ACT-like protein tyrosine kinase family protein
A_84_P565337	0,0286969	0,0010109	2,30227	1,203057	AT4G21865		
A_84_P21673	0,04475471	0,0030545	2,296892	1,199683	AT1G52400	ATBG1, BGL1, BGL	ATBG1_BGL1_BGLU18__beta glucosidase 18
A_84_P21603	0,01176281	7,81E-05	2,288224	1,194228	AT5G46330	FLS2	FLS2__Leucine-rich receptor-like protein kinase family protein
A_84_P181994	0,00857965	1,91E-05	2,284846	1,192097	AT3G02040	AtGDPD1, GDPD1,	AtGDPD1_GDPD1_SRG3__senescence-related gene 3
A_84_P108412	0,01686909	2,29E-04	2,284373	1,191798	AT4G22690	CYP706A1	CYP706A1__cytochrome P450, family 706, subfamily A, polypeptide 1
A_84_P20775	0,00464882	2,78E-06	2,284192	1,191684	AT5G58400		Peroxidase superfamily protein
A_84_P212918	0,02720185	9,01E-04	2,284103	1,191628	AT4G39030	EDS5, SCORD3, S	EDS5_SCORD3_SID1__MATE efflux family protein
A_84_P277930	0,02184876	4,96E-04	2,282945	1,190896	AT2G02680		Cysteine/Histidine-rich C1 domain family protein
A_84_P16068	0,01785415	2,85E-04	2,282311	1,190496	AT1G33790		jacalin lectin family protein
A_84_P816095	0,01774115	2,74E-04	2,282243	1,190453	AT4G01026	PYL7, RCAR2	PYL7_RCAR2__PYR1-like 7
A_84_P182114	0,02226756	5,14E-04	2,281288	1,189849	AT5G02950		Tudor/PWWP/MBT superfamily protein

A_84_P519221	0,01961223	3,78E-04	2,280608	1,189418	AT4G14860	AtOFP11, OFP11	AtOFP11_OFP11__ovate family protein 11
A_84_P869434	0,03184718	0,0013427	2,277785	1,187632	AT4G23600	CORI3, JR2	CORI3_JR2__Tyrosine transaminase family protein
A_84_P189784	0,02069154	4,37E-04	2,276053	1,186534	AT3G18690	MKS1	MKS1__MAP kinase substrate 1
A_84_P18737	0,04234786	0,0026625	2,274057	1,185268	AT5G38710		Methylenetetrahydrofolate reductase family protein
A_84_P784441	0,0325659	0,001427	2,272636	1,184366	AT4G18950		Integrin-linked protein kinase familyIntegrin-linked protein kinase family
A_84_P805118	0,029931	0,0011617	2,269276	1,182232	AT3G15450		Aluminium induced protein with YGL and LRDR motifs
A_84_P815327	0,02400674	6,36E-04	2,266853	1,180691	AT1G27130	ATGSTU13, GST12	ATGSTU13_GST12_GSTU13__glutathione S-transferase tau 13
A_84_P537920	0,01686909	2,30E-04	2,264265	1,179043	AT4G33985		Protein of unknown function (DUF1685)
A_84_P21728	0,01462891	1,55E-04	2,263773	1,178729	AT1G20490		AMP-dependent synthetase and ligase family protein
A_84_P814684	0,01769782	2,63E-04	2,263524	1,178571	AT1G21110;	IGMT3,IGMT4	
A_84_P12206	0,01830757	3,05E-04	2,26074	1,176795	AT5G61810	APC1	APC1__Mitochondrial substrate carrier family protein
A_84_P810995	0,04831925	0,0037049	2,260141	1,176413	AT2G41430	CID1, ERD15, LSR	CID1_ERD15_LSR1__dehydration-induced protein (ERD15)
A_84_P15182	0,03364271	0,0015513	2,258459	1,175339	AT1G60260	BGLU5	BGLU5__beta glucosidase 5
A_84_P852295	0,03624299	0,001841	2,255902	1,173704	AT3G47340	ASN1, AT-ASN1, D	ASN1_AT-ASN1_DIN6__glutamine-dependent asparagine synthase 1
A_84_P22597	0,03884352	0,0021489	2,255885	1,173694	AT5G59550		AtRDUF2_RDUF2__zinc finger (C3HC4-type RING finger) family protein
A_84_P17674	0,02493108	7,45E-04	2,253785	1,17235	AT1G27130	ATGSTU13, GST12	ATGSTU13_GST12_GSTU13__glutathione S-transferase tau 13
A_84_P17031	0,00894727	3,11E-05	2,253709	1,172301	AT1G03850	ATGRXS13, GRXS	ATGRXS13_GRXS13__Glutaredoxin family protein
A_84_P259140	0,01798792	2,92E-04	2,249105	1,169351	AT1G28050		BBX13__B-box type zinc finger protein with CCT domain
A_84_P12153	0,01386093	1,30E-04	2,247369	1,168237	AT5G47910	ATRBOHD, RBOH	ATRBOHD_RBOHD__respiratory burst oxidase homologue D
A_84_P248365	0,04831925	0,0037045	2,246696	1,167805	AT4G37240		
A_84_P805073	0,02695982	8,87E-04	2,239347	1,163078	AT3G15450		Aluminium induced protein with YGL and LRDR motifs
A_84_P846967	0,02075475	4,41E-04	2,237025	1,161581	AT5G53050		alpha/beta-Hydrolases superfamily proteinalpha/beta-Hydrolases superfamily protein
A_84_P15156	0,04008859	0,0023517	2,236603	1,161309	AT1G61470		Polynucleotidyl transferase, ribonuclease H-like superfamily protein
A_84_P22445	0,02577352	8,02E-04	2,235833	1,160812	AT5G04720	ADR1-L2, PHX21	ADR1-L2_PHX21__ADR1-like 2
A_84_P859574	0,03053011	0,0012168	2,235738	1,160751	AT5G04720	ADR1-L2, PHX21	ADR1-L2_PHX21__ADR1-like 2
A_84_P755699	0,03359263	0,0015343	2,233412	1,15925	AT2G34580		
A_84_P144119	0,03926466	0,002229	2,23331	1,159184	AT4G17250		
A_84_P849068	0,04469125	0,0030285	2,233185	1,159102	AT3G06760		Drought-responsive family proteinDrought-responsive family protein
A_84_P510552	0,03916847	0,0022138	2,229786	1,156905	AT5G41100		
A_84_P17955	0,03025034	0,0011882	2,229298	1,15659	AT1G22380	AtUGT85A3, UGT8	AtUGT85A3_UGT85A3__UDP-glucosyl transferase 85A3
A_84_P21886	0,00857212	1,87E-05	2,229261	1,156566	AT1G55920	ATSERAT2;1, SAT	ATSERAT2;1_SAT1_SAT5_SERAT2;1__serine acetyltransferase 2;1
A_84_P15536	0,01871661	3,22E-04	2,228236	1,155902	AT3G16470	JAL35, JR1	JAL35_JR1__Mannose-binding lectin superfamily protein
A_84_P12293	0,00882356	2,35E-05	2,219093	1,14997	AT1G11330		S-locus lectin protein kinase family protein
A_84_P197484	0,02951533	0,0011166	2,217134	1,148696	AT2G38310	PYL4, RCAR10	PYL4_RCAR10__PYR1-like 4
A_84_P15219	0,04942583	0,0039277	2,212806	1,145877	AT1G02860	BAH1, NLA	BAH1_NLA__SPX (SYG1/Pho81/XPR1) domain-containing protein
A_84_P22019	0,03899062	0,0021661	2,211227	1,144847	AT2G44390		Cysteine/Histidine-rich C1 domain family protein
A_84_P273770	0,01163687	6,94E-05	2,210556	1,144409	AT1G28380	NSL1	NSL1__MAC/Perforin domain-containing protein
A_84_P844839	0,04086231	0,0024725	2,209603	1,143787	AT4G39030	EDS5, SCORD3, S	EDS5_SCORD3_SID1__MATE efflux family protein
A_84_P11755	0,02430013	6,76E-04	2,208952	1,143362	AT3G14990	AtDJ1A, DJ1A	AtDJ1A_DJ-1a_DJ1A__Class I glutamine amidotransferase-like superfamily protein
A_84_P589129	0,03133682	0,001296	2,207034	1,142109	AT2G40095		Alpha/beta hydrolase related protein
A_84_P131945	0,00894727	3,36E-05	2,206865	1,141998	AT5G53060		RCF3_SHI1__RNA-binding KH domain-containing protein
A_84_P14143	0,02359227	5,98E-04	2,203991	1,140119	AT5G13550	SULTR4;1	SULTR4;1__sulfate transporter 4.1
A_84_P89489	0,02429591	6,74E-04	2,203869	1,140039	AT3G16330		
A_84_P565178	0,01830757	3,04E-04	2,197584	1,135919	AT3G25882	NIMIN-2	NIMIN-2__NIM1-interacting 2
A_84_P21875	0,03308225	0,0014772	2,196975	1,135518	AT1G63180	UGE3	UGE3__UDP-D-glucose/UDP-D-galactose 4-epimerase 3
A_84_P272750	0,01386093	1,30E-04	2,196947	1,1355	AT2G22300	CAMTA3, SR1	CAMTA3_SR1__signal responsive 1CAMTA3_SR1__signal responsive 1
A_84_P254190	0,00971693	4,37E-05	2,196283	1,135064	AT1G75230		DNA glycosylase superfamily protein
A_84_P14972	0,00178308	2,87E-07	2,191738	1,132075	AT5G44070	ARA8, ATPCS1, CA	ARA8_ATPCS1_CAD1_PCS1__phytochelatin synthase 1 (PCS1)
A_84_P10688	0,04362199	0,0028285	2,191377	1,131838	AT1G30070		SGS domain-containing protein
A_84_P24037	0,0145606	1,51E-04	2,188676	1,130058	AT3G18830	ATPLT5, ATPMT5,	ATPLT5_ATPMT5_PMT5__polyol/monosaccharide transporter 5
A_84_P109922	0,01634308	2,13E-04	2,188611	1,130015	AT4G17900		PLATZ transcription factor family protein

A_84_P13942	0,02449762	6,93E-04	2,187364	1,129193	AT1G06520	ATGPAT1, GPAT1	ATGPAT1_GPAT1_sn-2-GPAT1__glycerol-3-phosphate acyltransferase 1
A_84_P15324	0,01560944	1,81E-04	2,18504	1,12766	AT1G33560	ADR1	ADR1__Disease resistance protein (CC-NBS-LRR class) family
A_84_P78279	0,0320088	0,0013662	2,184396	1,127235	AT1G67920		
A_84_P813323	0,03913938	0,0021956	2,17921	1,123805	AT1G70780; CPuORF28		
A_84_P785683	0,03959857	0,0022951	2,177729	1,122825	AT1G27770	ACA1, PEA1	ACA1_PEA1__autoinhibited Ca2+-ATPase 1
A_84_P532349	0,00466105	3,16E-06	2,177452	1,122641	AT3G09520	ATEXO70H4, EXO	ATEXO70H4_EXO70H4__exocyst subunit exo70 family protein H4
A_84_P16128	0,01020095	4,85E-05	2,175282	1,121203	AT1G60270	BGLU6	BGLU6__beta glucosidase 6BGLU6__beta glucosidase 6
A_84_P97266	0,03800573	0,0020552	2,175144	1,121111	AT4G18510	CLE2	CLE2__CLAVATA3/ESR-related 2
A_84_P21159	0,03636191	0,0018572	2,173139	1,119781	AT3G04010		O-Glycosyl hydrolases family 17 protein
A_84_P249125	0,02095783	4,50E-04	2,171825	1,118908	AT1G68500		
A_84_P21889	0,02038725	4,11E-04	2,171567	1,118736	AT1G74360		Leucine-rich repeat protein kinase family protein
A_84_P22932	0,01771716	2,68E-04	2,169214	1,117172	AT2G22770	NAI1	NAI1__basic helix-loop-helix (bHLH) DNA-binding superfamily protein
A_84_P821329	0,04348974	0,0028056	2,167369	1,115945	AT3G44190		FAD/NAD(P)-binding oxidoreductase family protein
A_84_P190534	0,04806924	0,0036159	2,167053	1,115734	AT1G68450	PDE337	PDE337__VQ motif-containing protein
A_84_P19576	0,02237896	5,24E-04	2,164362	1,113942	AT4G39940	AKN2, APK2	AKN2_APK2__APS-kinase 2
A_84_P836958	0,03225273	0,0013985	2,162703	1,112835	AT1G61470		Polynucleotidyl transferase, ribonuclease H-like superfamily protein
A_84_P13248	0,01830757	3,05E-04	2,161595	1,112096	AT1G03800	ATERF10, ERF10	ATERF10_ERF10__ERF domain protein 10
A_84_P750244	0,04598934	0,0032541	2,161464	1,112009	AT1G69140		
A_84_P20445	0,01065349	5,40E-05	2,160613	1,111441	AT4G21410	CRK29	CRK29__cysteine-rich RLK (RECEPTOR-like protein kinase) 29
A_84_P212328	0,0184221	3,11E-04	2,159282	1,110551	AT3G50010		Cysteine/Histidine-rich C1 domain family protein
A_84_P859177	0,03051006	0,0012111	2,158004	1,109697	AT4G22780	ACR7	ACR7__ACT domain repeat 7ACR7__ACT domain repeat 7
A_84_P22084	0,04465805	0,0030177	2,157833	1,109583	AT3G11580		AP2/B3-like transcriptional factor family protein
A_84_P312543	0,02524157	7,67E-04	2,15743	1,109314	AT3G52870		IQ calmodulin-binding motif family protein
A_84_P89769	0,02612251	8,35E-04	2,151389	1,105269	AT2G35930	PUB23	AtPUB23_PUB23__plant U-box 23
A_84_P505223	0,01686909	2,30E-04	2,15087	1,10492	AT5G35732		
A_84_P22039	0,01156977	6,70E-05	2,149966	1,104314	AT2G31010		Protein kinase superfamily protein
A_84_P23152	0,03178847	0,0013312	2,14981	1,104209	AT3G47380		Plant invertase/pectin methylesterase inhibitor superfamily protein
A_84_P596065	0,00894727	2,47E-05	2,149805	1,104206	AT1G49520		SWIB complex BAF60b domain-containing protein
A_84_P816283	0,03818448	0,0020738	2,148263	1,10317	AT1G53280	AtDJ1B, DJ1B	AtDJ1B_DJ-1b_DJ1B__Class I glutamine amidotransferase-like superfamily protein
A_84_P230289	0,03518269	0,0017091	2,145975	1,101633	AT2G44080	ARL	ARL__ARGOS-like
A_84_P119322	0,02430013	6,79E-04	2,142498	1,099294	AT3G14060		
A_84_P24136	0,02114772	4,60E-04	2,139821	1,09749	AT3G55940		Phosphoinositide-specific phospholipase C family protein
A_84_P808847	0,01504028	1,64E-04	2,139649	1,097374	AT2G23320	WRKY15	AtWRKY15_WRKY15__WRKY DNA-binding protein 15
A_84_P13943	0,01526442	1,74E-04	2,138164	1,096373	AT5G07460	ATMSRA2, PMSR2	ATMSRA2_PMSR2__peptidemethionine sulfoxide reductase 2
A_84_P597426	0,02894719	0,0010505	2,137677	1,096044	AT4G21320	HSA32	HSA32__Aldolase-type TIM barrel family protein
A_84_P23998	0,01320943	1,08E-04	2,136488	1,095242	AT1G53430		Leucine-rich repeat transmembrane protein kinase
A_84_P14116	0,01861906	3,20E-04	2,134052	1,093596	AT5G66790		Protein kinase superfamily protein
A_84_P192974	0,01066107	5,47E-05	2,133877	1,093477	AT5G65660		hydroxyproline-rich glycoprotein family protein
A_84_P203128	0,02300682	5,62E-04	2,132088	1,092267	AT3G29575	AFP3	AFP3__ABI five binding protein 3
A_84_P23923	0,03399409	0,0015858	2,131501	1,091869	AT2G37900		Major facilitator superfamily protein
A_84_P784302	0,03939561	0,0022518	2,129073	1,090225	AT1G01720	ANAC002, ATAF1	ANAC002_ATAF1__NAC (No Apical Meristem) domain transcriptional regulator superfamily protein
A_84_P14449	0,0242297	6,71E-04	2,125369	1,087713	AT2G34810		FAD-binding Berberine family protein
A_84_P824439	0,00894727	3,29E-05	2,125032	1,087484	AT2G22300	CAMTA3, SR1	CAMTA3_SR1__signal responsive 1
A_84_P571306	0,02991192	0,0011546	2,123456	1,086414	AT2G38500		2-oxoglutarate (2OG) and Fe(II)-dependent oxygenase superfamily protein
A_84_P21994	0,01592639	1,95E-04	2,122978	1,086089	AT2G26440		PME12__Plant invertase/pectin methylesterase inhibitor superfamily
A_84_P286620	0,02497593	7,51E-04	2,120676	1,084524	AT4G33940		RING/U-box superfamily protein
A_84_P816321	0,03768138	0,0020177	2,118493	1,083038	AT5G44070	ARA8, ATPCS1, CA	ARA8_ATPCS1_CAD1_PCS1__phytochelatin synthase 1 (PCS1)
A_84_P796756	0,04234786	0,0026626	2,1174	1,082293	AT1G79245		
A_84_P11807	0,04025845	0,0023943	2,116581	1,081736	AT3G47800		Galactose mutarotase-like superfamily protein
A_84_P22614	0,01958881	3,59E-04	2,110794	1,077786	AT5G63320	NPX1	NPX1__nuclear protein X1
A_84_P68194	0,04538051	0,003142	2,107592	1,075596	AT5G46710		PLATZ transcription factor family protein

A_84_P294564	0,02324895	5,75E-04	2,106822	1,075069	AT3G11420		Protein of unknown function (DUF604)Protein of unknown function (DUF604)
A_84_P17200	0,04418246	0,0029286	2,105115	1,073899	AT1G16110	WAKL6	WAKL6__wall associated kinase-like 6
A_84_P588557	0,00894727	2,98E-05	2,104569	1,073525	AT4G36830	HOS3-1	HOS3-1__GNS1/SUR4 membrane protein family
A_84_P828208	0,02469361	7,30E-04	2,104473	1,073459	AT5G53060		RCF3_SHI1__RNA-binding KH domain-containing protein
A_84_P19785	0,04811797	0,0036293	2,103174	1,072568	AT5G65500		U-box domain-containing protein kinase family protein
A_84_P163223	0,03636191	0,0018604	2,102561	1,072147	AT3G13760		Cysteine/Histidine-rich C1 domain family protein
A_84_P13481	0,01320943	1,10E-04	2,102203	1,071902	AT2G23320	WRKY15	AtWRKY15_WRKY15__WRKY DNA-binding protein 15
A_84_P832916	0,02430118	6,80E-04	2,098414	1,0693	AT2G44380		Cysteine/Histidine-rich C1 domain family protein
A_84_P21166	0,01830757	3,06E-04	2,096378	1,067899	AT3G09830		Protein kinase superfamily protein
A_84_P54290	0,03681569	0,0019221	2,095145	1,06705	AT3G19970		alpha/beta-Hydrolases superfamily protein
A_84_P608949	0,04788074	0,0035934	2,091447	1,064502	AT4G15450		Senescence/dehydration-associated protein-related
A_84_P803506	0,00387638	1,09E-06	2,088249	1,062294	AT3G30775	ATPDH, ATPOX, A	AT-POX_ATPDH_ERD5_PDH1_PRO1_PRODH__Methylenetetrahydrofolate reductase family protein
A_84_P53650	0,03359263	0,001546	2,087328	1,061657	AT5G57910		
A_84_P18467	0,03827128	0,0020864	2,086823	1,061308	AT3G57520	AtSIP2, RS2, SIP2	AtSIP2_RS2_SIP2__seed imbibition 2
A_84_P88579	0,02449762	6,98E-04	2,085612	1,060471	AT1G15430		Protein of unknown function (DUF1644)
A_84_P563858	0,0497107	0,0039875	2,084348	1,059596	AT4G38340		NLP3__Plant regulator RWP-RK family protein
A_84_P813213	0,02009357	3,96E-04	2,081168	1,057393	AT4G22690	CYP706A1	CYP706A1__cytochrome P450, family 706, subfamily A, polypeptide 1
A_84_P22967	0,03446271	0,0016322	2,080063	1,056627	AT2G22500	DIC1, ATPUMP5, U	ATPUMP5_DIC1_UCP5__uncoupling protein 5
A_84_P23167	0,02449762	6,99E-04	2,077801	1,055058	AT3G50950	ZAR1	ZAR1__HOPZ-ACTIVATED RESISTANCE 1
A_84_P11601	0,01872867	3,24E-04	2,076943	1,054461	AT2G39660	BIK1	BIK1__botrytis-induced kinase1
A_84_P823526	0,02178353	4,93E-04	2,076692	1,054287	AT5G04250		Cysteine proteinases superfamily protein
A_84_P52100	0,0227833	5,52E-04	2,075827	1,053686	AT4G21910		MATE efflux family protein
A_84_P274520	0,04954357	0,0039493	2,075162	1,053224	AT3G47980		Integral membrane HPP family protein
A_84_P808837	0,01185074	8,24E-05	2,074917	1,053054	AT2G23320	WRKY15	AtWRKY15_WRKY15__WRKY DNA-binding protein 15
A_84_P827290	0,04017467	0,002382	2,071514	1,050686	AT4G13110		BSD domain-containing protein
A_84_P522242	0,02409643	6,61E-04	2,071476	1,050659	AT1G07985		Expressed protein
A_84_P854328	0,04970967	0,0039798	2,070135	1,049725	AT5G02020	SIS	SIS__SIS__SIS__
A_84_P13841	0,01592639	1,96E-04	2,069877	1,049545	AT4G25380	AtSAP10, SAP10	AtSAP10_SAP10__stress-associated protein 10
A_84_P754645	0,0340082	0,0015885	2,06863	1,048676	AT1G31540		Disease resistance protein (TIR-NBS-LRR class) family
A_84_P127291	0,04321904	0,0027746	2,066848	1,047432	AT5G62865		
A_84_P19986	0,03944673	0,0022656	2,063735	1,045258	AT1G01720	ANAC002, ATAF1	ANAC002_ATAF1__NAC (No Apical Meristem) domain transcriptional regulator superfamily protein
A_84_P92089	0,0336938	0,001565	2,063111	1,044822	AT1G19310		RING/U-box superfamily protein
A_84_P21831	0,04989897	0,0040285	2,062548	1,044428	AT1G15380	GLYI4	GLYI4__Lactoylglutathione lyase / glyoxalase I family protein
A_84_P21390	0,04277083	0,00272	2,061704	1,043837	AT4G21200	ATGA2OX8, GA2O	ATGA2OX8_GA2OX8__gibberellin 2-oxidase 8
A_84_P571830	0,04413573	0,0029101	2,059866	1,04255	AT5G65925		
A_84_P14321	0,03533791	0,0017409	2,057364	1,040797	AT1G74440		Protein of unknown function (DUF962)
A_84_P20148	0,02403026	6,50E-04	2,056926	1,04049	AT2G30870	ATGSTF10, ATGST	ATGSTF10_ATGSTF4_ERD13_GSTF10__glutathione S-transferase PHI 10
A_84_P870134	0,03117012	0,0012714	2,056679	1,040317	AT1G60270	BGLU6	BGLU6__beta glucosidase 6BGLU6__beta glucosidase 6
A_84_P852060	0,04811797	0,0036294	2,056495	1,040188	AT1G19770	ATPUP14, PUP14	ATPUP14_PUP14__purine permease 14
A_84_P845406	0,04387216	0,0028764	2,049024	1,034937	AT3G47340	ASN1, AT-ASN1, D	ASN1_AT-ASN1_DIN6__glutamine-dependent asparagine synthase 1
A_84_P750962	0,01971263	3,85E-04	2,04538	1,032369	AT1G18200	AtRABA6b, RABA6	AtRABA6b_RABA6b__RAB GTPase homolog A6B
A_84_P15150	0,03359263	0,0015412	2,044461	1,03172	AT1G24100	UGT74B1	UGT74B1__UDP-glucosyl transferase 74B1
A_84_P22153	0,03789915	0,0020486	2,040776	1,029118	AT3G30775	ATPDH, ATPOX, A	AT-POX_ATPDH_ERD5_PDH1_PRO1_PRODH__Methylenetetrahydrofolate reductase family protein
A_84_P848526	0,02018128	4,02E-04	2,039846	1,028461	AT3G17120		
A_84_P13013	0,01921593	3,46E-04	2,039038	1,027888	AT1G18390		Protein kinase superfamily proteinProtein kinase superfamily protein
A_84_P58430	0,02728939	9,07E-04	2,038989	1,027854	AT3G17120		
A_84_P158205	0,0403545	0,0024019	2,038049	1,027189	AT1G22470		
A_84_P750311	0,01872867	3,26E-04	2,037992	1,027148	AT1G72120		AtNPF5.14_NPF5.14__Major facilitator superfamily protein
A_84_P218298	0,03490096	0,0016866	2,037426	1,026748	AT2G42760		
A_84_P186194	0,04813688	0,0036466	2,035825	1,025614	AT2G35640		Homeodomain-like superfamily protein
A_84_P11922	0,02511608	7,61E-04	2,028394	1,020338	AT4G18280		glycine-rich cell wall protein-related

A_84_P12018	0,00387638	1,20E-06	2,027538	1,019729	AT4G15420		Ubiquitin fusion degradation UFD1 family protein
A_84_P502958	0,01989875	3,90E-04	2,025796	1,018489	AT2G21500		RING/U-box superfamily protein
A_84_P22649	0,00894727	3,17E-05	2,025425	1,018225	AT5G13110	G6PD2	G6PD2__glucose-6-phosphate dehydrogenase 2
A_84_P157325	0,02189142	4,99E-04	2,02396	1,017181	AT1G69360		Plant protein of unknown function (DUF863)Plant protein of unknown function (DUF863)
A_84_P19763	0,01663725	2,20E-04	2,023675	1,016977	AT5G60300	LecRK-I.9	DORN1_LecRK-I.9__Concanavalin A-like lectin protein kinase family protein
A_84_P20789	0,00918073	3,89E-05	2,02262	1,016225	AT1G71400	AtRLP12, RLP12	AtRLP12_RLP12__receptor like protein 12
A_84_P11083	0,02454013	7,19E-04	2,021431	1,015377	AT4G36900	DEAR4, RAP2.10	DEAR4_RAP2.10__related to AP2 10
A_84_P822179	0,02342488	5,80E-04	2,021241	1,015242	AT5G02020	SIS	SIS__SIS__SIS__
A_84_P23020	0,03270588	0,0014445	2,020978	1,015054	AT2G22850	AtbZIP6, bZIP6	AtbZIP6_bZIP6__basic leucine-zipper 6
A_84_P13306	0,04527197	0,0031223	2,018107	1,013002	AT1G03090	MCCA	MCCA_methylcrotonyl-CoA carboxylase alpha chain, mitochondrial 3-methylcrotonyl-CoA carboxylase 1
A_84_P13455	0,03187662	0,0013483	2,01475	1,010601	AT2G30360	CIPK11, PKS5, SIP	CIPK11_PKS5_SIP4_SNRK3.22__SOS3-interacting protein 4
A_84_P304080	0,01163687	7,15E-05	2,00996	1,007167	AT4G36930	SPT	SPT__basic helix-loop-helix (bHLH) DNA-binding superfamily protein
A_84_P12054	0,01830757	3,05E-04	2,009852	1,00709	AT5G07580		Integrase-type DNA-binding superfamily protein
A_84_P11868	0,01673145	2,22E-04	2,009152	1,006587	AT3G62260		Protein phosphatase 2C family protein
A_84_P97076	0,01560944	1,81E-04	2,008572	1,00617	AT1G80380		P-loop containing nucleoside triphosphate hydrolases superfamily protein
A_84_P510878	0,04831925	0,0037152	2,008487	1,006109	AT1G75000		GNS1/SUR4 membrane protein family
A_84_P12385	0,02745852	9,21E-04	2,008202	1,005904	AT1G80110	ATPP2-B11, PP2-B	ATPP2-B11_PP2-B11__phloem protein 2-B11
A_84_P87289	0,02069154	4,37E-04	2,00592	1,004264	AT1G24807;	ASB1,TRP4,WEI7	
A_84_P18377	0,04695471	0,0034309	2,003492	1,002517	AT3G24420		alpha/beta-Hydrolases superfamily protein
A_84_P833963	0,03822881	0,0020797	1,995415	0,996689	AT3G11850		Protein of unknown function, DUF593
A_84_P92929	0,03612883	0,0018272	1,99399	0,995658	AT5G19240		Glycoprotein membrane precursor GPI-anchored
A_84_P812231	0,03187662	0,0013484	1,993965	0,99564	AT1G03220;	0	
A_84_P868911	0,03473818	0,001667	1,991404	0,993786	AT5G05590	PAI2	PAI2__phosphoribosylanthranilate isomerase 2
A_84_P849451	0,03490096	0,0016869	1,990562	0,993176	AT3G26910		hydroxyproline-rich glycoprotein family protein
A_84_P17672	0,03025034	0,0011884	1,989678	0,992535	AT4G36150		Disease resistance protein (TIR-NBS-LRR class) family
A_84_P23992	0,02100477	4,54E-04	1,988682	0,991813	AT3G05640		Protein phosphatase 2C family protein
A_84_P787112	0,02353903	5,89E-04	1,987547	0,990989	AT5G56490		AtGulLO4_GulLO4__D-arabinono-1,4-lactone oxidase family protein
A_84_P17641	0,01386093	1,33E-04	1,987291	0,990803	AT4G29050		LecRK-V.9__Concanavalin A-like lectin protein kinase family protein
A_84_P832631	0,04972693	0,0039936	1,987284	0,990798	AT1G11330		S-locus lectin protein kinase family proteinS-locus lectin protein kinase family protein
A_84_P845699	0,03258821	0,0014332	1,984587	0,988839	AT3G18830	ATPLT5, ATPMT5,	ATPLT5_ATPMT5_PMT5__polyol/monosaccharide transporter 5
A_84_P22952	0,03197693	0,0013626	1,981325	0,986465	AT2G46650	ATCB5-C, B5 #1, C	ATCB5-C_B5 #1_CB5-C_CYTB5-C__cytochrome B5 isoform C
A_84_P17213	0,02728939	9,06E-04	1,98031	0,985726	AT1G58410		Disease resistance protein (CC-NBS-LRR class) family
A_84_P15244	0,04180804	0,0025939	1,979483	0,985124	AT1G75030	ATLP-3, TLP-3	ATLP-3_TLP-3__thaumatin-like protein 3
A_84_P848857	0,00950448	4,13E-05	1,977661	0,983795	AT3G07090		PPPDE putative thiol peptidase family protein
A_84_P89509	0,0373915	0,0019905	1,977596	0,983748	AT5G18490		Plant protein of unknown function (DUF946)
A_84_P95119	0,03571476	0,0017899	1,976463	0,982921	AT3G14840		Leucine-rich repeat transmembrane protein kinase
A_84_P10568	0,01786949	2,88E-04	1,97584	0,982466	AT1G07000	ATEXO70B2, EXO7	ATEXO70B2_EXO70B2__exocyst subunit exo70 family protein B2
A_84_P195774	0,00900545	3,48E-05	1,969759	0,978019	AT1G30320		Remorin family protein
A_84_P75444	0,02353903	5,88E-04	1,966591	0,975697	AT2G24100	ASG1	ASG1__
A_84_P18359	0,03975394	0,00231	1,963451	0,973392	AT3G25250	AGC2, AGC2-1, At	AGC2_AGC2-1_AtOXI1_AGC (cAMP-dependent, cGMP-dependent and protein kinase C) kinase protein
A_84_P161083	0,01771716	2,67E-04	1,962659	0,97281	AT5G52410		
A_84_P14345	0,01323236	1,11E-04	1,962454	0,972659	AT1G76040	CPK29	CPK29__calcium-dependent protein kinase 29
A_84_P107092	0,03308225	0,0014843	1,962322	0,972562	AT1G69050		
A_84_P538274	0,02751414	9,27E-04	1,958174	0,969509	AT1G30755		Protein of unknown function (DUF668)Protein of unknown function (DUF668)
A_84_P503493	0,0237224	6,07E-04	1,957649	0,969122	AT5G49015		Expressed protein
A_84_P788959	0,0296875	0,0011291	1,956408	0,968207	AT5G57910		
A_84_P308213	0,01492891	1,61E-04	1,954468	0,966776	AT3G03020		
A_84_P500277	0,04550704	0,0031586	1,953712	0,966218	AT2G17705		
A_84_P250505	0,02612251	8,29E-04	1,950549	0,963881	AT5G46780		VQ motif-containing protein
A_84_P823769	0,03076559	0,0012334	1,945815	0,960375	AT3G58980		F-box family protein
A_84_P819063	0,02582126	8,10E-04	1,945449	0,960103	AT3G46640	LUX, PCL1	LUX_PCL1__Homeodomain-like superfamily protein

A_84_P19788	0,01719517	2,42E-04	1,944603	0,959476	AT5G66210	CPK28	CPK28__calcium-dependent protein kinase 28
A_84_P21825	0,03014083	0,0011808	1,942328	0,957787	AT1G13210	ACA.l	ACA.l__autoinhibited Ca2+/ATPase II
A_84_P23186	0,01246891	9,60E-05	1,939654	0,955799	AT3G55110	ABCG18	ABCG18__ABC-2 type transporter family protein
A_84_P13692	0,0241966	6,69E-04	1,938157	0,954686	AT3G46710		NB-ARC domain-containing disease resistance protein
A_84_P15558	0,02883385	0,001027	1,937318	0,954061	AT3G20660	OCT4, AtOCT4	AtOCT4_OCT4__organic cation/carnitine transporter4
A_84_P10820	0,02047121	4,16E-04	1,935538	0,952735	AT3G13430		RING/U-box superfamily protein
A_84_P23180	0,04844125	0,0037566	1,928637	0,947581	AT3G53800	Fes1B	Fes1B__Fes1B
A_84_P11232	0,00903297	3,64E-05	1,928045	0,947139	AT5G54810	ATTSB1, TRP2, TR	ATTSB1_TRP2_TRPB_TSB1__tryptophan synthase beta-subunit 1
A_84_P123632	0,02454009	7,10E-04	1,927539	0,94676	AT1G70780;	CPuORF28	
A_84_P561086	0,03102973	0,0012626	1,925307	0,945088	AT5G44050		MATE efflux family protein
A_84_P18131	0,01066107	5,60E-05	1,92508	0,944919	AT1G07240	UGT71C5	UGT71C5__UDP-glucosyl transferase 71C5
A_84_P156895	0,04262674	0,0027039	1,924733	0,944658	AT3G47210		Plant protein of unknown function (DUF247)
A_84_P20006	0,01582691	1,92E-04	1,923072	0,943413	AT1G76380		DNA-binding bromodomain-containing protein
A_84_P168493	0,02850911	9,96E-04	1,922251	0,942797	AT3G46620		AtRDUF1_RDUF1__zinc finger (C3HC4-type RING finger) family protein
A_84_P259710	0,03831658	0,0020976	1,91909	0,940422	AT3G18930		RING/U-box superfamily protein
A_84_P814679	0,01771716	2,71E-04	1,918487	0,939969	AT3G62420;	ATBZIP53,BZIP53,CPuORF3	
A_84_P23294	0,03152039	0,0013147	1,917984	0,93959	AT4G24230	ACBP3	ACBP3__acyl-CoA-binding domain 3
A_84_P18591	0,02991192	0,0011583	1,917885	0,939516	AT4G29950		Ypt/Rab-GAP domain of gyp1p superfamily protein
A_84_P550411	0,00857965	1,89E-05	1,916685	0,938613	AT5G20190		Tetratricopeptide repeat (TPR)-like superfamily protein
A_84_P24127	0,03234271	0,0014059	1,916481	0,938459	AT3G53990		Adenine nucleotide alpha hydrolases-like superfamily protein
A_84_P825746	0,0281065	9,67E-04	1,913627	0,93631	AT4G21320	HSA32	HSA32__Aldolase-type TIM barrel family proteinHSA32__Aldolase-type TIM barrel family protein
A_84_P560703	0,02430013	6,75E-04	1,913023	0,935854	AT3G07150		
A_84_P21822	0,02477091	7,35E-04	1,912916	0,935774	AT1G21000		PLATZ transcription factor family protein
A_84_P19551	0,03999281	0,0023373	1,912536	0,935487	AT4G33300	ADR1-L1	ADR1-L1__ADR1-like 1
A_84_P123362	0,03211456	0,0013791	1,912072	0,935137	AT1G13740	AFP2	AFP2__ABI five binding protein 2
A_84_P256200	0,03120647	0,0012799	1,909599	0,93327	AT3G06760		Drought-responsive family proteinDrought-responsive family protein
A_84_P15341	0,02285099	5,57E-04	1,909018	0,932831	AT1G64200	VHA-E3	VHA-E3__vacuolar H+-ATPase subunit E isoform 3
A_84_P12104	0,01785633	2,87E-04	1,907605	0,931763	AT5G27380	GSH2, GSHB	AtGSH2_GSH2_GSHB__glutathione synthetase 2
A_84_P22312	0,04234786	0,002668	1,907347	0,931567	AT4G11360	RHA1B	RHA1B__RING-H2 finger A1B
A_84_P11862	0,0409187	0,0024804	1,906296	0,930772	AT3G60690		SAUR59__SAUR-like auxin-responsive protein family
A_84_P22159	0,02859729	0,0010001	1,906065	0,930597	AT3G13100	ABCC7, ATMRP7,	ABCC7_ATMRP7_MRP7__multidrug resistance-associated protein 7
A_84_P164953	0,02449762	6,93E-04	1,904194	0,92918	AT1G49720	ABF1	ABF1_AtABF1__abscisic acid responsive element-binding factor 1
A_84_P785537	0,03524169	0,0017216	1,904132	0,929133	AT5G40460		
A_84_P16258	0,0336938	0,0015653	1,899902	0,925925	AT1G49230		ATL78_AtATL78__RING/U-box superfamily protein
A_84_P281300	0,04465805	0,0030115	1,898538	0,924889	AT3G46640	LUX, PCL1	LUX_PCL1__Homeodomain-like superfamily protein
A_84_P750263	0,02376995	6,16E-04	1,898402	0,924786	AT1G17230		Leucine-rich receptor-like protein kinase family protein
A_84_P538776	0,03478254	0,0016715	1,898356	0,92475	AT4G24015		RING/U-box superfamily protein
A_84_P812038	0,02403887	6,58E-04	1,897513	0,924109	AT1G28330	DRM1, DYL1	AtDRM1_DRM1_DYL1__dormancy-associated protein-like 1
A_84_P12747	0,03529676	0,0017258	1,896174	0,923091	AT3G46700		UDP-Glycosyltransferase superfamily protein
A_84_P121232	0,0241966	6,69E-04	1,893508	0,921061	AT2G03240		EXS (ERD1/XPR1/SYG1) family protein
A_84_P531393	0,04181817	0,0026031	1,892646	0,920404	AT2G37210	LOG3	LOG3__lysine decarboxylase family protein
A_84_P17993	0,01961223	3,77E-04	1,892353	0,920181	AT1G61370		S-locus lectin protein kinase family protein
A_84_P856262	0,03645688	0,0018719	1,891678	0,919666	AT5G50200	ATNRT3.1, NRT3.1	ATNRT3.1_NRT3.1_WR3__nitrate transmembrane transporters
A_84_P298164	0,01163597	6,78E-05	1,890017	0,918399	AT5G65870	ATPSK5, PSK5	ATPSK5_PSK5__phytosulfokine 5 precursor
A_84_P815150	0,04348974	0,002806	1,88933	0,917874	AT2G36320		A20/AN1-like zinc finger family protein
A_84_P13039	0,03831641	0,002096	1,888914	0,917557	AT5G24420	PGL5	PGL5__6-phosphogluconolactonase 5
A_84_P818026	0,0151022	1,68E-04	1,888015	0,91687	AT4G26090	RPS2	RPS2__NB-ARC domain-containing disease resistance protein
A_84_P15176	0,01375994	1,23E-04	1,886798	0,91594	AT1G11960		ERD (early-responsive to dehydration stress) family protein
A_84_P218898	0,01961223	3,68E-04	1,886701	0,915866	AT5G27760		Hypoxia-responsive family protein
A_84_P15820	0,03988752	0,0023213	1,886149	0,915443	AT5G03630	ATMDAR2	ATMDAR2__Pyridine nucleotide-disulphide oxidoreductase family protein
A_84_P141359	0,01872867	3,25E-04	1,885462	0,914918	AT2G24550		

A_84_P13968	0,02195661	5,02E-04	1,885338	0,914824	AT5G16410		HXXXD-type acyl-transferase family protein
A_84_P19237	0,03051006	0,0012131	1,885	0,914564	AT2G27510	ATFD3, FD3	ATFD3_FD3__ferredoxin 3
A_84_P16662	0,02060719	4,29E-04	1,88297	0,91301	AT4G21570		Protein of unknown function (DUF300)
A_84_P810987	0,00606654	6,78E-06	1,881091	0,91157	AT2G41430	CID1, ERD15, LSR	CID1_ERD15_LSR1__dehydration-induced protein (ERD15)
A_84_P20465	0,0145606	1,51E-04	1,880572	0,911172	AT4G26090	RPS2	RPS2__NB-ARC domain-containing disease resistance protein
A_84_P17577	0,02910758	0,0010678	1,877991	0,90919	AT1G06180	ATMYB13, ATMYB	ATMYB13_ATMYBLFGN_MYB13__myb domain protein 13
A_84_P16738	0,02195661	5,02E-04	1,875028	0,906912	AT4G39890	AtRABH1c, RABH1	AtRABH1c_RABH1c__RAB GTPase homolog H1C
A_84_P123242	0,02646521	8,51E-04	1,874396	0,906426	AT5G40460		
A_84_P834403	0,02057283	4,27E-04	1,873945	0,906078	AT4G09150		T-complex protein 11T-complex protein 11
A_84_P848389	0,02896398	0,0010525	1,873577	0,905796	AT1G07890	APX1, ATAPX01, A	APX1_ATAPX01_ATAPX1_CS1_MEE6__ascorbate peroxidase 1
A_84_P14746	0,00961027	4,28E-05	1,873166	0,905478	AT4G11660	AT-HSFB2B, HSFB	AT-HSFB2B_HSF7_HSFB2B__winged-helix DNA-binding transcription factor family protein
A_84_P826004	0,01785415	2,84E-04	1,868904	0,902192	AT1G07000	ATEXO70B2, EXO7	ATEXO70B2_EXO70B2__exocyst subunit exo70 family protein B2
A_84_P535752	0,01320943	1,08E-04	1,868594	0,901953	AT2G13790	ATSERK4, BAK7, B	ATSERK4_BAK7_BKK1_SERK4__somatic embryogenesis receptor-like kinase 4
A_84_P19740	0,03537542	0,0017467	1,867599	0,901185	AT5G54300		Protein of unknown function (DUF761)
A_84_P604788	0,0491156	0,0038788	1,866795	0,900563	AT5G59510	DVL18, RTFL5	DVL18_RTFL5__ROTUNDIFOLIA like 5
A_84_P18315	0,04636379	0,0033158	1,864798	0,899019	AT3G09940	ATMDAR3, MDAR2	ATMDAR3_MDAR2_MDAR3_MDHAR__monodehydroascorbate reductase
A_84_P14868	0,02376995	6,18E-04	1,864795	0,899017	AT5G01830		ARM repeat superfamily protein
A_84_P10152	0,04639193	0,0033274	1,862771	0,89745	AT5G04760		Duplicated homeodomain-like superfamily protein
A_84_P550081	0,01375994	1,27E-04	1,862285	0,897074	AT3G09405		Pectinacetylesterase family protein
A_84_P798820	0,01375994	1,25E-04	1,861436	0,896416	AT2G41430	CID1, ERD15, LSR	CID1_ERD15_LSR1__dehydration-induced protein (ERD15)
A_84_P832013	0,04488314	0,0030705	1,860947	0,896037	AT5G07890		myosin heavy chain-related
A_84_P251265	0,01872867	3,26E-04	1,859908	0,895231	AT1G63720		
A_84_P784997	0,03533791	0,0017411	1,858849	0,894409	AT1G43886		transposable element gene
A_84_P127601	0,03827128	0,0020859	1,857877	0,893655	AT5G02940		Protein of unknown function (DUF1012)
A_84_P814940	0,04358541	0,0028142	1,854072	0,890697	AT4G30210	AR2, ATR2	AR2_ATR2__P450 reductase 2AR2_ATR2__P450 reductase 2
A_84_P103796	0,0373915	0,001985	1,851026	0,888325	AT3G51890		CLC3__Clathrin light chain proteinCLC3__Clathrin light chain protein
A_84_P22051	0,04614215	0,00327	1,848729	0,886534	AT2G19450	ABX45, AS11, ATD	ABX45_AS11_ATDGAT_AtDGAT1_RDS1_TAG1_membrane bound O-acyl transferase (MBOAT) protein
A_84_P555310	0,03330867	0,0014996	1,848614	0,886444	AT2G36650		
A_84_P222519	0,02544358	7,85E-04	1,847575	0,885633	AT1G21130	IGMT4	IGMT4__O-methyltransferase family protein
A_84_P19220	0,03688685	0,0019341	1,845863	0,884295	AT2G39210		Major facilitator superfamily protein
A_84_P13391	0,01492891	1,60E-04	1,84541	0,883942	AT1G34420		leucine-rich repeat transmembrane protein kinase family protein
A_84_P16698	0,01961223	3,66E-04	1,845251	0,883817	AT4G29700		Alkaline-phosphatase-like family protein
A_84_P16520	0,03181502	0,0013381	1,844985	0,883609	AT1G02640	ATBXL2, BXL2	ATBXL2_BXL2__beta-xylosidase 2
A_84_P20605	0,04784888	0,0035782	1,840491	0,880091	AT5G24530	DMR6	DMR6__2-oxoglutarate (2OG) and Fe(II)-dependent oxygenase superfamily protein
A_84_P16153	0,02894719	0,0010502	1,837108	0,877437	AT1G14130		2-oxoglutarate (2OG) and Fe(II)-dependent oxygenase superfamily protein
A_84_P552884	0,02906186	0,0010614	1,836306	0,876806	AT4G09150		T-complex protein 11T-complex protein 11
A_84_P13990	0,04970967	0,00398	1,83612	0,87666	AT5G26010		Protein phosphatase 2C family protein
A_84_P814037	0,01830216	3,01E-04	1,835812	0,876418	AT1G80380		P-loop containing nucleoside triphosphate hydrolases superfamily protein
A_84_P280930	0,02384917	6,27E-04	1,83508	0,875843	AT1G21670		
A_84_P15987	0,02237896	5,24E-04	1,834488	0,875378	AT5G61900;	BON,BON1,CPN1	
A_84_P15238	0,04826047	0,0036805	1,834137	0,875101	AT1G80320		2-oxoglutarate (2OG) and Fe(II)-dependent oxygenase superfamily protein
A_84_P23251	0,02943616	0,001103	1,833095	0,874282	AT4G09570	ATCPK4, CPK4	ATCPK4_CPK4__calcium-dependent protein kinase 4
A_84_P137359	0,02820842	9,76E-04	1,83274	0,874002	AT5G27070	AGL53	AGL53__AGAMOUS-like 53
A_84_P15928	0,04197278	0,0026226	1,832618	0,873906	AT5G46520		VICTR__Disease resistance protein (TIR-NBS-LRR class) family
A_84_P816799	0,02675365	8,69E-04	1,830923	0,872571	AT4G19880		Glutathione S-transferase family protein
A_84_P12695	0,04661662	0,0033746	1,827652	0,869991	AT3G25730	EDF3	EDF3__ethylene response DNA binding factor 3
A_84_P281740	0,03454188	0,0016456	1,827293	0,869708	AT1G78070		Transducin/WD40 repeat-like superfamily protein
A_84_P20025	0,02084717	4,46E-04	1,826485	0,86907	AT1G22360	AtUGT85A2, UGT8	AtUGT85A2_UGT85A2__UDP-glucosyl transferase 85A2
A_84_P812152	0,04838306	0,0037403	1,824638	0,86761	AT4G21850	ATMSRB9, MSRB9	ATMSRB9_MSRB9__methionine sulfoxide reductase B9
A_84_P236133	0,01686909	2,26E-04	1,823634	0,866817	AT1G70420		Protein of unknown function (DUF1645)
A_84_P22342	0,03270588	0,0014467	1,82351	0,866718	AT4G22780	ACR7	ACR7__ACT domain repeat 7

A_84_P118682	0,02943616	0,0011018	1,823327	0,866573	AT3G52430	ATPAD4, PAD4	ATPAD4_PAD4__alpha/beta-Hydrolases superfamily protein
A_84_P121882	0,04490265	0,0030802	1,822925	0,866255	AT4G30240		Syntaxin/t-SNARE family protein
A_84_P173901	0,04461956	0,0029913	1,820325	0,864196	AT5G22355		Cysteine/Histidine-rich C1 domain family protein
A_84_P819283	0,01323236	1,11E-04	1,816063	0,860814	AT4G36900	DEAR4, RAP2.10	DEAR4_RAP2.10__related to AP2 10DEAR4_RAP2.10__related to AP2 10
A_84_P16349	0,03746976	0,0019967	1,815829	0,860628	AT2G28080		UDP-Glycosyltransferase superfamily protein
A_84_P832358	0,01926563	3,47E-04	1,81559	0,860438	AT5G52410		
A_84_P10660	0,02208143	5,07E-04	1,814782	0,859797	AT2G29490	ATGSTU1, GST19,	ATGSTU1_GST19_GSTU1__glutathione S-transferase TAU 1
A_84_P556490	0,02237896	5,24E-04	1,813488	0,858767	AT4G23493		
A_84_P23354	0,04371693	0,0028488	1,812682	0,858126	AT4G38580	ATFP6, FP6, HIPP2	ATFP6_FP6_HIPP26__farnesylated protein 6
A_84_P562392	0,04372359	0,0028556	1,810314	0,85624	AT2G34355		Major facilitator superfamily protein
A_84_P77129	0,04657911	0,0033603	1,809002	0,855194	AT2G44370		Cysteine/Histidine-rich C1 domain family proteinCysteine/Histidine-rich C1 domain family protein
A_84_P505670	0,02038725	4,11E-04	1,807134	0,853704	AT2G36080		ABS2_NGAL1__AP2/B3-like transcriptional factor family protein
A_84_P554085	0,01564355	1,84E-04	1,806646	0,853313	AT1G02880	TPK1	TPK1__thiamin pyrophosphokinase1TPK1__thiamin pyrophosphokinase1
A_84_P513731	0,02369543	6,05E-04	1,805439	0,852349	AT3G12955		SAUR74__SAUR-like auxin-responsive protein family
A_84_P13281	0,0246688	7,26E-04	1,804504	0,851603	AT1G10050		glycosyl hydrolase family 10 protein / carbohydrate-binding domain-containing protein
A_84_P816633	0,04517826	0,0031085	1,804334	0,851466	AT5G27380	GSH2, GSHB	AtGSH2_GSH2_GSHB__glutathione synthetase 2
A_84_P13439	0,03541943	0,0017505	1,800746	0,848595	AT2G39980		HXXXD-type acyl-transferase family protein
A_84_P76134	0,01797131	2,91E-04	1,799786	0,847825	AT4G14270		
A_84_P21026	0,04308559	0,002758	1,798422	0,846731	AT2G33380	AtCLO3, CLO3, CL	AtCLO3_CLO-3_CLO3_RD20__Caleosin-related family protein
A_84_P820912	0,02559591	7,95E-04	1,797811	0,846241	AT3G02875	ILR1	ILR1__Peptidase M20/M25/M40 family protein
A_84_P182664	0,03359263	0,0015347	1,796727	0,845371	AT2G02710	PLP, PLPA, PLPB,	PLP_PLPA_PLPB_PLPC__PAS/LOV protein B
A_84_P12017	0,04103823	0,0024958	1,794466	0,843555	AT4G15270		glucosyltransferase-related
A_84_P15989	0,0373915	0,0019874	1,792985	0,842363	AT5G62350		Plant invertase/pectin methylesterase inhibitor superfamily protein
A_84_P81259	0,03665218	0,0019062	1,79277	0,842191	AT4G21510		AtFBS2_FBS2__F-box family protein
A_84_P16249	0,03255169	0,0014189	1,791898	0,841489	AT1G55510	BCDH BETA1	BCDH BETA1__branched-chain alpha-keto acid decarboxylase E1 beta subunit
A_84_P21190	0,02342488	5,82E-04	1,791671	0,841306	AT3G16350		Homeodomain-like superfamily protein
A_84_P186874	0,03021324	0,0011853	1,787399	0,837862	AT3G54020	AtIPCS1	AtIPCS1__Arabidopsis Inositol phosphorylceramide synthase 1
A_84_P534040	0,01320943	1,08E-04	1,785922	0,836669	AT2G31810		ACT domain-containing small subunit of acetolactate synthase protein
A_84_P246145	0,01647879	2,16E-04	1,784906	0,835848	AT4G32120		Galactosyltransferase family protein
A_84_P585178	0,03997699	0,002335	1,784847	0,8358	AT5G53895		
A_84_P22571	0,02400674	6,42E-04	1,781863	0,833386	AT5G52310	COR78, LTI140, LT	COR78_LTI140_LTI78_RD29A_low-temperature-responsive protein 78 /desiccation-responsive protein 29A
A_84_P840181	0,01874703	3,28E-04	1,781358	0,832977	AT3G48450		RPM1-interacting protein 4 (RIN4) family proteinRPM1-interacting protein 4 (RIN4) family protein
A_84_P20571	0,00894727	2,84E-05	1,781244	0,832885	AT1G68690	AtPERK9, PERK9	AtPERK9_PERK9__Protein kinase superfamily protein
A_84_P22517	0,03307353	0,0014714	1,781183	0,832836	AT5G37750		Chaperone DnaJ-domain superfamily protein
A_84_P11735	0,03993093	0,0023297	1,780875	0,832586	AT3G28930	AIG2	AIG2__AIG2-like (avirulence induced gene) family protein
A_84_P809109	0,02072643	4,40E-04	1,780716	0,832458	AT4G14270		
A_84_P21324	0,03359263	0,0015431	1,77915	0,831188	AT3G62420;	ATBZIP53,BZIP53,CPuORF3	
A_84_P188574	0,0427998	0,0027239	1,7788	0,830904	AT5G02020	SIS	SIS__SIS__SIS__
A_84_P14670	0,03331262	0,0015006	1,777766	0,830066	AT3G54200		Late embryogenesis abundant (LEA) hydroxyproline-rich glycoprotein family
A_84_P22953	0,04465805	0,003021	1,777406	0,829773	AT2G25140	CLPB4, CLPB-M, H	CLPB-M_CLPB4_HSP98.7__casein lytic proteinase B4
A_84_P814035	0,0265841	8,59E-04	1,776002	0,828633	AT1G80380		P-loop containing nucleoside triphosphate hydrolases superfamily protein
A_84_P99616	0,04176612	0,0025886	1,775381	0,828129	AT5G08360		Protein of unknown function (DUF789)
A_84_P14907	0,03523168	0,00172	1,775061	0,827868	AT5G13700	APAO, ATPAO1, P	APAO_ATPAO1_PAO1__polyamine oxidase 1
A_84_P245045	0,02067666	4,33E-04	1,774782	0,827642	AT5G64660	ATCMPG2, CMPG2	ATCMPG2_CMPG2__CYS, MET, PRO, and GLY protein 2
A_84_P18219	0,02390528	6,31E-04	1,774007	0,827012	AT1G04770		Tetratricopeptide repeat (TPR)-like superfamily protein
A_84_P17267	0,02740352	9,17E-04	1,771169	0,824702	AT2G41410		Calcium-binding EF-hand family protein
A_84_P17597	0,01926882	3,48E-04	1,770824	0,824421	AT4G18880	AT-HSFA4A, HSF A	AT-HSFA4A_HSF A4A__heat shock transcription factor A4A
A_84_P854510	0,03120647	0,0012808	1,770653	0,824282	AT5G02290	NAK	NAK__Protein kinase superfamily protein
A_84_P162193	0,04398862	0,0028882	1,766062	0,820536	AT5G62070	IQD23	IQD23__IQ-domain 23
A_84_P16834	0,03466453	0,0016626	1,764552	0,819302	AT5G28050		GSDA__Cytidine/deoxycytidylate deaminase family protein
A_84_P23105	0,01331538	1,12E-04	1,761843	0,817085	AT3G13110	ATSERAT2;2, SAT-	ATSERAT2;2_SAT-1_SAT-A_SAT-M_SAT3_SERAT2;2__serine acetyltransferase 2;2

A_84_P183994	0,04883185	0,0038135	1,760907	0,816318	AT3G14870		Plant protein of unknown function (DUF641)
A_84_P13308	0,04899432	0,0038572	1,759846	0,815449	AT1G79410	OCT5, AtOCT5	AtOCT5_OCT5__organic cation/carnitine transporter5
A_84_P817774	0,02676006	8,71E-04	1,758715	0,814522	AT5G61900;	BON,BON1,CPN1	
A_84_P579822	0,03172537	0,0013254	1,758058	0,813983	AT5G57880;	ATPRD2,MPS1,PRD2	
A_84_P830975	0,01731088	2,45E-04	1,757592	0,813601	AT1G30755		Protein of unknown function (DUF668)
A_84_P19628	0,02454009	7,13E-04	1,75705	0,813155	AT5G10820		Major facilitator superfamily protein
A_84_P110642	0,02277204	5,49E-04	1,755484	0,811869	AT2G36320		A20/AN1-like zinc finger family protein
A_84_P21264	0,04062048	0,0024375	1,75476	0,811274	AT3G48360	ATBT2, BT2	ATBT2_BT2__BTB and TAZ domain protein 2
A_84_P14621	0,02532245	7,78E-04	1,754397	0,810975	AT3G12520	SULTR4;2	SULTR4;2__sulfate transporter 4;2
A_84_P15984	0,03916847	0,0022098	1,75253	0,809439	AT5G61380	APRR1, AtTOC1, P	APRR1_AtTOC1_PRR1_TOC1__CCT motif -containing response regulator protein
A_84_P10998	0,04418246	0,0029216	1,752452	0,809375	AT4G23570	SGT1A	SGT1A__phosphatase-related
A_84_P806857	0,02524157	7,72E-04	1,752452	0,809375	AT5G28050		GSDA__Cytidine/deoxycytidylate deaminase family protein
A_84_P18708	0,0457815	0,0032323	1,752219	0,809183	AT5G23050	AAE17	AAE17__acyl-activating enzyme 17
A_84_P10638	0,02146564	4,74E-04	1,751707	0,808762	AT1G11260	ATSTP1, STP1	ATSTP1_STP1__sugar transporter 1
A_84_P830088	0,04017467	0,0023865	1,749064	0,806583	AT2G03240		EXS (ERD1/XPR1/SYG1) family protein
A_84_P97176	0,04856481	0,0037757	1,745036	0,803257	AT5G43190		Galactose oxidase/kelch repeat superfamily protein
A_84_P21538	0,03697815	0,0019423	1,744943	0,80318	AT5G18170	GDH1	GDH1__glutamate dehydrogenase 1
A_84_P23528	0,03317259	0,0014912	1,744134	0,802511	AT5G55700	BAM4, BMY6	BAM4_BMY6__beta-amylase 4
A_84_P20907	0,01564355	1,86E-04	1,738913	0,798185	AT1G49050		Eukaryotic aspartyl protease family protein
A_84_P571270	0,0282571	9,80E-04	1,737593	0,797091	AT2G28056	MIR172, MIR172A	MIR172_MIR172A__MIR172/MIR172A; miRNA
A_84_P93839	0,00877048	2,06E-05	1,737379	0,796912	AT1G78460		SOUL heme-binding family protein
A_84_P806863	0,01710836	2,38E-04	1,734841	0,794804	AT5G28050		GSDA__Cytidine/deoxycytidylate deaminase family protein
A_84_P22063	0,00894727	2,85E-05	1,734817	0,794784	AT2G48010	RKF3	RKF3__receptor-like kinase in in flowers 3
A_84_P13470	0,0313028	0,0012919	1,73436	0,794403	AT2G47890		B-box type zinc finger protein with CCT domain
A_84_P85169	0,01176281	7,78E-05	1,732777	0,793086	AT3G26600	ARO4	ARO4__armadillo repeat only 4
A_84_P241903	0,03438171	0,0016196	1,732716	0,793035	AT5G50200	ATNRT3.1, NRT3.1	ATNRT3.1_NRT3.1_WR3__nitrate transmembrane transporters
A_84_P18314	0,01065925	5,43E-05	1,732669	0,792996	AT3G10640	VPS60.1	VPS60.1__SNF7 family protein
A_84_P157795	0,01803394	2,94E-04	1,732505	0,792859	AT3G21070	ATNADK-1, NADK1	ATNADK-1_NADK1__NAD kinase 1
A_84_P15732	0,02532245	7,79E-04	1,730452	0,791149	AT4G25390		Protein kinase superfamily protein
A_84_P21970	0,04811797	0,0036322	1,729536	0,790385	AT2G22200		Integrase-type DNA-binding superfamily protein
A_84_P816956	0,01769782	2,64E-04	1,729453	0,790316	AT1G64190		6-phosphogluconate dehydrogenase family protein
A_84_P19863	0,02403887	6,54E-04	1,729295	0,790184	AT1G23830		
A_84_P816646	0,03954039	0,0022747	1,72713	0,788377	AT5G27380	GSH2, GSHB	AtGSH2_GSH2_GSHB__glutathione synthetase 2
A_84_P254390	0,04661662	0,0033712	1,726698	0,788015	AT2G30990		Protein of unknown function (DUF688)
A_84_P202508	0,03308225	0,0014848	1,725519	0,78703	AT1G73210		Protein of unknown function (DUF789)
A_84_P16794	0,04899432	0,0038536	1,725002	0,786598	AT1G18390		Protein kinase superfamily protein
A_84_P824802	0,03051006	0,0012073	1,724344	0,786048	AT2G44370		Cysteine/Histidine-rich C1 domain family protein
A_84_P88159	0,04538051	0,0031435	1,722204	0,784256	AT2G45360		Protein of unknown function (DUF1442)
A_84_P170233	0,01246891	9,27E-05	1,720364	0,782714	AT2G38000		chaperone protein dnaJ-related
A_84_P503984	0,0161733	2,03E-04	1,719128	0,781677	AT3G12510		MADS-box family protein
A_84_P862614	0,01188738	8,37E-05	1,718365	0,781036	AT3G22890	APS1	APS1__ATP sulfurylase 1
A_84_P82909	0,0467632	0,0034077	1,718289	0,780973	AT1G17830		Protein of unknown function (DUF789)
A_84_P273060	0,03308225	0,0014743	1,716116	0,779147	AT3G51090		Protein of unknown function (DUF1640)
A_84_P599034	0,01246891	9,46E-05	1,715161	0,778344	AT3G16860	COBL8	COBL8__COBRA-like protein 8 precursor
A_84_P854693	0,02612945	8,36E-04	1,713683	0,777101	AT5G63970		RGLG3__Copine (Calcium-dependent phospholipid-binding protein) family
A_84_P135625	0,03542483	0,0017563	1,711251	0,775051	AT4G25670;	CPuORF12	
A_84_P224559	0,04234786	0,0026691	1,706787	0,771283	AT5G13760		Plasma-membrane choline transporter family protein
A_84_P849522	0,01686909	2,28E-04	1,706371	0,770931	AT3G63010	ATGID1B, GID1B	ATGID1B_GID1B__alpha/beta-Hydrolases superfamily protein
A_84_P22207	0,03492962	0,0016899	1,705816	0,770462	AT3G47550		RING/FYVE/PHD zinc finger superfamily protein
A_84_P288524	0,03217042	0,001385	1,705339	0,770059	AT4G11850	MEE54, PLDGAMM	MEE54_PLDGAMMA1__phospholipase D gamma 1
A_84_P868111	0,02353903	5,91E-04	1,704156	0,769057	AT3G54020	AtIPCS1	AtIPCS1__Arabidopsis Inositol phosphorylceramide synthase 1

A_84_P21333	0,04572882	0,0032067	1,702465	0,767625	AT1G12200	FMO	FMO__Flavin-binding monooxygenase family protein
A_84_P257990	0,03178847	0,0013318	1,701722	0,766995	AT3G48350	CEP3	CEP3__Cysteine proteinases superfamily protein
A_84_P867087	0,03416876	0,0016007	1,699788	0,765355	AT5G54930		AT hook motif-containing protein
A_84_P561436	0,03916847	0,0022206	1,698545	0,764299	AT2G07749;	ORF251	
A_84_P810688	0,02362118	5,99E-04	1,697497	0,763409	AT5G15960	KIN1	KIN1__stress-responsive protein (KIN1) / stress-induced protein (KIN1)
A_84_P16701	0,02267799	5,40E-04	1,696147	0,762261	AT4G30350		SMXL2__Double Clp-N motif-containing P-loop nucleoside triphosphate hydrolases superfamily protein
A_84_P137419	0,03051635	0,0012156	1,695076	0,76135	AT1G21010		
A_84_P753864	0,00668285	8,51E-06	1,694665	0,761	AT1G67365		other RNA
A_84_P301020	0,03146277	0,0013111	1,694385	0,760761	AT4G25020		D111/G-patch domain-containing protein
A_84_P762519	0,04078834	0,0024636	1,690676	0,7576	AT3G21781		other RNA
A_84_P90109	0,0482928	0,0036917	1,68979	0,756844	AT3G05800	AIF1	AIF1__AtBS1(activation-tagged BRI1 suppressor 1)-interacting factor 1
A_84_P856001	0,03359263	0,0015367	1,686956	0,754422	AT5G17460		
A_84_P809392	0,01451456	1,46E-04	1,686218	0,753791	AT1G02880	TPK1	TPK1__thiamin pyrophosphokinase1TPK1__thiamin pyrophosphokinase1
A_84_P167973	0,02376995	6,19E-04	1,685983	0,75359	AT3G48450		RPM1-interacting protein 4 (RIN4) family proteinRPM1-interacting protein 4 (RIN4) family protein
A_84_P15372	0,03134441	0,0012987	1,685746	0,753387	AT2G38750	ANNAT4	ANNAT4_AtANN4__annexin 4
A_84_P852163	0,04387216	0,0028761	1,685675	0,753326	AT5G20250	DIN10, RS6	DIN10_RS6__Raffinose synthase family proteinDIN10_RS6__Raffinose synthase family protein
A_84_P761363	0,04311589	0,002762	1,685613	0,753274	AT3G13550	CIN4, COP10, EMB	CIN4_COP10_EMB144_FUS9__Ubiquitin-conjugating enzyme family protein
A_84_P159095	0,02445181	6,89E-04	1,68142	0,749681	AT1G33700		Beta-glucosidase, GBA2 type family protein
A_84_P21624	0,01156977	6,63E-05	1,681355	0,749624	AT1G64280	ATNPR1, NIM1, NP	ATNPR1_NIM1_NPR1_SAI1__regulatory protein (NPR1)
A_84_P12389	0,02067666	4,32E-04	1,681123	0,749425	AT1G14860	atnudt18, NUDT18	NUDT18_atnudt18__nudix hydrolase homolog 18
A_84_P821021	0,04927701	0,0039099	1,680366	0,748775	AT1G75020	LPAT4	LPAT4__lysophosphatidyl acyltransferase 4
A_84_P177674	0,0184221	3,11E-04	1,679499	0,748031	AT5G25210		
A_84_P765657	0,01504028	1,64E-04	1,677917	0,746672	AT4G40065		other RNA
A_84_P18514	0,03722991	0,0019627	1,677671	0,74646	AT1G06000		UDP-Glycosyltransferase superfamily protein
A_84_P13957	0,04141799	0,0025496	1,677585	0,746386	AT5G11650		alpha/beta-Hydrolases superfamily protein
A_84_P19477	0,02430013	6,79E-04	1,676546	0,745492	AT4G12080	AHL1, ATAHL1	AHL1_ATAHL1__AT-hook motif nuclear-localized protein 1
A_84_P754799	0,04603513	0,0032603	1,676209	0,745202	AT1G07780;	PAI1,TRP6,PAI2	
A_84_P785697	0,04368648	0,0028423	1,67508	0,74423	AT3G10260		Reticulon family protein
A_84_P19130	0,04387216	0,0028727	1,674623	0,743836	AT2G46270	GBF3	GBF3__G-box binding factor 3
A_84_P20210	0,02312453	5,69E-04	1,673013	0,742449	AT3G03190	ATGSTF11, ATGST	ATGSTF11_ATGSTF6_GSTF11__glutathione S-transferase F11
A_84_P833361	0,03681569	0,0019269	1,672622	0,742111	AT2G30100		pentatricopeptide (PPR) repeat-containing protein
A_84_P21398	0,02877405	0,001019	1,6693	0,739244	AT4G23270	CRK19	CRK19__cysteine-rich RLK (RECEPTOR-like protein kinase) 19
A_84_P19945	0,04572882	0,0032093	1,667122	0,73736	AT1G72850		Disease resistance protein (TIR-NBS class)
A_84_P529509	0,01971263	3,84E-04	1,66661	0,736917	AT1G77360		APPR6__Tetratricopeptide repeat (TPR)-like superfamily protein
A_84_P184384	0,01156977	6,65E-05	1,666043	0,736425	AT1G68440		
A_84_P861072	0,04254559	0,0026909	1,664049	0,734698	AT3G26740	CCL	CCL__CCR-likeCCL__CCR-like
A_84_P18041	0,01469936	1,56E-04	1,663158	0,733925	AT1G32690		
A_84_P715804	0,02681149	8,74E-04	1,662493	0,733348	AT5G18540		
A_84_P21584	0,02376995	6,13E-04	1,662449	0,73331	AT1G72210		bHLH096_bHLH96__basic helix-loop-helix (bHLH) DNA-binding superfamily protein
A_84_P761889	0,0145606	1,51E-04	1,65973	0,730948	AT3G16565		alanine-tRNA ligases;nucleic acid binding;ligases, forming aminoacyl-tRNA and related compounds
A_84_P852438	0,02454009	7,14E-04	1,659251	0,730532	AT5G24590	ANAC091, TIP	ANAC091_TIP__TCV-interacting proteinANAC091_TIP__TCV-interacting protein
A_84_P17654	0,03681569	0,0019256	1,659207	0,730494	AT4G31980		
A_84_P11048	0,02047567	4,18E-04	1,656537	0,72817	AT4G34810		SAUR5__SAUR-like auxin-responsive protein family
A_84_P82139	0,03959271	0,0022835	1,656263	0,727932	AT5G65920		ARM repeat superfamily protein
A_84_P67324	0,02883385	0,0010241	1,65555	0,72731	AT2G25930	ELF3, PYK20	ELF3_PYK20__hydroxyproline-rich glycoprotein family protein
A_84_P95179	0,03359263	0,0015326	1,654151	0,726091	AT1G44050		Cysteine/Histidine-rich C1 domain family protein
A_84_P817161	0,02684096	8,77E-04	1,653485	0,72551	AT4G30470		NAD(P)-binding Rossmann-fold superfamily proteinNAD(P)-binding Rossmann-fold superfamily protein
A_84_P17499	0,03474192	0,0016679	1,651308	0,723609	AT3G52800		A20/AN1-like zinc finger family protein
A_84_P766219	0,00877275	2,29E-05	1,650766	0,723136	AT5G26600		Pyridoxal phosphate (PLP)-dependent transferases superfamily protein
A_84_P20393	0,04473491	0,0030464	1,649941	0,722414	AT4G01910		Cysteine/Histidine-rich C1 domain family protein
A_84_P233289	0,03612883	0,0018274	1,64993	0,722405	AT1G80610		

A_84_P10413	0,01305407	1,05E-04	1,649713	0,722215	AT1G03905	ABCI19	ABCI19__P-loop containing nucleoside triphosphate hydrolases superfamily protein
A_84_P79549	0,00877275	2,21E-05	1,647751	0,720498	AT3G26090	ATRGS1, RGS1	ATRGS1_RGS1__G-protein coupled receptors;GTPase activators
A_84_P809384	0,04406328	0,0029002	1,646058	0,719015	AT1G76180	ERD14	ERD14__Dehydrin family proteinERD14__Dehydrin family protein
A_84_P833006	0,04418246	0,0029253	1,645951	0,718922	AT5G07730		
A_84_P851226	0,02951533	0,0011169	1,645702	0,718703	AT3G46640	LUX, PCL1	LUX_PCL1__Homeodomain-like superfamily protein
A_84_P79235	0,01498409	1,63E-04	1,643919	0,717139	AT3G11850		Protein of unknown function, DUF593Protein of unknown function, DUF593
A_84_P801314	0,03612883	0,001826	1,64258	0,715963	AT5G26600		Pyridoxal phosphate (PLP)-dependent transferases superfamily protein
A_84_P14271	0,04465805	0,0030097	1,642277	0,715697	AT1G66350	RGL, RGL1	RGL_RGL1__RGA-like 1
A_84_P19565	0,02676006	8,71E-04	1,640146	0,713824	AT4G37430	CYP81F1, CYP91A	CYP81F1_CYP91A2__cytochrome P450, family 91, subfamily A, polypeptide 2
A_84_P525365	0,03367786	0,0015556	1,638989	0,712806	AT3G57500		
A_84_P258390	0,04066901	0,0024491	1,638342	0,712236	AT4G25170		Uncharacterised conserved protein (UCP012943)
A_84_P789465	0,02955248	0,0011204	1,637404	0,711411	AT1G49720	ABF1	ABF1_AtABF1__abscisic acid responsive element-binding factor 1
A_84_P805290	0,04324035	0,0027809	1,63669	0,710781	AT1G75800		Pathogenesis-related thaumatin superfamily protein
A_84_P224479	0,02053168	4,20E-04	1,63641	0,710534	AT5G16650		Chaperone DnaJ-domain superfamily protein
A_84_P10858	0,01771716	2,71E-04	1,635349	0,709599	AT3G47160		RING/U-box superfamily protein
A_84_P816640	0,0243154	6,81E-04	1,634456	0,708811	AT5G27380	GSH2, GSHB	AtGSH2_GSH2_GSHB__glutathione synthetase 2
A_84_P11453	0,02445181	6,90E-04	1,63373	0,70817	AT1G53320	AtTLP7, TLP7	AtTLP7_TLP7__tubby like protein 7
A_84_P55070	0,02682222	8,75E-04	1,632891	0,707428	AT4G13030		P-loop containing nucleoside triphosphate hydrolases superfamily protein
A_84_P100746	0,01785415	2,81E-04	1,63274	0,707295	AT3G28220		TRAF-like family protein
A_84_P784699	0,04760732	0,0035326	1,63013	0,704987	AT5G41600	BTI3, RTNLB4	BTI3_RTNLB4__VIRB2-interacting protein
A_84_P13014	0,0364947	0,0018807	1,629889	0,704774	AT5G12110		Glutathione S-transferase, C-terminal-like;Translation elongation factor EF1B/ribosomal protein S6
A_84_P129666	0,03884352	0,0021491	1,629578	0,704498	AT5G07730		
A_84_P815258	0,01156977	6,70E-05	1,629353	0,704299	AT4G25690;	CPuORF13	
A_84_P13043	0,02507846	7,56E-04	1,629177	0,704144	AT5G25440		Protein kinase superfamily protein
A_84_P18693	0,03405143	0,0015914	1,628954	0,703946	AT1G18270		ketose-bisphosphate aldolase class-II family protein
A_84_P785373	0,02991192	0,0011546	1,628449	0,703499	AT1G78850		D-mannose binding lectin protein with Apple-like carbohydrate-binding domain
A_84_P183754	0,04181817	0,0026041	1,628319	0,703384	AT3G27420		
A_84_P11150	0,0308525	0,0012461	1,627381	0,702552	AT5G24590	ANAC091, TIP	ANAC091_TIP__TCV-interacting proteinANAC091_TIP__TCV-interacting protein
A_84_P107602	0,03875106	0,0021359	1,627369	0,702541	AT3G17860	JAI3, JAZ3, TIFY6B	JAI3_JAZ3_TIFY6B__jasmonate-zim-domain protein 3
A_84_P12615	0,02238792	5,26E-04	1,626652	0,701905	AT2G32235;	0	
A_84_P812535	0,01830757	3,03E-04	1,626203	0,701508	AT4G11650	ATOSM34, OSM34	ATOSM34_OSM34__osmotin 34ATOSM34_OSM34__osmotin 34
A_84_P11473	0,04799153	0,0036061	1,626075	0,701394	AT1G49650		alpha/beta-Hydrolases superfamily protein
A_84_P12764	0,04714022	0,0034525	1,625593	0,700966	AT3G50760	GATL2	GATL2__galacturonosyltransferase-like 2
A_84_P18117	0,02400674	6,46E-04	1,624354	0,699866	AT1G75800		Pathogenesis-related thaumatin superfamily protein
A_84_P765062	0,02943565	0,0010996	1,623314	0,698942	AT4G24415	MIR824A	MIR824A__MIR824a; miRNA
A_84_P17036	0,0145606	1,50E-04	1,622934	0,698605	AT1G77000	ATSKP2;2, SKP2B	ATSKP2;2_SKP2B__RNI-like superfamily protein
A_84_P22863	0,01565107	1,88E-04	1,621051	0,696929	AT1G22280	PAPP2C	PAPP2C__phytochrome-associated protein phosphatase type 2C
A_84_P205698	0,04572418	0,0031885	1,620705	0,696622	AT2G27260		Late embryogenesis abundant (LEA) hydroxyproline-rich glycoprotein family
A_84_P811421	0,03707299	0,0019498	1,620353	0,696308	AT5G20250	DIN10, RS6	DIN10_RS6__Raffinose synthase family proteinDIN10_RS6__Raffinose synthase family protein
A_84_P803838	0,03544915	0,0017626	1,618159	0,694353	AT4G25670;	CPuORF12CPuORF13	
A_84_P824252	0,03850592	0,0021143	1,614481	0,691071	AT3G08710	ATH9, TH9, TRX H	ATH9_TH9_TRX H9__thioredoxin H-type 9
A_84_P238313	0,04288919	0,0027335	1,61416	0,690784	AT4G26060		Ribosomal protein L18ae family
A_84_P23843	0,04261217	0,0026991	1,612606	0,689394	AT2G03200		Eukaryotic aspartyl protease family protein
A_84_P86519	0,04552032	0,0031627	1,61199	0,688843	AT5G04040	SDP1	SDP1__Patatin-like phospholipase family protein
A_84_P18500	0,03217042	0,0013846	1,611855	0,688722	AT4G01700		Chitinase family protein
A_84_P13049	0,01622046	2,05E-04	1,610694	0,687682	AT1G55850	ATCSLE1, CSLE1	ATCSLE1_CSLE1__cellulose synthase like E1
A_84_P562730	0,02039214	4,12E-04	1,609726	0,686815	AT4G38060		CCI2__
A_84_P10724	0,00230433	4,27E-07	1,60929	0,686424	AT2G30020		Protein phosphatase 2C family protein
A_84_P19752	0,02054225	4,24E-04	1,607769	0,68506	AT5G57900	SKIP1	SKIP1__SKP1 interacting partner 1
A_84_P16007	0,01958881	3,60E-04	1,607305	0,684644	AT5G66880	SNRK2.3, SNRK2-3	SNRK2-3_SNRK2.3_SRK2I__sucrose nonfermenting 1(SNF1)-related protein kinase 2.3
A_84_P198394	0,04461956	0,0029922	1,606945	0,68432	AT4G16670		Plant protein of unknown function (DUF828) with plant pleckstrin homology-like region

A_84_P848088	0,04556191	0,003174	1,60684	0,684226	AT1G63830		PLAC8 family proteinPLAC8 family protein
A_84_P764462	0,03773625	0,0020249	1,606574	0,683988	AT4G03510	ATRMA1, RMA1	ATRMA1_RMA1__RING membrane-anchor 1
A_84_P786348	0,03432886	0,0016155	1,605991	0,683464	AT1G69360		Plant protein of unknown function (DUF863)
A_84_P23887	0,04845812	0,0037607	1,605902	0,683384	AT2G22080		
A_84_P15331	0,03518269	0,0017113	1,604376	0,682013	AT2G43620		Chitinase family protein
A_84_P18852	0,02400674	6,46E-04	1,604175	0,681831	AT5G15870		glycosyl hydrolase family 81 protein
A_84_P16468	0,04418246	0,0029372	1,603715	0,681418	AT3G26740	CCL	CCL__CCR-likeCCL__CCR-like
A_84_P13801	0,02100365	4,52E-04	1,602835	0,680626	AT4G11650	ATOSM34, OSM34	ATOSM34_OSM34__osmotin 34
A_84_P848912	0,01775137	2,78E-04	1,602225	0,680077	AT5G42050		DCD (Development and Cell Death) domain protein
A_84_P857541	0,04813688	0,003646	1,60065	0,678658	AT4G26750	EXT-like	EXT-like_LIP5__hydroxyproline-rich glycoprotein family protein
A_84_P11479	0,02115263	4,62E-04	1,600444	0,678472	AT1G01260		JAM2__basic helix-loop-helix (bHLH) DNA-binding superfamily protein
A_84_P10767	0,01320943	1,09E-04	1,599281	0,677424	AT3G02990	ATHSFA1E, HSFA1	ATHSFA1E_HSFA1E__heat shock transcription factor A1E
A_84_P858372	0,03529944	0,0017304	1,596299	0,674731	AT1G75800		Pathogenesis-related thaumatin superfamily protein
A_84_P514578	0,04042752	0,0024193	1,596251	0,674687	AT2G48060		
A_84_P515753	0,03258517	0,0014312	1,596203	0,674644	AT4G31510		
A_84_P12278	0,03359263	0,0015442	1,59552	0,674027	AT1G12320		Protein of unknown function (DUF1442)
A_84_P830480	0,0364947	0,0018764	1,594789	0,673366	AT5G58040	ATFIP1[V], ATFIPS	ATFIP1[V]_ATFIPS5_FIP1[V]_FIPS5__homolog of yeast FIP1 [V]
A_84_P19320	0,03949743	0,0022695	1,593715	0,672394	AT3G16510		Calcium-dependent lipid-binding (CaLB domain) family protein
A_84_P567376	0,02452861	7,06E-04	1,592345	0,671153	AT5G66050		Wound-responsive family proteinWound-responsive family protein
A_84_P17510	0,04152048	0,0025578	1,592232	0,67105	AT1G23870	ATTPS9, TPS9	ATTPS9_TPS9__trehalose-phosphatase/synthase 9
A_84_P761677	0,03507878	0,0017004	1,592227	0,671046	AT3G45638		other RNA
A_84_P22255	0,03051006	0,001209	1,591696	0,670565	AT3G58710	ATWRKY69, WRKY	ATWRKY69_WRKY69__WRKY DNA-binding protein 69
A_84_P17345	0,02354743	5,93E-04	1,591464	0,670355	AT1G44790		ChaC-like family protein
A_84_P846313	0,0457815	0,0032268	1,591035	0,669966	AT3G11420		Protein of unknown function (DUF604)
A_84_P23665	0,03076559	0,0012383	1,589834	0,668876	AT1G03610		Protein of unknown function (DUF789)
A_84_P23239	0,0227833	5,52E-04	1,589633	0,668694	AT4G04220	AtRLP46, RLP46	AtRLP46_RLP46__receptor like protein 46
A_84_P21167	0,04444991	0,002972	1,588555	0,667715	AT3G02875	ILR1	ILR1__Peptidase M20/M25/M40 family protein
A_84_P573251	0,03206014	0,0013751	1,588419	0,667591	AT3G47200		Plant protein of unknown function (DUF247)
A_84_P796327	0,048729	0,0037986	1,588209	0,6674	AT5G20900	JAZ12, TIFY3B	JAZ12_TIFY3B__jasmonate-zim-domain protein 12
A_84_P609756	0,01386738	1,33E-04	1,586999	0,666301	AT3G50030		ARM-repeat/Tetratricopeptide repeat (TPR)-like protein
A_84_P826661	0,0364947	0,0018839	1,584987	0,664471	AT3G51890		CLC3__Clathrin light chain proteinCLC3__Clathrin light chain protein
A_84_P22526	0,04922931	0,0039004	1,584974	0,664459	AT5G40100		Disease resistance protein (TIR-NBS-LRR class) family
A_84_P12986	0,00772467	1,41E-05	1,584548	0,664071	AT5G04020		calmodulin binding
A_84_P86089	0,01163687	7,35E-05	1,582942	0,662608	AT4G25030		
A_84_P790810	0,02454009	7,11E-04	1,582816	0,662493	AT5G02200	FHL	FHL__far-red-elongated hypocotyl1-like
A_84_P724318	0,02551475	7,91E-04	1,58206	0,661804	AT5G06865		other RNA
A_84_P76794	0,02390528	6,30E-04	1,579719	0,659668	AT3G26680	ATSNM1, SNM1	ATSNM1_SNM1__DNA repair metallo-beta-lactamase family protein
A_84_P533074	0,04994319	0,0040396	1,579068	0,659073	AT1G78895		Reticulon family protein
A_84_P75484	0,04521387	0,0031124	1,578977	0,65899	AT3G14590	NTMC2T6.2, NTMC	NTMC2T6.2_NTMC2TYPE6.2__Calcium-dependent lipid-binding (CaLB domain) family protein
A_84_P13407	0,01592639	1,97E-04	1,577642	0,65777	AT1G18590	ATSOT17, ATST5C	ATSOT17_ATST5C_SOT17__sulfotransferase 17
A_84_P868662	0,03187662	0,0013471	1,57683	0,657027	AT4G30470		NAD(P)-binding Rossmann-fold superfamily protein
A_84_P845383	0,01947035	3,54E-04	1,575417	0,655734	AT3G51090		Protein of unknown function (DUF1640)
A_84_P11179	0,03076559	0,0012368	1,574926	0,655284	AT5G40170	AtRLP54, RLP54	AtRLP54_RLP54__receptor like protein 54
A_84_P511815	0,04103823	0,0024953	1,57434	0,654747	AT2G18193		P-loop containing nucleoside triphosphate hydrolases superfamily protein
A_84_P21622	0,03134441	0,0012999	1,572689	0,653233	AT5G51480	SKS2	SKS2__SKU5 similar 2
A_84_P824199	0,04418246	0,0029374	1,572425	0,652991	AT5G66050		Wound-responsive family proteinWound-responsive family protein
A_84_P582979	0,03916847	0,002211	1,570941	0,651629	AT3G15340	PPI2	PPI2__proton pump interactor 2
A_84_P11244	0,01331538	1,12E-04	1,567933	0,648864	AT5G58430	ATEXO70B1, EXO7	ATEXO70B1_EXO70B1__exocyst subunit exo70 family protein B1
A_84_P219858	0,04669211	0,0033903	1,566688	0,647718	AT5G13190	AtGILP, GILP	AtGILP_GILP__
A_84_P23085	0,0362616	0,0018465	1,566567	0,647607	AT3G25500	AFH1, AHF1, ATFH	AFH1_AHF1_ATFH1_FH1__formin homology 1
A_84_P809423	0,0487809	0,003805	1,566463	0,647511	AT1G76180	ERD14	ERD14__Dehydrin family protein

A_84_P571809	0,030758	0,0012302	1,566343	0,6474	AT5G58787		RING/U-box superfamily proteinRING/U-box superfamily protein
A_84_P10689	0,04418246	0,0029244	1,565611	0,646726	AT2G18750		Calmodulin-binding protein
A_84_P826018	0,01989875	3,90E-04	1,565531	0,646652	AT4G30240		Syntaxin/t-SNARE family protein
A_84_P16892	0,02376995	6,19E-04	1,565388	0,646521	AT1G56140		Leucine-rich repeat transmembrane protein kinase
A_84_P16856	0,03044238	0,0012006	1,564749	0,645931	AT5G41600	BTI3, RTNLB4	BTI3_RTNLB4__VIRB2-interacting protein 3
A_84_P171153	0,04917615	0,0038939	1,563376	0,644665	AT2G37940	AtIPCS2, ERH1	AtIPCS2_ERH1__Arabidopsis Inositol phosphorylceramide synthase 2
A_84_P15422	0,02230205	5,17E-04	1,563223	0,644524	AT2G23450		Protein kinase superfamily protein
A_84_P785057	0,02023179	4,06E-04	1,562928	0,644251	AT2G13790	ATSERK4, BAK7, B	ATSERK4_BAK7_BKK1_SERK4__somatic embryogenesis receptor-like kinase 4
A_84_P24061	0,04633552	0,0032936	1,562764	0,6441	AT3G19010		2-oxoglutarate (2OG) and Fe(II)-dependent oxygenase superfamily protein
A_84_P509060	0,04176612	0,0025841	1,561248	0,642699	AT1G63830		PLAC8 family proteinPLAC8 family protein
A_84_P857361	0,02026665	4,07E-04	1,560733	0,642223	AT4G28400		Protein phosphatase 2C family protein
A_84_P121962	0,04769728	0,0035547	1,560642	0,642139	AT3G27880		Protein of unknown function (DUF1645)
A_84_P14902	0,03850592	0,0021144	1,560615	0,642115	AT5G11670	ATNADP-ME2, NA	ATNADP-ME2_NADP-ME2__NADP-malic enzyme 2
A_84_P16129	0,04017467	0,002379	1,56003	0,641574	AT1G60140	ATTPS10, TPS10	ATTPS10_TPS10__trehalose phosphate synthase
A_84_P825682	0,04641205	0,0033372	1,558116	0,639803	AT5G66070		RING/U-box superfamily protein
A_84_P562314	0,0453766	0,0031366	1,557658	0,639379	AT2G04080		MATE efflux family protein
A_84_P515273	0,02091737	4,49E-04	1,557165	0,638922	AT1G61255		
A_84_P826495	0,04633552	0,0032966	1,555966	0,637811	AT3G55450	PBL1	PBL1__PBS1-like 1PBL1__PBS1-like 1
A_84_P716286	0,01276785	1,00E-04	1,555452	0,637334	AT5G48530		
A_84_P286360	0,03533791	0,0017416	1,553794	0,635796	AT3G03310	ATLCAT3, LCAT3	ATLCAT3_LCAT3__lecithin:cholesterol acyltransferase 3
A_84_P858684	0,01961223	3,64E-04	1,553267	0,635305	AT4G39090	RD19, RD19A	RD19_RD19A__Papain family cysteine protease
A_84_P23854	0,00772467	1,30E-05	1,552514	0,634606	AT2G31810		ACT domain-containing small subunit of acetolactate synthase protein
A_84_P20252	0,01592639	1,95E-04	1,550593	0,63282	AT3G26690	ATNUDT13, ATNU	ATNUDT13_ATNUDX13_NUDX13__nudix hydrolase homolog 13
A_84_P295744	0,01961223	3,71E-04	1,549467	0,631772	AT2G36310	NSH1, URH1	NSH1_URH1__uridine-ribohydrolase 1
A_84_P846636	0,01652713	2,17E-04	1,549271	0,63159	AT3G47550		RING/FYVE/PHD zinc finger superfamily protein
A_84_P23679	0,04521387	0,0031148	1,54825	0,630638	AT1G80920	AtJ8, AtToc12, J8,	AtJ8_AtToc12_DJC22_J8_Toc12__Chaperone DnaJ-domain superfamily protein
A_84_P23188	0,02740352	9,17E-04	1,547531	0,629969	AT3G55450	PBL1	PBL1__PBS1-like 1PBL1__PBS1-like 1
A_84_P824693	0,02511608	7,60E-04	1,544336	0,626987	AT5G58787		RING/U-box superfamily proteinRING/U-box superfamily protein
A_84_P23929	0,02449762	6,95E-04	1,543559	0,626261	AT2G18700	ATTPS11, ATTPSB	ATTPS11_ATTPSB_TPS11__trehalose phosphatase/synthase 11
A_84_P852053	0,03529944	0,0017286	1,542529	0,625298	AT4G25030		
A_84_P787591	0,03533791	0,0017405	1,540692	0,623578	AT4G15450		Senescence/dehydration-associated protein-related
A_84_P19881	0,02020968	4,04E-04	1,539853	0,622792	AT1G03740		Protein kinase superfamily protein
A_84_P16434	0,04421492	0,0029481	1,538734	0,621744	AT3G08710	ATH9, TH9, TRX H	ATH9_TH9_TRX H9__thioredoxin H-type 9
A_84_P18545	0,04991401	0,0040343	1,537353	0,620448	AT1G29280	ATWRKY65, WRKY	ATWRKY65_WRKY65__WRKY DNA-binding protein 65
A_84_P23535	0,02477556	7,37E-04	1,53516	0,618389	AT5G57630	CIPK21, SnRK3.4	CIPK21_SnRK3.4__CBL-interacting protein kinase 21
A_84_P20352	0,00894727	2,95E-05	1,533905	0,617209	AT3G55890		Yippee family putative zinc-binding protein
A_84_P17180	0,02342488	5,81E-04	1,532202	0,615606	AT1G18210		Calcium-binding EF-hand family protein
A_84_P818289	0,03367786	0,001558	1,531973	0,615391	AT3G47550		RING/FYVE/PHD zinc finger superfamily protein
A_84_P823703	0,0288939	0,0010353	1,53157	0,615011	AT5G52882		P-loop containing nucleoside triphosphate hydrolases superfamily protein
A_84_P592683	0,02497593	7,50E-04	1,531167	0,614632	AT2G30720		Thioesterase/thiol ester dehydrase-isomerase superfamily protein
A_84_P816721	0,03076559	0,0012361	1,530983	0,614458	AT4G36988;	CPuORF49,ATHSF4,AT-HSFB1,HSF4,HSFB1	
A_84_P271010	0,03006957	0,0011748	1,529913	0,613449	AT4G02550		
A_84_P23695	0,02991109	0,0011466	1,529087	0,61267	AT1G09250		AIF4__basic helix-loop-helix (bHLH) DNA-binding superfamily protein
A_84_P600173	0,03454188	0,0016551	1,528688	0,612294	AT5G03490		UDP-Glycosyltransferase superfamily protein
A_84_P11377	0,04181817	0,0026013	1,527671	0,611334	AT1G22890		
A_84_P848098	0,02381684	6,25E-04	1,522123	0,606085	AT3G08710	ATH9, TH9, TRX H	ATH9_TH9_TRX H9__thioredoxin H-type 9
A_84_P102836	0,02140161	4,71E-04	1,520263	0,604321	AT3G54620	ATBZIP25, BZIP25,	ATBZIP25_BZIP25_BZO2H4__basic leucine zipper 25
A_84_P532550	0,02100365	4,52E-04	1,519573	0,603666	AT4G18140	SSP4b	SSP4b__SCP1-like small phosphatase 4b
A_84_P16726	0,03585444	0,0018047	1,519003	0,603125	AT4G36140		disease resistance protein (TIR-NBS-LRR class), putative
A_84_P247395	0,01386093	1,32E-04	1,518802	0,602934	AT3G26470		Powdery mildew resistance protein, RPW8 domain
A_84_P13876	0,03438211	0,0016204	1,517646	0,601835	AT4G33160		F-box family protein

A_84_P11368	0,01658668	2,19E-04	1,516155	0,600417	AT1G61260		Protein of unknown function (DUF761)
A_84_P104016	0,03075464	0,0012272	1,515679	0,599964	AT1G05805		AKS2__basic helix-loop-helix (bHLH) DNA-binding superfamily protein
A_84_P563023	0,0362616	0,0018465	1,514719	0,599051	AT1G17145		RING/U-box superfamily protein
A_84_P601724	0,01565107	1,87E-04	1,513274	0,597673	AT3G25070	RIN4	RIN4__RPM1 interacting protein 4
A_84_P24015	0,02991192	0,0011549	1,511968	0,596428	AT3G17700	ATCNGC20, CNBT	ATCNGC20_CNBT1_CNGC20__cyclic nucleotide-binding transporter 1
A_84_P560796	0,02546071	7,87E-04	1,510989	0,595493	AT3G49550		
A_84_P190014	0,02693361	8,82E-04	1,51036	0,594892	AT4G36030	ARO3	ARO3__armadillo repeat only 3
A_84_P527116	0,02167651	4,88E-04	1,508931	0,593527	AT3G48180		
A_84_P817922	0,0407948	0,0024649	1,508367	0,592987	AT5G39410		Saccharopine dehydrogenase
A_84_P14067	0,04896518	0,0038439	1,50828	0,592904	AT5G54860		Major facilitator superfamily protein
A_84_P210718	0,04533307	0,0031308	1,508174	0,592803	AT3G60200		
A_84_P268440	0,03991389	0,0023248	1,508117	0,592749	AT2G15270		
A_84_P195794	0,04176612	0,0025827	1,505281	0,590033	AT4G19390		Uncharacterised protein family (UPF0114)
A_84_P306090	0,019105	3,41E-04	1,505148	0,589905	AT2G05260		alpha/beta-Hydrolases superfamily protein
A_84_P145439	0,04473491	0,0030442	1,50365	0,588469	AT2G31865	PARG2	PARG2__poly(ADP-ribose) glycohydrolase 2
A_84_P15196	0,03134441	0,0013002	1,503363	0,588193	AT1G03080		NET1D__kinase interacting (KIP1-like) family protein
A_84_P822818	0,04975333	0,0040029	1,502816	0,587669	AT3G03310	ATLCAT3, LCAT3	ATLCAT3_LCAT3__lecithin:cholesterol acyltransferase 3
A_84_P17328	0,02189142	4,99E-04	1,502294	0,587167	AT2G39350	ABCG1	ABCG1__ABC-2 type transporter family protein
A_84_P826468	0,03359263	0,0015334	1,501221	0,586136	AT1G21010		
A_84_P22022	0,04917615	0,0038908	1,501039	0,585961	AT2G22330	CYP79B3	CYP79B3__cytochrome P450, family 79, subfamily B, polypeptide 3
A_84_P66154	0,0145606	1,51E-04	1,500872	0,585801	AT5G63880	VPS20.1	VPS20.1__SNF7 family protein
A_84_P10582	0,02277204	5,48E-04	1,50043	0,585376	AT1G78600	BBX22, DBB3, LZF	BBX22_DBB3_LZF1_STH3__light-regulated zinc finger protein 1
A_84_P171853	0,01163687	7,08E-05	1,500097	0,585055	AT1G13390		
A_84_P103326	0,02449767	7,01E-04	-1,50047	-0,58541	AT1G61990		Mitochondrial transcription termination factor family protein
A_84_P597006	0,03355331	0,0015169	-1,50197	-0,58686	AT1G66250		O-Glycosyl hydrolases family 17 protein
A_84_P20046	0,0322775	0,0014009	-1,50441	-0,5892	AT1G14280	PKS2	PKS2__phytochrome kinase substrate 2
A_84_P219518	0,04473491	0,003047	-1,50485	-0,58962	AT1G65295		
A_84_P833726	0,03014083	0,0011813	-1,50514	-0,5899	AT1G66730	AtLIG6, LIG6	AtLIG6_LIG6__DNA LIGASE 6
A_84_P249845	0,03960313	0,0022977	-1,50591	-0,59063	AT3G46870		Pentatricopeptide repeat (PPR) superfamily protein
A_84_P820158	0,04418246	0,0029296	-1,50729	-0,59195	AT2G18050	HIS1-3	HIS1-3__histone H1-3
A_84_P135105	0,02612251	8,32E-04	-1,50775	-0,59239	AT3G17640		Leucine-rich repeat (LRR) family protein
A_84_P21908	0,0451422	0,0031029	-1,50784	-0,59249	AT1G51830		Leucine-rich repeat protein kinase family protein
A_84_P597910	0,04633552	0,0032962	-1,50811	-0,59274	AT1G68870	ATSOFL2, SOFL2	ATSOFL2_SOFL2__SOB five-like 2
A_84_P274710	0,04173238	0,0025776	-1,50832	-0,59294	AT4G14510	ATCFM3B, CFM3B	ATCFM3B_CFM3B__CRM family member 3B
A_84_P16440	0,03628755	0,0018514	-1,5093	-0,59388	AT3G04140		Ankyrin repeat family protein
A_84_P814976	0,02167651	4,88E-04	-1,50984	-0,5944	AT2G21970	SEP2	SEP2__stress enhanced protein 2
A_84_P16685	0,04636379	0,0033204	-1,51131	-0,5958	AT4G26790		GDSL-like Lipase/Acylhydrolase superfamily protein
A_84_P199044	0,03927432	0,0022339	-1,51182	-0,59629	AT1G63150		Tetratricopeptide repeat (TPR)-like superfamily protein
A_84_P848439	0,04416341	0,002914	-1,51262	-0,59705	AT1G11860		Glycine cleavage T-protein family
A_84_P254330	0,03739099	0,0019835	-1,51277	-0,59719	AT4G17600	LIL3:1	LIL3:1__Chlorophyll A-B binding family protein
A_84_P15056	0,038253	0,0020837	-1,51368	-0,59806	AT5G65710	HSL2	HSL2__HAESA-like 2
A_84_P502211	0,04006887	0,002348	-1,51496	-0,59928	AT3G18970	MEF20	MEF20__mitochondrial editing factor 20
A_84_P852804	0,04017467	0,0023723	-1,51576	-0,60004	AT5G21430	CRRL, NdhU	CRRL_NdhU__Chaperone DnaJ-domain superfamily protein
A_84_P792605	0,0342136	0,0016069	-1,5158	-0,60008	AT3G61310		AHL11__AT hook motif DNA-binding family protein
A_84_P520864	0,02991192	0,0011505	-1,51653	-0,60078	AT3G23370		RNA-binding (RRM/RBD/RNP motifs) family protein
A_84_P22024	0,01902633	3,38E-04	-1,51675	-0,60098	AT1G07640	OBP2	OBP2_URP3__Dof-type zinc finger DNA-binding family protein
A_84_P269540	0,04636379	0,0033192	-1,51692	-0,60114	AT2G18500	ATOFP7, OFP7	ATOFP7_OFP7__ovate family protein 7
A_84_P187824	0,04521387	0,0031152	-1,51754	-0,60173	AT2G31625;	ATDPB2,CYL2,DPB2	
A_84_P19654	0,01504028	1,66E-04	-1,51765	-0,60184	AT5G23070		AtTK1b_TK1b__Thymidine kinase
A_84_P10143	0,04006887	0,0023487	-1,51774	-0,60192	AT5G01930	AtMAN6, MAN6	AtMAN6_MAN6__Glycosyl hydrolase superfamily protein
A_84_P21919	0,03910996	0,002191	-1,51794	-0,60212	AT1G25440		BBX15__B-box type zinc finger protein with CCT domain

A_84_P242453	0,0362341	0,0018344	-1,51816	-0,60232	AT5G22020		Calcium-dependent phosphotriesterase superfamily protein
A_84_P784376	0,01633501	2,12E-04	-1,5189	-0,60302	AT3G61550		RING/U-box superfamily protein
A_84_P22494	0,03884352	0,0021488	-1,52094	-0,60497	AT5G23730	EFO2, RUP2	EFO2_RUP2__Transducin/WD40 repeat-like superfamily protein
A_84_P823506	0,04418246	0,0029406	-1,52108	-0,6051	AT1G06690		NAD(P)-linked oxidoreductase superfamily protein
A_84_P18709	0,04461956	0,0029978	-1,52111	-0,60512	AT5G23300	PYRD	PYRD__pyrimidine d
A_84_P19909	0,03764553	0,0020148	-1,52128	-0,60529	AT1G04180	YUC9	YUC9__YUCCA 9
A_84_P863005	0,04317679	0,0027689	-1,52141	-0,60541	AT1G80030		DJA7__Molecular chaperone Hsp40/DnaJ family protein
A_84_P814482	0,03999281	0,0023384	-1,52358	-0,60747	AT2G43710	FAB2, SSI2	AtSSI2_FAB2_LDW1_SSI2__Plant stearoyl-acyl-carrier-protein desaturase family protein
A_84_P16824	0,00884543	2,41E-05	-1,52381	-0,60768	AT5G25280		serine-rich protein-related
A_84_P841750	0,04636379	0,003312	-1,52436	-0,6082	AT5G15980		Pentatricopeptide repeat (PPR) superfamily protein
A_84_P231009	0,02894387	0,0010463	-1,52491	-0,60873	AT1G01070		UMAMIT28__nodulin MtN21 /EamA-like transporter family protein
A_84_P17580	0,03359263	0,0015368	-1,52718	-0,61087	AT4G10770	ATOPT7, OPT7	ATOPT7_OPT7__oligopeptide transporter 7
A_84_P810803	0,02951533	0,0011147	-1,52933	-0,6129	AT3G55360	ATTSC13, CER10,	ATTSC13_CER10_ECR_GLH6_TSC13__3-oxo-5-alpha-steroid 4-dehydrogenase family protein
A_84_P229999	0,04455438	0,002981	-1,52992	-0,61346	AT4G31330		Protein of unknown function, DUF599
A_84_P832601	0,04691907	0,0034228	-1,53085	-0,61433	ATCG01010	NDHF	NDHF__NADH-Ubiquinone oxidoreductase (complex I), chain 5 protein
A_84_P798859	0,04831925	0,0037132	-1,53094	-0,61442	AT1G73970		
A_84_P814104	0,02991192	0,001159	-1,53114	-0,6146	AT5G23060	CaS	CaS__calcium sensing receptor
A_84_P176234	0,03090113	0,001254	-1,53174	-0,61517	AT2G36070	ATTIM44-2, TIM44-	ATTIM44-2_TIM44-2__translocase inner membrane subunit 44-2
A_84_P832189	0,04811797	0,0036324	-1,53269	-0,61607	AT5G67030	ABA1, ATABA1, AT	ABA1_ATABA1_ATZEP_IBS3_LOS6_NPQ2_ZEP__zeaxanthin epoxidase (ZEP) (ABA1)
A_84_P796549	0,03959642	0,0022876	-1,53299	-0,61634	AT3G06868		
A_84_P551820	0,03454188	0,0016479	-1,53385	-0,61716	AT3G04770	RPSAb	RPSAb__40s ribosomal protein SA B
A_84_P244465	0,03358237	0,001526	-1,53398	-0,61728	AT3G28920	AtHB34, HB34, ZH	AtHB34_HB34_ZHD9__homeobox protein 34
A_84_P13830	0,04669211	0,0033867	-1,53413	-0,61742	AT4G22910	CCS52A1, FZR2	CCS52A1_FZR2__FIZZY-related 2
A_84_P751425	0,04831925	0,0037181	-1,5344	-0,61768	AT1G64770	NDF2, NDH45, Pns	NDF2_NDH45_PnsB2__NDH-dependent cyclic electron flow 1
A_84_P17816	0,03026108	0,0011907	-1,53508	-0,61831	AT5G45428;	CPuORF24	
A_84_P52410	0,04418246	0,002932	-1,53508	-0,61831	AT4G37080		Protein of unknown function, DUF547
A_84_P22890	0,0312771	0,0012901	-1,53527	-0,61849	AT1G14410	ATWHY1, PTAC1,	ATWHY1_PTAC1_WHY1__ssDNA-binding transcriptional regulator
A_84_P21158	0,02943565	0,0010994	-1,53594	-0,61912	AT3G04550		
A_84_P20800	0,02342488	5,81E-04	-1,53617	-0,61934	AT1G17700	PRA1.F1	PRA1.F1__prenylated RAB acceptor 1.F1
A_84_P786032	0,04991401	0,0040314	-1,53671	-0,61985	AT4G26850	VTC2	VTC2__mannose-1-phosphate guanylyltransferase (GDP)s;
A_84_P200084	0,01198826	8,55E-05	-1,53701	-0,62012	AT5G22090		Protein of unknown function (DUF3049)
A_84_P15878	0,0320905	0,0013771	-1,53746	-0,62055	AT5G25265		
A_84_P18535	0,04368648	0,0028415	-1,53781	-0,62088	AT4G13020	MHK	MHK__Protein kinase superfamily protein
A_84_P13453	0,01610925	2,00E-04	-1,53835	-0,62139	AT2G34060		Peroxidase superfamily protein
A_84_P835993	0,02780123	9,50E-04	-1,539	-0,62199	AT3G07610	IBM1	IBM1__Transcription factor jumonji (jmjC) domain-containing protein
A_84_P826941	0,04488314	0,0030738	-1,53919	-0,62217	AT1G03400		2-oxoglutarate (2OG) and Fe(II)-dependent oxygenase superfamily protein
A_84_P13380	0,03010546	0,0011771	-1,5398	-0,62275	AT1G79890		RAD3-like DNA-binding helicase protein
A_84_P13476	0,02009357	3,99E-04	-1,53997	-0,62291	AT2G18230	AtPPa2, PPa2	AtPPa2_PPa2__pyrophosphorylase 2
A_84_P16395	0,04292951	0,0027411	-1,54004	-0,62297	AT2G03480	QUL2	QUL2__QUASIMODO2 LIKE 2
A_84_P558547	0,04838306	0,0037401	-1,5408	-0,62368	AT5G65850		F-box and associated interaction domains-containing protein
A_84_P23671	0,02069154	4,36E-04	-1,54309	-0,62582	AT1G22850		SNARE associated Golgi protein family
A_84_P21554	0,02892086	0,0010409	-1,54343	-0,62614	AT5G25380	CYCA2;1	CYCA2;1__cyclin a2;1
A_84_P173411	0,03927432	0,0022348	-1,54364	-0,62633	AT3G22210		
A_84_P17664	0,04482194	0,0030622	-1,54375	-0,62644	AT4G34510	KCS17	KCS17__3-ketoacyl-CoA synthase 17
A_84_P829818	0,02695145	8,86E-04	-1,54404	-0,62671	AT4G39470		Tetratricopeptide repeat (TPR)-like superfamily protein
A_84_P533478	0,02436664	6,85E-04	-1,54422	-0,62687	AT4G27510		
A_84_P816178	0,03003507	0,0011721	-1,54463	-0,62727	AT1G76080	ATCDSP32, CDSP	ATCDSP32_CDSP32__chloroplastic drought-induced stress protein of 32 kD
A_84_P12263	0,04636379	0,0033053	-1,54481	-0,62743	AT5G38460		ALG6, ALG8 glycosyltransferase family
A_84_P525958	0,03557096	0,0017704	-1,54536	-0,62794	AT1G77630	LYM3	LYM3_LYP3__Peptidoglycan-binding LysM domain-containing protein
A_84_P792532	0,04639575	0,0033295	-1,54585	-0,6284	AT1G16489		other RNA
A_84_P758952	0,03219107	0,0013867	-1,54659	-0,62909	AT3G13062		Polyketide cyclase/dehydrase and lipid transport superfamily protein

A_84_P15712	0,03189056	0,001356	-1,54895	-0,63129	AT1G29170	ATSCAR3, SCAR3,	ATSCAR3_SCAR3_WAVE2__SCAR family protein
A_84_P15048	0,04465805	0,0030141	-1,54912	-0,63145	AT5G63710		Leucine-rich repeat protein kinase family protein
A_84_P512133	0,04648656	0,0033515	-1,54949	-0,6318	AT4G15810		P-loop containing nucleoside triphosphate hydrolases superfamily protein
A_84_P14035	0,03542483	0,0017535	-1,5505	-0,63274	AT5G45960		GDSL-like Lipase/Acylhydrolase superfamily protein
A_84_P519451	0,03091118	0,0012557	-1,55126	-0,63344	AT5G52950		
A_84_P846263	0,03173109	0,0013264	-1,55146	-0,63362	AT1G11860		Glycine cleavage T-protein familyGlycine cleavage T-protein family
A_84_P17110	0,04829036	0,0036839	-1,55179	-0,63393	AT1G77850	ARF17	ARF17__auxin response factor 17
A_84_P814302	0,03959271	0,0022859	-1,55325	-0,63529	AT5G11420		Protein of unknown function, DUF642
A_84_P819943	0,0443487	0,0029617	-1,55391	-0,63591	AT3G14400	UBP25	UBP25__ubiquitin-specific protease 25
A_84_P837815	0,00904516	3,77E-05	-1,55438	-0,63634	AT5G44410		FAD-binding Berberine family protein
A_84_P200834	0,04972693	0,0039951	-1,55494	-0,63686	AT1G58070		
A_84_P283520	0,04478252	0,0030585	-1,55502	-0,63694	AT4G28740		
A_84_P10351	0,03001025	0,0011687	-1,55533	-0,63722	AT5G20380	PHT4;5	PHT4;5__phosphate transporter 4;5
A_84_P820541	0,04831884	0,0037018	-1,55577	-0,63763	AT3G02640		
A_84_P15584	0,04327241	0,002785	-1,55611	-0,63794	AT3G47250		Plant protein of unknown function (DUF247)
A_84_P21608	0,02584636	8,12E-04	-1,55631	-0,63813	AT5G47630	mtACP3	mtACP3__mitochondrial acyl carrier protein 3
A_84_P127121	0,03569937	0,0017858	-1,55639	-0,63821	AT5G44650	AtCEST, CEST, Y3	AtCEST_CEST_Y3IP1__
A_84_P15095	0,03014083	0,00118	-1,55737	-0,63911	AT5G04140	FD-GOGAT, GLS1,	FD-GOGAT_GLS1_GLU1_GLUS__glutamate synthase 1
A_84_P166003	0,03681569	0,001924	-1,55868	-0,64032	AT3G13510		Protein of Unknown Function (DUF239)
A_84_P18937	0,0317688	0,0013295	-1,55925	-0,64085	AT1G08640	CJD1	CJD1__Chloroplast J-like domain 1
A_84_P787659	0,03120647	0,0012794	-1,56015	-0,64169	AT4G09970		
A_84_P12807	0,04780289	0,0035726	-1,56119	-0,64264	AT3G60720	PDLP8	PDLP8__plasmodesmata-located protein 8
A_84_P16721	0,0475861	0,0035275	-1,56141	-0,64285	AT4G35030		Protein kinase superfamily protein
A_84_P547377	0,0340082	0,0015886	-1,56178	-0,64319	AT2G43110		
A_84_P11745	0,03907514	0,0021864	-1,56196	-0,64336	AT3G29200	ATCM1, CM1	ATCM1_CM1__chorismate mutase 1
A_84_P11371	0,02417585	6,66E-04	-1,56309	-0,6444	AT1G64680		
A_84_P764999	0,03916847	0,0022195	-1,56309	-0,6444	AT4G26795		other RNA
A_84_P17948	0,02924256	0,001081	-1,56385	-0,6451	AT1G01860	PFC1	PFC1__Ribosomal RNA adenine dimethylase family protein
A_84_P19075	0,01163597	6,79E-05	-1,56482	-0,64599	AT1G19920	APS2, ASA1	APS2_ASA1__Pseudouridine synthase/archaeosine transglycosylase-like family protein
A_84_P819016	0,02826573	9,81E-04	-1,56575	-0,64685	AT2G17695		
A_84_P764875	0,01961223	3,72E-04	-1,56583	-0,64693	AT4G37925	NdhM, NDH-M	NDH-M_NdhM__subunit NDH-M of NAD(P)H:plastoquinone dehydrogenase complex
A_84_P22819	0,03727133	0,0019683	-1,5661	-0,64717	AT1G35910	TPPD	TPPD__Haloacid dehalogenase-like hydrolase (HAD) superfamily protein
A_84_P763808	0,01375994	1,26E-04	-1,56614	-0,64722	AT4G08940		Ubiquitin carboxyl-terminal hydrolase family protein
A_84_P56690	0,01375994	1,27E-04	-1,56659	-0,64763	AT4G32770	ATSDX1, VTE1	ATSDX1_VTE1__tocopherol cyclase, chloroplast/vitamin E deficient 1 (VTE1) / sucrose export defective 1
A_84_P824668	0,01742975	2,51E-04	-1,56706	-0,64806	AT3G01140	AtMYB106, MYB10	AtMYB106_MYB106_NOK__myb domain protein 106
A_84_P750079	0,01163687	6,86E-05	-1,56727	-0,64825	AT1G75150		
A_84_P813537	0,02894387	0,0010464	-1,56758	-0,64854	AT3G55800	SBPASE	SBPASE__sedoheptulose-bisphosphatase
A_84_P835427	0,04066901	0,0024472	-1,56852	-0,64941	AT1G66250		O-Glycosyl hydrolases family 17 protein
A_84_P223799	0,02948737	0,0011068	-1,56903	-0,64987	AT5G22100		RNA cyclase family protein
A_84_P858457	0,02381684	6,23E-04	-1,57074	-0,65144	AT4G28450		nucleotide binding;protein binding
A_84_P268710	0,0390369	0,0021804	-1,57166	-0,65229	AT2G47910	CRR6	CRR6__chlororespiratory reduction 6
A_84_P238393	0,04521387	0,0031149	-1,57188	-0,65249	AT4G22900		Protein of unknown function (DUF1191)
A_84_P762707	0,03264978	0,0014382	-1,57431	-0,65472	AT3G06868		
A_84_P13335	0,03963988	0,0023015	-1,57497	-0,65533	AT1G08280		GALT29A__Glycosyltransferase family 29 (sialyltransferase) family protein
A_84_P568326	0,03010546	0,0011776	-1,57511	-0,65546	AT1G09812		
A_84_P20506	0,04730906	0,0034714	-1,57524	-0,65558	AT4G35290	ATGLR3.2, ATGLU	ATGLR3.2_ATGLUR2_GLR3.2_GLUR2__glutamate receptor 2
A_84_P13126	0,03333252	0,001503	-1,57548	-0,65579	AT5G56040		SKM2__Leucine-rich receptor-like protein kinase family protein
A_84_P819331	0,04830764	0,0036964	-1,57601	-0,65628	AT5G48790		Domain of unknown function (DUF1995)
A_84_P763996	0,04555509	0,0031723	-1,57611	-0,65637	AT4G25700	B1, BCH1, BETA-O	B1_BCH1_BETA-OHASE 1_chy1__beta-hydroxylase 1
A_84_P23556	0,03891045	0,0021537	-1,57627	-0,65652	AT5G62230	ERL1	ERL1__ERECTA-like 1
A_84_P11751	0,01132469	6,26E-05	-1,57793	-0,65804	AT3G13810	AtIDD11, IDD11	AtIDD11_IDD11__indeterminate(ID)-domain 11

A_84_P13730	0,03411908	0,0015954	-1,57798	-0,65808	AT3G55340	PHIP1	PHIP1__phragmoplastin interacting protein 1
A_84_P841956	0,01634308	2,13E-04	-1,57875	-0,65878	AT5G48790		Domain of unknown function (DUF1995)
A_84_P18482	0,00857212	1,84E-05	-1,5801	-0,66002	AT3G61460	BRH1	BRH1__brassinosteroid-responsive RING-H2
A_84_P11357	0,03895907	0,0021582	-1,58027	-0,66017	AT1G62500		Bifunctional inhibitor/lipid-transfer protein/seed storage 2S albumin superfamily protein
A_84_P786301	0,02915839	0,001071	-1,581	-0,66084	AT3G13940		DNA binding;DNA-directed RNA polymerases
A_84_P756542	0,01004329	4,58E-05	-1,58139	-0,66119	AT2G20724		
A_84_P817921	0,01774115	2,76E-04	-1,58141	-0,66121	AT1G68830	STN7	STN7__STT7 homolog STN7
A_84_P772575	0,01742975	2,51E-04	-1,58149	-0,66128	AT1G62250		
A_84_P10436	0,02929986	0,0010857	-1,58347	-0,66309	AT1G09890		Rhamnogalacturonate lyase family protein
A_84_P20048	0,03785144	0,0020358	-1,58377	-0,66337	AT1G14345		NAD(P)-linked oxidoreductase superfamily protein
A_84_P811308	0,03914714	0,0022024	-1,58441	-0,66395	AT5G54770	THI1, THI4, TZ	THI1_THI4_TZ__thiazole biosynthetic enzyme, chloroplast (ARA6) (THI1) (THI4)
A_84_P847474	0,04092497	0,0024823	-1,58683	-0,66615	AT1G54385		ARM repeat superfamily proteinARM repeat superfamily protein
A_84_P849653	0,0362616	0,0018463	-1,58695	-0,66626	AT2G01680		Ankyrin repeat family protein
A_84_P788379	0,01768366	2,61E-04	-1,58755	-0,6668	AT3G14740		RING/FYVE/PHD zinc finger superfamily protein
A_84_P823140	0,02820842	9,76E-04	-1,58757	-0,66682	AT5G51110		Transcriptional coactivator/pterin dehydratase
A_84_P602807	0,0145606	1,48E-04	-1,58761	-0,66686	AT4G31400	CTF7	AtCTF7_CTF7_ECO1__damaged DNA binding;DNA-directed DNA polymerases
A_84_P186644	0,04418246	0,0029325	-1,5877	-0,66694	AT2G37240		Thioredoxin superfamily protein
A_84_P22703	0,0145606	1,50E-04	-1,58822	-0,66741	AT1G31050		basic helix-loop-helix (bHLH) DNA-binding superfamily protein
A_84_P294634	0,01961223	3,75E-04	-1,58869	-0,66784	AT5G53500		Transducin/WD40 repeat-like superfamily protein
A_84_P16435	0,04403443	0,0028972	-1,58924	-0,66834	AT3G07820		Pectin lyase-like superfamily protein
A_84_P23174	0,03258517	0,0014323	-1,59031	-0,66931	AT3G52720	ACA1, ATACA1, CA	ACA1_ATACA1_CAH1__alpha carbonic anhydrase 1
A_84_P186514	0,02454009	7,16E-04	-1,59061	-0,66958	AT5G45100	BRG1	BRG1__SBP (S-ribonuclease binding protein) family protein
A_84_P18751	0,0390369	0,0021773	-1,59147	-0,67036	AT1G68570		AtNPF3.1_NPF3.1__Major facilitator superfamily protein
A_84_P10327	0,04234786	0,0026648	-1,5923	-0,67111	AT5G64840	ABCF5, ATGCN5,	ABCF5_ATGCN5_GCN5__general control non-repressible 5
A_84_P11672	0,04799153	0,0036061	-1,59274	-0,67151	AT2G22920	SCPL12	SCPL12__serine carboxypeptidase-like 12
A_84_P856078	0,02084717	4,45E-04	-1,59305	-0,67179	AT3G01500	ATBCA1, ATSABP3	ATBCA1_ATSABP3_CA1_SABP3__carbonic anhydrase 1
A_84_P15425	0,03913154	0,0021932	-1,59305	-0,67179	AT1G67750		Pectate lyase family protein
A_84_P810038	0,04262674	0,0027035	-1,59318	-0,67191	AT5G14740	BETA CA2, CA18,	BETA CA2_CA18_CA2__carbonic anhydrase 2
A_84_P10692	0,02507846	7,58E-04	-1,59337	-0,67208	AT2G36880	MAT3	MAT3__methionine adenosyltransferase 3
A_84_P785818	0,03003507	0,0011713	-1,5943	-0,67292	AT3G28200		Peroxidase superfamily protein
A_84_P20345	0,02381684	6,23E-04	-1,59547	-0,67398	AT3G54280	ATBTAF1, BTAF1,	ATBTAF1_BTAF1_CHA16_CHR16_RGD3__DNA binding;ATP binding;nucleic acid binding
A_84_P847105	0,02612251	8,31E-04	-1,5955	-0,67401	AT5G53020		Ribonuclease P protein subunit P38-related
A_84_P575740	0,03220695	0,0013898	-1,59658	-0,67498	AT2G35550	ATBPC7, BBR, BP	ATBPC7_BBR_BPC7__basic pentacysteine 7
A_84_P23100	0,0485757	0,0037809	-1,59817	-0,67643	AT3G15570		Phototropic-responsive NPH3 family protein
A_84_P13702	0,0286969	0,0010094	-1,59818	-0,67643	AT3G49240	emb1796	emb1796__Pentatricopeptide repeat (PPR) superfamily protein
A_84_P727905	0,04294266	0,0027434	-1,59924	-0,67739	AT1G14650		SWAP (Suppressor-of-White-APricot)/surp domain-containing protein / ubiquitin family protein
A_84_P562243	0,04831925	0,0037107	-1,60027	-0,67832	AT1G62350		Pentatricopeptide repeat (PPR) superfamily protein
A_84_P10702	0,02494938	7,48E-04	-1,60028	-0,67832	AT2G18570		UDP-Glycosyltransferase superfamily protein
A_84_P17178	0,03897839	0,002162	-1,60176	-0,67966	AT1G66520;	pde194	
A_84_P527692	0,03134441	0,0013001	-1,60259	-0,6804	AT1G62110		Mitochondrial transcription termination factor family protein
A_84_P308973	0,03367786	0,0015591	-1,60346	-0,68119	AT3G52040		
A_84_P18364	0,03830155	0,0020941	-1,60363	-0,68134	AT3G12750	ZIP1	AtZIP1_ZIP1__zinc transporter 1 precursor
A_84_P14396	0,0215952	4,82E-04	-1,60386	-0,68155	AT1G29950;	AJAX2,CPuORF35,AJAX2,CPuORF34,AJAX2	
A_84_P20849	0,01526442	1,73E-04	-1,60492	-0,6825	AT1G27480		alpha/beta-Hydrolases superfamily protein
A_84_P261020	0,02170344	4,91E-04	-1,60528	-0,68283	AT3G10150	ATPAP16, PAP16	ATPAP16_PAP16__purple acid phosphatase 16
A_84_P854905	0,02196731	5,03E-04	-1,60722	-0,68456	AT1G68010	ATHPR1, HPR	ATHPR1_HPR__hydroxypyruvate reductase
A_84_P12819	0,04017467	0,0023621	-1,60738	-0,68472	AT3G44820		Phototropic-responsive NPH3 family protein
A_84_P23779	0,0274646	9,23E-04	-1,60753	-0,68485	AT1G68520		BBX14__B-box type zinc finger protein with CCT domain
A_84_P77579	0,01633501	2,11E-04	-1,60813	-0,68538	AT3G22968;	CPuORF59	
A_84_P191924	0,04994319	0,0040402	-1,60827	-0,68551	AT5G46690	bHLH071	bHLH071__beta HLH protein 71
A_84_P832800	0,02898836	0,0010574	-1,60878	-0,68597	AT4G35270		NLP2__Plant regulator RWP-RK family protein

A_84_P585522	0,04831925	0,0037134	-1,60881	-0,686	AT2G20980	MCM10	MCM10__minichromosome maintenance 10
A_84_P786152	0,02751567	9,31E-04	-1,60957	-0,68668	AT1G77630	LYM3	LYM3_LYP3__Peptidoglycan-binding LysM domain-containing protein
A_84_P784916	0,04669211	0,0033893	-1,60997	-0,68704	AT1G10370	ATGSTU17, ERD9,	ATGSTU17_ERD9_GST30_GST30B_GSTU17__Glutathione S-transferase family protein
A_84_P503065	0,04528285	0,0031241	-1,61011	-0,68716	AT3G05470		Actin-binding FH2 (formin homology 2) family protein
A_84_P178514	0,01961223	3,68E-04	-1,61015	-0,68719	AT1G22030		
A_84_P251085	0,04473491	0,003039	-1,61065	-0,68764	AT2G47840	AtTic20-II, Tic20-II	AtTic20-II_Tic20-II__Uncharacterised conserved protein ycf60
A_84_P23286	0,03278848	0,0014549	-1,61139	-0,68831	AT4G22240		Plastid-lipid associated protein PAP / fibrillin family protein
A_84_P227839	0,01156977	6,60E-05	-1,61264	-0,68942	AT1G67050		
A_84_P605175	0,04312844	0,0027638	-1,61342	-0,69012	AT2G39370	MAKR4	MAKR4__
A_84_P808801	0,04400296	0,0028932	-1,61521	-0,69172	AT2G31660	EMA1, SAD2, URM	EMA1_SAD2_URM9__ARM repeat superfamily protein
A_84_P13999	0,03308225	0,0014754	-1,6154	-0,69189	AT5G35220	EGY1	AMOS1_EGY1__Peptidase M50 family protein
A_84_P753739	0,03902999	0,0021695	-1,61616	-0,69257	AT1G51680	4CL.1, 4CL1, AT4C	4CL.1_4CL1_AT4CL1__4-coumarate:CoA ligase 1
A_84_P861164	0,0380066	0,0020562	-1,61661	-0,69297	AT2G23790		Protein of unknown function (DUF607)
A_84_P540376	0,04730906	0,003474	-1,61676	-0,69311	AT3G23290	LSH4	LSH4__Protein of unknown function (DUF640)
A_84_P20759	0,04829221	0,0036885	-1,61786	-0,69409	AT5G28500		
A_84_P16477	0,03358237	0,0015217	-1,61853	-0,69468	AT3G26590		MATE efflux family protein
A_84_P19904	0,04648082	0,00335	-1,62124	-0,69709	AT1G10370	ATGSTU17, ERD9,	ATGSTU17_ERD9_GST30_GST30B_GSTU17__Glutathione S-transferase family protein
A_84_P834131	0,01937779	3,51E-04	-1,62209	-0,69786	AT4G14650		
A_84_P285270	0,03687182	0,0019324	-1,62361	-0,69921	AT3G51750		
A_84_P15158	0,03913938	0,0021968	-1,62672	-0,70197	AT1G62250		
A_84_P817496	0,02951533	0,001112	-1,62759	-0,70274	AT1G55960		Polyketide cyclase/dehydrase and lipid transport superfamily protein
A_84_P15294	0,03367786	0,001556	-1,62835	-0,70341	AT1G17920	HDG12	HDG12__homeodomain GLABROUS 12
A_84_P704286	0,04465805	0,0030211	-1,6293	-0,70425	AT4G01037	AtWTF1, WTF1	AtWTF1_WTF1__Ubiquitin carboxyl-terminal hydrolase family protein
A_84_P599010	0,02400674	6,42E-04	-1,63213	-0,70675	AT3G10525	LGO, SMR1	LGO_SMR1__LOSS OF GIANT CELLS FROM ORGANS
A_84_P10343	0,04857402	0,0037776	-1,63249	-0,70707	AT5G16000	NIK1	AtNIK1_NIK1__NSP-interacting kinase 1
A_84_P869349	0,02376995	6,17E-04	-1,63255	-0,70712	AT2G21860		violaxanthin de-epoxidase-relatedviolaxanthin de-epoxidase-related
A_84_P756553	0,02376995	6,18E-04	-1,633	-0,70752	AT2G35550	ATBPC7, BBR, BP	ATBPC7_BBR_BPC7__basic pentacysteine 7
A_84_P148568	0,0243154	6,83E-04	-1,63473	-0,70905	AT5G02180		Transmembrane amino acid transporter family protein
A_84_P193384	0,04311589	0,0027615	-1,63497	-0,70926	AT5G67385		Phototropic-responsive NPH3 family protein
A_84_P93009	0,02991192	0,0011505	-1,63608	-0,71024	AT2G14880		SWIB/MDM2 domain superfamily protein
A_84_P820856	0,0390369	0,0021798	-1,63918	-0,71297	AT1G64770	NDF2, NDH45, Pns	NDF2_NDH45_PnsB2__NDH-dependent cyclic electron flow 1
A_84_P18880	0,04775265	0,0035624	-1,63928	-0,71306	AT1G35250		ALT2__Thioesterase superfamily protein
A_84_P823999	0,01340841	1,14E-04	-1,63976	-0,71349	AT5G23920		
A_84_P19078	0,04899432	0,0038642	-1,64006	-0,71375	AT1G19190		alpha/beta-Hydrolases superfamily protein
A_84_P752571	0,01742975	2,49E-04	-1,64016	-0,71384	AT1G80030		DJA7__Molecular chaperone Hsp40/DnaJ family protein
A_84_P21670	0,04641205	0,0033408	-1,64036	-0,71401	AT5G63800	BGAL6, MUM2	BGAL6_MUM2__Glycosyl hydrolase family 35 protein
A_84_P221816	0,02355661	5,96E-04	-1,64043	-0,71407	AT2G21860		violaxanthin de-epoxidase-relatedviolaxanthin de-epoxidase-related
A_84_P820316	0,03270588	0,0014461	-1,64115	-0,71471	AT4G26790		GDSL-like Lipase/Acylhydrolase superfamily protein
A_84_P206348	0,04489678	0,0030788	-1,64585	-0,71883	AT1G60060		Serine/threonine-protein kinase WNK (With No Lysine)-related
A_84_P67034	0,03822321	0,0020785	-1,64586	-0,71884	AT1G55910	ZIP11	ZIP11__zinc transporter 11 precursor
A_84_P868534	0,02237896	5,20E-04	-1,64636	-0,71928	AT3G01060		
A_84_P582063	0,00884543	2,42E-05	-1,6465	-0,7194	AT3G11090	LBD21	LBD21__LOB domain-containing protein 21
A_84_P760300	0,01871915	3,23E-04	-1,64706	-0,7199	AT3G28160;	0	
A_84_P825671	0,031304	0,0012934	-1,64847	-0,72112	AT4G08940		Ubiquitin carboxyl-terminal hydrolase family protein
A_84_P19650	0,03828945	0,0020908	-1,64857	-0,72122	AT1G49560		Homeodomain-like superfamily protein
A_84_P848405	0,01775137	2,77E-04	-1,65019	-0,72263	AT2G17695		
A_84_P17021	0,02544358	7,85E-04	-1,65036	-0,72278	AT1G50250	FTSH1	FTSH1__FTSH protease 1
A_84_P856852	0,02849884	9,94E-04	-1,65298	-0,72507	AT3G46870		Pentatricopeptide repeat (PPR) superfamily protein
A_84_P855921	0,03272725	0,0014484	-1,65365	-0,72566	AT1G50250	FTSH1	FTSH1__FTSH protease 1
A_84_P19460	0,04661662	0,0033741	-1,65387	-0,72584	AT4G05410	YAO	YAO__Transducin/WD40 repeat-like superfamily protein
A_84_P10051	0,03359263	0,0015332	-1,65458	-0,72646	AT4G23300	CRK22	CRK22__cysteine-rich RLK (RECEPTOR-like protein kinase) 22

A_84_P848914	0,04811797	0,0036297	-1,6546	-0,72648	AT4G17840		
A_84_P847471	0,04320978	0,0027725	-1,65471	-0,72658	AT1G33720	CYP76C6	CYP76C6__cytochrome P450, family 76, subfamily C, polypeptide 6
A_84_P589834	0,04742935	0,0035093	-1,65495	-0,72679	AT1G54385		ARM repeat superfamily proteinARM repeat superfamily protein
A_84_P20003	0,02285082	5,56E-04	-1,6558	-0,72753	AT1G68130	AtIDD14, IDD14, ID	AtIDD14_IDD14_IDD14alpha_IDD14beta__indeterminate(ID)-domain 14
A_84_P15477	0,0274646	9,23E-04	-1,65648	-0,72812	AT3G10000	EDA31	EDA31__Homeodomain-like superfamily protein
A_84_P19769	0,01900532	3,36E-04	-1,65701	-0,72858	AT5G61570		Protein kinase superfamily protein
A_84_P23649	0,04017467	0,002372	-1,65758	-0,72907	AT1G31050		basic helix-loop-helix (bHLH) DNA-binding superfamily protein
A_84_P12706	0,0364947	0,0018793	-1,65848	-0,72986	AT3G20240		Mitochondrial substrate carrier family protein
A_84_P763517	0,01830757	3,03E-04	-1,65852	-0,72989	AT4G07725		transposable element gene
A_84_P243195	0,03076559	0,0012382	-1,65885	-0,73018	AT4G29310		Protein of unknown function (DUF1005)
A_84_P15647	0,02364189	6,02E-04	-1,66141	-0,73241	AT3G62110		Pectin lyase-like superfamily protein
A_84_P21757	0,03828945	0,0020885	-1,66183	-0,73277	AT1G31040		PLATZ transcription factor family protein
A_84_P13934	0,03086358	0,00125	-1,66226	-0,73315	AT5G05270		AtCHIL_CHIL__Chalcone-flavanone isomerase family protein
A_84_P755262	0,01681458	2,24E-04	-1,66277	-0,73359	AT2G18260	ATSYP112, SYP11	ATSYP112_SYP112__syntaxin of plants 112
A_84_P115622	0,01375994	1,22E-04	-1,66283	-0,73364	AT4G28230		
A_84_P610677	0,04324035	0,002778	-1,6637	-0,7344	AT3G57200		
A_84_P595350	0,03808665	0,0020649	-1,66578	-0,7362	AT2G32100	ATOFP16, OFP16	ATOFP16_OFP16__ovate family protein 16
A_84_P831367	0,0364947	0,0018834	-1,6659	-0,7363	AT1G14430		glyoxal oxidase-related protein
A_84_P11394	0,03484798	0,0016778	-1,66682	-0,73709	AT1G10270	GRP23	GRP23__glutamine-rich protein 23
A_84_P829677	0,01020095	4,87E-05	-1,66692	-0,73719	AT5G23420	HMGB6	HMGB6__high-mobility group box 6
A_84_P23747	0,00894727	2,94E-05	-1,668	-0,73812	AT1G10900		Phosphatidylinositol-4-phosphate 5-kinase family protein
A_84_P22031	0,0418366	0,002607	-1,66902	-0,739	AT2G22990	SCPL8, SNG1	SCPL8_SNG1__sinapoylglucose 1
A_84_P805176	0,04461956	0,0029976	-1,66968	-0,73957	AT3G61490		Pectin lyase-like superfamily protein
A_84_P13867	0,04113878	0,0025085	-1,67197	-0,74154	AT4G30980	LRL2	LRL2__LJRHL1-like 2
A_84_P12757	0,01386093	1,32E-04	-1,67418	-0,74346	AT3G49220		Plant invertase/pectin methylesterase inhibitor superfamily
A_84_P240075	0,02248672	5,33E-04	-1,67444	-0,74368	AT5G51670		Protein of unknown function (DUF668)
A_84_P123932	0,02929986	0,0010851	-1,67505	-0,74421	AT1G79510		Uncharacterized conserved protein (DUF2358)
A_84_P11458	0,02400674	6,47E-04	-1,67637	-0,74534	AT1G80270	PPR596	PPR596__PENTATRICOPEPTIDE REPEAT 596
A_84_P23848	0,03569937	0,0017857	-1,67794	-0,74669	AT2G25060	AtENODL14, ENOD	AtENODL14_ENODL14__early nodulin-like protein 14
A_84_P307040	0,01608974	2,00E-04	-1,67796	-0,7467	AT4G00370	ANTR2, PHT4;4	ANTR2_PHT4;4__Major facilitator superfamily protein
A_84_P521249	0,0325659	0,0014256	-1,67819	-0,74691	AT5G54400		S-adenosyl-L-methionine-dependent methyltransferases superfamily protein
A_84_P853567	0,04234786	0,0026664	-1,68015	-0,74859	AT5G28500		
A_84_P755523	0,02877405	0,0010186	-1,68023	-0,74866	AT2G41950		
A_84_P13191	0,02909376	0,0010659	-1,68074	-0,7491	AT5G21100		Plant L-ascorbate oxidase
A_84_P840305	0,03664915	0,001897	-1,68075	-0,74911	AT3G28960		Transmembrane amino acid transporter family protein
A_84_P845813	0,02077349	4,42E-04	-1,68098	-0,7493	AT4G14120		
A_84_P15342	0,038253	0,0020836	-1,68175	-0,74996	AT2G41820		PXC3__Leucine-rich repeat protein kinase family protein
A_84_P20023	0,00884543	2,39E-05	-1,68197	-0,75015	AT1G07180	ATNDI1, NDA1	ATNDI1_NDA1__alternative NAD(P)H dehydrogenase 1
A_84_P13171	0,03103756	0,0012644	-1,68211	-0,75027	AT5G66770		GRAS family transcription factor
A_84_P10220	0,01961223	3,73E-04	-1,68411	-0,75198	AT5G35970		P-loop containing nucleoside triphosphate hydrolases superfamily protein
A_84_P809951	0,02763937	9,39E-04	-1,68432	-0,75217	AT4G23490		Protein of unknown function (DUF604)
A_84_P810121	0,04017467	0,0023738	-1,68515	-0,75288	AT1G58360	AAP1, NAT2	AAP1_AtAAP1_NAT2__amino acid permease 1
A_84_P549559	0,03929059	0,0022412	-1,68521	-0,75293	AT5G38100		S-adenosyl-L-methionine-dependent methyltransferases superfamily protein
A_84_P821540	0,02054225	4,23E-04	-1,68572	-0,75337	AT3G55010	ATPURM, EMB281	PUR5__phosphoribosylformylglycinamidine cyclo-ligase, chl/phosphoribosyl-aminoimidazole synthetase
A_84_P861375	0,02146564	4,74E-04	-1,68582	-0,75345	AT1G32060	PRK	PRK__phosphoribulokinase
A_84_P248025	0,03308225	0,0014823	-1,68672	-0,75422	AT2G42800	AtRLP29, RLP29	AtRLP29_RLP29__receptor like protein 29
A_84_P828254	0,02644849	8,49E-04	-1,68674	-0,75424	AT5G63040		
A_84_P16470	0,01504028	1,64E-04	-1,68885	-0,75604	AT3G23000	ATSR2, ATSRPK1,	ATSR2_ATSRPK1_CIPK7_PKS7_SnRK3.10__CBL-interacting protein kinase 7
A_84_P18661	0,04371872	0,0028504	-1,68965	-0,75672	AT5G04660	CYP77A4	CYP77A4__cytochrome P450, family 77, subfamily A, polypeptide 4
A_84_P22168	0,03450806	0,0016383	-1,68969	-0,75676	AT3G21010		transposable element gene
A_84_P721249	0,03387075	0,0015759	-1,68972	-0,75678	AT5G41612		other RNA

A_84_P800891	0,03916847	0,0022108	-1,69015	-0,75715	AT2G32480	ARASP	ARASP__ARABIDOPSIS SERIN PROTEASE
A_84_P12127	0,04371553	0,0028459	-1,69381	-0,76027	AT5G40820	ATATR, ATR, ATR	ATATR_ATR_ATRAD3__Ataxia telangiectasia-mutated and RAD3-related
A_84_P15747	0,04234786	0,0026693	-1,69383	-0,76029	AT4G28630	ABCB23, ATATM1,	ABCB23_ATATM1_ATM1__ABC transporter of the mitochondrion 1
A_84_P21618	0,04889452	0,0038286	-1,69394	-0,76038	AT5G50160	ATFRO8, FRO8	ATFRO8_FRO8__ferric reduction oxidase 8
A_84_P530419	0,02737199	9,13E-04	-1,69467	-0,761	AT2G01990		
A_84_P11494	0,01961223	3,70E-04	-1,69481	-0,76113	AT1G67870		glycine-rich protein
A_84_P766073	0,04422265	0,0029496	-1,69538	-0,76161	AT5G35796		
A_84_P787140	0,04963833	0,0039648	-1,69585	-0,762	AT5G49730;	ATFRO6,FRO6,ATFRO7,FRO7	
A_84_P12759	0,03916847	0,0022136	-1,69979	-0,76536	AT3G49670	BAM2	BAM2__Leucine-rich receptor-like protein kinase family protein
A_84_P151138	0,02883385	0,0010263	-1,70155	-0,76685	AT3G63210	MARD1	MARD1__Protein of unknown function (DUF581)
A_84_P11901	0,03543342	0,0017586	-1,7035	-0,7685	AT1G06100		Fatty acid desaturase family protein
A_84_P20503	0,04641205	0,003337	-1,70544	-0,77015	AT4G34760		SAUR50__SAUR-like auxin-responsive protein family
A_84_P760791	0,02353903	5,92E-04	-1,70603	-0,77064	AT3G54060		
A_84_P758763	0,02612251	8,34E-04	-1,70792	-0,77224	AT3G28160;	0	
A_84_P841211	0,03359263	0,0015317	-1,70804	-0,77234	AT3G25570;	CPuORF11	
A_84_P847435	0,02740352	9,15E-04	-1,70868	-0,77289	AT3G08600		Protein of unknown function (DUF1191)
A_84_P777695	0,02991192	0,0011559	-1,71528	-0,77845	AT3G23290	LSH4	LSH4__Protein of unknown function (DUF640)
A_84_P22740	0,00894727	2,76E-05	-1,71737	-0,7802	AT1G77200		Integrase-type DNA-binding superfamily protein
A_84_P579017	0,04641205	0,0033409	-1,71775	-0,78052	AT1G07490	DVL9, RTFL3	DVL9_RTFL3__ROTUNDIFOLIA like 3
A_84_P12616	0,01436057	1,42E-04	-1,71797	-0,78071	AT2G32220		Ribosomal L27e protein family
A_84_P761712	0,03750303	0,0020003	-1,71844	-0,7811	AT3G51075		other RNA
A_84_P12750	0,03993093	0,0023299	-1,71881	-0,78141	AT3G47430	PEX11B	PEX11B__peroxin 11B
A_84_P830397	0,02449762	6,94E-04	-1,71917	-0,78171	AT3G24080		KRR1 family proteinKRR1 family protein
A_84_P575291	0,04899432	0,0038574	-1,7192	-0,78173	AT5G36740		Acyl-CoA N-acyltransferase with RING/FYVE/PHD-type zinc finger protein
A_84_P19829	0,04742935	0,0035099	-1,71949	-0,78198	AT5G58390		Peroxidase superfamily protein
A_84_P16534	0,03359263	0,0015466	-1,72011	-0,7825	AT3G48160	DEL1, E2FE, E2L3	DEL1_E2FE_E2L3__DP-E2F-like 1
A_84_P23531	0,01774115	2,75E-04	-1,72079	-0,78307	AT1G33240	AT-GTL1, GTL1	AT-GTL1_ATGTL1_GTL1__GT-2-like 1
A_84_P845749	0,01175392	7,73E-05	-1,72186	-0,78397	AT3G06770		Pectin lyase-like superfamily protein
A_84_P826969	0,02275215	5,45E-04	-1,72208	-0,78415	AT1G65030		Transducin/WD40 repeat-like superfamily protein
A_84_P12412	0,02376995	6,11E-04	-1,72218	-0,78424	AT1G60890		Phosphatidylinositol-4-phosphate 5-kinase family protein
A_84_P22205	0,02237896	5,24E-04	-1,72289	-0,78483	AT1G48460		
A_84_P808242	0,02732394	9,10E-04	-1,72352	-0,78535	AT1G14345		NAD(P)-linked oxidoreductase superfamily protein
A_84_P750030	0,02033809	4,09E-04	-1,72414	-0,78588	AT1G73445		transposable element gene
A_84_P71224	0,04488314	0,0030731	-1,72531	-0,78685	AT2G35350	PLL1	PLL1__poltergeist like 1
A_84_P23328	0,02342488	5,84E-04	-1,72568	-0,78716	AT4G31600		UTr7__UDP-N-acetylglucosamine (UAA) transporter family
A_84_P19279	0,03665218	0,0019059	-1,72793	-0,78904	AT3G07050	NSN1	NSN1__GTP-binding family protein
A_84_P284250	0,03454188	0,0016547	-1,72938	-0,79025	AT5G27360	SFP2	SFP2__Major facilitator superfamily protein
A_84_P600900	0,02595606	8,19E-04	-1,73042	-0,79113	AT3G56870		
A_84_P17147	0,03786849	0,0020416	-1,73079	-0,79143	AT1G28670	ARAB-1	ARAB-1__GDSL-like Lipase/Acylhydrolase superfamily protein
A_84_P105006	0,03220695	0,001394	-1,73124	-0,7918	AT5G40830		S-adenosyl-L-methionine-dependent methyltransferases superfamily protein
A_84_P824287	0,01246891	9,62E-05	-1,7316	-0,79211	AT1G70230	AXY4, TBL27	AXY4_TBL27__TRICHOME BIREFRINGENCE-LIKE 27
A_84_P17807	0,02316882	5,71E-04	-1,73257	-0,79292	AT5G43080	CYCA3;1	CYCA3;1__Cyclin A3;1
A_84_P11330	0,04611502	0,003267	-1,73336	-0,79358	AT1G11545	XTH8	XTH8__xyloglucan endotransglucosylase/hydrolase 8
A_84_P18896	0,04115374	0,0025145	-1,73421	-0,79428	AT1G71480		Nuclear transport factor 2 (NTF2) family protein
A_84_P11254	0,02226756	5,15E-04	-1,73575	-0,79556	AT5G60450	ARF4	ARF4__auxin response factor 4
A_84_P851252	0,03184718	0,0013431	-1,73627	-0,79599	AT4G31400	CTF7	AtCTF7_CTF7_ECO1__damaged DNA binding;DNA-directed DNA polymerases
A_84_P816308	0,04572882	0,00321	-1,73696	-0,79656	AT5G05200		Protein kinase superfamily protein
A_84_P20911	0,03523168	0,00172	-1,73762	-0,79711	AT1G69780	ATHB13	ATHB13__Homeobox-leucine zipper protein family
A_84_P14745	0,01513611	1,69E-04	-1,73793	-0,79737	AT4G11440		Mitochondrial substrate carrier family protein
A_84_P23234	0,00894727	2,91E-05	-1,73815	-0,79755	AT4G02630		Protein kinase superfamily protein
A_84_P21952	0,03788604	0,0020458	-1,73876	-0,79806	AT2G43710	FAB2, SSI2	AtSSI2_FAB2_LDW1_SSI2__Plant stearoyl-acyl-carrier-protein desaturase family protein

A_84_P547725	0,04887474	0,0038195	-1,74083	-0,79977	AT5G09580		
A_84_P812373	0,02512251	7,62E-04	-1,74112	-0,80002	AT5G01410	ATPDX1, ATPDX1.	ATPDX1_ATPDX1.3_PDX1_PDX1.3_RSR4__Aldolase-type TIM barrel family protein
A_84_P15323	0,02894719	0,0010487	-1,74247	-0,80114	AT1G32240	KAN2	KAN2__Homeodomain-like superfamily protein
A_84_P757718	0,01989875	3,90E-04	-1,74262	-0,80126	AT2G24755		other RNA
A_84_P15700	0,03941842	0,002258	-1,74307	-0,80163	AT4G13710		Pectin lyase-like superfamily protein
A_84_P810878	0,01520549	1,70E-04	-1,7431	-0,80166	AT3G14420		GOX1__Aldolase-type TIM barrel family protein
A_84_P751365	0,01768366	2,59E-04	-1,74352	-0,802	AT1G45201	ATTLL1, TLL1	ATTLL1_TLL1__triacylglycerol lipase-like 1
A_84_P606916	0,02752188	9,34E-04	-1,74457	-0,80287	AT2G30890;	TBL43	
A_84_P182154	0,03188377	0,0013513	-1,74667	-0,80461	AT5G49730	ATFRO6, FRO6	ATFRO6_FRO6__ferric reduction oxidase 6
A_84_P85719	0,04198026	0,0026241	-1,74773	-0,80548	AT3G44940		Protein of unknown function (DUF1635)
A_84_P587896	0,04742935	0,0035106	-1,74968	-0,80709	AT1G05420	ATOFP12, OFP12	ATOFP12_OFP12__ovate family protein 12
A_84_P542466	0,02774078	9,46E-04	-1,74995	-0,80731	AT5G36710;	0	
A_84_P598030	0,02883385	0,0010246	-1,75045	-0,80773	AT2G31270	ATCDT1A, CDT1, C	ATCDT1A_CDT1_CDT1A__homolog of yeast CDT1 A
A_84_P549710	0,00466105	3,99E-06	-1,7514	-0,80851	AT1G05950		
A_84_P573880	0,03122214	0,0012842	-1,75264	-0,80953	AT1G79150		binding
A_84_P830261	0,01771716	2,71E-04	-1,75389	-0,81055	AT3G05480	ATRAD9, RAD9	ATRAD9_RAD9__cell cycle checkpoint control protein family
A_84_P190804	0,04927701	0,003911	-1,75426	-0,81086	AT5G09460;	AJAX3,CPuORF43,	AJAX3,CPuORF42,AJAX3,CPuORF41,AJAX3
A_84_P22043	0,03189056	0,0013532	-1,75429	-0,81088	AT2G37560	ATORC2, ORC2	ATORC2_ORC2__origin recognition complex second largest subunit 2
A_84_P232159	0,038253	0,0020836	-1,75444	-0,81101	AT2G32530	ATCSLB03, ATCSL	ATCSLB03_ATCSLB3_CSLB03__cellulose synthase-like B3
A_84_P816662	0,01768366	2,60E-04	-1,75477	-0,81128	AT2G47930	AGP26, ATAGP26	AGP26_ATAGP26__arabinogalactan protein 26
A_84_P825582	0,01911949	3,43E-04	-1,75538	-0,81178	AT2G41040		S-adenosyl-L-methionine-dependent methyltransferases superfamily protein
A_84_P21335	0,02487969	7,43E-04	-1,75817	-0,81407	AT4G01030		pentatricopeptide (PPR) repeat-containing protein
A_84_P22412	0,01130293	6,20E-05	-1,76049	-0,81597	AT4G39410	ATWRKY13, WRKY	ATWRKY13_WRKY13__WRKY DNA-binding protein 13
A_84_P824302	0,04086231	0,0024731	-1,76437	-0,81915	AT4G29310		Protein of unknown function (DUF1005)
A_84_P13857	0,04017467	0,0023693	-1,76659	-0,82097	AT4G28780		GDSL-like Lipase/Acylhydrolase superfamily protein
A_84_P11957	0,01592639	1,96E-04	-1,76688	-0,8212	AT4G26540		Leucine-rich repeat receptor-like protein kinase family protein
A_84_P815188	0,04831925	0,0037143	-1,76716	-0,82144	AT2G25080	ATGPX1, GPX1	ATGPX1_GPX1__glutathione peroxidase 1
A_84_P813506	0,04465805	0,003012	-1,76778	-0,82194	AT4G22570	APT3	APT3__adenine phosphoribosyl transferase 3
A_84_P290554	0,04303499	0,0027538	-1,76814	-0,82223	AT3G14740		RING/FYVE/PHD zinc finger superfamily protein
A_84_P838518	0,01642861	2,15E-04	-1,76904	-0,82297	AT1G50280		Phototropic-responsive NPH3 family protein
A_84_P24138	0,00530427	4,79E-06	-1,77078	-0,82438	AT3G56330		N2,N2-dimethylguanosine tRNA methyltransferase
A_84_P18868	0,00903297	3,58E-05	-1,77084	-0,82443	AT5G19730		Pectin lyase-like superfamily protein
A_84_P610685	0,03086358	0,0012499	-1,7718	-0,82522	AT3G59670		
A_84_P848652	0,01403995	1,37E-04	-1,77236	-0,82567	AT1G32060	PRK	PRK__phosphoribulokinasePRK__phosphoribulokinase
A_84_P827727	0,02156671	4,78E-04	-1,77384	-0,82688	AT5G56860	GATA21, GNC	GATA21_GNC__GATA type zinc finger transcription factor family protein
A_84_P12408	0,03124189	0,0012858	-1,77397	-0,82698	AT1G73630		EF hand calcium-binding protein family
A_84_P21684	0,0151022	1,68E-04	-1,77398	-0,82699	AT5G67200		Leucine-rich repeat protein kinase family protein
A_84_P186234	0,01202061	8,63E-05	-1,7753	-0,82806	AT3G25590		
A_84_P761052	0,02103692	4,56E-04	-1,77696	-0,82941	AT3G52720	ACA1, ATACA1, CA	ACA1_ATACA1_CAH1__alpha carbonic anhydrase 1
A_84_P753742	0,03506512	0,0016989	-1,7817	-0,83325	AT1G04778		
A_84_P16381	0,03748751	0,0019986	-1,78434	-0,83539	AT2G34190		Xanthine/uracil permease family protein
A_84_P231649	0,01320943	1,08E-04	-1,78518	-0,83607	AT3G24080		KRR1 family proteinKRR1 family protein
A_84_P15998	0,03454188	0,0016543	-1,78533	-0,83619	AT5G64630	FAS2, MUB3.9, NF	FAS2_MUB3.9_NFB01_NFB1__Transducin/WD40 repeat-like superfamily protein
A_84_P819038	0,0291012	0,0010669	-1,78872	-0,83892	AT1G33240	AT-GTL1, GTL1	AT-GTL1_ATGTL1_GTL1__GT-2-like 1
A_84_P22318	0,02665718	8,65E-04	-1,79012	-0,84005	AT4G12830		alpha/beta-Hydrolases superfamily protein
A_84_P13781	0,03268509	0,0014413	-1,79325	-0,84258	AT1G23340		Protein of Unknown Function (DUF239)
A_84_P15740	0,04695471	0,0034278	-1,79411	-0,84327	AT4G27030	FAD4, FADA	FAD4_FADA__fatty acid desaturase A
A_84_P15126	0,02084717	4,46E-04	-1,79421	-0,84334	AT1G69160		
A_84_P540304	0,02272896	5,44E-04	-1,79606	-0,84483	AT3G02500		
A_84_P835299	0,03524169	0,0017221	-1,79633	-0,84505	AT2G41510	ATCKX1, CKX1	ATCKX1_CKX1_cytokinin oxidase/dehydrogenase 1ATCKX1_CKX1__cytokinin oxidase/dehydrogenase 1
A_84_P806618	0,02384919	6,27E-04	-1,79671	-0,84536	AT2G26080	AtGLDP2, GLDP2	AtGLDP2_GLDP2__glycine decarboxylase P-protein 2

A_84_P194524	0,01775137	2,77E-04	-1,79719	-0,84574	AT2G29760	OTP81	OTP81__Tetratricopeptide repeat (TPR)-like superfamily protein
A_84_P12173	0,01872867	3,26E-04	-1,79829	-0,84663	AT5G53730		NHL26__Late embryogenesis abundant (LEA) hydroxyproline-rich glycoprotein family
A_84_P592388	0,02376995	6,14E-04	-1,7985	-0,84679	AT5G43250	NF-YC13	NF-YC13__nuclear factor Y, subunit C13
A_84_P21472	0,04875428	0,0038017	-1,80112	-0,84889	AT4G14790	ATSUV3, EDA15	ATSUV3_EDA15__ATP-dependent RNA helicase, mitochondrial (SUV3)
A_84_P23199	0,0288939	0,0010367	-1,80229	-0,84983	AT3G58070	GIS	GIS__C2H2 and C2HC zinc fingers superfamily protein
A_84_P539380	0,04269926	0,0027143	-1,80302	-0,85042	AT2G35075		
A_84_P13779	0,02400674	6,47E-04	-1,80469	-0,85175	AT4G03270	CYCD6;1	CYCD6;1__Cyclin D6;1
A_84_P762563	0,03930434	0,0022438	-1,80495	-0,85196	AT3G57157		other RNA
A_84_P13494	0,04361687	0,0028213	-1,80578	-0,85262	AT2G36690		2-oxoglutarate (2OG) and Fe(II)-dependent oxygenase superfamily protein
A_84_P788639	0,04896518	0,0038443	-1,80607	-0,85285	AT3G03770		Leucine-rich repeat protein kinase family protein
A_84_P856045	0,02507846	7,56E-04	-1,80638	-0,8531	AT2G25080	ATGPX1, GPX1	ATGPX1_GPX1__glutathione peroxidase 1
A_84_P21617	0,03133682	0,0012962	-1,80737	-0,85389	AT5G49910	cpHsc70-2, HSC70	HSC70-7_cpHsc70-2__chloroplast heat shock protein 70-2
A_84_P12842	0,04130216	0,0025281	-1,80751	-0,854	AT4G08150	BP, BP1, KNAT1	BP_BP1_KNAT1__KNOTTED-like from Arabidopsis thaliana
A_84_P240205	0,02449762	6,97E-04	-1,80806	-0,85445	AT2G27840	HDA13, HDT04, HD	HD2D_HDA13_HDT04_HDT4__histone deacetylase-related / HD-related
A_84_P10678	0,04091296	0,0024778	-1,80808	-0,85446	AT2G28050		Pentatricopeptide repeat (PPR) superfamily protein
A_84_P11318	0,03786849	0,0020407	-1,80817	-0,85453	AT1G35310	MLP168	MLP168__MLP-like protein 168
A_84_P292434	0,01686448	2,25E-04	-1,80997	-0,85597	AT2G47930	AGP26, ATAGP26	AGP26_ATAGP26__arabinogalactan protein 26
A_84_P20132	0,03450806	0,0016382	-1,81012	-0,85609	AT2G21210		SAUR6__SAUR-like auxin-responsive protein family
A_84_P843020	0,02507846	7,57E-04	-1,81077	-0,8566	AT1G07010	AtSLP1, SLP1	AtSLP1_SLP1__Calcineurin-like metallo-phosphoesterase superfamily protein
A_84_P802670	0,03206014	0,0013744	-1,81087	-0,85669	AT4G08150	BP, BP1, KNAT1	BP_BP1_KNAT1__KNOTTED-like from Arabidopsis thaliana
A_84_P10906	0,04917615	0,0038923	-1,81506	-0,86002	AT3G58120	ATBZIP61, BZIP61	ATBZIP61_BZIP61__Basic-leucine zipper (bZIP) transcription factor family protein
A_84_P800839	0,03313515	0,0014887	-1,81524	-0,86016	AT1G22710	ATSUC2, SUC2, S	ATSUC2_SUC2_SUT1__sucrose-proton symporter 2
A_84_P10011	0,01961223	3,74E-04	-1,81585	-0,86064	AT4G09350	CRRJ, NdhT	CRRJ_DJC75_NdhT__Chaperone DnaJ-domain superfamily protein
A_84_P20990	0,02998172	0,0011658	-1,81756	-0,862	AT1G71850		Ubiquitin carboxyl-terminal hydrolase family protein
A_84_P837093	0,03818448	0,0020746	-1,8213	-0,86497	AT1G14280	PKS2	PKS2__phytochrome kinase substrate 2PKS2__phytochrome kinase substrate 2
A_84_P753729	0,04787055	0,0035844	-1,82271	-0,86608	AT1G48745		
A_84_P767998	0,03172537	0,0013255	-1,82275	-0,86612	AT5G42146		
A_84_P11240	0,04473491	0,0030409	-1,82638	-0,86899	AT1G56110	NOP56	NOP56__homolog of nucleolar protein NOP56
A_84_P843303	0,04156374	0,0025615	-1,82903	-0,87108	AT3G02500		
A_84_P825382	0,03518269	0,001713	-1,82913	-0,87116	AT3G51895	AST12, SULTR3;1	AST12_SULTR3;1__sulfate transporter 3;1
A_84_P815691	0,04456152	0,0029825	-1,82926	-0,87126	AT3G49670	BAM2	BAM2__Leucine-rich receptor-like protein kinase family protein
A_84_P577221	0,02400674	6,34E-04	-1,83027	-0,87205	AT5G24330	ATXR6, SDG34	ATXR6_SDG34__ARABIDOPSIS TRITHORAX-RELATED PROTEIN 6
A_84_P848773	0,04176612	0,0025878	-1,83077	-0,87245	AT4G15393;	CYP72A5,CYP72A6	
A_84_P66124	0,04418246	0,0029332	-1,83162	-0,87312	AT4G09900	ATMES12, MES12	ATMES12_MES12__methyl esterase 12
A_84_P520907	0,04780289	0,0035725	-1,83182	-0,87328	AT3G48250	BIR6	BIR6__Pentatricopeptide repeat (PPR) superfamily protein
A_84_P16281	0,03929059	0,0022397	-1,83264	-0,87392	AT2G24820	AtTic55, Tic55, TIC	AtTic55_TIC55-II_Tic55__translocon at the inner envelope membrane of chloroplasts 55-II
A_84_P19225	0,01718834	2,40E-04	-1,83366	-0,87472	AT1G07370	ATPCNA1, PCNA1	ATPCNA1_PCNA1__proliferating cellular nuclear antigen 1
A_84_P99496	0,01633501	2,12E-04	-1,83949	-0,87931	AT5G23420	HMGB6	HMGB6__high-mobility group box 6HMGB6__high-mobility group box 6
A_84_P12766	0,02582126	8,10E-04	-1,83959	-0,87938	AT3G51240	F3H, F3'H, TT6	F3'H_F3H_TT6__flavanone 3-hydroxylase
A_84_P10101	0,01835125	3,09E-04	-1,84091	-0,88042	AT4G34610	BLH6	BLH6__BEL1-like homeodomain 6
A_84_P11118	0,03959857	0,0022923	-1,84213	-0,88137	AT5G10390		H3.1__Histone superfamily protein
A_84_P127561	0,0293697	0,0010915	-1,8434	-0,88237	AT4G15680		Thioredoxin superfamily protein
A_84_P867201	0,0457815	0,0032337	-1,84342	-0,88238	AT5G23750		Remorin family protein
A_84_P18061	0,04057087	0,0024317	-1,84412	-0,88293	AT1G10790		
A_84_P560726	0,03333965	0,0015041	-1,84413	-0,88294	AT3G13980		
A_84_P525105	0,02894719	0,0010482	-1,84463	-0,88333	AT2G04790		
A_84_P533182	0,04986016	0,0040208	-1,84471	-0,88339	AT2G37380	MAKR3	MAKR3__
A_84_P750345	0,03278848	0,001454	-1,85026	-0,88773	AT1G49370		
A_84_P24069	0,02612251	8,30E-04	-1,85067	-0,88805	AT3G16870	GATA17	GATA17__GATA transcription factor 17
A_84_P525765	0,04953547	0,0039456	-1,85071	-0,88808	AT1G07270		Cell division control, Cdc6Cell division control, Cdc6
A_84_P21871	0,0145606	1,51E-04	-1,85105	-0,88834	AT1G66540		Cytochrome P450 superfamily protein

A_84_P804260	0,02277204	5,49E-04	-1,854	-0,89064	AT5G09460;	AJAX3,CPuORF43,AJAX3,CPuORF42,AJAX3,CPuORF41,AJAX3	
A_84_P256710	0,04538051	0,0031396	-1,85527	-0,89163	AT3G57940		Domain of unknown function (DUF1726)
A_84_P17063	0,01492891	1,61E-04	-1,85666	-0,89271	AT1G30840	ATPUP4, PUP4	ATPUP4_PUP4__purine permease 4
A_84_P819249	0,02720185	9,01E-04	-1,86093	-0,89603	AT5G42720		Glycosyl hydrolase family 17 protein
A_84_P65224	0,02830536	9,83E-04	-1,86545	-0,89952	AT2G28350	ARF10	ARF10__auxin response factor 10
A_84_P18040	0,02725007	9,04E-04	-1,86615	-0,90006	AT1G11600	CYP77B1	CYP77B1__cytochrome P450, family 77, subfamily B, polypeptide 1
A_84_P23290	0,04899432	0,0038616	-1,86824	-0,90168	AT4G23290	CRK21	CRK21__cysteine-rich RLK (RECEPTOR-like protein kinase) 21
A_84_P11463	0,04208476	0,0026335	-1,87075	-0,90362	AT1G73620		Pathogenesis-related thaumatin superfamily protein
A_84_P20899	0,01769782	2,63E-04	-1,87765	-0,90893	AT1G10640		Pectin lyase-like superfamily protein
A_84_P10523	0,03454188	0,0016516	-1,87887	-0,90986	AT1G34040		Pyridoxal phosphate (PLP)-dependent transferases superfamily protein
A_84_P806838	0,04826047	0,0036785	-1,87974	-0,91053	AT3G15400	ATA20	ATA20__anther 20
A_84_P23582	0,04198548	0,0026254	-1,88487	-0,91446	AT5G15948;	CPuORF1	
A_84_P14983	0,01774115	2,75E-04	-1,88551	-0,91496	AT5G46740	UBP21	UBP21__ubiquitin-specific protease 21
A_84_P181494	0,02118828	4,65E-04	-1,88744	-0,91643	AT3G48280	CYP71A25	CYP71A25__cytochrome P450, family 71, subfamily A, polypeptide 25
A_84_P10755	0,03543911	0,0017605	-1,88852	-0,91726	AT3G03060		P-loop containing nucleoside triphosphate hydrolases superfamily protein
A_84_P14533	0,03533791	0,0017402	-1,88942	-0,91795	AT3G05600		alpha/beta-Hydrolases superfamily protein
A_84_P15547	0,04572882	0,0031947	-1,88995	-0,91835	AT3G22560		Acyl-CoA N-acyltransferases (NAT) superfamily protein
A_84_P224349	0,04474596	0,0030498	-1,89282	-0,92054	AT2G46040		ARID/BRIGHT DNA-binding domain;ELM2 domain protein
A_84_P238483	0,03364271	0,0015506	-1,89925	-0,92543	AT5G04895		ABO6__DEA(D/H)-box RNA helicase family protein
A_84_P800447	0,00895168	3,38E-05	-1,89948	-0,9256	AT3G46940	DUT1	DUT1__DUTP-PYROPHOSPHATASE-LIKE 1DUT1__DUTP-PYROPHOSPHATASE-LIKE 1
A_84_P13693	0,02430013	6,80E-04	-1,89961	-0,9257	AT3G46940	DUT1	DUT1__DUTP-PYROPHOSPHATASE-LIKE 1DUT1__DUTP-PYROPHOSPHATASE-LIKE 1
A_84_P23169	0,0394248	0,0022616	-1,90056	-0,92643	AT3G51420	ATSSL4, SSL4	ATSSL4_SSL4__strictosidine synthase-like 4
A_84_P105556	0,03076559	0,0012331	-1,9019	-0,92744	AT5G63100		S-adenosyl-L-methionine-dependent methyltransferases superfamily protein
A_84_P786857	0,02991192	0,001155	-1,90209	-0,92759	AT4G26600		S-adenosyl-L-methionine-dependent methyltransferases superfamily protein
A_84_P23359	0,02226756	5,14E-04	-1,90256	-0,92794	AT4G39770	TPPH	TPPH__Haloacid dehalogenase-like hydrolase (HAD) superfamily protein
A_84_P17249	0,04633552	0,0032928	-1,90273	-0,92807	AT2G47490	ATNDT1, NDT1	ATNDT1_NDT1__NAD+ transporter 1
A_84_P10370	0,03895907	0,0021575	-1,90391	-0,92897	AT5G04230	ATPAL3, PAL3	ATPAL3_PAL3__phenyl alanine ammonia-lyase 3
A_84_P19878	0,02075475	4,41E-04	-1,90716	-0,93143	AT1G64640	AtENODL8, ENODL	AtENODL8_ENODL8__early nodulin-like protein 8AtENODL8_ENODL8__early nodulin-like protein 8
A_84_P155915	0,04408735	0,0029028	-1,90771	-0,93184	AT5G43370	APT1, PHT1;2, PH	APT1_PHT1;2_PHT2__phosphate transporter 2
A_84_P21681	0,02118828	4,65E-04	-1,91189	-0,935	AT5G66460	AtMAN7, MAN7	AtMAN7_MAN7__Glycosyl hydrolase superfamily protein
A_84_P19887	0,02951533	0,0011137	-1,91352	-0,93623	AT1G80760	NIP6, NIP6;1, NLM	NIP6_NIP6;1_NLM7__NOD26-like intrinsic protein 6;1
A_84_P19966	0,04324035	0,0027808	-1,91682	-0,93872	AT1G69200	FLN2	FLN2__fructokinase-like 2
A_84_P22105	0,01592639	1,96E-04	-1,91863	-0,94007	AT3G04030		MYR2__Homeodomain-like superfamily protein
A_84_P14327	0,04762339	0,0035371	-1,91956	-0,94078	AT1G78090	ATTPPB, TPPB	ATTPPB_TPPB__trehalose-6-phosphate phosphatase
A_84_P209948	0,02680561	8,73E-04	-1,92318	-0,9435	AT2G32870		TRAF-like family proteinTRAF-like family protein
A_84_P605036	0,02454009	7,15E-04	-1,92673	-0,94616	AT1G70120		Protein of unknown function (DUF1163)
A_84_P838032	0,04674462	0,0034036	-1,93005	-0,94864	AT1G68570		AtNPF3.1_NPF3.1__Major facilitator superfamily protein
A_84_P18765	0,0457815	0,0032298	-1,9341	-0,95166	AT5G46280	MCM3	MCM3__Minichromosome maintenance (MCM2/3/5) family protein
A_84_P281450	0,03665218	0,0019073	-1,93719	-0,95396	AT1G21270	WAK2	WAK2__wall-associated kinase 2
A_84_P819143	0,03949811	0,0022708	-1,93856	-0,95499	AT5G49910	cpHsc70-2, HSC70	HSC70-7_cpHsc70-2__chloroplast heat shock protein 70-2
A_84_P764604	0,01066107	5,66E-05	-1,93916	-0,95543	AT4G18501		
A_84_P17549	0,02581204	8,05E-04	-1,94022	-0,95622	AT4G00165		Bifunctional inhibitor/lipid-transfer protein/seed storage 2S albumin superfamily protein
A_84_P23533	0,0286969	0,0010108	-1,94194	-0,9575	AT5G57190	PSD2	PSD2__phosphatidylserine decarboxylase 2
A_84_P740964	0,03818448	0,0020739	-1,94278	-0,95812	AT5G08760		
A_84_P18056	0,03624299	0,0018374	-1,94482	-0,95963	AT1G77870	MUB5	MUB5__membrane-anchored ubiquitin-fold protein 5 precursor
A_84_P131376	0,01771716	2,68E-04	-1,94953	-0,96312	AT5G19190		
A_84_P563710	0,03189056	0,0013553	-1,94984	-0,96336	AT5G27780		SAUR75__SAUR-like auxin-responsive protein family
A_84_P124012	0,03076559	0,0012379	-1,951	-0,96422	AT5G26790		
A_84_P826337	0,02820842	9,76E-04	-1,95334	-0,96594	AT2G12462		
A_84_P510106	0,02609744	8,26E-04	-1,95397	-0,96641	AT2G35840;	0	
A_84_P10969	0,02184876	4,97E-04	-1,95408	-0,96649	AT4G12390	PME1	PME1__pectin methylesterase inhibitor 1PME1__pectin methylesterase inhibitor 1

A_84_P14999	0,01961223	3,75E-04	-1,95445	-0,96676	AT1G64370		
A_84_P566307	0,01902633	3,38E-04	-1,95447	-0,96678	AT5G06790		
A_84_P59580	0,01782063	2,79E-04	-1,95593	-0,96786	AT4G34560		
A_84_P812952	0,02991192	0,0011535	-1,95868	-0,96988	AT5G45350		proline-rich family protein
A_84_P23341	0,02895624	0,0010515	-1,96221	-0,97248	AT4G34790		SAUR3__SAUR-like auxin-responsive protein family
A_84_P24132	0,0274646	9,22E-04	-1,96536	-0,97479	AT3G55120	A11, CFI, TT5	A11_AtCHI_CFI_CHI_TT5__Chalcone-flavanone isomerase family protein
A_84_P23550	0,02454009	7,17E-04	-1,96603	-0,97529	AT5G61000	ATRPA70D, RPA70	ATRPA70D_RPA1D_RPA70D__Replication factor-A protein 1-related
A_84_P808727	0,03670938	0,0019112	-1,97076	-0,97875	AT1G15760		Sterile alpha motif (SAM) domain-containing protein
A_84_P770243	0,0485757	0,0037805	-1,97209	-0,97972	ATMG01060	ORF107G	ORF107G__
A_84_P17551	0,02118828	4,65E-04	-1,97252	-0,98004	AT4G00880		SAUR31__SAUR-like auxin-responsive protein family
A_84_P23806	0,04572882	0,0031974	-1,97288	-0,9803	AT1G13600	AtbZIP58, bZIP58	AtbZIP58_bZIP58__basic leucine-zipper 58
A_84_P15874	0,03307353	0,001471	-1,97656	-0,98299	AT5G24150	SQE5, SQP1	SQE5_SQP1__FAD/NAD(P)-binding oxidoreductase family protein
A_84_P567338	0,04555509	0,0031713	-1,97721	-0,98347	AT5G55570		
A_84_P16293	0,02551475	7,91E-04	-1,98013	-0,98559	AT2G46570	LAC6	LAC6__laccase 6
A_84_P826445	0,01163687	7,31E-05	-1,98104	-0,98626	AT4G12390	PME1	PME1__pectin methylesterase inhibitor 1PME1__pectin methylesterase inhibitor 1
A_84_P253555	0,0364947	0,0018828	-1,98322	-0,98784	AT4G14090		UDP-Glycosyltransferase superfamily protein
A_84_P855355	0,04294266	0,0027439	-1,98491	-0,98908	AT5G49730;	ATFRO6,FRO6,ATFRO7,FRO7	
A_84_P22499	0,0409498	0,0024866	-1,98494	-0,9891	AT5G25120	CYP71B11	CYP71B11__ytochrome p450, family 71, subfamily B, polypeptide 11
A_84_P21289	0,01564355	1,86E-04	-1,98633	-0,9901	AT3G53940		Mitochondrial substrate carrier family protein
A_84_P113332	0,03258517	0,0014308	-1,98887	-0,99195	AT2G31070	TCP10	TCP10__TCP domain protein 10
A_84_P556476	0,04572882	0,0032034	-1,98906	-0,99209	AT4G18750	DOT4	DOT4__Pentatricopeptide repeat (PPR) superfamily protein
A_84_P13642	0,01769782	2,64E-04	-1,9907	-0,99328	AT3G28040		Leucine-rich receptor-like protein kinase family protein
A_84_P21252	0,04066901	0,002446	-1,99341	-0,99524	AT3G45680		Major facilitator superfamily protein
A_84_P10591	0,03220695	0,0013948	-1,99503	-0,99641	AT1G25360		Pentatricopeptide repeat (PPR) superfamily protein
A_84_P20381	0,03727133	0,0019676	-1,99657	-0,99752	AT3G63110	ATIPT3, IPT3	ATIPT3_IPT3__isopentenyltransferase 3
A_84_P805355	0,02376995	6,20E-04	-2,0018	-1,0013	AT1G12460		Leucine-rich repeat protein kinase family protein
A_84_P752347	0,02906338	0,0010628	-2,00584	-1,00421	AT1G62835		
A_84_P20876	0,02454009	7,11E-04	-2,00637	-1,00459	AT1G64780	AMT1;2, ATAMT1;2	AMT1;2_ATAMT1;2__ammonium transporter 1;2
A_84_P828102	0,02891722	0,0010387	-2,01778	-1,01277	AT5G62140		
A_84_P820256	0,04641205	0,0033347	-2,01874	-1,01346	AT2G24820	AtTic55, Tic55, TIC	AtTic55_TIC55-II_Tic55__translocon at the inner envelope membrane of chloroplasts 55-II
A_84_P792003	0,04813784	0,0036478	-2,0204	-1,01464	AT4G25845;	ORP4B	
A_84_P519713	0,0153101	1,75E-04	-2,02389	-1,01713	AT1G66840	PMI2, WEB2	PMI2_WEB2__Plant protein of unknown function (DUF827)
A_84_P13912	0,0364947	0,0018813	-2,02845	-1,02038	AT4G16730	TPS02	TPS02_TPS02-Ws__-Ws
A_84_P830783	0,0286969	0,0010082	-2,02983	-1,02136	AT5G16500		LIP1__Protein kinase superfamily protein
A_84_P12781	0,04741487	0,003503	-2,03055	-1,02187	AT3G54400		Eukaryotic aspartyl protease family protein
A_84_P515118	0,0293167	0,0010877	-2,03262	-1,02334	AT5G56200		C2H2 type zinc finger transcription factor family
A_84_P539632	0,03233584	0,0014049	-2,03501	-1,02504	AT4G13990		Exostosin family proteinExostosin family protein
A_84_P273780	0,02411081	6,63E-04	-2,04066	-1,02904	AT1G49470		Family of unknown function (DUF716)
A_84_P535510	0,0497107	0,003988	-2,04111	-1,02935	AT3G53680		Acyl-CoA N-acyltransferase with RING/FYVE/PHD-type zinc finger domain
A_84_P836109	0,0390369	0,0021776	-2,04219	-1,03012	AT4G13990		Exostosin family proteinExostosin family protein
A_84_P831659	0,0215952	4,81E-04	-2,04569	-1,03259	AT4G28680	TYRDC, TYRDC1	AtTYDC_TYDC_TYRDC_TYRDC1__L-tyrosine decarboxylase
A_84_P17185	0,02532245	7,77E-04	-2,04569	-1,03259	AT1G07270		Cell division control, Cdc6Cell division control, Cdc6
A_84_P827163	0,03416876	0,0016018	-2,05131	-1,03654	AT1G55910	ZIP11	ZIP11__zinc transporter 11 precursorZIP11__zinc transporter 11 precursor
A_84_P15502	0,03368684	0,0015619	-2,05598	-1,03982	AT3G14370	WAG2	WAG2__Protein kinase superfamily protein
A_84_P825578	0,01560944	1,81E-04	-2,05687	-1,04045	AT2G41040		S-adenosyl-L-methionine-dependent methyltransferases superfamily protein
A_84_P769220	0,04002055	0,0023422	-2,06003	-1,04267	AT5G18404		
A_84_P110322	0,02277204	5,50E-04	-2,06171	-1,04384	AT3G14900	EMB3120	EMB3120__
A_84_P292024	0,01851141	3,16E-04	-2,0633	-1,04495	AT4G03292		Polynucleotidyl transferase, ribonuclease H-like superfamily protein
A_84_P17819	0,04411166	0,0029066	-2,06614	-1,04694	AT5G46270		Disease resistance protein (TIR-NBS-LRR class) family
A_84_P112722	0,01592639	1,95E-04	-2,06659	-1,04725	AT2G41040		S-adenosyl-L-methionine-dependent methyltransferases superfamily protein
A_84_P17526	0,04789742	0,0035963	-2,06662	-1,04727	AT3G58810	ATMTP3, ATMTPA	ATMTP3_ATMTPA2_MTP3_MTPA2__metal tolerance protein A2

A_84_P788935	0,02848171	9,93E-04	-2,06742	-1,04783	AT2G20180	PIF1, PIL5	PIF1_PIL5__phytochrome interacting factor 3-like 5
A_84_P161803	0,0242297	6,71E-04	-2,07139	-1,0506	AT4G29150	IQD25	IQD25__IQ-domain 25
A_84_P15258	0,03256498	0,0014223	-2,07453	-1,05279	AT1G20120		GDSL-like Lipase/Acylhydrolase superfamily protein
A_84_P22161	0,01564355	1,84E-04	-2,07782	-1,05507	AT3G24300	AMT1;3, ATAMT1;3	AMT1;3_ATAMT1;3__ammonium transporter 1;3
A_84_P12761	0,04737008	0,0034896	-2,07875	-1,05572	AT3G50130		Plant protein of unknown function (DUF247)
A_84_P202108	0,02414743	6,64E-04	-2,08193	-1,05792	AT3G20015		Eukaryotic aspartyl protease family protein
A_84_P12918	0,04830702	0,0036942	-2,08203	-1,05799	AT4G30120	ATHMA3, HMA3	ATHMA3_HMA3__heavy metal atpase 3
A_84_P14379	0,03536541	0,0017454	-2,08442	-1,05964	AT1G14440	AtHB31, HB31, ZH	AtHB31_FTM2_HB31_ZHD4__homeobox protein 31
A_84_P14137	0,02916541	0,0010726	-2,09101	-1,0642	AT5G13170	AtSWEET15, SAG2	AtSWEET15_SAG29_SWEET15__senescence-associated gene 29
A_84_P790814	0,03359263	0,0015404	-2,09429	-1,06646	AT5G05810	ATL43	ATL43__RING/U-box superfamily protein
A_84_P23490	0,03367786	0,0015583	-2,0983	-1,06922	AT5G45070	AtPP2-A8, PP2-A8	AtPP2-A8_PP2-A8__phloem protein 2-A8
A_84_P756272	0,04086231	0,0024738	-2,09861	-1,06944	AT2G27395		
A_84_P543622	0,02054225	4,22E-04	-2,10421	-1,07328	AT1G52530		
A_84_P15308	0,01177365	8,04E-05	-2,10465	-1,07358	AT1G16090	WAKL7	WAKL7__wall associated kinase-like 7
A_84_P85229	0,02150118	4,76E-04	-2,11067	-1,0777	AT4G28310		
A_84_P15532	0,01185074	8,27E-05	-2,11283	-1,07917	AT3G14450	CID9	CID9__CTC-interacting domain 9
A_84_P842922	0,04138362	0,0025408	-2,11874	-1,08321	AT3G13980		
A_84_P556074	0,01989875	3,91E-04	-2,12083	-1,08463	AT1G70985		hydroxyproline-rich glycoprotein family protein
A_84_P21737	0,02812162	9,70E-04	-2,14612	-1,10173	AT3G13065	SRF4	SRF4__STRUBBELIG-receptor family 4
A_84_P21361	0,03058917	0,0012199	-2,14979	-1,1042	AT4G10120	ATSPS4F	ATSPS4F__Sucrose-phosphate synthase family protein
A_84_P21370	0,02704814	8,94E-04	-2,15293	-1,1063	AT4G12320	CYP706A6	CYP706A6__cytochrome P450, family 706, subfamily A, polypeptide 6
A_84_P845538	0,02582126	8,09E-04	-2,1533	-1,10655	AT2G36630		Sulfite exporter TauE/SafE family protein
A_84_P14418	0,02342488	5,84E-04	-2,15722	-1,10917	AT2G40230		HXXXD-type acyl-transferase family protein
A_84_P17772	0,04262674	0,0027036	-2,16194	-1,11233	AT5G25810	tny	tny__Integrase-type DNA-binding superfamily protein
A_84_P825068	0,04484528	0,0030649	-2,16261	-1,11277	AT2G41940	ZFP8	ZFP8__zinc finger protein 8ZFP8__zinc finger protein 8
A_84_P11644	0,03431221	0,0016139	-2,16479	-1,11422	AT2G37460		UMAMIT12__nodulin MtN21 /EamA-like transporter family protein
A_84_P12717	0,04361687	0,0028206	-2,16491	-1,11431	AT3G18610	ATNUC-L2, NUC-L	ATNUC-L2_NUC-L2_NUC2_PARLL1__nucleolin like 2
A_84_P22576	0,02376995	6,20E-04	-2,1669	-1,11563	AT5G53950	ANAC098, ATCUC	ANAC098_ATCUC2_CUC2_NAC No Apical Meristem domain transcriptional regulator superfamily protein
A_84_P528745	0,02586423	8,14E-04	-2,17384	-1,12024	AT2G39230	LOJ	LOJ__LATERAL ORGAN JUNCTION
A_84_P16094	0,04831884	0,0037008	-2,17819	-1,12313	AT1G23130		Polyketide cyclase/dehydrase and lipid transport superfamily protein
A_84_P861913	0,02951044	0,0011092	-2,17973	-1,12415	AT1G64640	AtENODL8, ENODL	AtENODL8_ENODL8__early nodulin-like protein 8
A_84_P20256	0,02400674	6,45E-04	-2,19095	-1,13155	AT3G12820	AtMYB10, MYB10	AtMYB10_MYB10__myb domain protein 10
A_84_P11953	0,01961223	3,65E-04	-2,19995	-1,13747	AT4G25780		CAP Cysteine-rich secretory proteins, Antigen 5, and Pathogenesis-related 1 protein superfamily protein
A_84_P16823	0,04970967	0,0039801	-2,2006	-1,1379	AT1G01060	LHY, LHY1	LHY_LHY1__Homeodomain-like superfamily protein
A_84_P14743	0,04017467	0,002366	-2,20234	-1,13904	AT4G11050	AtGH9C3, GH9C3	AtGH9C3_GH9C3__glycosyl hydrolase 9C3
A_84_P20729	0,03929059	0,0022399	-2,20357	-1,13984	AT5G65010	ASN2	ASN2__asparagine synthetase 2
A_84_P286230	0,02160571	4,83E-04	-2,20713	-1,14217	AT3G25905	CLE27	CLE27__CLAVATA3/ESR-RELATED 27
A_84_P17658	0,04017467	0,0023722	-2,21641	-1,14823	AT4G33010	AtGLDP1, GLDP1	AtGLDP1_GLDP1__glycine decarboxylase P-protein 1
A_84_P10036	0,03665218	0,0019046	-2,22179	-1,15172	AT4G19590		Chaperone DnaJ-domain superfamily protein
A_84_P94599	0,04844125	0,0037583	-2,22707	-1,15515	AT3G56290		
A_84_P12595	0,04036515	0,0024119	-2,22958	-1,15677	AT2G32610	ATCSLB01, ATCSL	ATCSLB01_ATCSLB1_CSLB01__cellulose synthase-like B1
A_84_P21423	0,04880985	0,0038083	-2,2315	-1,15801	AT4G28680	TYRDC, TYRDC1	AtTYDC_TYDC_TYRDC_TYRDC1__L-tyrosine decarboxylase
A_84_P819992	0,04510453	0,0030972	-2,2353	-1,16047	AT4G32340		Tetratricopeptide repeat (TPR)-like superfamily protein
A_84_P15766	0,01871661	3,22E-04	-2,24804	-1,16867	AT4G32980	ATH1	ATH1__homeobox gene 1
A_84_P15327	0,0442149	0,002947	-2,25229	-1,17139	AT2G41940	ZFP8	ZFP8__zinc finger protein 8ZFP8__zinc finger protein 8
A_84_P22292	0,02060719	4,30E-04	-2,25905	-1,17571	AT4G04020	FIB	FIB_PGL35__fibrillinFIB_PGL35__fibrillin
A_84_P761488	0,03594406	0,0018106	-2,26058	-1,1767	AT3G01329		ECA1-like gametogenesis related family protein
A_84_P18822	0,01743021	2,52E-04	-2,26516	-1,17962	AT5G61420	AtMYB28, HAG1, M	AtMYB28_HAG1_MYB28_PMG1__myb domain protein 28
A_84_P21758	0,03959857	0,0022964	-2,27554	-1,18621	AT1G62630		Disease resistance protein (CC-NBS-LRR class) family
A_84_P21154	0,03542483	0,0017552	-2,2819	-1,19023	AT1G01390		UDP-Glycosyltransferase superfamily protein
A_84_P12740	0,03359263	0,0015457	-2,28387	-1,19148	AT1G02630		Nucleoside transporter family protein

A_84_P813422	0,0373717	0,0019811	-2,28876	-1,19456	AT3G48740	AtSWEET11, SWE	AtSWEET11_SWEET11__Nodulin MtN3 family protein
A_84_P311583	0,00904516	3,72E-05	-2,3005	-1,20194	AT5G42445		
A_84_P21901	0,04826047	0,0036688	-2,30843	-1,20691	AT1G06830		Glutaredoxin family protein
A_84_P22686	0,02695982	8,87E-04	-2,30948	-1,20757	AT1G15760		Sterile alpha motif (SAM) domain-containing proteinSterile alpha motif (SAM) domain-containing protein
A_84_P815182	0,0312771	0,0012895	-2,31089	-1,20845	AT3G27060	ATTSO2, TSO2	ATTSO2_TSO2__Ferritin/ribonucleotide reductase-like family protein
A_84_P23195	0,01454446	1,47E-04	-2,32002	-1,21414	AT3G57130	BOP1	BOP1__Ankyrin repeat family protein / BTB/POZ domain-containing protein
A_84_P92099	0,02507846	7,58E-04	-2,3217	-1,21518	AT2G32880		TRAF-like family protein
A_84_P87419	0,03308225	0,0014797	-2,34244	-1,22801	AT3G25290		Auxin-responsive family protein
A_84_P531612	0,03913858	0,0021945	-2,34972	-1,23249	AT4G04745		
A_84_P768303	0,01642861	2,15E-04	-2,35021	-1,23279	AT5G18407		Defensin-like (DEFL) family protein
A_84_P809484	0,03454188	0,0016538	-2,35336	-1,23472	AT5G15948;	CPuORF1	
A_84_P21449	0,03691384	0,0019381	-2,38002	-1,25097	AT4G34770		SAUR1__SAUR-like auxin-responsive protein family
A_84_P13826	0,04831925	0,0037301	-2,4032	-1,26496	AT4G21760	BGLU47	BGLU47__beta-glucosidase 47
A_84_P11955	0,03359263	0,0015449	-2,40422	-1,26557	AT4G26150	CGA1, GATA22, G	CGA1_GATA22_GNL__cytokinin-responsive gata factor 1
A_84_P566577	0,01232764	9,08E-05	-2,40536	-1,26625	AT1G16730	UP6	UP6__unknown protein 6
A_84_P22322	0,01771716	2,72E-04	-2,42757	-1,27951	AT4G13810	AtRLP47, RLP47	AtRLP47_RLP47__receptor like protein 47
A_84_P17296	0,04362199	0,0028277	-2,43572	-1,28435	AT2G42990		GDSL-like Lipase/Acylhydrolase superfamily protein
A_84_P11583	0,04234786	0,0026657	-2,44188	-1,28799	AT2G40900		UMAMIT11__nodulin MtN21 /EamA-like transporter family protein
A_84_P22129	0,03484798	0,0016807	-2,44812	-1,29167	AT3G27660	OLE3, OLEO4	OLE3_OLEO4__oleosin 4
A_84_P90919	0,04181083	0,0025951	-2,4529	-1,29449	AT3G61950		basic helix-loop-helix (bHLH) DNA-binding superfamily protein
A_84_P12889	0,03978182	0,0023125	-2,45669	-1,29672	AT4G23780		
A_84_P19357	0,04181817	0,0026043	-2,45844	-1,29775	AT3G44990	AtXTH31, ATXTR8,	ATXTR8_AtXTH31_XTH31_XTR8__xyloglucan endo-transglycosylase-related 8
A_84_P760435	0,0362616	0,0018457	-2,47559	-1,30777	AT3G31993		transposable element gene
A_84_P575477	0,02532245	7,79E-04	-2,47786	-1,3091	AT1G14630		
A_84_P571785	0,02524157	7,67E-04	-2,48436	-1,31287	AT5G51920		Pyridoxal phosphate (PLP)-dependent transferases superfamily protein
A_84_P812958	0,01526442	1,74E-04	-2,48559	-1,31359	AT4G04020	FIB	FIB_PGL35__fibrillinFIB_PGL35__fibrillin
A_84_P19925	0,02067666	4,34E-04	-2,48989	-1,31608	AT1G03020		Thioredoxin superfamily protein
A_84_P20159	0,04017467	0,0023769	-2,50083	-1,3224	AT2G32540	ATCSLB04, ATCSL	ATCSLB04_ATCSLB4_CSLB04__cellulose synthase-like B4
A_84_P12058	0,03308225	0,0014824	-2,50956	-1,32743	AT5G08640	ATFLS1, FLS, FLS	ATFLS1_FLS_FLS1__flavonol synthase 1
A_84_P12677	0,0484796	0,0037635	-2,51514	-1,33064	AT3G23630	ATIPT7, IPT7	ATIPT7_IPT7__isopentenyltransferase 7
A_84_P21145	0,03665218	0,0019067	-2,5408	-1,34528	AT3G03480	CHAT	CHAT__acetyl CoA:(Z)-3-hexen-1-ol acetyltransferase
A_84_P11358	0,01830757	3,06E-04	-2,56729	-1,36024	AT1G03820		
A_84_P14510	0,04019184	0,0023885	-2,57538	-1,36479	AT2G03090	ATEXP15, ATEXPA	ATEXP15_ATEXPA15_ATHEXP ALPHA 1.3_EXP15_EXPA15__expansin A15
A_84_P20589	0,02248672	5,33E-04	-2,57934	-1,367	AT5G16530	PIN5	PIN5__Auxin efflux carrier family protein
A_84_P18118	0,02071601	4,39E-04	-2,59026	-1,3731	AT1G56430	ATNAS4, NAS4	ATNAS4_NAS4__nicotianamine synthase 4
A_84_P11065	0,04669211	0,003388	-2,63119	-1,39572	AT4G39480	CYP96A9	CYP96A9__cytochrome P450, family 96, subfamily A, polypeptide 9
A_84_P210848	0,02836969	9,88E-04	-2,63385	-1,39717	AT5G22930		Protein of unknown function (DUF1635)
A_84_P305070	0,00894727	3,11E-05	-2,63712	-1,39896	AT2G15020		
A_84_P857350	0,03484798	0,0016803	-2,64117	-1,40118	AT1G23130		Polyketide cyclase/dehydrase and lipid transport superfamily protein
A_84_P786557	0,02991109	0,0011478	-2,66592	-1,41463	AT2G25510		
A_84_P10228	0,01177365	8,13E-05	-2,69213	-1,42875	AT5G38820		Transmembrane amino acid transporter family protein
A_84_P584694	0,04066901	0,0024512	-2,70486	-1,43556	AT2G40390		
A_84_P15108	0,0241966	6,68E-04	-2,72333	-1,44537	AT1G23205		Plant invertase/pectin methylesterase inhibitor superfamily protein
A_84_P12302	0,03181502	0,0013372	-2,72671	-1,44716	AT1G62510		Bifunctional inhibitor/lipid-transfer protein/seed storage 2S albumin superfamily protein
A_84_P60560	0,03828945	0,0020918	-2,72974	-1,44877	AT2G25510		
A_84_P102716	0,03089017	0,0012527	-2,73354	-1,45077	AT4G18630		Protein of unknown function (DUF688)
A_84_P586938	0,04362199	0,0028265	-2,73702	-1,45261	AT5G49740	ATFRO7, FRO7	ATFRO7_FRO7__ferric reduction oxidase 7
A_84_P824811	0,01731088	2,45E-04	-2,75188	-1,46042	AT2G32870		TRAF-like family proteinTRAF-like family protein
A_84_P10285	0,00606654	7,02E-06	-2,75834	-1,4638	AT5G54510	DFL1, GH3.6	DFL1_GH3.6__Auxin-responsive GH3 family protein
A_84_P13165	0,03569937	0,0017874	-2,76202	-1,46572	AT5G65320		basic helix-loop-helix (bHLH) DNA-binding superfamily protein
A_84_P762597	0,04636379	0,0033133	-2,77645	-1,47324	AT3G27329;		0

A_84_P819560	0,03418483	0,001604	-2,78754	-1,47899	AT4G00780		TRAF-like family protein
A_84_P13124	0,02256138	5,36E-04	-2,79955	-1,4852	AT5G55340		MBOAT (membrane bound O-acyl transferase) family protein
A_84_P768492	0,03681569	0,0019258	-2,80266	-1,4868	AT5G63087		Plant thionin family protein
A_84_P255460	0,04371872	0,0028525	-2,81363	-1,49243	AT2G28340	GATA13	GATA13__GATA transcription factor 13
A_84_P524292	0,04197278	0,0026219	-2,81454	-1,4929	AT2G32530	ATCSLB03, ATCSL	ATCSLB03_ATCSLB3_CSLB03__cellulose synthase-like B3
A_84_P18331	0,02884718	0,00103	-2,81674	-1,49403	AT3G04530	ATPPCK2, PEPCK	ATPPCK2_PEPCK2_PPCK2__phosphoenolpyruvate carboxylase kinase 2
A_84_P760178	0,02612251	8,31E-04	-2,81727	-1,4943	AT3G28540		P-loop containing nucleoside triphosphate hydrolases superfamily protein
A_84_P18215	0,0286969	0,0010059	-2,8184	-1,49487	AT2G32290	BAM6, BMY5	BAM6_BMY5__beta-amylase 6
A_84_P12165	0,04603513	0,0032595	-2,86803	-1,52006	AT5G51310		2-oxoglutarate (2OG) and Fe(II)-dependent oxygenase superfamily protein
A_84_P761356	0,00461552	2,46E-06	-2,88402	-1,52808	AT3G61898		
A_84_P605859	0,0380408	0,0020589	-2,88648	-1,52931	AT1G47485		
A_84_P14878	0,04831925	0,0037053	-2,92152	-1,54672	AT5G04950	ATNAS1, NAS1	ATNAS1_NAS1__nicotianamine synthase 1
A_84_P757781	0,03959642	0,0022899	-3,00497	-1,58735	AT2G37555		other RNA
A_84_P16207	0,02477556	7,37E-04	-3,01615	-1,59271	AT1G68360		C2H2 and C2HC zinc fingers superfamily protein
A_84_P10779	0,03044238	0,0012021	-3,06119	-1,61409	AT3G30530	ATBZIP42, bZIP42	ATBZIP42_bZIP42__basic leucine-zipper 42
A_84_P599886	0,02040626	4,13E-04	-3,13189	-1,64704	AT3G06145		
A_84_P767462	0,02038725	4,12E-04	-3,13786	-1,64978	AT5G59990		CCT motif family proteinCCT motif family protein
A_84_P598547	0,03089017	0,0012524	-3,19463	-1,67565	AT5G55040		DNA-binding bromodomain-containing protein
A_84_P761618	0,03542483	0,0017544	-3,20758	-1,68149	AT3G26816;	MIR169L,MIR169N	
A_84_P10289	0,029931	0,0011631	-3,2375	-1,69488	AT5G55720		Pectin lyase-like superfamily protein
A_84_P12422	0,03897839	0,0021614	-3,29209	-1,71901	AT1G48670		auxin-responsive GH3 family protein
A_84_P10781	0,02821329	9,77E-04	-3,34102	-1,74029	AT3G15650		alpha/beta-Hydrolases superfamily protein
A_84_P16880	0,0364947	0,0018792	-3,43768	-1,78144	AT5G47980		HXXXD-type acyl-transferase family protein
A_84_P22462	0,03497349	0,0016936	-3,46949	-1,79472	AT5G09930	ABCF2	ABCF2__ABC transporter family protein
A_84_P543942	0,03187662	0,0013467	-3,57641	-1,83851	AT3G30725	AtGDU6, GDU6	AtGDU6_GDU6__glutamine dumper 6
A_84_P16647	0,01874703	3,28E-04	-3,59072	-1,84427	AT4G13900	AtRLP49, RLP49	AtRLP49_RLP49__
A_84_P13969	0,03916847	0,0022168	-3,60796	-1,85118	AT5G17220	ATGSTF12, GST26	ATGSTF12_GST26_GSTF12_TT19__glutathione S-transferase phi 12
A_84_P19540	0,03518269	0,0017115	-3,61873	-1,85548	AT1G43800		FTM1_SAD6__Plant stearoyl-acyl-carrier-protein desaturase family protein
A_84_P847244	0,04730906	0,0034787	-3,68644	-1,88223	AT2G36610	ATHB22, HB22	ATHB22_HB22__homeobox protein 22
A_84_P788914	0,03645025	0,001869	-3,68729	-1,88256	AT2G40900		UMAMIT11__nodulin MtN21 /EamA-like transporter family protein
A_84_P604856	0,01375994	1,23E-04	-3,73262	-1,90019	AT5G59990		CCT motif family proteinCCT motif family protein
A_84_P753015	0,03439173	0,0016225	-3,77963	-1,91825	AT1G76952	IDL5	IDL5__inflorescence deficient in abscission (IDA)-like 5
A_84_P54840	0,01246891	9,53E-05	-3,81315	-1,93098	AT3G19270	CYP707A4	CYP707A4__cytochrome P450, family 707, subfamily A, polypeptide 4
A_84_P12179	0,00894727	2,56E-05	-3,86271	-1,94961	AT5G55330		MBOAT (membrane bound O-acyl transferase) family protein
A_84_P846994	0,04139227	0,0025432	-3,97266	-1,99011	AT2G40900		UMAMIT11__nodulin MtN21 /EamA-like transporter family protein
A_84_P592665	0,00918073	3,88E-05	-3,99169	-1,997	AT2G24762	AtGDU4, GDU4	AtGDU4_GDU4__glutamine dumper 4
A_84_P81559	0,03914714	0,0022031	-4,07614	-2,0272	AT4G33560		Wound-responsive family protein
A_84_P768727	0,01961223	3,78E-04	-4,21251	-2,07468	AT5G53486		
A_84_P554758	0,0145606	1,51E-04	-4,52834	-2,17898	AT4G37810		
A_84_P761647	0,04899432	0,0038533	-4,83826	-2,27449	AT3G26818	MIR169M	MIR169M__MIR169M; miRNA
A_84_P21430	0,01177365	8,11E-05	-4,90102	-2,29308	AT4G30250		P-loop containing nucleoside triphosphate hydrolases superfamily protein
A_84_P294924	0,0364524	0,0018708	-5,13764	-2,36111	AT2G38920		SPX (SYG1/Pho81/XPR1) domain-containing protein/zinc finger (C3HC4-type RING finger) protein-related
A_84_P14421	0,02732394	9,10E-04	-5,15854	-2,36696	AT2G41510	ATCKX1, CKX1	ATCKX1_CKX1__cytokinin oxidase/dehydrogenase 1
A_84_P784337	0,02512251	7,62E-04	-7,33864	-2,87551	AT1G65480	FT	FT_RSB8__PEBP (phosphatidylethanolamine-binding protein) family protein
A_84_P14793	0,04254959	0,0026922	-8,15501	-3,02769	AT1G21890		UMAMIT19__nodulin MtN21 /EamA-like transporter family protein

Supplemental Table 1. Differential transcript levels in TPT-RAP2.3 lines treated with -estradiol. Levels at 1h after treatment with a NO pulse (E1) versus those at 0 time (E0).

ProbeName	p (Corr)	p	FC	Log FC	AGI	Symbol	Corrected annoatation
A_84_P11046	0,04968483	5,50E-04	493,9474	8,948214	AT4G34410	RRTF1	RRTF1__redox responsive transcription factor 1
A_84_P21769	0,03177396	1,08E-04	272,0891	8,087935	AT1G61120	GES, TPS04, TPS4	GES_TPS04_TPS4__terpene synthase 04
A_84_P595141	0,02561561	2,76E-05	222,51181	7,797738	AT1G30135	JAZ8, TIFY5A	JAZ8_TIFY5A__jasmonate-zim-domain protein 8
A_84_P21573	0,03263922	1,34E-04	111,84534	6,8053613	AT5G38120	4CL8	4CL8__AMP-dependent synthetase and ligase family protein
A_84_P761749	0,01254327	4,34E-06	91,743805	6,519539	AT3G22275		
A_84_P18289	0,01203481	1,57E-06	77,07201	6,268135	AT2G44810	DAD1	DAD1__alpha/beta-Hydrolases superfamily protein
A_84_P851247	0,032583	1,31E-04	69,98376	6,128948	AT5G28237		Pyridoxal-5'-phosphate-dependent enzyme family protein
A_84_P521598	0,03157461	1,03E-04	63,441887	5,987364	AT2G22760		basic helix-loop-helix (bHLH) DNA-binding superfamily protein
A_84_P610481	0,03364056	1,61E-04	57,627926	5,848696	AT2G34600	JAZ7, TIFY5B	JAZ7_TIFY5B__jasmonate-zim-domain protein 7
A_84_P14748	0,03263667	1,32E-04	52,879234	5,7246294	AT1G17420	ATLOX3, LOX3	ATLOX3_LOX3__lipoxygenase 3ATLOX3_LOX3__lipoxygenase 3
A_84_P17584	0,02725945	4,86E-05	52,255585	5,7075133	AT1G17380	JAZ5, TIFY11A	JAZ5_TIFY11A__jasmonate-zim-domain protein 5
A_84_P20976	0,03937708	2,68E-04	48,03467	5,5860043	AT1G19210		Integrase-type DNA-binding superfamily protein
A_84_P785475	0,02775724	6,21E-05	46,777004	5,5477276	AT1G17420	ATLOX3, LOX3	ATLOX3_LOX3__lipoxygenase 3ATLOX3_LOX3__lipoxygenase 3
A_84_P17546	0,04905209	5,24E-04	46,38127	5,5354705	AT3G44860	FAMT	FAMT__farnesoic acid carboxyl-O-methyltransferase
A_84_P592948	0,03162822	1,06E-04	41,518867	5,375695	AT4G11911		
A_84_P524680	0,01254327	4,34E-06	41,0063	5,357774	AT5G13220	JAS1, JAZ10, TIFY9	JAS1_JAZ10_TIFY9__jasmonate-zim-domain protein 10
A_84_P16173	0,03545904	1,84E-04	40,13306	5,3267193	AT1G28480	GRX480, roxy19	GRX480_roxy19__Thioredoxin superfamily protein
A_84_P10627	0,03498028	1,76E-04	37,747044	5,2382917	AT2G20880	AtERF53, ERF53	AtERF53_ERF53__Integrase-type DNA-binding superfamily protein
A_84_P18072	0,03624293	2,14E-04	36,203068	5,17804	AT1G72520	ATLOX4, LOX4	ATLOX4_LOX4__PLAT/LH2 domain-containing lipoxygenase family protein
A_84_P847119	0,02065646	1,41E-05	35,206936	5,137788	AT5G62360		Plant invertase/pectin methylesterase inhibitor superfamily protein
A_84_P823221	0,01417998	5,23E-06	33,437576	5,0633984	AT5G13220	JAS1, JAZ10, TIFY9	JAS1_JAZ10_TIFY9__jasmonate-zim-domain protein 10
A_84_P502791	0,03545904	2,03E-04	32,893456	5,0397286	AT1G32910		HXXXD-type acyl-transferase family protein
A_84_P17881	0,03265593	1,45E-04	32,795807	5,0354395	AT5G62360		Plant invertase/pectin methylesterase inhibitor superfamily protein
A_84_P11564	0,02725945	5,24E-05	32,35481	5,0159082	AT1G64160		AtDIR5_DIR5__Disease resistance-responsive (dirigent-like protein) family protein
A_84_P15993	0,01997895	1,12E-05	31,351526	4,9704638	AT5G63450	CYP94B1	CYP94B1__cytochrome P450, family 94, subfamily B, polypeptide 1
A_84_P611898	0,04834748	4,92E-04	30,85118	4,9472537	AT5G59580	UGT76E1	UGT76E1__UDP-glucosyl transferase 76E1
A_84_P788408	0,02065646	1,43E-05	30,409632	4,9264565	AT2G22760		basic helix-loop-helix (bHLH) DNA-binding superfamily protein
A_84_P20120	0,03263922	1,42E-04	25,755907	4,6868315	AT2G27690	CYP94C1	CYP94C1__cytochrome P450, family 94, subfamily C, polypeptide 1
A_84_P832235	0,04834748	4,96E-04	21,1765	4,4043922	AT3G44860;	FAMT	
A_84_P23179	0,00821229	2,74E-07	20,134415	4,3315916	AT3G53600		C2H2-type zinc finger family protein
A_84_P16877	0,03839359	2,45E-04	18,979265	4,246352	AT5G47240	atnudt8, NUDT8	NUDT8_atnudt8__nudix hydrolase homolog 8
A_84_P18113	0,02725945	4,88E-05	17,729317	4,148065	AT1G76640		CML39__Calcium-binding EF-hand family protein
A_84_P812834	0,03137732	9,55E-05	17,47696	4,1273823	AT1G28480	GRX480, roxy19	GRX480_roxy19__Thioredoxin superfamily protein
A_84_P558681	0,02065646	1,37E-05	17,238531	4,107565	AT1G53885;		0
A_84_P826417	0,03287368	1,46E-04	16,93389	4,0818415	AT5G24110	ATWRKY30, WRKY30	ATWRKY30_WRKY30__WRKY DNA-binding protein 30
A_84_P789698	0,01203481	2,73E-06	15,82814	3,9844198	AT1G72416		Chaperone DnaJ-domain superfamily protein
A_84_P853664	0,01203481	2,41E-06	15,815641	3,9832802	AT2G06050	AtOPR3, DDE1, OPR3	AtOPR3_DDE1_OPR3__oxophytodienoate-reductase 3
A_84_P715317	0,02725945	5,34E-05	15,674281	3,9703274	AT1G72416		Chaperone DnaJ-domain superfamily protein
A_84_P611334	0,04793091	4,71E-04	15,29613	3,9350948	AT2G22880		VQ motif-containing protein
A_84_P232439	0,03157461	9,85E-05	15,201731	3,9261637	AT4G31800	ATWRKY18, WRKY18	ATWRKY18_WRKY18__WRKY DNA-binding protein 18
A_84_P17343	0,03066272	8,40E-05	15,199038	3,925908	AT2G44840	ATERF13, EREBP, ERF13	ATERF13_EREBP_ERF13__ethylene-responsive element binding factor 13
A_84_P785932	0,04367585	3,50E-04	15,114456	3,9178572	AT1G25400		
A_84_P19028	0,02459617	2,06E-05	14,740016	3,8816662	AT1G74930	ORA47	ORA47__Integrase-type DNA-binding superfamily protein
A_84_P76184	0,02358327	1,79E-05	14,440209	3,8520198	AT5G24110	ATWRKY30, WRKY30	ATWRKY30_WRKY30__WRKY DNA-binding protein 30
A_84_P67084	0,03983375	2,78E-04	14,163812	3,8241377	AT1G25400		
A_84_P15340	0,03545904	2,07E-04	14,054783	3,8129892	AT2G06050	AtOPR3, DDE1, OPR3	AtOPR3_DDE1_OPR3__oxophytodienoate-reductase 3
A_84_P818172	0,03903778	2,63E-04	13,979904	3,8052826	AT1G15040		GAT_GAT1_2.1__Class I glutamine amidotransferase-like superfamily protein

A_84_P14985	0,03545904	2,01E-04	13,779772	3,78448	AT5G47220	ATERF2, ATERF-2, ERF2	ATERF-2_ATERF2_ERF2__ethylene responsive element binding factor 2
A_84_P13031	0,01203481	3,23E-06	13,7481	3,7811604	AT5G19110		Eukaryotic aspartyl protease family protein
A_84_P11822	0,03116852	8,89E-05	13,690612	3,775115	AT3G51450		Calcium-dependent phosphotriesterase superfamily protein
A_84_P181974	0,03954257	2,72E-04	13,470726	3,7517557	AT1G20310		
A_84_P852628	0,032583	1,25E-04	12,645198	3,6605177	AT5G02600	NAKR1, NPCC6	NAKR1_NPCC6__Heavy metal transport/detoxification superfamily protein
A_84_P542646	0,032583	1,23E-04	12,62653	3,6583862	AT1G15040		GAT_GAT1_2.1__Class I glutamine amidotransferase-like superfamily protein
A_84_P217688	0,03866172	2,53E-04	12,450544	3,6381369	AT1G76600		
A_84_P840907	0,03545904	2,07E-04	11,791884	3,5597224	AT5G56880		
A_84_P19845	0,03866172	2,58E-04	11,764797	3,5564046	AT3G27810	ATMYB21, ATMYB3, MYB2	ATMYB21_ATMYB3_MYB21__myb domain protein 21
A_84_P586962	0,03117324	9,16E-05	11,694893	3,5478067	AT5G56880		
A_84_P529724	0,03498028	1,75E-04	11,3272085	3,5017204	AT3G20340		
A_84_P832673	0,03188318	1,09E-04	10,763261	3,4280434	AT3G20340		
A_84_P196584	0,04985619	5,54E-04	10,613109	3,4077754	AT3G48650		
A_84_P10611	0,0436378	3,44E-04	9,422673	3,2361364	AT2G43530		Scorpion toxin-like knottin superfamily protein
A_84_P137619	0,0282656	6,54E-05	8,372727	3,0656977	AT5G54490	PBP1	PBP1__pinoid-binding protein 1
A_84_P704033	0,02725945	3,46E-05	8,275334	3,0488176	AT1G11185		other RNA
A_84_P97916	0,04715346	4,40E-04	8,26751	3,047453	AT4G29780		
A_84_P236643	0,032583	1,20E-04	8,170585	3,0304394	AT1G44350	ILL6	ILL6__IAA-leucine resistant (ILR)-like gene 6
A_84_P820417	0,04292386	3,22E-04	8,059987	3,0107775	AT4G17490	ATERF6, ERF6, ERF-6-6	ATERF6_ERF-6-6_ERF6__ethylene responsive element binding factor 6
A_84_P15450	0,04418976	3,64E-04	7,737815	2,9519262	AT2G32120	HSP70T-2	HSP70T-2__heat-shock protein 70T-2
A_84_P18859	0,04796798	4,73E-04	7,677764	2,9406862	AT5G28630		glycine-rich protein
A_84_P216248	0,03839359	2,46E-04	7,540287	2,9146194	AT1G69890		Protein of unknown function (DUF569)
A_84_P22053	0,03866172	2,51E-04	7,483406	2,903695	AT2G41100	ATCAL4, TCH3	ATCAL4_TCH3__Calcium-binding EF hand family protein
A_84_P537220	0,04764787	4,58E-04	7,469642	2,9010391	AT5G57510		
A_84_P16821	0,03866172	2,57E-04	7,2578816	2,8595486	AT5G24470	APRR5, PRR5	APRR5_PRR5__pseudo-response regulator 5
A_84_P17140	0,03954257	2,72E-04	7,2034364	2,8486853	AT1G32640	ATMYC2, JAI1, JIN1, MYC2	ATMYC2_JAI1_JIN1_MYC2_ZBF1__Basic helix-loop-helix DNA-binding protein
A_84_P169283	0,04963683	5,42E-04	7,100398	2,8279	AT5G06570		alpha/beta-Hydrolases superfamily protein
A_84_P13216	0,03545904	2,02E-04	6,917477	2,790246	AT1G20510	OPCL1	OPCL1__OPC-8:0 CoA ligase1
A_84_P18976	0,022797	1,63E-05	6,9162197	2,7899837	AT1G30730		FAD-binding Berberine family protein
A_84_P858725	0,03687087	2,23E-04	6,8956404	2,7856846	AT1G72450	JAZ6, TIFY11B	JAZ6_TIFY11B__jasmonate-zim-domain protein 6
A_84_P562774	0,04834748	4,95E-04	6,8833942	2,7831202	AT5G12340		
A_84_P20831	0,02686399	3,07E-05	6,872378	2,7808094	AT1G61340		AtFBS1_FBS1__F-box family protein
A_84_P759481	0,032583	1,23E-04	6,8531885	2,7767754	AT3G12145	FLOR1, FLR1	FLOR1_FLR1_FTM4__Leucine-rich repeat (LRR) family protein
A_84_P255510	0,03966834	2,74E-04	6,797904	2,76509	AT1G72450	JAZ6, TIFY11B	JAZ6_TIFY11B__jasmonate-zim-domain protein 6
A_84_P769565	0,032583	1,28E-04	6,687007	2,7413607	AT5G44585		
A_84_P869292	0,03263922	1,43E-04	6,6748314	2,7387314	AT4G17500	ATERF-1, ERF-1	ATERF-1_ERF-1__ethylene responsive element binding factor 1
A_84_P267120	0,02561561	2,77E-05	6,615539	2,7258587	AT1G74950	JAZ2, TIFY10B	JAZ2_TIFY10B__TIFY domain/Divergent CCT motif family protein
A_84_P860087	0,03157461	1,01E-04	6,6047897	2,7235126	AT1G27020		
A_84_P10561	0,03973117	2,76E-04	6,524381	2,705841	AT1G51780	ILL5	ILL5__IAA-leucine resistant (ILR)-like gene 5
A_84_P12419	0,03116852	8,95E-05	6,492836	2,6988487	AT1G51760	IAR3, JR3	IAR3_JR3__peptidase M20/M25/M40 family protein
A_84_P811808	0,03545904	1,90E-04	6,463502	2,692316	AT3G12145	FLOR1, FLR1	FLOR1_FLR1_FTM4__Leucine-rich repeat (LRR) family protein
A_84_P811806	0,02745376	5,74E-05	6,430457	2,6849213	AT3G12145	FLOR1, FLR1	FLOR1_FLR1_FTM4__Leucine-rich repeat (LRR) family protein
A_84_P789539	0,04430861	3,71E-04	6,418689	2,6822786	AT4G06746	DEAR5, RAP2.9	DEAR5_RAP2.9__related to AP2 9
A_84_P92059	0,04866988	5,06E-04	6,3683405	2,6709175	AT5G67480	ATBT4, BT4	ATBT4_BT4__BTB and TAZ domain protein 4
A_84_P813646	0,03117324	9,34E-05	6,234517	2,6402779	AT2G26530	AR781	AR781__Protein of unknown function (DUF1645)
A_84_P10039	0,03066272	8,29E-05	6,123644	2,6143904	AT1G27020		
A_84_P23398	0,03263922	1,35E-04	6,0850153	2,6052608	AT5G06870	ATPGIP2, PGIP2	ATPGIP2_PGIP2__polygalacturonase inhibiting protein 2
A_84_P503480	0,032583	1,23E-04	6,064253	2,6003299	AT5G45630		Protein of unknown function, DUF584
A_84_P18211	0,032583	1,30E-04	6,037292	2,5939016	AT2G26530	AR781	AR781__Protein of unknown function (DUF1645)
A_84_P14882	0,03624293	2,13E-04	5,979535	2,5800333	AT1G06620		2-oxoglutarate (2OG) and Fe(II)-dependent oxygenase superfamily protein

A_84_P12418	0,02801358	6,33E-05	5,8875475	2,5576668	AT1G49530	GGPS6	GGPS6__geranylgeranyl pyrophosphate synthase 6
A_84_P154615	0,0436378	3,43E-04	5,808375	2,5381346	AT1G76590		PLATZ transcription factor family protein
A_84_P503102	0,03545904	2,06E-04	5,736511	2,5201735	AT3G15440		
A_84_P19516	0,03364056	1,60E-04	5,7081337	2,513019	AT4G25470	ATCBF2, CBF2, DREB1C, F	ATCBF2_CBF2_DREB1C_FTQ4__C-repeat/DRE binding factor 2
A_84_P13376	0,03364056	1,59E-04	5,6514235	2,4986143	AT1G74430	ATMYB95, ATMYBCP66, M	ATMYB95_ATMYBCP66_MYB95__myb domain protein 95
A_84_P224809	0,01254327	4,16E-06	5,640257	2,495761	AT2G38790		
A_84_P515468	0,03545904	1,95E-04	5,5587335	2,4747562	AT2G45940		Protein of unknown function (DUF295)
A_84_P174151	0,032583	1,23E-04	5,4836364	2,455133	AT2G40330	PYL6, RCAR9	PYL6_RCAR9__PYR1-like 6
A_84_P786720	0,03209353	1,11E-04	5,4800906	2,4541998	AT5G08790	anac081, ATAF2	ATAF2_anac081__NAC No Apical Meristem domain transcriptional regulator protein
A_84_P785249	0,03545904	2,07E-04	5,416209	2,4372835	AT4G31800	ATWRKY18, WRKY18	ATWRKY18_WRKY18__WRKY DNA-binding protein 18
A_84_P541993	0,03263922	1,37E-04	5,3921638	2,4308643	AT2G27310		F-box family protein
A_84_P857687	0,03157461	9,96E-05	5,3083034	2,4082508	AT1G73500	ATMKK9, MKK9	ATMKK9_MKK9__MAP kinase kinase 9
A_84_P259470	0,00821229	3,79E-07	5,1318836	2,3594885	AT1G61890		MATE efflux family protein
A_84_P22892	0,02686399	3,10E-05	5,0725274	2,3427048	AT1G73500	ATMKK9, MKK9	ATMKK9_MKK9__MAP kinase kinase 9
A_84_P608981	0,03116852	8,78E-05	5,036675	2,3324716	AT4G24600		
A_84_P13913	0,03645221	2,16E-04	5,0225487	2,3284197	AT1G19380		Protein of unknown function (DUF1195)
A_84_P11731	0,04793091	4,72E-04	4,7087526	2,235345	AT3G24500	ATMBF1C, MBF1C	ATMBF1C_MBF1C__multiprotein bridging factor 1C
A_84_P19561	0,02840631	6,81E-05	4,7005453	2,2328281	AT4G35480	RHA3B	RHA3B__RING-H2 finger A3B
A_84_P17388	0,04589367	4,04E-04	4,5260463	2,1782513	AT3G06500	A/N-InvC	A/N-InvC__Plant neutral invertase family protein
A_84_P751526	0,02686399	3,09E-05	4,4877424	2,1659899	AT1G72920		Toll-Interleukin-Resistance (TIR) domain family protein
A_84_P834641	0,02725945	3,23E-05	4,3908973	2,1345158	AT3G29000		Calcium-binding EF-hand family proteinCalcium-binding EF-hand family protein
A_84_P10171	0,03510382	1,78E-04	4,36874	2,1272173	AT5G10300	AtHNL, ATMES5, HNL, MES	ATMES5_AtHNL_HNL_MES5__methyl esterase 5
A_84_P23164	0,02995629	7,48E-05	4,366982	2,1266365	AT3G50260	ATERF#011, CEJ1, DEAR1	ATERF#011_CEJ1_DEAR1__cooperatively regulated by ethylene and jasmonate 1
A_84_P15741	0,04367585	3,55E-04	4,3414803	2,118187	AT4G27280		Calcium-binding EF-hand family protein
A_84_P862058	0,03157461	1,02E-04	4,3406134	2,117899	AT3G12145	FLOR1, FLR1	FLOR1_FLR1_FTM4__Leucine-rich repeat (LRR) family protein
A_84_P603728	0,04345628	3,35E-04	4,2791715	2,0973315	AT5G02600	NAKR1, NPCC6	NAKR1_NPCC6__Heavy metal transport/detoxification superfamily protein
A_84_P13173	0,03364056	1,62E-04	4,248639	2,0870008	AT5G67300	ATMYB44, ATMYBR1, MYB	ATMYB44_ATMYBR1_MYB44_MYBR1__myb domain protein r1
A_84_P210868	0,04944391	5,34E-04	4,171626	2,0606098	AT4G16146		cAMP-regulated phosphoprotein 19-related protein
A_84_P504929	0,02995629	7,57E-05	4,164958	2,058302	AT3G29000		Calcium-binding EF-hand family proteinCalcium-binding EF-hand family protein
A_84_P807259	0,02840631	6,79E-05	4,1259584	2,0447292	AT5G67300	ATMYB44, ATMYBR1, MYB	ATMYB44_ATMYBR1_MYB44_MYBR1__myb domain protein r1
A_84_P787617	0,04905209	5,22E-04	3,9813547	1,9932594	AT5G03270	LOG6	LOG6__lysine decarboxylase family protein
A_84_P12086	0,03157461	1,04E-04	3,9647171	1,9872179	AT5G19100		Eukaryotic aspartyl protease family protein
A_84_P501308	0,02725945	5,19E-05	3,92415	1,9723802	AT3G14260		Protein of unknown function (DUF567)
A_84_P282640	0,02745376	5,67E-05	3,8140407	1,9313202	AT2G23170	GH3.3	GH3.3__Auxin-responsive GH3 family protein
A_84_P23526	0,03545904	1,94E-04	3,7528946	1,9080038	AT5G55090	MAPKKK15	MAPKKK15__mitogen-activated protein kinase kinase kinase 15
A_84_P765048	0,03839359	2,45E-04	3,7421644	1,9038728	AT4G33467		
A_84_P18856	0,032583	1,22E-04	3,7176847	1,8944044	AT5G17490	AtRGL3, RGL3	AtRGL3_RGL3__RGA-like protein 3
A_84_P193944	0,04589367	4,04E-04	3,7046678	1,8893442	AT5G66650		Protein of unknown function (DUF607)
A_84_P10148	0,03263922	1,39E-04	3,687331	1,882577	AT5G03270	LOG6	LOG6__lysine decarboxylase family protein
A_84_P765109	0,03866172	2,56E-04	3,6716042	1,8764105	AT4G36052		other RNA
A_84_P23394	0,02725945	4,69E-05	3,6571116	1,8707047	AT5G05730	AMT1, ASA1, JDL1, TRP5,	AMT1_ASA1_JDL1_TRP5_WEI2__anthranilate synthase alpha subunit 1
A_84_P10136	0,01203481	2,47E-06	3,653376	1,8692303	AT4G36670	AtPLT6, AtPMT6, PLT6, PM	AtPLT6_AtPMT6_PLT6_PMT6__Major facilitator superfamily protein
A_84_P12969	0,03319501	1,50E-04	3,6518743	1,8686371	AT4G17230	SCL13	SCL13__SCARECROW-like 13
A_84_P230699	0,04367585	3,55E-04	3,6216953	1,8566651	AT5G05530		RING/U-box superfamily protein
A_84_P72634	0,02725945	3,40E-05	3,5925968	1,845027	AT4G36500		
A_84_P63594	0,03263922	1,39E-04	3,5852706	1,842082	AT4G18205		Nucleotide-sugar transporter family protein
A_84_P15965	0,04418976	3,63E-04	3,5069664	1,8102236	AT5G56980		
A_84_P16285	0,04292386	3,23E-04	3,41793	1,7731228	AT2G29720	CTF2B	CTF2B__FAD/NAD(P)-binding oxidoreductase family protein
A_84_P784166	0,04905209	5,18E-04	3,3979995	1,7646856	AT5G45340	CYP707A3	CYP707A3__cytochrome P450, family 707, subfamily A, polypeptide 3
A_84_P12726	0,0487499	5,08E-04	3,3720498	1,7536259	AT3G11020	DREB2, DREB2B	DREB2_DREB2B__DRE/CRT-binding protein 2B

A_84_P146199	0,04492016	3,83E-04	3,3702714	1,7528647	AT5G05440	PYL5, RCAR8	PYL5_RCAR8__Polyketide cyclase/dehydrase and lipid transport superfamily protein
A_84_P819483	0,02725945	4,12E-05	3,362552	1,7495565	AT1G72920		Toll-Interleukin-Resistance (TIR) domain family protein
A_84_P12143	0,03545904	1,98E-04	3,3614874	1,7490997	AT5G45340	CYP707A3	CYP707A3__cytochrome P450, family 707, subfamily A, polypeptide 3
A_84_P786905	0,02725945	3,62E-05	3,33497	1,7376738	AT5G41120		Esterase/lipase/thioesterase family protein
A_84_P242895	0,02725945	3,90E-05	3,301954	1,72332	AT1G66160	ATCMPG1, CMPG1	ATCMPG1_CMPG1__CYS, MET, PRO, and GLY protein 1
A_84_P852047	0,02725945	3,51E-05	3,3007145	1,7227783	AT5G05440	PYL5, RCAR8	PYL5_RCAR8__Polyketide cyclase/dehydrase and lipid transport superfamily protein
A_84_P817892	0,02745376	5,57E-05	3,2935677	1,7196512	AT5G05440	PYL5, RCAR8	PYL5_RCAR8__Polyketide cyclase/dehydrase and lipid transport superfamily protein
A_84_P286390	0,04985619	5,55E-04	3,2902992	1,7182188	AT3G25780	AOC3	AOC3__allene oxide cyclase 3
A_84_P18141	0,04280318	3,19E-04	3,25511	1,7027063	AT1G55450		S-adenosyl-L-methionine-dependent methyltransferases superfamily protein
A_84_P856402	0,04793091	4,70E-04	3,2451842	1,6983004	AT3G50950	ZAR1	ZAR1__HOPZ-ACTIVATED RESISTANCE 1
A_84_P522895	0,03545904	1,93E-04	3,2442985	1,6979065	AT5G10210		
A_84_P19214	0,04920762	5,29E-04	3,2377703	1,6950006	AT2G32510	MAPKKK17	MAPKKK17__mitogen-activated protein kinase kinase kinase 17
A_84_P17683	0,03162822	1,06E-04	3,2228677	1,688345	AT4G39580		Galactose oxidase/kelch repeat superfamily protein
A_84_P762419	0,032583	1,16E-04	3,177133	1,6677254	AT3G15518		
A_84_P16568	0,03545904	1,82E-04	3,1707025	1,6648024	AT3G55840		Hs1pro-1 protein
A_84_P135945	0,04715346	4,36E-04	3,0907733	1,6279678	AT3G11840	PUB24	PUB24__plant U-box 24
A_84_P826913	0,04758364	4,52E-04	3,0673645	1,6169996	AT3G50950	ZAR1	ZAR1__HOPZ-ACTIVATED RESISTANCE 1
A_84_P17609	0,03263922	1,42E-04	3,0241826	1,5965452	AT4G21870		HSP20-like chaperones superfamily protein
A_84_P14664	0,04367585	3,47E-04	2,9995308	1,5847368	AT3G53160	UGT73C7	UGT73C7__UDP-glucosyl transferase 73C7
A_84_P16077	0,03984243	2,82E-04	2,9893405	1,5798272	AT1G05100	MAPKKK18	MAPKKK18__mitogen-activated protein kinase kinase kinase 18
A_84_P20474	0,04715346	4,39E-04	2,9811866	1,5758867	AT4G28000		P-loop containing nucleoside triphosphate hydrolases superfamily protein
A_84_P836721	0,03364056	1,62E-04	2,9658854	1,5684628	AT4G19520		disease resistance protein (TIR-NBS-LRR class) family
A_84_P10473	0,04963683	5,48E-04	2,9100313	1,5410347	AT1G59870	ABCG36, ATABCG36, ATP	ABCG36_ATABCG36_ATPDR8_PEN3__ABC-2 Plant PDR ABC-type transporter protein
A_84_P22522	0,03995023	2,90E-04	2,9090292	1,5405378	AT5G39020		Malectin/receptor-like protein kinase family protein
A_84_P18091	0,0282656	6,58E-05	2,9027019	1,5373964	AT1G63040		
A_84_P12431	0,04492016	3,84E-04	2,9020267	1,5370607	AT1G74420	ATFUT3, FUT3	ATFUT3_FUT3__fucosyltransferase 3
A_84_P11802	0,04791181	4,66E-04	2,8997235	1,5359154	AT3G46690		UDP-Glycosyltransferase superfamily protein
A_84_P23923	0,03545904	1,90E-04	2,8560324	1,5140123	AT2G37900		Major facilitator superfamily protein
A_84_P241449	0,04680056	4,22E-04	2,8517444	1,5118446	AT1G28190		
A_84_P608304	0,03736534	2,28E-04	2,8506021	1,5112667	AT5G54710		Ankyrin repeat family protein
A_84_P11679	0,03263922	1,38E-04	2,832755	1,5022058	AT2G23680		Cold acclimation protein WCOR413 family
A_84_P596065	0,03476378	1,73E-04	2,827343	1,4994469	AT1G49520		SWIB complex BAF60b domain-containing protein
A_84_P19584	0,03319501	1,51E-04	2,818578	1,4949675	AT4G15975		RING/U-box superfamily protein
A_84_P97466	0,04605175	4,09E-04	2,8143814	1,4928178	AT2G27830		
A_84_P790545	0,04706127	4,32E-04	2,8054786	1,4882469	AT1G49520		SWIB complex BAF60b domain-containing protein
A_84_P857480	0,03345015	1,55E-04	2,8033059	1,4871291	AT1G20450	ERD10, LTI29, LTI45	ERD10_LTI29_LTI45__Dehydrin family protein
A_84_P19057	0,02725945	4,45E-05	2,7929404	1,4817847	AT1G67970	AT-HSFA8, HSFA8	AT-HSFA8_HSFA8__heat shock transcription factor A8
A_84_P785967	0,02995629	7,64E-05	2,792778	1,4817009	AT5G54940		Translation initiation factor SUI1 family protein
A_84_P15109	0,02725945	4,89E-05	2,7734554	1,4716845	AT1G20450	ERD10, LTI29, LTI45	ERD10_LTI29_LTI45__Dehydrin family protein
A_84_P23396	0,03157461	1,04E-04	2,768429	1,4690676	AT5G06320	NHL3	NHL3__NDR1/HIN1-like 3
A_84_P15958	0,04357103	3,38E-04	2,7383487	1,4533062	AT5G54940		Translation initiation factor SUI1 family protein
A_84_P17461	0,04726939	4,43E-04	2,7376068	1,4529152	AT3G43430		RING/U-box superfamily protein
A_84_P12990	0,04791181	4,65E-04	2,7213573	1,4443264	AT5G05490	ATREC8, DIF1, REC8, SYN	AtREC8_DIF1_REC8_SYN1__Rad21/Rec8-like family protein
A_84_P114372	0,01997895	1,15E-05	2,7183206	1,4427156	AT5G53050		alpha/beta-Hydrolases superfamily protein
A_84_P23419	0,04341499	3,30E-04	2,7114112	1,4390439	AT5G13200		GRAM domain family protein
A_84_P816929	0,03954257	2,71E-04	2,6990616	1,4324579	AT5G54170		Polyketide cyclase/dehydrase and lipid transport superfamily protein
A_84_P813874	0,02960254	7,30E-05	2,6988564	1,4323481	AT4G12720	AtNUDT7, GFG1, NUDT7	AtNUDT7_GFG1_NUDT7__MutT/nudix family protein
A_84_P16642	0,02725945	5,26E-05	2,6948738	1,4302177	AT4G12720	AtNUDT7, GFG1, NUDT7	AtNUDT7_GFG1_NUDT7__MutT/nudix family protein
A_84_P12575	0,02745376	5,76E-05	2,6869955	1,4259939	AT2G23030	SNRK2.9, SNRK2-9	SNRK2-9_SNRK2.9__SNF1-related protein kinase 2.9
A_84_P18180	0,03347359	1,57E-04	2,6693485	1,4164877	AT2G31880	EVR, SOBIR1	EVR_SOBIR1__Leucine-rich repeat protein kinase family protein

A_84_P19740	0,03434476	1,68E-04	2,6352463	1,3979378	AT5G54300		Protein of unknown function (DUF761)
A_84_P13235	0,04993777	5,62E-04	2,6289027	1,3944607	AT1G13260	EDF4, RAV1	AtRAV1_EDF4_RAV1__related to ABI3/VP1 1
A_84_P13740	0,04680056	4,25E-04	2,5941815	1,3752794	AT3G57740		Protein kinase superfamily protein
A_84_P819884	0,04834748	4,97E-04	2,5927722	1,3744955	AT4G38550		Arabidopsis phospholipase-like protein (PEARLI 4) family
A_84_P21661	0,02065646	1,29E-05	2,581782	1,3683672	AT5G61590		Integrase-type DNA-binding superfamily protein
A_84_P16735	0,03329087	1,53E-04	2,5734754	1,3637179	AT4G39070		BBX20_BZS1__B-box zinc finger family protein
A_84_P823703	0,04715346	4,39E-04	2,5656297	1,359313	AT5G52882		P-loop containing nucleoside triphosphate hydrolases superfamily protein
A_84_P786801	0,04605175	4,08E-04	2,5640743	1,358438	AT5G13210		Uncharacterised conserved protein UCP015417, vWA
A_84_P23992	0,02725945	5,07E-05	2,5617168	1,357111	AT3G05640		Protein phosphatase 2C family proteinProtein phosphatase 2C family protein
A_84_P166733	0,04993777	5,63E-04	2,5440683	1,3471375	AT5G17350		
A_84_P24091	0,04357103	3,39E-04	2,4709506	1,3050661	AT3G45960	ATEXLA3, ATEXPL3, ATHE	ATEXLA3_ATEXPL3_ATHEXP BETA 2.3_EXLA3_EXPL3__expansin-like A3
A_84_P15703	0,032583	1,30E-04	2,453968	1,2951164	AT4G18340		Glycosyl hydrolase superfamily protein
A_84_P278240	0,0479263	4,67E-04	2,4509275	1,2933278	AT3G29040		Domain of unknown function (DUF26)
A_84_P17400	0,04944391	5,35E-04	2,4429362	1,2886162	AT3G14050	ATRSH2, AT-RSH2, RSH2	AT-RSH2_ATRSH2_RSH2__RELA/SPOT homolog 2
A_84_P19431	0,03545904	2,06E-04	2,4340978	1,2833871	AT3G62150	ABCB21, PGP21	ABCB21_PGP21__P-glycoprotein 21
A_84_P18342	0,03839359	2,46E-04	2,408123	1,267909	AT3G16050	A37, ATPDX1.2, PDX1.2	A37_ATPDX1.2_PDX1.2__pyridoxine biosynthesis 1.2
A_84_P819063	0,04905209	5,23E-04	2,4044883	1,2657299	AT3G46640	LUX, PCL1	LUX_PCL1__Homeodomain-like superfamily protein
A_84_P55660	0,01750383	6,86E-06	2,400437	1,2632971	AT3G56880		VQ motif-containing protein
A_84_P127601	0,04686994	4,27E-04	2,3992488	1,2625828	AT5G02940		Protein of unknown function (DUF1012)
A_84_P158475	0,032583	1,29E-04	2,38777	1,2556639	AT2G41640		Glycosyltransferase family 61 protein
A_84_P793477	0,032583	1,19E-04	2,3632765	1,2407885	AT5G52882		P-loop containing nucleoside triphosphate hydrolases superfamily protein
A_84_P281300	0,04968483	5,51E-04	2,3574302	1,237215	AT3G46640	LUX, PCL1	LUX_PCL1__Homeodomain-like superfamily protein
A_84_P564716	0,02995629	7,73E-05	2,3456824	1,2300076	AT1G03850	ATGRXS13, GRXS13	ATGRXS13_GRXS13__Glutaredoxin family protein
A_84_P259140	0,04905209	5,22E-04	2,3317509	1,2214136	AT1G28050		BBX13__B-box type zinc finger protein with CCT domain
A_84_P19413	0,02459617	2,10E-05	2,3285053	1,2194041	AT3G57530	ATCPK32, CDPK32, CPK32	ATCPK32_CDPK32_CPK32__calcium-dependent protein kinase 32
A_84_P14864	0,04920762	5,30E-04	2,322025	1,2153835	AT4G37260	ATMYB73, MYB73	ATMYB73_MYB73__myb domain protein 73
A_84_P796587	0,03677519	2,21E-04	2,283834	1,1914577	AT2G27389		
A_84_P20977	0,04418976	3,65E-04	2,2757728	1,1863565	AT1G14480		Ankyrin repeat family protein
A_84_P21825	0,03263922	1,41E-04	2,2708888	1,1832571	AT1G13210	ACA.I	ACA.I__autoinhibited Ca2+/ATPase II
A_84_P510552	0,03263922	1,38E-04	2,2424476	1,1650742	AT5G41100		
A_84_P233859	0,03545904	1,98E-04	2,2225354	1,1522064	AT2G28570		
A_84_P127291	0,01203481	1,66E-06	2,2088308	1,1432829	AT5G62865		
A_84_P828333	0,04514324	3,95E-04	2,2076542	1,1425142	AT2G29740	UGT71C2	UGT71C2__UDP-glucosyl transferase 71C2
A_84_P15729	0,04332435	3,28E-04	2,1981933	1,1363182	AT1G32460		
A_84_P17279	0,04367585	3,54E-04	2,184822	1,1275158	AT2G25090	CIPK16, SnRK3.18	AtCIPK16_CIPK16_SnRK3.18__CBL-interacting protein kinase 16
A_84_P22597	0,0345411	1,70E-04	2,173714	1,120162	AT5G59550		AtRDUF2_RDUF2__zinc finger (C3HC4-type RING finger) family protein
A_84_P15341	0,03117324	9,21E-05	2,149713	1,1041441	AT1G64200	VHA-E3	VHA-E3__vacuolar H+-ATPase subunit E isoform 3
A_84_P843872	0,03016915	7,86E-05	2,1364977	1,0952477	AT1G53430		Leucine-rich repeat transmembrane protein kinase
A_84_P799914	0,03545904	2,04E-04	2,1283474	1,0897336	AT3G05640		Protein phosphatase 2C family protein
A_84_P175641	0,04834748	4,83E-04	2,0755057	1,0534629	AT3G19660		
A_84_P538776	0,03839359	2,43E-04	2,0744553	1,0527326	AT4G24015		RING/U-box superfamily protein
A_84_P538274	0,02757152	5,92E-05	2,0676796	1,0480126	AT1G30755		Protein of unknown function (DUF668)
A_84_P16882	0,03866172	2,55E-04	2,0597782	1,0424889	AT5G48540		receptor-like protein kinase-related family protein
A_84_P202508	0,04834748	4,91E-04	2,0573874	1,0408134	AT1G73210		Protein of unknown function (DUF789)
A_84_P13043	0,04726939	4,45E-04	2,0551188	1,0392218	AT5G25440		Protein kinase superfamily protein
A_84_P767643	0,01203481	1,17E-06	2,053523	1,0381012	AT1G29620;	0	
A_84_P118232	0,02737991	5,43E-05	2,0428433	1,0305786	AT5G16360		NC domain-containing protein-related
A_84_P15979	0,04514324	3,92E-04	2,0288744	1,0206796	AT5G60270		LecRK-I.7__Concanavalin A-like lectin protein kinase family protein
A_84_P87289	0,04834748	4,87E-04	2,003949	1,0028458	AT1G24807;	ASB1,TRP4,WEI7	
A_84_P16108	0,02561561	2,64E-05	2,0025756	1,0018567	AT1G09940	HEMA2	HEMA2__Glutamyl-tRNA reductase family protein

A_84_P23998	0,03177396	1,07E-04	1,9864762	0,9902115	AT1G53430		Leucine-rich repeat transmembrane protein kinase
A_84_P13968	0,03319501	1,52E-04	1,9713829	0,979208	AT5G16410		HXXXD-type acyl-transferase family protein
A_84_P798820	0,03984243	2,84E-04	1,9696114	0,977911	AT2G41430	CID1, ERD15, LSR1	CID1_ERD15_LSR1__dehydration-induced protein (ERD15)
A_84_P89769	0,03545904	2,05E-04	1,9542948	0,9666481	AT2G35930	PUB23	AtPUB23_PUB23__plant U-box 23
A_84_P17009	0,03677519	2,21E-04	1,9475461	0,96165746	AT1G20823		RING/U-box superfamily protein
A_84_P612207	0,03545904	1,91E-04	1,9426678	0,9580392	AT2G18196		Heavy metal transport/detoxification superfamily protein
A_84_P18782	0,03995023	2,88E-04	1,9260719	0,94566154	AT1G64380		Integrase-type DNA-binding superfamily protein
A_84_P16068	0,04367585	3,50E-04	1,919927	0,9410514	AT1G33790		jacalin lectin family protein
A_84_P852460	0,04605175	4,12E-04	1,9185543	0,9400196	AT3G03020		
A_84_P20325	0,03319501	1,50E-04	1,9122261	0,9352531	AT3G50060	MYB77	MYB77__myb domain protein 77
A_84_P14972	0,03839359	2,43E-04	1,9091052	0,93289655	AT5G44070	ARA8, ATPCS1, CAD1, PCS	ARA8_ATPCS1_CAD1_PCS1__phytochelatin synthase 1 (PCS1)
A_84_P828208	0,04367585	3,55E-04	1,9024699	0,9278736	AT5G53060		RCF3_SHI1__RNA-binding KH domain-containing protein
A_84_P599750	0,03347359	1,57E-04	1,8927684	0,9204979	AT2G07779		
A_84_P832916	0,04087757	2,99E-04	1,8911864	0,9192915	AT2G44380		Cysteine/Histidine-rich C1 domain family protein
A_84_P16701	0,02505797	2,25E-05	1,8864268	0,9156561	AT4G30350		SMXL2__Double Clp-N motif-containing P-loop nucleoside triphosphate hydrolases protein
A_84_P11230	0,032583	1,24E-04	1,8629879	0,8976183	AT5G54190	PORA	PORA__protochlorophyllide oxidoreductase A
A_84_P553302	0,03263667	1,32E-04	1,8568221	0,8928356	AT1G25500		Plasma-membrane choline transporter family protein
A_84_P11150	0,02725945	5,20E-05	1,8558993	0,89211845	AT5G24590	ANAC091, TIP	ANAC091_TIP__TCV-interacting proteinANAC091_TIP__TCV-interacting protein
A_84_P10316	0,03984243	2,84E-04	1,8522642	0,88928986	AT5G62020	AT-HSFB2A, HSFB2A	AT-HSFB2A_HSFB2A__heat shock transcription factor B2A
A_84_P22972	0,04343475	3,33E-04	1,8432426	0,882246	AT2G42980		Eukaryotic aspartyl protease family protein
A_84_P833361	0,04292386	3,22E-04	1,8329258	0,87414837	AT2G30100		pentatricopeptide (PPR) repeat-containing protein
A_84_P23624	0,02725945	4,88E-05	1,8303626	0,87212944	AT1G71697	ATCK1, CK, CK1	ATCK1_CK_CK1__choline kinase 1
A_84_P839512	0,04993777	5,60E-04	1,8275504	0,8699112	AT4G10845		
A_84_P852438	0,04341499	3,32E-04	1,8163341	0,8610296	AT5G24590	ANAC091, TIP	ANAC091_TIP__TCV-interacting protein
A_84_P10224	0,04357103	3,39E-04	1,7917385	0,8413601	AT5G37770	CML24, TCH2	CML24_TCH2__EF hand calcium-binding protein family
A_84_P527116	0,03973117	2,77E-04	1,7884418	0,83870316	AT3G48180		
A_84_P20795	0,032583	1,30E-04	1,7716016	0,82505417	AT1G15890		Disease resistance protein (CC-NBS-LRR class) family
A_84_P19320	0,04196317	3,11E-04	1,7682612	0,82233137	AT3G16510		Calcium-dependent lipid-binding (CaLB domain) family protein
A_84_P785283	0,03116852	8,78E-05	1,7679036	0,82203954	AT1G78070		Transducin/WD40 repeat-like superfamily protein
A_84_P18540	0,04834748	4,98E-04	1,754464	0,8110304	AT4G18170	ATWRKY28, WRKY28	ATWRKY28_WRKY28__WRKY DNA-binding protein 28
A_84_P840152	0,02725945	4,21E-05	1,7544409	0,8110113	AT5G13190	AtGILP, GILP	AtGILP_GILP__
A_84_P19551	0,02725945	4,99E-05	1,7541347	0,8107595	AT4G33300	ADR1-L1	ADR1-L1__ADR1-like 1
A_84_P272750	0,04348327	3,36E-04	1,7454746	0,8036193	AT2G22300	CAMTA3, SR1	CAMTA3_SR1__signal responsive 1
A_84_P245045	0,04834748	4,84E-04	1,7222108	0,7842617	AT5G64660	ATCMPG2, CMPG2	ATCMPG2_CMPG2__CYS, MET, PRO, and GLY protein 2
A_84_P20605	0,04866988	5,06E-04	1,7153732	0,77852243	AT5G24530	DMR6	DMR6__2-oxoglutarate (2OG) and Fe(II)-dependent oxygenase superfamily protein
A_84_P17672	0,04993777	5,63E-04	1,7120031	0,7756853	AT4G36150		Disease resistance protein (TIR-NBS-LRR class) family
A_84_P16180	0,04430861	3,70E-04	1,7079643	0,77227783	AT1G11050		Protein kinase superfamily protein
A_84_P13957	0,03545904	2,04E-04	1,7032583	0,7682972	AT5G11650		alpha/beta-Hydrolases superfamily protein
A_84_P21190	0,04726939	4,44E-04	1,7014836	0,76679325	AT3G16350		Homeodomain-like superfamily protein
A_84_P20006	0,032583	1,23E-04	1,7005234	0,7659788	AT1G76380		DNA-binding bromodomain-containing protein
A_84_P10152	0,03677519	2,21E-04	1,6998737	0,76542753	AT5G04760		Duplicated homeodomain-like superfamily protein
A_84_P22312	0,04379721	3,57E-04	1,6839865	0,7518806	AT4G11360	RHA1B	RHA1B__RING-H2 finger A1B
A_84_P15820	0,04920762	5,29E-04	1,6825356	0,75063705	AT5G03630	ATMDAR2	ATMDAR2__Pyridine nucleotide-disulphide oxidoreductase family protein
A_84_P21553	0,04503756	3,87E-04	1,6560607	0,72775555	AT5G25110	CIPK25, SnRK3.25	CIPK25_SnRK3.25__CBL-interacting protein kinase 25
A_84_P159575	0,0345411	1,70E-04	1,6242286	0,69975466	AT4G15765		FAD/NAD(P)-binding oxidoreductase family protein
A_84_P18077	0,04963683	5,47E-04	1,614544	0,69112676	AT1G67560	ATLOX6, LOX6	ATLOX6_LOX6__PLAT/LH2 domain-containing lipoxygenase family protein
A_84_P156715	0,03116852	8,68E-05	1,6140692	0,69070244	AT5G62770		Protein of unknown function (DUF1645)
A_84_P766219	0,01997895	1,15E-05	1,5954776	0,67398834	AT5G26600		Pyridoxal phosphate (PLP)-dependent transferases superfamily protein
A_84_P12249	0,04834748	4,98E-04	1,5714763	0,65212053	AT1G28010	ABCB14, ATABCB14, MDR	ABCB14_ATABCB14_MDR12_PGP14__P-glycoprotein 14
A_84_P17501	0,04605175	4,10E-04	1,5606717	0,6421671	AT3G53180	NodGS	NodGS__glutamate-ammonia ligases;catalytics;glutamate-ammonia ligases

A_84_P21946	0,02725945	4,07E-05	1,5567553	0,6385422	AT1G73540	atnudt21, NUDT21	NUDT21_atnudt21__nudix hydrolase homolog 21
A_84_P22448	0,03937708	2,67E-04	1,5515846	0,63374233	AT1G06640		2-oxoglutarate (2OG) and Fe(II)-dependent oxygenase superfamily protein
A_84_P599935	0,04963683	5,47E-04	1,5245023	0,6083383	AT3G19830	NTMC2T5.2, NTMC2TYPE5	NTMC2T5.2_NTMC2TYPE5.2__Calcium-dependent lipid-binding (CaLB domain) protein
A_84_P18223	0,04758364	4,51E-04	1,502241	0,5871163	AT2G32800	AP4.3A	AP4.3A_LecRK-S.2__protein kinase family protein
A_84_P10812	0,032583	1,24E-04	-1,5010667	-0,58598804	AT3G13150		Tetratricopeptide repeat (TPR)-like superfamily protein
A_84_P808242	0,03545904	1,87E-04	-1,5020751	-0,5869569	AT1G14345		NAD(P)-linked oxidoreductase superfamily protein
A_84_P12750	0,04905209	5,23E-04	-1,5058012	-0,5905313	AT3G47430	PEX11B	PEX11B__peroxin 11B
A_84_P14719	0,04805315	4,76E-04	-1,5200204	-0,60409063	AT4G02070	ATMSH6, MSH6, MSH6-1	ATMSH6_MSH6_MSH6-1__MUTS homolog 6
A_84_P557318	0,04706127	4,30E-04	-1,530575	-0,61407375	AT4G04790		Tetratricopeptide repeat (TPR)-like superfamily protein
A_84_P603012	0,04514324	3,95E-04	-1,5468154	-0,629301	AT5G59360		
A_84_P606916	0,04993777	5,63E-04	-1,5604345	-0,64194775	AT2G30890;	TBL43	
A_84_P294634	0,04430861	3,72E-04	-1,5648938	-0,64606476	AT5G53500		Transducin/WD40 repeat-like superfamily protein
A_84_P75044	0,04446041	3,77E-04	-1,571464	-0,65210915	AT5G02830		Tetratricopeptide repeat (TPR)-like superfamily protein
A_84_P22890	0,04238424	3,15E-04	-1,5726548	-0,65320206	AT1G14410	ATWHY1, PTAC1, WHY1	ATWHY1_PTAC1_WHY1__ssDNA-binding transcriptional regulator
A_84_P788949	0,04834748	4,97E-04	-1,58142	-0,6612205	AT3G28100		UMAMIT45__nodulin MtN21 /EamA-like transporter family protein
A_84_P15631	0,04196317	3,10E-04	-1,5903727	-0,66936487	AT3G57830		Leucine-rich repeat protein kinase family protein
A_84_P519713	0,04805315	4,76E-04	-1,5977954	-0,6760827	AT1G66840	PMI2, WEB2	PMI2_WEB2__Plant protein of unknown function (DUF827)
A_84_P19998	0,01822007	7,98E-06	-1,5984154	-0,67664236	AT1G70550		Protein of Unknown Function (DUF239)
A_84_P16203	0,01203481	2,96E-06	-1,6029801	-0,68075657	AT1G48630	RACK1B, RACK1B_AT	RACK1B_RACK1B_AT__receptor for activated C kinase 1B
A_84_P525958	0,03670782	2,18E-04	-1,6037549	-0,68145365	AT1G77630	LYM3	LYM3_LYP3__Peptidoglycan-binding LysM domain-containing protein
A_84_P18915	0,04834748	4,95E-04	-1,610567	-0,68756866	AT1G51460	ABCG13	ABCG13__ABC-2 type transporter family protein
A_84_P814458	0,032583	1,18E-04	-1,6148211	-0,6913743	AT1G72970	EDA17, HTH	EDA17_HTH__Glucose-methanol-choline (GMC) oxidoreductase family protein
A_84_P756180	0,04514324	3,92E-04	-1,6263505	-0,7016382	AT2G14890	AGP9	AGP9__arabinogalactan protein 9
A_84_P13735	0,02459617	2,04E-05	-1,6550156	-0,7268448	AT3G56370		Leucine-rich repeat protein kinase family protein
A_84_P828891	0,03302845	1,48E-04	-1,6658808	-0,73628515	AT3G28100		UMAMIT45__nodulin MtN21 /EamA-like transporter family protein
A_84_P20046	0,02561561	2,78E-05	-1,6663269	-0,73667145	AT1G14280	PKS2	PKS2__phytochrome kinase substrate 2
A_84_P610685	0,02553658	2,42E-05	-1,6737278	-0,7430649	AT3G59670		
A_84_P23174	0,03839359	2,46E-04	-1,7165121	-0,77948	AT3G52720	ACA1, ATACA1, CAH1	ACA1_ATACA1_CAH1__alpha carbonic anhydrase 1
A_84_P16459	0,03839359	2,44E-04	-1,737366	-0,79690164	AT3G14570	ATGSL04, atgsl4, gsl04	ATGSL04_GSL04_GSL4_atgsl4__glucan synthase-like 4
A_84_P15327	0,04706127	4,31E-04	-1,7497976	-0,80718803	AT2G41940	ZFP8	ZFP8__zinc finger protein 8
A_84_P19743	0,03545904	1,82E-04	-1,7528561	-0,8097076	AT5G55250	AtIAMT1, IAMT1	AtIAMT1_IAMT1__IAA carboxylmethyltransferase 1
A_84_P292434	0,03498028	1,77E-04	-1,7646543	-0,8193855	AT2G47930	AGP26, ATAGP26	AGP26_ATAGP26__arabinogalactan protein 26
A_84_P224349	0,03407956	1,66E-04	-1,7719564	-0,82534313	AT2G46040		ARID/BRIGHT DNA-binding domain;ELM2 domain protein
A_84_P837561	0,02725945	4,04E-05	-1,7828845	-0,8342132	AT5G06790		
A_84_P23459	0,02725945	5,32E-05	-1,7854155	-0,83625984	AT5G35960		Protein kinase family protein
A_84_P21962	0,04430861	3,72E-04	-1,7864089	-0,83706236	AT2G31830		5PTase14__endonuclease/exonuclease/phosphatase family protein
A_84_P21617	0,02745376	5,59E-05	-1,7899876	-0,83994955	AT5G49910	cpHsc70-2, HSC70-7	HSC70-7_cpHsc70-2__chloroplast heat shock protein 70-2
A_84_P556476	0,02553658	2,47E-05	-1,8061285	-0,8529005	AT4G18750	DOT4	DOT4__Pentatricopeptide repeat (PPR) superfamily protein
A_84_P10579	0,03995023	2,86E-04	-1,8061941	-0,8529529	AT1G78970	ATLUP1, LUP1	ATLUP1_LUP1__lupeol synthase 1
A_84_P13774	0,04834748	4,95E-04	-1,8081007	-0,854475	AT4G02060	MCM7, PRL	MCM7_PRL__Minichromosome maintenance (MCM2/3/5) family protein
A_84_P12918	0,04845032	5,00E-04	-1,8207784	-0,8645553	AT4G30120	ATHMA3, HMA3	ATHMA3_HMA3__heavy metal atpase 3
A_84_P15930	0,04430861	3,70E-04	-1,8238839	-0,8670139	AT1G29460		SAUR65__SAUR-like auxin-responsive protein family
A_84_P16879	0,04715346	4,36E-04	-1,8380351	-0,8781643	AT5G47800		Phototropic-responsive NPH3 family protein
A_84_P11901	0,03736534	2,29E-04	-1,8434998	-0,88244724	AT1G06100		Fatty acid desaturase family protein
A_84_P599886	0,04418976	3,66E-04	-1,8572689	-0,8931827	AT3G06145		
A_84_P23912	0,03263922	1,41E-04	-1,8782952	-0,90942377	AT2G38940	ATPT2, PHT1;4	ATPT2_PHT1;4__phosphate transporter 1;4
A_84_P14379	0,03866172	2,52E-04	-1,9066913	-0,9310713	AT1G14440	AtHB31, HB31, ZHD4	AtHB31_FTM2_HB31_ZHD4__homeobox protein 31
A_84_P525765	0,04479766	3,81E-04	-1,9177188	-0,93939114	AT1G07270		Cell division control, Cdc6
A_84_P830586	0,03984243	2,83E-04	-1,9280196	-0,9471197	AT5G22310		
A_84_P13857	0,03545904	1,90E-04	-2,0062153	-1,0044764	AT4G28780		GDSL-like Lipase/Acylhydrolase superfamily protein

A_84_P15700	0,04834748	4,89E-04	-2,0230672	-1,0165442	AT4G13710	Pectin lyase-like superfamily protein
A_84_P815691	0,04905209	5,23E-04	-2,0243142	-1,0174332	AT3G49670 BAM2	BAM2__Leucine-rich receptor-like protein kinase family protein
A_84_P826247	0,03995023	2,88E-04	-2,0565464	-1,0402236	AT4G18960 AG	AG__K-box region and MADS-box transcription factor family protein
A_84_P286230	0,04905209	5,16E-04	-2,0649412	-1,0461006	AT3G25905 CLE27	CLE27__CLAVATA3/ESR-RELATED 27
A_84_P284680	0,032583	1,29E-04	-2,0658257	-1,0467185	AT3G01730	
A_84_P785044	0,03954257	2,73E-04	-2,0822313	-1,0581303	AT2G27840 HDA13, HDT04, HDT4	HD2D_HDA13_HDT04_HDT4__histone deacetylase-related / HD-related
A_84_P18411	0,03839359	2,44E-04	-2,1690044	-1,117033	AT3G44970	Cytochrome P450 superfamily protein
A_84_P15097	0,02725945	4,23E-05	-2,224122	-1,1532359	AT1G35290	ALT1__Thioesterase superfamily protein
A_84_P564094	0,03839359	2,43E-04	-2,3109784	-1,2085037	AT2G10920	
A_84_P12766	0,04605175	4,08E-04	-2,3183165	-1,2130775	AT3G51240 F3H, F3'H, TT6	F3'H_F3H_TT6__flavanone 3-hydroxylase
A_84_P592665	0,03157461	9,73E-05	-2,357402	-1,2371979	AT2G24762 AtGDU4, GDU4	AtGDU4_GDU4__glutamine dumper 4
A_84_P827741	0,032583	1,16E-04	-2,3619843	-1,2399993	AT3G12820 AtMYB10, MYB10	AtMYB10_MYB10__myb domain protein 10
A_84_P756272	0,04715346	4,40E-04	-2,5115683	-1,3285885	AT2G27395	
A_84_P609989	0,04514324	3,95E-04	-2,5272398	-1,3375626	AT5G18720	Domain of unknown function (DUF3444)
A_84_P18634	0,04715346	4,35E-04	-2,7114186	-1,4390478	AT4G14700 ATORC1A, ORC1A	ATORC1A_ORC1A__origin recognition complex 1
A_84_P21135	0,02561561	2,63E-05	-2,7293327	-1,4485482	AT3G03820	SAUR29__SAUR-like auxin-responsive protein family
A_84_P15502	0,04905209	5,22E-04	-2,7771978	-1,47363	AT3G14370 WAG2	WAG2__Protein kinase superfamily protein
A_84_P13212	0,04359596	3,42E-04	-2,8259041	-1,4987125	AT2G27395	
A_84_P815182	0,04367585	3,46E-04	-3,0570955	-1,6121616	AT3G27060 ATTSO2, TSO2	ATTSO2_TSO2__Ferritin/ribonucleotide reductase-like family protein
A_84_P10228	0,04680056	4,25E-04	-3,060963	-1,6139855	AT5G38820	Transmembrane amino acid transporter family protein
A_84_P769679	0,03545904	1,90E-04	-3,146212	-1,653616	AT5G49615 TAS3b	TAS3b__TAS3b (trans-acting siRNA 3b); other RNA
A_84_P828605	0,03117324	9,41E-05	-3,5074313	-1,8104148	AT4G25010 AtSWEET14, SWEET14	AtSWEET14_SWEET14__Nodulin MtN3 family protein
A_84_P10285	0,02725945	4,06E-05	-3,8586605	-1,9481001	AT5G54510 DFL1, GH3.6	DFL1_GH3.6__Auxin-responsive GH3 family protein
A_84_P21169	0,04905209	5,25E-04	-4,6126404	-2,2055929	AT3G04280 ARR22, RR22	ARR22_RR22__response regulator 22